National Research Council Canada
Conseil national de recherches Canada

ASSOCIATE COMMITTEE ON GEOTECHNICAL RESEARCH

WORKSHOP ON EXTREME ICE FEATURES

NOVEMBER 3-5, 1986
BANFF, ALBERTA

SPONSORED BY

SNOW AND ICE SUBCOMMITTEE
ASSOCIATE COMMITTEE ON GEOTECHNICAL RESEARCH

COMPILED BY:

G.R. PILKINGTON
AND
B.W. DANIELEWICZ

TECHNICAL MEMORANDUM 141

NRCC 28003

JUNE 1987

PRICE $20.00

Canada

88-04443/

The Associate Committee on Geotechnical Research is one of about thirty special committees which assist the National Research Council in its work. Formed in 1945 to deal with an urgent wartime problem involving soil and snow, the Commiteee is now performing its intended task of coordinating Canadian research studies concerned with the physical and mechanical properties of Snow and Ice, Peatlands, Permafrost, Urban Engineering Terrain Problems, Soil and Rock Engineering, and Marine Geotechnical Engineering. The Committee consists of about twenty Canadians appointed as individuals and not as representatives, each for a three-year term. Enquiries will be welcomed and should be addressed to: The Secretary, Associate Committee on Geotechnical Research, c/o Institute for Research in Construction, National Research Council of Canada, Ottawa, Ontario, K1A 0R6.

This publication is one of a series being produced by the Associate Committee on Geotechnical Research of the National Research Council of Canada. It may therefore be reproduced without amendment, provided that the Institute is told in advance and that full and due acknowledgement of this publication is always made. No abridgment of this report may be published without the written authority of the Secretary of the ACGR. Extracts may be published for purposes of review only.

****

Le Comité associé de recherches géotechniques est l'un des quelque trente comités spécieux qui assistent le Conseil national de recherches dans ses fonctions. Créé en 1945 pour s'occuper de problèmes ayant trait aux sols et à la neige et urgents par suite de la guerre, le Comité remplit maintenant le rôle qui lui était destiné, celui de coordonner au Canada les recherches portant sur les propriétes physiques et mécaniques du sol canadien. Il s'acquitte de ses fonctions par l'intermédiaire des sous-comités de la neige et de la glace, des marécages, du pergélisol, des problèmes l'ingénierie urbaine relatifs au terrain et de génie du sol et des roches, et de génie géotechnique marin. Le Comité se compose d'environ vingt canadiens nommés à titre individuel, et répondrons avec plaisir à vos demandes de renseignement. Veuillez les adresser à:

Le Secrétaire
Comité associé de recherches géotechniques
a/s Institut de recherche en construction
Conseil national de recherches
Ottawa, Ontario K1A 0R6

La présente publication fait partie d'une série réalisée par le Comité associé de recherches géotechniques du Conseil national de recherches. Elle peut donc être reproduite telle quelle à condition que l'institut en soit prévenue au préalable et que l'on mentionne toujours la présente publication. Il est interdit de publier tout résume du présent rapport sans le consentement écrit du secrétaire du CARG, seule sont authorisée les extraits cités dans un comptes rendus.

NATIONAL RESEARCH COUNCIL OF CANADA
CONSEIL NATIONAL DE RECHERCHES CANADA

Associate Committee on Geotechnical Research

WORKSHOP ON EXTREME ICE FEATURES

November 3 - 5, 1986
Banff, Alberta

Sponsored by

Snow and Ice Subcommittee
Associate Committee on Geotechnical Research

Compiled by

G.R. Pilkington
and
B.W. Danielewicz

TECHNICAL MEMORANDUM NO. 41

NRCC 28003

TABLE OF CONTENTS

Page

OPENING REMARKS 1

EXTREME ICE FEATURES 3

SUMMARY OF PRESENTATIONS 5

SUGGESTIONS FOR WHAT TO DO WITH THE CONCLUSIONS OF WORKSHOP 9

BEAUFORT GYRE ICE TRAJECTORIES by S. Cornett 11

STRUCTURE AND GROWTH OF ARCTIC ICE SHELVES AND ICE ISLANDS by M.O. Jeffries 39

LOSS, DECAY, AND RECENT DRIFT OF ICE ISLANDS by W.M. Sackinger and M. Yan 53

MECHANICAL PROPERTIES OF SHELF ICE by R. Frederking and N.K. Sinha 67

* MULTI-YEAR HUMMOCK FIELDS by B. Wright 79

MULTI-YEAR ICE STATISTICS by L.G. Spedding & M.C. Hill 81

MECHANICAL PROPERTIES OF MULTI-YEAR SEA ICE by J.A. Richter-Menge and G.F.N. Cox 121

SURVEY OF PHYSICAL AND MECHANICAL PROPERTIES OF ICEBERGS by J-P. Nadreau 155

FRACTURE MECHANICS AND DAMAGE THEORY AS A BASIS FOR CALCULATION OF ICE-STRUCTURE LOADS by I.J. Jordaan 193

EXTREME ICE FEATURES - STRUCTURE INTERACTION by K.R. Croasdale 233

ICE/STRUCTURE INTERACTION RESEARCH NEEDS by T. Zimmerman ... 279

METHODS OF RISK ANALYSIS by F.G. Bercha 305

REMOTE SENSING OF EXTREME ICE HAZARDS by E. Leavitt and R. Lowry 335

OPERATIONAL RESPONSE TO HAZARDOUS ICE FEATURES by G.R. Pilkington 349

Page

ICE PRESSURES DURING THE IMPACT OF AN ICE MASS by H.R. Kivisild 359

THE ULTIMATE EXTREME ICE FEATURE-ANTARCTIC ICEBERGS by R.B. Thomson 369

EXTREME ICE FEATURE MAPS OF THE ARCTIC OCEAN DERIVED FROM DATA RECORDED BY NUCLEAR SUBMARINES by L.A. LeSchack 373

THE SURFACE WAVE FORMS ON THE ELLESMERE ISLAND ICE SHELVES AND ICE ISLANDS by G. Holdsworth 385

OXYGEN ISOTOPE EVIDENCE OF FRESHWATER POOLS AND ICE ACCRETION BELOW MULTIYEAR LANDFAST SEA ICE, NORTHERN ELLESMERE ISLAND by M.O. Jeffries 405

PRELIMINARY OBSERVATIONS ON COMPRESSIVE STRENGTH, DEFORMATION AND POISSON'S RATIO OF ICEBERG ICE by N.K. Sinha and R. Frederking 413

* ICE INTERACTIONS WITH THE MOLIKPAQ by B. Wright and G.R. Pilkington 431

NORWEGIAN PETROLEUM DIRECTORATE by Vegar Steiro and Stein Storli 433

CURRENT RELEVANT RESEARCH ACTIVITIES OF THE ATTENDEES AT THE WORKSHOP by G.R. Pilkington 447

List of Workshop Attendees 451

List of Technical Memoranda by the Associate Committee on Geotechnical Research 455

---

* Papers not included in these proceedings

WORKSHOP ON EXTREME ICE FEATURES

This workshop is sponsored by the National Research Council of Canada Subcommittee for Snow and Ice. This Subcommittee has the mandate to keep abreast of developments in the field of snow and ice and provide reports to its parent committee the Associate Committee for Geotechnical Research which reports to the Head of the NRCC. The Subcommittees also have an educational role and in this capacity the Snow and Ice Subcommittee has run several workshops covering different current topics on snow and ice to establish the state of the field, the current major problems, and who is doing what. Proceedings of these workshops are available from the NRCC for a nominal charge in the form of Technical Memoranda. (A complete listing of all the T.M.'s put out by the NRCC ACGR is attached at the back of these proceedings.).

An undertaking of this kind relies on contributions from numerous people. First, I would like to thank my co-chairman Ben Danielewicz, for his assistance in putting together this workshop. Secondly, both Ben and I would like to thank our companies, Canmar Ltd. and Gulf Canada Resources Ltd. (my former company), for letting us take the time from our daily schedules to organize the workshop and for letting us use the company secretarial services. Next I would like to thank the authors for taking the time to prepare and present papers; I am extremely impressed by the high standard of the papers. Finally, I would like to thank all the delegates for coming and providing lively discussions; I feel that we had a good interchange of ideas.

Thanks must also go to the Banff Springs Hotel for providing us with such excellent facilities and friendly service; certainly this location helped in ensuring the success of the workshop.

Finally, I would like to say how much I have enjoyed running this workshop, and I hope that all those who attended benefitted as much as I did from the presentations and discussion.

Roger Pilkington
Workshop Chairman, and
Chairman of the N.R.C.
Subcommittee for Snow and Ice

EXTREME ICE FEATURES

The purpose of this workshop on Extreme Ice Features is to discuss all aspects of extreme ice features to try to establish the state of the field, the major problems, and where we should be going from here. Despite the drop in the price of oil and the resulting reduction in Arctic activity, most companies are moving ahead at a reduced pace and, as research funds are scarce, it is essential to know what the priorities are.

An "extreme ice feature" is a feature which causes a problem for an offshore structure, however, in this workshop we will be concentrating mainly on ice features which present a serious problem for fixed offshore production structures which have to remain in place for about 25 years. The design and operation of such structures depends on the number, distribution, and shape of ice islands and hummock fields in the Beaufort Sea and icebergs off the east coast of Canada. Ice strength, modes of failure and effective ice pressures are also necessary information required for such features, along with their velocities and trajectories.

In this workshop papers will be presented to cover all the abovementioned aspects of extreme ice features. At the end of the presentations we will attempt to write down the state of knowledge and what are considered to be the remaining major problems to be resolved in each area before we can say that we have adequate information to design a structure for the Arctic offshore.

Following the formal workshop presentations, a few contributed papers will be presented covering some recent work in the area of extreme ice features.

SUMMARY OF PRESENTATIONS

In this summary we have attempted to identify the areas which are in need of more information from an offshore development point of view. Over the past two days we have heard papers on all aspects of extreme ice features from ice islands to hummock fields to icebergs, and their trajectories and modes of interaction with fixed structures. Below we have taken each extreme ice feature type and summarized what information is needed to allow a proper evaluation of the risk of ice feature-structure impact which is needed for the design of structures, calculation of impact loads for operational situations, detection, monitoring, and development of the means of handling the features to reduce the risk. The items below are compiled from suggestions and discussions by workshop attendees, who are recognized experts in the field.

ICE ISLANDS

For the calculation of the risk of impact of an ice island with a structure and the resulting magnitude of the load, we need the following information.

1. We require more information on the number and sizes of all ice islands.
2. Instantaneous velocities of ice islands.
3. Small- and large-scale ice strengths.
4. Effective strength of entire ice island.
5. Reduction in size of islands as they move south from Ellesmere Island, where they are produced, to the southern Beaufort Sea.

For operational purposes:

6. We need to tag all ice islands that would be considered hazardous for offshore production structures with satellite tracking buoys.
7. Conduct a survey with side looking airborne radar along the west coast of the Arctic Islands from Banks Island to Ward Hunt Island every 2 to 3 years to identify any ice islands in this area, any significant reductions in the area of the ice shelves, and to determine the regrowth of the shelves.

8. Revise models to predict the risk of ice islands or hummock field impact with structures in light of new ice drift information.

9. We need to investigate methods of breaking up extreme features (e.g., ships, explosives, coal dusting, etc.).

MULTI-YEAR HUMMOCK FIELDS AND MULTI-YEAR FLOES

There features will probably be the design criterion for offshore structures as they are far more abundant than ice islands, even though they are, in general, not as big.

1. We need more information on the number, size, shape (3 dimensions), thickness (average thickness, deepest ridges, and edge thickness), depth of consolidation, and small-scale and large-scale strength of multi-year hummock fields. There are only two data sets available at present (1981 and 1982).

   It was felt that many of the above items could be obtained by reviewing old SLAR or SAR data collected by the Atmospheric Environment Service and industry.

2. Are multi-year hummock fields and multi-year floes from the same basic distribution?

3. Instantaneous (1 hour average) velocity distributions.

   Again essentially for operational purposes:

4. Tag very large hummock fields with satellite tracking buoys, if they are moving into the southern Beaufort Sea.

STRENGTH OF MULTI-YEAR ICE

This area is covered in the PERD Workshop on Ice Structure Interaction which was summarized by Tom Zimmerman in this workshop. The items below were particularly emphasized at this workshop.

1. Standardize ice testing techniques.

2. Investigate scale effects.

3. Investigate the application of small-scale test data for the calculation of global and local (10 to 100 sq. m) loads.

ICEBERGS

1. There is a considerable quantity of information on the horizontal velocities of icebergs and their strength and more is being collected by the drill rigs. Unfortunately, most of the data are confidential to industry. Release of these data should be encouraged by Government.

2. We need information on vertical velocities of bergy bits to obtain their total kinetic energy and for comparison with the models being developed by C-CORE.

3. We need more information on the numbers of icebergs (again a lot of this information is confidential to industry). The information must be compiled and analysed in a standard form.

4. We need information on the three-dimensional shape and size of icebergs, in particular their local shape to investigate ice. contact loads.

5. There is no information on iceberg-structure interaction. (qualitative or quantitative).

ICE-STRUCTURE INTERACTION

Again this aspect was covered in the review of the Ice Loads on Structures workshop by Tom Zimmerman. However, it is felt that the conclusions below are worthwhile repeating:

1. Continue the development of fracture mechanics and damage theory for calculations of crushing loads on offshore structures for thick multi-year ice and dynamic loading situations. Damage theory requires a study of the viscosity of the pulverized ice as it extrudes from the damage zone between ice and structure.

2. Calibrate theories and laboratory test with full-scale data.

3. Continue work on pack ice driving forces (i.e., in situ field tests).

4. Continue the work on limit stress pressures and scale effects.

5. Study dynamic loading - the ice, the structure, and the geotechnical problems.

6. Obtain full-scale data on local (10 to 100 sq. m) pressures both confined and unconfined.

REMOTE SENSING

1. Continue to improve understanding of SAR and SLAR images of ice to allow a better interpretation of ice types. This must be backed up with ground truthing.
2. Develop a manual for SAR and SLAR interpretation including time of year and location.
3. Develop standards for quality control of data.
4. Continue development of devices to remotely measure ice thickness.
5. Continue development of marine and over-the-horizon radar systems for ice, and search radar for icebergs.
6. Continue development of other systems for ice detection.
7. Continue working on ice forecast models for the 1 to 3 days periods.

SUGGESTIONS FOR WHAT TO DO WITH THE CONCLUSIONS OF WORKSHOP

After presenting the summaries for each of the papers presented, the participants discussed what should or could be done with these ideas. The following suggestions were made:

1. As the workshop was organized under the NRC Snow and Ice Subcommittee, the Chairman of this Subcommittee, G.R. Pilkington, should forward them to the Chairman of the parent committee, the Associate Committee for Geotechnical Research, and request that he forward them to the head of NRC as being the recommendations of experts in the field.

2. It was felt that the recommendations should also be forwarded to COGLA who would be in a position to bring pressure to bear on AES to follow through with some of the recommendations.

3. Tom Zimmerman of C-FER indicated that Peter Adams, the Head of C-FER, presented the findings of the Ice-Structure Workshop to PERD (Maurice Ruel). It was suggested that we attempt to do the same.

4. Bill Sackinger suggested that we send the conclusions to Fred Roots who has been given the job of forming an Arctic Research Department. Bill also offered to send a list of other people to whom we should send the recommendations.

5. It was suggested that we should publish an article in a public document on the recommendations.

6. Brian Wright suggested that we should form an ad hoc co-op or working group to follow the recommendations. The group would formulate the recommendations into a research program and then go to the most appropriate agencies, such as CPA, ESRF, NOGAP, PERD, NSERC, COGLA (Don Dempster).

   We might get data from industry, then request a matching grant from NSERC, for example.

7. The feeling was that we must lobby, as other groups that lobby get listened to.

8. John Sykes indicated that he was finding it harder and harder to get NSERC funds, as they generally depended on getting industrial funds and these had dried up due to other priorities such as social, economic, and space programs.

9. It was pointed out that industry have equipment and people that are under-utilized at present, hence we should look into joint university/industry programs.

10. We need a statement as to why we need the information at this time and cannot wait until industry is again interested. The reason is that we have to continue data collection as any data lost can never be recovered. We should also stress sovereignty.

BEAUFORT GYRE ICE TRAJECTORIES

by

S. Cornett
Dome Petroleum
Box 200
Calgary, Alberta

ABSTRACT

This paper deals with regional ice movement in the Beaufort Gyre. A brief summary of the driving forces and publicly available ice drift data is followed by a detailed discussion of the trajectories including average speeds and directions, seasonal and geographical variations and distributions of velocities.

It was noted that the speed and direction of ice drift shows definite variation according to geographical location in the Gyre. Further, the influence of synoptic atmospheric circulation patterns was found to be related to seasonal variations in ice conditions. Seasonal trends in ice drift speeds and meadering coefficients were also observed.

An assessment of the current state of research on the topic and suggestions for future work will conclude the paper.

1.0 INTRODUCTION

The Arctic Ocean is usually considered to encompass the area roughly north of 75° latitude. In the general surface circulation of the Arctic Ocean two dominant currents can be identified, namely the Transpolar Drift and the Beaufort Gyre (Figure 1.1). The Transpolar Drift enters the Arctic Ocean via the Bering Strait, swings slightly west following a path several hundred kilometres off the USSR coast. It exits through the Greenland Sea and the Denmark Strait. It is fed by the smaller currents of the East Siberian Sea and the Laptev Sea which receive fluvial outflow from the many rivers along the coast.

The second major current is the Beaufort Gyre which circulates in a clockwise direction with its center located at approximately 80°N latitude and 140°W longitude. It has been estimated that the area included in the Beaufort Gyre varies from 40 to 60 percent of the total area of the polar basin (Vinje, 1982). It is by the means of the Beaufort Gyre, that extreme ice features from the Arctic Ocean are capable of entering the Beaufort Sea.

2.0 DRIVING FORCES

2.1 Atmospheric Circulation

On a macroscale, sea ice movement is a result of synoptic scale atmospheric circulation which, in turn, moves the pack ice by wind stresses on the ice surface. It also indirectly drives ocean circulation beneath the ice.

In the winter, the low level atmospheric circulation is driven by subsidence over the cold continental masses. It produces four large pressure cells, two continental highs and two oceanic lows (Figure 2.1).

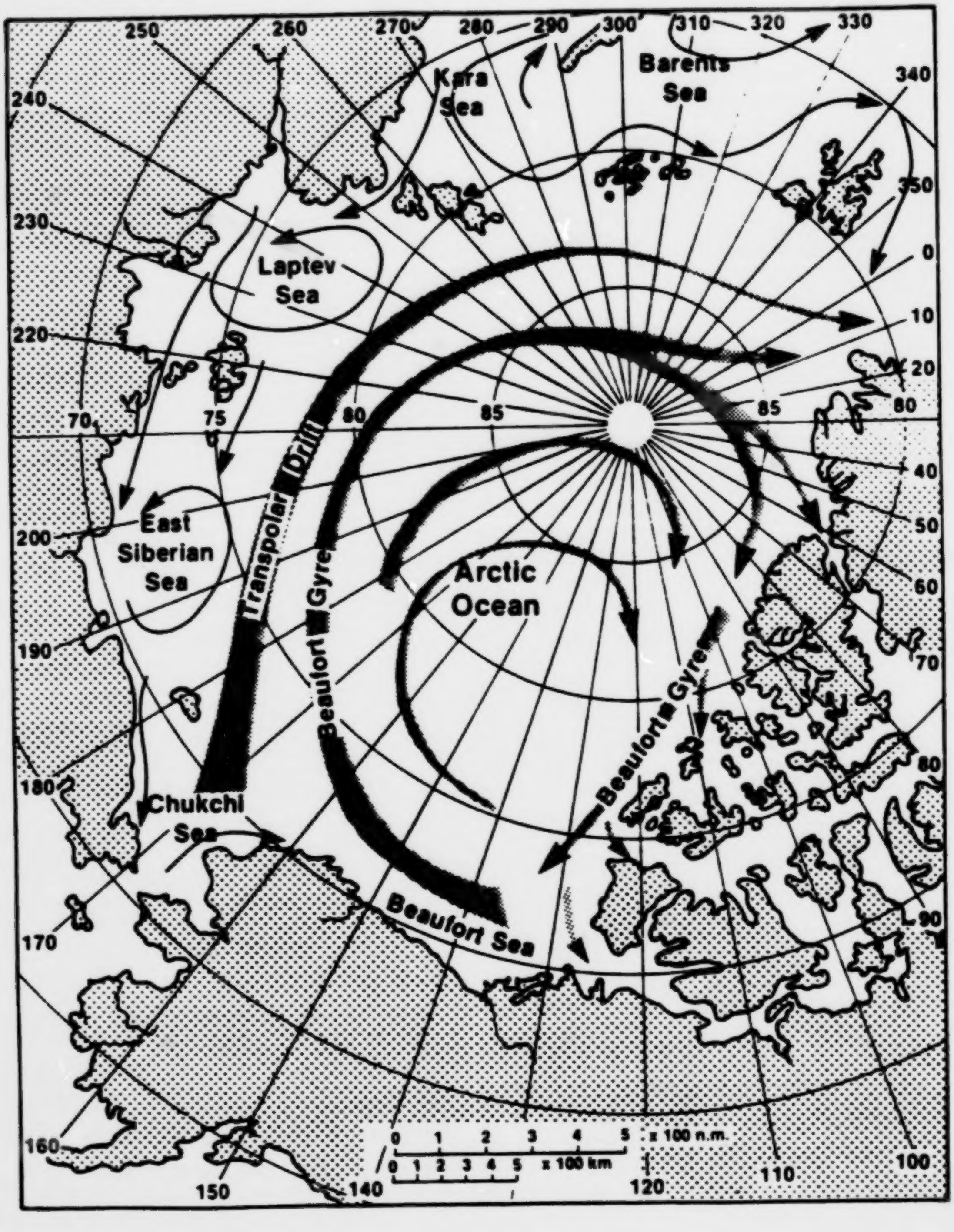
250
260
270
280
290
300
310
320
330
340
350
0
10
20
40
50
60
70
80
90
100
110
120
140
150
160
170
180
190
200
220
230
240
70
75
80
85
85
80
Kara Sea
Barents Sea
Laptev Sea
East Siberian Sea
Transpolar Drift
Beaufort Gyre
Arctic Ocean
Beaufort Gyre
Chukchi Sea
Beaufort Sea
0 1 2 3 4 5 x 100 n.m.
0 1 2 3 4 5 x 100 km

Figure 1.1

General Surface Circulation Patterns Of The Arctic Ocean

The Siberian high is joined to the second smaller high over the Mackenzie Basin by an elongated ridge across the Pacific side of the Arctic ice cap. The Icelandic low controls the circulation over northern Scandinavia and the sea area on the Eurasian side of the Pole. A trough extends from the Icelandic low through the Norwegian Sea into the Barents Sea along which secondary lows travel. Another trough exists over the Davis Strait. The second low, the Aleutian low, lies over the north Pacific but is not as dominant a feature as the Icelandic low.

There is no specific Arctic high on the mean map for January (Figure 2.1) as has been suggested in the past, however, strong anti-cyclones are common over the Arctic Basin and the main air stream is from the middle and western Siberian coast, across the Pole and the south across the Greenland-Spitzbergen area. From the eastern Siberian coast the air mass mixes with Alaska-Yukon air and crosses the Arctic Ocean into the Canadian Archipelago. In summary then, there is no significantly mean driving force provided by the synoptic scale atmospheric patterns for the Beaufort Gyre in the winter.

The January pattern usually persists into March but then changes rapidly with the commencement of solar heating over the continent. The low cells and the Siberian continental high weaken and a region of high pressure dominates the central Arctic Ocean resulting in a clockwise circulation (Figure 2.2). It is during this period in the spring, that the average pressure patterns provide the greatest driving force for the circulation of the Beaufort Gyre.

In the summer the Arctic Ocean is covered by a rather low pressure gradient with a weak low pressure area over the central region and weak anti-cyclones over the peripheral regions including the region of the Beaufort Gyre (Figure 2.3). The result is a generally, sluggish mean flow. However, this period coincides with the period of mobile ice

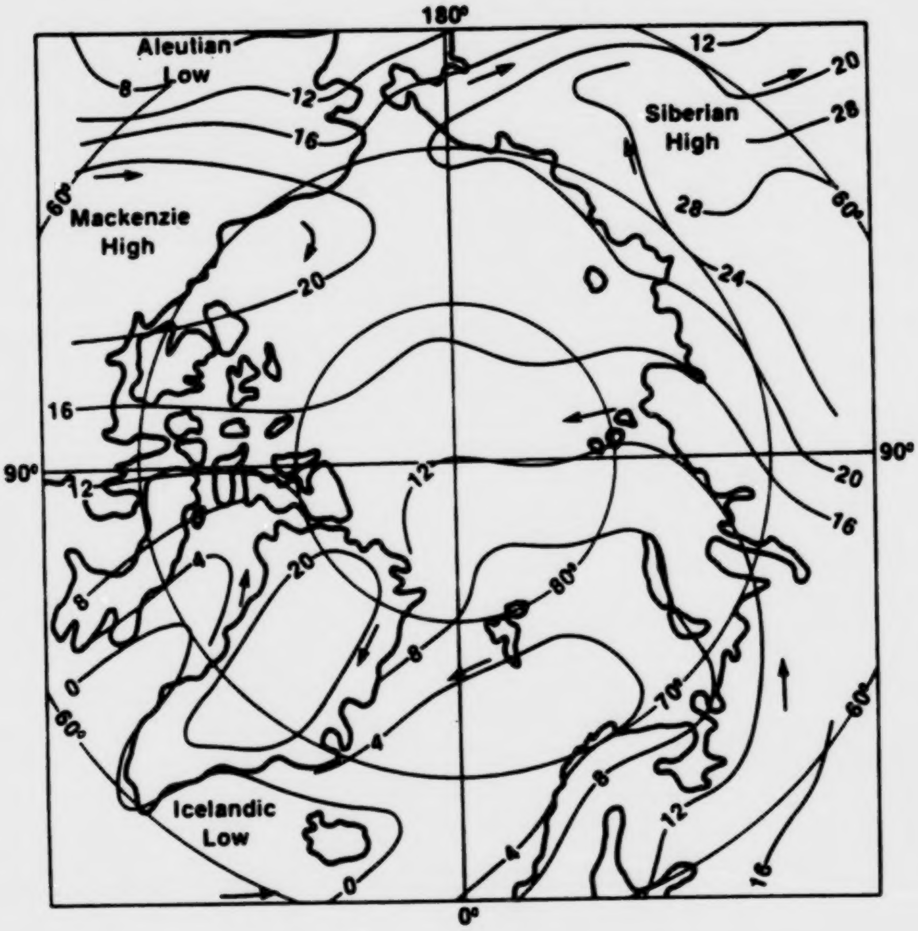
180°
Aleutian Low
8
12
16
12
20
28
Siberian High
28
60°
Mackenzie High
20
24
16
90°
90°
12
20
12
16
60°
8
4
20
8
0
60°
70°
60°
4
8
12
Icelandic Low
0
4
16
0°

Figure 2.1

Mean Air Pressure (mbar), January

(from Vowinckel E. and S. Orvig, 1970)

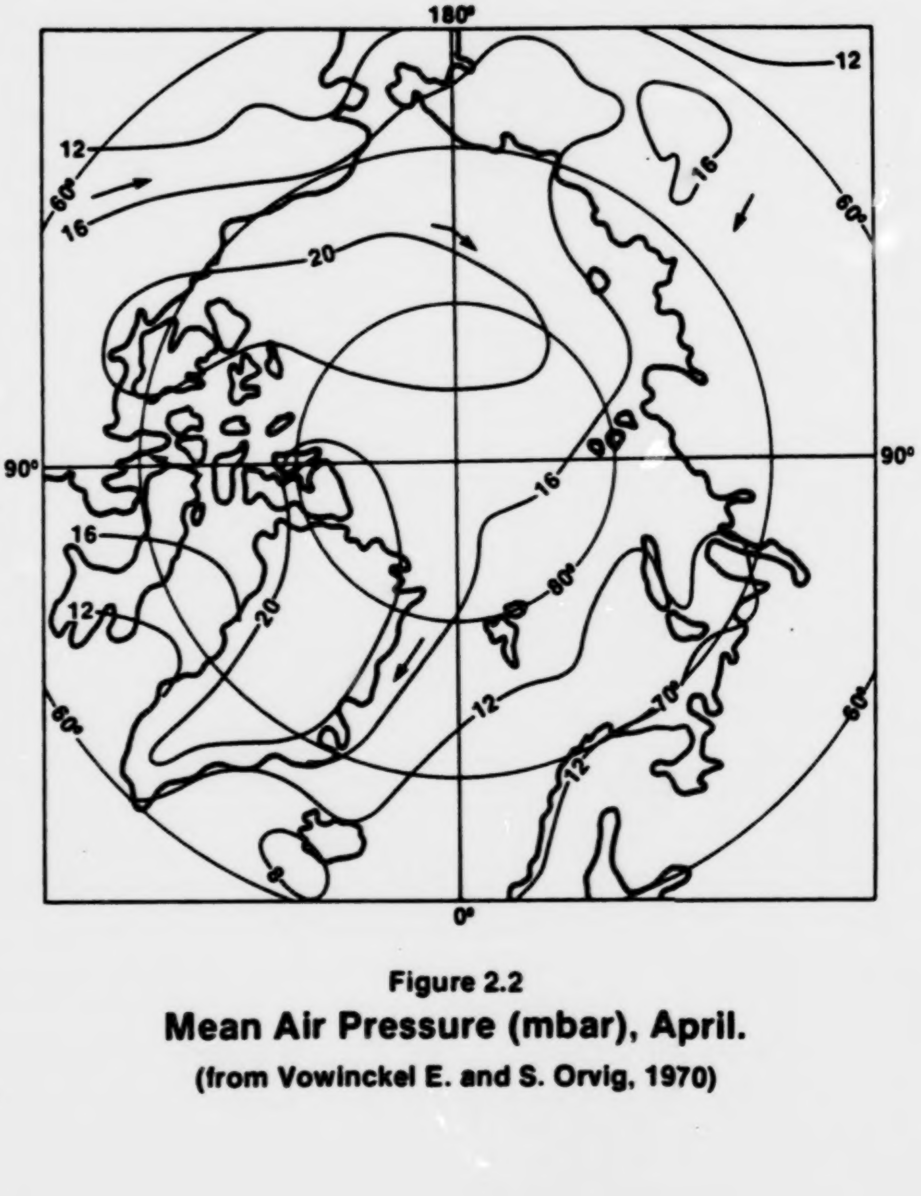
180°
12
12
60°
16
60°
16
20
90°
90°
16
16
90°
12
20
80°
60°
12
70°
12
60°
0°

Figure 2.2

Mean Air Pressure (mbar), April.

(from Vowinckel E. and S. Orvig, 1970)

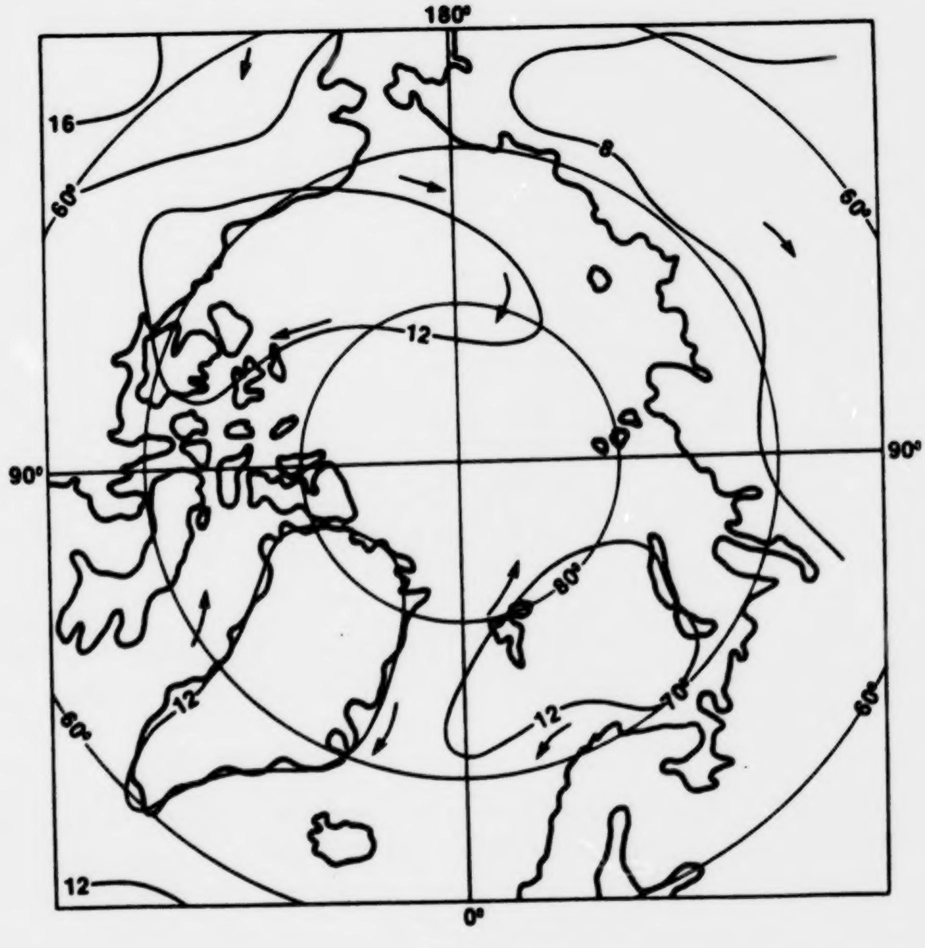
180°
16
8
60°
60°
12
90°
90°
80°
70°
12
12
60°
60°
12
0°

Figure 2.3

Mean Air Pressure (mbar), July.

(from Vowinckel E. and S. Orvig, 1970)

conditions and therefore, the most pronounced clockwise circulation of the Beaufort Gyre. In the autumn changes occur which cause the pattern to slip again towards the winter arrangement. The Aleutian low and then the Icelandic low begin to regain their intensity and the Siberian high begins to rebuild as temperatures drop rapidly over the land masses. This period, therefore is often characterized by alternating strong cyclonic activity and calm anti-cyclonic conditions.

In summary, it can be seen that, although there is no one dominant pressure system over the Arctic Ocean, the anti-cyclonic system during mobile ice conditions serves to drive the clockwise circulation pattern of the ice movement in the Beaufort Gyre.

2.2 Oceanic Circulation

A second driving force in the movement of ice in the Arctic Ocean, albeit closely linked to atmospheric circulation, is the circulation of Arctic water. It, in turn, is driven by both wind (pressure) and density differences. The pattern is comprised of a slow, surface drift, a few centimetres per second, from the eastern side of the Arctic Ocean, across the Pole and out through the Greenland Sea and the clockwise pattern of the Beaufort Gyre in the western part of the Arctic Ocean (Figure 1.1).

The two largest volumes of water inflow are the currents entering from the Atlantic Ocean (approximately 140,000 km^3/yr) and the current entering through the Bering Strait (approximately 20,000 km^3/yr). The Atlantic water has little effect on the surface circulation as it is sufficiently cool and dense to sink below the Arctic water. The inflow from the Bering Strait, however, has a direct effect on the movement of ice in the Beaufort Gyre, providing the eastern section with a significant driving force. Inflow due to river runoff and precipitation has relatively little influence (3,800 km^3/yr) on the large scale surface circulation of the Arctic Ocean.

The most important avenue for outflow is the Denmark Strait (112,000 km^3/yr) followed by the Davis Strait (31,400 km^3/yr). These straits are important due to the fact that they provide "escape routes" for extreme ice features from the Beaufort Gyre. This has been suggested as the fate of the ice islands, T-1 and T-2.

2.3 Other Influences on Ice Drift Trajectories

On a smaller scale, ice involvement is affected locally by land masses, bottom topography, surface roughness of the ice and local currents which may be generated by changes in the temperature and salinity of the water and river outflow. Other regional influences include the degree of convergence of ice in a region and the tilt of the ocean surface due to synoptic scale pressure systems.

The direction of ice movement, when unrestricted, is generally 25° to 40° to the right of the surface wind direction (Zubov, 1945 and others). Surface wind movement, however, is generally to the left of the geostrophic winds by the same amount due to surface friction drag, and Coriolis force (Sobczak, 1977). The result is that ice drift is generally aligned with geostrophic wind, i.e. parallel to isobars. However, ice which is in close proximity to a land mass such as an island or a shallow bottom topography, shoals, may move up to 20° to the left of the surface wind due to frictional drag (Zubov, 1945; Sobczak, 1977).

The degree of compactness or divergence of the ice pack can have a significant effect on the speed and direction of ice drift. In areas of convergence, caused by restrictive geography and a subsequent increase concentration of ice, ice speed will generally be reduced and drift directions altered. A consequence of this scenario is often ridge building and a resultant increase in surface roughness. In divergent conditions, ice will be more likely to follow the patterns of free drift.

Another driving force which may be seen on a regional scale is the effect of regional currents resulting from the inflow from rivers. The effect of increased river discharge in early summer due to inland melting is noticeable on satellite imagery of ice in the Southern Beaufort Sea and in some areas along the Siberian coast.

Surface roughness of ice can influence the speed of ice movement by affecting the wind drag on a piece of ice. It was found, on T-3 (Browne and Crary, 1959) that wind stresses on the ice island were somewhat smaller than those of the surrounding pack ice due to the smoothness of the surface of the ice island.

Changes in the level of the sea due to passing local atmospheric pressure systems can set up a sloping sea-surface which can impose a gravitational component onto normal ice drift movements. In the region of the Bering Strait this has been postulated as one of the contributing factors to the northward oceanic transport from the Bering Sea to the Arctic Ocean (Coachman and Aagaard, 1981).

Inertial oscillations have been found to be another influence affecting the movement of ice. These are frequently observed as looping clockwise motions in the horizontal plane and are a result of inertial water mass movement resulting from the Coriolis effect (Colony, R. and A.S. Thorndike, 1980). A similar effect on ice drift can be caused by tidal currents.

3.0 ICE DRIFT DATA SOURCES

The collection of ice movement data in the Arctic Ocean effectively began when wreckage from the JEANNETTE was found washed ashore in southwest Greenland a few years after the ship was wrecked near the New Siberian Islands in 1879. It has been suggested that this gave Nansen the idea of a drift voyage across the Arctic Ocean and so led to the

FRAM expedition (1893-1896), (Dunbar, M., 1963). From that expedition it was discovered that ice movement in the Arctic Ocean occurred (in part) from the east Siberian coast to the Atlantic Ocean by way of the Pole and the Greenland and Norwegian Sea. Later, the drift patterns of the Russian ship SEDOV (1937-1940) verified and added to the initial findings of the FRAM. Since then, documentation of ice movement in the Arctic Ocean has increased through the use of drifter buoys, aircraft flights, satellite imagery, various ships, ice islands and manned scientific drifting stations situation on large floes.

The Soviet Union established the first drifting station, North Pole-1 (NP-1), in 1937 by aircraft. Systematic work on drifting stations and on high-altitude aircraft expeditions really began in 1950-54 with the stations of NP-2 and NP-3, NP-4 (1954). From then, until 1973, there were, on average, 2 Russian drifting stations in operation each year.

The first ice island was discovered, identified and named in 1946 T-1 by the United States Air Force. The ice islands named T-2 and T-3 were discovered in 1950 and 1947 respectively and all three were tracked by aerial reconnaissance for several years. The Ward Hunt ice islands, WH-1, WH-2, WH-3 and WH-4, were tracked by aerial reconnaissance for various periods between 1963 and 1967.

The Arctic Ice Dynamics Joint Experiment (AIDJEX) was initiated in the late 1960s and the final scientific plan was established to take place in 1975/76 to provide the means to acquire a set of synoptic data about the basic nature of pack ice dynamics. Of the various types of data and studies that came out of the project (many of which are still being analyzed), the drift tracks of four manned ice stations and 14 RAMS drifter buoys are the most useful in the assessment of general ice drift trajectories of the Beaufort Gyre. RAMS (Random Access Measurement System), buoys were drifter buoys that transmitted position data to the Nimbus to Satellite. The four manned stations were tracked using NavSat (Navy Navigation Satellite System).

Most recently, ice drift data has been collected using drifting data buoys in conjunction with the Argos positioning system. The system is managed by Service Argos of the French National Centre for Space Studies (CNES) and uses weather satellites of NOAA (United States National Oceanic and Atmospheric Administration) to relay location transmissions and any data collected between buoys in the field and a central processing facility in France. A total of 26 Argos buoys provided usable location data from the Beaufort Sea between 1979 and 1985. This data, however, is proprietary to participants in APOA Project #222 until 1990.

4.0 ICE DRIFT TRAJECTORIES: GEOGRAPHICAL VARIATIONS

4.0 Results

The data from the above sources was analyzed to determine the average drift rates of pack ice in different sections of the Arctic Ocean and in particular the Beaufort Gyre. The drift tracks were plotted and vector distances calculated between positions with known dates and/or times. Small scale meandering was not included in the calculation of net distances.

The average period of time used in arriving at the net speed was in the order of several weeks to months. This was required because much of the data, specifically the North Pole drifting stations and the early ice islands (the Ward Hunt islands and T-1, T-2 and T-3), is only available on this scale. All data, consequently, was taken to the same time base. The same vector plots were used to determine mean drift direction in each region. The results of the plots are shown in Figure 4.1.

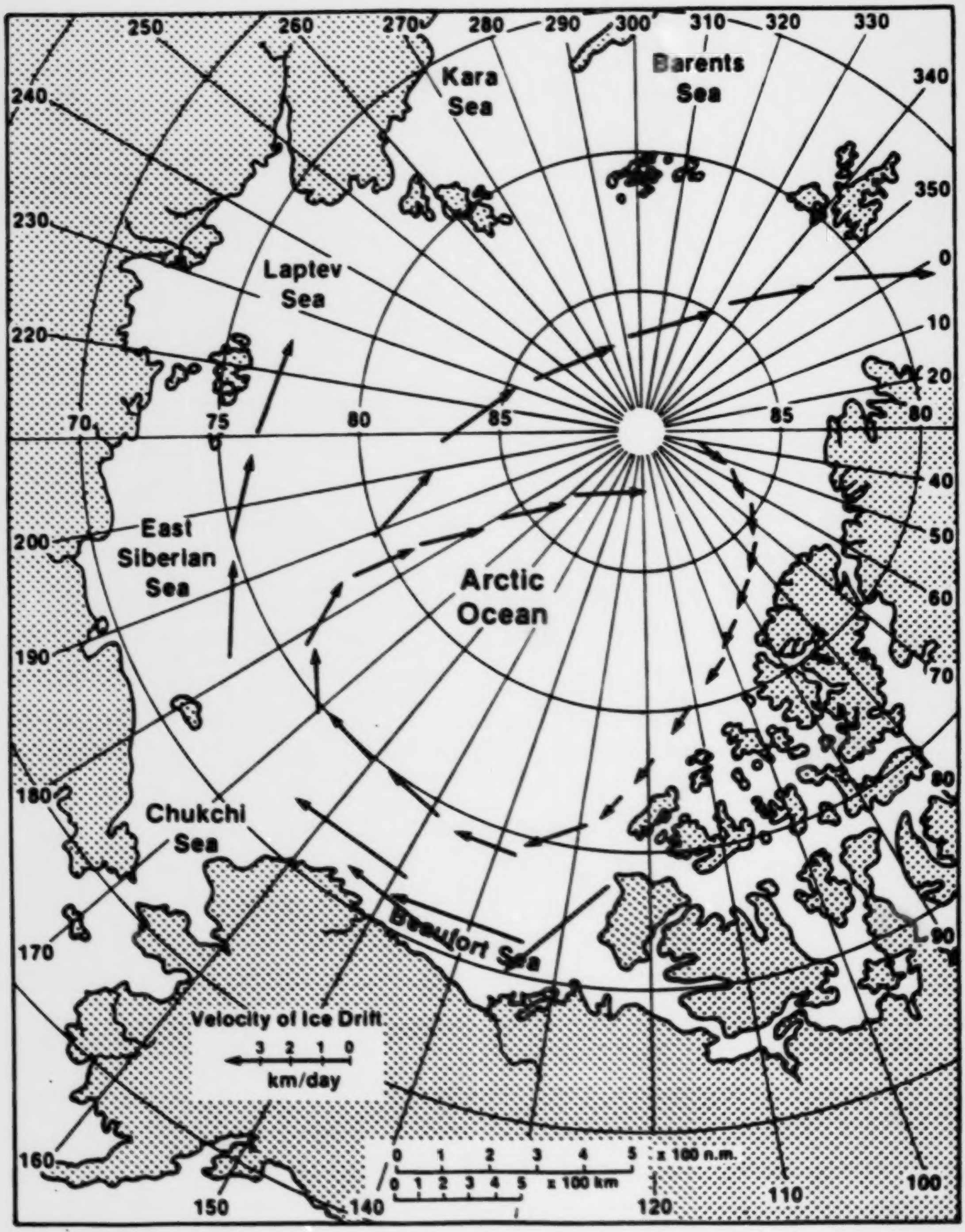
250
260
270
280
290
300
310
320
330
340
350
0
10
20
240
230
220
200
190
180
170
160
150
140
120
110
100
90
80
70
60
50
40
Kara
Sea
Barents
Sea
Laptev
Sea
East
Siberian
Sea
Arctic
Ocean
Chukchi
Sea
Beaufort Sea
70
75
80
85
85
80
Velocity of Ice Drift
3 2 1 0
km/day
0 1 2 3 4 5 x 100 n.m.
0 1 2 3 4 5 x 100 km

Figure 4.1

Mean Velocities Of Ice Drift In
The Arctic Ocean (km/day)

The direction of ice drift trajectories in the Beaufort Gyre can be divided into several regions. The first region describes an arc starting at Banks Island and continuing southwest then west and northwest along the Beaufort Sea coast to about 73° latitude. Drift data here was provided mainly by the RAMS and Argos drifter buoys. The average drift speeds were found to be 4.6 km/day (2.5 nm/day, 5.5 cm/s). This region is the area of the Beaufort Gyre which is commonly referred to as the seasonal pack. In summer, melting of first-year ice occurs and areas of open water become dominant producing extremely divergent ice conditions.

Further offshore a region extending west from at about N75° and W130°, then north along W180° and north and east to about N85° and W120°. Data in this region includes ice islands T-1, T-2 and T-3, the Aidjex manned ice stations and several of the North Pole stations. The average ice drift speed is about 2.3 km/day (1.2 nm/day or 2.8 cm/s). This section of the Gyre parallels the Transpolar Drift.

Another section of the Gyre moves along the coast of Ellesmere Island and the Queen Elizabeth Islands, beginning in the region of W30° and N88° has an average ice drift speed of 1.0 km/day (0.5 nm/day or 1.2 cm/s). Data for this region is taken from the drift tracks of the Ward Hunt ice islands and T-1, T-2 and T-3.

Data on the speed of the Transpolar Drift comes from the North Pole stations and drifting vessels such as the Fram and the Sedov. The mean speed of the drift, from the region around N85° and W200° to the Greenland Sea, averages about 2.9 km/day (1.6 nm/day or 3.5 cm/sec). The mean speed of the Transpolar Drift is somewhat higher than that of the Beaufort Gyre due to higher local speeds at the entrance to the Greenland Strait. The last region that was identified was the area offshore of the Chukchi, East Siberian and Laptev Seas. From several of the North Pole stations and the voyages of the Maud and the JEANNETTE it was found that the average ice drift speed was somewhat higher than that of the Transpolar Drift and the Beaufort Gyre, but not quite as high as that of the near shore Beaufort Sea ice drift. The average speed was 3.3 km/day (1.8 n./day or 2.2 cm/sec) and can be attributed in part to the influence of summer ice melt and subsequent open water conditions similar to these found in the Beaufort Sea.

4.2 Discussion

The mean drift speed based on the data described above,is 2.6 km/day (1.4 nm/day or 3.1 cm/sec). A given ice feature could be expected to complete one rotation of the Gyre in 4 to 10 years, depending primarily upon its starting position and trajectory. This compares favourably with mean speeds cited in the literature(Browne and Crary, 1959; DePaoli et al, 1982; Dunbar and Wittman, 1962 etc). However, a mean ice drift speed for the entire Beaufort Gyre is not an extremely useful statistic because of the wide variations in drift speed according to geographical location. It is more appropriate to discuss speed in the context of each particular region of concern.

The mean ice drift speed offshore of Ellesmere and the Queen Elizabeth Islands is considerably lower than in the rest of the Beaufort Gyre. As the pack begins to move toward the northern coast of the Canadian Archipelago, convergent conditions become dominant due to the increasing compactness of the ice causing a significant reduction in the effective ice drift speed. The degree of compactness in the field will have an effect on the distances over which perturbations in ice velocity can be observed. Effects over distances up to 150-200 km were reported by Basuev in 1967 (Vinje, 1982). During AIDJEX, velocity correlations were observed over distances as great as 800 km (Thorndike and Colony, 1977).

Another by product of convergent ice conditions is increased ridging activity. Consequently, data pertaining to the distribution of sea ice roughness was reviewed. Ridge keel statistics which were derived from submarine sonar profiles indicate that the highest probability of encountering ridge keels occurred offshore of Northern Greenland, Ellesmere Island and the Queen Elizabeth Islands (LeSchack, 1983). These were also areas where the deepest keels were found. Hudson, et al, (1980) also identified this area as the origin of multi-year hummock fields, large floes made up of heavily ridged multi-year ice which had undergone severe deformation due to convergence. In contrast, several areas of open water due to ice divergence are regularly observed in the Arctic Ocean and are known as to recurring polynas. The Bathurst polyna is located offshore of the eastern Beaufort Sea coast, near Banks Island and the Chukchi Sea polyna is located at the outflow of the Bering Strait in the Chukchi Sea. The divergent ice conditions are primarily a result of changes in the orientation of the coastline and landfast ice edge which allows the ice pack to expand.

5.0 ICE DRIFT TRAJECTORIES: SEASONAL VARIATIONS

Ice drift speeds and, to a lesser extent, drift directions also show variations according to season. Contributing factors to seasonal variation in drift speeds are numerous. In general, mean ice drift speeds are higher in the summer season than in the winter. (See Table 5.1)

As noted earlier, the synoptic atmospheric circulation pattern in its winter configuration, does not produce an effective driving force for the Beaufort Gyre. It is not until the spring pattern develops in March and April that a predominant anti-cyclonic stress is felt. This allows drift speeds in the Beaufort Gyre to increase through the spring

TABLE 5.1

SUMMARY OF SEASONAL VARIATION IN ICE DRIFT TRAJECTORIES

LOCATION	WINTER (KM/DAY) (October through June)	SUMMER (KM/DAY) (July through September)
Mean Ice Drift Speed		
Ellesmere Island and Canadian Archipelago	0.9	1.9
Western and Northwestern Sector	1.2	1.2
Beaufort Sea	4.6	5.7
Meandering Coefficient		
Beaufort Sea	4.5	2.4

N.B. The data for the Beaufort Sea does not include drift trajectories of isolated floes. In addition summer data in the Beaufor Sea includes the month of October (which is, therefore, from the winter data set). This has been done to more accurately reflect the beginning of freeze-up in the different regions of the Beaufort Gyre.

and summer. In the winter, increased overall ice thickness in the cold months reduces the amount of ridge building that can take place under limited driving forces. This consequently limits the possibility for floe movement. In addition, leads which do form quickly freeze over, inhibiting further down ice movements.

In the summer, the melting process decreases the total ice concentration, allowing the ice pack to diverge under appropriate conditions. The trend towards higher drift speeds in summer is most evident in the Beaufort Sea due to the reduced concentration and dissipation of the seasonal pack ice. This effect can also be observed offshore of the Canadian Archipelago and in the western and north western sectors of the Beaufort Gyre although there is less differentiation between mean drift speeds in the summer and winter. This is a result of the minimal amount of summer melting that takes place and the high degree of compactness of the ice in the region.

Seasonal variations in drift direction are specifically rated to the degree of meandering that exists. The coefficient of meandering is used to describe the relationship between the total distance travelled and the net displacement. It is defined as the ratio of the total distance travelled to the net distance travelled in a given time period and, as referred to by Dunbar and Wittman (1962), it provides an index of the deviation from the general direction of movement. In the Beaufort Gyre daily meandering coefficients can vary between 1.5 and 10.0 with a mean of 3.9 (Wadham, 1975).

Meandering coefficients tend to be higher during periods of low ice drift speeds, i.e. the winter period (Dunbar and Wittman, 1962). In the Beaufort Sea, meandering coefficients of 4.5 in the winter and 2.4 in the summer have been reported (Danielewicz and Pilkington, 1980).

A further indication of the differences between summer and winter ice movement patterns was identified by Rothrock (1975), during AIDJEX when he noted the "restrained step-like behaviour" of floes in winter in comparison to the "more nearly continuous rotation" of floes in summer.

Seasonal variations in drift speed and direction may also exist locally where a specific feature, such as the river outflow, has an impact on drift patterns for a limited period of time. For example, the Mackenzie River discharges large volumes of fresh water into the Beaufort Sea during spring runoff. It is a common occurrence to see eddies, up to 35 kilometres in diameter, break away and continue to drift through the area as relatively isolated bodies creating local currents from varying directions. These currents can be among the strongest in the Beaufort Sea, approaching 2 kts (Horizon, 1984).

Although the centre of the Beaufort Gyre is located at approximately 150°W and 78°N it can shift with the Transpolar Drift. It undergoes slow lateral displacements between the Eurasian and American side of the Arctic Ocean which are, in turn, probably due to variations in the general atmospheric circulation patterns (Vinje, 1982). Browne and Crary (1959) noted that there are large variations in wind systems from year to year, which affect ice drift. A specific example of this was the variation in the drift tracks of NP-2 and T-3 in 1952 and 1953 which corresponded to variations in the respective average pressure patterns.

6.0 BEAUFORT SEA DRIFT TRAJECTORIES

As a result of the recent commercial interest in the Beaufort Sea, that region of the Beaufort Gyre has been studied in greater than the rest detail. The primary means of ice drift data collection has been the remotely interrogated drifter buoys, specifically Rams and Argos

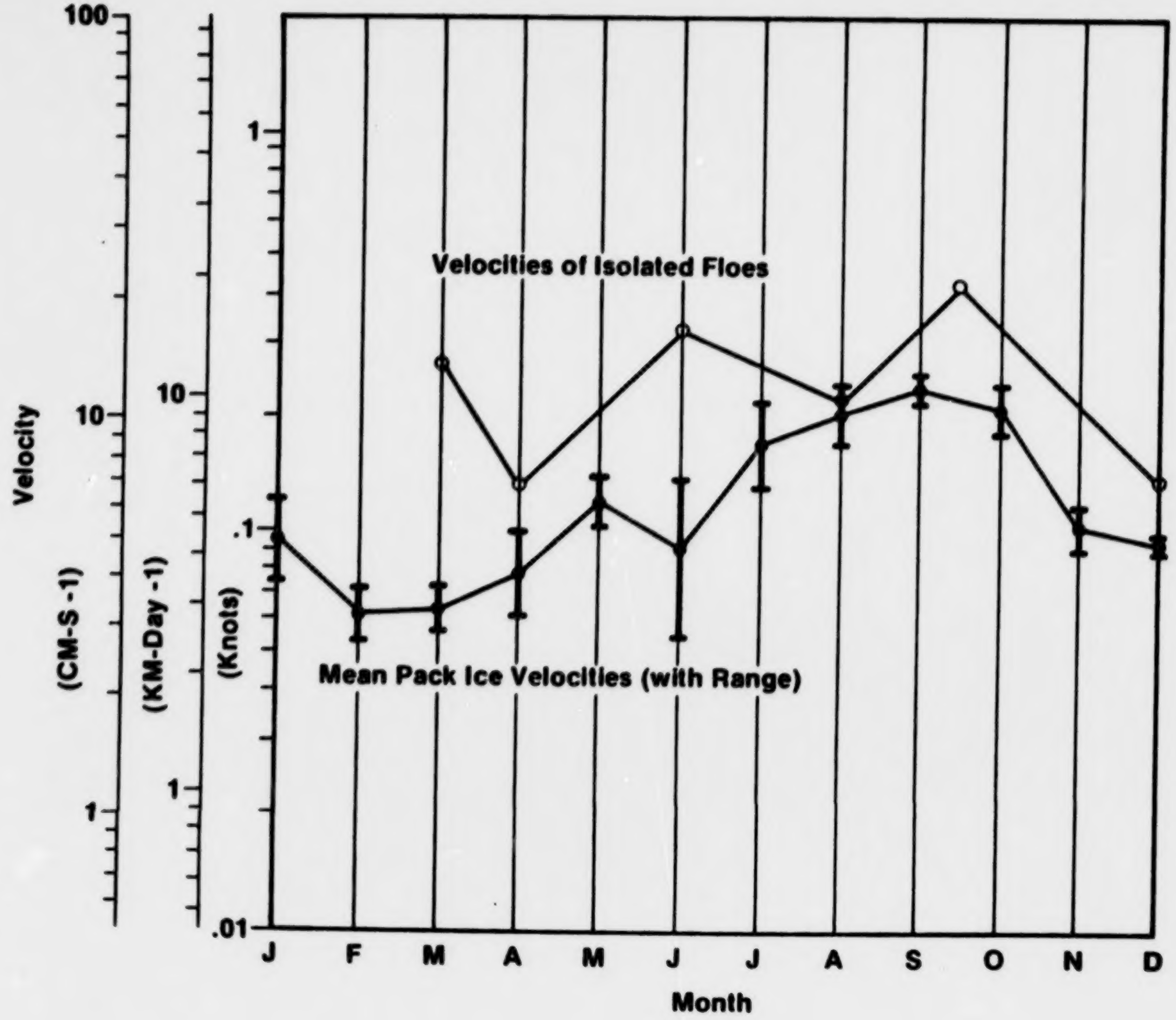

Figure 6.1
Mean Monthly Ice Drift Velocities In The Beaufort Sea
(After Danielewicz and Pilkington, 1980)

drifter buoys. Other studies have used Landsat and NOAA imagery. Mean ice drift speeds for the Beaufort Sea are shown in Figure 6.1. The seasonal variation of ice drift speed is evident, ranging from 3 km/day in February to 10 km/day in September. It can also be seen that the mean velocity for free (isolated) floes is greater than that for (concentrated) pack ice.

A trend has also been observed which shows mean daily ice displacements increasing in magnitude from the eastern region of the Beaufort Sea to the Chukchi Sea. The directional frequency of low velocity displacements was relatively evenly distributed among all of the quadrant whereas the high velocity movements were oriented predominantly towards the west. Meandering coefficient were lower with high daily velocities.

7.0 CONCLUSIONS

Ice drift trajectories in the Beaufort Gyre follow an anti-cyclonic drift path. They are governed primarily by the synoptic atmospheric circulation patterns which move the pack by virtue of wind stresses on the rough surface of the ice and by the ocean circulation patterns. The relationship between the seasonal variation in atmospheric circulation and seasonal variation in ice conditions has been shown to have a significant effect on the circulation of the Beaufort Gyre. Although the atmospheric pressure gradients over the Arctic Ocean in the spring and summer are not as strong as those of the winter pressure patterns, they are aligned with the shoreline and occur during more mobile ice conditions. They, therefore, have a greater influence on the motion of ice in the Beaufort Gyre.

Drift trajectories also show variations in speed and direction according to their position in the Beaufort Gyre. The fastest moving ice is in the Beaufort Sea where ice conditions are more divergent due to the shape of the coast and the substantial decrease in ice concentration in summer. The lowest speeds are seen in the pack offshore of the northern tip of Greenland and Ellesmere Island, a result of the convergence caused by the coastal shape. Other driving influences include bottom topography, local currents or tides, the time of year and therefore ice thickness and the amount of refreezing occurring in leads, the slope of the sea surface due to passing pressure cells and inertial oscillations. All of these influences are inter-related and can have an effect on the speed and/or direction of drift trajectories.

8.0 AREAS FOR FUTURE RESEARCH

Continued deployment and analysis of drifter buoys would add to the existing data base thereby enabling a higher level of confidence to be placed on existing statistics of ice drift trajectories. The majority of public data available is more than 10 years old. However, because of the close relationship between ice drift and atmospheric circulation, efforts should be made to collect atmospheric pressure data at the same time. This is possible with drifter buoys.

Special emphasis should be placed on verifying the drift trajectories of the pack as it moves southward along the Canadian Archipelago and into the Beaufort Sea. This is the means by which extreme ice features such as ice islands and hummock fields, make their way into the Beaufort Sea where they could pose a hazard to commercial operations. A useful corollary to this would be an attempt to estimate the volumes of old ice transferred into and out of the Beaufort Gyre annually. This would provide a means of assessing the amount of old ice that could be expected to affect offshore operations in the Beaufort Sea.

Further attempts should be made to collect data on ice drift trajectories over short time periods, especially in the northern extremes of the Beaufort Gyre where the data base is particularly sparce.

The inter-relationships of the various driving forces and the degree of their influence on ice drift trajectories should continue to be investigated. The relative importance of synoptic scale atmosphere circulation needs to be compared with the effects of smaller scale influences such as local currents, internal stresses within the pack, coastal geography and bottom topography and the characteristics of the ice features themselves. This can best be achieved through reasonably comprehensive field investigations, similar in philosophy to AIDJEX, but not necessarily on such a grand scale. Results of these types of investigations could have a significant impact on offshore operations in terms of establishing more accurate risk levels and possible avoiding the costs of overly conservative assumptions.

REFERENCES & BIBLIOGRAPHY

Barnes, P.W., D. M. Schell, E. Reimnitz (ed.), 1984, The Alaskan Beaufort Sea Ecosystems and Environments. Academic Press Inc., Toronto.

Boucher, K., 1975, Global Climate, The English Universities Press Ltd., London, Great Britain.

Browne, I.M. and A.P. Crary, 1959, The Movement of Ice in the Arctic Ocean in Arctic Sea Ice (Thurston, W.R. ed.), National Academy of Sciences, Washington, D.C.

Colony, R. and A.S. Thorndike, 1980, The Horizontal Coherency of the Motion of Summer Arctic Sea Ice, Journal of Physical Oceanography Vol. 10, Aug. 1980.

Cornett, S. and R. Kowalchuk, 1985, Statistical Analysis of Ice Movement in the Beaufort Sea Using Argos Buoy Data, A.P.O.A. Project No. 222.

Danielewicz, B.W. and G.R. Pilkington, 1980, Selected Environmental Characteristics of Beaufort Sea Ice, report for Dome Petroleum Limited.

DePaoli, S., T.B. Morrison, R.W. Marcellus, 1982, Analysis of Interaction Probabilities Between Large Ice Features and Offshore Structures in the Canadian Beaufort Sea, report for Canadian Marine Drilling Ltd.,

Dunbar, M. and W. Wittman, 1963, Some Features of Ice Movement in the Arctic Basin in Proceedings of the Arctic Basin Symposium, October, 1962, Arctic Institute of North American, Washington, D.C.

Horison Offshore Services, 1984, An Examination of Beaufort Sea Ocean Currents 1981-1983, report for Canadian Marine Drilling Ltd.

Hudson, R.D. et al, 1980, Final Report on the Field Studies and Aerial Mapping Along the North West Edge of the Canadian Archipelago, report for Dome Petroleum Limited.

Koenig, L.S., K.R. Greenaway, M. Dunbar, G. Hattersley-Smith, 1952, Arctic Ice Islands, Arctic, Vol. 5, Issue 2.

Kozo, T.L., 1984, Short Term Prediction (Nowcasting) of Net Daily Sea Ice Movement in the Bering Strait with a Mesoscale Meteorological Network, Final Report, Outer Continental Shelf Environmental Assessment Program, Research Unit 519.

Lee, R., 1970, The Circulation of the Arctic in Weather and Climate, (Nelson J.G. and W.J. Chambers, eds.) Methuen Publications, Toronto.

LeSchack, L.A., 1983, Arctic Ocean Ice Deformation Chart Using Sonar Data Recorded from Nuclear Submarines, POAC 83, Finland, Vol. 1.

Lindsay, D., W. Seifert, N. Anderson, 1968, Ice Islands, 1967, Arctic Vol. 21, Issue 2.

Lockwood, J.G., 1974, World Climatology, An Environmental Approach, Edward Arnold (Publishers) Ltd., London, Great Britain.

McLaren, A.S., P. Wadham , R. Weintraub, 1984, The Sea Ice Topography of M'Clure Strait in Winter and Summer of 1960 from Submarine Profiles, Arctic, Vol. 37, No. 2.

McPhee, M.G., L. Mangum, P. Martin, 1978, Performance of Met/Ocean Buoys in Aidjex, Aidjex Bulletin No. 40, University of Washington, Seattle, Wash.

Michel, B., 1985, Element of Ice Dynamics in the Arctic Ice Pack, POAC 85, Greenland, Vol. 1.

Muench, R.D., G.R. Stegen, L.E. Hachmeister, 1983, Prediction of Ice Distribution and Movement in the Outer Marginal Ice Zone, POAC 83, Finland, Vol. 1.

Norcor Engineering, 1977, Probable Behavior and Fate of a Winter Oil Spill in the Beaufort Sea, Norcor Engineering, Yellowknife, N.W.T.

Nordlund, O.P., W.M. Sackinger, M. Yan, 1985, Ice Features and Movement North of Ellesmere Island, Canada, POAC 85, Greenland, Vol. 1.

Pritchard, R.S. (ed.), 1980, Sea Ice Processes and Models, Proceedings of AIDJEX Symposium, University of Washington Press, Seattle, Wash.

Reimer, R.W., J.C. Schedvin, R.S. Pritchard, 1983, Chukchi Sea Ice Motion, POAC 83, Finland, Vol. 2.

Reimnitz, E., L. Toimil, P. Barnes, 1977, Arctic Continental Shelf Processes and Morphology Related to Sea Ice Zonation, Beaufort Sea, Alaska, AIDJEX Bulletin No. 36, University of Washington, Seattle, Wash.

Rothrock, D.A., 1975, The Steady Drift of an Incompressible Arctic Ice Cover, Journal of Geophysical Research, Vol. 80 (30).

Sackinger, W.M., et al, 1985, Ice Island Generation and Trajectories North of Ellesmere Island, Canada, POAC 85, Greenland, Vol. 2.

Sobczak, L.W., 1977, Ice Movements in the Beaufort Sea, Journal of Geophysical Research, Vol. 82, No. 9.

Treshnikov, A.F., Ye. G. Nikiforov, N.I. Blinov, 1977, Results of Oceanological Investigations by the "North Pole" Drifting Stations, Polar Geography, Jan-Mar. 1977.

Vinje, T.E., 1982, the Drift Pattern of Sea Ice in the Arctic with Particular Reference to the Atlantic Approach in *The Arctic Ocean, the Hydrographic Environment and the Fate of Pollutants*, (Roy, L., ed.) MacMillan Press Ltd., London, Great Britain.

Vowinckel E. and S. Orvig, 1970, the Climate of the North Polar Basin in *Climates of the Polar Regions*, World Survey of Climatology, Vol. 14.

Wadham , P., 1975, Sea Ice Morphology in the Beaufort Sea, Technical Report 36, Beaufort Sea Project, Dept. Environment, Victoria, B.C.

Zubov, N.N., 1945, Arctic Ice, Translation No. 108, Air Force Geophysics Laboratory, Jan. 1979, Mass., U.S.

NRC WORKSHOP ON EXTREME ICE FEATURES

Questions and Discussions Form

AUTHOR: S. Cornett

PAPER: Beaufort Gyre Ice Trajectories

DISCUSSION BY: G. Holdsworth

DISCUSSION:

Is there enough data to study any shifts in the position of bifurcation of the N.E. limb of the Beaufort Gyre where it is directed towards Northern Ellesmere Island. This question has relevance to the drift paths of ice islands in this region (off Ward Hunt ice shelf).

AUTHOR'S REPLY:

No. At this time there is not enough data. To study this, position data for a number of targets as well as other information such as pressure patterns, both local and regional, currents, ice concentration, etc. for the same time period is required. I don't think there is a sufficient data base at this time. However, it should be mentioned that drifter buoys are now being used in the Arctic Ocean by the Norwegians and the Polar Science Centre at the University of Washington. These may provide more data in the near future.

DISCUSSION BY: G.R. Pilkington

DISCUSSION:

Do we have enough information to predict the drift paths of ice islands and hummock fields into the southern Beaufort Sea?

AUTHOR'S REPLY:

No. But we can say that they will eventually come down into the area.

STRUCTURE AND GROWTH OF ARCTIC ICE SHELVES AND ICE ISLANDS

by

Martin O. Jeffries
Geophysical Institute
University of Alaska
Fairbanks, Alaska 99775-0800
U.S.A.

ABSTRACT Our knowledge of the growth and structure of Arctic ice shelves and ice islands is the result of sporadic investigations since the early 1950s. This paper is a brief review of that work. Present ice shelf extent is outlined and it is shown that the seven remaining ice shelves owe their origin to a variety of growth processes. The largest ice shelf, Ward Hunt Ice Shelf, has grown *in situ* and it is shown that the internal structure is not homogeneous due to spatial variations in the flow of freshwater and seawater - and associated ice accretion below the ice. Calving of ice from the ice shelves creates ice islands but the causes of calving are unknown. There are presently about 25 ice islands off Axel Heiberg and Ellesmere islands.

INTRODUCTION

Ice islands are among the largest ice features known in the Arctic Ocean. For example, T-2, first sighted in July 1946, remains the largest recorded ice island (about 700km^2). It is now generally accepted that the ice islands were originally part of the extensive Ellesmere Ice Shelf that perhaps once fringed the northern coast coast of Ellesmere Island, from Point Moss to Nansen Sound (Fig.1). Today, the remains of the Ellesmere Ice Shelf are to be found in a number of small, individual ice shelves. Ice shelves and ice islands have been studied sporadically since they were first discovered 40 years ago. This paper is a brief review of studies of the structure and growth of these extreme ice features.

PRESENT ICE SHELF EXTENT

The actual area and extent of the Ellesmere Ice Shelf will never be known. But, with the disintegration of the ice shelf and the creation of ice islands, the total area of shelf ice has decreased to about 1400km^2. Most of the remaining shelf ice is to be found at seven locations; Markham I.S., Ward Hunt I.S., Ayles I.S., Milne I.S., Hanson I.S., Alfred Ernest I.S. and Armstrong I.S. (Fig. 1). The largest of the present ice shelves is the Ward Hunt Ice Shelf which has an area of about 440km^2. The thickness of Ward Hunt I.S. varies between 40m and 50m, but the greatest known shelf ice thickness is 100m, in Milne I.S. The ice shelves are noted for their distinctive undulating surface topography of ridges and troughs that are particularly recognizable in summer when meltwater accumulates in the troughs as long, narrow lakes. Hattersley-Smith (1957) coined the term "rolls" to describe the undulations.

STRUCTURE AND GROWTH OF ARCTIC ICE SHELVES

Originally, the ice shelves grew by two processes; 1) glaciers flowed off the land and remained afloat as glacier tongues in fiords and inlets and, 2) thick sea ice grew (by deformation or congelation) and remained fast to the coast. Large areas of Milne I.S. and Alfred Ernest I.S. originated as a result of the first process (Jeffries 1986a) while Ward Hunt I.S. originated as a result of the second process (Hattersley-Smith 1960). The glacier tongues and the sea ice acted as stable platforms for subsequent thickening by; 1) surface accumulation of snow and ice and, 2) undersurface accretion of fresh, brackish or saline ice, related to water stratification associated with ice dams across the mouths of bays and inlets. In addition, after an ice island calving the shelf ice is often quickly replaced by multiyear landfast sea ice that grows *in situ* in a manner analogous to the original growth of some ice shelves. Milne Re-entrant, at the front of Milne I.S., is an example of sea ice growth, to as much as 10m thickness, after an ice island calving (Jeffries 1986b and Jeffries this volume). The most extensive studies of the growth and structure of arctic ice shelves have been undertaken on Ward Hunt I.S. The results of this work are summarised in the next section.

IN SITU ICE SHELF GROWTH: ICE CORE STUDIES OF WARD HUNT ICE SHELF

The first ice cores were drilled in Ward Hunt I.S. in 1954 (Marshall 1955) and since that time many cores have been drilled in attempts to study the internal structure of the shelf (Ragle and others 1964; Lyons et al. 1971; Jeffries 1985). These studies have revealed that the shelf ice has grown *in situ* rather than from glaciers, but there are considerable lateral inhomogeneities, with the greatest contrast being between the east and west parts of the shelf. This is described below.

Radio-echo sounding of Ward Hunt I.S. has encountered problems with internal reflections and low permittivity that have been attributed to the presence of saline ice (Hattersley-Smith et al. 1969; Prager 1983). This problem is especially apparent in the west shelf where there is a considerable amount of saline ice (Fig. 2). Jeffries (1985) described the four-layer stratigraphy of alternating non-saline and saline layers and described the growth of each layer as follows:

> Stratum 2: the remains of the original thick sea ice that grew *in situ*. Mean salinity of 2.12o/oo; mean electrical conductivity, 3.07 mS cm^{-1} (milli-Siemens per centimetre).
>
> Stratum 1: freshwater ice or iced-firn that accumulated at the surface of Stratum 2 as a result of the percolation and refreezing of meltwater in snowpack. Mean salinity, <0.01 o/oo; mean electrical conductivity, 0.008 mS cm^{-1}.
>
> Stratum 3: freshwater ice that accreted from freshwater at the undersurface of the ice shelf . Mean salinity, 0.18 o/oo; mean electrical conductivity, 0.274 mS cm^{-1}.
>
> Stratum 4: saline ice that accreted from seawater at the undersurface of the ice shelf . Mean salinity, 3.89 o/oo; mean electrical conductivity, 5.3 mS cm^{-1}.

Prager (1983) obtained good bottom reflections from east Ward Hunt I.S. where the ice is 40-50m thick. Subsequently, from studies of "Hobson's Ice Island", it was discovered that the east shelf (from which the ice island calved) is composed of an apparently homogeneous mass of non-saline ice (Sackinger et al. 1986; Jeffries et al. in press). The ice has a very low electrical conductivity of 0.005 mS cm^{-1} (Fig. 3), i.e. three orders of magnitude lower than the saline ice of the west shelf. The ice is believed to have grown as a result of bottom freezing of freshwater and has entirely replaced the sea ice that originally grew in this area. This assumes a continual loss of ice from the ice shelf surface; available evidence suggests that this has been the case for the last 100-400 years.

The marked contrast in the internal structure of the east and west shelf is attributed to differences in water circulation below the ice (Jeffries et al. in press). The west shelf is underlain entirely by seawater that flows into Disraeli Fiord (Fig. 1). The fiord is stratified, with a permanent, 44m deep layer of freshwater overlying deeper seawater (Keys 1978; Jeffries 1985). The outflow of freshwater from the fiord is believed to occur predominantly beneath the east shelf, from which fresh ice accretes onto the bottom of the ice shelf.

ICE ISLAND CALVINGS SINCE 1959

Ice islands T-1, T-2, T-3, T-4 and T-5 were discovered during the period 1946-50. The immense size of these particular ice islands suggests that the greater part of the disintegration of the Ellesmere Ice Shelf occurred only 1 or 2 decades prior to 1950. However, there have been further calvings since that time, most of them documented since 1959 when extensive vertical aerial photographic coverage of the ice shelves was obtained by the RCAF. The largest calving took place in 1961-62 when almost $600km^2$ of ice broke away from Ward Hunt I.S. (Hattersley-Smith 1963). Between 1962 and 1966 a number of events occurred: M'Clintock I.S. disintegrated, although a number of large pieces of shelf ice remain in M'Clintock Inlet; about $15km^2$ of ice broke off Ayles I.S. which in turn moved about 5km out of Ayles Fiord (the ice shelf remains in place at the mouth of the fiord) (Jeffries 1986b); about $35km^2$ of ice calved from Milne I.S. (Jeffries 1986b). More recently, in 1982-83, about $40km^2$ of ice calved from east Ward Hunt I.S. (Jeffries and Serson 1983).

The causes of ice island calvings are not yet well understood, but numerous possibilities have been suggested. These include crack initiation and propagation by the actions of winds, tides and pack ice pressure, seismic shocks and resonant motions and vibrations within the ice. (See Holdsworth in this volume for further discussion of vibrations).

ICE ISLAND POPULATION

In the early 1970s efforts were made to determine the number of ice islands in the Beaufort Sea (Spedding 1977). Over 400 ice islands were counted but the subsequent fate of these is unknown. After the calving from Ward Hunt I.S. in 1982-83, eight ice islands were located on SLAR (side-looking airborne radar) imagery of 11 May 1983 (Sackinger et al. 1986). During an aerial photographic mission in July 1984, Jeffries and Sackinger observed nine old ice islands that they believed to be unrelated to the 1982-83 calving. In spring 1986, between 23 and 25 ice islands were counted from an aircraft flying at 3000m close to the northern coasts of Axel Heiberg and Ellesmere Islands (Jeffries unpublished data).

The increase in the number of ice islands since 1983 is due either to the disintegration of some of those that calved in 1983 and/or an "invasion" of older ice islands into this area. The largest of the known ice islands is "Hobson's Ice Island" which has dimensions of 4 x 9km, an area of 26km^2 and a mean thickness of 42.5m. Three deep ice cores have now been drilled in this ice island; two of these are presently being studied at the Geophysical Institute, University of Alaska-Fairbanks. The smallest ice island has dimensions of only 70 x 60m with an estimated thickness of 30m. Like the ice shelves from which they calved, the ice islands have an undulating topography of ridges and troughs. In addition, they tend to be elongated with a high length-width ratio.

Ice island calvings have occurred quite regularly since 1959. This raises the question of whether further calvings are likely in the future. As noted earlier in this section, Ayles I.S. moved about 5km out of Ayles Fiord. Although the shelf remains at the mouth of the fiord it is now in a more precarious position from which it could calve, under the right circumstances. The inner part of Alfred Ernest I.S. is part of a glacier tongue which appears to have pushed the outer shelf seaward. A further advance (perhaps a surge) of the glacier might cause a calving and the loss of a large part of Alfred Ernest I.S.

SUMMARY

Despite considerable disintegration, probably during the last 100 years, ice shelves remain important features on the north coast of Ellesmere Island. The structure of these shelves is quite variable owing to different growth mechanisms and processes that give rise to considerable variations in ice salinity (and, by implication, crystallography). The inhomogeneous structure of the ice shelves would be evident in ice islands, depending on their source. The largest ice island known at the present time is composed entirely of freshwater ice, but other ice islands might contain sea ice.

In the interval 1983-86, about 25 ice islands have been sighted along the coastal margins of the northern Queen Elizabeth Islands. However, this is only a small part of the Arctic Ocean, for which the total number of ice islands remains unknown. Although the area of shelf ice is much smaller than it once was, the potential for further ice island calvings remains. Furthermore, the shelf ice lost at the time of calving is quickly replaced by multiyear landfast sea ice; new ice shelves regenerate and ice islands calve from these areas.

ACKNOWLEDGEMENTS

My work on the ice shelves began at the University of Calgary, Department of Geography, and was made possible with the support of the Polar Continental Shelf Project, Defence Research Establishment Pacific, Arctic Institute of North America, Gulf Canada, Dome Petroleum and Petro-Canada. Work at the Geophysical Institute, University of Alaska is supported by the U.S. Dept. of Energy, Morgantown Energy Technology Centre, W.Virginia.

REFERENCES

Hattersley-Smith, G. 1957. Arctic 10 : 32-44.

....1960. Geografiska Annaler 42 : 45-38.

....1963. Journal Of Glaciology 4 : 415-444.

...., Fuzesy, A. and Evans, S. 1969. Defence Research Establishment Ottawa, Technical Note 69-6.

Jeffries, M.O. 1985. PhD Thesis, University of Calgary.

............................1986a. Arctic and Alpine Research 18 :

............................1986b. Arctic 39 : 15-19

.... and Serson, H.V. 1983. Arctic 36 :289-290.

.... et al. in press. Annals of Glaciology 10:

Keys, J.E. 1978. Defence Research Establishment Ottawa, Report No. 792.

Lyons et al. 1971. Journal of Glaciology 10 : 93-100.

Marshall, E.W. 1955. Arctic 8 : 109-114.

Prager, B.T. 1983. MSc Thesis, University of British Columbia.

Ragle, R.H. et al. 1964. Journal of Glaciology 5 : 39-59.

Sackinger, W.M. et al. 1986. U.S. Dept. of Energy, Morgantown Energy Technology Centre, Contractor's Review Meeting.

Spedding, G. 1977. Report IPRT-21ME-74 of APOA Project 99-1.

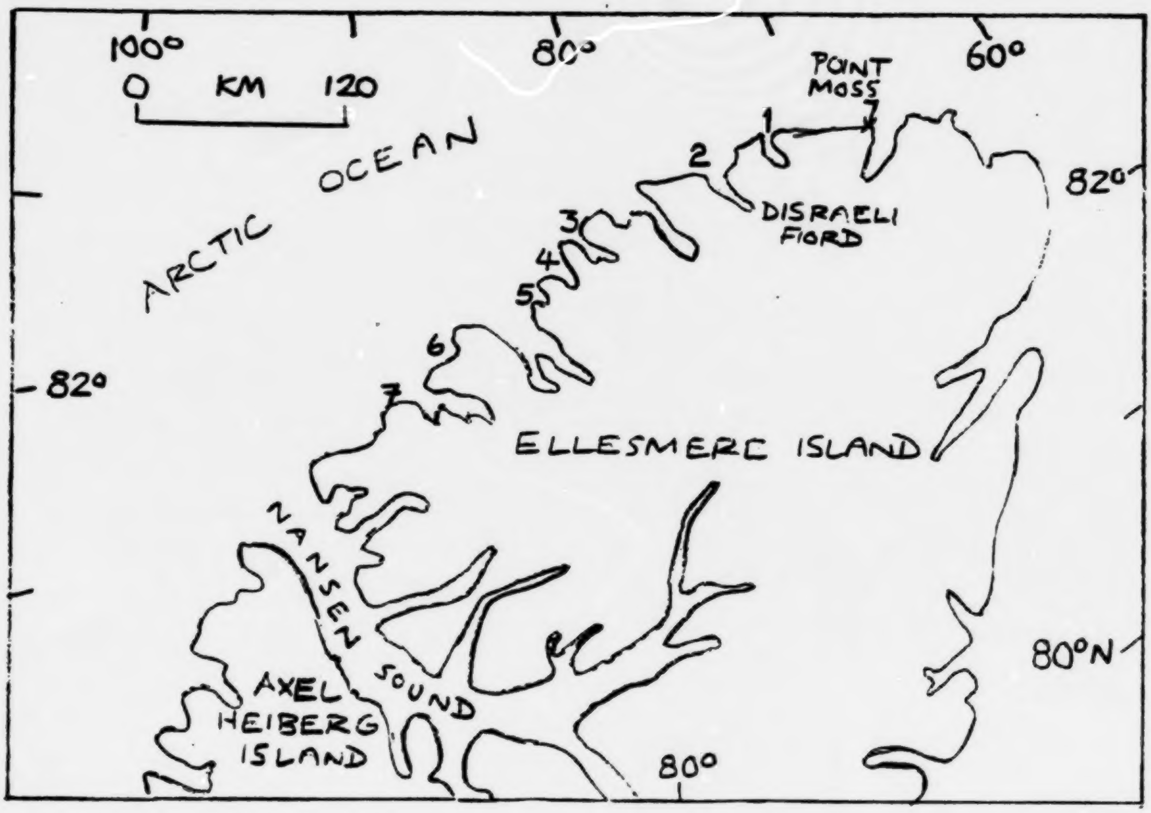
100°
80°
60°
0 KM 120
POINT MOSS
1
2
3
4
5
6
7
82°
82°
80°N
80°
ARCTIC OCEAN
DISRAELI FIORD
ELLESMERE ISLAND
NANSEN SOUND
AXEL HEIBERG ISLAND

FIGURE 1. Location map of ice shelves off the north coast of Ellesmere Island
1: Markham; 2: Ward Hunt; 3: Ayles; 4: Milne; 5: Hanson;
6: Alfred Ernest; 7: Armstrong.

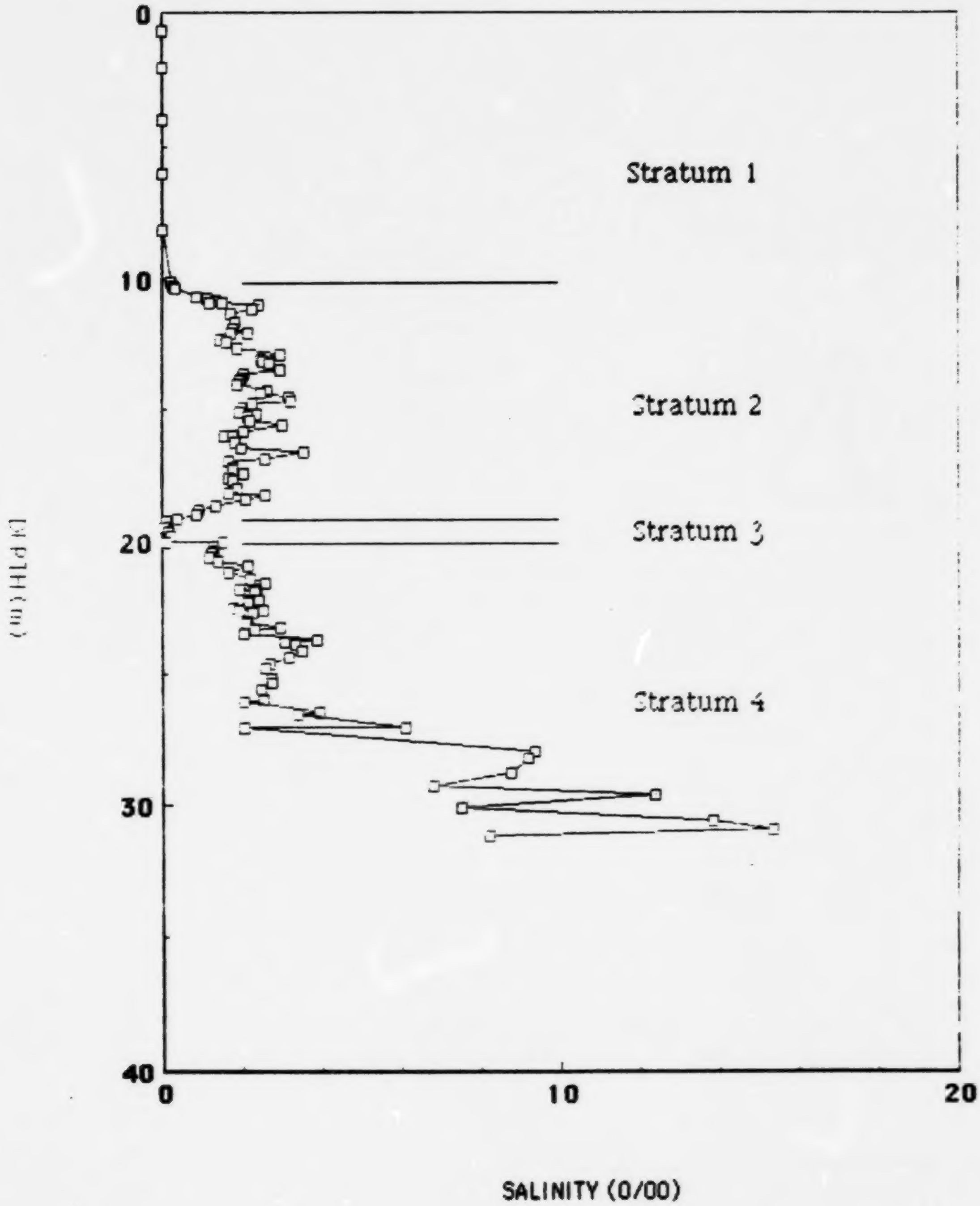

Fig. 2: Salinity profile, ice core 83-1.

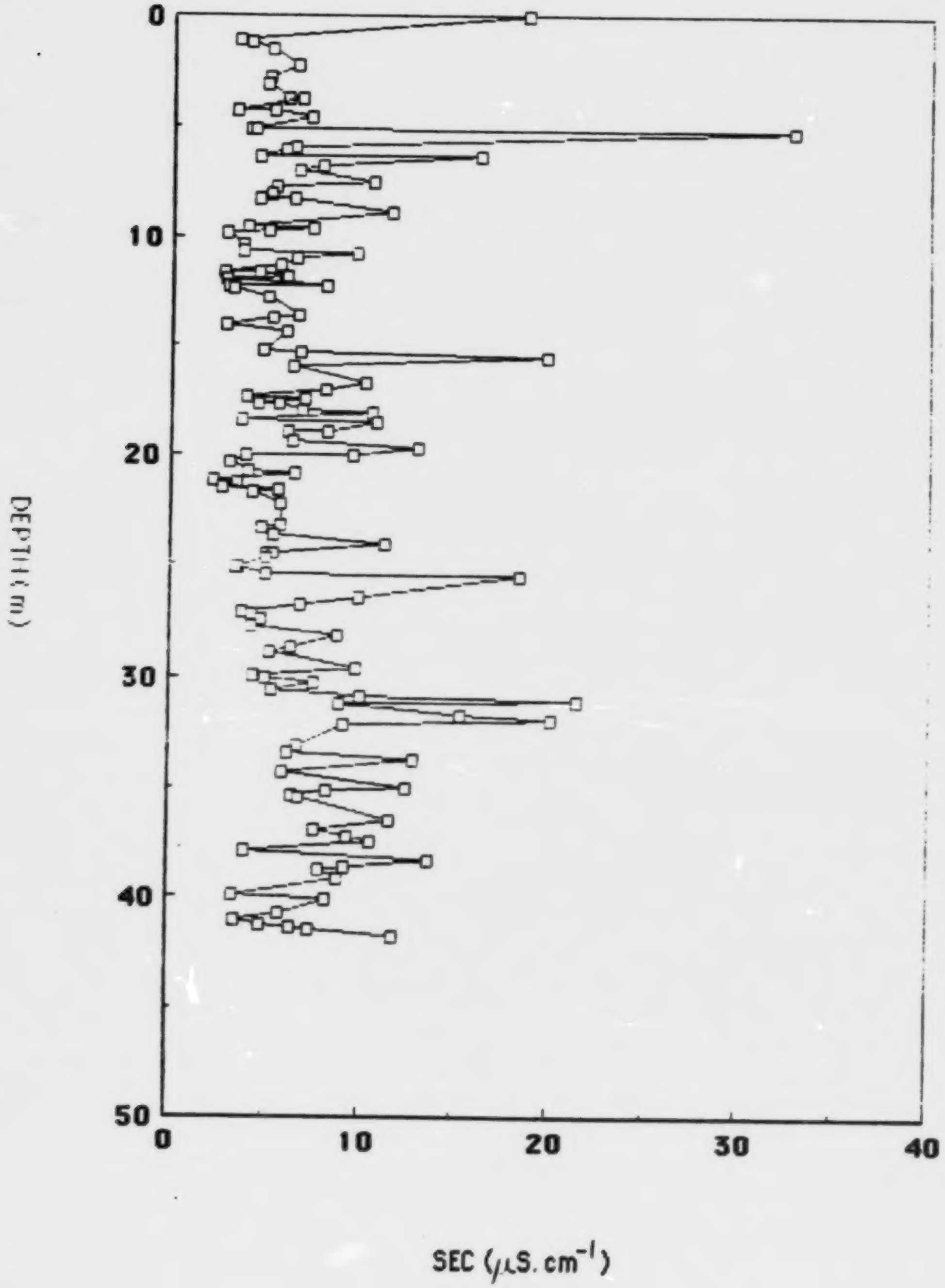

Fig. 3: Conductivity profile, ice core 85-10

NRC WORKSHOP ON EXTREME ICE FEATURES

Questions and Discussions Form

AUTHOR:	M.O. Jeffries
PAPER:	Structure and Growth of Arctic Ice Shelves and Ice Islands
DISCUSSION BY:	G.R. Pilkington

DISCUSSION:

1. Are there many large areas that might calve at this time? How big are they? How many are there?

2. Are ice shelves in a steady-state at this time or are they relics of a colder period?

AUTHOR'S REPLY:

1. Ayles Ice Shelf and the outer part of the Alfred Ernest Ice Shelf, each about 50 km^2 in area, are potential sources of ice islands. Perhaps it might be better to say that at these locations there appears to be a greater potential for calving than at other locations. There exists a potential for calving from any of the remaining ice shelves, but we know so little about the calving mechanism and calving conditions that it is difficult, if not impossible, to predict where and when a calving will occur.

2. In terms of the areal extent, the ice shelves are certainly not in steady-state, due of course to the calving of the ice and creation of ice islands. On the other hand, our ice core evidence suggests, at least for the Ward Hunt Ice Shelf, that the ice shelves are in steady-state thickness, i.e., surface ice loss by ablation in summer is balanced by bottom accretion. The ice shelves were almost certainly in existence during the Little Ice Age; in the High Arctic this was approximately the period 330 BP to 100 BP (years before present). The ice shelves might be as little as 300-400 years old, but are probably much older. It has been suggested that the ice shelves as we know them today, began to grow 3000-4000 years ago. This is based on radio-carbon dating of driftwood which became stranded on the shores of fiords on the north coast of Ellesmere Island.

DISCUSSION BY: M. Nessim

DISCUSSION:

1. From your observations to date, is the size distribution of ice islands biomodal?

2. Can you make a comment on the shape and geometry of the edges of ice islands?

AUTHOR'S REPLY:

1. In May 1986 we counted 23-25 ice islands off the NW coast of Axel Heiberg Island. There was no systematic examination of their size distribution, geometry, etc., but on the basis of subsequent examination of oblique aerial photographs I would say that there is a bimodal size distribution with the majority of ice islands being at the smaller end of the distribution, i.e., $< 1 \text{ km}^2$ in area.

2. Ice islands tend to be long and narrow, i.e., a high length-ratio, but my observations do not suggest that the smaller the ice island, the lower the length-width ratio (more equidimensional). The edges of the ice islands tend to be quite straight. Soon after calving the edges are actually ice cliffs, the height or freeboard being dependent on ice thickness. The ice cliffs are very steep, and close to vertical. However, with time the ice island edge is overridden by pack ice rubble and pressure ridges and the cliff is no longer evident. If a fragment breaks off the ice island, then a new cliff will appear.

DISCUSSION BY: W.M. Sackinger

DISCUSSION:

From your measurements of Tritium in the ice shelf and ice island cores, what is the average rate of ice accretion from beneath for the past 30 years?. Are there any indications of year-to-year variability in the under-ice accretion rate?

AUTHOR'S REPLY:

The Tritium data that I have available suggest a mean annual bottom accretion rate of almost 100 mm per annum. While the available data are sufficient to allow a mean annual accretion rate to be determined, it would require more data to assess the interannual variability in the bottom accretion. Unfortunately, because of the nature of the ice core drilling program, the ice that would allow us to fill in the data gaps is not available to us.

COMMENT BY: G. Holdsworth

Some progress has been made regarding the modelling of the Ward Hunt ice shelf in terms of free vibrations. The fifth mode of vibration (period unavailable) gives the right geometry for explaining (qualitatively) the 1962 calving event. Oscillation in this mode for a sufficient time interval might have led to fatigue in the ice.

LOSS, DECAY, AND RECENT DRIFT OF ICE ISLANDS

by

W.M. Sackinger
M. Yan*

Geophysical Institute
University of Alaska
Fairbanks, Alaska 99775-0800 USA

I. Introduction

There have been few records kept of the paths of ice islands, their reduction in thickness and size, and their ultimate fate. Except for the eastern movement of WH-5 shortly after its creation in 1962 from the Ward Hunt Ice Shelf, ice islands have been observed or presumed to move towards the southwest after their creation by calving from the ice shelves of Ellesmere Island. They have been carried around the Beaufort Gyre (Cornett, 1986) and when they reach the region near the North Pole, there is an unknown probability that they may join the trans-Polar drift stream, an average drift of sea ice towards the Fram Strait. If so, they are ejected into the North Atlantic, where they move around the southern tip of Greenland and disappear in the warmer waters of the Labrador Sea. In Figure 1, the path of Arlis II illustrates this. If the ice islands are subject to a certain sequence of wind conditions near the Pole (as yet to be determined) they rejoin the mass of low-average-drift-velocity multi-year ice north of Ellesmere Island, and begin another circuit of the Beaufort Gyre. The ice island T-3 executed three circuits of the Beaufort Gyre from 1950 until it was finally ejected into the Greenland Sea in June 1984. The trajectory of T-3 also

---

Presented at the Workshop on Extreme Ice Features, National Research Council of Canada, Banff, November 3-5, 1986.

*Present Address:4F-4, No.83, Wen-chow St, Taipei, Taiwan, 10768 ROC.

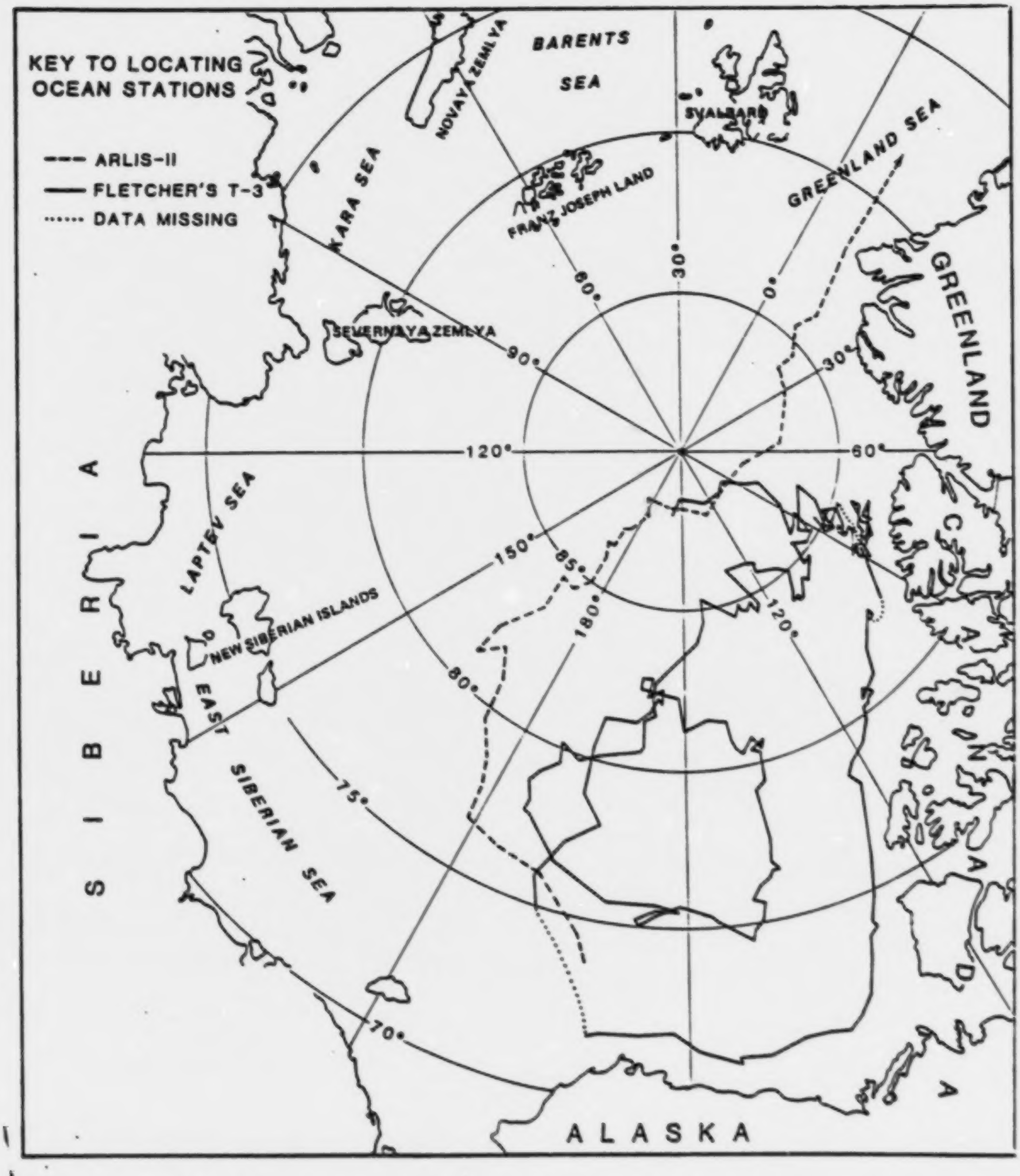
KEY TO LOCATING OCEAN STATIONS
--- ARLIS-II
— FLETCHER'S T-3
...... DATA MISSING
BARENTS SEA
NOVAYA ZEMLYA
KARA SEA
SVALBARD
FRANZ JOSEPH LAND
GREENLAND SEA
GREENLAND
SEVERNAYA ZEMLYA
90°
60°
30°
0°
30°
120°
60°
150°
85°
180°
120°
80°
75°
70°
SIBERIA
LAPTEV SEA
NEW SIBERIAN ISLANDS
EAST SIBERIAN SEA
CANADA
ALASKA

FIGURE 1. Drift tracks of ice islands T-3 and Arlis-II in the Arctic Ocean. For many years the drift of T-3 followed the clockwise motion of the Beaufort Gyre while Arlis-II drifted directly across the Arctic Ocean in the Trans-Polar Drift Stream.

is shown in Figure 1. Most of the residence time was in regions north of 83°N, where average summer ablation is low. In contrast, in the region of the southern Beaufort Sea, ablation rates in the range 2m to 3m per year occur. In the case of T-3, with a thickness of 50m when first occupied (Crary, 1954), its thickness was reduced to 30m after 20 years (Holdsworth and Traetteberg, 1973).

Ice islands also become grounded in the coastal waters of the Beaufort and Chukchi Seas, where tidally-induced stresses cause them to fragment. The industry study reported by Spedding (1977) found 433 such fragments in 1972, 299 fragments in 1973, and 27 ice island fragments in 1974. Ice islands and fragments have also been observed in the channels between the Queen Elizabeth Islands, which provide other pathways for ice island loss, but which are blocked by multi-year sea ice during most summers.

II. Recent Drift of Ice Islands

Some of the ice islands produced at the Ward Hunt Ice Shelf in 1983 (Jeffries and Serson, 1983; Jeffries, 1986) have been instrumented and tracked on a daily basis using the System Argos buoys. The recent comprehensive work by Yan (1986) gives details of the trajectory of the largest island of the cluster, upon which the permanent field station of the Polar Continental Shelf Project (PCSP) was established by G.D. Hobson. A brief overview of the results of Yan's trajectory analysis is given here; for additional details, the reader is referred to the original report (Yan, 1986).

In August 1983, G.D. Hobson deployed buoy 3831 on the largest ice island, which has been measured to be 10km long, 5km wide, and which has a thickness of 42.6 ± 0.9m on the shelf ice portion (Jeffries 1986, pers. comm.). The average shelf ice density is 870 kg/m^3 and the surface area of the island is 1.65×10^7 m^2; the average density of the old sea ice portion of the island is 910 kg/m^3, and the surface area is 0.95×10^7 m^2 (Jeffries 1986, pers. comm.). Thus the total surface area

A of the island is 2.6×10^7 m^2, and the total mass of the island is approximately 6.9×10^{11}kg.

For an ice island, the equation of motion may be written as

$$M \frac{dv}{dt} = F_{ai} + F_{ap} + F_{wi} + F_{wp} + F_{co} + F_g$$

where M is ice island mass, dv/dt is its acceleration, F_{ai} is the wind drag force on the ice island, F_{ap} is the wind drag force on the pack ice adjacent to the island, F_{wi} is the water drag force on the ice island, F_{wp} is the water drag force on the pack ice adjacent to the island, F_{co} is the Coriolis force on the island, and F_g is the pressure gradient force. The wind drag F_{ai} is given as $F_{ai} = C_{ai}\rho_a V_a^2 A_i$ where C_{ai} is the air drag coefficient on the ice island, ρ_a is the air density, V_a^2 is the relative speed between the wind and the island, and A_i is the area of the island. A similar expression may be written for the water drag, $F_{wi} = C_w\rho_w V_w^2 A_i$ where C_w is the water drag coefficient on the ice island, ρ_w is the water density and V_w is the relative speed between the water (below the boundary layer) and the ice island. Similar expressions may be written for the pack ice area in intimate contact with the ice island. The Coriolis force is $F_{co} = M\,(2\omega\sin\phi)\,k \times V$ with ϕ as the latitude and ω as the angular velocity of the earth.

In choosing the drag coefficients, it was recognized that the upper and lower surfaces of the ice islands are relatively smooth, leading to the choice of $C_{ai} = 1.1 \times 10^{-3}$ and $C_{wi} = 1.32 \times 10^{-3}$, taken from Banke et al. (1980) and Langleben (1982), respectively. For the adjacent pack ice, drag coefficients $C_{ap} = 2.7 \times 10^{-3}$ and $C_{wp} = 5.5 \times 10^{-3}$ were used (McPhee, 1980) in recognition of the greater surface roughness. A model was chosen, for initial comparison with actual trajectories, in which an area A_p of pack ice immediately upwind of the island was set equal to the island area, and the angle between the water drag forces and the velocity was chosen to be 24 degrees (McPhee, 1982), for purposes of initial calculations. Observations of fully-developed ice ridges around circular artificial islands suggested that this choice of area would be an appropriate initial assumption.

Three types of movement episodes were observed. Major movements parallel to the coastline in the southwest direction were more than 10km per day, with average speed greater than 0.1 m/sec. An example is shown in Figure 2a. Smaller movement episodes (1-10 km/day) with average speeds of .01 to 0.1 m/sec also took place, first towards the southwest, then back towards the northeast (Fig. 2b). Random movement directions (less than 1 km/day) were observed 90% of the time, most of which were thought to be positioning system statistical variations.

Geostrophic winds were calculated for major movement episodes and were compared with observed trajectories as shown, for example, in Figure 3. The ratio of ice island speed to geostrophic wind speed was 0.44%, 1.1%, 1.4%, 1.5%, 1.3%, 1.5%, and 0.93% for this major episode from Day 334 to 344, 1983. The ice island in this observed episode moved at an average angle of 20 ± 10 degrees to the left of the geostrophic wind direction. Geostrophic windspeeds of 18.1 m/sec and 25.0 m/sec on Days 334-336 initiated this movement. The surface pressure map for Day 336 shows the polar weather pattern responsible for this, with a large high pressure area near the pole and a low pressure over northern Greenland (Fig. 4).

The force balance on the island was calculated for each day, using the methods described above; each force plus their vector sum is shown in Figure 5 for this particular episode. Because of insufficient data between any two daily positions, it was not possible to calculate the acceleration term. Once the island acquired appreciable velocity (Day 335-336) the Coriolis force term becomes very large and should have turned the island velocity to the right. This did not occur; a possible explanation is that an additional pack ice force (a reaction force) was present on the ice island boundary, shown in Figure 5 as a residual force F_r. This could be caused by a very slight consolidation of the pack ice on the right side of the direction of ice island motion, allowing water drag and air drag forces on an additional region of pack ice to affect the island motion. A similar result was reported by Hunkins (1975), who found that there was an internal ice force directed 135° to the left of the ice motion. In our case, the average direction

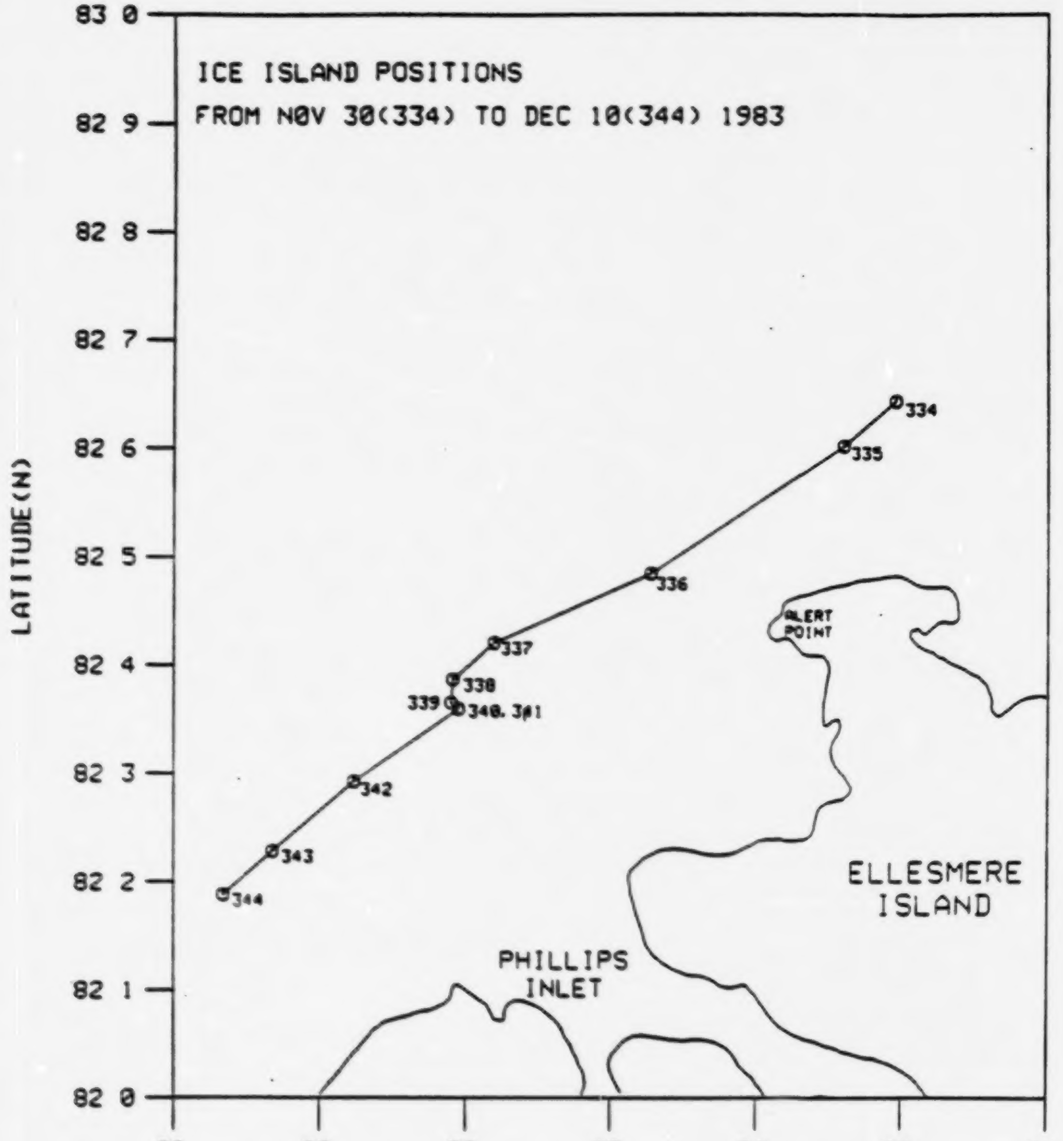
ICE ISLAND POSITIONS
FROM NOV 30(334) TO DEC 10(344) 1983
LATITUDE(N)
83 0
82 9
82 8
82 7
82 6
82 5
82 4
82 3
82 2
82 1
82 0
334
335
336
337
338
339
340, 341
342
343
344
ALERT POINT
ELLESMERE ISLAND
PHILLIPS INLET
90
89
88
87
86
85
84
0
10(Km)
LONGITUDE(W)

FIGURE 2a. The daily positions for ice island 3831 from Nov. 30 (Day-334) to Dec. 10 (Day-344) 1983.

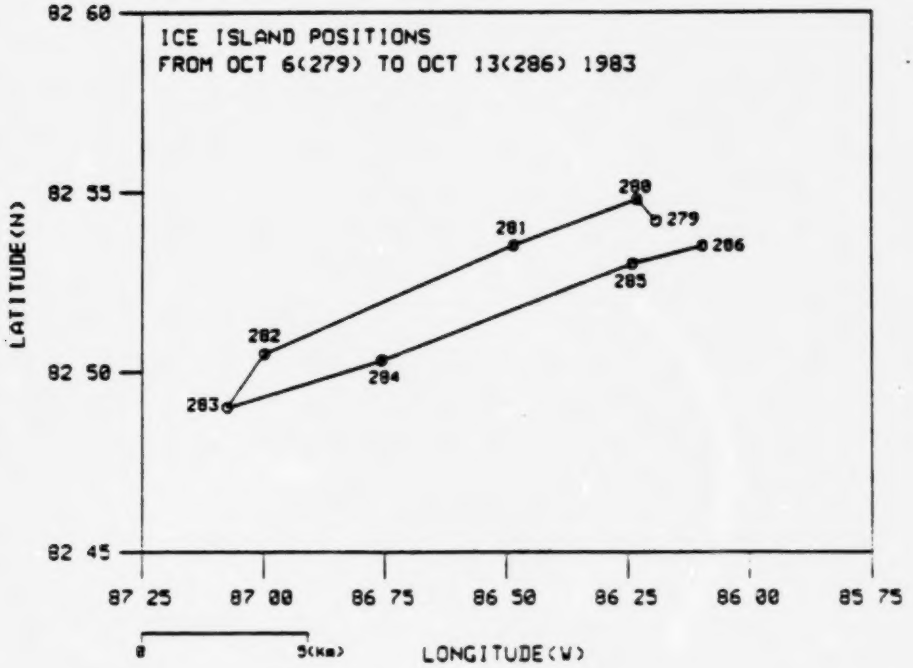

FIGURE 2b. The daily positions for ice island 3831 from October 6 (Day-279) to October 13 (Day-386) 1983.

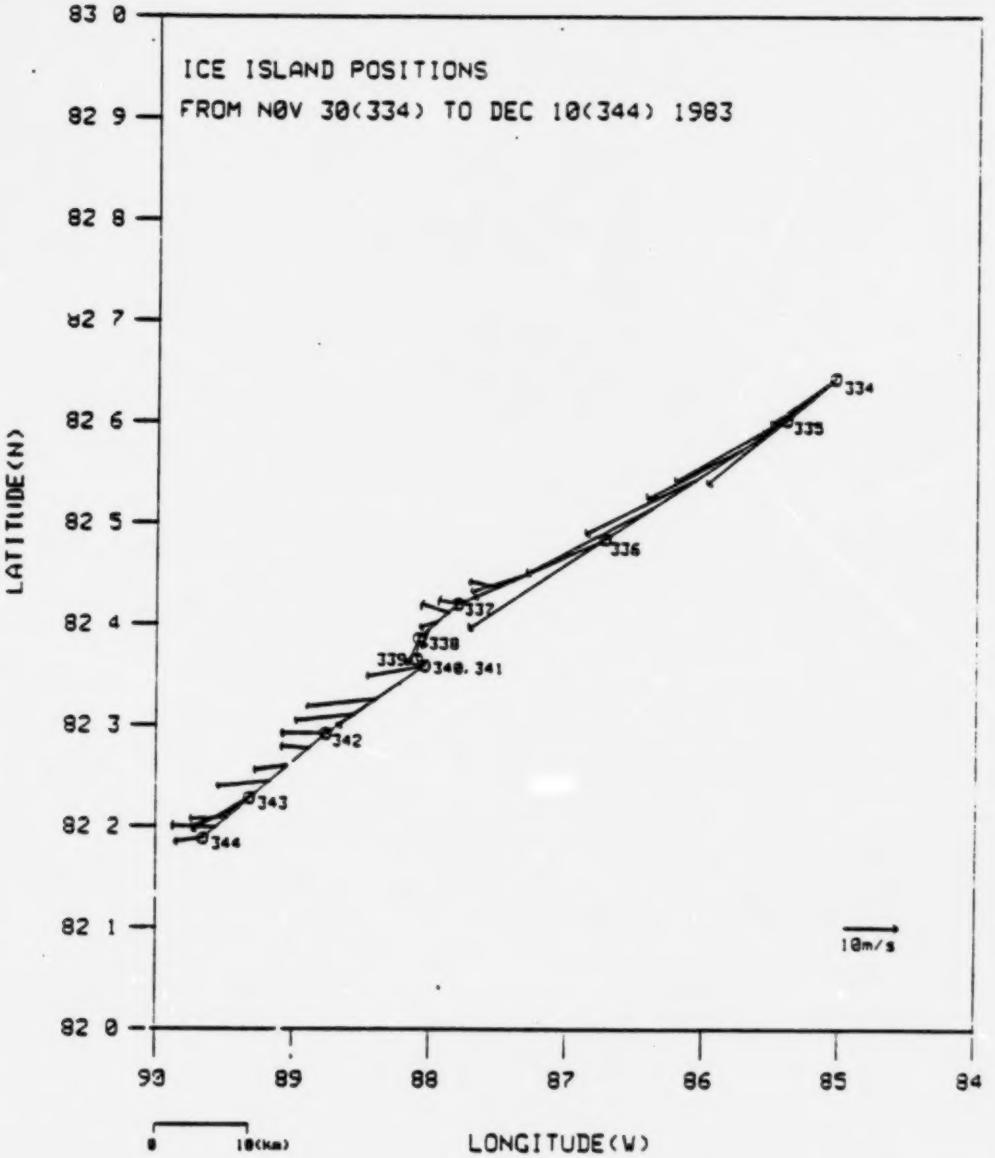

FIGURE 3. The ice island positions and the geostrophic wind vectors from Day-334 to 344, 1983.

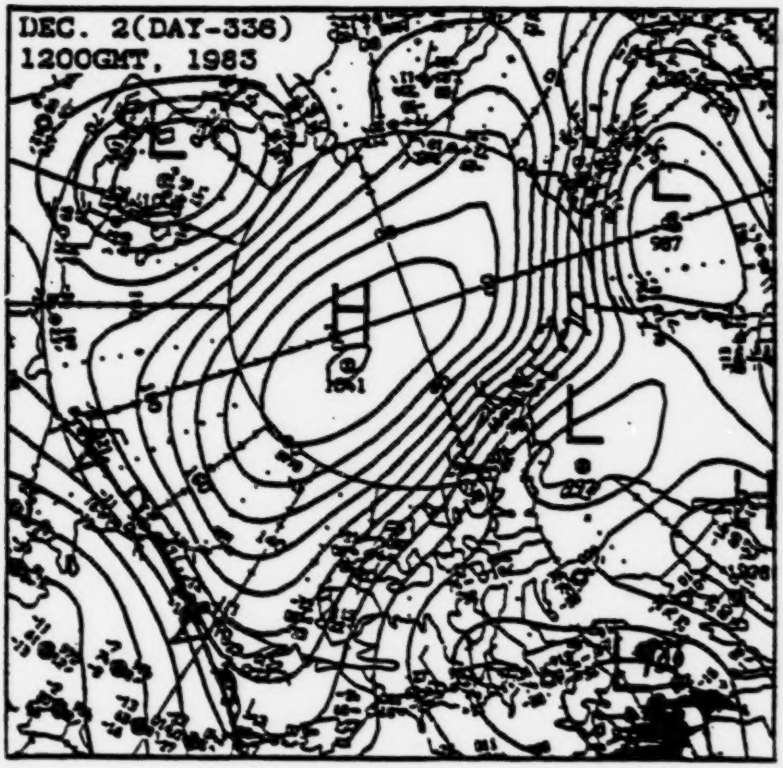
DEC. 2(DAY-336)
1200GMT, 1983
L
H
L
L
987
1041

FIGURE 4. Surface weather map for Dec. 2 (Day-336) 1200 GMT, 1983.

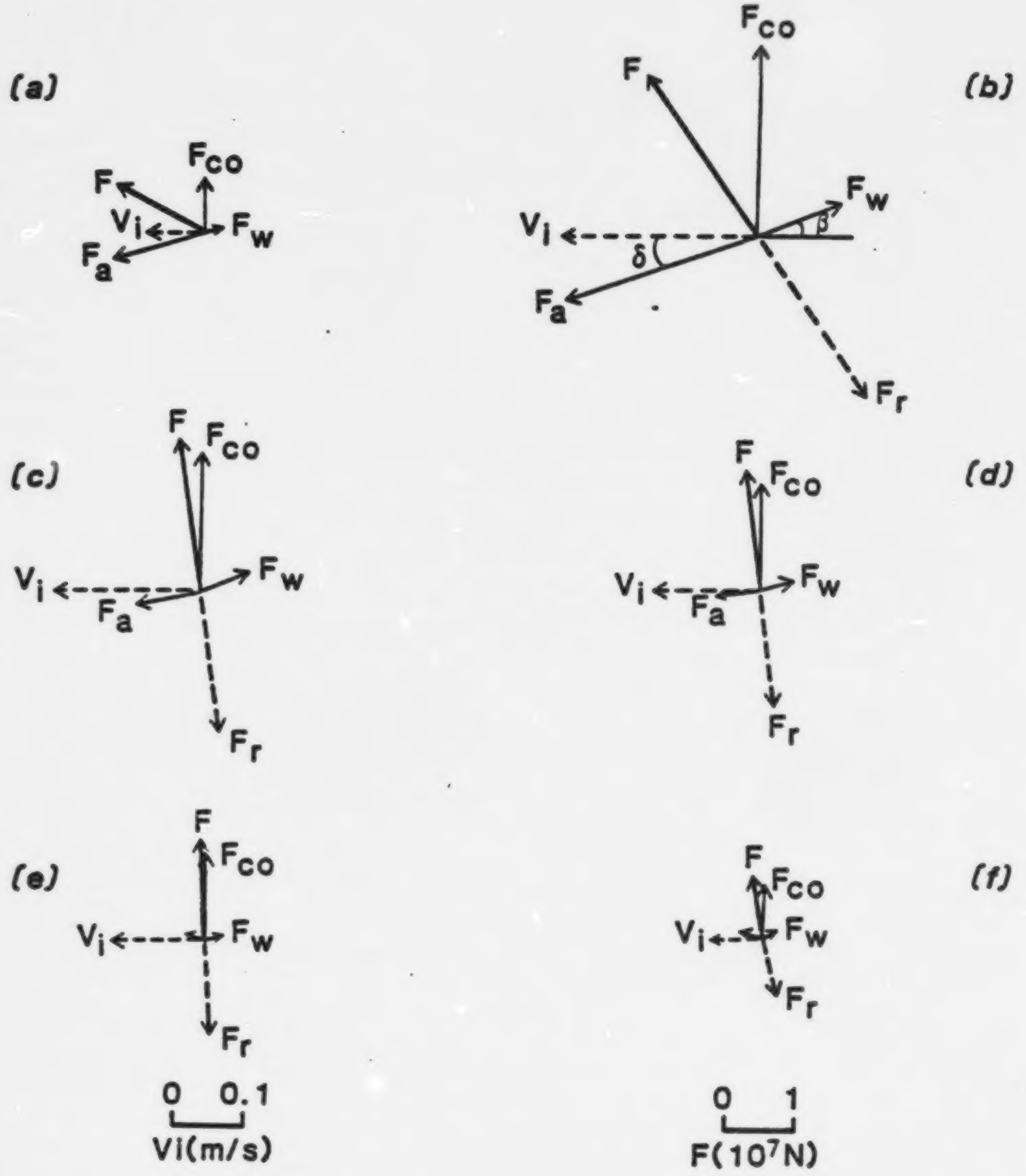
(a)
F
Fco
Vi
Fw
Fa
(b)
Fco
F
Fw
β
Vi
δ
Fa
Fr
(c)
F
Fco
Vi
Fw
Fa
Fr
(d)
F
Fco
Vi
Fw
Fa
Fr
(e)
F
Fco
Vi
Fw
Fr
(f)
F
Fco
Vi
Fw
Fr
0 0.1
Vi(m/s)
0 1
F(10⁷N)

FIGURE 5. Force balance among wind drag force (F_a), water drag force (F_w) and Coriolis force (F_{co}) for
(a) Day 334-335, (b) Day 335-336,
(c) Day 336-337, (d) Day 341-342,
(e) Day 342-343, (f) Day 343-344.
$F=F_a+F_w+F_{co}$, F_r: residual force.
V_i: ice island velocity(m/s).
β=24 degrees (after McPhee, 1982), $\delta=\gamma-\theta$.

of the pack ice reaction force is 103 ± 12 degrees to the left of the ice island velocity. This may be due to the greater Coriolis force caused by the mass of the ice island, which is much larger than that of an equal area of pack ice.

III. Conclusions

The trajectory of Hobson's ice island near the coast of Ellesmere Island shows three categories of movement episodes: (1) large movements ($\geq$10 km) towards the southwest; (2) medium movements (1-10 km) in two sequentially opposite directions along the coastline; and (3) small random movements (<1 km) in any direction. Evidence from surface pressure maps shows that an offshore geostrophic wind component is a necessary condition in the initial stages of the large and medium movements in the southwest direction. Ratios of ice island speed to geostrophic wind speed range from 1.0% to 1.5% for the first type of movement. The average angle between ice island movement direction and geostrophic wind direction ranges from 20 to 26 degrees counterclockwise from the geostrophic wind direction. Force balance calculations show that the large Coriolis force on the massive, moving ice island is balanced by a reaction force from the pack ice acting upon the ice island boundary, at an angle 103 ± 12 degrees to the left of the ice island velocity.

IV. Acknowledgements

The support of this research by the U.S. Department of Energy, Morgantown Energy Technology Center, under Contract No. DE-AC21-83MC20037, and also by the Canadian Polar Continental Shelf Project is greatly appreciated. Valuable discussions took place with M.O. Jeffries, G.D. Hobson, H.V. Serson, H. Tippens, H.O. Shoemaker, T. Kozo, and others in the course of this study.

References

Banke, E.G., S.D. Smith and R.J. Anderson, 1980. Drag coefficients at AIDJEX from sonic anemometer measurements. Sea Ice Processes and Models, R.S. Pritchard (ed.), University of Washington Press, 430-442.

Cornett, S., 1986. Beaufort Gyre ice trajectories. NRC Workshop on Extreme Ice Features, Banff, November 3-5, 1986.

Crary, A.P., 1954. Seismic studies on Fletcher's Ice Island, T-3. Trans. Am. Geophys. Union, 35: 293-300.

Holdsworth, G. and A. Traetteberg, 1973. The deformation of an Arctic ice island. Proc. of the 2nd International Conference on Port and Ocean Engineering under Arctic Conditions, University of Iceland, 419-440.

Hunkins, K., 1975. The oceanic boundary layer and stress beneath a drifting ice floe. J. Geophys. Res., 80(24): 3425-3433.

Jeffries, M.O. 1986. Personal communication.

Jeffries, M.O. and H.V. Serson, 1983. Recent changes at the front of Ward Hunt Ice Shelf, Ellesmere Island, N.W.T. Arctic, 36(3): 289-290.

Langleben, M.P., 1982. Water drag coefficient of first-year sea ice. J. Geophys. Res., 87(C1): 573-578.

McPhee, M.G., 1982. Sea ice drag laws and simple boundary layer concepts, including application to rapid melting. USA Cold Regions Research and Engineering Laboratory, CRREL Report 82-4, 52 pp.

McPhee, M.G., 1980. An analysis of pack ice drift in summer. Sea Ice Processes and Models, R.S. Pritchard (ed.), University of Washington Press, 62-75.

Spedding, L.G., 1977. Ice island count southern Beaufort Sea 1976. APOA #99, IPRT-13ME-77, Imperial Oil Limited, 50pp.

Yan, M.-H., 1986. The relationship between ice island movement and weather conditions. M.S. thesis, University of Alaska, Fairbanks, 91pp.

NRC WORKSHOP ON EXTREME ICE FEATURES

Questions and Discussions Form

AUTHOR: W. Sackinger and M. Yan

PAPER: Loss, Decay and Recent Drift of Ice Islands

DISCUSSION BY: G. Holdsworth

DISCUSSION:

1. Please comment on discussion of L. LeSchack: if an ice island entered the shear zone it could rotate as well as be translated.
2. Did you try running your numerical trajectory model for an ice island without including the pack ice?

AUTHOR'S REPLY:

1. The shift of wind direction should cause the pack ice to push the island from a new direction, and the open water often observed near the ice island should close (nonuniformly) and open on another side. Slowly, the island would change its orientation. As yet, we have not acquired data to confirm this.
2. Yes. Results are as one would expect, with the island speed increasing to an asymptotic value, when a step-function of wind is applied. The transient decay of velocity was also checked as were the Coriolis Force effects. Results will be reported in a future publication.

DISCUSSION BY: Martin Jefferies

DISCUSSION:

Our experience on the north coast of Ellesmere Island indicates winds blowing parallel to shore. Yet, you suggest that onshore winds are the normal case. What would account for this? It is worth noting that the surface undulations on the ice shelves are commonly parallel to the shoreline.

AUTHOR'S REPLY:

Orographic effects due to the high coastal mountain range are one explanation as a mesoscale geostrophic wind towards the shoreline forces the pack ice to be crowded next to the shore over distances of hundreds of kilometers, still, deflection of winds by the mountains can cause winds parallel to shore on the ice shelves, within 10-20 km of the shoreline mountain range. Mountain barrier baroclinicity is an additional probable effect during this most common case. It is worth noting that the melt ponds on ice shelves deeper within the fjords of Ellesmere Island are aligned with the long axis of the fjord, thus indicating a dominant effect of orographic winds during summer in orienting the melt ponds.

MECHANICAL PROPERTIES OF SHELF ICE

by

R. Frederking and Nirmal K. Sinha
Institute for Research in Construction
National Research Council of Canada
Ottawa, Ontario, K1A 0R6

1.0 Introduction

Ice islands, as discussed at this Workshop, constitute one of the extreme ice features for which account must be taken in the planning of operations and design of offshore structures for the Beaufort Sea. Information on the size, distribution, movements and physical and mechanical properties of ice island are needed. This contribution focuses on the mechanical properties. The other factors are addressed elsewhere by the Workshop.

Ice islands have their source in the remnant ice shelves of northern Ellesmere Island (Crary, 1960). Therefore it is assumed that the mechanical properties of ice islands and shelf ice are the same. Hereafter ice island ice will be taken to be synonymous with shelf ice. A review of the literature has revealed that there is very little information on the mechanical properties of shelf ice. The work which has been done in this area has concentrated on the determination of very low load level creep (stresses of the order of 100 kPa or less) primarily in the course of the study of the behaviour of ice shelves; i.e. influence of ice shelves on the motion of glaciers and the calving of ice islands and icebergs. Literature on the behaviour of Antarctic ice shelves is quite extensive in contrast to the relatively few articles on Arctic ice shelves.

The work in the Arctic has mostly addressed the Ward-Hunt and Milne ice shelves (Marshall, 1955; Jefferies, 1985) or the behaviour of ice islands (Muguruma and Higuchi, 1963). In an ice island, Holdsworth and Traetteberg (1974) carried out measurements which suggested strain rates, generally compressive, in the range 10^{-12} to 10^{-10} s^{-1}. Associated stress levels were estimated to be about 10 kPa.

Because of the absence of any direct information on mechanical properties of shelf ice, this review will examine indirect methods for predicting properties. This will be done by combining knowledge of the physical properties of shelf ice with knowledge of the mechanical properties of other types of ice which have similar physical characteristics. While this approach is not completely satisfactory, it does provide a means for bracketing the expected mechanical properties of shelf ice. Also some of the alternative approaches for direct measurement of mechanical properties will be considered.

2.0 Prediction of Mechanical Properties from Physical Properties

It is possible to predict mechanical properties of ice based on certain information on the physical properties, e.g. temperature, salinity, grain size, grain structure, density, etc. Since no direct data are available on mechanical properties of shelf ice, methods for estimating them will be discussed here.

2.1 Physical characteristics of shelf ice

The first step is to consider the physical properties and characteristics of shelf ice. The work of Jeffries (1985) on the Ward Hunt and Milne ice shelves provides a wealth of information. He indicated that ice shelves form as a result of sea ice growth, surface accumulation of precipitation, and movement of glacier tongues. The non-saline ice types were identified as Ice, Trough and Fijord. They comprised granular ice with grain sizes ranging from a few mm to 10's of mm. Densities were in the range 880 to 900 kg/m^3. These ice types would appear to be similar to glacial ice and snow ice found on rivers and lakes. Saline ice in ice shelves was identified as Reentrant or multi-year, Basement I and II, and Basement III. These saline ice types had a structure which was characterized as being similar to old sea ice; i.e. evidence of brine inclusions and a similar grain shape. Reentrant ice had a salinity of

1 °/oo and a density of 870 kg/m^3. Basement I and II which was deeper in the shelf had a salinity of about 2 °/oo and densities of 910 to 920 kg/m^3. Basement III which comprised about the bottom 6 m for the shelf had a salinity of about 8 °/oo and a density of about 920 kg/m^3. This Basement ice was estimated to be about 4000 years old. Currently the ice shelf is at a minimum following 400 to 500 years of regression.

Holdsworth and Traetteberg (1974) provided information on the temperature, salinity and density profile of Fletcher's Ice Island. The total thickness of the island was about 30 m. Their results on the characteristics of ice showed the top 5/6 of the thickness to have densities in the range 900 to 910 kg/m^3. Salinities in this level were also extremely low, < 0.01 °/oo. There was no information on the grain structure, however with the very low salinities it could be assumed that this ice was glacial in origin. The salinity of the lower 1/6 of the island was about 1 °/oo, which would suggest old multi-year ice. The temperature gradient in the lower part of the ice was 0.3 to 0.4°C/m.

From the above two sources it is clear that there is no universal description of shelf ice and that each occurrence of it must be characterized separately.

Given the above information on the temperature gradient, the growth rate at the bottom surface of an ice cover $\dot{h}$ can be approximated by

$$\dot{h} = \frac{k_i}{L\rho} G \qquad (1)$$

where G is temperature gradient, k_i is thermal conductivity, ρ is density and L is latent heat. The above equation, from Sinha and Nakawo (1981), suggested $L = 300$ J/g, $\rho = 910$ kg/m^3 and $k_i = 2$ W/m°C for first-year sea ice. With these parameters and the observed temperature gradient, an accretion rate of 50 to 100 mm per year could be expected on the bottom of an ice island. This low growth rate could explain the very low salinities observed on the bottom of the ice island and suggests that the lower part could be described as multi-year. Depending on the age of an ice island, it is conceivable that a significant proportion of the island could be composed of old multi-year ice.

2.1 Prediction Equations

The prediction equations for strength are generally empirical. There are for example the brine volume equations for strength and elasticity of sea ice (Schwarz and Weeks, 1977). The flexural strength of sea ice is given by

$$\sigma_f = 750\left(1 - \left(\frac{\nu_b}{0.202}\right)^{\frac{1}{2}}\right) \text{ [kPa]} \qquad (2)$$

where ν_b is the brine volume ($\nu_b < 0.33$). The elastic modulus as a function of brine volume was given by

$$E = 10\left(1 - \nu_b^{\frac{1}{2}}\right)^4 \text{ [GPa]} \qquad (3)$$

for $\nu_b < 0.1$. The brine volume fraction, ν_b, (a function of ice temperature and salinity) is given by

$$\nu_b = \frac{S}{1000}\left\{- \frac{49.185}{T} + 0.532\right\} \qquad (4)$$

where $-0.5 > T > -23°C$ and S is ice salinity in parts per thousand. The above equations are commonly used to predict the flexural strength and elastic modulus of sea ice sheets.

More recently, Cox and Weeks (1983) have pointed out that since the air content in sea ice can be significant, total porosity is a better factor to which strength and elasticity properties should be related. The total porosity is a function of temperature, salinity and density. Recently this porosity approach was applied to the characterization of compressive strength (Timco and Frederking, 1986). For compressive strength, the total porosity effect was found to be of the form

$$\frac{\sigma}{\sigma_0} = 1 - \sqrt{\frac{\nu_T}{\nu_0}} \qquad (5)$$

where σ is the strength, σ_0 is the strength at the reference porosity ν_0, and ν_T is the total porosity. The reference porosity was found to be about 0.25 and equation (5) to apply for porosities up to about 0.2.

A number of investigators have found a rate effect on strength of the form

$$\frac{\sigma}{\sigma_0} = A \left(\frac{\dot{\varepsilon}}{\dot{\varepsilon}_0}\right)^m \qquad (6)$$

in terms of strain rate, or

$$\frac{\sigma}{\sigma_0} = B \left(\frac{\dot{\sigma}}{\dot{\sigma}_0}\right)^n \qquad (7)$$

in terms of stress rate. A, B, m and n are experimental constants and $\dot{\varepsilon}_0$ is unit strain rate, σ_0 is unit stress and $\dot{\sigma}_0$ is unit stress rate.

The total porosity ν_T discussed above is a function of both salinity and temperature. For ice with a very low salinity, say less than 0.5 °/₀₀, equation (5) is possibly no longer applicable. For these low salinities, an equation of the type proposed by Michel (1978) could be considered. He proposed upper yield strength of various fresh water ice types in terms of strain rate and temperature

$$\sigma = A\, \dot{\varepsilon}^m \exp\,(Q/R\,\theta\,) \qquad (8)$$

where R is the universal gas constant, θ is temperature in Kelvin and A, m and Q are experimental parameters determined for each ice type.

A number of predictor equations of uniaxial compressive strength for various ice types, are summarized in Table 1. This is not meant to be an exhaustive listing, but is an indication of the range of uniaxial strength properties that could be encountered. Note that these are empirical equations which have been established from measurements in the stress rate range of approximately 10^{-2} MPa s^{-1} to 10^{-1} MPa s^{-1} and the strain rate range of approximately 10^{-5} s^{-1} to 10^{-3} s^{-1}. Extrapolating much beyond these ranges is not recommended. The strength vs strain rate equations have been plotted in Figure 1 for comparative purposes. Some of the differences in results are due to differences in test techniques, but certain definite trends are evident. For sea ice at -10°C (curves 1 to 4) both columnar-grained and frazil structures give generally similar results. In contrast, fresh water columnar-grained ice containing no air bubbles (high density) has a significantly higher strength at the same temperature of -10°C (curve 8). On the other hand warm ice having a substantial air content (low density) has a significantly lower strength (curve 7). Curves 5 and 6, which are for multi-year ridge ice, show strengths at the upper range measured for sea ice and the trend of increasing strength with decreasing temperature. These two curves also show the hazards in extrapolating beyond the range of the measurements, in this case at strain rates decreasing towards 10^{-6} s^{-1} the curves cross, inferring higher strengths at higher temperatures.

In terms of predicting deformation (creep or effective elastic modulus), the creep equation proposed by Sinha (1979) offers a good representation of uniaxial behaviour

$$\varepsilon = \frac{\sigma}{E_o} + c\left(\frac{d_1}{d}\right)\left(\frac{\sigma}{E_o}\right)\{1-\exp(-(a_T t)^{\frac{1}{n}})\} + \dot{\varepsilon}_{v_o}\left(\frac{\sigma}{\sigma_o}\right)^n t$$

$$a_T = \exp - \left(\frac{Q}{R\theta} + a\right)\ [s]$$

$$\dot{\varepsilon}_v = A \exp\left(\frac{-Q}{R\theta}\right) [s^{-1}] \qquad (9)$$

where d is the grain size, σ is the stress, t is time, θ is temperature, E_0 is Young's modulus (9.5 GPa), and n, c, Q, a and A are experimentally determined constants, σ_0 is unit stress (= 1 MPa) and d_1 is unit of grain diameter (= 1 m).

3.0 Testing Methods

Because of the great thickness of ice islands, carrying out mechanical property investigations is not a simple matter. The first problem is to obtain representative samples of the material. Obtaining block or core samples from the full thickness is a major task. The variability in ice types which can be expected to be found in shelf ice requires any investigation to devote considerable effort to characterizing ice types that are present. Parameters should include not only salinity and grain structure, but also air bubble determinations. Samples for physical testing should be obtained from representative locations in the ice. The tests can be carried out in the field in improvised laboratory facilities or the samples can be transported back to the laboratory. Another alternative which offers promise is to use in situ testing techniques such as the borehole jack or a pressuremeter. This approach essentially eliminates the requirement for sampling. The interpretation of in situ test results is still open to some questions, particularly in relation to conventional tests such as uniaxial compression. Some progress, however, is being made (Sinha, 1986b).

The primary engineering purpose of strength testing, in the laboratory, or in situ is to obtain a relative strength for comparison with other ice types. Uniaxial loading with strain rate control is the most reasonable basis for comparison since this test is among the most straightforward and is most commonly reported in literature. Confined compression and fracture toughness are also relevant bases for comparison.

Another direction which has been less explored is the examination of flaws, cracks or imperfections in ice features. For large ice features such as ice islands these factors may be as important or more so than conventional mechanical properties.

4.0 Conclusions

Comparisons can be made between the physical characteristics of shelf ice outlined in Section 2.1 and the physical properties of the various ice types tabulated in Table 1. This shows that shelf ice generally falls within our range of experience in terms of physical properties; i.e. density, salinity, temperature and grain structure. Therefore it is unlikely that the mechanical properties of shelf will fall outside those measured for other ice types. The predictor equations available are useful for establishing relative values for mechanical properties but not making estimates of absolute values. A more desirable approach, however, would be to conduct mechanical property investigations directly on ice island ice. Any such investigations must have a parallel effort in which physical characteristics of ice islands (e.g. temperatures, salinities, grain structure) are determined.

5.0 References

Cox, G.F.N. and Weeks, W.F. (1983). Equations for determining the gas and brine volumes in sea ice samples. J. Glaciol., Vol. 29, pp. 306-316.

Cox, G.F.N., Richter-Menge, J.A., Weeks, W.F., Bosworth, H., Perron, Mellor, M. and Durell, G. (1985). Mechanical properties of multi-year sea ice. Phase II: Test results. CRREL Report 85-16, 81 pp.

Crary, A.P. (1960). Arctic ice islands and ice shelf studies, Part II. Arctic, Vol. 13, No. 1, pp. 32-50.

Frederking, R.M.W. and Timco, G.W. (1983). Uniaxial compressive strength and deformation of Beaufort Sea ice. Proc. POAC'83, Helsinki, Finland, Vol. 1, pp. 89-98.

Holdsworth, G. and Traetteberg, A. (1974). The deformation of an arctic ice island. Proc. POAC '73, Reykjavik, Aug. 27-30, 1973, pp. 419-440.

Jeffries, M.O. (1985). Physical, chemical and isotropic investigations of Ward Hunt ice shelf and Milne ice shelf. Ph.D. Thesis, University of Calgary.

Marshall, E.W. (1955). Structural and stratigraphic studies of the northern Ellesmere Ice Shelf. Arctic, Vol. 8, No. 2, pp. 109-114.

Michel, B. (1978). Ice mechanics. Les Presses de l'Universitē Laval, Quebec, 1978.

Muguruma, J. and Higuchi, K. (1963). Glaciological studies on ice island T-3. J. Glaciol. Vol. 4, No. 36, pp. 709-730.

Schwarz, J. and Weeks, W.F. (1977). Engineering properties of sea ice. J. Glaciol., Vol. 19, No. 81, pp. 499-531.

Sinha, N.K. (1979). Grain boundary sliding in polycrystalline materials. Philosophical Magazine A, 40(6), pp. 825-842.

Sinha, N.K. and Nakawo, M. (1981). Growth of first-year sea ice. Eclipse Sound, Baffin Island, Canada. Can. Geotech. J., Vol. 18, No. 1, pp. 17-23.

Sinha, N.K. (1981). Rate sensitivity of compressive strength of columnar-grained ice. Experimental Mechanics, Vol. 21, No. 6, pp. 209-218.

Sinha, N.K. (1983). Field test 1 of compressive strength of first-year sea ice. Annals of Glaciology, Vol. 4, pp. 253-259.

Sinha, N.K. (1984). Uniaxial compressive strength of first-year and multi-year sea ice. Can. Journal of Civ. Eng., Vol. 11, pp. 82-91.

Sinha, N.K. (1986a). Young Arctic frazil sea ice: field and laboratory strength tests. Journal of Materials Science, Vol. 21, No. 5, pp. 1533-1546.

Sinha, N.K. (1986b). The borehole jack. Is it a useful Arctic tool? Proc. 5th OMAE, Tokyo 13-17 April 1986, Vol. IV, pp. 328-335.

Timco, G.W. and Frederking, R. (1986). Confined compression tests: Outlining the failure envelope of columnar sea ice. Cold Reg. Sci. Technol., Vol. 12, No. 1, pp. 12-28.

Wang, Y.S. (1979). Crystallographic studies and strength tests of field ice in the Alaskan Beaufort Sea. Proc. 5th Int. Conf. on Port and Ocean Engineering under Arctic Conditions (POAC-79), August, Trondheim, Norway, Vol. 1, pp. 346-355.

TABLE 1
Equations for calculating uniaxial compressive strength of ice

Temp. °C	Salinity °/oo	Density kg/m^3	Grain Structure	Equation	Curve No. +	Source
(a) Strength as a function of stress rate						
-10	6-9	910	c-g	$\sigma = 4.5\,\dot{\sigma}^{0.28}$		Sinha (1983)
-10	5-7	910	frazil	$\sigma = 6.7\,\dot{\sigma}^{0.30}$		Sinha (1984)
-11	4-5	900	c-g	$\sigma = 5.2\,\dot{\sigma}^{0.36}$		Frederking and Timco (1983)
-10	0	918	c-g	$\sigma = 11.7\,\dot{\sigma}^{0.30}$		Sinha (1981)
(b) Strength as a function of strain rate						
-10	5-6	-	c-g	$\sigma = 26.4\,\dot{\varepsilon}^{0.23}$	1	Wang (1979)
-10	5-6	910	frazil	$\sigma = 49\,\dot{\varepsilon}^{0.275}$	2	Sinha (1984)
-10	5-6	910	frazil	$\sigma = 70.6\,\dot{\varepsilon}^{0.335}$	3	Sinha (1986a)
-10	4-8	910	c-g	$\sigma = 45\,\dot{\varepsilon}^{0.32}$	4	Sinha (1984)
-5	2	870	m**	$\sigma = 28\,\dot{\varepsilon}^{0.23}$	5	Cox et al (1985)
-20	2	870	m	$\sigma = 151\,\dot{\varepsilon}^{0.37}$	6	Cox et al (1985)
-2	1-2	830	c-g	$\sigma = 11\,\dot{\varepsilon}^{0.26}$	7	Timco and Frederking (1986)
-10	0	918	c-g	$\sigma = 177\,\dot{\varepsilon}^{0.328}$	8	Sinha (1981)

Note: units of stress MPa
stress rate Mpa s^{-1}
strain rate s^{-1}
+ Refers to curves numbered in Figure 1
* c-g = columnar grained
** m = mixed columnar grained and granular

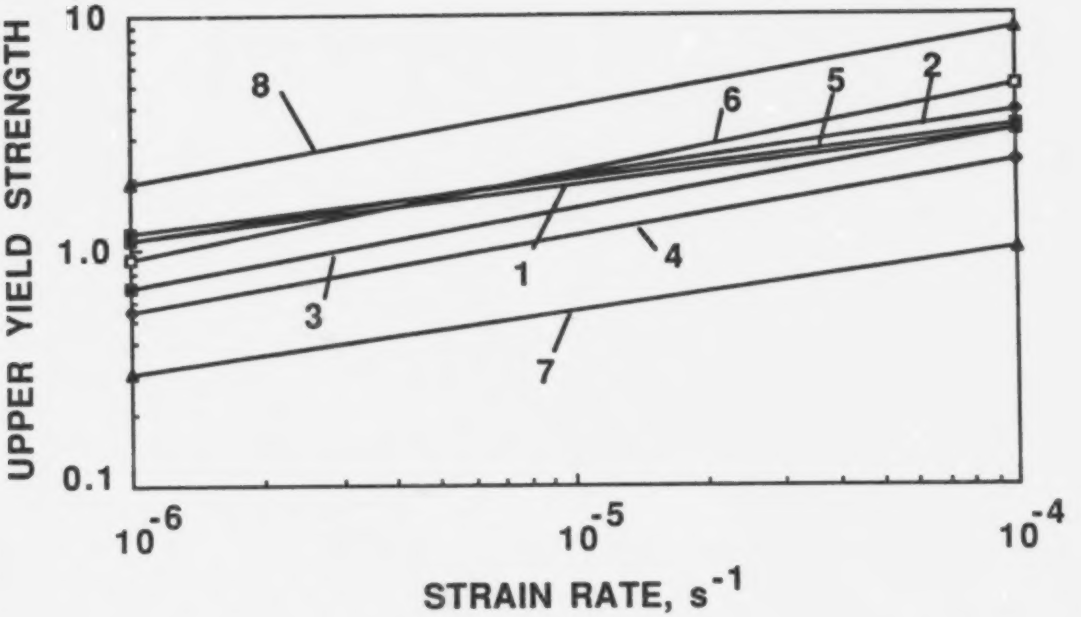

FIGURE 1

COMPARISON OF A NUMBER OF PREDICTOR EQUATIONS FOR UNIAXIAL COMPRESSIVE STRENGTH AS A FUNCTION AT STRAIN RATE (NOTE: NUMBERS REFER TO EQUATIONS IN TABLE 1(b))

NRC WORKSHOP ON EXTREME ICE FEATURES

Questions and Discussions Form

AUTHOR: R. Frederking and Nirmal K. Sinha

PAPER: Mechanical Properties of Shelf Ice

DISCUSSION BY: W.M. Sackinger

DISCUSSION:

From your discussion of the importance of microstructure of ice as a determining factor in mechanical properties, is it a fair statement that you would encourage (1) more examination of microstructure of ice-island ice, and (2) actual measurements of the mechanical properties of samples of ice-island ice?

AUTHOR'S REPLY:

Yes. Microstructural analysis and small-scale testing should, however, be complemented with large-scale detailed observations and in situ mechanical tests.

MULTI-YEAR HUMMOCK FIELDS

by

B. Wright
Gulf Canada Corp. Ltd.

(Paper not included in this Proceedings)

MULTI-YEAR ICE STATISTICS

by

L.G. Spedding, Esso Resources Canada Limited
M.C. Hill, Geographical Services
by Chris Hill

ABSTRACT

Multi-year ice incursions into southern Beaufort Sea coastal waters of less than 100 metres tend to be both irregular and sporadic in their occurrence and severity. However, the largest regular forces likely to be encountered by an offshore structure will be exerted by multi-year ice.

Within the past decade, numerous studies of the multi-year ice environment have been conducted in order to determine probabilistic ice design loads. These studies have examined multi-year ice frequency of occurrence, concentrations, floe size distributions, surface morphology, ridge height, and keel depths along with mean ice thicknesses. The intent of this paper is to summarize and review the present publicly available data covering these subject areas.

1.0 INTRODUCTION

The permanent polar pack ice which covers the Central Arctic Basin and extends into the Beaufort Sea is composed predominantly of multi-year ice. This central mass of multi-year ice, which has survived numerous summers, slowly circulates in a clockwise direction throughout the year in the Beaufort Gyre. In coastal waters, at depths less than 100 metres, annual or "first-year" ice prevails.

Normally, the southern boundary of the polar ice zone lies between 71°30' and 73°N in the southeastern Beaufort Sea. Annual fluctuations in the southern limit of the polar pack take place. This can result in varying concentrations of multi-year ice drifting into water depths as shallow as 5 m.

The return of multi-year ice into coastal waters of less than 100 m depth tends to be both irregular and sporadic in its occurrence and severity. As the largest regular forces likely to be encountered by an offshore structure will be exerted by multi-year ice, characterization of the multi-year ice environment is essential for design load estimation.

Numerous studies of the multi-year ice environment have been conducted this past decade. Data quantity, quality, and analysis techniques vary widely. Combining these variables with the sporadic nature of the multi-year ice incursion into coastal waters complicates the derivation of design ice loads. The intent of this paper is to:

- Provide a summary of the various aspects of the multi-year ice environment.
- Place in the correct context the occurrence of multi-year ice in coastal waters and statistics describing such occurrence.

It should be noted at this point that only information available in the public domain is presented in this paper. A considerable body of proprietary data does exist, which may address or alter opinions herein expressed.

2.0 GLOBAL MULTI-YEAR ICE DISTRIBUTION

As the occurrence of multi-year (including second-year) ice in coastal waters of the southern Beaufort Sea is transitory in nature, it is worthwhile reviewing its global distribution in the adjacent Arctic Basin. It is the Central Arctic Basin that is predominantly multi-year ice covered. Old ice concentrations decrease, in general, as one approaches the coast, with first-year ice predominating in the seas covering the bordering continental shelves. Precise statistics on multi-year ice distributions across the Arctic basin are not available at this time. However, estimates of the multi-year ice fractions have been made.

One estimate of the multi-year ice concentrations across the Arctic has been made from data collected during a two-year aerial survey of the Arctic (Wittman and Schule, 1966). The ice type distributions derived from their study for the winter (January - May) is given in Table 1. The geographical regions to which the distributions apply are illustrated in Figure 1. The Arctic ice cover is categorized by Wittman and Schule according to the following thickness criteria:

- new ice: less than 0.3 m thickness,
- thick winter ice: between 0.3 m and 2.0 m thickness,
- polar ice: thickness varying around 3 m.

The results indicate that multi-year ice concentrations vary significantly across the Arctic. Polar ice fractions range from 23% in the Greenland Sea to 90% in the Canadian Basin. The trend to higher concentrations in the central basin compared to the coastal areas is apparent.

In recent years, further information on Arctic sea ice boundaries, concentrations, and types has started to emerge from the analyses of passive microwave imagery acquired by the Nimbus satellites (Gloersen et al., 1978 and Carsey, 1982).

The Nimbus microwave data tend to substantiate the earlier observed global multi-year ice distribution trends. The central core of predominantly multi-year ice is readily apparent in Nimbus 7 Scanning Multi-channel Microwave Radiometer (SMMR) imagery. In this imagery, the changes in the emitted microwave radiation correspond to multi-year ice concentration changes.

General comparisons of the Nimbus SMMR multi-year ice determined fraction with the Wittman and Schule data show the SMMR estimates to be the lower, by around 20% (Cavalieri et al., 1984). The reasons for this are not fully understood at this time. While further studies are required to improve accuracy and understanding of the SMMR data, they do substantiate observations regarding polar ice distribution trends.

3.0 SOUTHERN LIMIT OF POLAR PACK

The dynamics of the polar pack result in the southern edge of the pack never remaining static in one location. Northward and southward shifts of the polar pack edge take place, both inter-annually and throughout a season. The majority of the time there is no sharp boundary between the polar pack and the seasonal coastal ice, but rather a gradual increase in the old ice concentrations. The width of the boundary zone varies and is highly dependent on prevailing meteorological conditions.

This inter-annual variability, in both the southern limit and boundary zone width, is illustrated in the data from two studies. Both studies rely on the analysis of the Atmospheric Environment Service's (AES) weekly ice charts to determine the southern limits of the multi-year ice.

The limits of 2/10 and 5/10 multi-year ice concentrations for the years 1973 to 1978, as determined by Hill (1979) in his analyses of the ice charts, are shown in Figures 2 and 3. If the 5/10 concentration boundary is regarded as marking the polar ice edge, it is clear that multi-year ice concentrations drop gradually towards shore in certain years, i.e. 1973, 1975, and 1976. In these years there is a distinct separation between the 2/10 and 5/10 isopleths. In other years, i.e. 1974, 1977, and 1978, the 2/10 and 5/10 isopleths are almost coincident and there is a distinct drop in the concentration of multi-year ice past a particular point.

A more recent analysis (De Paoli et al., 1982) of the AES ice charts, though using slightly different concentration criteria, confirms the general trends. In this analysis the polar pack edge (multi-year ice concentrations greater than 7/10) and 1/10 multi-year concentration boundaries were plotted from the first and last charts of the season (Figures 4 and 5).

With regard to the southeastern Beaufort Sea, the following conclusions can be drawn from the data:

- The southern limit of the polar pack can be expected to run between latitudes 71°N and 73°N.
- Considerable annual variability in the location of the southern limit of the polar pack can be expected. In adverse years, if 5/10 multi-year ice concentrations are considered to denote pack edge, it can be expected as far south as 70°30'N.
- The latter study indicates that in approximately 3 out of 10 years the pack edge has moved towards the coast during the winter months and for other years it has moved seaward. This last conclusion, however, should be treated with caution due to the uncertainties in determining the polar ice edge from the data base.

4.0 MULTI-YEAR ICE OCCURRENCE IN COASTAL WATERS

It is during southerly migrations of the polar pack edge that invasions of multi-year ice into coastal waters take place. Again, it is the AES ice charts that provide the long-term, consistently prepared, data base from which statistics on multi-year ice have been derived. Over the years a number of analyses of these data have been carried out.

One of the earliest analyses of these data was carried out by Fenco in 1975. In this study, the southern Beaufort Sea was divided into six areas (Figure 6) and frequency of occurrence of a given old ice composition determined. For the nearshore area, the analysis indicated an almost 100% probability of old ice concentrations less than 10%. The risk of encountering larger old ice concentrations increased with progression into the deeper outer zones (Figure 7).

More recent industry analyses of the ice charts have examined both the site specific and regional aspects of multi-year ice occurrence. The senior author (Spedding, 1978) examined the occurrence of multi-year ice during the summer open water season. In this analysis, the longitudinal occurrence at the 200, 100, 70, 50, and 30 foot water depths between 129°W and 140°W was examined.

An example of some of the data from this analysis is illustrated in Figure 8. Here, the total number of weeks of each summer (for the years 1967-1977) that old ice was present at the 50-foot water depth for longitudes 130°W, 136°W, and 140°W is plotted. For this paper, a further eight years of data were added. The number of weeks in Figure 8 is the total number of weeks during the open water season in which any old ice concentration was present. Old ice concentrations could have ranged from a trace (>1/10) to 10/10. It is obvious from the data that wide fluctuations in both the annual severity and presence of old ice occur.

With decreasing water depth, a reduction in the frequency of multi-year ice occurrence can be expected (Figure 9). Here the cumulative weekly ice totals for all the nineteen summer seasons for the various water depths are plotted by longitude. For example, at the 30-foot water depth, longitude 130°W, multi-year ice was present for only seven seeks during the summer seasons in the 19 years. Knowing the average summer open water season length (12 weeks at this site), estimates of percentage time that ice was present can be made (3% in this instance). For the 200-foot water depth, this increases to the 14-29% range.

The invasion of multi-year ice into coastal waters is most likely in late summer, when a large proportion of the first-year ice has melted or before sufficient new ice growth is established to halt its progress. This tendency is reflected by the October maximum in the mean multi-year ice concentrations presented in Figure 10.

All the analyses indicate wide fluctuations in both the length and annual occurrence of multi-year ice in coastal waters. Typical durations of multi-year ice presence are in the order of weeks, but ice that descends late in the season may remain trapped throughout the winter in the landfast ice zone. This happened in the winters of 1974-75, 1975-76, and 1983-84. At most water depths, the data indicate that some multi-year ice concentrations can be ex-pected one year in two. The wide fluctuations in multi-year occurrence, however, limit such generalizations. Quite often, a particular site may experience a number of ice-free years followed by a series of severe ice years.

5.0 VARIATIONS IN CONCENTRATIONS AND OCCURRENCE

Both old ice concentration and occurrence vary widely on a weekly basis throughout a season, as well as annually. Within a season, ice concentrations can vary with water depth and longitude. These points are illustrated in observations from the 1985 summer (Tables 2 and 3). Data in Table 4 illustrate the annual variability that can occur at specific offshore drill sites. It can be seen that concentrations vary from 0 to 10/10.

Site specific and regional probability of exceedence statistics have been derived from analysis of the ice charts (Hill, 1979). The annual and weekly exceedence probabilities of multi-year ice concentrations are shown in Figures 11 and 12. As durations of multi-year ice at any one site are in the order of several weeks, the weekly probabilities of occurrence are understandably lower than the annual probabilities. These data have also been presented graphically in Figures 13 and 14. For coastal waters south of latitude 71^{o}N, the weekly 2/10 and 5/10 multi-year probability of exceedence percentages are low, being 10 and 15 percent respectively.

Averaging of concentration data (Figure 15) is representative in showing mean annual multi-year ice concentrations for the area. The increasing probability of occurrence with distance from shore and to the northwest is in agreement with other study results. However, due to the large variations in old ice occurrence, mean or average, values do not adequately describe the phenomena.

From the various analyses of the AES data, there is general agreement that observed multi-year ice, along with concentrations involved, vary significantly both throughout a season and annually. The trend is to higher frequency of occurrence with increasing water depth. Also there is higher risk of ice incursion from the northwest.

Old ice invasion patterns, along with their variability, are adequately described by the ice chart analyses. It must, however, be remembered that averaging and smoothing of the observations take place during chart preparation. Operational experience and observations indicate that concentrations and occurrence vary significantly within short distances. While the data show past trends, it is not possible to use these data in a predictive mode.

6.0 MULTI-YEAR FLOE SIZE DISTRIBUTIONS

It is floes along the southern edge of the polar pack that are swept into coastal waters during incursions. Thus, in this region, a knowledge of multi-year floe sizes and their distribution is required for mass and kinetic energy determinations.

In recent years, a number of studies has been conducted to examine floe size distributions. A variety of methods has been used to acquire this information. The data sources have consisted of ice charts, satellite imagery, aerial photography, side-looking airborne radar (SLAR), and synthetic aperture radar (SAR).

Some of the major studies that have been conducted are as follows:

Fenco, 1975: Frequency of occurrence of medium size floes (100-500 m diameter) was determined, by month, for each of the six zones in Figure 6. Analysis was based on ice chart data for years 1953-1973. Results of the study, while showing regional trends, is of little value for structural design purposes.

Spedding, 1979: Aerial photographs from 56 flight lines along the ice edge were analysed. Three flights were conducted in 1973 by Esso, while the remainder comes from AES flights conducted in 1974 and 1975. Photographic coverage is between 120°W and 136°W and from shore out to 72°N. Thirty-five of the flight lines were over concentrations of multi-year ice ranging from one to nine-tenths. Floes were categorized by average diameters into size ranges of 0-250 ft, 250-500 ft, 500-1000 ft, 1000-2500 ft, and 2500-5000 ft.

Arsenault, 1981: Multi-year floe distributions in the 1-2, 2-3, 3-4, 4-5, and >5 km size classes were determined from four SLAR flights conducted in September and October, 1980. Floes less than 1 km in diameter were ignored since discrimination of such floes across the full 100 km SLAR swath width was not possible. Floe size distributions were made for five areas along the pack edge between 126°W - 137°W longitude and 70°N - 72°N latitude. Separate area measurements were made to avoid repeat population counts. Floe size was based on major axis length.

Intera, 1981: The Canada Centre for Remote Sensing SAR-equipped Convair 580 airplane made five flights, October 6-10, 1980, over the Orvilruk and Kopanoar drill sites. Multi-year floe size distributions were estimated from the SAR real time processor imagery. Floe distributions for each day were calculated for the entire SAR mosaic. Areas of all floes with diameters greater than 300 m (0.25 km^2) were measured by electronic planimeter. Distributions were based on area, bin sizes incrementing by 0.25 km^2. Data seem to fit an exponential distribution.

Hudson et al., 1982: 4000 km^2 of aerial photography were taken along the edge of the polar pack from 73°N, on Banks Island, to 83°N, on Ellesmere Island. Photographic lines were flown parallel and perpendicular to coastlines. Floe size determinations, based on average floe diameter, were summed in 300 m increments. Floes were classified by type of ice, subjectively described as smooth, bumpy, or extremely bumpy. Separate floe distributions were presented for these three categories for both the parallel and perpendicular flight lines.

Gulf, 1983: Floe sizes were determined from analysis of 300 km^2 of aerial photography covering three regions at approximate latitude 72°N, between longitudes 131°30'W and 133°25'W. Photographs were stereoscopically scanned to place each floe into a category of low, medium, or high freeboards, corresponding to total floe thicknesses of 4 to 7 m, 7 to 12 m, and greater then 12 m. This classification of floes by freeboard was based on a thickness of freeboard algorithm developed by Kovacs (1977). Floes were measured in two directions to obtain long (a) and short (b) axes. Axis measurements were used to calculate floe size, assuming floes to be in the shape of an ellipse. The "a" length increments were plotted in various forms to find the most accurate fit. The best fit in all cases was exponential.

From all of the above studies, floe size distributions are available. Each of the studies, however, had a different minimum floe size cutoff and bin size. Correlation and normalization of the data from the different studies were undertaken for the Beaufort Sea Environmental Impact Panel submission (Marcellus and Morrison, 1982). Exceedence plots of the size distributions generated are illustrated in Figure 16.

With the exception of the Hudson data, which were collected along the edge of the Canadian Archipelago, all data were obtained in the southern Beaufort Sea. From Figure 16 it is seen that floe sizes vary considerably from study to study. It should also be noted that the second Esso distribution in Figure 16 is based on analysis of Landsat (satellite) imagery. There are a number of possible reasons for the differences:

- differences in geographical location,
- time of year or spatial differences,
- different types of imagery used; different interpretation and floe size categories used.

The scatter may even be a factual representation of the variation in size distribution of multi-year ice in the area. Examination of satellite and SLAR imagery certainly indicates that floe size distributions can vary significantly over short distances. Quite often these are quantitative trends that emerge from analysis of the data bases and are not always evident in the statistics.

There is evidence of spatial variability along with regional variability, i.e. large floes are swept into the region off Banks Island and a gradual breakdown occurs during their westerly drift. An increase in the proportion of smaller floes is evident with progression of summer, numbers peaking in late August. Large floes, however, are always present, indicating a continuing flux of large floes into the area.

Imagery types may account for some of the differences. Spatial coverage of aerial photography is less than that of SLAR, resulting in possible bias in distributions toward smaller sizes. On the other hand, discrimination of small floes below certain thresholds is difficult on SLAR and SAR. In high ice concentrations floe size determination is difficult in all imagery due to merging of floe boundaries.

In both the determination of floe dimensions and size categories, techniques differ widely, i.e. area, average diameter, maximum diameter, elliptical shape. Use of different minimum cutoffs and bin sizes can distort data set comparisons. This is evident in Figure 17 where distributions from three cases are plotted; the

1974-75 summer distribution (Spedding, 1979), data for 1974-75 landfast ice zone determined from SLAR (Spedding, 1979), data from the 19 March 1979 aerial photo flight into the polar pack (C-CORE, 1980). The shift in two distributions due to the large floe size cutoff limits for the 1974-74 winter and March 1979 data is clearly visible when compared with the 1974-75 summer data (Figure 17).

Differences in collection and analysis methods are certainly factors contributing to the observed variability in the distributions. However, in the authors' opinion, some of the difference is also due to annual variability. In the analyses of the 1974 and 1975 aerial photographs (Spedding, 1979) a possible trend to larger floe sizes is indicated for these poor ice years. The occurrence in coastal waters of large floes with diameters in excess of 10 km cannot be ignored. Such floes are clearly visible in all the observational bases. While such large floes may be considered to be composite floes, i.e. conglomerates of smaller floes frozen together, they are structurally strong enough to remain as identifiable features for periods of months. In poor ice years, such as 1974, multi-year floes kilometres in diameter may reach water depths of 10 m. The concentrations of multi-year ice trapped in coastal waters that year are given in Table 5, while floe sizes are given in Table 6.

While existing floe size distributions depict trends, standardization of size categorization is desirable. Also, the spatial and temporal variabilities require further investigation.

7.0 MULTI-YEAR ICE CHARACTERISTICS

Multi-year ice is distinguished from first-year ice by a number of physical characteristics. Level first-year ice generally attains a maximum thickness of around 2 m by the end of the winter, whereas multi-year ice thickness ranges from 2 m to 4 m throughout the year. Also, the surface topography of multi-year ice is more undulating than that of first-year ice due to its having survived a number of melt seasons.

In addition, the salinity of multi-year ice is lower as a result of the ice undergoing a number of melting and refreezing cycles. Due to the melting and refreezing processes, voids in the ice become filled with melt water. As a result, multi-year floes are essentially solid ice.

It is the intent of this section to review available information on multi-year floe thicknesses, ridge keel depths, and ridge sail heights.

7.1 MEAN ICE THICKNESS

Multi-year floes are characterized by extreme irregularities in both their surface and underwater topographies, which result in large variations in their ice thicknesses. Even for so-called level or undeformed floes, thickness can vary significantly over distances of metres. Quite often, on this type of floe, there is no discernible correlation between surface and subsurface topographical features. The topography and thickness of floes depend on formation processes, geographical location, drift, and melt season histories. As a result, the physical characteristics of adjacent floes may vary significantly. Despite the variations apparent in individual floe thicknesses, a number of estimates of the mean multi-year ice thickness are available.

One such estimate (Potocsky, 1975) of mean multi-year ice thickness throughout the year is illustrated in Figure 18. This indicates a growth rate of 0.1 to 0.2 m per month from October through April with the mean thickness reaching a maximum of 3 m.

Estimates of the probability of exceedence of ice thickness by month in the Beaufort Sea (after Maykut, 1977) are illustrated in Figure 19. These estimates are based on thermodynamic calculations of the regional heat and mass balances of the central Arctic ice cover. A mean multi-year ice thickness of between 2.0 and 3.2 m throughout the year is indicated.

More recently, multi-year ice thickness distributions have been estimated from submarine sonar data (Wadhams and Horne, 1978) and from impulse radar measurements (C-CORE, 1980). The resulting thickness distributions from both studies are plotted in Figure 20. Mean thickness of 3.7 m with standard deviation of 1.5 m are derived from the radar data, while for the sonar data the mean and standard deviation are 3.9 m and 2.1 m respectively. There is reasonable agreement between the two distributions even though measurement techniques and measurement sample sizes differ. The Wadhams and Horne probability density function curve is composed of three overlapping ice thickness distributions: an initial peak caused by thin ice, a broader peak due to undeformed first-year and multi-year ice, and a tail due to ice in ridges and hummocks.

The impulse radar probability density function (PDF) shows only the multi-year portion of the undeformed ice peak and deformed tail. There is no contribution by first-year ice as there is no penetration by the impulse radar. There could be several factors contributing to the lower radar PDF in the thickness range beyond 5.5 m; the ice thickness distributions may be different, no penetration of deformed ice, different floe populations because of data collected in different regions. Impulse radar data were collected from 27 km of bottom echoes, while sonar data were recorded over a 1400 km profile.

In spite of the difference in measurement techniques and record lengths, the mean thickness estimates from the sonar and impulse radar are in close agreement. The measured data tend to indicate higher mean thicknesses than the earlier two theoretical studies. Results from more recent field drilling studies tend to support observations regarding underestimation of mean ice thickness in earlier studies. Further work, however, is required to clarify this trend to increasing mean thickness. Also, the trend in field programs is toward collection of information on the more extreme type of multi-year features which may bias mean thickness estimates to the higher side.

7.2 MULTI-YEAR RIDGE CHARACTERISTICS

Ridges in multi-year ice are the remnants of ridges formed during the first year of ice development. Over a cycle of two or more seasonal melt and freeze episodes, such ridges consolidate as melt water refreezes in ridge voids (see section 7.0). Seasonal melt from the ridge surface also results in a ridge of more attenuated relief than is encountered in first-year ice ridges.

It has been estimated (Kovacs, 1973) that two seasons of ice melt and refreezing should suffice to produce a fully consolidated ridge, free of voids. The complete absence of such voids is confirmed by observation of exposed cross sections of split ridges (Mellor and Kovacs, 1971; Kovacs et al., 1975).

In addition to the surface pressure ridge remnant, the multi-year ridge complex also consists of a broad, bowl-shaped subsea keel structure. Figures 21 and 22 are profiles of actual measured ridge and keel complexes, from two different studies, which illustrate the normal relationship between surface and subsea components. The great thickness of ice at a multi-year ridge complex poses some problems in actually obtaining direct keel depth measurements. Due to the excessive time and energy expended in augering the measuring holes in several ridges, the technique of side-looking sonar ranging has been used to obtain nearly all of the more than 70 keel profiles presently available in the public domain. The sonar ranging technique does, however, necessitate the drilling of holes in less thick ice either side of the ridge complex in order to permit entry of the sonar equipment. Thus, in seeking multi-year ridge complexes which are more easily accessible for purposes of measurement, an element of sampling bias may exist in the limited amount of measured profile data.

Attention has been paid to the ratio of sail height to keel depth in the few measured complexes. Figure 23 illustrates one attempt at correlating the two measurements. Forty-four of the publicly available data points were plotted, representing ridges of up to 11 m height and keels up to 32 m depth. The apparently close correlation of sail height and keel depth points to the more easily measured sail being a predictive index of the total mass of multi-year ice which may impact a given structure.

As indicated previously, however, not all of the publicly available ridge and keel measurements mave been plotted together. Dickins (1976) profiled multi-year ridge complexes in the Queen Elizabeth Islands and Vaudrey (1981) has presented measurements for features off the Alaskan coast. In both studies, sail to keel ratios regularly exceeded 1:5 compared with the mean of 1:3.25 for the ridges of Figure 23. It is desirable that a more rigorous statistical analysis be performed on all available ridge and keel data in order to provide a better basis for use of ridge height measurement as a predictive index of the whole.

7.3 RIDGE AND KEEL DISTRIBUTIONS

A knowledge of ridge/keel distributions is required for the design of offshore structures and for determination of mean ice thicknesses. While the surface relief is relatively easy to measure, there is the problem of deducing keel drafts and their distributions from the data. To help in this regard, theoretical distribution functions for ridge sail heights and keel depths based on the randomness of ridges have been derived (Hibler et al., 1977). The distribution functions are in the form of negative exponentials. Typical results from using the model to compare observed and predicted keel depth distributions are illustrated in Figure 24.

Typical ridge height distributions are illustrated in Figures 25 and 26. In Figure 25, data are from a 77 km flight line north of Alert, on the north coast of Ellesmere Island (Lowry and Wadhams, 1979). While the second distribution (Figure 26) is for first-year ridges, similarities emerge from the data. In both cases, the majority of ridges are less than 3.5 m high, ridges over this height being infrequent events.

Keel draft measurements derived from the analysis of submarine sonar data is the other information base for the determination of ridge distributions. Much of the presently unclassified information from this source was collected in the deeper waters of the Arctic basin. Although work has been carried out toward developing distribution probability functions from these data, satisfactory conclusions remain forthcoming.

8.0 CONCLUSION

Concentration and occurrence of multi-year ice varies across the Arctic basin, with significant annual and within-year fluctuations occurring along the edge of the polar pack in the southeastern Beaufort Sea. In general, multi-year concentrations and probability of occurrence increase with water depth and distance from shore.

Some spatial and regional variability trends appear in the size distribution of multi-year floes. Difficulty in developing usable distributions continues to be encountered due to differences in data measurement conventions among the various studies done.

Data on the dimensions and frequency of occurrence of multi-year ridges and keels are required for estimation of ice loads. Further work can be carried out on derivation of satisfactory probability statistics from existing over-ice laser profiles and from subsea sonar data. Greater work still would be possible should access be had to the significant amount of as yet proprietary data not presented in this paper.

REFERENCES

Arsenault, L.D. (1981), SLAR qualitative evaluation and multi-year ice floe size distribution, Cold Regions Remote Sensing, report prepared for Dome Petroleum Limited.

C-CORE (Oct. 1981), Multi-year ice thickness distribution in the Beaufort Sea determined by airborne impulse radar, Centre for Cold Ocean Resources Engineering, publication no. 80-11.

Carsey, F.D. (20 July 1982), Arctic sea ice distribution at end of summer 1973-76 from satellite data, Journal of Geophysical Research, vol. 87, no. C8, pp. 5804-5835.

Cavalieri, D.J. and P. Gloersen, W.J. Campbell (30 June 1984), Determination of sea ice parameters with the Nimbus 7 SMMR, Journal of Geophysical Research, vol. 89, no. D4, pp. 5355-5369.

De Paoli, S. and T.B. Morrison, R.W. Marcellus (March 1982), Analysis of interaction probabilities between large ice features and offshore structures in the Canadian Beaufort Sea, Dome Petroleum Limited.

Dickins, D.F. (Oct 1976), Multi-year pressure ridge study, Queen Elizabeth Islands, APOA project no. 102, for Sun Oil Company.

Fenco (April 1975), Project G-1 Beaufort Sea Project ice information study, volumes 1 and 2, Foundation of Canada Engineering Corporation Ltd.

Francois, R.E. (March 1977), High resolution observations of under-ice morphology, Naval Surface Weapons Center, Maryland, report no. APL-UW-7712.

Gladwell, R.W. (1977), Field studies of the strength and physical properties of a multi-year pressure ridge in the southern Beaufort Sea, APOA report no. 91, by Imperial Oil Limited, Calgary, Alberta.

Gloersen, P. and H.J. Zwally, A.T.C. Chang, D.K. Hall, W.J. Campbell, R.O. Ramseier (1978), Time-dependence of sea ice concentration and multi-year ice fraction in the Arctic basin, Boundary Layer Meteorology, no. 13, pp. 339-359.

Gulf Canada Resources Inc. (1983), personal communication on 1980 Multi-year Ice Study.

Hibler, W.D. III and S.J. Mock, W.B. Tucker III (1972), Statistical aspects of sea ice ridge distributions, Journal of Geophysical Research, vol. 77 (30), pp. 5954-5970.

Hill, M.C. (1979), Annual limits of multi-year ice concentrations in the Beaufort Sea, internal data analysis, Canadian Marine Drilling Ltd.

Hudson, R.D. and G.R. Pilkington, M. Metge, B. Wright, D. McGonigal, D. Schwab (1980), Final report on the field studies and aerial mapping along the northwest edge of the Canadian Archipelago, joint project, Dome Petroleum Limited and Gulf Canada Resources Inc.

Intera Environmental Consultants Ltd. (1980), Multi-year floe size distribution from the airborne real time processor data, prepared for Dome Petroleum Limited.

Kovacs, A. and M. Mellor (Aug. 1971), Sea ice pressure ridges and ice islands, Creare Inc., technical note TN-122, APOA project no. 17.

Kovacs, A, and M. Mellor (1974), Sea ice morphology and ice as a geologic agent in the southern Beaufort Sea, Arctic Institute of North America, Coast and Shelf of the Southern Beaufort Sea Symposium.

Kovacs, A. and D. Dickins, B. Wright (Oct. 1975), An investigation of multi-year pressure ridges and shore pileups, Norcor Engineering, APOA project no. 89.

Kovacs, A. and W.S. Weeks, S. Ackley, W.D. Hibler III (1973), Structure of a multi-year pressure ridge, Arctic, vol. 26, no. 1.

Kovacs, A. (1983), Characteristics of multi-year pressure ridges, 7th International Conference on Port and Ocean Engineering under Arctic Conditions, vol. 13, pp. 173-182.

Lowry, R.T. and P. Wadhams (20 May 1979), On the statistical distributions of pressure ridges in sea ice, Journal of geophysical Research, vol. 84, no. C5, pp. 2487-2494.

Marcellus, R.W. and T.B. Morrison (April 1982), Ice design statistics for the Canadian Beaufort Sea, Canada Marine Engineering Ltd., prepared for the EIS partners.

Maykut, G.A. (Sept. 1977), Estimates of the regional heat mass balance of the ice cover in the central Arctic, Proceedings, AIDJEX Symposium on Sea Ice Processes and Models.

Potocsky, G.J. (1975), Alaskan area 15 and 30 day forecasting guide, NTIS AD-A010527, Naval Oceanographic Office, Washington, DC.

Spedding, L.G. (Feb. 1978), Statistics on Beaufort Sea summer ice cover for ice/structure collision assessment, Imperial Oil Limited internal report IPRT-2ME78.

Spedding, L.G. and P. McLellen, C. Soares (Jan. 1979), Summer ice floe size and distribution in the southern Beaufort Sea, Imperial Oil Limited, internal report IPRT-1ME-78.

Wadhams, P. and R.J. Horne (1978), An analysis of ice profiles obtained by submarine sonar in the AIDJEX area of the Beaufort Sea, Scott Polar Research Institute, technical report 78-1, Cambridge, UK.

Vaudrey, K.D. (Oct. 1981), Beaufort Sea multi-year ice feature survey, AOGA project no. 139.

Voelker, R.P. et al. (1981), Trafficability tests of Polar Sea, volume II, Maritime Administration, Office of Research and Development, report no. MA-RD-940-82018, Washington, DC.

Wittman, W.I. and J.J. Schule jr. (1966), Comments on the mass budget of Arctic pack ice, Proceedings of the Symposium on the Arctic Heat Budget and Atmospheric Circulation, edited by J.O. Fletcher, pp. 215-246, memo RM-5233-NSF, Rand Corporation, Santa Monica, Calif.

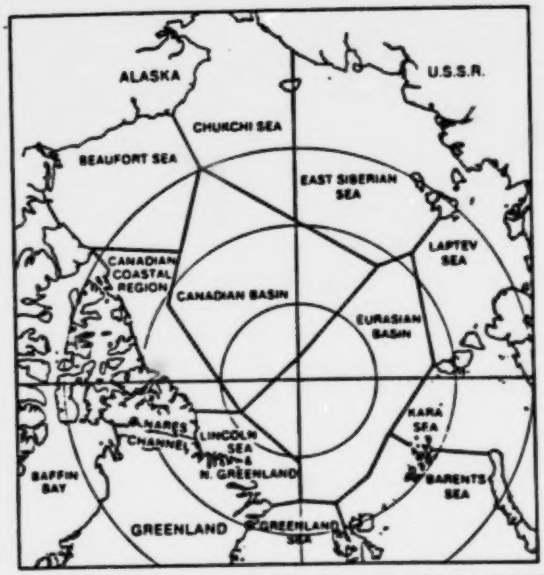
ALASKA
U.S.S.R.
CHUKCHI SEA
BEAUFORT SEA
EAST SIBERIAN SEA
LAPTEV SEA
CANADIAN COASTAL REGION
CANADIAN BASIN
EURASIAN BASIN
KARA SEA
NARES CHANNEL
LINCOLN SEA & N. GREENLAND
BAFFIN BAY
BARENTS SEA
GREENLAND
GREENLAND SEA

Base map of the Arctic from *Wittmann and Schule* [1966].

FIGURE I

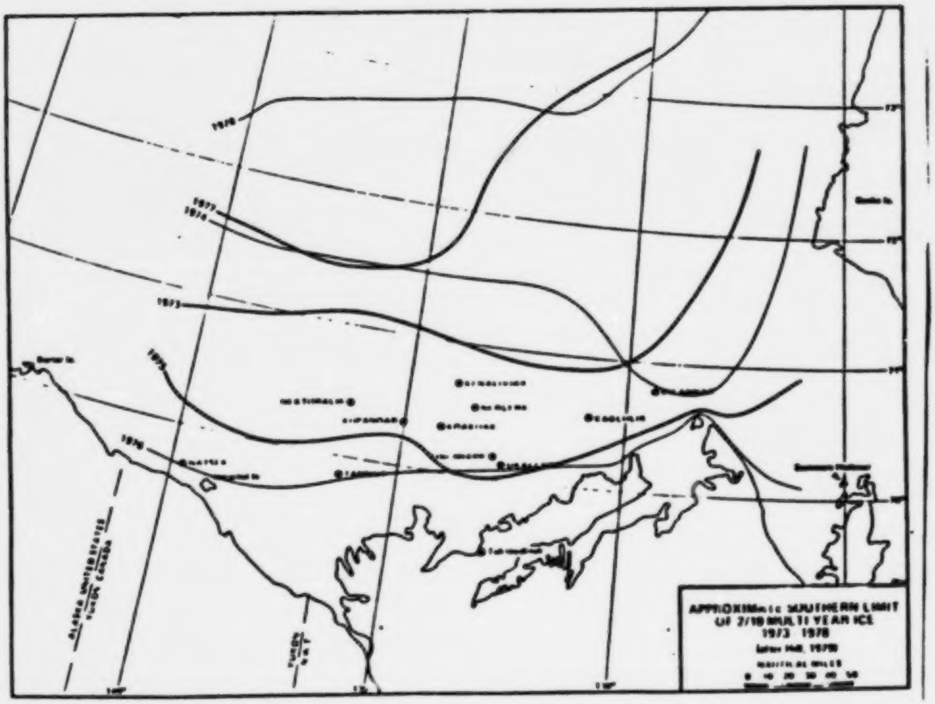
APPROXIMATE SOUTHERN LIMIT
OF 7/10 MULTI YEAR ICE
1973 1978
NAUTICAL MILES
0 10 20 30 40 50
ALASKA UNITED STATES
YUKON CANADA

FIGURE 2

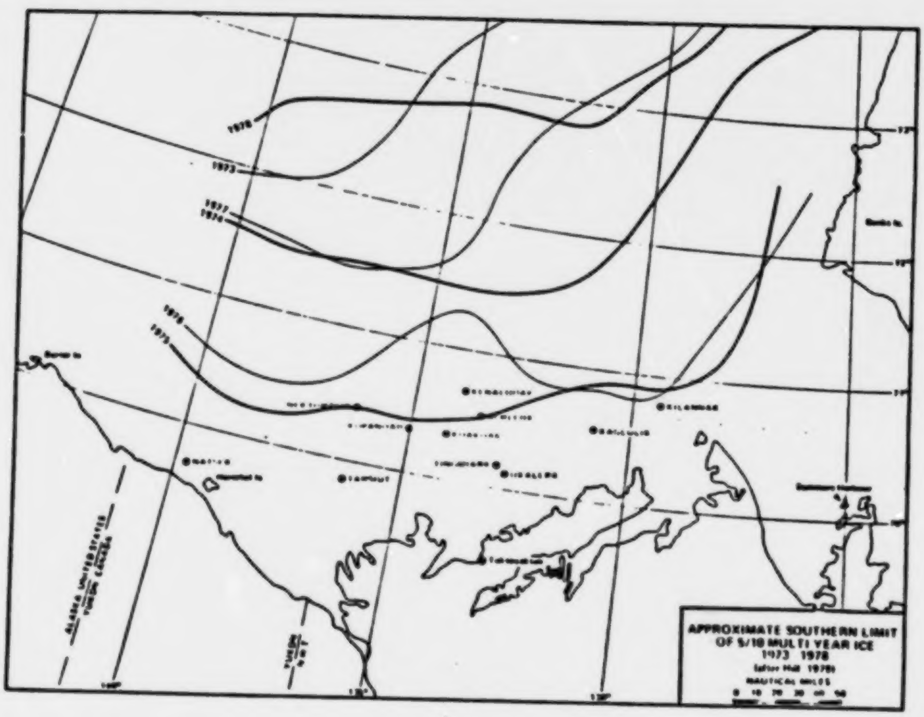
1978
1973
1977
1976
1975
ALASKA UNITED STATES
YUKON CANADA
APPROXIMATE SOUTHERN LIMIT
OF 5/10 MULTI YEAR ICE
1973 1978
(after Hill 1978)
NAUTICAL MILES
0 10 20 30 40 50

FIGURE 3

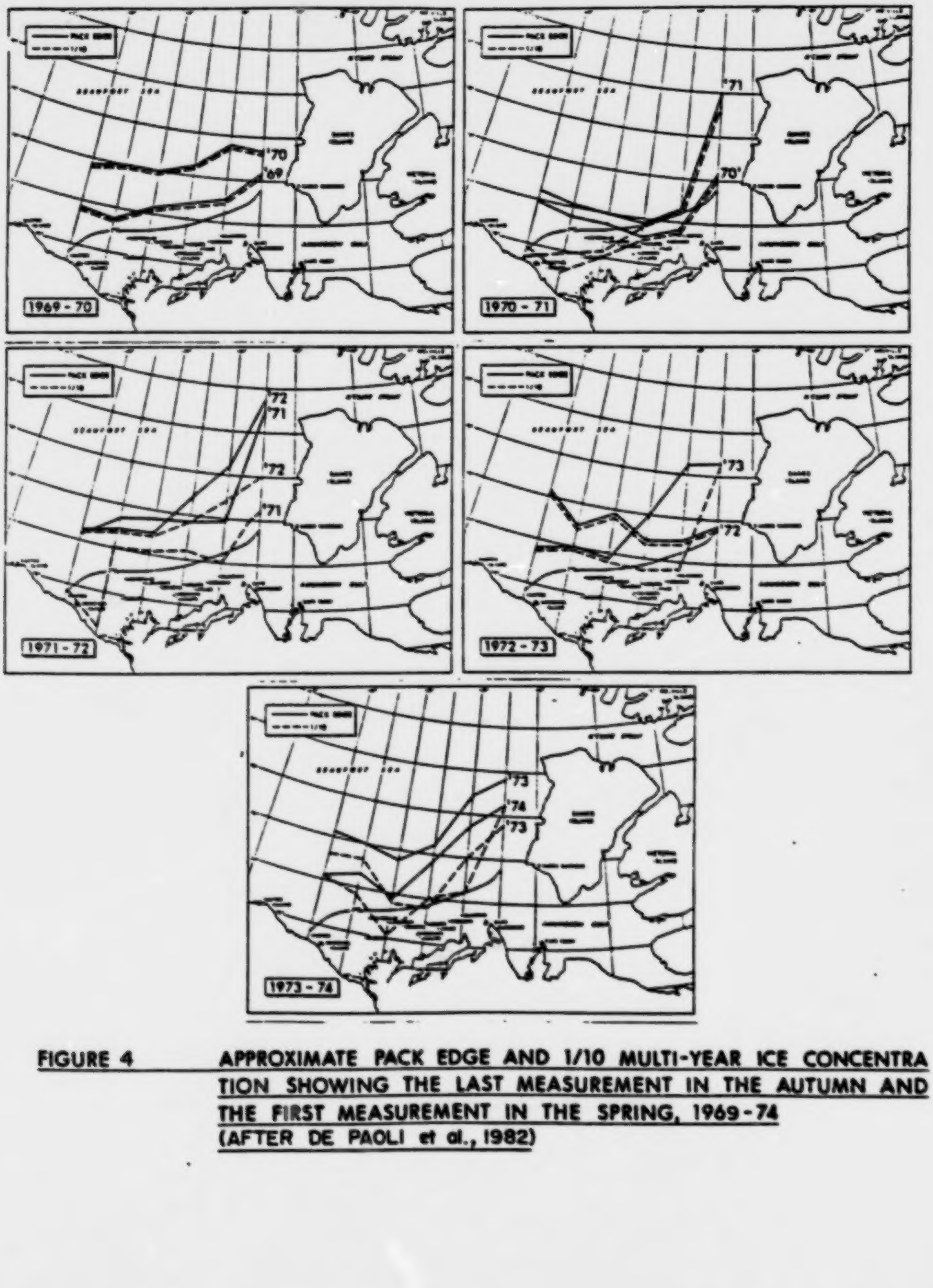
1969 - 70
'70
'69
1970 - 71
'71
70'
1971 - 72
'72
'71
'72
'71
1972 - 73
'73
'72
1973 - 74
'73
'74
'73

FIGURE 4 APPROXIMATE PACK EDGE AND 1/10 MULTI-YEAR ICE CONCENTRATION SHOWING THE LAST MEASUREMENT IN THE AUTUMN AND THE FIRST MEASUREMENT IN THE SPRING, 1969-74 (AFTER DE PAOLI et al., 1982)

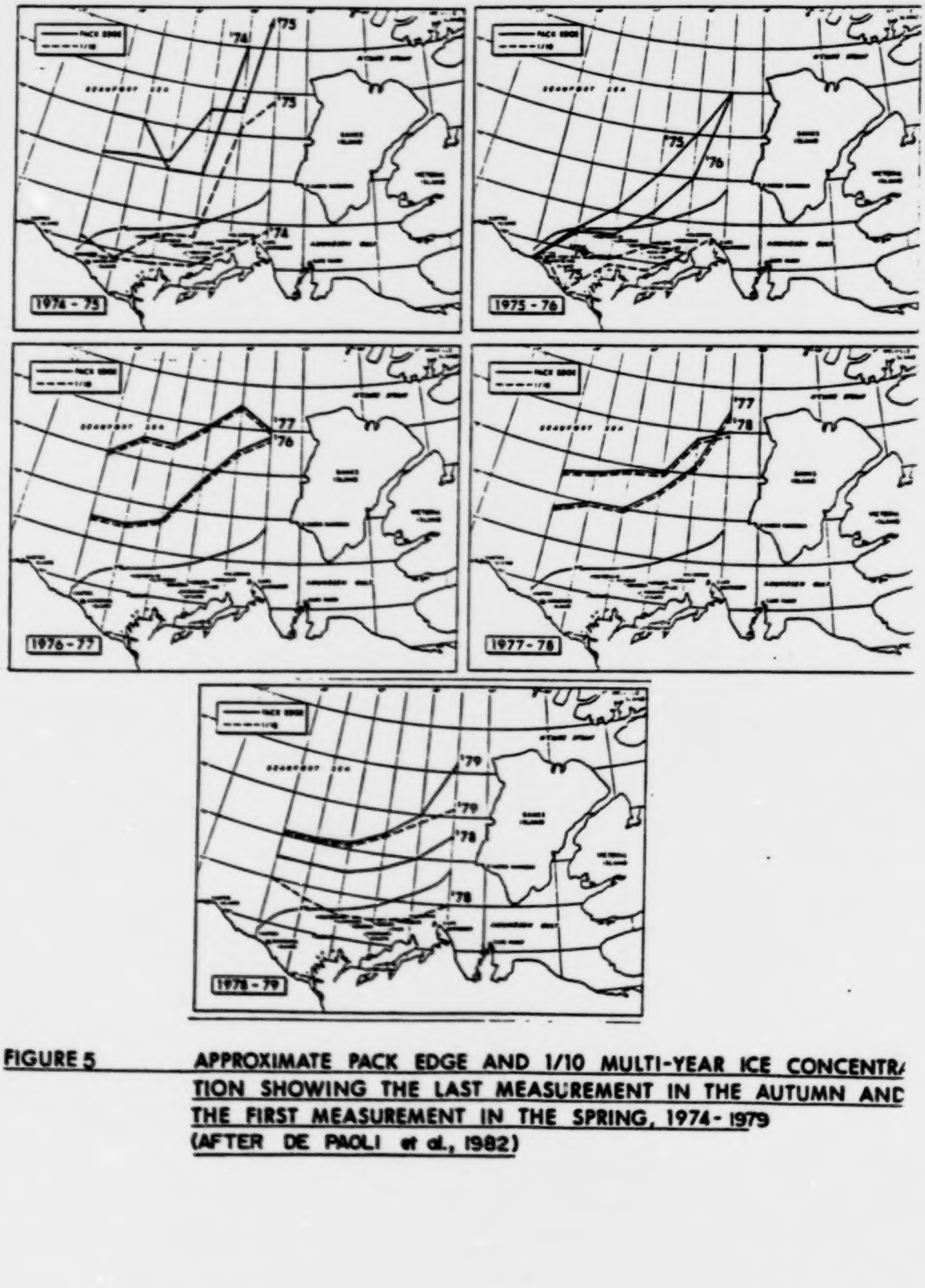
PACK EDGE
1/10
'74
'75
'75
'74
1974 - 75
'75
'76
1975 - 76
'77
'76
1976 - 77
'77
'78
1977 - 78
'79
'79
'78
'78
1978 - 79

FIGURE 5 APPROXIMATE PACK EDGE AND 1/10 MULTI-YEAR ICE CONCENTR TION SHOWING THE LAST MEASUREMENT IN THE AUTUMN AN THE FIRST MEASUREMENT IN THE SPRING, 1974- 1979 (AFTER DE PAOLI et al., 1982)

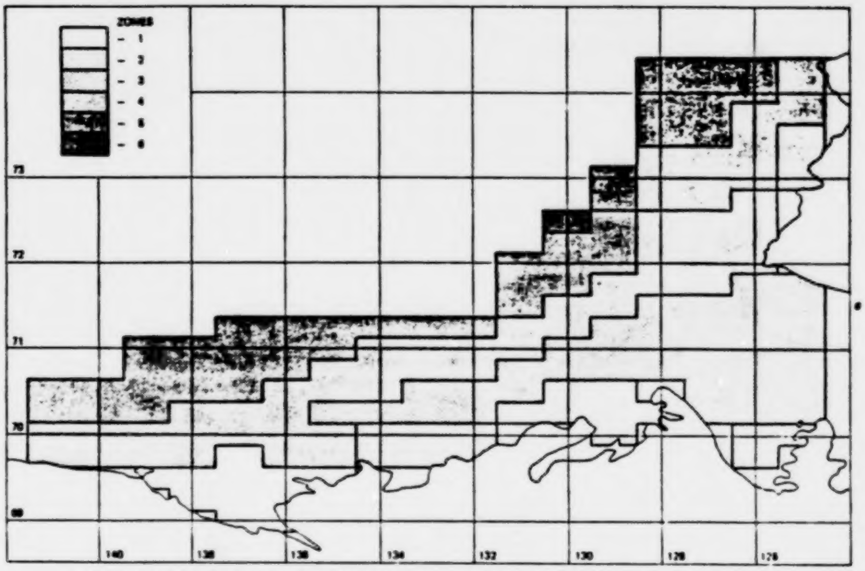
ZONES
- 1
- 2
- 3
- 4
- 5
- 6
73
72
71
70
69
140
138
136
134
132
130
128
126

THE SIX AREAS THE BEAUFORT SEA WAS DIVIDED INTO FOR THE ANALYSIS OF THE HISTORICAL ICE DATA GATHERED BY THE CANADIAN GOVERNMENT ICE PATROL Fenco (1975)

FIGURE 6

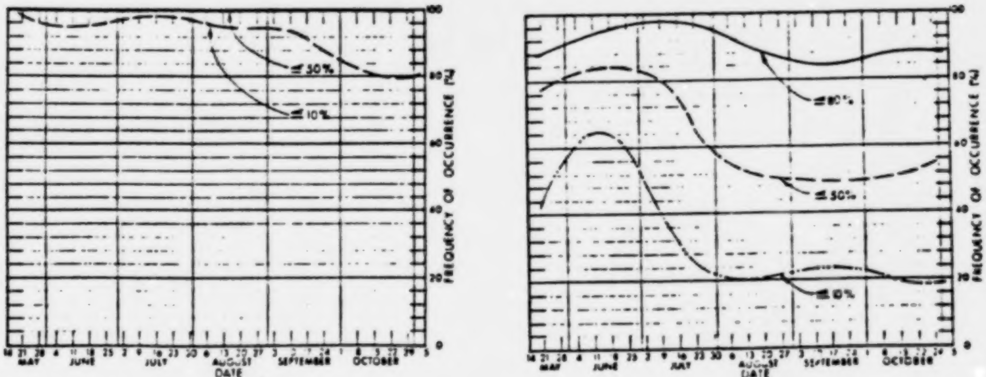

AREA 1

AREA 6

FIGURE 7

FREQUENCY OF OCCURRENCE OF OLD ICE COMPOSITION FOR BEAUFORT SEA (1953-1973 DATA)

58-218

No. OF WEEKS ICE CHARTS REPORT MULTI-YEAR ICE CONCENTRATION AT 50' WATER DEPTH DURING SUMMER OPEN WATER SEASON FOR LONGITUDES 140°, 136° AND 130°W YEARS 1967 - 1985

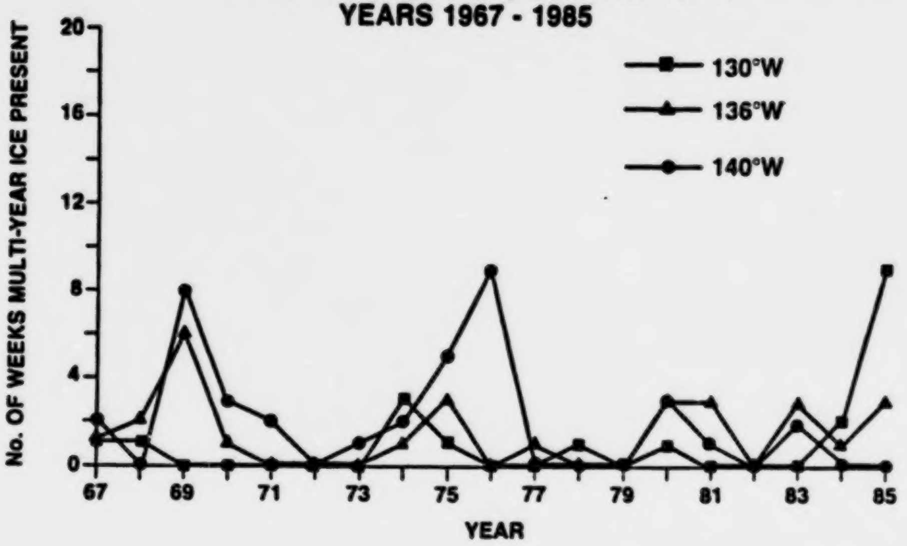

FIGURE 8

58-217

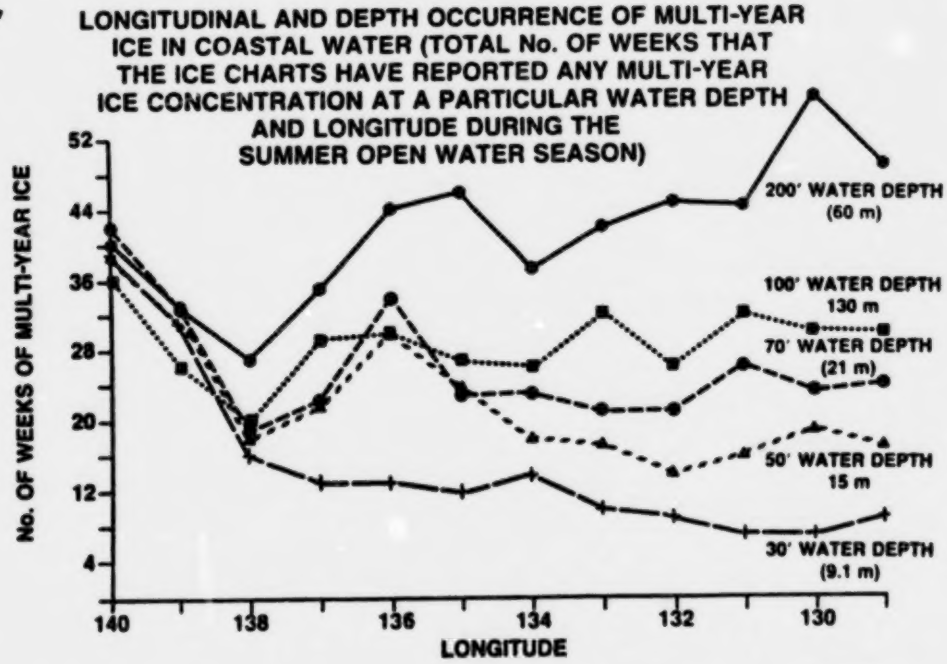

LONGITUDINAL AND DEPTH OCCURRENCE OF MULTI-YEAR ICE IN COASTAL WATER (TOTAL No. OF WEEKS THAT THE ICE CHARTS HAVE REPORTED ANY MULTI-YEAR ICE CONCENTRATION AT A PARTICULAR WATER DEPTH AND LONGITUDE DURING THE SUMMER OPEN WATER SEASON)

FIGURE 9

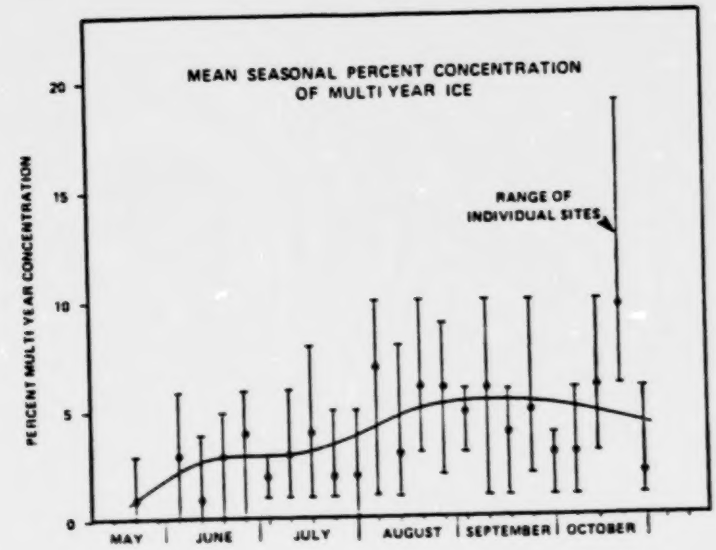

FIGURE 10

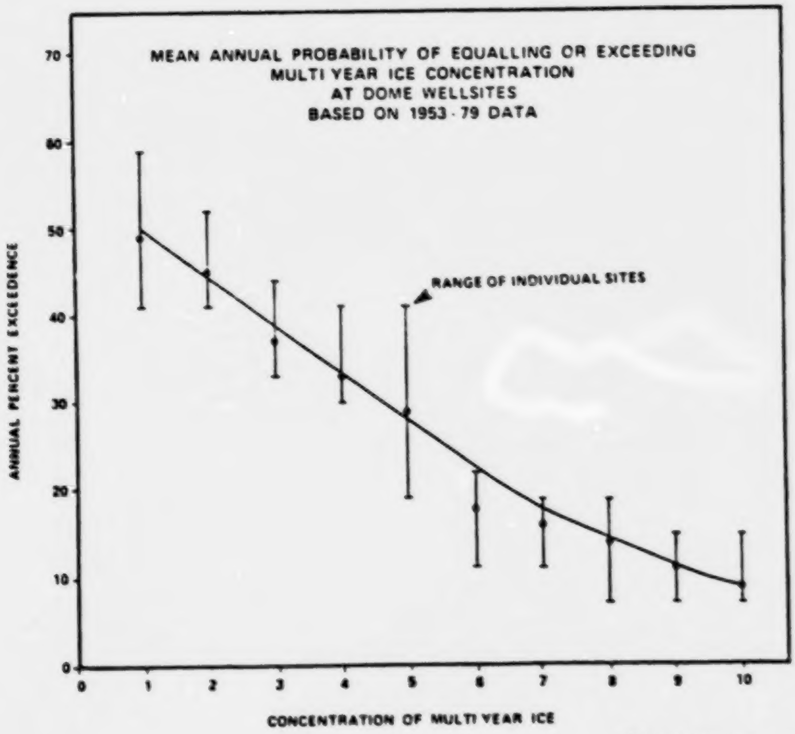

FIGURE 11

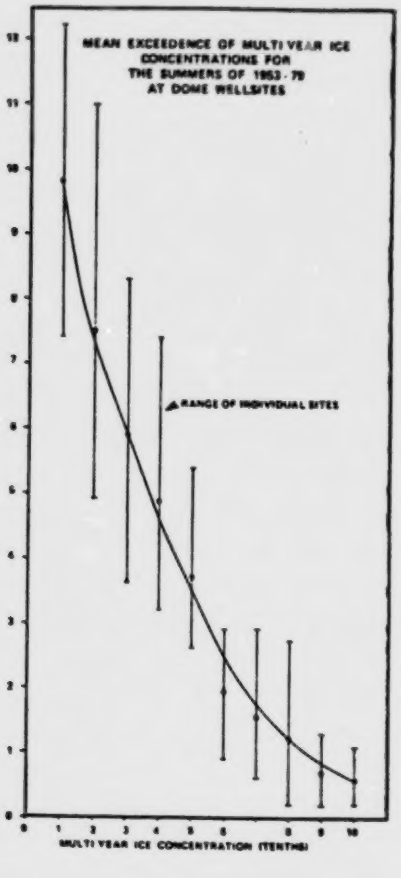

FIGURE 12

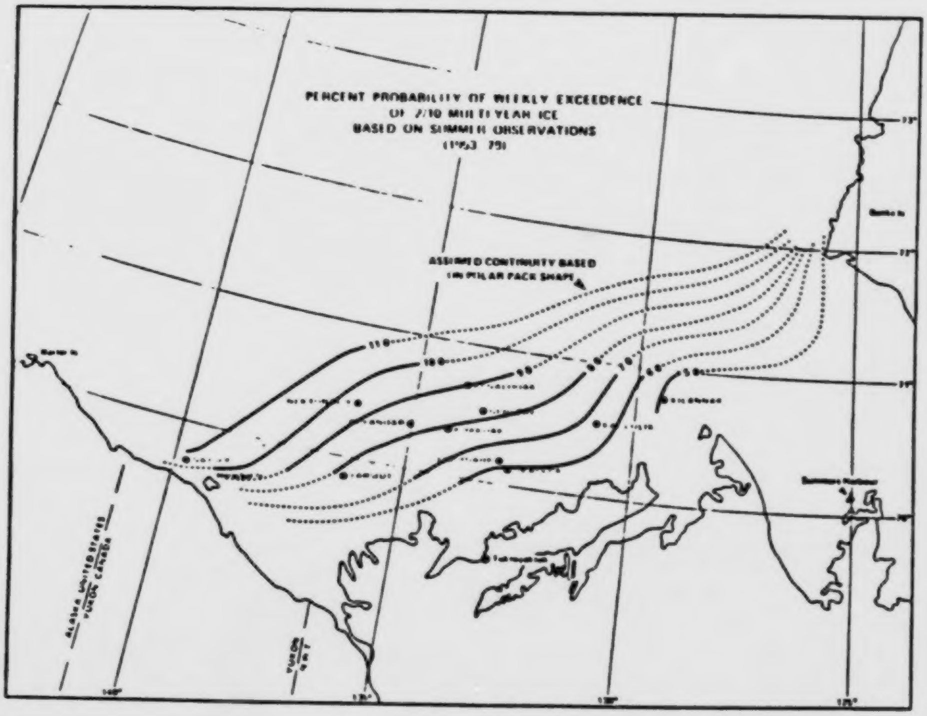
PERCENT PROBABILITY OF WEEKLY EXCEEDENCE
OF 7/10 MULTI YEAR ICE
BASED ON SUMMER OBSERVATIONS
(1953 79)
ASSUMED CONTINUITY BASED
ON POLAR PACK SHAPE
11.0
10.0
9.0
8.0
7.0
6.0
5.0
73°
72°
71°
70°
ALASKA UNITED STATES
YUKON CANADA
YUKON
N.W.T.
140°
135°
130°
125°

FIGURE 13

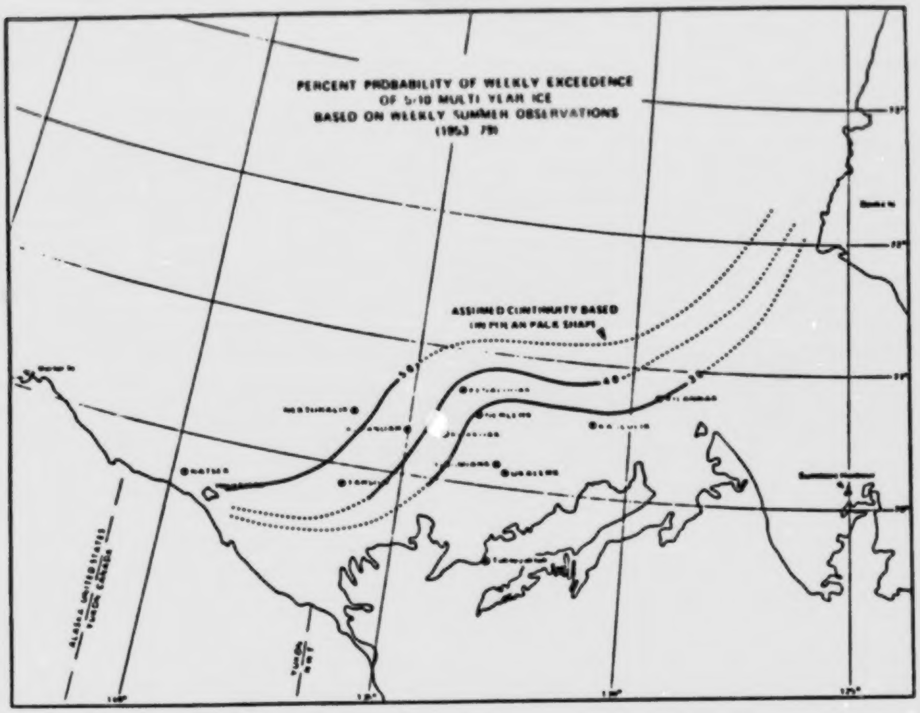
PERCENT PROBABILITY OF WEEKLY EXCEEDENCE
OF 5/10 MULTI YEAR ICE
BASED ON WEEKLY SUMMER OBSERVATIONS
(1953 79)
ASSUMED CONTINUITY BASED
ON MEAN PACK SHAPE
ALASKA UNITED STATES
YUKON CANADA
YUKON
N.W.T.

FIGURE 14

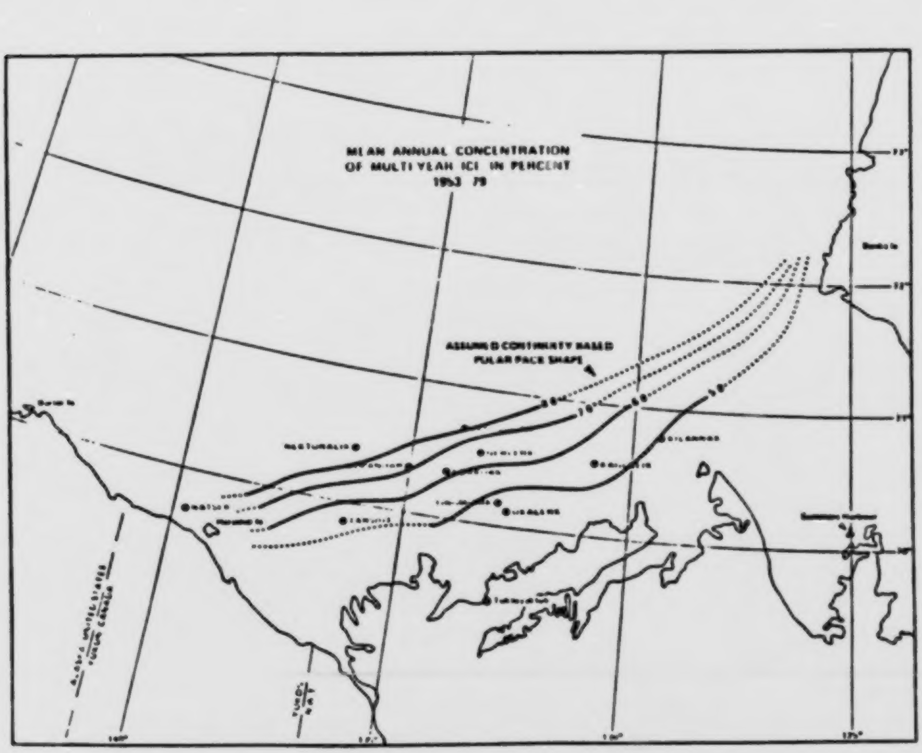
MEAN ANNUAL CONCENTRATION
OF MULTI YEAR ICE IN PERCENT
1953 79
ASSUMED CONTINUITY BASED
POLAR PACK SHAPE
ALASKA UNITED STATES
YUKON CANADA
YUKON
N.W.T.

FIGURE 15

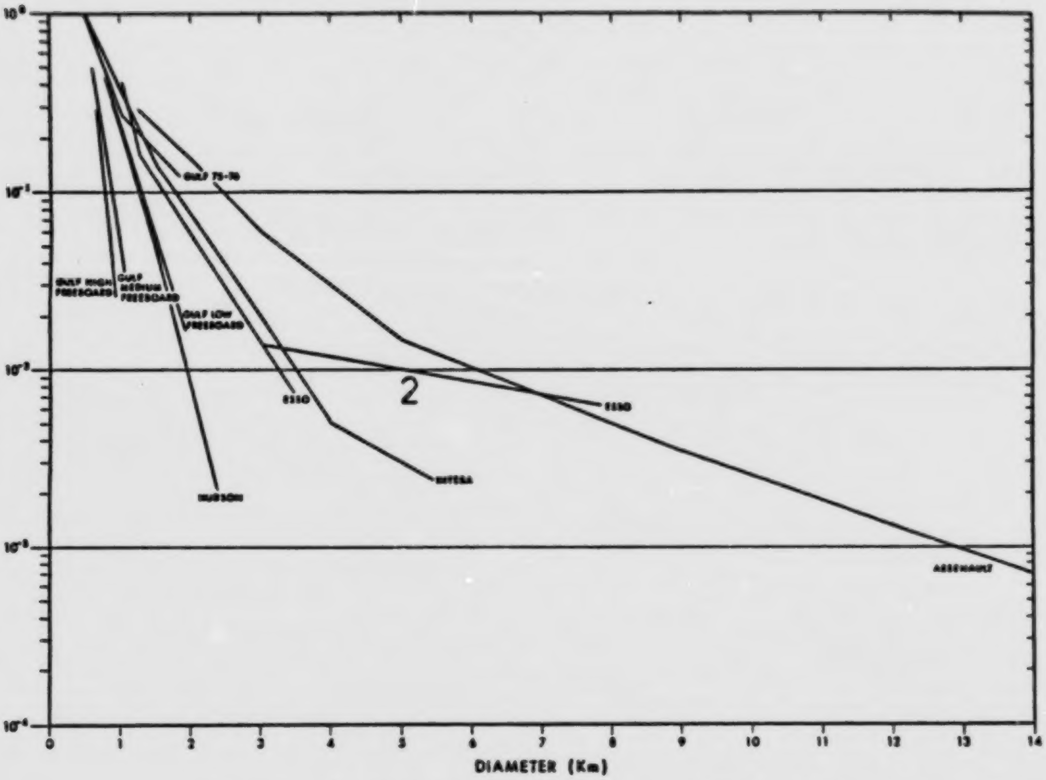

MEASURED MULTI-YEAR FLOE SIZE DISTRIBUTIONS FOR FLOES >500m IN DIAMETER

FIGURE 16

58-218

COMPARISON OF DISTRIBUTIONS FROM THREE DATA SETS ALONG WITH MODIFIED 79 03 17 DATA SET

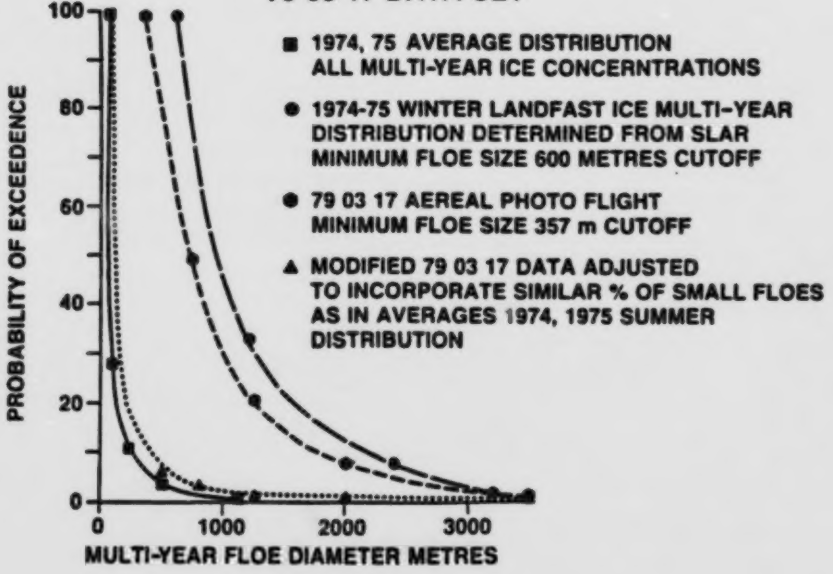

FIGURE 17

THE MEAN THICKNESS OF MULTI YEAR ICE
IN THE BEAUFORT SEA
(AFTER POTOCKY, 1975)

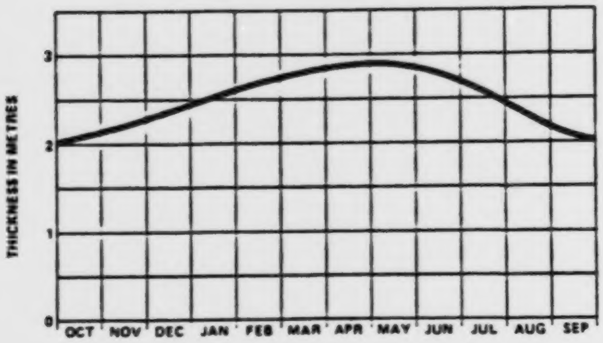

FIGURE 18

THE PROBABILITY OF EXCEEDENCE OF ICE THICKNESS
BY MONTH IN THE BEAUFORT SEA
(AFTER MAYKUT, 1977)

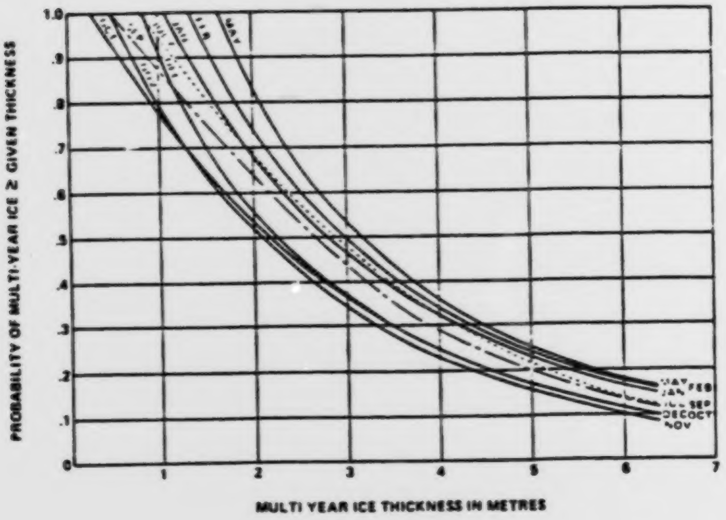

FIGURE 19

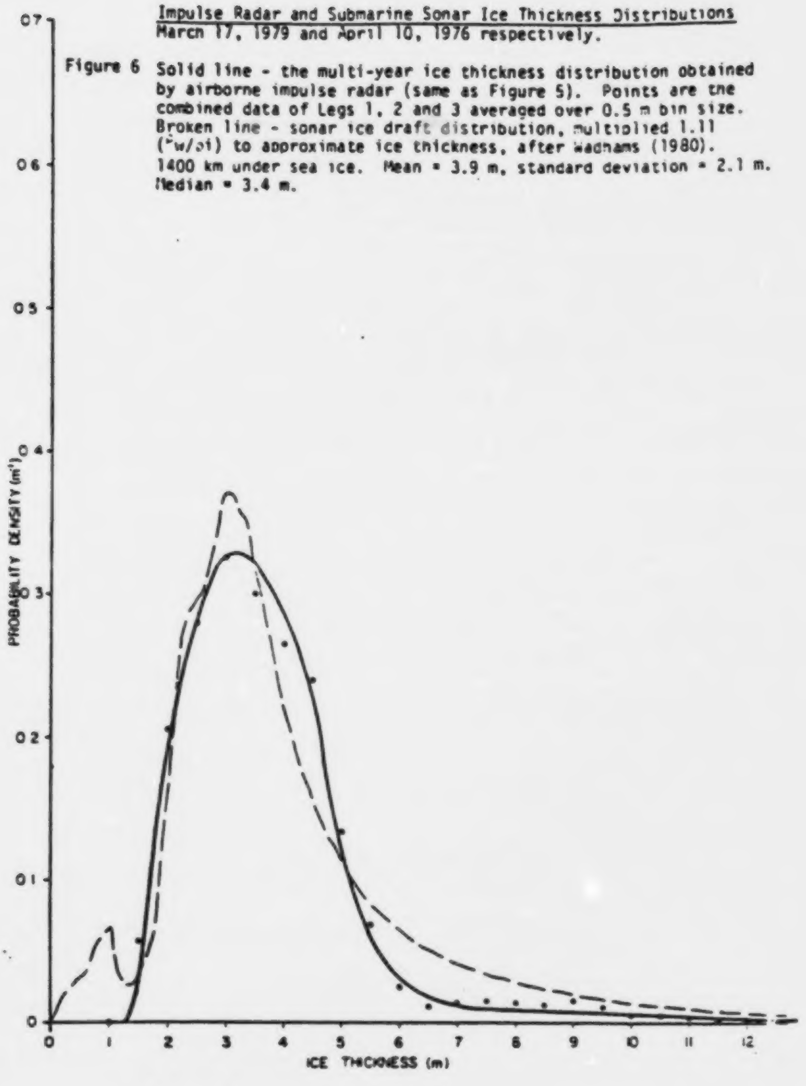

Impulse Radar and Submarine Sonar Ice Thickness Distributions
March 17, 1979 and April 10, 1976 respectively.

Figure 6 Solid line - the multi-year ice thickness distribution obtained by airborne impulse radar (same as Figure 5). Points are the combined data of Legs 1, 2 and 3 averaged over 0.5 m bin size. Broken line - sonar ice draft distribution, multiplied 1.11 (ρ_w/ρ_i) to approximate ice thickness, after Wadhams (1980). 1400 km under sea ice. Mean = 3.9 m, standard deviation = 2.1 m. Median = 3.4 m.

FIGURE 20

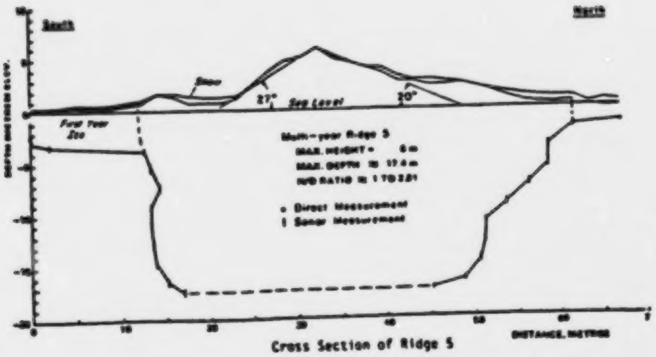
South
North
DEPTH (METRES) ELEV.
Snow
27°
Sea Level
20°
First Year Ice
Multi-year Ridge 5
MAX. HEIGHT = 6 m
MAX. DEPTH ≈ 17.4 m
H/D RATIO ≈ 1 TO 2.91
Direct Measurement
Sonar Measurement
DISTANCE, METRES

Cross Section of Ridge 5

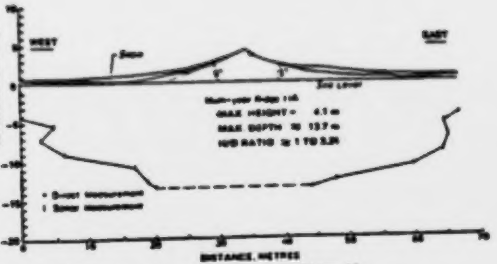
WEST
EAST
DEPTH (METRES) ELEV.
Snow
Sea Level
Multi-year Ridge 11A
MAX. HEIGHT = 4.1 m
MAX. DEPTH ≈ 13.7 m
H/D RATIO ≈ 1 TO 3.34
Direct Measurement
Sonar Measurement
DISTANCE, METRES

Figure 18. Cross Section A of Ridge 11.

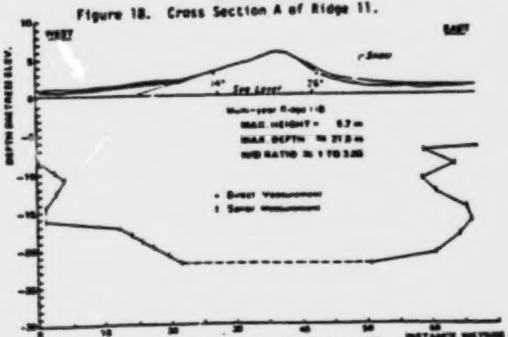
WEST
EAST
DEPTH (METRES) ELEV.
Snow
14°
Sea Level
25°
Multi-year Ridge 11B
MAX. HEIGHT = 5.7 m
MAX. DEPTH ≈ 21.0 m
H/D RATIO ≈ 1 TO 3.69
Direct Measurement
Sonar Measurement
DISTANCE, METRES

Cross Section A of Ridge 11.

FIGURE 21

From Wright et al 1979

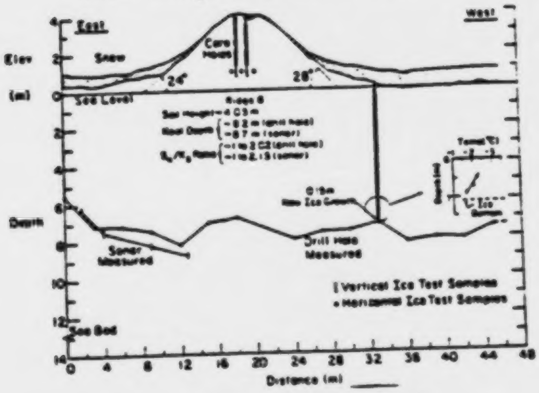
East
West
Elev
(m)
Snow
Core Holes
24°
28°
Sea Level
Ridge 8
Sail Height ~4.03 m
Keel Depth { ~8.2 m (drill hole) / ~8.7 m (sonar)
S_h/K_d Ratio { ~1 to 2.02 (drill hole) / ~1 to 2.15 (sonar)
Temp (°C)
Depth (m)
0.15 m New Ice Growth
Ice Bottom
Depth
Sonar Measured
Drill Hole Measured
Vertical Ice Test Samples
Horizontal Ice Test Samples
Sea Bed
Distance (m)

Cross section of ridge 8.

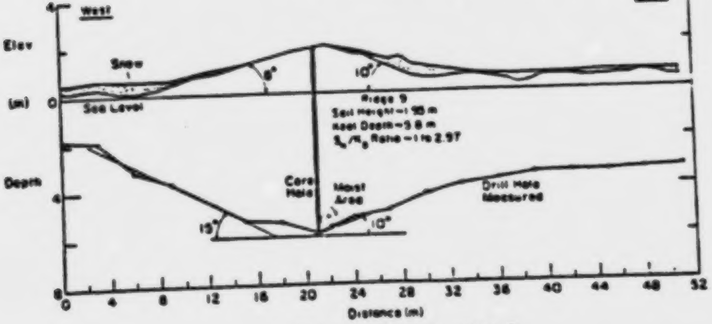
West
East
Elev
(m)
Snow
8°
10°
Sea Level
Ridge 9
Sail Height ~1.95 m
Keel Depth ~5.8 m
S_h/K_d Ratio ~1 to 2.97
Depth
Core Hole
Moist Area
Drill Hole Measured
15°
10°
Distance (m)

Cross section of ridge 9.

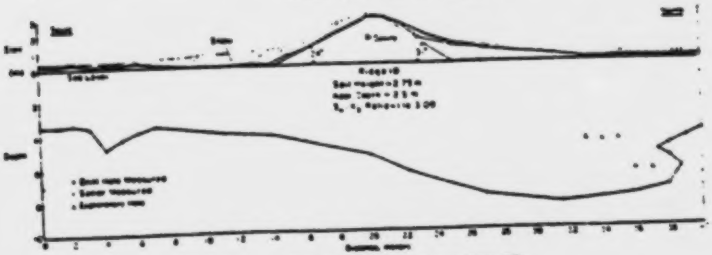
Snow
Sea Level
Ridge 10
Depth
Drill Hole Measured
Sonar Measured
Exploratory Hole

Cross section of ridge 10.

FIGURE 22

From Kovacs 1985

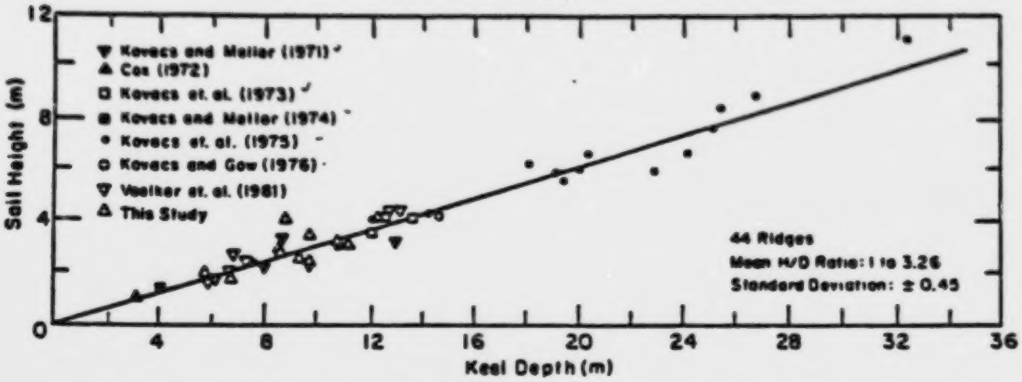

Relationship between multi-year pressure ridge sail height and keel depth.

FIGURE 23

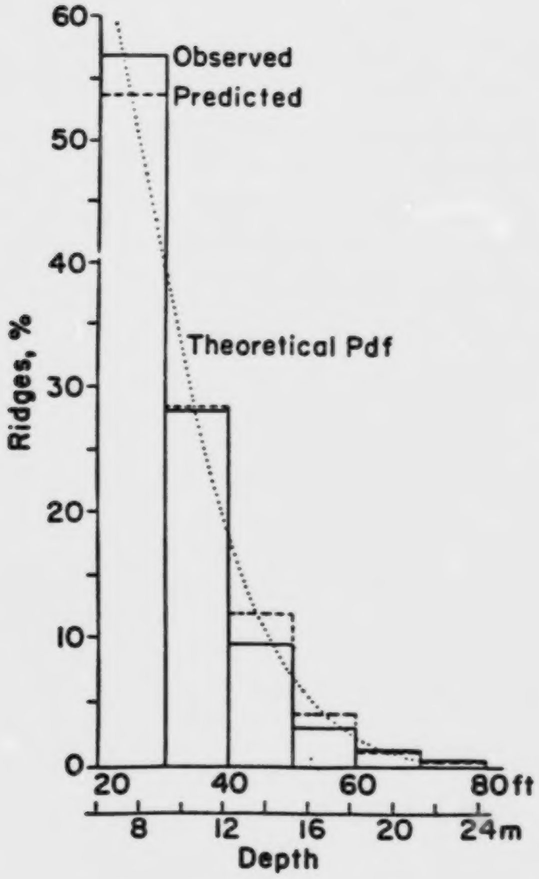

Figure 5. Observed and predicted percentage ridge keel depth distributions. The dotted line is the theoretical probability density function normalized so that its average value over any category gives the predicted percentage for that category, which is also shown. The normalized probability density function (NPdf) for ridge keels deeper than 6.1 m is listed in each subcaption (with h measured in meters). The last category includes all ridges with depths between the category lower limit and ∞.

a) Central Arctic Basin Province, 5702 ridges, NPdf: $P(h)dh = .346 \exp(-.01167h^2)dh$.

FIGURE 24

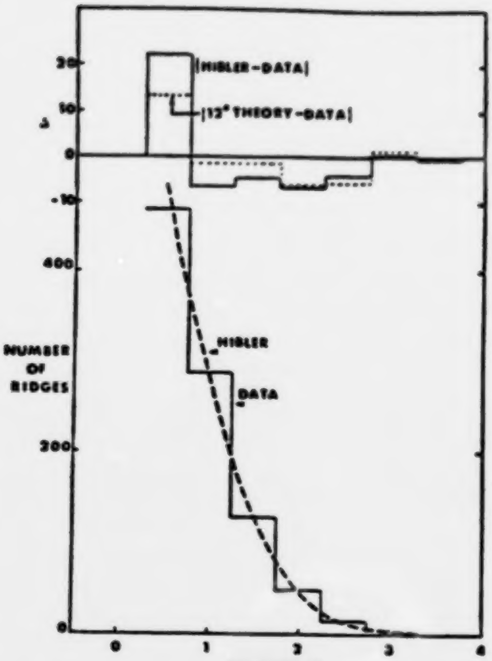

Fig. 5. Argus laser profile data, 1973. Observed ridge heights compared with Hibler theory. The bin size is 0.5 m. and the cutoff is 0.5 m. The upper histogram is the difference Δ between the data and the original and modified Hibler theories.

FIGURE 25

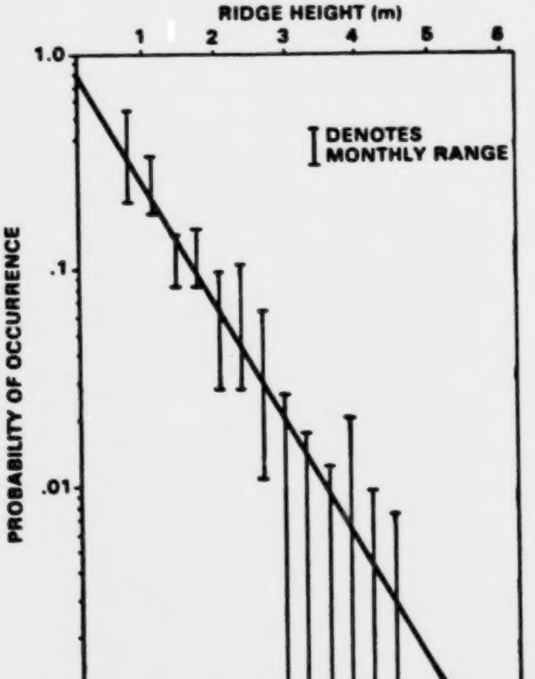

FIGURE 1.1-7 *Probability of finding first year ridges of a given height in the seasonal ice zone in winter (1973-1979) based on Wright and Schwab (1979). The seasonal ice zone can be 50 km wide or greater in some winters. This figure shows that only 1 ridge in 1,000 is likely to be higher than 5 m in the zone.*

FIGURE 26

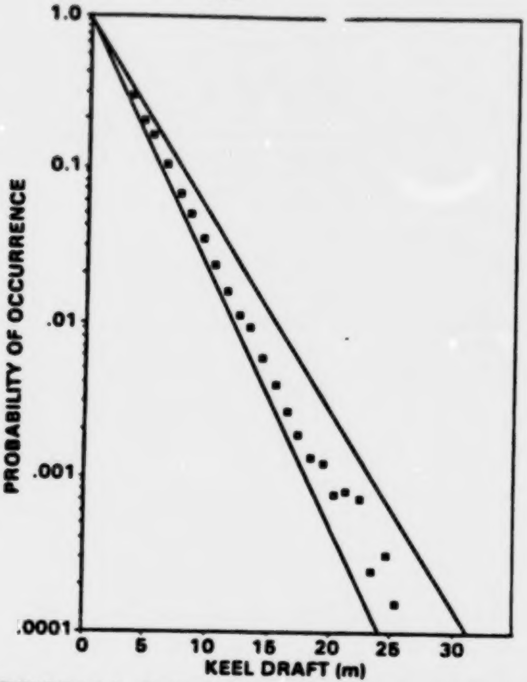

FIGURE 1.1-8 *Probability of finding pressure ridge keels of a given draft during submarine transects in the polar ice zone (based on Wadhams and Horne, 1978). This figure shows that the probability of finding a pressure-ridge keel with a draft of 20 m, along a transect in the polar ice zone, is about 1 in 1,000.*

FIGURE 27

TABLE I

Arctic Ice Thickness Distribution

Region	Polar Ice	Winter Ice	New Ice
Canadian Basin	90%	7%	3%
Canadian Coastal	86%	9%	5%
Beaufort Sea	65%	26%	9%
Chukchi Sea	53%	38%	9%
East Siberian Sea	45%	43%	12%
Eurasian Basin	86%	10%	4%
Barents Sea	59%	23%	18%
Greenland Sea	23%	47%	30%
North Greenland	71%	24%	6%

Based on the published work of *Wittmann and Schule* [1966].

TABLE 2

WEEKLY VARIATION IN MULTI-YEAR ICE CONCENTRATIONS LONGITUDE 131°, SUMMER 1985

MULTI-YEAR ICE CONCENTRATION (IN TENTHS) AT VARIOUS DEPTHS

DATE	200'(60 M)	100'(30 M)	70'(21 M)	50'(15 M)	30'(9 M)
JULY 7	TRACE	TRACE	0	0	0
14	TRACE	TRACE	TRACE	TRACE	0
21	2	0	0	0	0
29	2	0	0	0	0
AUG. 4	3	3	3	3	2
11	1	1	3	3	0
18	4	1	TRACE	0	0
25	8	0	1	0	0
SEPT. 1	4	4	3	0	0
5	3	3	1	0	0
15	8	3	3	1	0
22	0	1	1	1	1
29	9	3	4	2	9
OCT. 6	9	5	5	1	1
13	9	3	3	3	1

TABLE 3

LONGITUDINAL VARIABILITY IN MULTI-YEAR ICE CONCENTRATIONS FOR WEEK OF SEPTEMBER 15, 1985

ICE CONCENTRATIONS IN TENTHS

WATER DEPTH	140°	139°	138°	137°	136°	135°	134°	133°	132°	131°	130°	129°
200'	0	0	0	0	1	3	0	8	8	8	8	8
100'	0	0	0	0	0	3	3	3	3	3	3	3
70'	0	0	0	0	0	0	1	3	0	3	1	1
50'	0	0	0	0	0	0	1	3	1	1	1	1
30'	0	0	0	0	0	0	0	0	0	0	0	0

Table 4.

Maximum Concentration of Multi-Year Ice (in tenths)

At Dome Wellsites 1953-79

Site	53	54	55	56	57	58	59	60	61	62	63	64	65	66	67	68	69	70	71	72	73	74	75	76	77	78	79
	Year																										
Kilannak	10	5	0	10	10	0	0	0	10	0	0	0	0	3	0	0	0	2	0	0	3	3	6	4	0	8	0
Kaglulik	10	5	5	5	9	0	9	0	0	0	0	0	0	3	0	0	2	2	0	0	0	5	6	4	0	2	0
Nerlerk	10	5	5	10	10	0	0	0	0	0	0	0	0	0	2	0	7	2	2	0	2	5	4	4	0	3	0
Ting./Uklk.	10	5	5	5	10	0	0	0	0	0	0	0	0	0	0	0	7	1	0	0	0	5	3	4	0	1	0
Kopanoar	10	5	5	5	10	0	1	0	5	0	0	0	0	0	10	0	8	3	2	0	2	5	7	6	0	1	0
Tarsiut	5	5	5	10	10	0	0	0	3	0	0	0	0	0	0	0	10	8	0	0	2	1	7	6	0	0	0
Natsek	0	5	5	0	10	0	3	0	2	0	0	0	0	0	10	0	8	9	2	0	2	2	8	4	0	0	0

TABLE 5
MULTI-YEAR ICE CONCENTRATIONS BY LONGITUDE AND WATER DEPTH LANDFAST ICE ZONE WINTER 1974-75
(Spedding, 1978)

Longitude	% Multi-year Ice Between Shore & 12m Water Depth	% Multi-year Ice 12m isobath to Ice Edge
128 - 129	0	17
129 - 130	0	20
130 - 131	10	56
131 - 132	7.6	34
132 - 133	1.0	7.0
133 - 134	0	23
134 - 135	10	50
135 - 136	4	47
136 - 137	2	20

TABLE 6

FLOE SIZE DISTRIBUTION BY LONGITUDE FOR LANDFAST ICE ZONE WINTER 1974/75

(Spedding, 1978)

Floe Size Distribution

Longitude	1/4-1/2 mile	1/2-1 mile	1-2 mile	2 mile +
128 - 129	24	3	0	
129 - 130	39	5	2	1
130 - 131	90+	36	8	3
131 - 132	59	17	9	
132 - 133	33	19	2	
133 - 134	31	4	1	2
134 - 135	70+	19	7	4
135 - 136	60+	34	3	1
136 - 137	49+	34	8	2

TABLE 7A
SAIL & KEEL MEASUREMENTS BEAUFORT SEA STUDIES

Source	Ridge No.	Sail Ht(m)	Keel Depth(m)	Sail to Keel Ratio
Kovacs & Mellor 1971 (APOA 17)	1a	3.4	8.5	2.50
	2	2.4	7.9	3.29
	3	5.5	13.4	2.44
	4	3.4	12.9	3.76
Kovacs et al 1973 Section	A	3.9	12.0	3.1
	B	3.9	13.0	3.30
	C	3.4	11.5	3.40
Kovacs and Mellor, 1974		1.5	4.1	2.7
Kovacs, Dickens, Wright, 1975 (APOA 89)	1	10.6	31	2.94
	2	8.0	24.4	3.04
	3	5.8	13.2	3.3
	4	3.9	11.6	2.95
	5	6.0	17.4	2.91
	6	5.7	18.3	3.22
	7	6.4	19.5	3.05
	8	2.9	10.4	3.62
	9	6.3	23.2	3.65
	10	2.3	7.3	3.20
	11A	4.1	13.7	3.31
	11B	5.7	21.9	3.85
Cox 1972		0.9	2.9	3.10
Gladwell (APOA 91)		4.6	11.3	2.46
Kovac 1983	1	2.5	9.3	3.72
	2	3.1	11.1	3.58
	3	2.4	9.6	4.00
	4	3.15	10.8	3.48
	5	1.8	6.7	3.72
	6	3.4	9.8	2.88
	7	4.08	12.2	3.01
	8	4.05	8.7	2.15
	9	1.95	5.8	2.97
	10	2.75	8.5	3.09
	11	3.0	8.5	2.83
Francois 1977		1.9	9.9	1:8.6

TABLE 7 B
SAIL AND KEEL MEASUREMENTS
QUEEN ELIZABETH ISLANDS
Source: Dickins, 1976

Ridge id.	Sail Height (m)	Keel Depth (m)	Keel/Soil Ratio
1	4.8	26	5.4
3	3.7	26	7.0
4	2.6	15.0	5.7
6	4.0	9.5	2.4
9	5.9	27.0	4.6
9	5.9	31.0	9.7
7	2.8	6.5	2.4
8	3.3	12.5	3.8
10	2.6	14.5	5.6
10	2.3	8.0	3.5
10	2.6	13.0	4.9
11	4.5	16.0	3.6
12	5.5	22.5	4.1
12	3.3	14.0	4.2
13	5.3	22.0	4.1
13	6.4	37.0	5.8
13	3.0	32.0	10.7
13	3.7	31.8	8.7
14	5.0	27.0	5.4
14	3.5	22.5	6.4

NRC WORKSHOP ON EXTREME ICE FEATURES

Questions and Discussions Form

AUTHOR L.G. Spedding and M.C. Hill

PAPER: Multi-year Ice Statistics

DISCUSSION BY: B. Wright

DISCUSSION:

I would like to compliment you on an excellent contribution. In terms of the discrepancies in the multi-year floe size distributions that you have outlined, you have pointed out that the method of analysis (e.g., bin size) has a significant effect. Clearly, the definition of "a multi-year floe" also has a significant effect and is very much related to the resolution of the imagery comprising the data base (e.g., landsat imagery vs SLAR vs high quality aerial photography. In our experience, large "multi-year floes" in the order of 5-10 km in extent are almost invariably a matrix of first-year, second-year and multi-year ice. We refer to them as conglomerate floes. Often during ice/structure interactions these floes fail or fracture along "thinner ice lines (first-year ice)" and they are fairly easy to "ice manage" with icebreakers in open water or thin ice environments. Could you comment on conglomerate floes as opposed to very large multi-year floes?

AUTHOR'S REPLY:

There is no doubt that the large floes with diameters in the order of tens of kilometers, observed in satellite and SLAR imagery are conglomerate floes, i.e., multi-year floes cemented together by first year ice. However, at the present time our knowledge of the ice composition and structural integrity of these floes is limited.

It is interesting to note that the Gulf, Hudson et al., Esso and Intera studies indicate multi-year floe maximum diameter ranging between 2.5 - 5.5 km. Possibly this is an indication of the maximum diameter discrete multi-floes can be expected to attain in the southern Beaufort Sea. On the other hand, observations indicate the large conglomerate floes are structurally strong enough to survive considerable (months) periods in coastal waters. Regarding the development of structural interaction and loading scenarios for these conglomerate floes, we need to know more about their structural integrity and potential fracture patterns.

DISCUSSION BY: W.M. Sackinger

DISCUSSION:

An important factor in multi-year ridge mechanical properties on a large-scale is the thickness of the consolidated ice zone in the core of the ridge. Data from the early 1980's suggests that a maximum asymptotic value of 12 metres thickness may be applicable for such multi-year ridge consolidated zones, regardless of the initial keel depth which consists of unconsolidated zones, A plausible reason for this is found by considering summer melting processes in the sail of large annual ridges. First, brine drainage occurs. Then, fresh meltwater is generated which drains into the ridge core where it encounters a zero-degree isotherm and freezes. The freshwater will also pool on top of the interstitial seawater within the ridge, which is as -1.8°C and which permits freezing of a nearly-freshwater core layer of ice between the blocks, thus tending to seal off the interstices between blocks. Ultimately this leads to a broad, consolidated zone in the ridge core, of limited thickness, and the limited amount of surface meltwater in successive years will escape laterally on the surface to adjacent meltponds on top of the ice surface. Subsequent movement and grounding of the consolidated ice ridge would probably remove the remaining loosely-consolidated ice blocks from the ice ridge keel. Thus deep-water old ridges may be displaying unconsolidated deep keels but old ridges which have grounded would not have unconsolidated deep keels. In either case, there should be an asymptotic value for consolidated zone thickness, for this type of ice ridges. Is this explanation consistent with your experience, or can you cite exceptions.

AUTHOR'S REPLY:

At this point in time I do not think we have enough evidence to confirm or disapprove your theory. Examination of published profiles indicates examples of ridges in which consolidation of keels is indicated to depths greater than as well as for other ridges with unconsolidated blocks at less than 12 m.

One problem to date is limited number of ridges profiled, as well as variability in quality of profile information. The ridges profiled to date have also occurred in widely different geographical areas. Variation may be due to regional geographical differences, ridge formation and melt histories. Quite often we even lack descriptions on estimates of type of ridge profiled, i.e., second- or multi-year.

MECHANICAL PROPERTIES OF MULTI-YEAR SEA ICE

J.A. Richter-Menge* and G.F.N. Cox*

SUMMARY

For considerable time, little was known about the mechanical properties of multi-year (≥ second-year) sea ice. This was rather surprising, as multi-year ridges and floes are considered to be "design" ice features for drilling structures in exposed areas of the Beaufort and Chukchi Seas. Five years ago, with combined support from the petroleum industry and the Minerals Management Service (U.S. Department of the Interior), a major effort was initiated at the Cold Regions Research and Engineering Laboratory (CRREL) to determine the mechanical properties and structure of ice samples from multi-year pressure ridges in the Alaska Beaufort Sea. Uniaxial compression tests were performed on both vertical and horizontal ridge samples (Cox et al. 1984 and 1985). A statistical analysis of the strength of vertical ice samples from ten of the ridges, between cores located side by side on the same ridge, and between samples from the same core, indicated that the main factor contributing to the variance in ice strength of a data set was the variation in ice strength within each core. In effect, the strength of vertical ice samples from different ridges was not statistically different (Weeks, 1985). This was not surprising as the internal structure in each ridge was highly variable (Richter-Menge et al. 1986 and 1987a). However, in most of the sampled ridges, many of the individual ice blocks were oriented in a near horizontal position (Richter-

---

*U.S. Army Cold Regions Research and Engineering Laboratory, Hanover, New Hampshire.

Menge and Cox, 1985a). Consequently, vertical ice samples from the ridge generally gave a higher mean comressive strength than horizontal ice samples taken from near the same location (Richter-Menge and Cox, 1985b). Uniaxial tension tests and confined compression tests ($\sigma_1 > \sigma_2 = \sigma_3$) were also done during the program. The tensile strength of vertical ridge samples showed little variation with either temperature or strain rate (Cox and Richter-Menge, 1985). The confined compressive strength data indicated that, for confinement ratios (σ_2/σ_1) up to 0.50, there was little variation in the deviatric yield stress ($\sigma_1 - \sigma_2$) at a given strain rate and temperature (Cox and Richter-Menge, 1986).

A few multi-year floe samples were also tested during this program, however, more extensive testing of multi-year floe ice has been done in Canada (Frederking and Timco, 1981 and Sinha, 1983 and 1985). Like undeformed first-year sea ice, the multi-year floe ice is predominately columnar. The multi-year ice has undergone desalination however, leaving many air-filled voids throughout the material. It is still unclear what the effect of desalination has on the mechanical behavior of this ice.

Available literature on the in situ testing of multi-year is scarce. The most popular tests involve the use of a hydraulic press placed down a hole or excavated cavity (e.g. borehole jack). Sinha (1986) recently reviewed the use of the borehole jack to measure the in situ strength of first-year, multi-year ridge, and multi-year floe ice. Based on the results of Sinha's work it appears that this test technique is insensitive to variations in ice type. It's usefulness therefore, remains in question.

This paper will focus on the results of the multi-year ridge ice sample tests. The authors do not feel that the available data on multi-year floe ice is sufficient to describe the mechanical properties of this ice type. We find ourselves in a similar situation with respect to the in situ testing of multi-year floe and ridge ice.

INTRODUCTION

Multi-year pressure ridges are thick accumulations of broken ice blocks that have survived at least one melt season. Surface melting and subsequent freezing of the water in the ridge cavities produce a massive ice feature with few or no voids. Multi-year pressure ridges in excess of 30 meters thick have been observed off the Beaufort Sea coast (Kovacs 1976).

Data on the mechanical properties of multi-year sea ice are necessary for developing arctic structures and vessels that must be designed to withstand the impact of a multi-year pressure. Recently we completed a study that involved testing over 500 multi-year ridge ice samples. This study was designed to help us understand the structure and mechanical properties of the ice. The program consisted of two phases. The first phase included collecting samples of 10 different multi-year pressure ridges in the southern Beaufort Sea, developing a variety of test techniques, and performing 282 uniaxial compression, tension and confined compression tests on vertically cored samples (Cox et al 1984 and Mellor et al 1984). The majority of the tests were uniaxial constant-strain-rate compression tests. The results of the Phase I tests indicated that there was no significant difference in the mean compressive strength between samples taken from different pressure ridges (Weeks 1985). The main factor contributing to variations in the strength from test to test was associated with the extreme local variability of ice structure within a ridge (Richter-Menge et al 1986 and 1987).

The second phase of the program also included a field sampling program in the Alaskan Beaufort Sea (Cox et al 1985). Vertically cored ice samples were collected from four different multi-year ridges. Matched horizontal and vertical pairs were also collected from one ridge to investigate the effect of sample orientation on the mean compressive strength. A total of 188 tests were completed. In Phase II the tests were equally divided among unconfined constant-strain-rate compression and tension tests and confined compression tests.

This paper briefly describes the sample preparation and test techniques developed in the program. Data on the compressive, tensile and confined compressive strength of the multi-year ridge ice samples will also be summarized. Additional results on the initial tangent modulus, residual strength and failure strain are given in Cox et al. (1984, 1985).

ICE DESCRIPTION

Thin sections of each ice sample and two continuous vertical multi-year ridge cores revealed that the ice structure in a multi-year pressure ridge is highly variable (Richter-Menge and Cox 1985) . This variation is a result of the ridge building and consolidation processes that take place during the formation of a multi-year ridge. In general the ice structure in a multi-year ridge sample can be classified according to one of three major ice texture categories: granular, columnar, or a mixture of columnar and granular. The number of samples of a given ice structure varied from one test condition to another. It is important to note this variation since work on multi-year ridge samples has shown that the mean compressive strength is significantly influenced by the percentage of columnar test specimens and the orientation of the ice crystals in these samples

(Richter-Menge et al 1986 and 1987). Further analysis of the crystal orientation of columnar samples within the ridge has also shown that, in the ridges we sampled, most of the columnar blocks were lying in a nearly horizontal position; in other words, with the direction of crystal elongation nearly vertical (Richter-Menge and Cox 1985a). A frequency histogram of the number of columnar ridge samples at a given σ:z angle (the angle between the direction of crystal elongation and the vertical) illustrates this tendency (Fig. 1).

The average salinity and density of the ice samples are presented in Table 1. In general, the ice collected in the first phase of the program had a slightly higher density than the ice collected in the second phase. The average salinity of the samples collected during the first and second phases were similar.

SAMPLE PREPARATION AND TEST TECHNIQUES

Dumbbell specimens were prepared from 10.8-cm-diameter ice cores. Samples were first rough-cut on a bandsaw, and the ends were milled square on a milling machine to produce a 25.4-cm-long test specimen. Synthane end caps were then bonded to the sample using fresh water to freeze them to the milled end planes. The endcapped samples were turned on a lathe to a dumbbell shape. Compression samples had a neck diameter of 10.2 cm, and the tension samples had a neck diameter of 8.9 cm. The form tools used to prepare both the dumbbelled compression and tension samples had a radius of curvature equal to twice the diameter of the finished neck. This radius was chosen to minimize stress concentrations near the sample end planes. Every effort was made to produce properly sized, precision-machined test samples using recommended methods (Hawkes and Mellor 1970 and Schwarz et al 1981).

All of the tests -- compression, tension and confined compression -- were performed on a closed-loop electrohydraulic testing machine. The machine had two actuators with capacities of 1.1 and 0.11 MN and a fast-response, high-flow-rate servo-valve.The load frame of the machine had a capacity of 2.2 MN. Test temperatures were controlled within 0.5°C by placing the sample in an environmental chamber mounted between the columns of the testing machine. The lower machine platen was also refrigerated to eliminate any thermal gradient problems. Load and sample strain data were recorded on an XY plotter, a strip chart, and an FM magnetic tape recorder.

Strain rates in the unconfined uniaxial compression and tension tests were controlled by monitoring the full sample strain with an extensometer, which was attached to the synthane end caps bonded to the test specimen (Fig. 2). Strains on the necks of the specimens were also monitored with a pair of direct current displacement transducers (DCDTs) to provide accurate strain, strain rate and modulus data. The unconfined tests were programmed to continue to 5% full sample strain to examine post-yield behavior and the residual strength of the ice. Since this resulted in considerable deformation of the test specimen, strain rates could not be controlled by the transducers mounted on the ice.

Confined compression tests ($\sigma_1 > \sigma_2 = \sigma_3$) were performed using the triaxial cell shown schematically in Figure 3. The cell was designed so that the confining radial pressure ramped in constant proportion to the applied axial stress (σ_2/σ_1 = constant). For a right circular cylindrical specimen, the ratio of the confining pressure to the axial stress is determined by the ratio of the diameter of the piston entering the cell (10.8 cm) to the diameter of the piston in the upper cylinder. Two ratios of confining pressure to axial stress were used, 0.25 and 0.50. The larger ratio was obtained by placing a reduction collar in the upper piston and using a correspondingly smaller diameter piston. Hydraulic fluid was used as the confining medium. A latex membrane was placed around the test specimen to prevent hydraulic fluid from permeating into the sample void spaces. The strain rate in the confined compression tests was controlled by the averaged output of two extensometers mounted on the shaft going into the triaxial cell (Fig. 4).

Details of the sample preparation and test techniques are given in Mellor et al (1984).

RESULTS AND DISCUSSION

Constant-Strain-Rate Uniaxial Compression Tests

A total of 222 constant-strain-rate uniaxial compression tests were performed on vertically cored multi-year ridge ice samples in the first phase of the program. The tests in Phase I were conducted at two strain rates (10^{-5} and 10^{-3} s^{-1}) and two temperatures (-20° and -5°C). In Phase II, 69 uniaxial compression tests were performed. These samples were tested at the same temperature but at different strain rates (10^{-4} and 10^{-2} s^{-1}) to compliment the tests performed in Phase I. Unlike Phase I, the Phase II unconfined compression tests at a strain rate of 10^{-4} s^{-1} were performed on both horizontal and vertical samples to assess the effect of sample orientation on ice strength. A summary of the compressive strength data for both phases of the project is given in Table 2. The mean compressive strength of the ice is plotted against strain rate in Figure 5.

At a given temperature and strain rate, the compressive strength data show considerable scatter. These large variations in strength can be explained by large variations in the ice structure and porosity (Richter-Menge et al 1986 and 1987). The strength of each specimen depends not only on the type of ice present in the specimen, which is highly variable from sample to sample, but also on the ice grain size and crystal orientation. Strength variations are further increased by variations in the ice porosity.

The transition from predominantly ductile behavior to brittle occurred between the strain rates of 10^{-3} and 10^{-2} at both test temperatures. Based on our understanding of the variation of ice strength with strain rate, we would expect a power law relationship between ice strength and strain rate in the ductile range (Mellor 1983). On log-log paper, strength versus strain rate would plot as a straight line. The combined average test results of Phases I and II at -5°C do not show this tendency. The average strength of the 10^{-4} s^{-1} is lower than anticipated. However, at -20°C the 10^{-4} s^{-1} Phase II test average is in reasonable agreement with the 10^{-5} s^{-1} averages obtained in Phase I.

Since the strength of sea ice decreases with increasing porosity, it appears that the above observations can be explained in terms of the average ice porosity of the samples tested at each strain rate and temperature. In Table 2 mean porosities are given for the samples tested at each test condition. At -5°C the 10^{-4} s^{-1} tests have a much higher porosity than the tests conducted at 10^{-5} and 10^{-3} s^{-1}. At -20°C the mean porosities of the 10^{-5}, 10^{-4} and 10^{-3} s^{-1} tests are similar, and the average strength values do show a power law relationship.

In addition to the variation in average ice porosity, we also note that at the 10^{-4} s^{-1} test condition, the mean compressive strength was obtained using both horizontal and vertical samples. At a given test temperature the mean compressive strength of the 10^{-4} s^{-1} horizontal samples alone is lower than the strength of the vertical samples (Table 2). The variation is a result of the preferred orientation of the columnar ice blocks within the ridge, which we discussed in the ice description section. Since the columnar blocks tend to lie in a near horizontal position, the vertically cored columnar ridge samples are generally load parallel to the elongated crystal axis. Horizontal samples are loaded normal to the direction of crystal elongation. Results from tests on first-year sea ice samples indicate that the hard fail direction in columnar sea ice occurs when loads are applied parallel to the direction of elongation of the crystals (Peyton 1966 and Wang 1979). Consequently, the overall mean compressive strength of vertically cored multi-year ridge samples will generally be higher than the mean compressive strength of horizontal ridge samples. The variation will depend on the number of columnar ice samples and their exact crystal orientation with respect to the loading direction. A high percentage of vertical columnar ice samples will be reflected in a relatively high mean compressive strength. The effect of sample orientation results in a lower mean compressive strength when the vertical and horizontal test data at 10^{-4} s^{-1} are combined as done in Figure 5.

In both the -5° and -20°C tests done at a strain rate of 10^{-2} s^{-1} the ice failed in a brittle manner. It would appear from Figure 5 that there is an apparent decrease in ice strength relative to the tests conducted at 10^{-3} s^{-1}. We attribute this decrease in strength to the much larger porosity of the 10^{-2} s^{-1} samples and to variations in the overall structural composition between test groups. There were very few columnar ice samples in the 10^{-2} s^{-1} test groups. We would anticipate a leveling off in strength between 10^{-3} and 10^{-2} s^{-1} based on work by Richter-Menge et al (1987) on first-year sea ice and by Blair (1986) on transversely isotropic columnar saline ice grown in the laboratory.

Constant-Strain-Rate Uniaxial Tension Tests

Thirty-six constant-strain-rate tension tests were performed on vertically oriented multi-year pressure ridge samples during the second phase of the program. The tests were done at two strain rates (10^{-5} and 10^{-3} s^{-1}) and two temperatures (-20° and -5°C). Nine tests were done at each test condition. A summary of the tensile strength data is given in Table 3. Strength data are plotted against strain rate in Figure 6.

In general, the mean tensile strength shows no significant variation with strain rate or temperature. This behavior is consistent with data on the tensile strength of freshwater polycrystalline ice summarized by Mellor (1983). At strain rates greater than 10^{-5} s^{-1}, the tensile strength of freshwater polycrystalline ice shows little or no variation with strain rate, and from -5° to -20°C, the strength only shows a very small increase. In contrast the results from Dykins' (1970) uniaxial tensile tests on first-year sea ice show a strong temperature dependency. However, this large strength variation is not due to changes in temperature of the pure ice matrix but rather a change in the ice brine volume or porosity. Since the salinity of the multi-year test specimens is very low, the brine porosity and strength of the ice show little variation with temperature.

The effect of ice crystal structure was also evident in the tensile tests on multi-year ridge samples. While the strength of the sample was not greatly influenced by the structural composition of the sample, the location of the failure plane was dependent on structural variability. For all test conditions, there was a definite tendency for the ice to fail in the part of the specimen containing the coarsest grains. This tendency has been observed in tensile tests on freshwater polycrystalline ice (Hawkes and Mellor 1972, Haynes 1978, Currier and Schulson 1982, and Schulson et al 1984). There were exceptions, however. For example, in a few tests containing brecciated ice (ice composed of columnar fragments in a granular matrix), failure occurred in the finer-grained granular ice when the columnar fragments were oriented with the direction of crystal elongation parallel to the load. In some ice samples containing both fine and coarse grains, failure was not associated with grain size. Instead, flaws in the specimen such as large voids and structure discontinuities controlled the fracture location (Fig. 7). Low strength values were usually associated with large voids and cavities in the specimen.

Confined Compression Constant-Strain-Rate Tests

A total of 55 confined compression or conventional triaxial tests ($\sigma_1 > \sigma_2 = \sigma_3$) were performed on multi-year pressure ridge samples at different test temperatures, strain rates and confining pressures during Phase II of the program. The number of tests at each test condition is summarized along with the confined compressive strength data in Table 4. The mean confined compressive strength of the ice, σ_1, for each test condition is plotted against the confining pressure ($\sigma_2=\sigma_3$) at failure in Figure 8. Mean uniaxial (unconfined) compressive strength data from the first phase of the test program are included for comparison. In making comparisons between the unconfined and confined compressive strength data, it should again be noted that the Phase I ridge samples generally had a lower porosity. There was also a tendency for the Phase II confined compression test groups to have a lower percentage of columnar ice. Both of these factors act to reduce the mean strengths.

The confined compressive strength increases with increasing temperature, increasing strain rate, and increasing confining pressure. Due to variability of the ice structure between samples, the data show considerable scatter. At both 10^{-5} s^{-1} and 10^{-3} s^{-1} the yield surface appears to parallel the hydrostat ($\sigma_2/\sigma_1 = 1$) suggesting that failure of the ridge ice samples at these strain rates may be approximately described by Tresca or von Mises yield criteria. Tests on first-year sea ice samples at the same strain rates indicate that at an increased confining ratio of 0.75, the deviatoric stress ($\sigma_1-\sigma_2$) at peak load begins to decrease (Richter-Menge 1987). Similar observations have been made by Jones (1982), who investigated the confined compressive strength of freshwater polycrystalline ice. We would anticipate the same to be true of multi-year ice. This behavior is more accurately described by a Smith yeild criterion (Hausler 1981).

CONCLUSIONS

The combined test results of this extensive test program provide a foundation for developing constitutive laws and failure criteria for multi-year pressure ridges. These results are incomplete, however, without a thorough examination of the influence of ice structure on the test results. Structure analyses of the multi-year ridge ice samples have shown that the structure has a profound effect on the mechanical properties of the ice (Richter-Menge et al 1986 and 1987). This must be considered when data sets are combined in the attempt to establish characteristic behavior.

It does appear that, in multi-year pressure ridges containing a large proportion of columnar sheet ice blocks, the horizontal ice strength may be significantly less than the vertical ice strength. This is because there may be preference for ice blocks to lie in a nearly horizontal position during ridge formation. The results of this study and those of earlier investigators (Peyton 1966 and Wang 1979) have shown that horizontal sheet ice samples are significantly weaker than vertical sheet ice samples. More field studies of the internal structure of first-year and multi-year pressure ridges are needed to capitalize on this finding. Using ice strength data from vertically oriented ridge specimens may be conservative in horizontal ridge loading problems.

In general the compressive strength of multi-year ridge ice samples increases significantly with an increase in strain rate from 10^{-5} to 10^{-3} s^{-1}. Beyond 10^{-3} s^{-1}, where the ice is failing in a brittle manner, the compressive strength appears to level off. At a given strain rate, there is an increase in the compressive strength with a decrease in temperature and a decrease in porosity. An increase in the confining pressure surrounding the ice sample also results in an increase in strength.

The mean tensile strength of the multi-year ridge samples shows little variation with strain rate or temperature. Variations in strength are generally the result of the highly variable ice structure. There is a tendency for the tensile ice strength to decrease with increasing porosity.

Finally we note that one important addition to this series of test data still remains to be completed. This involves an investigation of the mechanical properties of multi-year ridge ice at high temperatures (-2°C). Information in this region of temperatures is needed to define the mechanical properties of pressure ridge keels.

ACKNOWLEDGEMENTS

The mechanical properties of multi-year pressure ridge ice program study was sponsored by Shell Development Company and the Minerals Management Service of the Department of the Interior with support from Amoco Production Company, Arco Oil and Gas Company, Chevron Oil Field Research Company, Exxon Production Research Company, Gulf Research and Development Company, Mitsui Engineering and Shipbuilding Company, the National Science Foundation, Sohio Petroleum Company, Texaco, the U.S. Department of Energy and the U.S. Coast Guard.

REFERENCES

Blair, S.C., 1986. Confined compressive strength of saline ice at intermediate strain rates. In Proceedings of the Second Ice Penetration Technology Workshop, 16-19 June 1986, Monterey, California.

Cox, G.F.N. and J.A. Richter-Menge, 1986. Confined compressive strength of multi-year pressure ridge sea ice samples. OMAE '86, Vol. 4, pp. 365-373.

Cox, G.F.N. and J.A. Richter-Menge, 1985. Tensile strength of multi-year pressure ridge sea ice samples. ASME Journal of Energy Resources Technology, Vol. 107, No. 3, pp. 375-380.

Cox, G.F.N., J.A. Richter-Menge, W.F. Weeks, M. Mellor, H.W. Bosworth, G. Durell and N. Perron, 1985. Mechanical properties of multi-year sea ice, Phase II: Test results. U.S. Army Cold Regions Research and Engineering Laboratory, CRREL Report 85-16.

Cox, G.F.N., J.A. Richter-Menge, W.F. Weeks, M. Mellor and H.W. Bosworth, 1984. Mechanical properties of multi-year sea ice, Phase I: Test results. U.S. Army Cold Regions Research and Engineering Laboratory, CRREL Report 84-9.

Currier, J.H. and E.M. Schulson, 1982. The tensile strength of ice as a function of grain size. Acta Metallurgica, vol. 30, pp. 1511-1514.

Dykins, J.E., 1970. Ice engineering: Tensile properties of sea ice grown in a confined system. Naval Civil Engineering Laboratory, Technical Report R689.

Frederking, R.M.W. and G.W. Timco, 1981. Mid-winter mechanical properties of ice in the southern Beaufort Sea. POAC '81, Vol. 1, pp. 225-234.

Hawkes, I. and M. Mellor, 1972. Deformation and fracture of ice under uniaxial stress. Journal of Glaciology, vol. 11, no. 61, pp. 103-131.

Hawkes, I. and M. Mellor, 1970. Uniaxial testing in rock mechanics laboratories. Engineering Geology, 1970, vol. 4, pp. 177-285.

Haynes, F.D., 1978. Effect of temperature on the strength of snow ice. U.S. Army Cold Regions Research and Engineering Laboratory, CRREL Report 78-27.

Jones, S.J., 1982. The confined compressive strength of polycrystalline ice. Journal of Glaciology, vol. 28, no. 98, pp. 171-178.

Kovacs, A., 1976. Grounded ice in the fast ice zone along the Beaufort Sea coast of Alaska. U.S. Army Cold Regions Research and Engineering Laboratory, CRREL Report 76-32.

Mellor, M., G.F.N. Cox and H.W. Bosworth, 1984. Mechanical properties of multi-year sea ice: Testing techniques. U.S. Army Cold Regions Research and Engineering Laboratory, CRREL Report 84-8.

Mellor, M., 1983. Mechanical behavior of sea ice. U.S. Army Cold Regions Research and Engineering Laboratory, Monograph 83-1.

Peyton, H.R., 1966. Sea ice strength. Geophysical Institute, University of Alaska, Report UAG-182.

Richter-Menge, J.A. and N.M. Perron, 1987. The mechanical properties of multi-year sea ice, Phase II: Ice structure analysis. U.S. Army Cold Regions Research and Engineering Laboratory. CRREL Report.

Richter-Menge, J.A., 1987. Confined compressive strength of horizontal first-year sea ice samples. Accepted for presentation at the 6th International Symposium on Offshore Mechanics and Arctic Engineering, Houston, 1-5 March 1987.

Richter-Menge, J.A., G.F.N. Cox and N. Perron, 1986. The mechanical properties of multi-year sea ice, Phase I: Ice structure analysis. U.S. Army Cold Regions Research and Engineering Laboratory, CRREL Report.

Richter-Menge, J.A. and G.F.N. Cox, 1985a. Structure, salinity, and density of multi-year sea ice pressure ridges. ASME Journal of Energy Resources Technology, Vol. 107 (No. 4), pp. 493-497.

Richter-Menge, J.A. and G.F.N. Cox, 1985b. The effect of sample orientation on the compressive strength of multi-year pressure ridge ice samples. Proceedings, ASCE Arctic '85 Conference, San Francisco, CA., 1985.

Schulson, E.M., P.N. Lim and R.E. Lee, 1984. A brittle to ductile transition in ice under tension. Philosophical Magazine, vol. 49, pp. 353-363.

Schwarz, J., R. Frederking, V. Gavrillo, I.G. Petrov, K.I. Hirayama, M. Mellor, P. Tryde and K.D. Vaudrey, 1981. Standardized testing methods for measuring mechanical properties of ice. Cold Regions Science and Technology, vol. 4, pp. 245-253.

Sinha, N.K., 1986. The borehole jack, is it a useful arctic tool? OMAE '86, Vol. 4, pp. 328-335.

Sinha, N.K., 1985. Confined strength and deformation of second-year columnar-grained sea ice in Mould Bay. OMAE '85, Vol. 2, pp. 209-218.

Sinha, N.K., 1984. Uniaxial compressive strength of first-year and multi-year sea ice. Canadian Journal of Civil Engineering, Vol. 11, No. 1, pp. 82-91.

Wang, Y.S., 1979. Crystallographic studies and strength tests of field ice in the Alaskan Beaufort Sea. Proceedings, Fifth International Conference on Port and Ocean Engineering under Arctic Conditions, Trondheim, Norway, 1979, vol. 1, pp. 651-665.

Weeks, W.F., 1984. Variation of ice strength within and between multi-year pressure ridges in the Beaufort Sea. ASME Journal of Energy Resource Technology, Vol. 107, (No. 2), pp. 167-172.

Table 1. Average salinity and density (-20°C) of ice samples obtained from ridges A, B and C during Phase II and all ridges from Phase I.

		Phase II			
	Phase I	Ridge A	Ridge B	Ridge C	Three ridges
Salinity ($^{o}/oo$)	1.26±0.82	0.38±0.49	1.29±0.87	2.29±1.19	1.34±1.18
Density (Mg/m^3)	0.891±0.026	0.834±0.046	0.870±0.035	0.888±0.024	0.865±0.042

Table 2. Summary of compressive strength data for Phases I and II.

		Maximum		Minimum		Mean		Mean porosity (o/oo)	Number of samples
		(MPa)	(lbf/in.^{2})	(MPa)	(lbf/in.^{2})	(MPa)	(lbf/in.^{2})		
					-5°C (23°F)				
10^{-5} s^{-1}	V*	7.52	1090	0.47	68	2.34±1.08	340±157	44	71
10^{-4} s^{-1}	V	5.52	800	1.87	271	3.07±1.23	445±179	69	9
10^{-4} s^{-1}	H	3.87	561	1.21	175	2.35±0.74	341±108	78	10
10^{-4} s^{-1}	all	5.52	800	1.21	175	2.69±1.04	390±151	73	19
10^{-3} s^{-1}	V	10.90	1580	2.39	346	6.06±1.63	879±237	46	69
10^{-2} s^{-1}	V	6.42	931	2.69	390	4.67±1.17	677±169	68	9
					-20°C (-4°F)				
10^{-5} s^{-1}	V	4.26	617	1.17	170	2.79±0.69	404±100	36	41
10^{-4} s^{-1}	V	12.73	1846	3.34	485	6.17±3.10	894±450	50	13
10^{-4} s^{-1}	H	7.02	1018	1.68	243	3.74±1.67	543±242	33	12
10^{-4} s^{-1}	all	12.73	1846	1.68	243	5.00±2.70	725±392	42	25
10^{-3} s^{-1}	V	12.68	1838	7.03	1020	9.63±1.39	1396±202	39	41
10^{-2} s^{-1}	V	10.48	1520	4.12	597	8.24±2.05	1195±297	74	9

*H - horizontal; V - vertical.

Table 3. Summary of uniaxial tensile strength data for Phase II.

	Maximum		Minimum		Mean		Mean porosity	Number of
	(MPa)	(lbf/in.^{2})	(MPa)	(lbf/in.^{2})	(MPa)	(lbf/in.^{2})	(o/oo)	samples
				-5°C (23°F)				
10^{-5} s^{-1} V*	1.03	149	0.57	82	0.82±0.17	119±24	78	9
10^{-3} s^{-1} V	0.83	120	0.41	60	0.61±0.16	89±23	108	9
				-20°C (-4°F)				
10^{-5} s^{-1} V	0.92	134	0.49	71	0.71±0.16	103±23	82	9
10^{-3} s^{-1} V	0.92	134	0.48	69	0.75±0.16	109±23	77	9

*V - vertical.

Table 4. Summary of confined strength data for different strain rates, temperatures and confining-pressure-to-axial-stress ratios (σ_2/σ_1).

		σ_2/σ_1	Maximum (MPa)	Maximum (lbf/in.^{2})	Minimum (MPa)	Minimum (lbf/in.^{2})	Mean (MPa)	Mean (lbf/in.^{2})	Mean porosity (o/oo)	Number of samples
						-5°C (23°F)				
10^{-5} s^{-1}	V*	0.25	3.95	573	1.14	166	2.86±0.98	415±142	79	10
10^{-5} s^{-1}	V	0.50	6.61	959	2.28	330	3.81±1.59	552±231	86	9
10^{-3} s^{-1}	V	0.50	17.94	2602	5.43	788	11.70±3.41	1697±495	78	9
						-20°C (-4°F)				
10^{-3} s^{-1}	V	0.25	17.07	2475	11.58	1679	14.77±1.90	2141±275	77	9
10^{-5} s^{-1}	V	0.50	11.03	1600	3.95	573	6.59±1.97	956±286	82	9
10^{-3} s^{-1}	V	0.50	38.63	5602	8.34	1210	23.50±8.73	3408±1266	57	9

* V - Vertical.

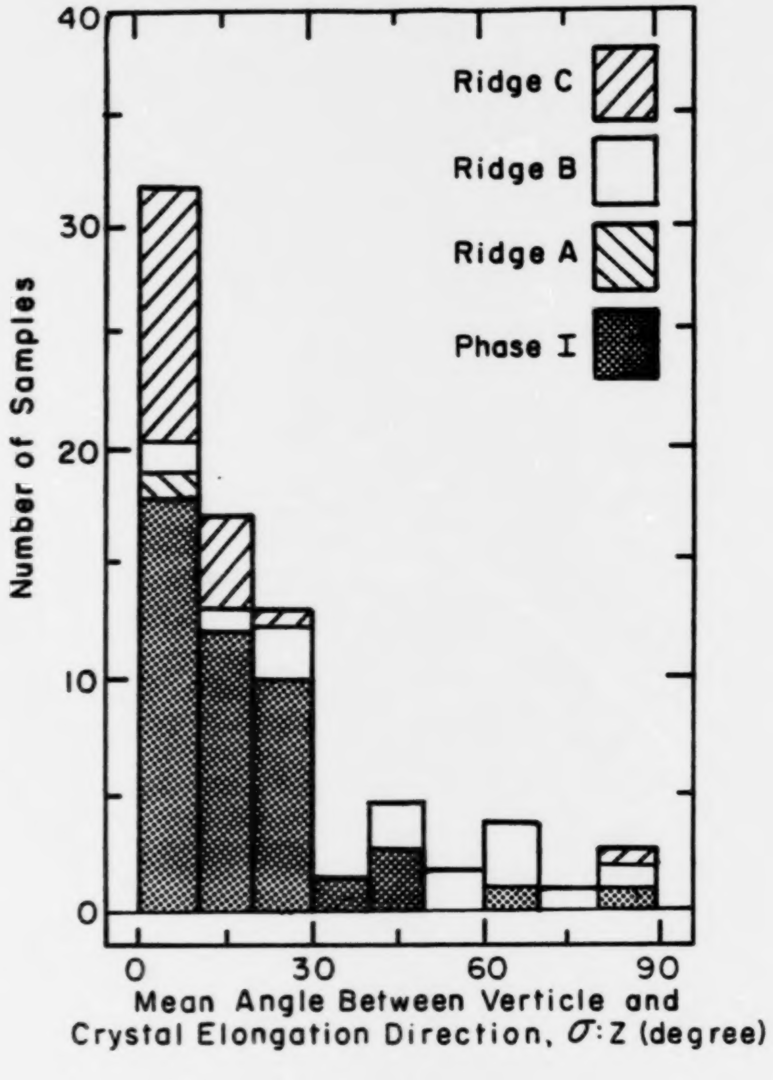

Figure 1. Frequency histogram of the multi-year ridge columnar ice samples in a given σ:z orientation.

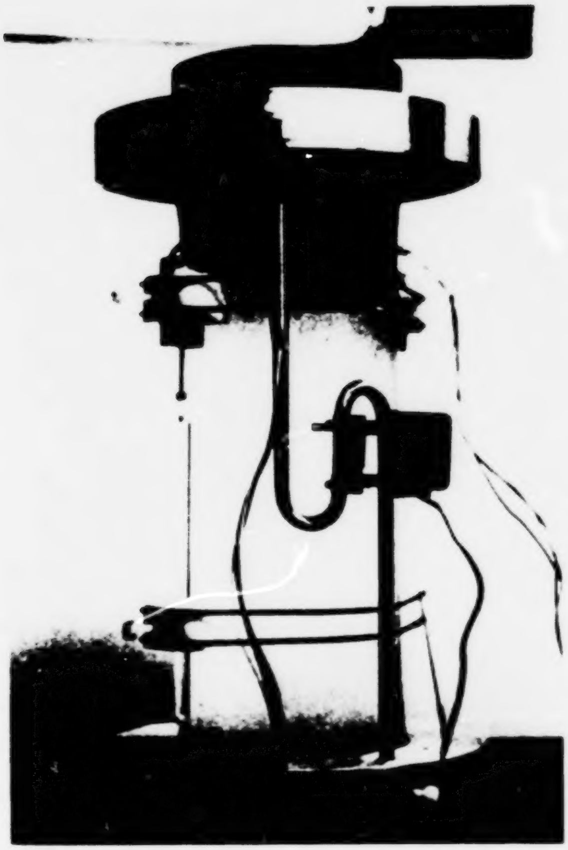

Figure 2. Instrumented unconfined uniaxial compression test. The same instrumentation was used in the uniaxial tension tests.

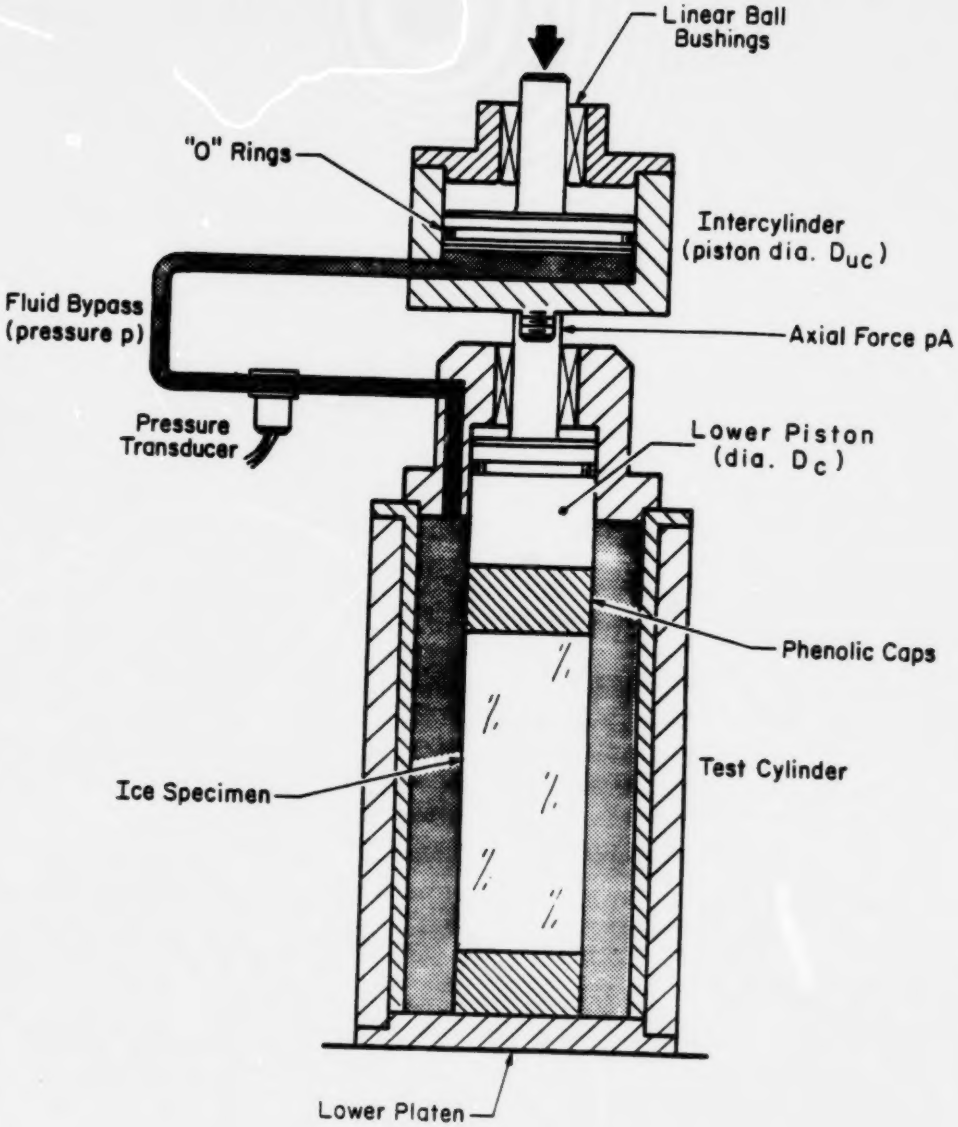
Linear Ball Bushings
"O" Rings
Intercylinder (piston dia. D_{uc})
Fluid Bypass (pressure p)
Axial Force pA
Pressure Transducer
Lower Piston (dia. D_c)
Phenolic Caps
Test Cylinder
Ice Specimen
Lower Platen

Figure 3. Schematic diagram of triaxial cell used for confined compression tests.

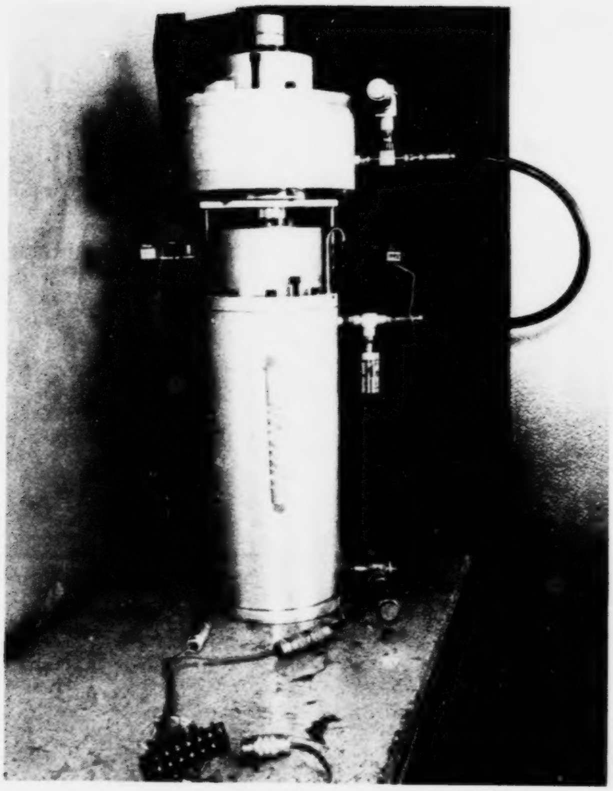

Figure 4. Triaxial cell used for confined compression tests.

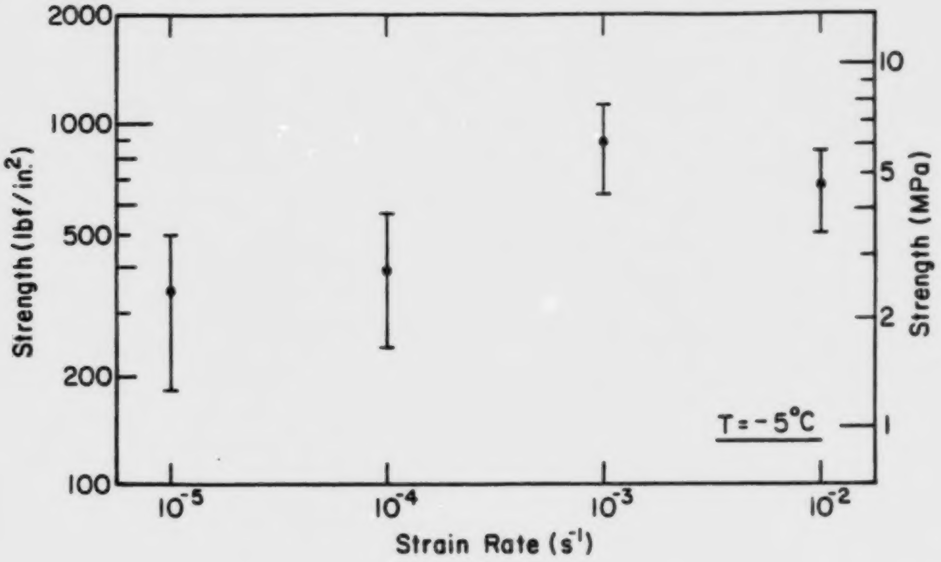

a. Samples tested at -5°C.

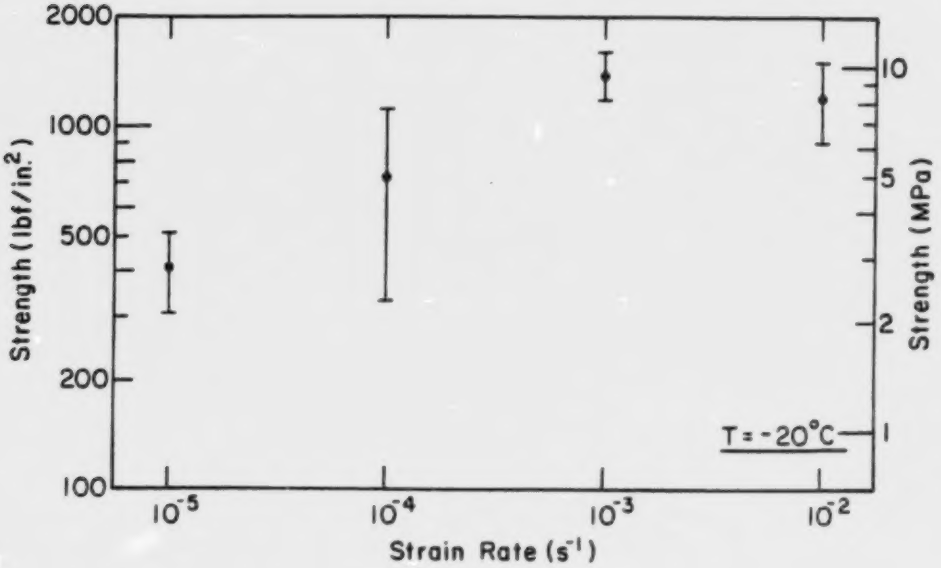

b. Samples tested at -20°C.

Figure 5. Mean uniaxial compressive strength versus strain rate for multi-year ridge samples. The bars denote one standard deviation.

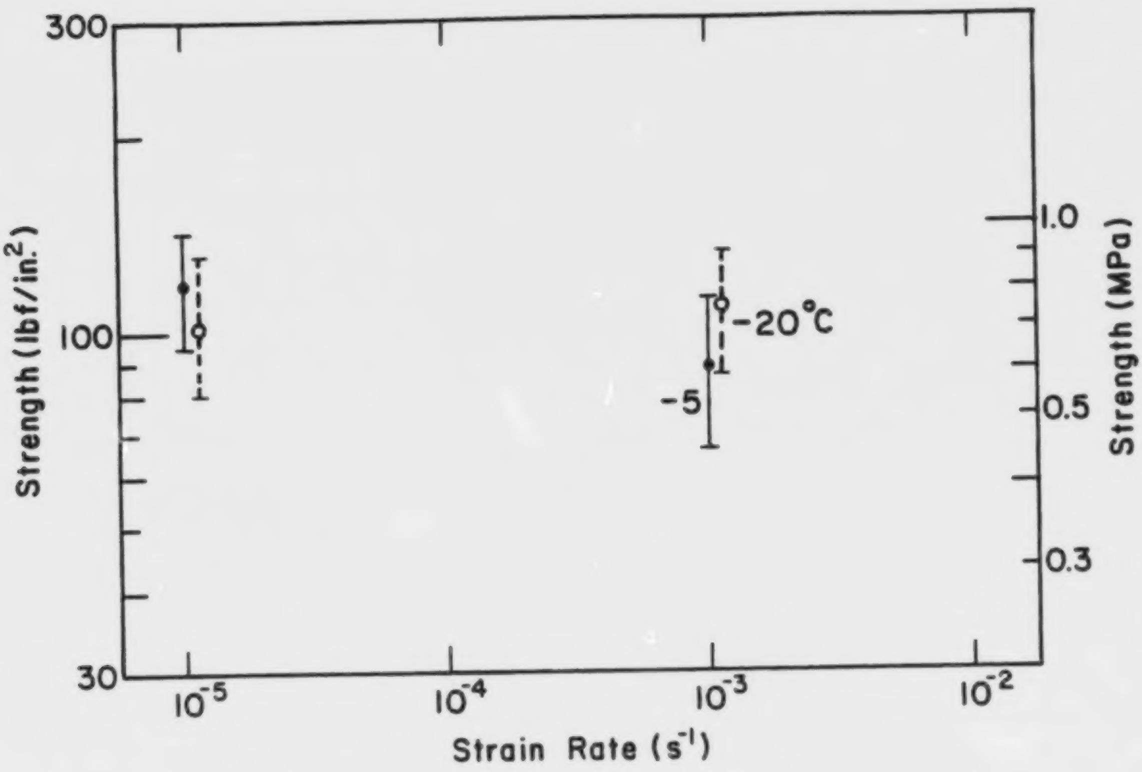

Figure 6. Mean uniaxial tensile strength versus strain rate for multi-year ridge samples tested at -20° and -5°C. The bars denote one standard deviation.

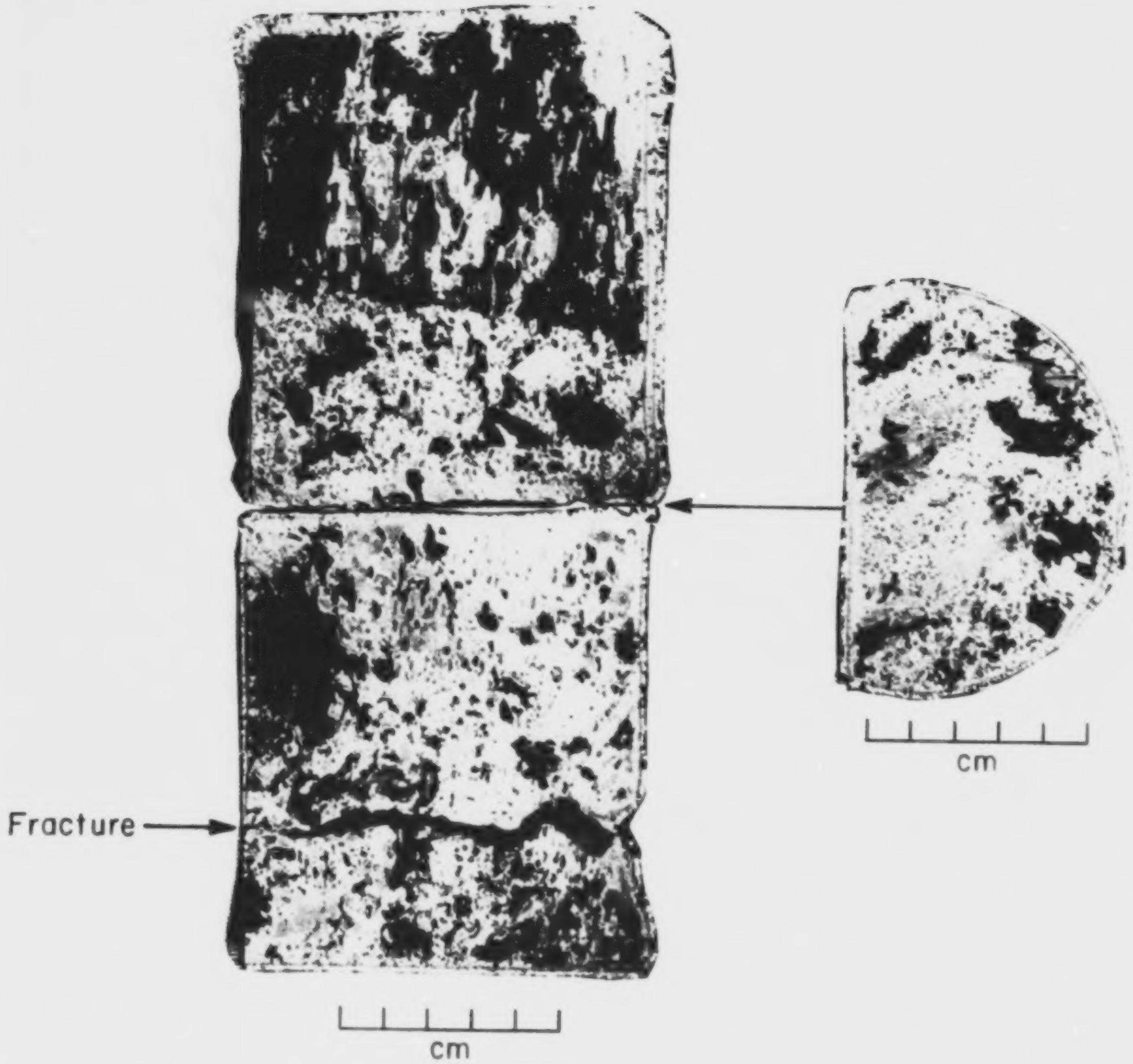

Figure 7. Photographs of ice thin sections taken in crossed polarized light to illustrate the location of fracture plane with respect to ice structure in a tension sample.

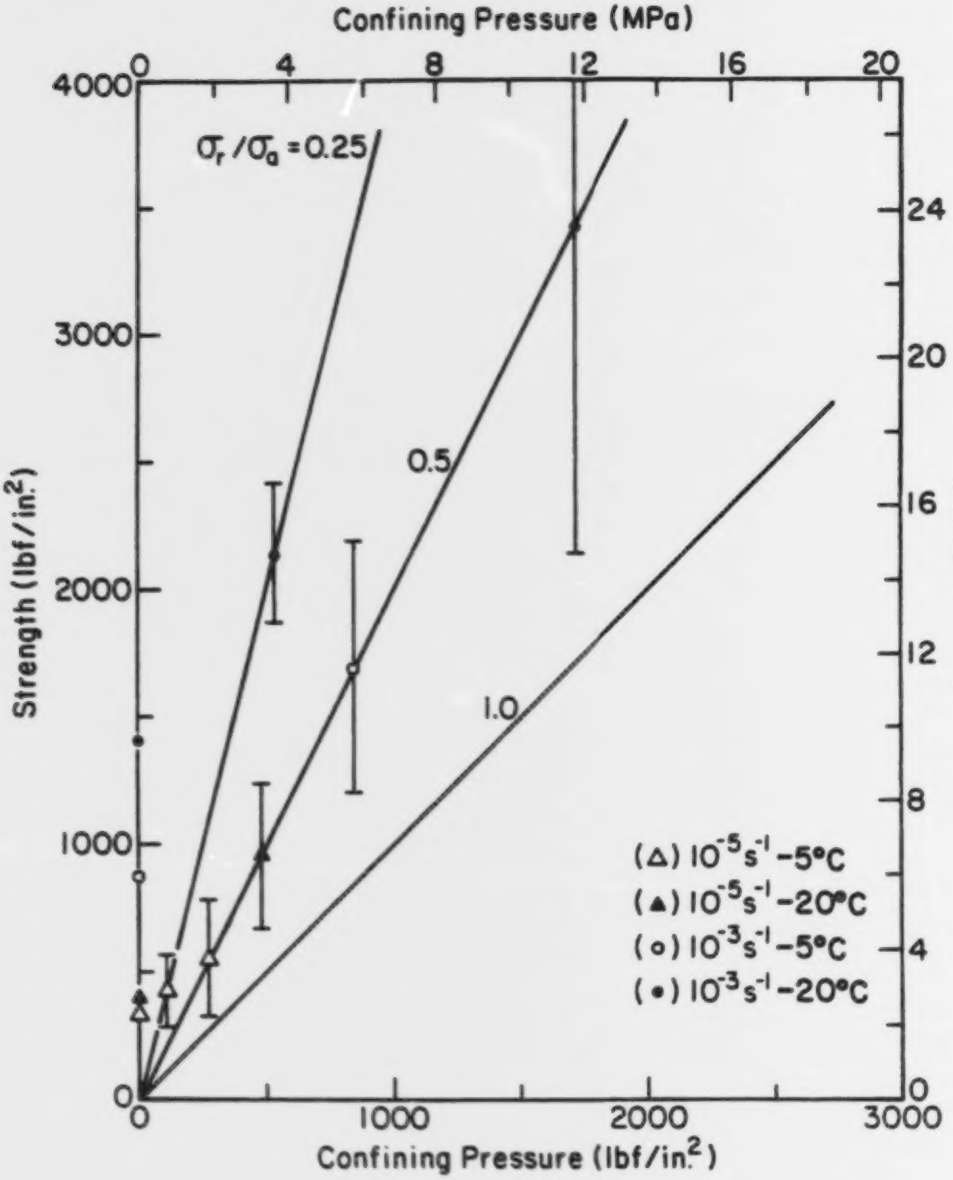

Figure 8. Mean compressive strength versus confining pressure for multi-year ridge samples at different temperatures and strain rates. The bars denote one standard deviation.

NRC WORKSHOP ON EXTREME ICE FEATURES

Questions and Discussions Form

AUTHOR: J.A. Richter-Menge and G.F.N. Cox

PAPER: Mechanical Properties of Multi-year Sea Ice

DISCUSSION BY: Ken Croasdale

DISCUSSION:

The author and her colleagues are to be commended on providing a very valuable data set on the small-scale properties of multi-year ice. I agree with the author that the issue of using small-scale data in ice load predictions is a difficult one. I further agree that small-scale crushing strength may well be appropriate for local ice pressure criteria, but not for global loads. However, the rationale for using the tensile strength for large-scale ice crushing pressure is not clear. Would the author care to comment.

AUTHOR'S REPLY:

When making the comment I was not considering the large-scale crushing pressure, rather I was focusing on flexural failure of the ice feature. Two scenarios can be imagined:

1. ride-up of a multi-year floe on a conical base. If a keel grounds on the side, the edges of the floe will see an increase in freeboard without support. This will cause bending out of plane.
2. impact of a ridge against the side of a structure could see the centre pinned while edges are free. Again, flexure of the feature will occur, but this time in plane.

Flexural failure of the ice feature is controlled by the tensile strength; hence the comment.

DISCUSSION BY: Ian Jordaan

DISCUSSION:

I would question the use of Tresca/von Mises plasticity - basis yield criteria. Would not a creep law apply for ice under hydrostatic confining pressure? That is at pressures high enough to suppress microcracking.

AUTHOR's REPLY:

First, let me (hopefully) add some clarity to my presentation by stating that by yield criteria I am speaking only of the mathematical expression that describes the failure envelop of the ice--failure being the peak stress the sample reaches during loading. This description is independent of the mechanism(s) of deformation involved in attaining that peak load. I consider the constitutive equation to be the expression of the ice behaviour along the loading curve. The latter is obviously much more complicated and highly dependent on deformational mechanisms. Based on this, when I was reviewing the use of the Tresca/von Mises yield criteria and the Smith yield criteria I was interested in determining which yield criteria best described the relationship between the deviatoric stress at peak load and the confining pressure. Again the deformational behaviour of the ice, be it plasticity or creep, did not enter into this review.

The use of the Tresca/von Mises yield criteria does appear to be a good approximation of the deviatoric stress versus confining pressure up to the peak in this curve (see Figure 9, Reference 1). It does not describe the drop in the deviatoric stress beyond this point, however. The Smith yield criteria appears to give a better overall description of the failure envelope.

A creep law may be an appropriate means of explaining the loading behaviour of the ice when subject to hydrostatic confining pressure. I cannot comment on this with any accuracy as the efforts of Gordon Cox and myself have focused only on the failure envelop of the ice. Work on the constitutive behaviour will likely begin this year.

One final note, Ralston (2) has modeled the behaviour of ice indentation using plasticity theory with some success. I'm sure you are aware of this work.

References

(1) RICHTER-MENGE, J.A. Confined compressive strength of horizontal first-year sea ice samples. Accepted for presentation at the 6th International Symposium on Offshore Mechanics and Arctic Engineering (OMAE '87), Houston, 1-5 March 1987.

(2) RALSTON, T.D. Yield and plasticity deformation in ice crushing failure. Proceedings, Symposium on Sea Ice Processes and Models, University of Washington, Seattle, Vol. 2, pp. 147-156, 6-9, September 1977.

DISCUSSION BY: Maher Nessim

DISCUSSION:

Have you made a comparison between the properties of deformed and undeformed multi-year ice, and if so do you think that the difference warrants treating them as two different materials in ice-structure interaction problems?

AUTHOR'S REPLY:

I have not made a comparison between the properties of deformed and undeformed multi-year ice in my tests, but I would still like to comment.

Undeformed multi-year ice is predominately columnar in structure. Deformed multi-year ice is a much more complicated beast. The deformed ice tends to be a mixture of columnar and granular ice, resulting from the process of deformation. We have done an extensive amount of work on the multi-year ridge ice and first-year sea ice. The latter has a columnar ice structure like the undeformed multi-year ice and gives us a good indication of the properties of the undeformed ice. *Comparing the results of these tests we find that the columnar first-year ice has a much higher degree of anisotropy than the multi-year ridge ice. The standard deviation of the strength in tests done on first-year ice tends to be smaller indicating a much more uniform composition. The mean strength of a test series done on horizontal first-year and multi-year is comparable, but the vertical strength shows a much higher strength for the first-year ice. The highest strength multi-year ridge samples are those made up of columnar ice, loaded parallel to the columns. The strength of these samples decreases with an increase in the amount of granular ice included in the sample.

Based on this, I would venture to say that you must consider the design problem in order to decide whether to treat undeformed and deformed multi-year ice as the same material. I expect that it would be a valid approximation in the determination of global ice loads in a horizontal loading problem. I would consider them as separate materials, however, if I was interested in determining ice loads in a vertical loading scenario (e.g., bearing capacity) or for any local impact loading forces. One further observation, since the undeformed multi-year ice is columnar, the strength of these samples would give you a conservative design load in the ice loads on offshore structures problem.

---

* Initially it was anticipated that the undeformed multi-year columnar ice would have a strength higher than the first-year ice due to brine drainage. The little work done on multi-year undeformed ice shows a strength comparable to first-year ice, however. This is probably due to a comparable porosity (combined air and brine content) between the two. More work needs to be done in this regard.

Survey of physical and mechanical properties of icebergs.

Jean-Paul Nadreau
Centre for Cold Ocean Resources Engineering
Memorial University of Newfoundland
St John's, NF, Canada, A1B 3X5

1.0 Introduction

In the North Atlantic Ocean, icebergs have always been looked at as a threat to shipping. The sinking of the Titanic is the most well-known example of disaster caused by icebergs. Since 1914, the International Ice Patrol has been monitoring the ice and iceberg conditions in the North Atlantic Ocean.

Offshore exploratory drilling in Eastern Canada has shown hydrocarbon reserves large enough to be exploited in a near future should oil prices be economically attractive. However, the production of oil in this region requires offshore structures able to cope with the hostile environment created by the presence of icebergs.

The ice cover in Eastern Canada is not as threatening as in Beaufort sea, but icebergs, growlers and bergy bits are a definite hazard for exploration and production platforms. They can interact with the offshore structure and can also scour the sea floor endangering any shallowly buried pipelines.

This review deals only with icebergs found in Eastern Canadian waters. It excludes references to ice islands which are found in the Arctic Ocean and offshore Elizabeth Islands and it also excludes icebergs originating from Antarctica.

2.0 Environmental Data

2.1 Origin

The vast majority of icebergs which are encountered offshore Newfoundland and Labrador originate from Greenland. Greenland is covered with an ice sheet of nearly 2 million km^2 which has a maximum thickness of 3300 m. The scientific literature states that the Greenland ice cap produces between 10,000 and 30,000 icebergs each year. Although glaciers from both the east and west shores of Greenland are active, the vast majority of icebergs calve from the west coast glaciers. As an example of extremes, one can cite the Jacobshavn Glacier for its "flowing" speed of 22 m/day (8 km/year) and the Rinks Glacier for producing icebergs over 600 m thick (Robe, 1980).

2.2 Calving

Icebergs are known to exhibit picturesque shapes and features. This is due to ablation, melting or fragmentation experienced during their journey southwards. When the bergs calve from the parent glacier they more or less look like each other, the essential difference being their size. The origin of the iceberg will determine most of its characteristics : glaciers which are not afloat will produce small icebergs; ice streams with a floating tongue will produce larger icebergs whose length is several times their thickness; and finally, ice shelves will produce the largest bergs.

Several theories have been used to explain the rate of calving and the size of the bergs. Reeh (1968) proposed the first model based on the force balance experienced by the ice tongue. The ice "hydrostatic" pressure and the water pressure create a couple M and a tensile axial force N at the end of the floating ice slab (Figure 1). This basic model has been improved by Holdsworth (1977) to explain various mechanisms of calving. Finite-element techniques have also been used to include different parameters such as temperature-dependent relaxation functions, tidal actions and bedrock geometries (Reddy *et al.*, 1980).

2.3 Drift patterns

Once icebergs have calved from the parent glaciers, they begin a journey which may last for two or three years before the bergs finally deteriorate and melt. As shown in Figure 2, icebergs follow the West Greenland current to the North end of Baffin Bay where they turn southwards along with the Baffin Island current. Icebergs from the East coast pass round the South tip of Greenland to follow the same route as those bergs produced by the West Greenland glaciers.

Figure 3 shows that, on the icebergs' way south, they can be diverted by secondary currents and spend some time in sounds and straits. They finally continue their journey by following the Labrador current (Figure 4) which lead them to the Grand Banks of Newfoundland. At this point they can drift either eastwards north of Flemish Cap or southwards between Flemish Cap and the Grand Banks. At these latitudes the effects of the warm North Atlantic current can be felt. Most icebergs deteriorate and melt. Figure 5 shows the maximum mean iceberg limit as well as some unusual reported sightings.

Tracking icebergs is now possible through techniques such as satellite imagery. Figures 3 and 4 show the tracks of bergs tracked by this technique. The remote detection of beacons like TIROS buoys used by the International Ice Patrol (IIP) for their 1983 TIROS Arctic Drifters (TAD) campaign (Figure 6) is another technique. The only problem in the interpretation of the results is the difficulty to determine when the buoy fell off the iceberg. It seems probable, for instance, that the last section of the trajectory of buoy #2611 (Figure 6) can be accounted for by the wind driven surface currents only. It is likely (Anderson, 1983) that a storm caused the TAD to fall off the iceberg and act as a surface drifter until it terminated transmission.

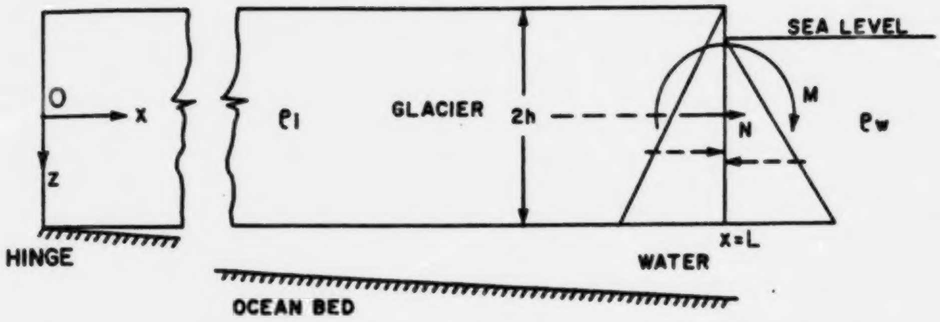
O
X
Z
HINGE
ρI
GLACIER
2h
SEA LEVEL
M
N
ρw
X=L
WATER
OCEAN BED

Figure 1. Model for marginal calving mechanism(Reeh,1968)

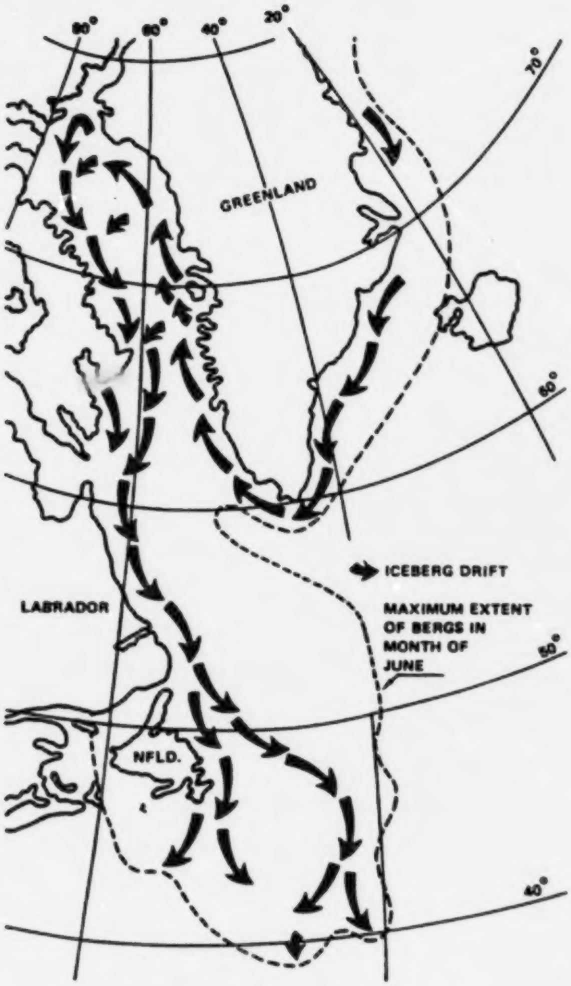
80°
60°
40°
20°
70°
60°
50°
40°
GREENLAND
LABRADOR
NFLD.
ICEBERG DRIFT
MAXIMUM EXTENT OF BERGS IN MONTH OF JUNE

Figure 2. Drift path of Greenland icebergs.
(Soulis,1975 modified by Robe,1980)

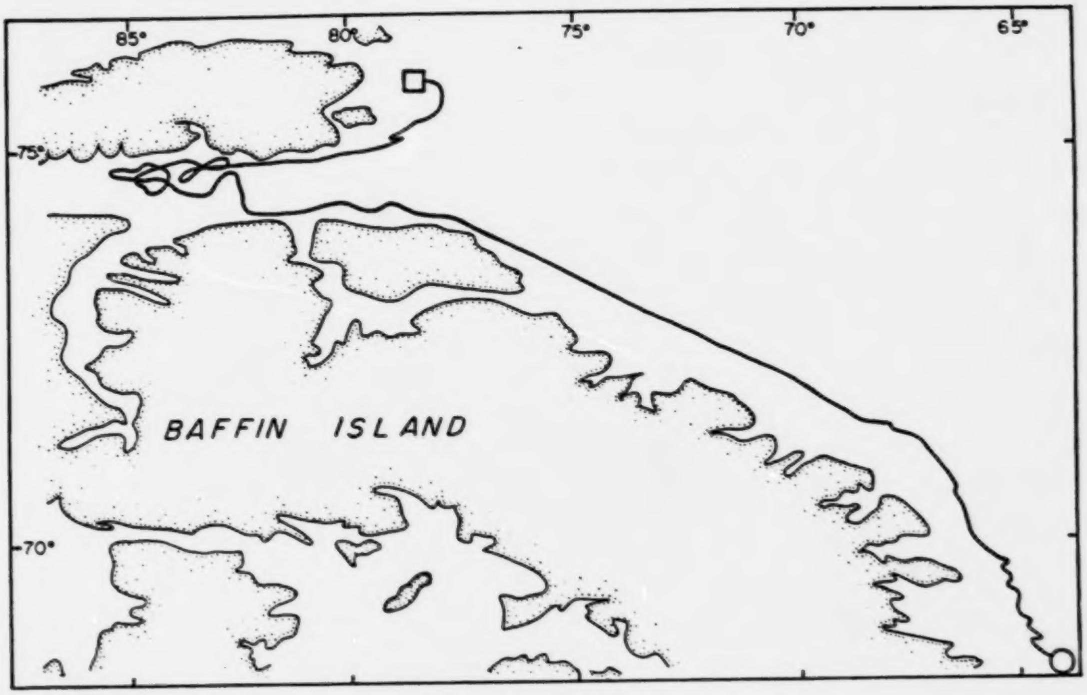
85°
80°
75°
70°
65°
75°
70°
BAFFIN ISLAND

Figure 3. Satellite track iceberg drift. (Fissel, 1981)

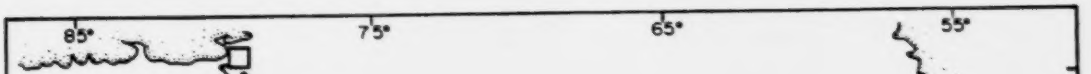
85°
75°
65°
55°
75°
65°
BAFFIN ISLAND

Figure 4. Satellite track iceberg drift. (Fissel, 1981)

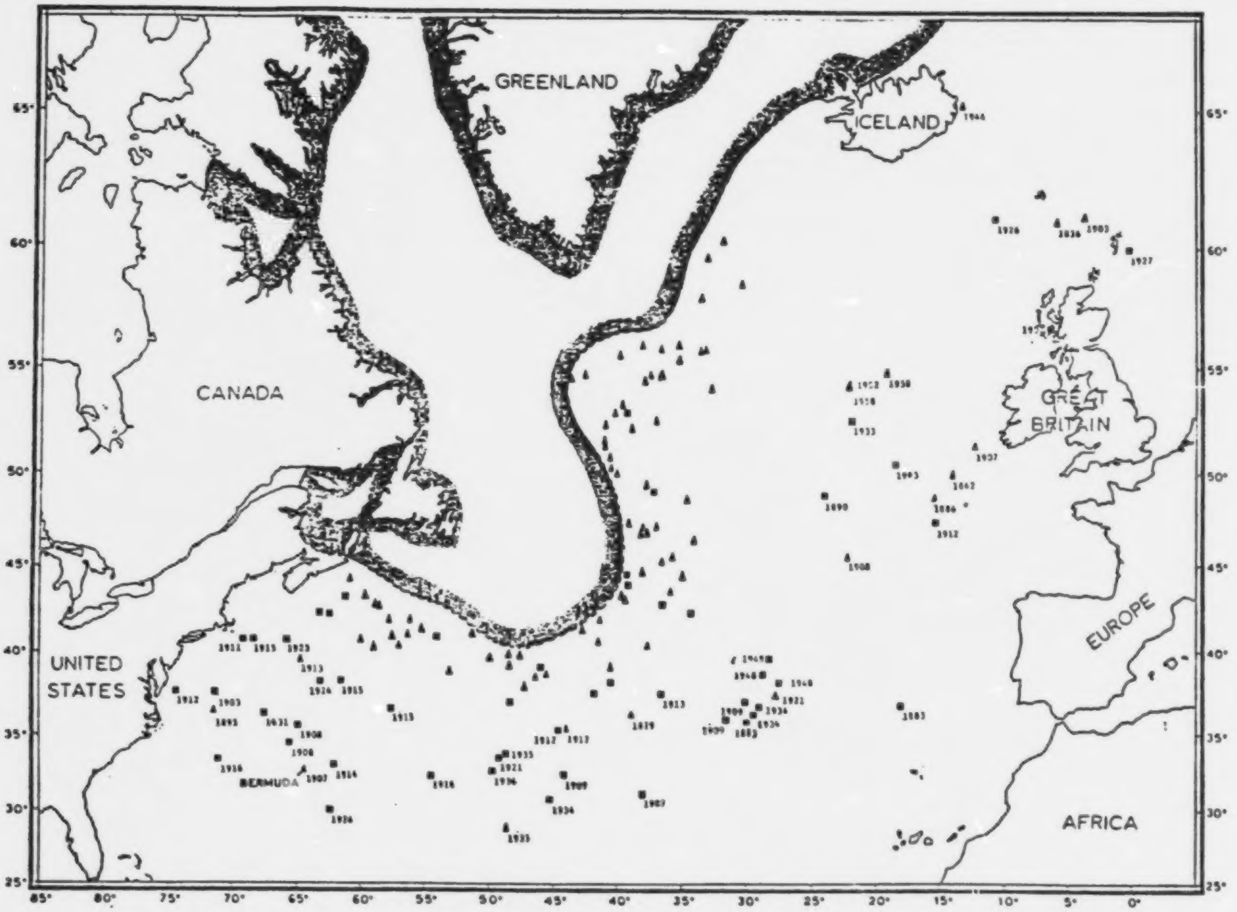
GREENLAND
ICELAND
CANADA
GREAT BRITAIN
UNITED STATES
EUROPE
AFRICA
BERMUDA
65°
60°
55°
50°
45°
40°
35°
30°
25°
85°
80°
75°
70°
65°
60°
55°
50°
45°
40°
35°
30°
25°
20°
15°
10°
5°
0°

Figure 5. Maximum mean iceberg limit and reported unusual iceberg sightings. (Ketchen and Hildenbrand, 1977)

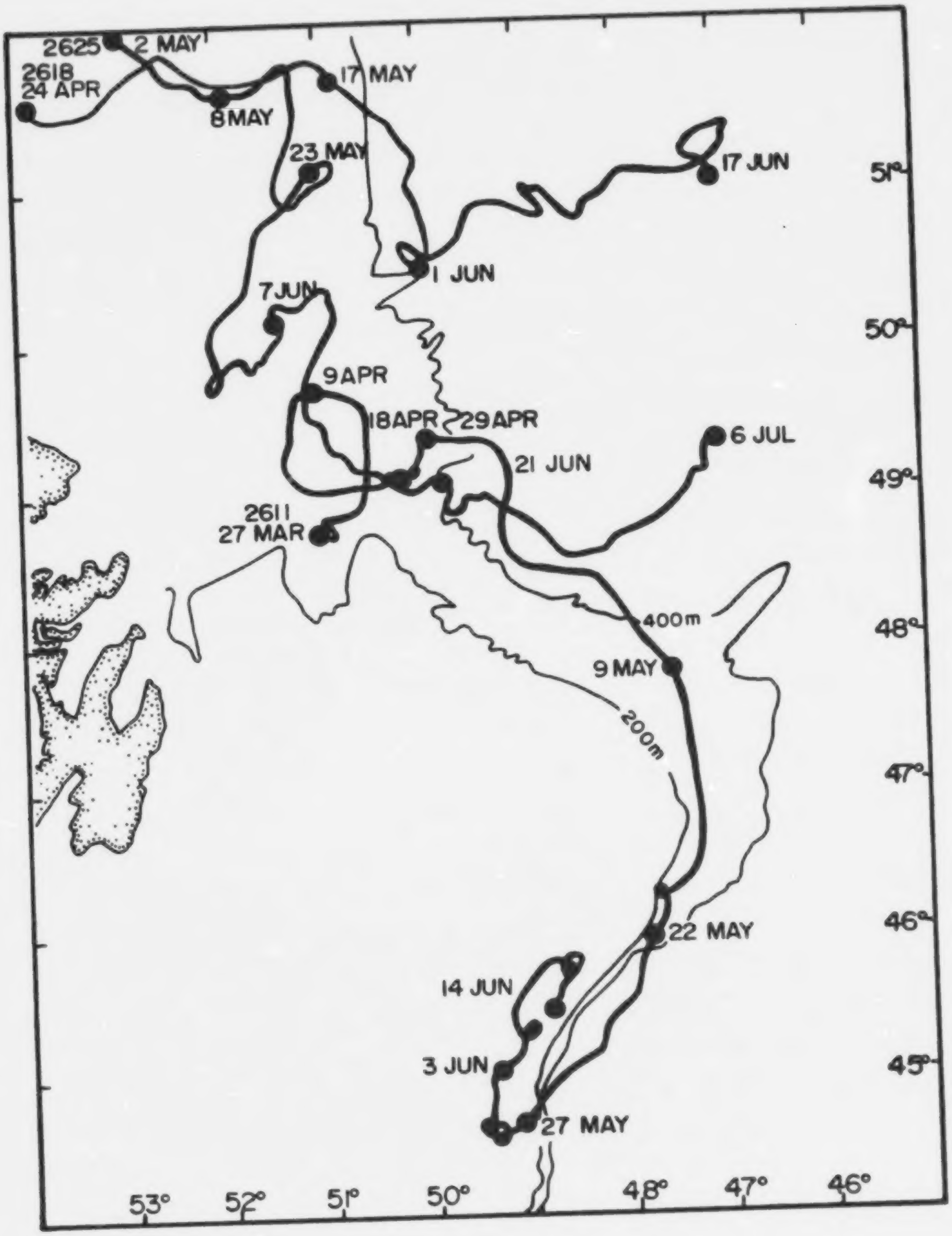
2625
2 MAY
2618
24 APR
8 MAY
17 MAY
23 MAY
17 JUN
1 JUN
7 JUN
9 APR
18 APR
29 APR
6 JUL
21 JUN
2611
27 MAR
400m
9 MAY
200m
22 MAY
14 JUN
3 JUN
27 MAY
51°
50°
49°
48°
47°
46°
45°
53°
52°
51°
50°
48°
47°
46°

Figure 6 Tracks of TIROS Arctic Drifters deployed by IIP during 1983. (Anderson, 1983)

2.4 Iceberg drift models

Any petroleum company operating offshore Newfoundland needs protect its drilling rigs from iceberg collision. Up to now, this has been achieved by towing the iceberg away from the drilling site or by moving the rig itself when the iceberg is too large to be towed. In all cases, a warning system is needed in order to initiate avoidance action. Besides the available International Ice Patrol forecasts, models have been developed to predict iceberg movements. El-Tahan and El-Tahan (1983) have studied the factors controlling iceberg motion. Based on field observations and theoretical studies they suggest that iceberg drift is affected by currents, winds, Coriolis acceleration, waves, ocean surface slope (pressure gradient) and iceberg sizes parameters.

Currents are clearly the most important factor affecting the direction and velocity of the berg. Figure 7 shows that water currents contribute about 50% to 65% of the iceberg motion.

These models remain limited in their application; their range of action and accuracy within that range depend greatly upon the parameters used to feed the model. Gaskill *et al.* (1984) think that standard models which use forecasted wind data and the last measured current at the considered site as inputs to the model to determine the velocity of the iceberg are not as accurate as models which are based on the past observed motion of the particular berg and on the long term velocity for the icebergs in the area of interest.

2.5 Fluxes

Data available on fluxes of icebergs are essentially due to observations by the U.S. Naval Hydrographic Office from 1900 until 1914, and from then on, by the International Ice Patrol which was

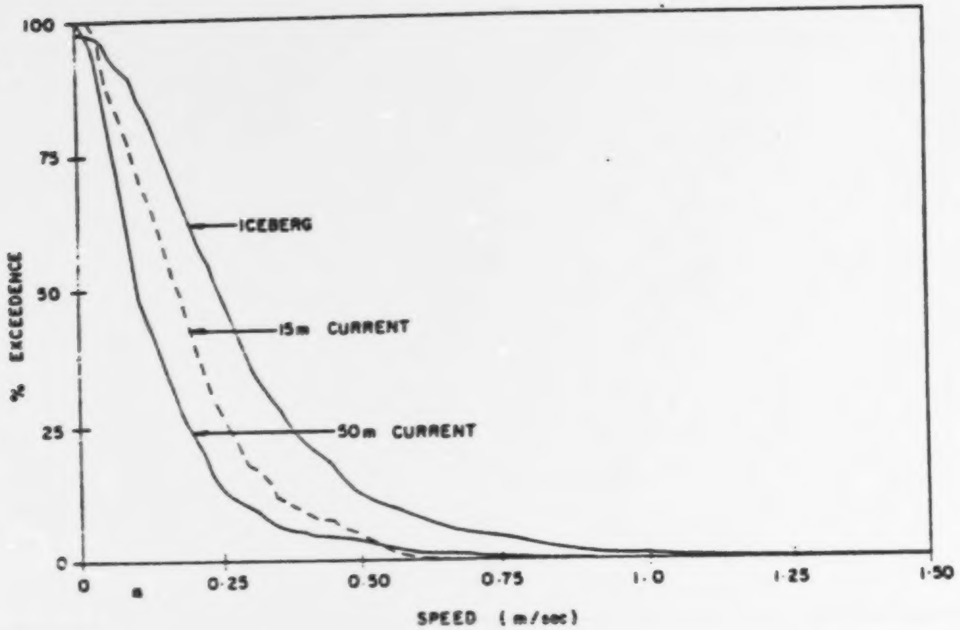

Figure 7. Iceberg speed and current velocity. (El Tahan and El Tahan, 1983)

created after the sinking of the Titanic. Figure 8 presents the estimated number of icebergs reported south of 48°N for the period 1900-1984. This data should be looked at with some reservation since the means to count the icebergs has evolved with time. The histogram presented in Figure 8 can be broken into three different data sets. The first set includes sightings from 1900 through 1945 where iceberg distributions were determined from surface observations made from Coast Guard cutters patrolling plus sightings by merchant and fishing vessels transiting the area. During the second period, which starts after World War II, aircraft reconnaissance became the primary method for locating and tracking icebergs (Ketchen, 1977). Finally, the third set begins in 1983 where Side-Looking Airborne Radar (SLAR) was introduced in reconnaissance flights (Thayer, 1984). It seems probable that elevated figures for 1983 and 1984 are primarily due to the new technology.

From these data and from similar sets obtained by the Canadian Atmospheric Environment Service, seasonal iceberg density distribution can be derived (Gustajtis and Buckley, 1977; Sutton and Mudry, 1983). They give indications of periods and locations where icebergs tend to recur. The histogram presented in Figure 9 shows the monthly average of icebergs crossing 48°N. The maximum tends to move earlier in the year as the considered location is upper North.

3.0 Physical properties

3.1 Mass and draft

As icebergs vary greatly in shape, classification of bergs is rather difficult. The International Ice Patrol describes icebergs by various types such as tabular, tilted tabular, blocky, pinnacled, drydock and domed. As far as size is concerned, growlers have a mass

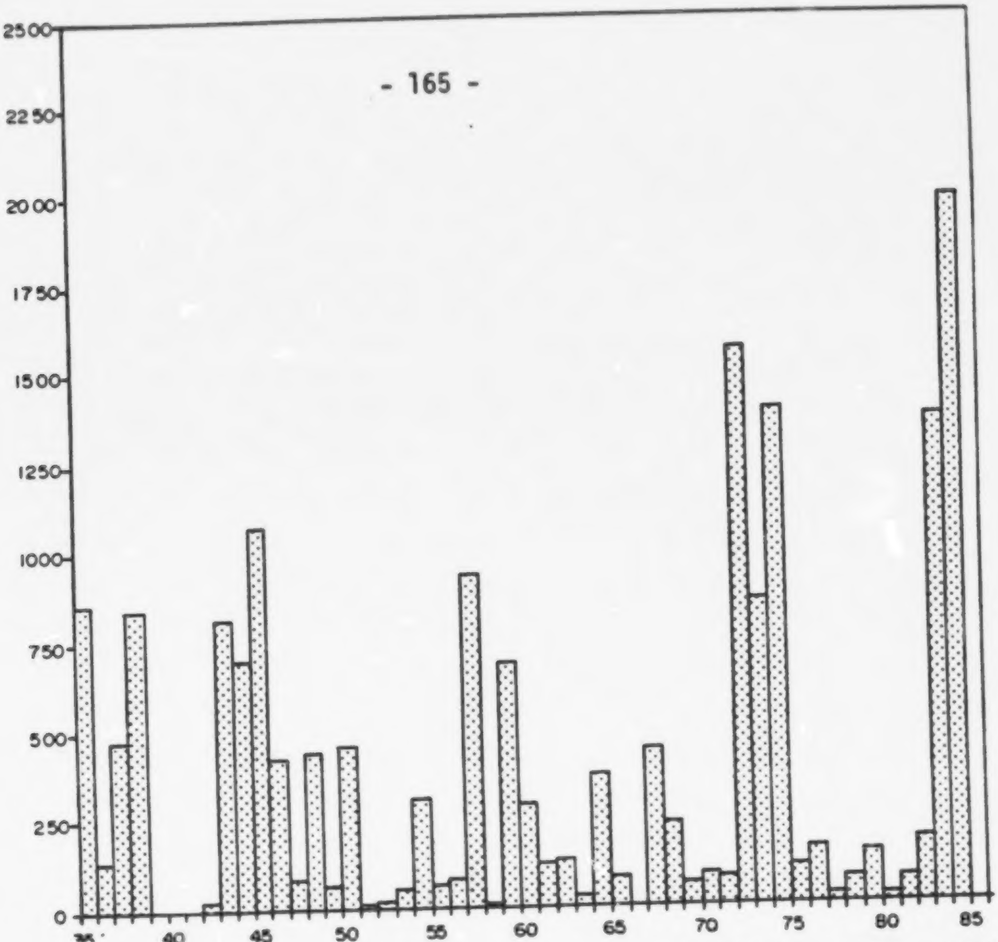

Figure 8. Number of icebergs south of 48° N. for 1935–1984 (U.S. Coast Guard data)

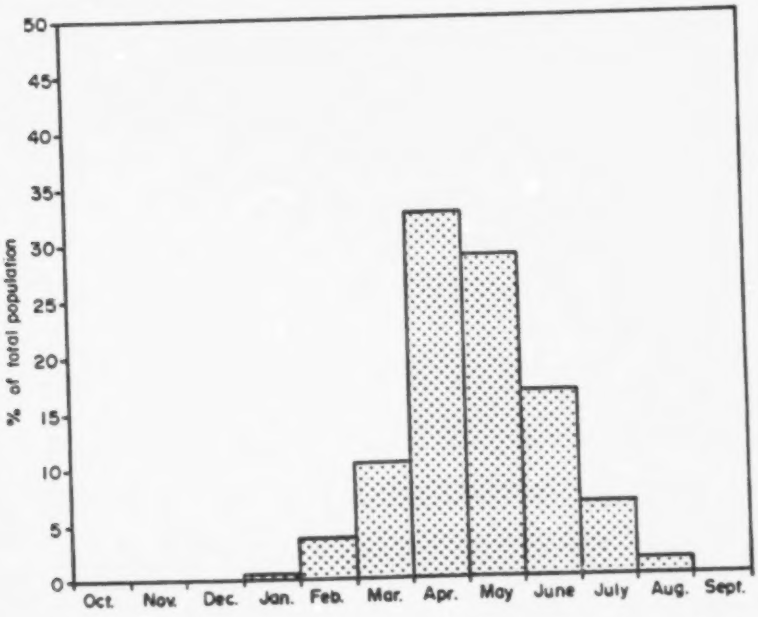

Figure 9. Monthly average of icebergs crossing 48° N. latitude for 1946–1984 (U.S. Coast Guard data)

up to 1,000 tonnes, bergy bits up to 10,000 tonnes and small bergs up to 100,000 tonnes.

Since the early seventies, iceberg surveys have been carried out systematically by oil companies who needed information on icebergs for design purposes. Mangor and Zorn (1983) presented the results of several extensive field programs undertaken offshore Greenland. The mass of almost 300 icebergs has been calculated and the draft of over 100 of them has been measured. The results are presented in Figures 10 and 11. The maximum estimated mass was found to be around 32 million tonnes and the maximum recorded draft was 187 m. Interesting relationships between draft and mass, and height and mass are presented in Figures 12 and 13.

Similar surveys undertaken offshore Labrador show that iceberg characteristics do not change radically during this first part of their journey. Histograms presented in Figures 14 and 15 show the same range for mass and draft (Berenger and Wright, 1980). The mean iceberg mass lies around 1 million tonnes, although a berg as large as 50 million tonnes was observed.

3.2 Temperatures

Very little is known on the internal temperature of an iceberg. This temperature depends essentially on the original temperature of the glacier from which the berg calved, the temperature of the water it has travelled in, and the length of time it has spent at sea (Diemand, 1984). Mocks and Weeks (1965) present ten-metre isotherms for the Greenland ice sheet as being between -12^oC and -31^oC depending on latitude and elevation. A round temperature of -20^oC can be considered as realistic for most of the calving glaciers.

Considering the low thermal conductivity of ice, it is reasonable to think that the core of an iceberg remains at the temperature of

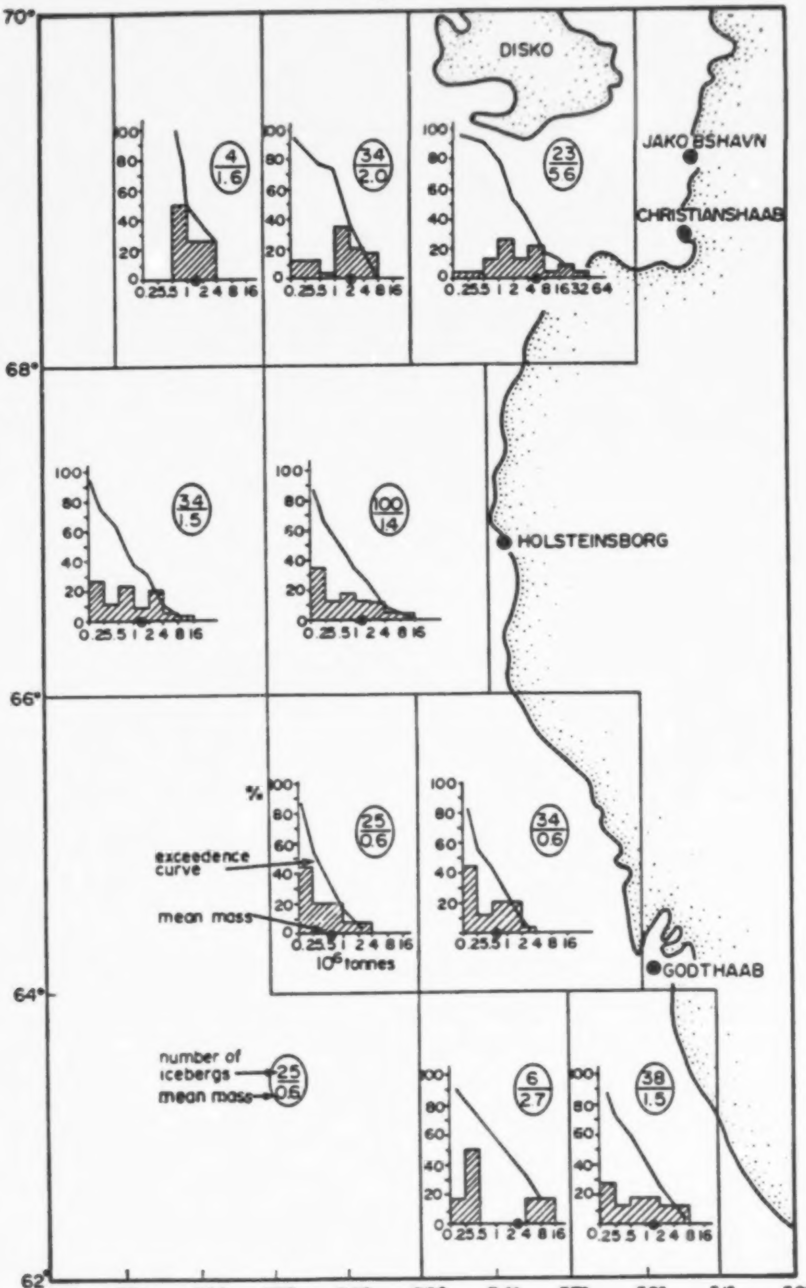
DISKO
JAKOBSHAVN
CHRISTIANSHAAB
HOLSTEINSBORG
GODTHAAB
4/1.6
34/2.0
23/5.6
34/1.5
100/14
25/0.6
34/0.6
6/2.7
38/1.5
%
exceedence curve
mean mass
10⁶ tonnes
number of icebergs
mean mass
70°
68°
66°
64°
62°
60°
59°
58°
57°
56°
55°
54°
53°
52°
51°
50°
0.25 .5 1 2 4 8 16 32 64

Figure 10. Iceberg mass distribution vs. latitude and longitude. (Mangor and Zorn, 1983)

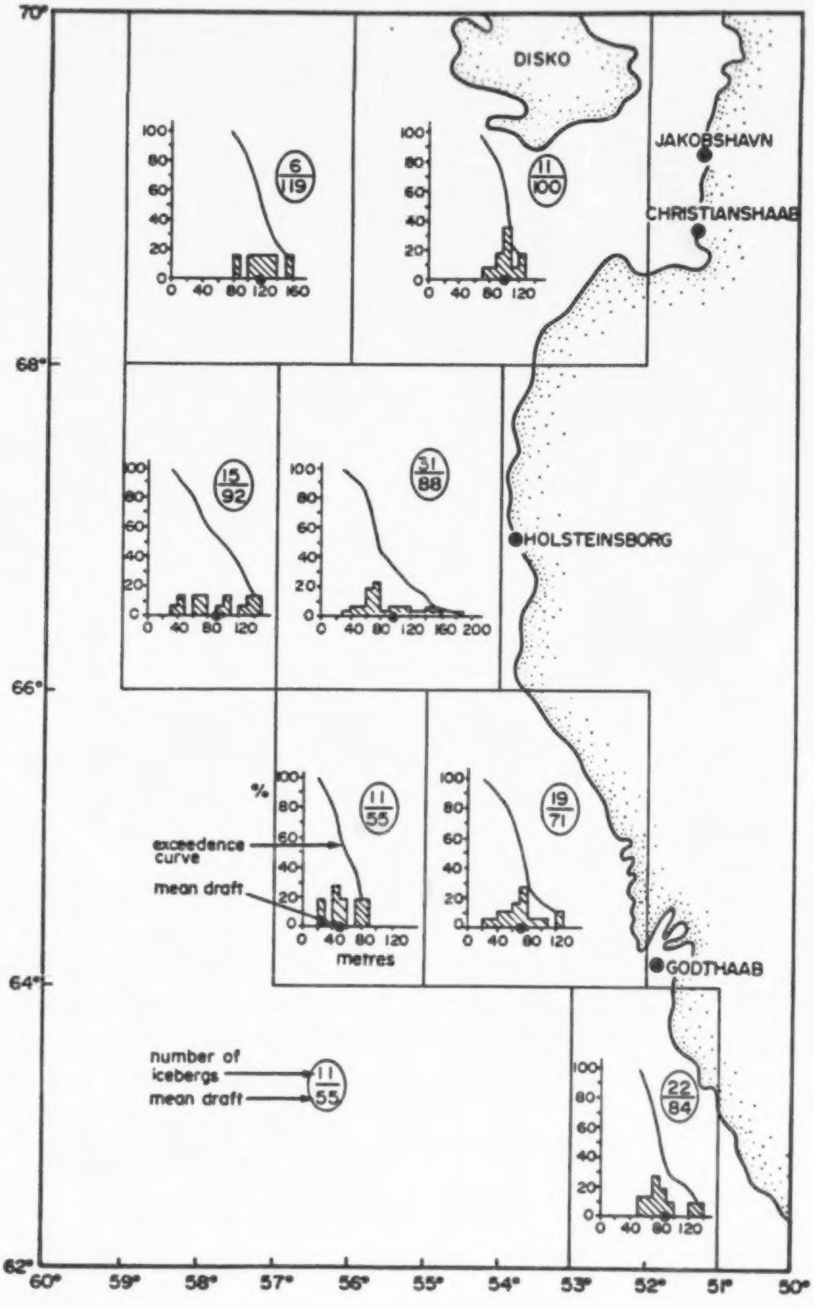
70°
68°
66°
64°
62°
60°
59°
58°
57°
56°
55°
54°
53°
52°
51°
50°
DISKO
JAKOBSHAVN
CHRISTIANSHAAB
HOLSTEINSBORG
GODTHAAB
6/119
11/100
15/92
31/88
11/55
19/71
22/84
%
exceedence curve
mean draft
metres
number of icebergs
mean draft
0
20
40
60
80
100
120
160
200

Figure 11. Iceberg draft distribution vs. latitude and longitude. (Mangor and Zorn, 1983)

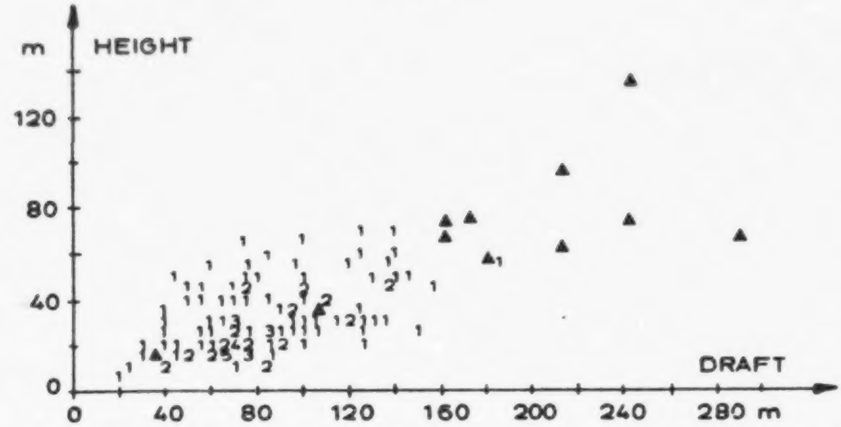

Figure 12. Relations between height and draft for East Greenland icebergs (marked ▲) and for West Greenland icebergs. (Mangor and Zorn, 1983)

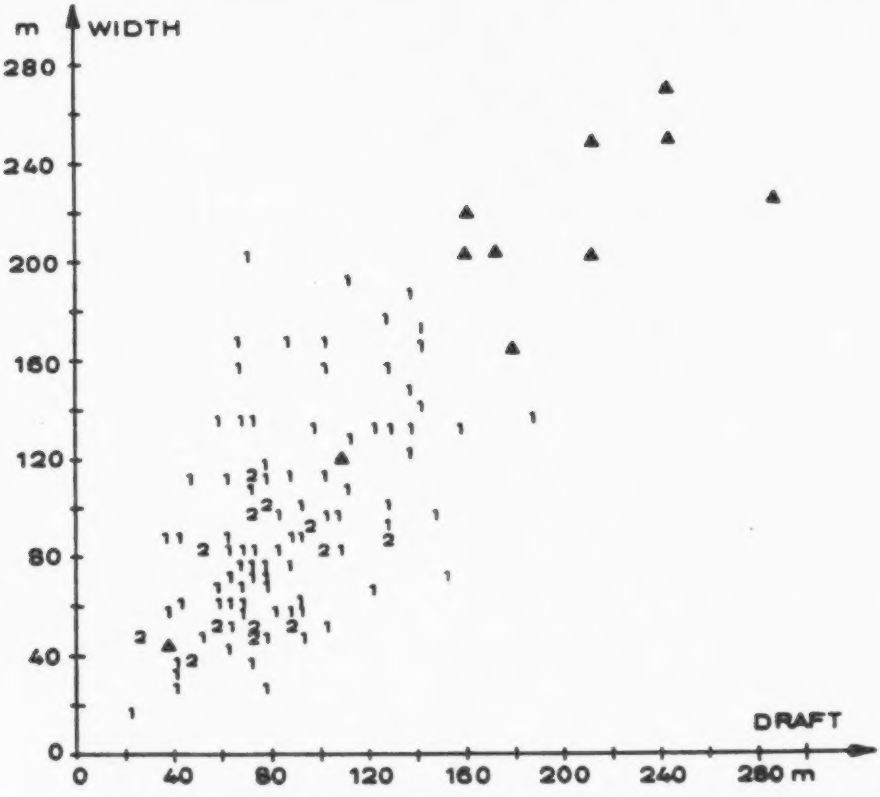

Figure 13. Relations between width and draft for East Greenland icebergs (marked ▲) and for West Greenland icebergs. (Mangor and Zorn, 1983)

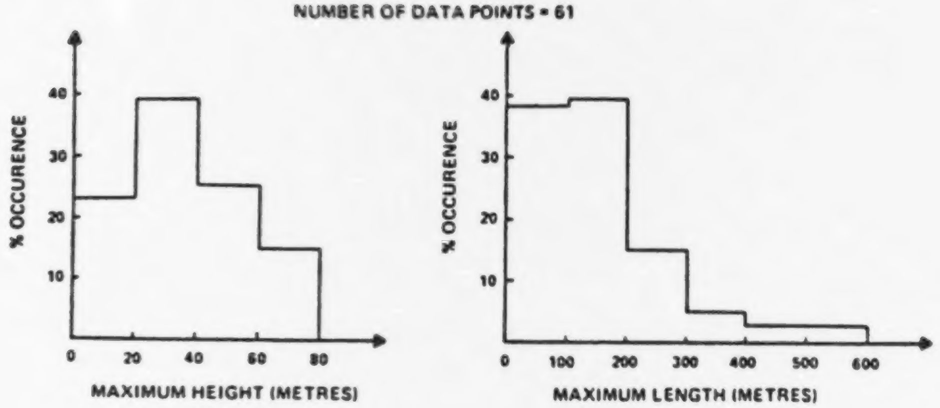

Figure 14. Histograms of maximum iceberg heights and lengths (Jul., Aug., Sept., 1974-75) (Berenger and Wright, 1980)

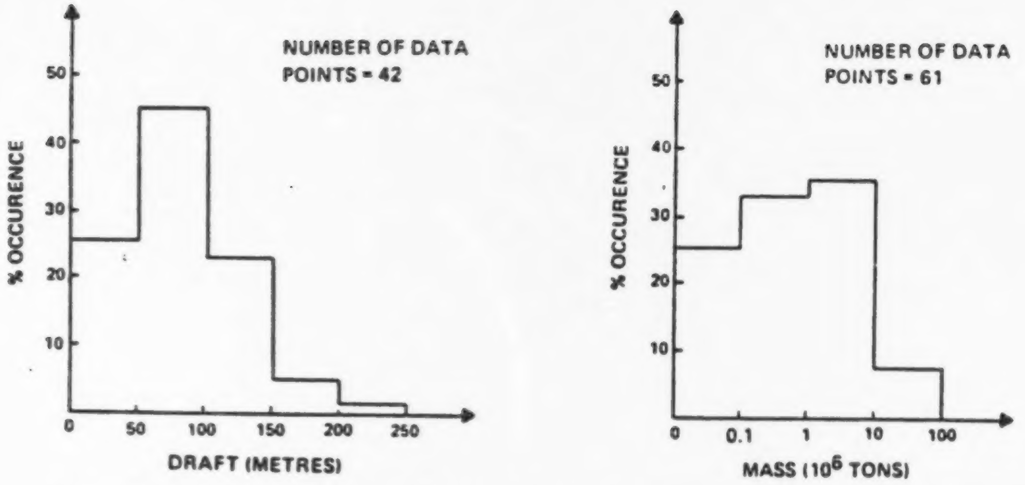

Figure 15. Histograms of maximum iceberg drafts and masses (Jul., Aug., Sept., 1974-75) (Berenger and Wright, 1980)

the parent glacier. Diemand (1984) showed that ablation which occurs in warm waters changes the temperature gradient from the ice-water interface toward the centre of the berg, but leaves the core virtually undisturbed (Figure 16). *In situ* temperature measurements show clearly this gradient and extrapolation of the steepest gradient leads to a possible minimum bulk temperature between -15°C and -20°C (Figure 17).

3.3 Stability

The icebergs which are encountered on the Grand Banks exhibit shapes of all kinds. The bergs usually have experienced several rollings caused by a gradual displacement of the centre of gravity as ablation occurs. The sequence presented in Figure 18 shows a typical example of an iceberg rolling which happened with no warning. Besides the fact that the eventuality is for an iceberg to roll, turns any helicopter landing on a berg and *in situ* measurements into a hazardous experience. It also presents the possibility of the berg increasing its draft during the process. This is a threat for sea-bed installations. Calculations by Bass and Peters (1984) show that a certain class of icebergs can increase their draft by as much as 50%, the average for the increase in draft being approximately 25%.

Mangor and Zorn (1983) state that the stability of an iceberg is dependent on width, height and draft but is independent of the length. Stability generally decreases with increasing width/draft ratio, increases with increasing width and decreases with increasing height.

The stability of icebergs is also affected by phenomena such as natural splitting (Figure 19). This type of splitting is caused by stresses which develop in the iceberg. Table 1 (Diemand *et al.*, 1987) shows the possible types of stresses present in an iceberg.

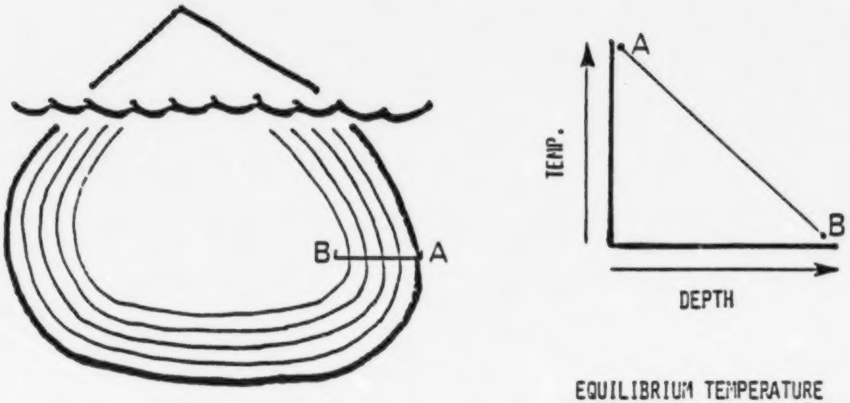
A
B
TEMP.
DEPTH

EQUILIBRIUM TEMPERATURE
(WATER TEMPERATURE -1.8°C.)

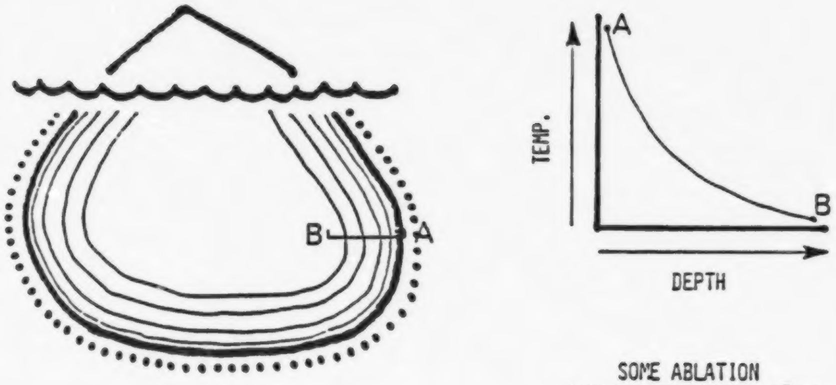
A
B
TEMP.
DEPTH

SOME ABLATION
(WATER TEMPERATURE 2°C.)

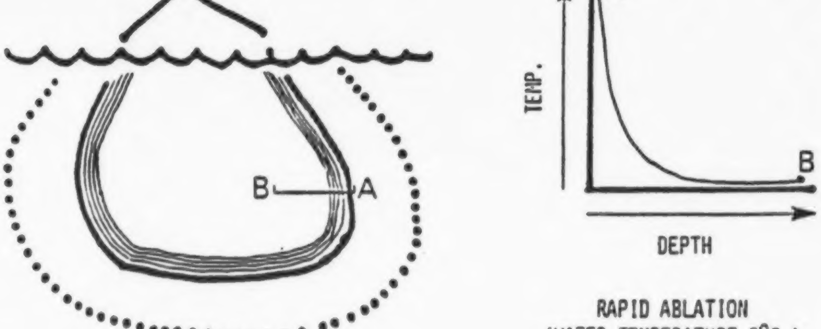
A
B
TEMP.
DEPTH

RAPID ABLATION
(WATER TEMPERATURE 6°C.)

Figure 16. Effect of increasing ablation rates on the thermal profile of an iceberg. (Diemand, 1984)

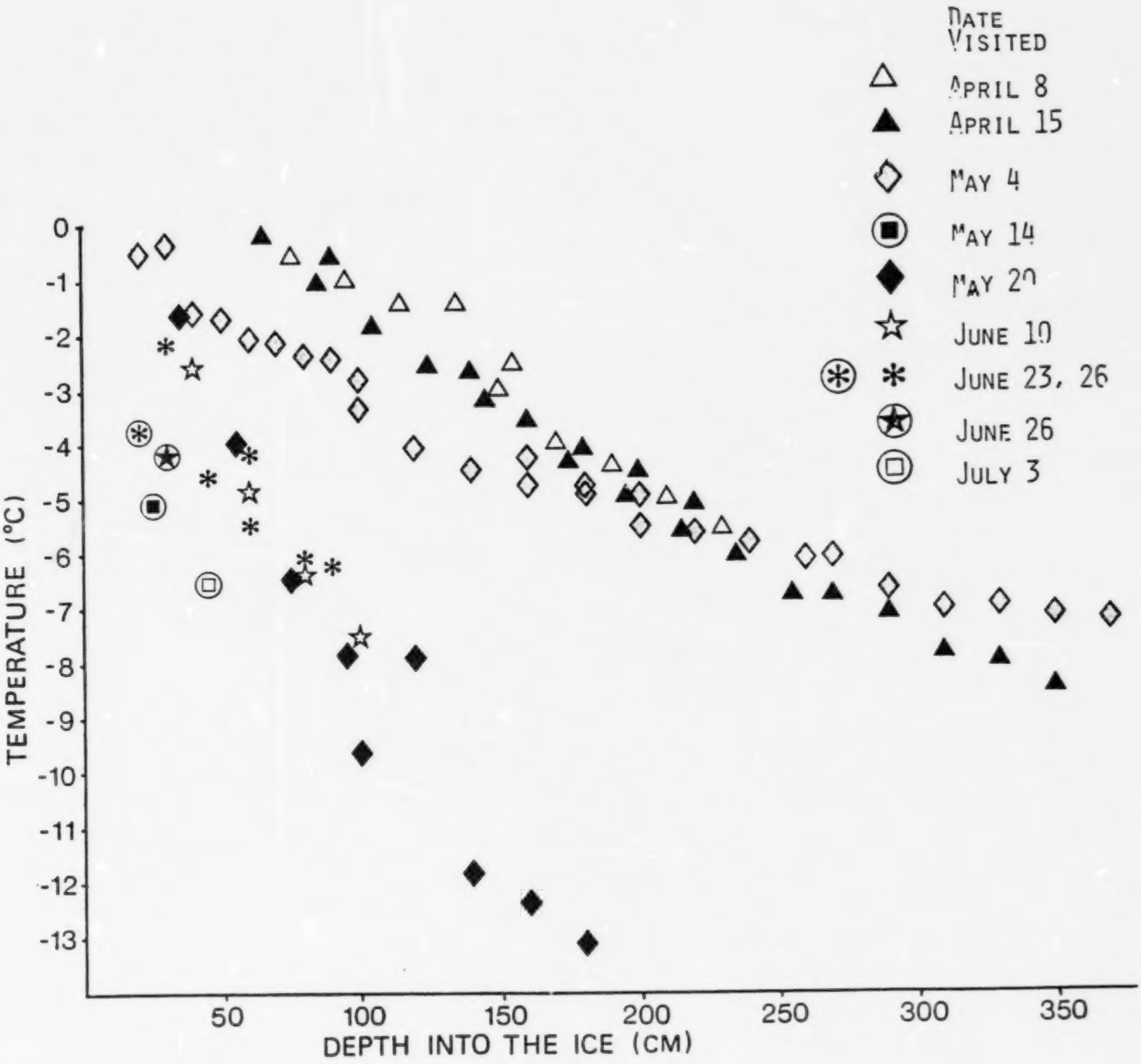

Figure 17. Temperature data obtained from icebergs near St. John's, Nfld., 1983. (Diemand, 1984)

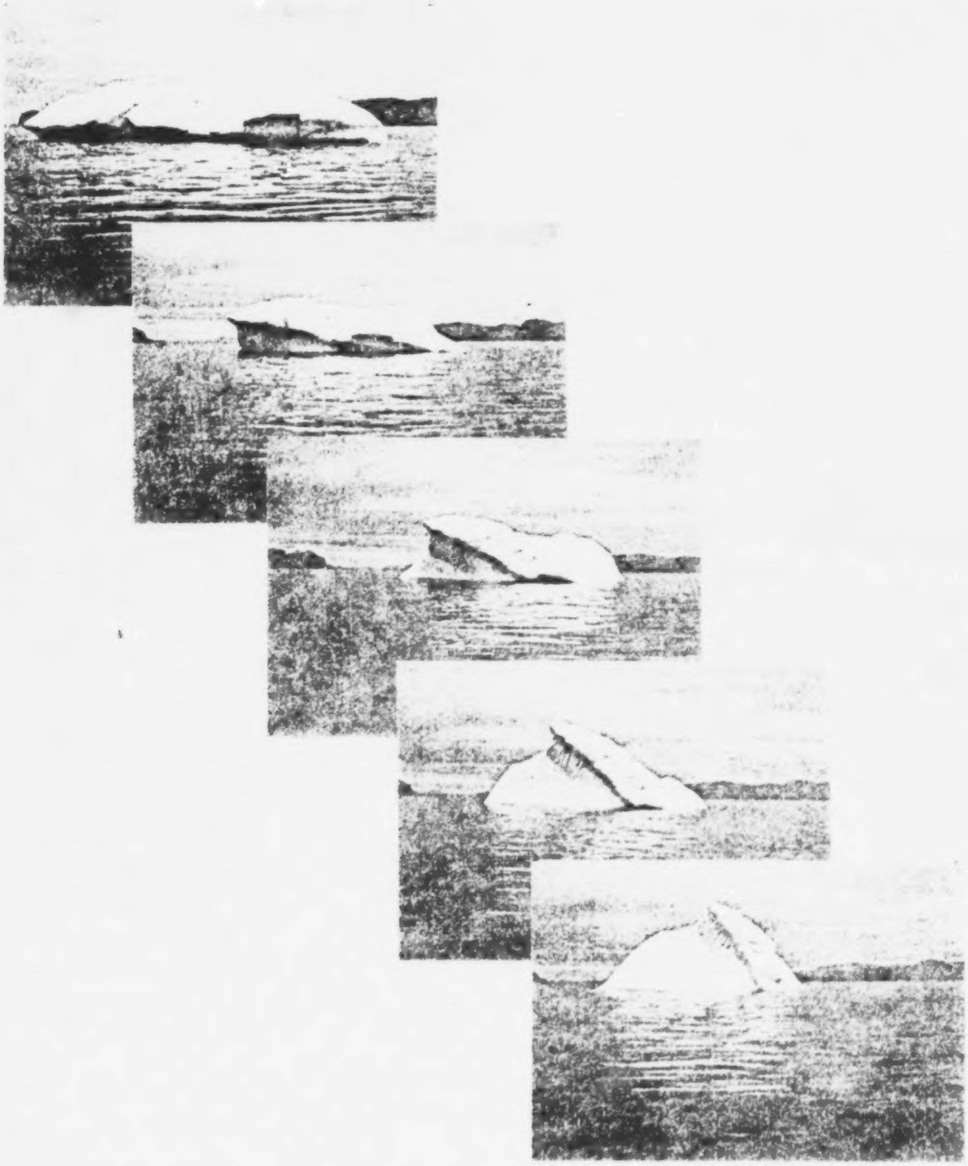

Figure 18. Iceberg rolling (C-CORE photos)

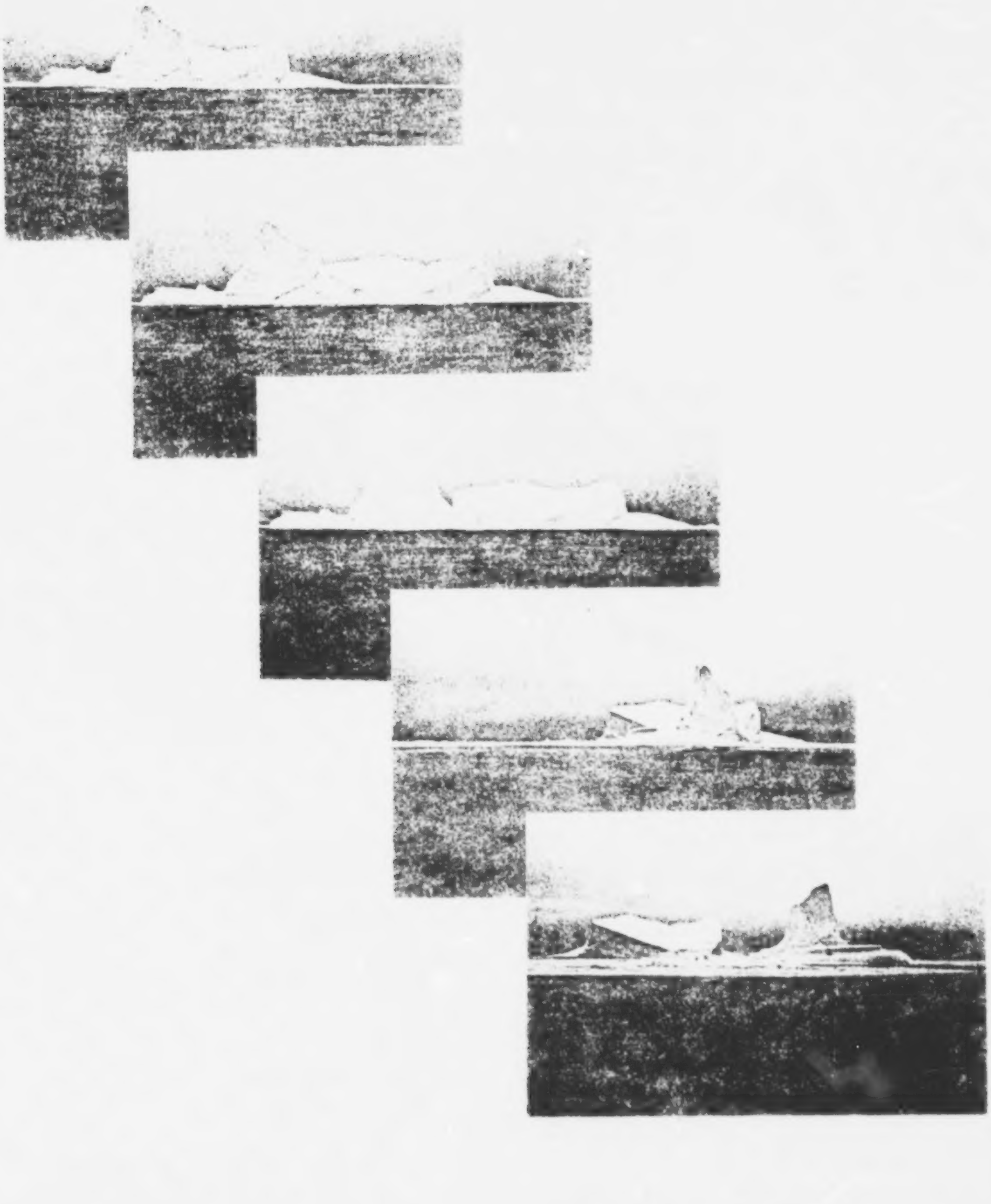

Figure 19. Iceberg splitting (C-CORE photos)

The approximate values associated with each of them show that thermal stresses are of the same order of magnitude as the tensile strength of ice. Next in magnitude are the stresses created by buoyancy forces which act on the underwater rams that tabular icebergs develop as they are eroded by waves.

	Expected Magnitudes	Occurrence in the ice	Governing factors	Probable Variability
Residual	0.1 MPa	Widespread	Glacier history	Unknown
Hydrostatic	small	Widespread	Iceberg history	Moderate
Thermal	2 MPa	Local	Water temperature	High
Buoyancy	0.5 MPa	Local	Underwater shape	High

Table 1. Types of stresses present in an iceberg. (Diemand *et al.*, 1987)

3.4 Velocity

The best data available on iceberg velocities are derived, for most of them, from tracking obtained on an hourly basis. Most authors (Berenger and Wright, 1980; Ball *et al.*, 1981) agree on average values about 0.2 m/s and maximum around 1.0 and 1.2 m/s. These values are obtained by assuming that icebergs travel along a straight line between two readings. Figure 20 shows how far from a straight line an iceberg track can be (Ball *et al.*,1981). Icebergs were observed to move in loops and spiral erratically (probably due

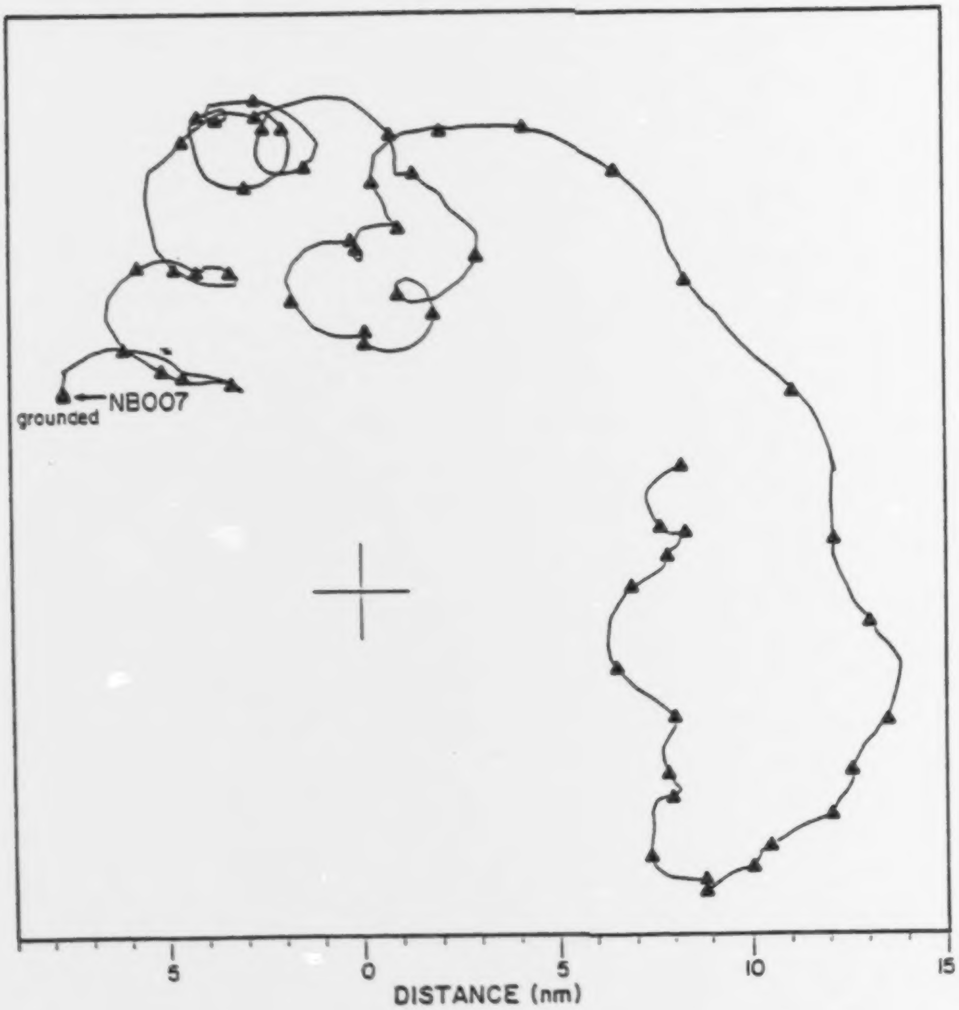

Figure 20. Track of iceberg (▲ are 6 hours apart) (Ball et al., 1981)

to tidal currents and Coriolis acceleration) and reverse the direction of their motion with no warning.

El-Tahan and El-Tahan (1983) have analyzed data obtained from 266 icebergs tracked at wellsites in 1978-79. The exceedence diagram (Figure 21) shows that about half of the iceberg population exhibit grounding at one time. From this set of data the highest recorded speed is 1.3 m/s. It should be noted that 7% of the total population reach speeds over 1 m/s. The authors infer from these results that the length of the iceberg trajectory is, in general, about 1.6 times the length of the straight line joining the trajectory ends.

As mentioned earlier the values presented above are average hourly drift speeds. In models of iceberg-structure interaction like those presented by Bass *et al.* (1985) and Arockiasamy *et al.* (1985), the force exerted on the structure is dependent on the velocity. What is needed in the model is the instantaneous velocity which can be dramatically different from the average drift speed of the berg. Large iceberg are not very sensitive to rough sea state but growlers and bergy bits can have their velocity substantially increased by swell. Sea state modifies the iceberg velocity in magnitude and direction. Lever and Sen (1986) present a model which takes into consideration the contribution of the significant surge velocity V_S of a given sea state. They define the total velocity V_T of the iceberg as being:

$$V_T = V_D + V_S$$

where V_D is the drift speed of the berg.

Figure 22 shows the total velocity exceedence curves for various sizes of icebergs. It is quite interesting to notice that the 1% exceedence velocity for a 600 tonne growler would be 2.14 m/s (i.e. 330% increase over the value based on drift velocity alone). For the same 1% exceedence, a 1 million tonne iceberg would see a 20% increase of its speed. Results of this type are extremely important for design criteria of floating or fixed platforms, but more work is needed in this direction.

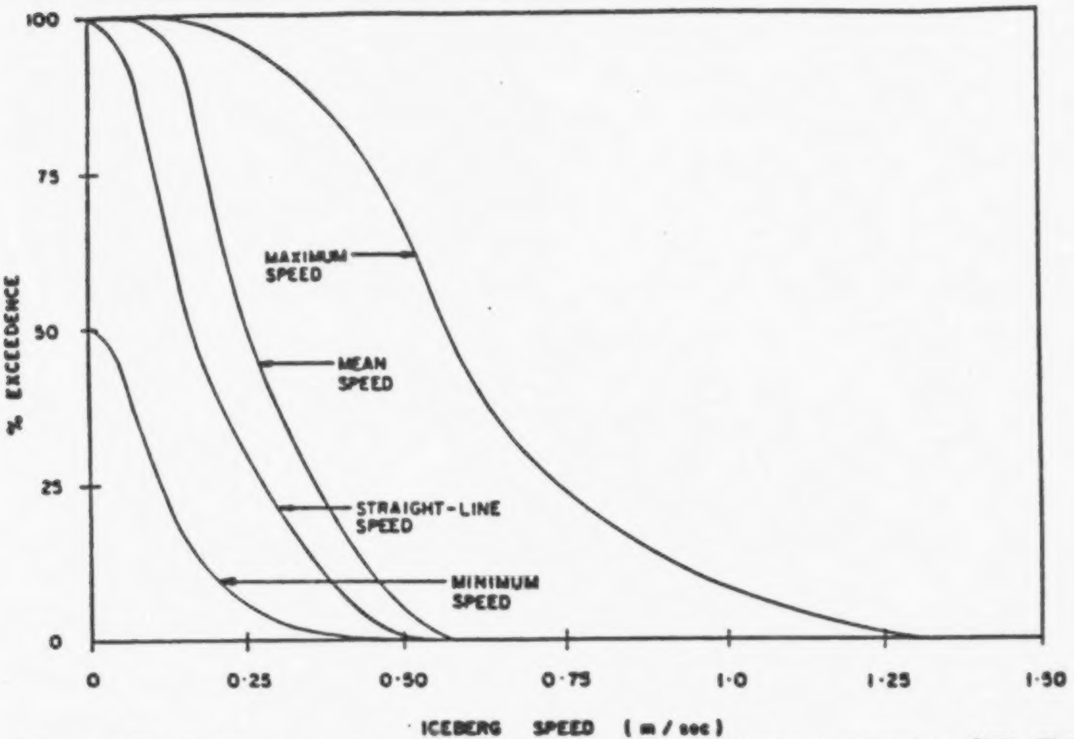

Figure 21. Drift speeds of 266 icebergs offshore Labrador (El-Tahan and El-Tahan, 1985)

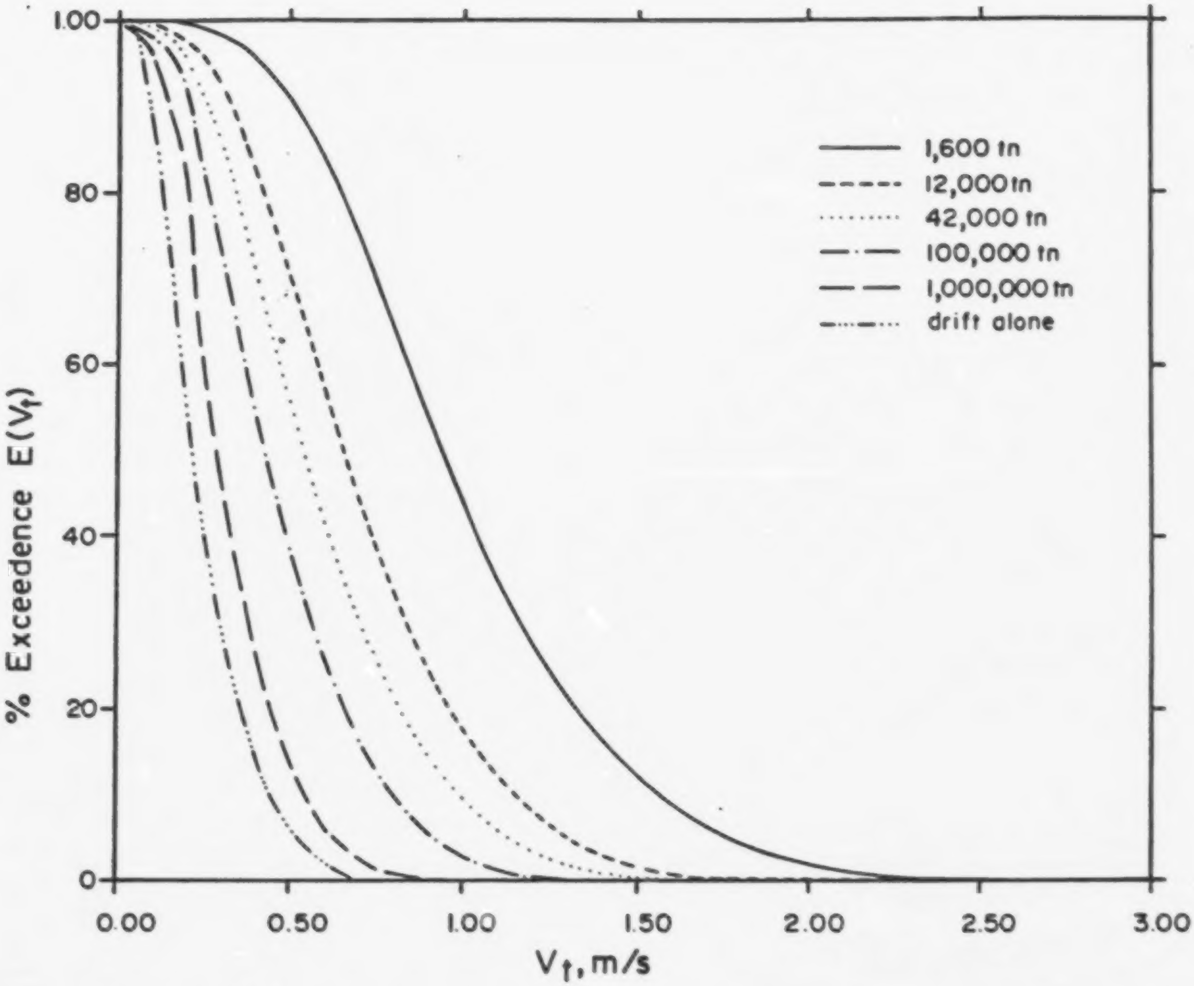

Figure 22. Total velocity exceedence curves. (Lever and Sen,1985)

4.0 Mechanical properties

Literature on mechanical properties of iceberg ice is rather scarce. As mentioned by Weeks and Mellor (1984), properties of most antarctic icebergs can reasonably be inferred from the properties of the parent shelves which are well documented. On the other hand, arctic icebergs calve from glaciers which have experienced strong deformation, resulting in recrystallization of the initial glacier ice. Changes in both the crystal orientation and the grain size are known to affect the mechanical characteristics and behaviour of ice.

4.1 Crystallography

The recrystallization of the ice can be visualized on the thin section presented in Figure 23 and in the fabric diagrams shown in Figure 24. The first diagram shows an extremely strong c-axis alignment; the second one exhibits a multimaximum pattern typical of Alpine glaciers. However, the last two diagrams have no definite orientation, indicating clearly that generalizations cannot be made on iceberg c-axis orientation.

Recrystallization is usually associated with a significant change in the crystal size. In Figure 23, it can be seen clearly that the crystal can be fairly large. Individual grain size can be several centimetres wide, leading to average grain size around one centimetre. Figure 25 shows a histogram representing the frequency distribution of iceberg ice grain size within a sample (Arockiasamy *et al.*, 1983).

One of the main characteristic feature of iceberg ice is the presence in the grains of elongated bubbles. These typical bubbles can be seen in Figure 23. They have diameters up to 0.2 mm and lengths up to 4 mm (Scholander and Nutt, 1960). The air which is in

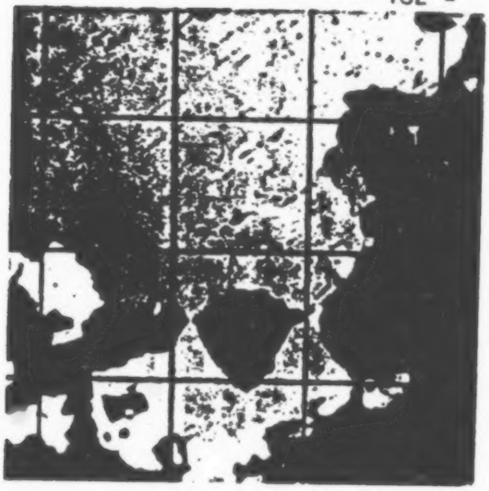

Figure 23. Iceberg ice (Nadreau, 1985)

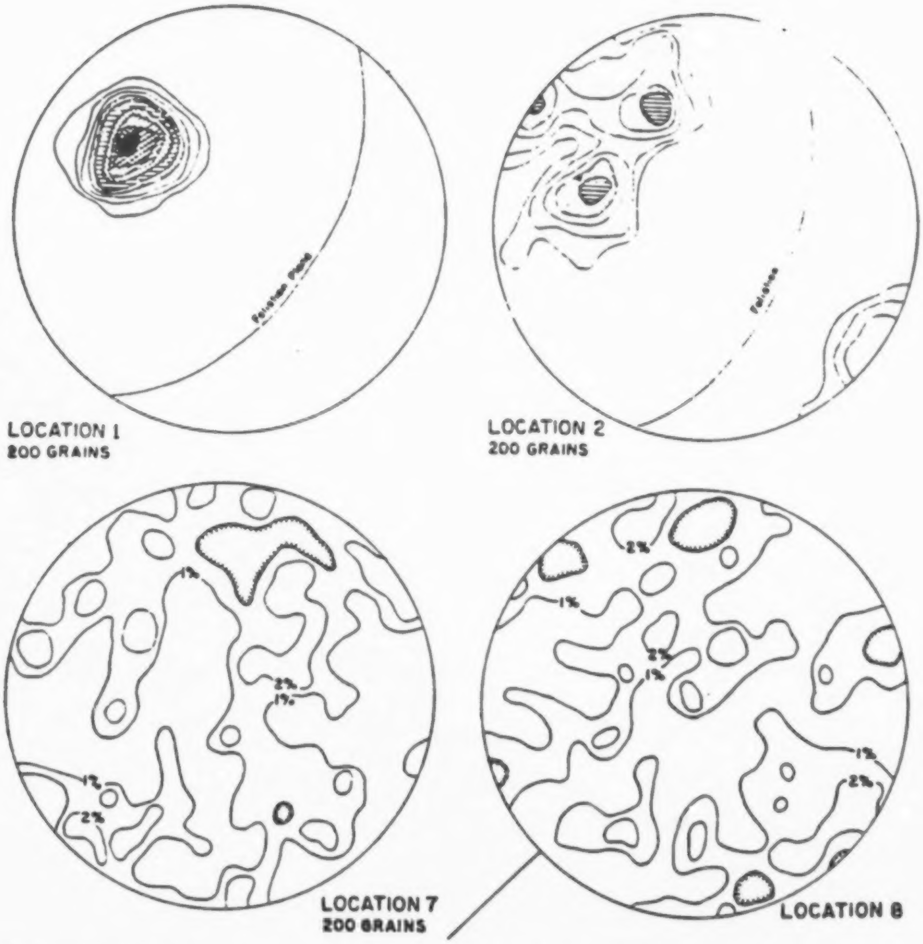
Foliation Plane
Foliation
LOCATION 1
200 GRAINS
LOCATION 2
200 GRAINS
1%
2%
1%
1%
2%
LOCATION 7
200 GRAINS
2%
1%
2%
1%
1%
2%
LOCATION 8

Figure 24. Four fabric diagrams of c-axis orientations in glacier ice from sites along the margin of the Greenland Ice Sheet (Rigsby, 1955 in Weeks and Mellor, 1984)

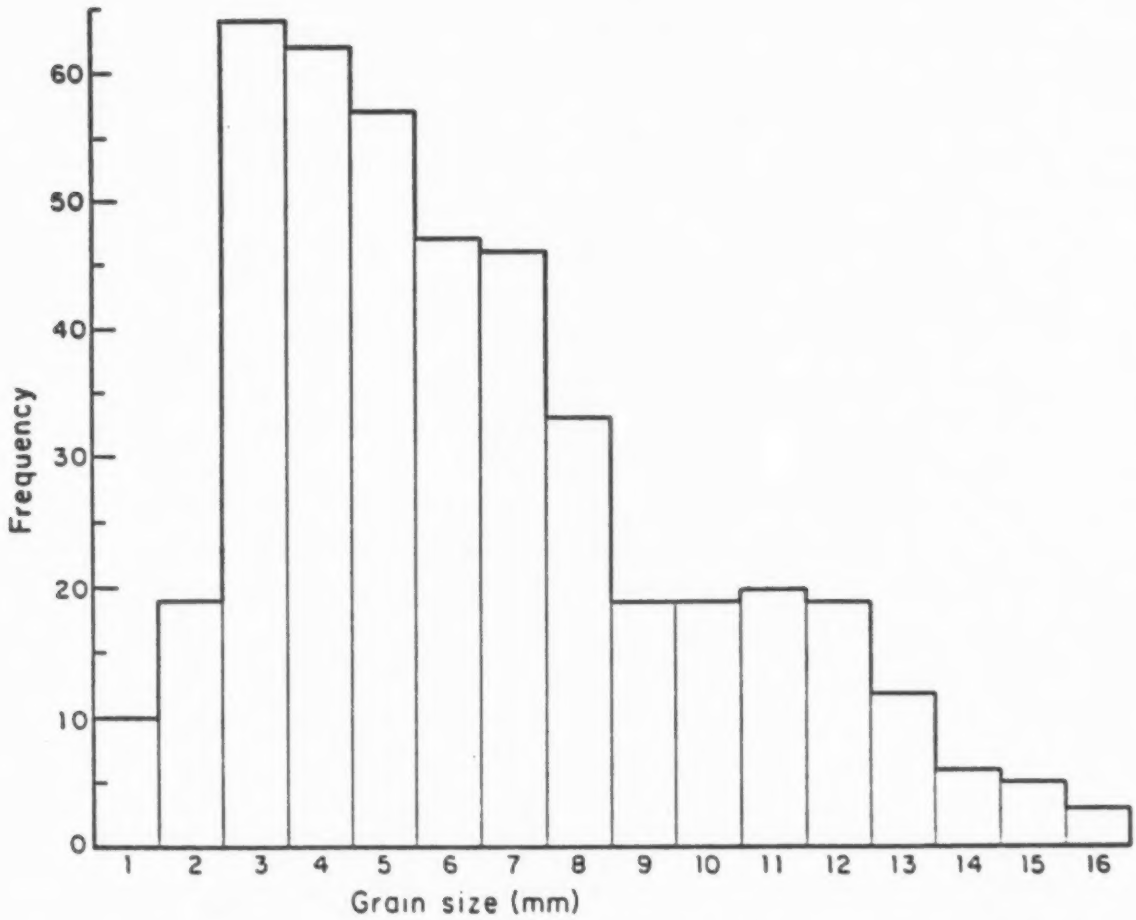

Figure 25. Frequency distribution of iceberg ice grain size. (Arockiasamy et. al., 1983)

these bubbles has been entrapped when the snow became ice. Depending on the depth at which the bubbles were located when the iceberg calved from the parent glacier, the pressure in these bubbles can be between .2 and 2 MPa. The tubular shape of the bubbles is due to the surrounding stress state. Nakawo and Wakahama (1981) obtained the same type of elongated bubbles when they applied a biaxial compression on an prismatic ice sample. The long axis of these elongated bubbles developed in the direction of free expansion. The presence of pressurized gas in the ice is probably one of the distinctive features of iceberg ice and it must be taken into consideration when analyzing its mechanical behaviour.

Entrapped air affects the density of the ice. Pure ice is known to have a density of 0.9167 Mg/m^3 (Hobbs, 1974). Density of iceberg ice is found to be as low as 0.88 Mg/m^3 (Lachance, 1985) which corresponds to a volume of entrapped air around 6-7%.

4.2 Uniaxial compressive strength

As already mentioned, the data available on iceberg ice is rather limited. Published results lead to a value for uniaxial compressive strength between 5 and 7 MPa at a temperature of -5 C and a strain rate of 10^{-3} s^{-1}. Figures 26 and 27 present the available results from various studies. They show the well-known dependency of ice strength on strain rate. The data have been divided in two sets on a temperature basis, although temperature does not seem to have a great influence in that range. The effect of temperature can be seen at lower temperatures as shown in Figure 28.

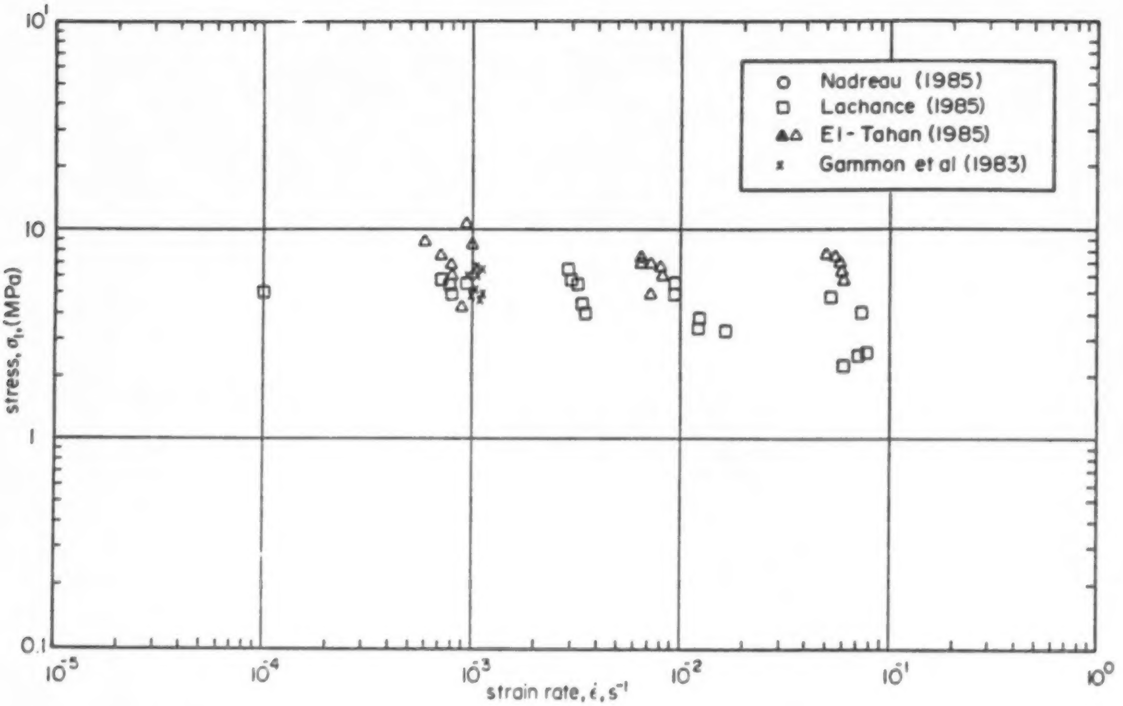

Figure 26. Stress dependence on strain rate, iceberg ice, $\theta = -5°C$

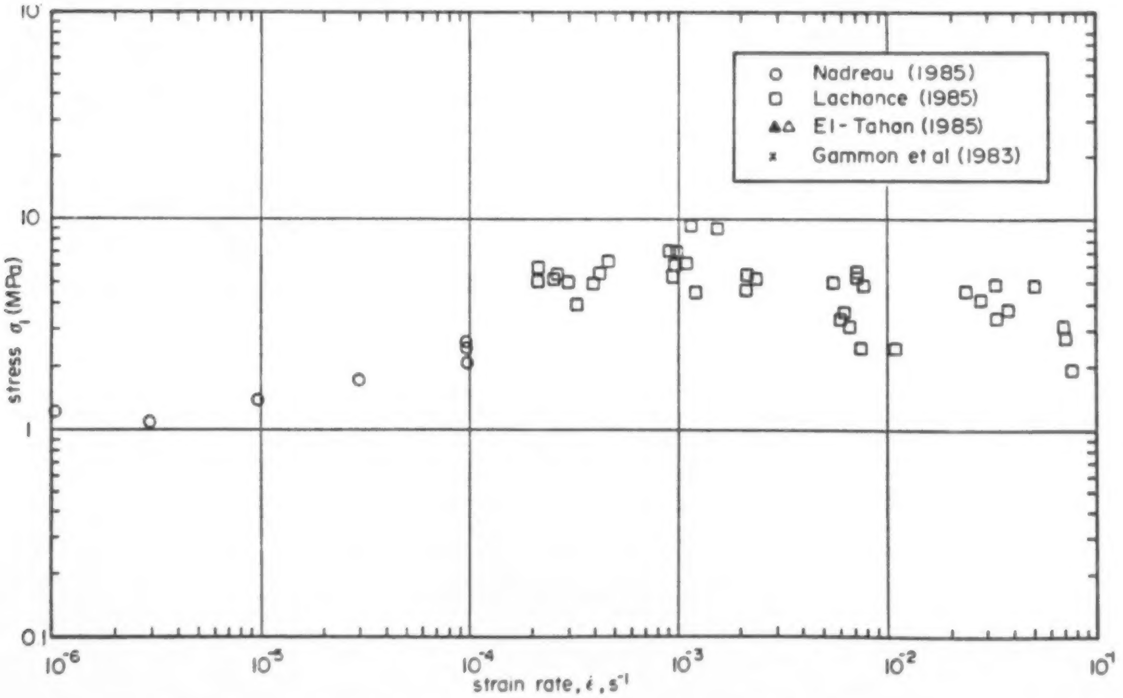

Figure 27. Stress dependence on strain rate, iceberg ice, $\theta = -10°C$.

4.3 Confined compressive strength

A few triaxial tests have been performed on iceberg ice (Nadreau, 1985). The confined behaviour of iceberg ice seems quite comparable to other types of ice. Glen's exponent has been found to be 3.22 in the strain rate range of 10^{-6} to 10^{-4} s^{-1} and for a confining pressure of 30 MPa (Nadreau and Michel, 1986). It is interesting to plot these results with those obtained by El-Tahan (1985) for indentation tests. He used a cylindrical indentor on blocks of iceberg ice which were either confined or unconfined. The open triangles (Figure 29) represent averages of the tests performed on confined blocks and the solid triangles, the results on unconfined blocks. The small number of data points and the different origins of the two sets of data should be noted. However, the "continuity" between the two sets and the effect of confinement created by the indentor is worth noting.

Some impact tests have also been carried out by El-Tahan *et al.* (1985). The maximum (average of seven values) was 17.35 MPa. The relation between this type of tests and uniaxial compressive strength of ice is not clearly established yet (Nevel, 1986).

5.0 Conclusion

Such a review paper shows clearly our limited knowledge about icebergs.

A great deal of information is needed on the morphological features of icebergs, especially their underwater shapes which are difficult to estimate. This morphological characteristic is extremely important since this is the part of the iceberg which will scour the seabed or hit the offshore structure.

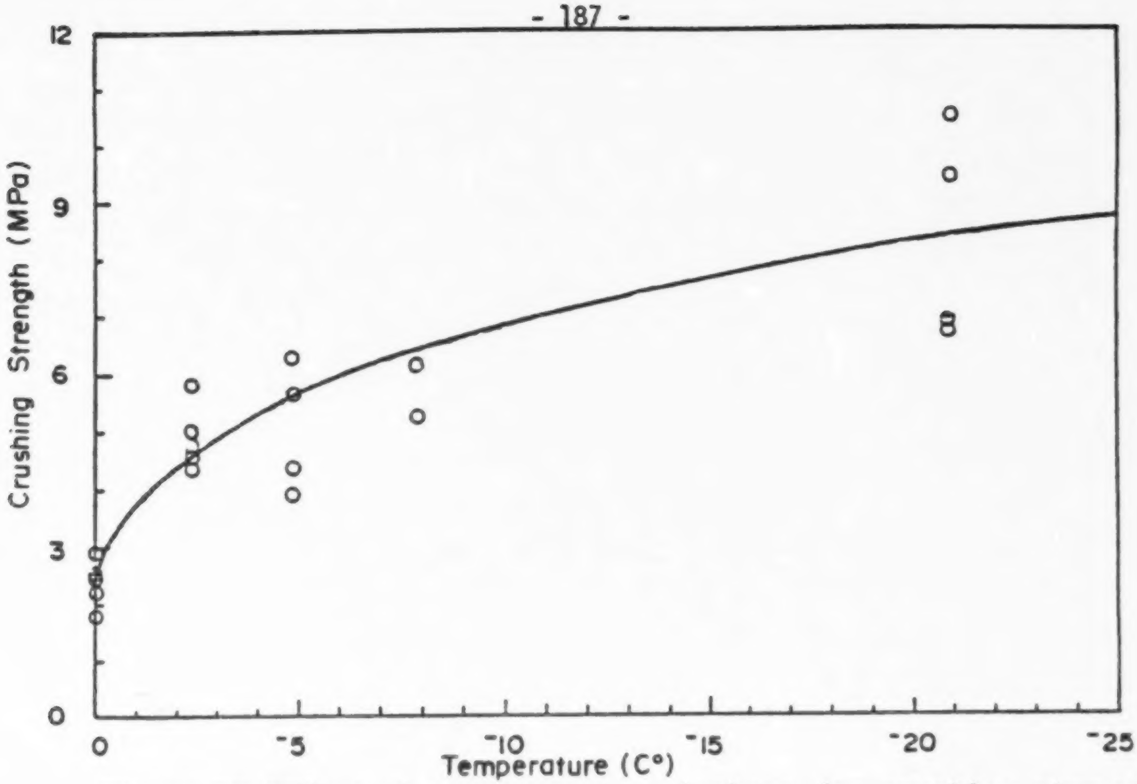

Figure 28. Effect of temperature on iceberg ice crushing strength. (Lachance, 1985)

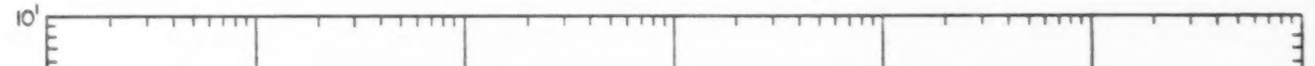

Figure 29. Stress dependence on strain rate, indentation and confined tests, iceberg ice.

The known velocities of icebergs are only approximated and to date, no instantaneous values in various sea states are available from field experiments. When used in models of iceberg-structure interaction, velocities are elevated to the power square when used in kinetic energy.

The iceberg strength at high strain rates and for large area of impact is virtually unknown.

It is these unknowns which make icebergs so threatening. The image is probably too easy but it is obvious that we know only "the tip of the iceberg". A lot of work is still needed to master these mastodons and to manage them in such a way that they do not endanger human life.

Acknowledgements

C-CORE would like to thank the Institute for Marine Dynamics for its financial support to the author for the preparation of this paper.

6.0 References

Anderson, I. (1983) "Oceanographic conditions on the Grand Banks during the 1983 International Ice Patrol season" Report of the International Ice Patrol in the North Atlantic, Bulletin No. 69, pp 51-66.

Arockiasamy, M., El-Tahan, H. and Swamidas, A.S.J. (1983) "Strength of iceberg and artificial snow ice under simulated impact loads" Faculty of Engineering and Applied Science, Memorial University, St John's, Newfoundland.

Arockiasamy, M., Swamidas, A.S.J., and El-Tahan, H. (1985) "Response of offshore structure to bergy-bit and iceberg impacts" Behaviour of Offshore Structures, Delft, The Netherlands, Proceedings, pp 951-961.

Ball, P., Gaskill, H.S. and Lopez, R.J. (1981) "Iceberg motion: an analysis of two data sets collected at drill sites in the Labrador sea" C-CORE Publication 81-2.

Bass, D., Gaskill, H. and Riggs, N. (1985) "Analysis of iceberg impacts with gravity base structures at Hibernia" OMAE 85, Dallas, Texas, Proceedings, Vol 2, pp 255-259.

Bass, D.W. and Peters, G.R. (1984) "Computer simulation of iceberg instability" Cold Regions Science and Technology, Vol 9, pp 163-169.

Berenger, D. and Wright, B.D. (1980) "Ice conditions affecting offshore Hydrocarbon production in the Labrador sea" Intermaritec'80, Hamburg, Germany, Proceedings, pp 390-402.

Diemand, D. (1984) "Iceberg temperatures in the North Atlantic-theoretical and measured" Cold Regions Science and Technology, Vol. 9, pp 171-178.

Diemand, D., Nixon, W.A. and Lever, J.H. (1987) "On the splitting of icebergs - Natural and induced" OMAE 87, Houston, Texas, Proceedings (in press).

El-Tahan, H.W. (1985) Dynamic response of a hydroelastic model of a typical semi-submersible to wave and bergy-bit impact" Ph.D. thesis, Memorial University, St John's, Newfoundland.

El-Tahan, M.S. and El-Tahan, H.W. (1983) "Forecast of iceberg ensemble drift" OTC 83, Houston, Texas, Proceedings, pp 151-158.

El-Tahan, H., Swamidas, A.S.J. and Arockiasamy, M. (1985) "Impact strength of iceberg and artificial snow ice" Canadian Coastal conference, St John's, Newfoundland, Proceedings, pp 363-381.

Fissel, D.B. (1981) "Data report No. 7, Satellite-tracked iceberg movements in Baffin Bay and Lancaster Sound, Summers 1978 and 1979" Report prepared for Petro-Canada by Arctic Sciences.

Gammon, P.H., Gagnon, R.E., Bobby, W. and Russell, W.E. (1983) "Physical and mechanical properties of icebergs" OTC 83, Houston, Texas, Proceedings, Vol 1, pp 143-150.

Gaskill, H.S., Terry, B. and Riggs, N. (1984) "Forecasting iceberg drift: a comparative study" Iceberg Research, No. 7, pp 8-13.

Gustajtis, K.A. and Buckley, T.J (1977) "A seasonal iceberg density distribution along the Labrador coast" POAC 77, St John's, Newfoundland, Proceedings, pp 972-983.

Hobbs, P.V. (1974) "Ice physics" Clarendon Press, Oxford, 837 p.

Holdsworth, G. (1977) "Some mechanisms for the calving of icebergs" Iceberg Utilization, Pergamon Press, pp 160-175.

Ketchen, H.G. (1977) "Iceberg population south of 48°N since 1900" Report of the International Ice Patrol in the North Atlantic, Bulletin No. 63.

Ketchen, H.G. and Hildenbrand, R.N. (1977) "Unusual iceberg sighting" Report of the International Ice Patrol in the North Atlantic, Bulletin No. 63.

Lachance, J. (1985) "Etude du comportement fragile de la glace d'iceberg et de la glace columnaire d'eau douce" M.Sc. thesis, Civil Engineering Department, Laval University, Quebec City.

Lever, J.H. and Sen, D. (1986) "A method to upgrade iceberg velocity statistics to include wave-induced motion" OMAE 86, Tokyo, Japan, Proceedings, Vol. 4, pp 320-327.

Mangor, K. and Zorn, R. (1983) "Iceberg conditions offshore Greenland" Iceberg Research, No. 4, pp 4-20.

Mocks, S.J. and Weeks, W.F. (1965) "The distribution of 10-metre snow temperatures on the Greenland ice sheet" U.S. Army CRREL Research Report 170, Hanover, N.H.

Nadreau, J.P. (1985) "Lois de comportement et de fluage de la glace granulaire simulée de crêtes de pression" Ph.D. thesis, Civil Engineering Department, Laval University, Quebec City.

Nadreau, J.P. and Michel, B. (1986) "Yield envelope for confined ice" ITC 86, MIT, Cambridge, Mass., Proceedings, pp 25-36.

Nakawo, M. and Wakahama, G. (1981) "Preliminary experiments on the formation of elongated air bubbles in glacier ice by stress"

Journal of Glaciology, Vol. 27, No. 95, pp 141-146.

Nevel, D.E. (1986) "Iceberg impact forces" IAHR 86, Iowa City, Iowa, Proceedings, Vol. 3.

Reddy, D.V., Bobby, W., Arockiasamy, M and Dempster, R.T. (1980) "Viscoelastic analysis of calving glaciers" Annals of Glaciology, Vol. 1, pp 37-41.

Reeh, N. (1968) "On the calving of ice from floating glaciers and ice shelves" Journal of Glaciology, Vol. 7, pp 215-232.

Robe, R.Q. (1980) "Iceberg drift and deterioration" in Dynamics of Snow and Ice Masses, Academic Press, Inc., pp 211-259.

Scholander, P. and Nutt, D.C. (1960) "Bubble pressure in Greenland icebergs" Journal of Glaciology, Vol. 3, pp 671-678.

Soulis, E.D. (1975) "Modelling of drift of nearby icebergs using wind and current measurements at a fixed station" Canadian Society of Petroleum Geologists, Mem. 4, pp 879-889.

Sutton, J. and Mudry, D. (1983) "Iceberg distribution in the Labrador Sea from SLAR imagery 1978 to 1980" POAC 83, Helsinki, Finland, Proceedings, pp 214-221.

Thayer, N. (1984) "Effects of Side Looking Airborne Radar (SLAR) on iceberg detection during the 1983 and 1984 International Ice Patrol seasons" Report of the International Ice Patrol in the North Atlantic, bulletin No. 70, pp 69-74.

Weeks, W.F., and Mellor, M. (1984) "Mechanical properties of ice in the arctic seas" in "Arctic Technology and Policy", Hemisphere Publishing Corp., pp 235-259.

FRACTURE MECHANICS AND DAMAGE THEORY AS A BASIS FOR CALCULATION OF ICE-STRUCTURE LOADS

Ian J. Jordaan

Faculty of Engineering and Applied Science, Memorial University of Newfoundland, St. John's, Newfoundland, Canada

ABSTRACT

Most events observed in large scale ice-structure interaction occur at high enough velocities to cause the ice to fracture. This occurs as propagation of tension cracks or as crushing of ice where the stresses are compressive. Analysis of the former can be carried out by linear elastic fracture mechanics; complex geometries and boundary conditions can be studied using finite element methods. A promising direction for analysis of compressive crushing lies in the area of damage mechanics, particularly using shear damage models. Crushed ice can be modelled as a viscoplastic extruding material. These directions of research are discussed as well as the implication for ice-structure interaction. The alternating crushing and clearing process in ice is of great importance and provides an explanation for reduced average ice pressures as well as dynamic action excited during the ice-structure interaction process. The excitation could result from cycles of ice crushing and clearing.

OVERVIEW AND MOTIVATION

The interaction of large ice features and fixed offshore structures poses some interesting problems in mechanics. Figure 1 illustrates some of these in a schematic manner (from Jordaan, 1986). Ice features are observed to split, with large tensile cracks appearing, Figure 1(a); crushing is observed along the interface of the structure and the ice feature, Figure 1(b); and flexural failures are observed in areal ice features, Figure 1(c). The present paper is concerned with the first two of these phenomena.

An important aspect to be considered along with the above is the clearing of the ice. Since the fracture events of Figure 1 occur generally in a sporadic manner, there is also the clearing process to be studied. In Figure 1(a), the large fragments of the floe are able to clear around the structure after the main crack has propagated sufficiently to create separate pieces. The process of clearing of the crushed ice, in Figure 1(b), is of particular importance, since it provides the explanation for the fact that the average pressure along the face of the structure is lower than the ice crushing strength. Since the crushing (pulverisation) events in the ice feature are generally non-simultaneous, and localised along the face of the structure, and also, as noted, sporadic, the average pressure is the average of a few crushing events and many clearing events. The clearing

Combining equations (1) and (2), we have (with the occurrence of a fracture event):

$$K_{1C}^2 = EG_{1C} \cdot \qquad (3)$$

The value of fracture toughness is determined by experiment and depends on the stress state, which affects the ease with which a crack will propagate; see for example Sih (1973). The critical flaw will have the combination of length and orientation which gives the lowest value of stress for all cracks in the sample of material in the body under consideration (at lower stresses, the material will creep without fracture). Generally the critical crack will propagate right through the specimen, leading to failure.Values of G_{1C} as well as surface energy (γ_s) are given in Table 1. It is apparent from this and other comparisons that ice is one of the most brittle materials on earth.

Table 1

Material	$2\gamma_s$ (both in J/m^2)	G_{1C}	$G_{1C}/(2\gamma_s)$ Approx.
Glass	0.5-0.6	2-4	2-5
Steel (Mild) at 0°C	36	43,200	1,200
Ice	0.2	1-2	5-10

process for crushed ice is a process of squeezing out of the crushed ice. This has been observed to result in 10 m high piles of "tooth-paste like" material, around the Molipaq structure in the Beaufort Sea during the 1985/86 winter, when a multiyear ice floe surrounded by first year ice interacted with the structure. The crushing process in reality involves two aspects

- the process of damage and fracture of the ice, and
- the subsequent process of ice clearing.

Before going into these aspects in more detail, global (tensile) cracking will be discussed.

GLOBAL (TENSILE) FRACTURES

Although ice creeps at any stress state or level, apart from purely hydrostatic states, it is usually dominated by the propensity to fracture. Under tensile states of stress, the critical flaw of length (2a) as shown in Figure 2 will propagate at a stress given by:

$$\sigma = \sqrt{(EG_{1C}/\pi a)} \qquad (1)$$

where E = elastic modulus, G_{1C} = energy requirement per unit area of crack and is essentially a material constant.

The original Griffith concept suggested the use of surface energy for G_{1C}, but it has been subsequently established that work is also expended in creep (plastic) deformation in the crack tip zone. Ice is brittle enough to make the assumption that this zone is small and to include the work in the energy requirement, that is, in G. For analysis purposes, it is appropriate to calculate the energy released during the perturbation of a crack length using linear elastic fracture mechanics (LEFM).

For a sharp crack in a wide plate under tension, the stress intensity factor K_1 is given by:

$$K_1 = \sigma\sqrt{\pi a} \qquad (2)$$

i.e. all stresses in the region of the crack are amplified in proportion to $a^{1/2}$. Experimentally it is found that the stress at which a crack becomes unstable occurs at a value of $K_1=K_{1C}$, the fracture toughness, which is essentially a material constant. Measurements of fracture toughness for ice have been carried out and reported by several investigators. Hamza and Muggeridge (1979) reviewed previous measurements and reported results of their own experiments. Other investigations of note have been carried out by Goodman (1980) and by Timco and Frederking (1983), the latter being concerned with sea ice.

In summary of the above, existing flaws or cracks will propagate at a value $(\sigma\sqrt{a})$ = constant. Clearly the flaw structure in field ice is of importance, dictating statistical distributions of "a"; other aspects such as the sharpness of crack tips "in nature" are of importance.

Analysis of crack propagation can be carried out in closed form for certain idealized crack and ice feature geometries (see Palmer et al., 1983, for an application). More generally, numerical methods are used; Figure 3 shows a typical finite element mesh around a crack, in which the propagation was studied using J-integral methods (Tomin et al., 1985).

Analysis of the kind just noted is potentially of great importance in studying improved ice-breaking techniques: various bow forms could be modelled and the potential for failing and splitting ice features evaluated.

CRUSHING OF ICE

Crushing describes the pulverisation of ice in predominantly macroscopically compressive fields of stress, by the joining together of myriads of cracks so that the crushed ice particles attain the possibility to move as separate entities. They eventually no longer form a solid continuum and behave more as a viscous fluid (Kheisin and Likhomanov, 1973; Kurdymov and

Kheisin, 1976; Likhomanov and Kheisin, 1971). The process of transformation of the virgin ice to a powder can be appreciated quite vividly by contrasting the final crushed ice with the initial solid ice mass. This process is one of progressive damage.

THE DAMAGE PROCESS

The heterogeneous structure of many materials includes dislocations, grain boundaries, microcracks and voids. These propagate and develop under compressive stresses. The propagation of large cracks in tension is not the concern of the present section - this has been considered above. Rather, the system of microcracks that develop under compressive stresses is the subject of the present discussion. An excellent study of crack development with time in ice under compressive states of stress was conducted by Gold (1972).

Consider a specimen of material, such as concrete, rock, or as we have seen ice, loaded in compression. If one subjects the material to a small increment of stress or strain, there can be several effects on the material. There may be an increase or decrease in elastic strain energy; there may be irreversible movements associated with creep or plastic flow; last, the microcrack system may extend and new microcracks could be nucleated: this is the essence of the damage process. Generally, the crack growth will be stable so that damage increases in a relatively orderly manner.

It is important to recognize that elasticity, creep or plastic flow do not of themselves result in material damage or degradation. Storage of elastic strain energy is a reversible process without any effect on the structure of the material. On the other hand, creep and plastic flow are irreversible (involving heat generation); nonetheless the structure of the material is restored after the movement of dislocations. Gross deformations will lead eventually to damage but this is not associated with the process itself. Further discussion regarding creep is appropriate. It is all too common in the literature in ice engineering to refer to creep and plasticity as if they were separate phenomena. In broad outline, both are associated with slip movements in which work is done in translating atoms along slip planes. The movements result from shear stress and are aided by movements of dislocations. Translational symmetry and periodicity of crystals results in restorability of structure. Grain boundary sliding is a special mechanism associated with primary creep (Sinha, 1984).

For materials at high homologous temperatures (such as ice) the movements discussed do not require a constant yield stress to be activated, and there is no evidence of such a yield stress for ice. The creep movements occur at all stresses, with a distinct non-linearity with stress. The secondary creep rate ϵ follows the relationship $\dot{\epsilon}=k\sigma^n$ where k and n are constants. There is therefore no point in developing yield surfaces, which would *ipso facto* be different for each strain rate.

The mechanism for the progress of damage above involves changes to the structure of the material; as the density and size of cracks increases, the response of a specimen of macroscopic size changes. Figure 4 shows the changes in the stress-strain curve for concrete under successive load cycles. This phenomenon is exhibited by many materials with a strain-softening descending branch, and one such material is ice. The damage can occur at a fast rate, without substantial time-dependent response of the ice, or slowly, leading to a gradual development of damage with time. In this case, the damage is referred to as creep damage (Leckie, 1978) although the resulting change to the material is damage, not creep (which occurs simultaneously).

ROLE OF ENERGY

It is appropriate to study the present subject with some of the fundamentals in mind. In particular, the behaviour of ice and other brittle materials depends very strongly on the amount of energy transferred to it during a given time interval. The first law of thermodynamics states that, for a given volume of material and interval of time:

$$dE = dW + dQ \qquad (4)$$

where dE = increase of internal energy of the volume

dW = work done on the volume by its surroundings, and

dQ = heat received by the volume from its surroundings.

The term "dW" causes profound changes to the behaviour and nature of the material so that it is preferable and convenient to consider small intervals of time, and also to consider small volumes of material (although this is not necessary, for the validity of equation (1)). The rate of work (power) by surface tractions on a small volume of material is readily calculated by means of the flux of mechanical energy $\vec{w}$ (Love, 1927; Bridgman, 1941) as -div $\vec{w}$ multiplied by the small volume ($dV=dx_1dx_2dx_3$) where the flux $\vec{w}$ is given by the vector with components $w_i=(-\sigma_{ij}\ v_j)$, $i=1,2,3$. The notation for stress is different from Love's; the first subscript i in σ_{ij} corresponds to the plane ($i=1,2,3$) under consideration. The energy entering a volume V in unit time ($\dot{W}=dW/dt$) is given by

$$\dot{W} = -\int_S \vec{w}.\bar{n}\ ds = -\int_V \mathrm{div}\ \vec{w}\ dV = \int_V (\sigma_{ij}v_j)_{,i} dV \qquad (5)$$

where $\bar{n}$ is the outward unit normal at the point under consideration and S denotes the surface of V.

In the present instance, we are less concerned with heat being transferred to our specimen than with the work term of equation (5), and the effect of the work done on a small volume of material in a unit of time will be considered. As noted in the preceding section, this will result in the following effects:

(1) There can be an increase in the elastic strain energy (basically an increase in internal energy).

(2) The work can be dissipated as heat during creep processes. These do not usually result per se in substantial changes to the structure of the material, although grain boundary sliding leads to stress concentrations and consequent crack initiation.

(3) The work can be used in processes resulting in damage to the material. We will be concerned primarily with the creation of new surfaces by cracking.

The damage processes discussed (item (3) above) represent a distinct case: the work is largely dissipated in the region of intense high stresses near the crack tip. Not all is dissipated, however. Some energy is conserved as surface energy, but this is a small percentage (about 10%) of the energy dissipated and cannot readily be regained. For practical purposes, the energy in damaging the material can be treated as being dissipated, but to refer to the energy as being entirely dissipated is not correct.

The growing network of cracks which constitutes damage of the material is characterized by phenomena which are addressed in the next section. The key point is that one does not wish to follow each individual crack, but rather "smear" the cracks out over the material. The rationale for this is sensible because the number of cracks is large; repetitive tests on similar specimens would yield quite different detailed crack patterns, though with similar "average" behaviour.

DAMAGE MECHANICS

The first clue to material behaviour is the dependence of the stress-strain relationship on the testing method. Two standard tests are shown in Figure 5. The test method has long been known to affect the result; for instance flexible test machines with load control can feed strain energy into a specimen that is beginning to be damaged, enhancing the rate of damage and possibly resulting in a sudden unstable failure. To the writer's knowledge, no systematic study of damage has been completed with the question of energy fluxes being considered as a basic aspect. It seems that this should be considered especially in planning experimental work and in setting up models of material behaviour.

The literature on damage mechanics, from the point of view of material modelling, is wide. An extended bibliography is appended after the references to the present paper. A review of continuum damage mechanics has been conducted recently by Krajcinovic (1984) and this provides an excellent starting point. It must be emphasized that almost all of the work in the area of damage mechanics has been computer-oriented, using for example finite element analysis. It is important also to develop some simple closed form techniques.

The first point to note in continuum damage mechanics is that the material damage is distributed uniformly in the volume (possibly small) of material under consideration. The damage results in a degradation of elastic properties. A simple bilinear stress-strain relationship is shown in Figure 6. It is important to note the change in elastic modulus after the onset of degradation, typified by the change in slope of the unloading curve, as illustrated in Figure 6. More sophisticated relationships are shown in Figure 7; it is important to note that after a certain amount of damage the material is unlikely to have memory of the origin so that unloading curves of kind illustrated in Figure 7(b) are more realistic. In order that the damage illustrated in Figures 6 and 7 can develop in a progressive fashion, the tests would be conducted with control of the incoming mechanical energy, for instance in a strain-controlled test. Various measures of damage have been proposed: generally they relate to the change of elastic modulus. The increasing network of cracks (damage) results in the formation of stress-free zones or voids, thereby causing higher effective stresses in the undamaged material. The "effective" elastic modulus, i.e. averaged over the damaged and undamaged zones is reduced. For the remainder of this section, the material will be considered elastic, although the inclusion of allowance can be made for work (creep or plastic) at small zones near the crack tip.

A formulation of damage evaluation for elastic bodies has been given by Dougill (1983), who started with the generalized Hooke's law:

$$\sigma_{ij} = C_{ijkm}\,\epsilon_{km} \qquad (6)$$

This can be differentiated with respect to time (denoted by superimposed dots) to give

$$\dot{\sigma}_{ij} = C_{ijkm}\,\dot{\epsilon}_{km} + \dot{C}_{ijkm}\,\epsilon_{km} \qquad (7)$$

Although the effects related to the two terms on the right of equation (7) occur during the same time interval, it is useful to consider them separately. The first is the elastic component (as if there was no degradation) and the second is related to the change in stiffness (modulus) of the material and was termed by Dougill the fracture stress decrement. Dougill developed a theory analogous to hardening plasticity, but with the use of Il'ilushin's postulate. These theories will not be pursued here; rather, a relatively tractable approach suggested by Resende and Martin (1983) will be described. In this, we consider only shear damage, omitting the dilational terms developed by Resende and Martin.

The deviatoric components of the stress and strain tensors are written as

$$s_{ij} = \sigma_{ij} - \frac{1}{3} \sigma_{kk} \delta_{ij}$$

and $$e_{ij} = \epsilon_{ij} - \frac{1}{3} \epsilon_{kk} \delta_{ij}$$

respectively, where δ_{ij} is the Kronecker delta. We consider now the effective shear stress s as

$$s = \left(\frac{1}{2} s_{ij} s_{ij}\right)^{1/2} \tag{8}$$

which is invariant, and can be thought of as a constant times the root mean square of the maximum shear stresses. The model considers the damage to be represented by the parameter λ, with $0 \le \lambda \le 1$; $\lambda = 0$ represents "no damage" while $\lambda = 1$ represents "total failure" and loss of shear stiffness. Formally, the value of λ decides the value of the shear modulus, i.e.

$$s = Ge = G_o(1-\lambda)e \qquad (9)$$

where G_o = initial shear modulus. From (9):

$$G = G_o(1-\lambda) \qquad (10)$$

and it is possible to derive the following rate forms of (9):

$$\begin{aligned} \dot{s} &= G_o(1-\lambda)\dot{e} - G_o e\dot{\lambda}, \text{ for loading } (\dot{\lambda}>0) \\ \text{and} \quad \dot{s} &= G_o(1-\lambda)e \text{ for unloading } (\dot{\lambda}=0) \end{aligned} \qquad (11)$$

It is important to note that unloading does not involve any progressive damage and that the model, in the structure of equations (9)-(11) embodies the assumption that the material returns to the origin (e=o) on unloading.

The summary above is intended to provide an overview of the direction of theoretical work that the writer feels to be potentially fruitful in the study of the pulverisation of ice. One application along the lines of the theory above has been conducted by Cormeau, Jordaan and Maes (1986). This included also the consideration of residual strains on unloading (loss of memory).

Further development of damage mechanics is necessary to the understanding of the crushing of ice. The work of Resende and Martin suggests that the damage rate $\dot{\lambda}$ be considered as a function of $\dot{e}$, e and p (= 1/3 σ_{ii}). In line with the reasoning in the present paper, it is proposed to consider

$$\dot{\lambda} = \dot{\lambda}\ (\dot{\omega}, E). \qquad (12)$$

where E is internal energy and $\dot{\omega} = d\omega/dt$ is the rate of work done on a unit volume by the surroundings, i.e. the value $\dot{\omega}$ corresponds to $\dot{W}$ of equation (5) except that it is the rate of work done on a unit volume. Clearly if $\dot{\omega}<0$ then $\dot{\lambda}=0$ (unloading) and for $\dot{\omega}>0$ there is energy available for the creation of new surfaces. A theory along these lines is being developed by the writer, taking into account the initiation of new cracks as well as the propagation of existing cracks; the densities and lengths are of importance.

In the above, a scalar damage function has been considered; this is an appropriate simplified starting point for the theory. Krajcinovic (1984) makes a good case for a vectorial representation. In the case of ice, the shear damage could be anisotropic and this would require directional information.

Two other aspects deserve attention: the effect of concurrent hydrostatic confining pressure on the damage process as well as the dilalational effects associated with this process. Above all, further experimental work is needed to study the damage process and to determine material parameters.

BEHAVIOUR OF PULVERISED ICE

The analysis of the clearing process requires the study of the behaviour of pulverised ice. The concept is shown in a general way in Figure 8, in which the energy of the pulverisation, i.e. the destruction of shear stiffness is identified. The quantity p is the hydrostatic pressure, i.e. $p = (1/3)\sigma_{ii}$. Subsequently the crushed ice will flow under shear stress with predominantly compressive stress states. The resulting material can be modelled as an incompressible viscous fluid since its ability to deform in shear is great compared to its compressibility. Neglecting the inertia terms and the body forces in the Navier-Stokes equations one obtains

$$\frac{\partial p}{\partial x_i} - \mu \nabla^2 v_i = o, \qquad (13)$$

where p = pressure in crushed ice

x_i = spatial coordinate

μ = viscosity

$\nabla^2(\cdot)$ = Laplacian

v_i = velocity at x_i .

The case of flow between two parallel plates, simulating an ice sheet crushing against a vertical surface, can be solved easily on this basis; the idea is illustrated in the top of Figure 9, with the crushed ice being ejected from the top and bottom surfaces at the interaction zone. The resulting force (per unit width), F, on the indenter can be shown to be

$$F = \mu V\left(\frac{h}{\ell}\right)^3 \qquad (14)$$

where V = rate of movement of ice sheet

h = thickness of ice sheet

ℓ = thickness of crushed layer.

This relationship and the associated theory has been used in Timco and Jordaan (1987) in an analysis of ice sheet indentation. The question of vibrations excited by the ice crushing-clearing process is being investigated, illustrated schematically in Figure 9. The clearing process is governed by equations of the kind illustrated in Equation (14).

An alternative analysis method for the flow of pulverised ice is possible if the analogy between Hooke's and Stokes' laws is exploited (Jordaan, 1986). This was done in an exploratory study by Cormeau et al. (1986).

CONCLUSIONS

(1) Future ice research would be much assisted if continuum plasticity theory is avoided. There is a role for viscoplasticity in the analysis of crushed ice under compressive stress states. Ice creeps at all levels of stress. Yield criteria do not provide a useful characterisation of ice failure.

(2) Fracture and damage mechanics offer useful representations of ice behaviour. It is important to distinguish between compressive cracking leading to crushed ice, and global (tensile) splitting of ice features. The concept of shear damage in compressive stress states offers a useful starting point and this is consistent with treating the flow of crushed ice as that of a material which can resist pressure but with no shear stiffness.

(3) Fracture mechanics computations, for instance with the finite element method, are potentially of great practical applicability in studying the breaking of ice, for instance in optimising bow forms for ice breakers.

(4) Characterisation of flaws and cracks in sea ice is of great importance.

(5) Experimental work on the damage and crushing phenomena in ice is greatly needed. Viscosities for the flow of crushed ice need to be determined.

(6) The alternate crushing and clearing of an ice sheet provides a possible explanation for dynamic excitation of structures during continuous interaction with ice; combined with the concept of non-simultaneous failure, an explanation for reduced average ice pressures is obtained.

ACKNOWLEDGEMENTS

Financial support for this research from the Natural Sciences and Engineering Research Council of Canada, as well as Mobil Oil Canada, Ltd., is gratefully acknowledged. Helpful discussions and collaboration with Ken Croasdale, Marc Maes and Garry Timco are acknowledged.

REFERENCES †

Bridgman, P.W. (1941): "The Nature of Thermodynamics". Harvard.

Cormeau, A., Jordaan, I.J. and Maes, M. (1986): "Development of a Model for Progressive Damage in Ice". Report prepared for Department of Public Works, Government of Canada, by Det norske Veritas (Canada) Ltd.

Cottrell, Alan. (1975): "An Introduction to Metallurgy". Edward Arnold.

Dougill, J.W. (1983): "Constitutive Relations for Concrete and Rock: Applications and Extensions of Elasticity and Plasticity Theory". William Prager Symposium on Mechanics of Geomaterials, Rocks, Concretes, Soils, September 11-15.

Gold, L.W. (1972): "The Failure Process in Columnar-Grained Ice". NRCC Paper No. 369.

Goodman, D.J. (1977): "Critical Stress Intensity Factor (K_{IC}) Measurements of High Loading Rates for Polycrystalline Ice". In: P. Tryde (Ed.), Physics and Mechanics of Ice, IUTAM Symp., pp. 129-146.

Hamza, H. and Muggeridge, D.B. (1979): "Plane-strain Fracture Toughness of Freshwater Ice". Proc. POAC-79, The Norwegian Institute of Technology, Trondheim, Norway.

Jordaan, I.J. (1986): "Numerical and Finite Element Techniques in Calculation of Ice-Structure Interaction". 8th. IAHR Symposium on Ice, Iowa City, August.

Kheisin, D.E., and Likhomanov, V.A. (1973): "An Experimental Determination of the Specific Energy of Mechanical Crushing in Ice by Impact". Problemy Arktiki i Antarktiki, Vol. 41, pp.55-61.

Krajcinovic, D. (1984): "Continuum Damage Mechanics". Applied Mechanics Reviews, Vol. 37, No. 1, pp.1-6.

Kurdyumov, V.A., and Kheisin, D.E. (1976): "Hydrodynamic Model of the Impact of a Solid on Ice". Prikladnaya Mekhanika, Vol. 12, No. 10, pp.103-109.

---

† An additional bibliography on damage mechanics is given after this section

Leckie, F.A. (1978): "The Constitutive Equations of Continuum Creep Damage Mechanics". Philosophical Transactions of the Royal Society, London, Series A, 288, 27-47.

Likhomanov, V.A., and Kheisin, D.E. (1971): "Experimental Investigation of Solid Body Impact on Ice". Problemy Arctiki i Antarktiki, Vol. 38, pp.105-111.

Love, A.E.H. (1927): "A Treatise on the Mathematical Theory of Elasticity". Cambridge University Press.

Palmer, A.C. et al. (1983): "Fracture and Its Role In Determining Ice Forces on Offshore Structures". Annals of Glaciology, Vol. 4, pp.216-221.

Resende, L., and Martin, J.B. (1983): "A Progressive Damage Continuum Model for Granular Materials". Computer Methods in Applied Mechanics and Engineering 42 (1984) 1-18 North Holland.

Sih, G.C. (1973): "A Special Theory of Crack Propagation in Mechanics of Fracture, Methods of Analysis and Solution of Crack Problems". Ed. G.C. Sih, Noordhoff.

Sinha, N.K. (1984): ""Intercrystalline Cracking, Grain-Boundary Sliding, and Delayed Elasticity at High Temperatures". Journal of Materials Science, Vol. 19, pp.359-376.

Spooner, D.C., and Dougill, J.W. (1975): "A Quantitative Assessment of Damage Sustained in Concrete During Compressive Loading". Reprinted from Magazine of Concrete Research, Vol. 27, No. 92, September, pp.151-160.

Timco, G.W. (1986): "Indentation and Penetration in Freshwater Ice". 5th. Symposium on Offshore Mechanics and Arctic Engineering, OMAE, Japan, April 13-17.

Timco, G.W. and Frederking, R.M.W. (1983): "Flexural Strength and Fracture Toughness of Sea Ice". Cold Regions Sci. and Technol., 8:35-41.

Timco, G.W. and Jordaan, I.J. (1987): "Dynamic Action of Ice Crushing in Rigid Indentation", in preparation.

Timoshenko, S.P., and Goodier, J.N. (1970): "Theory of Elasticity". Third Edition, McGraw Hill.

Tomin, M.J., Cormeau, A., Jordaan, I.J., (1985): "Development of Analytical Models Related to Experimental Work on Ice Structure Interaction". Report by Det norske Veritas to Department of Public Works, Government of Canada.

ADDITIONAL BIBLIOGRAPHY ON DAMAGE MECHANICS

Ashby, M.F. and Hallam, S.D. (Cooksley) (1986): "The Failure of Brittle Solids Containing Small Cracks Under Compressive Stress States". Acta. Metall., Vol. 34, No. 3, pp.497-510.

Bazant, Z.P., and Gambarova, P.G.: "Crack Shear in Concrete: Crack Band Microplane Model".

Bazant, Z.P. (1977): "Endochronic and Classical Theories of Plasticity in Finite Element Analysis". International Conference on Finite Elements in Nonlinear Solid and Structural Mechanics, Geilo, Norway, Aug. 29-Sept. 1, Vol. 1.

Bazant, Z.P. (1976): "Instability, Ductility, and Size Effect in Strain-Softening Concrete". Journal of the Engineering Mechanics Division, April.

Bazant, Z.P., and Bhat, P.D. (1976): "Endochronic Theory of Inelasticity and Failure of Concrete". Journal of the Engineering Division, August.

Bazant, Z.P., and Krizek, R.J. (1975): "Endochronic Constitutive Law for Inelastic Shear and Densification of Sand". Proceedings of the Fifth Canadian Congress of Applied Mechanics, Fredericton, New Brunswick.

Burt, N.J., and Dougill, J.W. (1977): "Progressive Failure in a Mode Heterogeneous Medium". Journal of the Engineering Mechanics Division, June.

Carpinteri, A., and Sih, G.C. (1983): "Damage Accumulation and Crack Growth in Bilinear Materials with Softening: Application of Strain Energy Density Theory". Lehigh University, Institute of Fracture and Solid Mechanics, Report No. IFSM-83-115.

Chaboche, J.L. (1979): "The Continuous Damage Mechanics: A Tool to Describe Phenomena Before Crack Initiation". 2nd. Int. Seminar on Incl. Analysis and Life Prediction in High Temp. Env., pp.C9-C14.

Chen, E.P., Kipp, M.E., and Grady, D.E. (1984): "A Strain-Rate Sensitive Rock Fragmentation Model". To appear in Mechanics of Oil Shale, edited by K.P. Chong and J.W. Smith, Applied Science Ltd.

Davison, L., and Stevens, A.I. (1973): "Thermomechanical Constitution of Spalling Elastic Bodies". Journal of Applied Physics, Vol. 44, pp. 667-674.

Dienes, J.K. (19): "Fracture, Failure, and Fragmentation". Theoretical Division, Group T-3, Los Alamos National Laboratory, Los Alamos, New Mexico.

Dougill, J.W. (19): "An Approximate Assessment of the Effects of Heterogeneity on the Strength and Mode of Failure of Concrete Systems". University of London King's College, Civil Engineering Department.

Dougill, J.W. (1983): "Path Dependence and a General Theory for the Progressively Fracturing Solid". Proc. R. Soc. Lond., A390, 341-351, Great Britain.

Dougill, J.W., Lau, J.C., and Burt, N.J. (1976): "Towards a Theoretical Model for Progressive Failure and Softening in Rock, Concrete and Similar Materials". To be presented at the American Society of Civil Engineering Mechanics Division Specialty Conference of Mechanics in Engineering University of Waterloo, Ontario, May 26-28.

Dougill, J.W. (1976): "On Stable Progressively Fracturing Solids". Reprint from Journal of Applied Mathematics and Physics, Vol. 27, Fasc. 4, ZAMP, pp. 423-437.

Dougill, J.W. (1975): "Some Remarks on Path Independence in the Small in Plasticity". Quarterly of Applied Mathematics, October.

Dougill, J.W., and Rida, M.A.M. (1980): "Further Consideration of Progressively Fracturing Solids". The Journal of Engineering Mechanics Division, October.

Hamza, H. (1986): "Application of Fracture Mechanics Techniques to Ice-structure Interaction Problems". IAHR Symposium, Iowa City, Vol. 1, pp.329-347.

Hayhurst, D.R., Dimmer, P.R., and Chernuka, M.W. (1975): "Estimates of the Creep Rupture Lifetime of Structures Using the Finite-Element Method". Journal of Mechanics and Physics of Solids, Vol. 23, pp.335-355.

Horii, H., and Nemat-Nasser, S. (1982): "Overall Moduli of Solids with Microcracks: :oad Induced Anisotropy". J. Mech. Phys. Solids, Vol. 31, pp.155-171.

Kachanov, L.M. (1958): "Time to Failure Under Creep Conditions". Isz. AN SSR OTN, No. 8.

Karr, D.G. (1985): "Constitutive Equations for Ice as a Damaging Material". Proc. Civil Eng. in the Arctic Offshore, ASCE, San Francisco, March 25-57.

Krajcinovic, D., and Fonseka, G.U. (1981): "The Continuing Damage Theory of Brittle Materials". Journal of Applied Mechanics, December, Vol. 48.

Leckie, F.A. and Hayhurst, D.R. (1974): "Creep Rupture of Structures". Proceedings of the Royal Society, London, Series A., Vol. 340, 1974, pp.323-347.

Lemaitre, J., and Chaboche, J.L. (1985): "Mecanique des Materieux Solides". First Edition, Dunod.

Lemaitre, J., and Chaboche, J.L. (1978): "Aspect Phenomenologique de la Rupture par Endommagement". Journal de Mecanique Appliquee, Vol. 2, pp.317-365.

Nemat-Nasser, S., and Horii, H. (1984): "Micro-Mechanics of Fracture and Failure of Geo-Materials in Compression". Advances in Fracture Research, Proceedings of the 6th International Conference on Fracture (ICF6), New Delhi, India, Dec. 4-10.

Nemat-Nasser, S., and Horii, H. (1984): "Rock Failure in Compression". Int. J. Engrg. Sci., Vol. 22, No. 8-10, pp.9499-1011.

Nemat-Nasser, S., and Horii, H. (1982): "Growth of Microcracks in Rocks, and Load-Induced Anisotropy". Symposium on Fracture Mechanics Approach to Hydraulic Fracturing and Geothermal Energy, Sendai, Japan, November 8.

Resende, L., and Martin, J.B.: "Constitutive Modelling and Finite Element Analysis in Rock Mechanics - Part I: The Internal Damage Model and Parameter Identification". AMRU Rep. No. 57 (to be published).

Resende, L., and Martin, J.B.: "Constitutive Modelling and Finite Element Analysis in Rock Mechanics - Part II: Finite Element Solution of Boundary Value Problems". AMRU Rep. No. 58 (to be published).

Resende, L., and Martin, J.B. (1983): "Damage Constitutive Model for Geotechnical Applications". University of Cape Town, Rondebosch, Cape Town, South Africa, Nonlinear Structural Mechanics Research Unit, Technical Report No. 44.

Stankowski, T., and Gerstle, K.H. (1983): "Simple Formulation of Concrete Behaviour Under Load Histories". Paper submitted for Publication in Jnl. A.C.I., September.

Vakulenko, A.A. and Kachanov, M.L. (1971): "Continuum Theory of Cracked Media". Mekh Tverdogo Tela, Vol. 6, pp.159-166.

Willam, K.J., and Sture, S. (1985): "A Composite Fracture Model for Localized Failure in Cementitious Materials". Paper presented at second Symposium on the Interaction of Non-Nuclear Munitions with Structures, Panama City Beach, Florida, April.

Willam, K.J., Bicanic, N., and Sture, S. (1984): "Constitutive and Computational Aspects of Strain-Softening and Localization in Solids". Presented at A.S.M.E. - WAM'84 Symposium on Constitutive Equations: Micro, Macro and Computational Aspects", New Orleans, December 10-14.

Zhurkov, S.N., and Sanfirova, T.P. (1958): "The Relationship Between Strength and Creep in Metals and Alloys". Zhurnal Teoreticheskoi Fyziki, Vol. 28, No. 8.

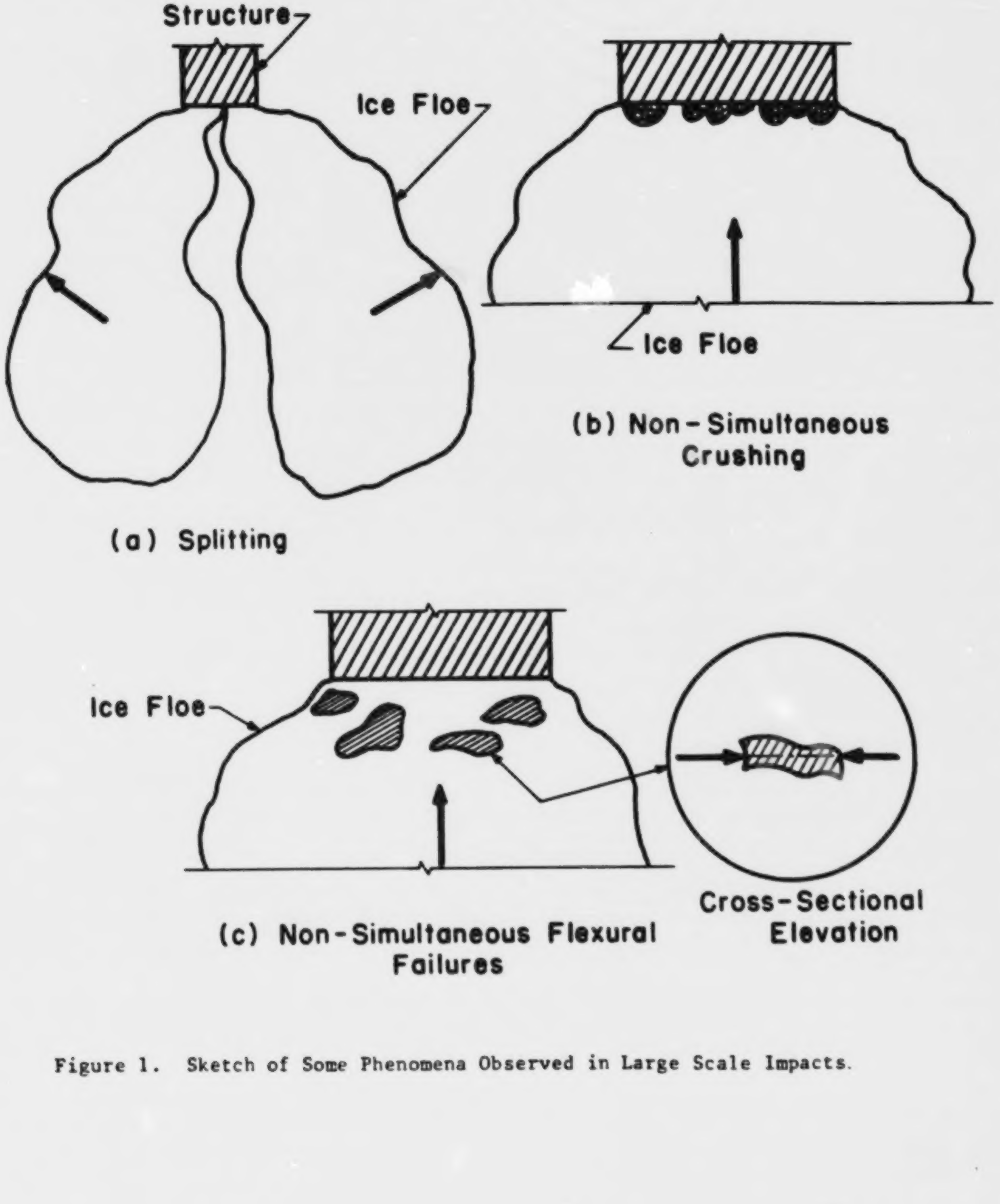
Structure
Ice Floe
(a) Splitting
Ice Floe
(b) Non-Simultaneous Crushing
Ice Floe
(c) Non-Simultaneous Flexural Failures
Cross-Sectional Elevation

Figure 1. Sketch of Some Phenomena Observed in Large Scale Impacts.

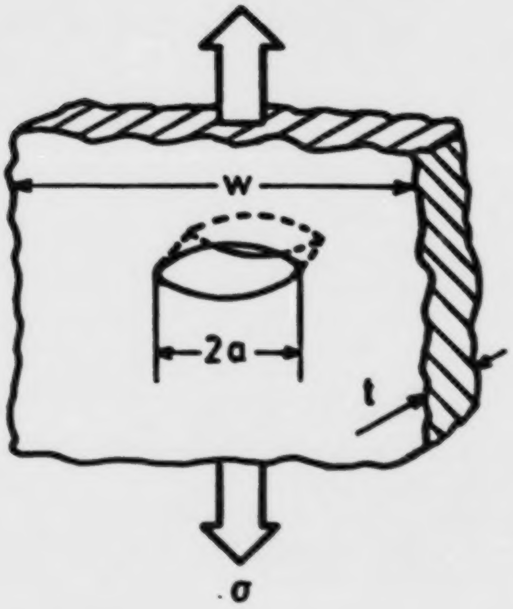

Figure 2. Crack in Tensile Stress Field

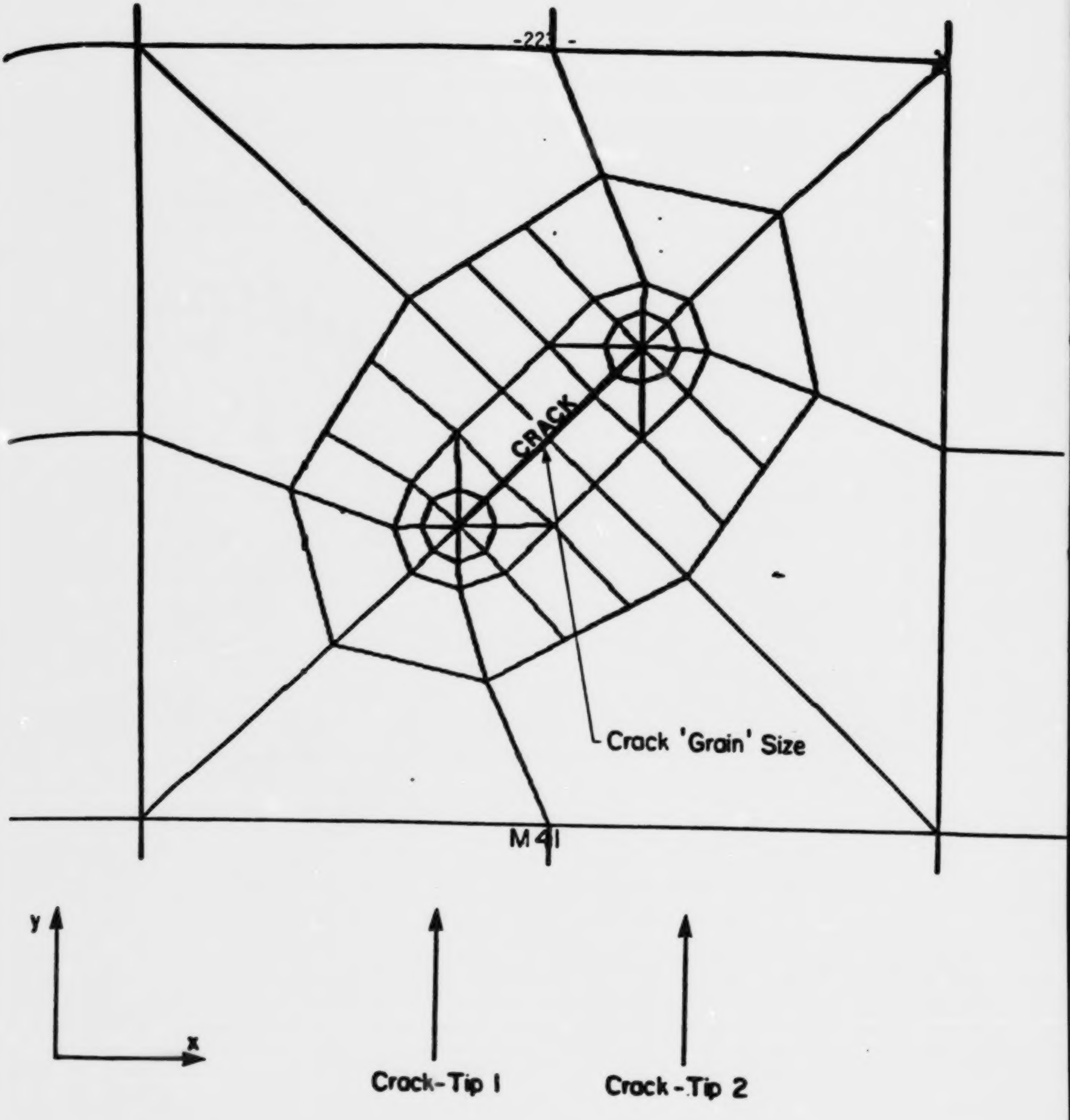
CRACK
Crack 'Grain' Size
M41
y
x
Crack-Tip 1
Crack-Tip 2

Figure 3. Grain-sized Crack in Study of Crack Propagation Accompanying Experimental Work of Timco (1986). Existing Cracks of Any Required Length can be Modelled.

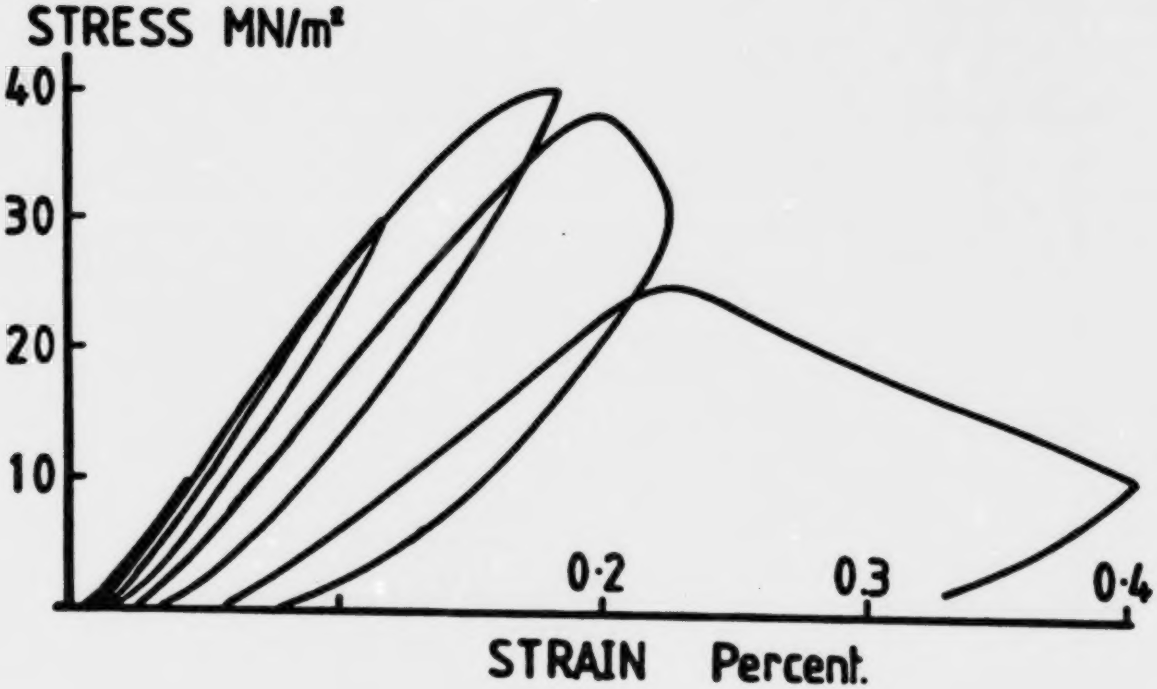

Figure 4. Cyclic Loading of Concrete in Compression Based on Work of Spooner and Dougill (1975).

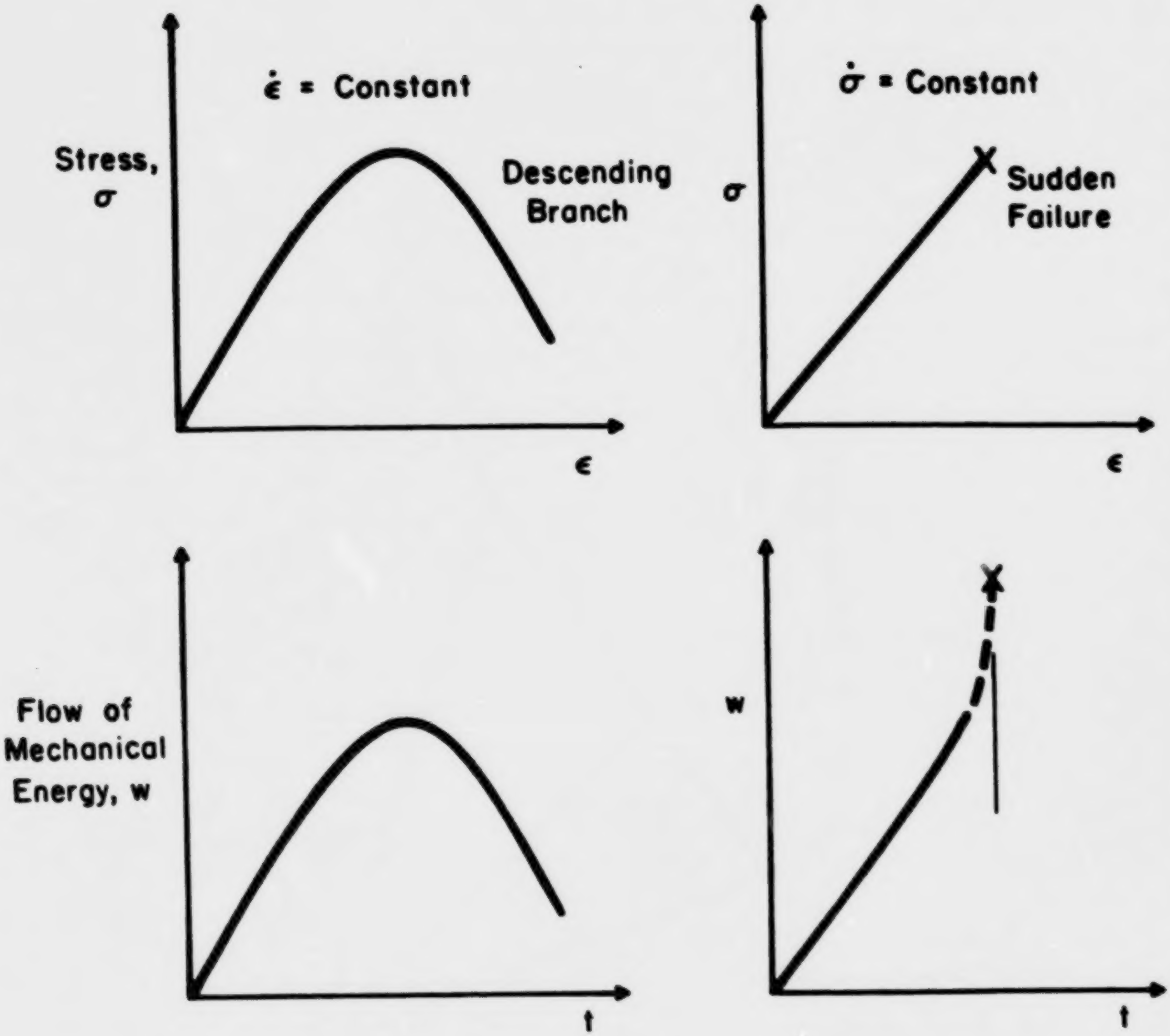
$\dot{\epsilon}$ = Constant
Stress, σ
Descending Branch
ϵ
$\dot{\sigma}$ = Constant
σ
Sudden Failure
ϵ
Flow of Mechanical Energy, w
t
w
t

Figure 5. Strain and Stress-controlled Tests and Associated Flow of Mechanical Energy into Specimen.

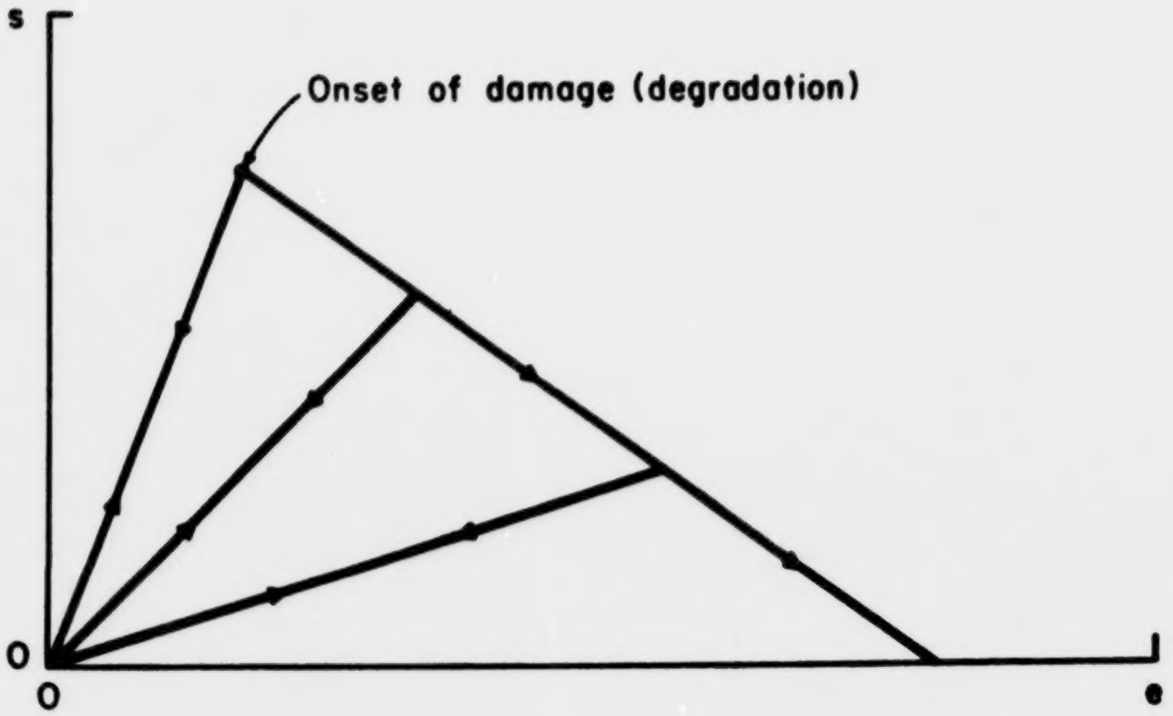
s
Onset of damage (degradation)
0
0
e

Figure 6. Simplified Bi-linear Damage Model.

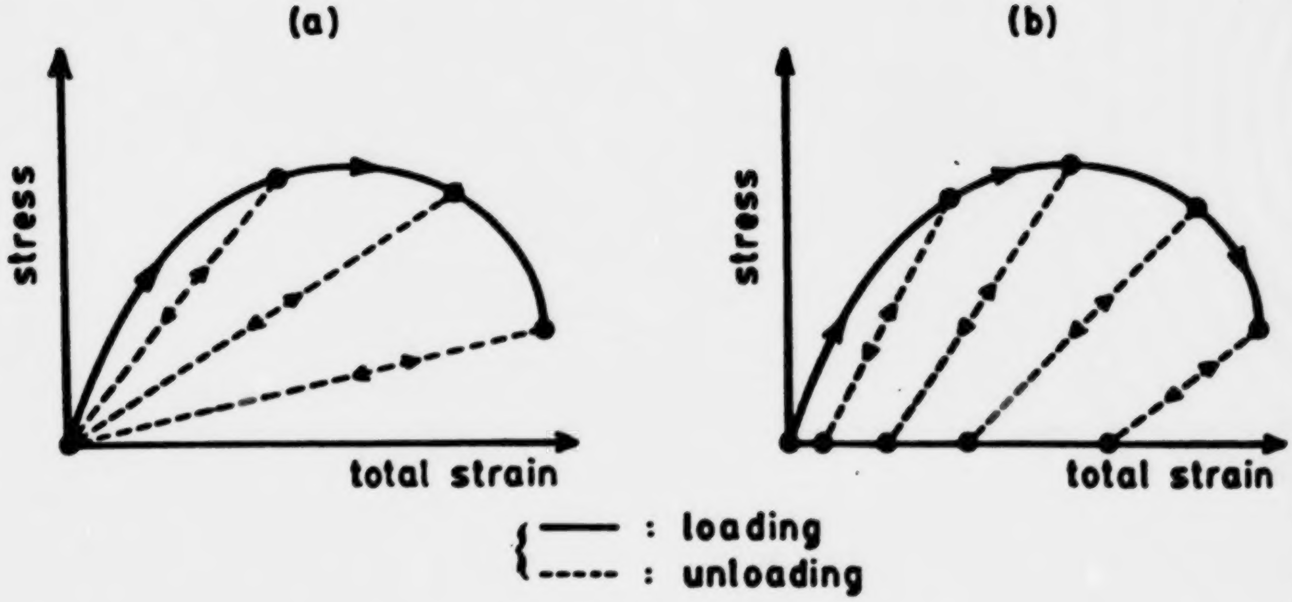
(a)
(b)
stress
total strain
stress
total strain
: loading
: unloading

Figure 7. Damage Relationships, (a) With Memory and (b) Without Memory of Origin.

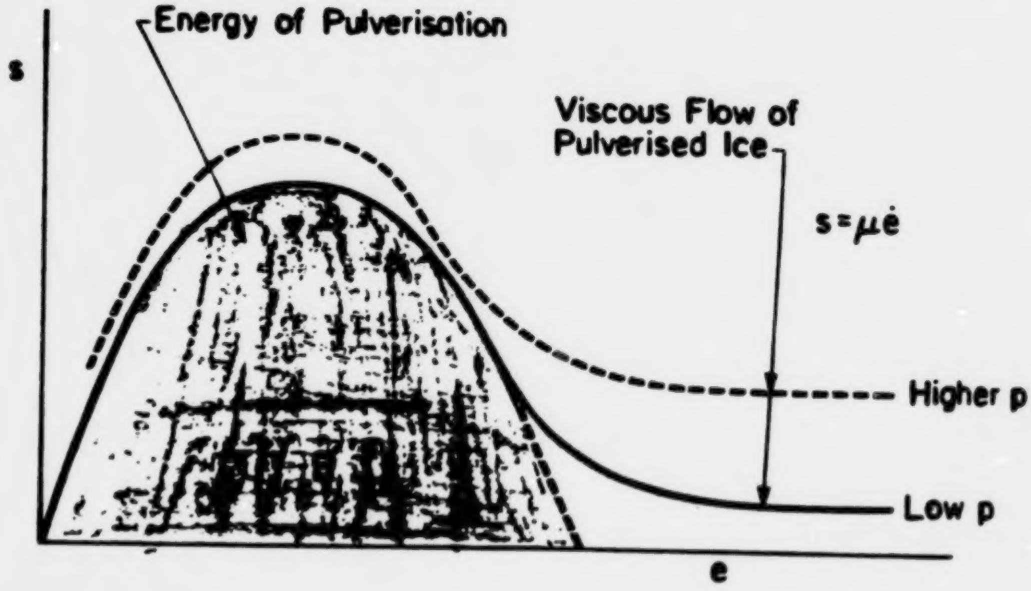
Energy of Pulverisation
s
Viscous Flow of Pulverised Ice
$s = \mu \dot{e}$
Higher p
Low p
e

Figure 8. Energy of Pulverisation and Subsequent Flow of Pulverised Ice. Hypothesized Effect of Hydrostatic Pressure, p.

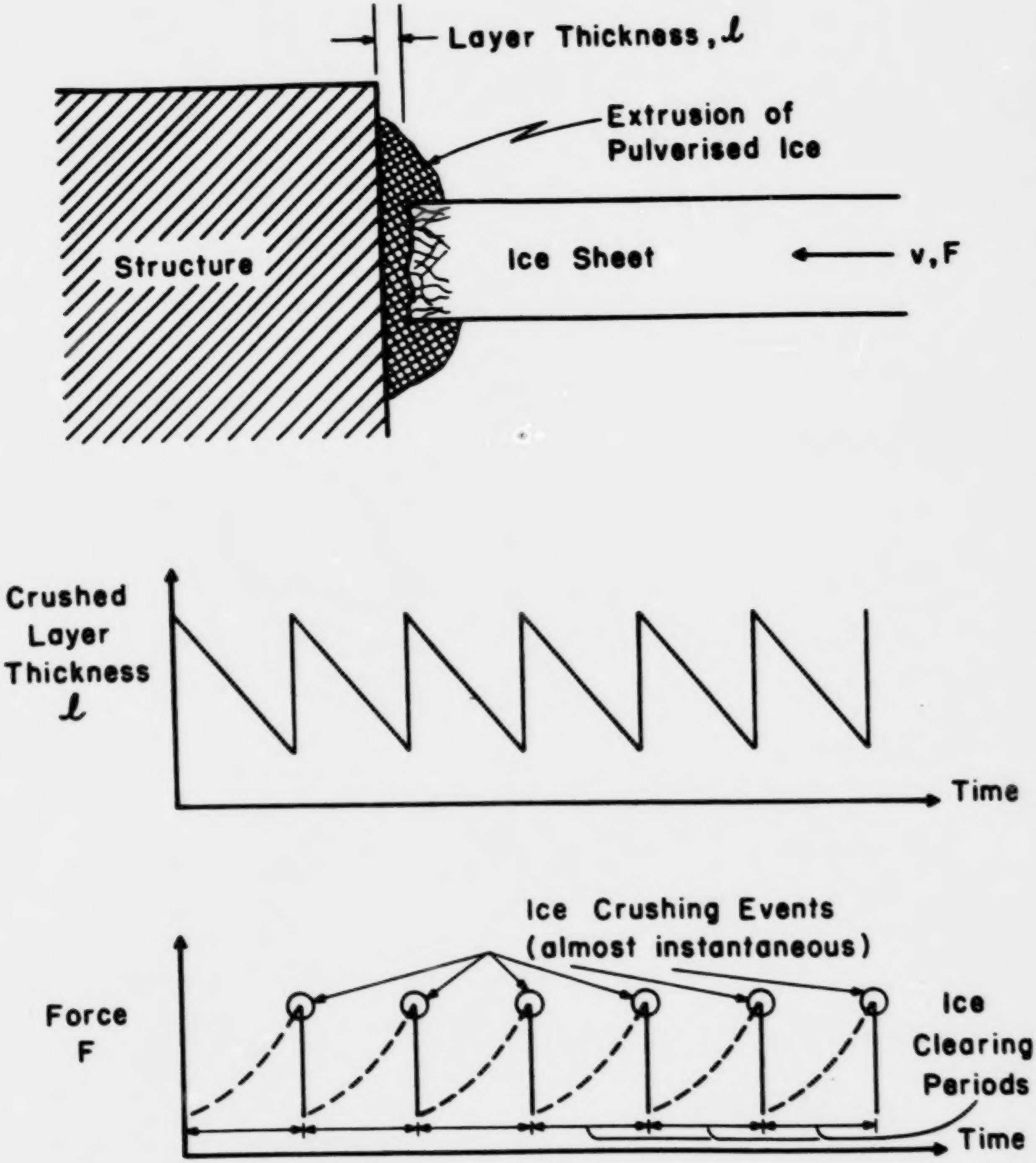
Layer Thickness, ℓ
Extrusion of Pulverised Ice
Structure
Ice Sheet
v, F
Crushed Layer Thickness ℓ
Time
Ice Crushing Events (almost instantaneous)
Force F
Ice Clearing Periods
Time

Figure 9. Schematic Illustration of Alternate Crushing (Pulverisation) of Ice Followed By Ejection (Clearing) Periods.

NRC WORKSHOP ON EXTREME ICE FEATURES

Questions and Discussions Form

AUTHOR: I.J. Jordaan

PAPER: Fracture Mechanics and Damage Theory as a Basis for Calculation of Ice-structure Loads

DISCUSSION BY: B. Wright

DISCUSSION:

I would like to compliment you on your excellent and forward looking presentation. I certainly agree with your comments on the relevance of fracture mechanics to ice/structure interaction and ice failure problems. I would like to note that our icebreakers, in carrying out their ice management duties around the Kulluk, select thin ice areas in rough multi-year floes, create a "flaw" by ramming and then slowly push on the flaw until a major fracture propagates through the floe. This technique is successful in floes to several kilometres in extent in an open water or thin ice environment.

AUTHOR'S REPLY:

I would like to thank Mr. Wright for his remarks and for the interesting observation on icebreaking. I believe that the numerical "tools" are available for analytical studies of icebreaking and consider that this would be a fruitful way to assist analysis of icebreaking.

DISCUSSION BY: G. Holdsworth

DISCUSSION:

Concerning the model that you showed illustrating a continuous crushing/spalling mode of failure, what were the 1) amplification factors on the stress spikes and 2) time intervals between stress peaks in the graph that accompanied the model geometry.

AUTHOR'S REPLY:

The peak stresses can be two times the average, or even more in some instances. The time intervals vary considerably depending on the scale. Small-scale tests in the laboratory would show intervals of a fraction of a second. The cyclic load on the Molikpaq structure apparently had a repetitive load at a frequency of about 1 Hz.

DISCUSSION BY: Hans R. Kivisild

DISCUSSION:

The formation of cracks under loads on an ice face are important for the application of fracture mechanics. Cracks can be shown to develop under compressive loads (as shown by Wang, Ralston, Iyer and Kivisild) with the sort of cracks more or less proportional to the linear dimensions of the loaded area.

AUTHOR'S REPLY:

I would like to thank Dr. Kivisild for his interesting comments. Generally I am in agreement with the statement regarding the size of the zone of cracking. However, the zone of compression cracking can be considerably less than the dimension of the loaded area, for large-scale interactions. Fracture and damage mechanics show more promise in developing a theory of ice failure than plasticity methods. The latter would tend to exaggerate the size of the zone. The crushed layer itself can be quite narrow.

DISCUSSION BY: R. Gerard

DISCUSSION:

Do you have any feel for the circumstances that exist in the vicinity of the peak load: it would seem the "pulverized ice" analysis would be more important in the off-peak circumstances.

AUTHOR'S REPLY:

The peak is likely to be associated with the peak build-up in strain energy in the ice just prior to and at pulverization. The subsequent clearing process would tend to correspond to off-peak circumstances. Taken together, and considering zones of non-simultaneous failure, this provides the explanation for the fact that the average load is less than the peak at crushing.

EXTREME ICE FEATURE - STRUCTURE INTERACTION

by

K.R. Croasdale

INTRODUCTION

Vugraphs 1-3

Generally under this topic, we can ask ourselves two questions;

1) Can offshore structures be designed for extreme ice features?
2) Should structures be designed for them?

The first of these two questions will be the topic of this presentation. The second question involves the broader issues of probability, risk and economics; it will not be addressed in this talk.

The outline of the presentation is as follows:

- overview of logic and mechanics of ice-structure interaction
- relevance of current methods to extreme ice feature interaction
- significance of field measurements and real-world experience
- speculation of typical extreme ice feature loads and whether they can be designed for

For the purpose of this presentation, extreme ice features will be defined as;

- greater than 15-20 m thick
- tabular or ridge-like
- discrete (i.e. limited in area and existing within thinner ice)

BACKGROUND AND LOGIC OF ICE-STRUCTURE INTERACTION

Vugraph 4

The classic problem in ice mechanics is that of ice crushing against a narrow pier. Up to about two decades ago this was the main ice-structure interaction problem addressed by civil engineers. The application of interest being the design of bridge piers.

Vugraph 5

The Russian engineer, Korzhavin, is usually credited for the development of the empirical equation for ice pressure against a vertical pier.

$p = Imk\sigma_c$ (see VG for definition of terms)

This equation was later adopted by engineers faced with the issue of specifying loads on arctic offshore platforms. A considerable amount of research was done to investigate and better quantify the parameters in Korzhavin's equation. The American Petroleum Institute (API), recommended the use of an equation similar to Korzhavin's for developing loads on offshore platforms.

It was recognized however that the approach had limitations and was likely conservative. Especially for wide structures (as is typical of arctic offshore platforms) (see Croasdale, 1985).

Vugraph 6

As illustrated conceptually in VG 6, the interaction with structures of extreme ice features such as large, thick ice islands or multi-year floes, can involve very different modes of ice failure than crushing against a narrow pier. The simple application of the Korzhavin type of equation to extreme ice features could be very misleading. A broader logic and methodology to ice loads has been developed and has particular relevance to the issue of extreme ice feature-structure interaction.

Vugraph 7

This broader logic for ice-structure interaction is illustrated in VG 7. The three limits to ice loads can be defined as:

- limit stress (ice fails locally at structure)
- limit momentum (load limited by momentum of ice feature)
- limit force (load limited by driving forces on ice).

The two latter limits may have particular significance for extreme ice features.

Vugraph 8

The limit stress load is the usually addressed ice load. It assumes that the ice force is governed by ice failure across the structure width (as in Korzhavin's approach). For a vertical structure the load is simply defined as the effective ice pressure (p) multiplied by structure width (D) and local ice thickness (t).

Vugraph 9

The limit stress load also covers other modes of ice failure. In addition to crushing against a vertical structure, the ice load could be governed by local bending failure against a sloping structure, and/or by a rubble-building mode of ice failure if a rubble field exists around a wide structure. Ice engineers have developed various approaches to quantifying these different modes of ice failure.

Vugraph 10

If the ice feature is of limited size and discrete, such as an iceberg, the ice load may be governed by the type of interaction defined as "limit momentum". In this situation, local ice failure occurs at the structure, but the ice feature is stopped before it fully envelops the structure. In this case the load is less than the limit-stress load.

Vugraph 11

The general approach to calculation of limit-momentum ice forces is given with the appropriate equations. These equations have been used to calculate iceberg impact loads for Canadian E. Coast structures. A major problem in this context is defining the large-scale ice crushing strength to be used in the equation (see Croasdale, 1983; and Cammaert and Wong, 1983).

Vugraph 12

When a locally very thick floe contacts a wide structure, the limit stress load may become so large that the driving forces on the floe may not be sufficient to generate such a large load. In this case the ice load would be governed by the sum of the driving forces.

Vugraph 13

The driving forces are the wind drag, the current drag and the pack ice forces acting across the back of the floe. It is generally accepted that pack ice forces are controlled by pressure ridging in the thinner ice within the pack ice.

Vugraph 14

Ridge building forces have been speculated-upon (as shown in the VG); but until recently no actual measurements of average ridge building forces across a wide front had been obtained. (A project to obtain such measurements will be described later.)

A major difficulty in specifying limit force loads has always been that of quantifying the ridging forces. As can be seen from the VG, the uncertainty in ridging forces spans several orders of magnitude.

Vugraph 15

Despite such uncertainties, work done several years ago indicated that limit force loads might control the design ice loads associated with extreme ice features (Croasdale, 1980). This early work created the incentive to further pursue the concept of limiting driving forces, especially in relation to extreme ice features such as ice islands and thick multi-year floes.

APPLICATION OF CURRENT METHODS TO PREDICTION OF ICE LOADS DUE TO EXTREME ICE FEATURES

Before proceeding further with the limit-force approach let use examine typical limit-stress ice loads associated with extreme ice features.

Vugraph 16

Assume for the moment that the structure has vertical sides and the

Korzhavin equation for ice crushing can be used (the API 2N equation as shown on the VG is the same).

Vugraph 17

If we further assume uniaxial crushing strengths obtained in the laboratory then strength values similar to those shown in this VG would apply. In the pack ice regime, the velocities are sufficient to cause deformation at strain rates greater than 10^{-3} $\sec^{-1}$, therefore peak ice strengths (say 800 psi for granular ice) must be used.

Vugraph 18

The effective ice pressures obtained using the indentation equation can now be calculated (assuming typical values for I and K). Typically they might be 1200 psi (8 MPa) for columnar ice and 600 psi (4 MPa) for granular ice.

Vugraph 19

If we assume the lower value of 600 psi (4 MPa) we can calculate typical loads generated against a 150 m wide structure by an ice island 40 m thick. (Based on limit-stress conditions). The load is 24,000 MN (or 2,400,000 tonnes or 4,800,000 kips).

This is obviously a gigantic load and would be difficult to design for. (For comparison a typical caisson structure currently in use for arctic exploration would have a sliding resistance no greater than about 100,000 tonnes.)

SIGNIFICANCE OF FIELD MEASUREMENTS AND REAL-WORLD EXPERIENCE

The previous calculation reflects current methodology as extrapolated from bridge pier experience and as presented in API 2N. However engineers involved in the design and operation of arctic structures have known for some time that the approach is conservative, especially for wide structures.

Measurements and observation at actual arctic structures, and results from large-scale experiments such as Hans Island have yielded lower global ice pressures than those obtained using indentation theory and small-scale ice strengths.

Vugraph 20

A speculative curve of ice crushing versus aspect ratio (diameter to ice thickness) was produced in 1981 for the Canadian Beaufort Sea Environmental Impact Statement (1982). It was drawn up recognizing actual experience and early results from Hans Island. It suggests global ice pressures on a wide structure of 1.0 MPa (or less). Reasons why global ice pressures could be lower than those derived from indentation theory are various, and have been discussed by several authors (e.g. Sanderson 1984, Croasdale 1985). The topic is beyond the scope of this presentation.

It is of interest however to adjust the typical global ice force previously calculated for a global ice pressure of say 1.0 MPa. The global force in the previous example reduces to 600,000 tonnes, which is still substantial and would be difficult to design for.

This brings us back to the limit force approach, and the need for real data on large-scale pack ice forces which could be used to better quantify limit force ice loads.

Vugraph 21

Earlier this year a pilot experiment was conducted in the southern Beaufort Sea to try to measure pack ice forces across a front of several km. The general scheme is shown in the VG. The concept was to instrument a multi-year floe close to its centre with arrays of ice stress sensors. The hypothesis being that when the floe was subject to converging ice conditions, pressure ridging would occur in the surrounding thinner ice, and the ice stress sensors would measure the average compressive stresses in the floe from which average ridging forces could be deduced.

Vugraph 22

During the experiment a suitable floe was selected and instrumented. The VG shows the movement of the floe during the experiment. No measurements of stress were recorded until the floe was driven south against the landfast ice edge.

Vugraph 23

When this occurred, ridging occurred on the NW edge of the floe and the stress events could be correlated to the ridging events.

Vugraph 24 and 25

A typical stress event is shown on VGs 24 and 25. The change in compressive stress was about 25 kPa.

Vugraph 26

If this compressive stress is converted to an average ridging force (w in N/m), a typical maximum value for the ridging events which occurred is 1.0×10^4 N/m.

If we allow a factor of 3.0 for errors and uncertainties, we obtain a value for w of about 3.0×10^4 N/m across the 5 km width of the floe.

Vugraph 27

Another source of data for pack ice driving forces suggests minimum values in the range 1.5 to 7.5×10^5 N/m across the back of a 1 km wide floe. These two sets of data are not necessarily in conflict, as one might expect higher average forces across a smaller floe than across a large one (due to spatial averaging).

Vugraph 28

This table speculates on typical pack ice forces as a function of floe width and presents the corresponding limit force load assuming a blocking floe in front of a structure with the pack ice ridging behind it. In this case, the limit force load of 100,000 tonnes is the same in all cases.

TYPICAL EXTREME ICE FEATURE LOADS

Vugraph 29

We can now compare limit stress and limit force ice loads for an ice feature 10 km in width acting on a structure 150 m in diameter. In this calculation a constant ice crushing strength of 1.0 MPa is assumed, and the pack ice driving force is assumed to be 10^5 N/m. The limit stress load varies with local ice thickness. As can be seen, for ice thicknesses greater than 10 m, the limit force ice load (speculative) will control.

Vugraph 30

With the previous typical ice loads in mind we can now compare them with the sliding resistance of a typical production platform resting on a sandy sea floor. The calculation shown in the VG suggests that the allowable ice load would be about 200,000 tonnes-force. Looking back at VG 29 we see that such a load would be exceeded using the limit stress approach when the ice thickness exceeds about 15 m. On the other hand if the limit force approach can be invoked, then the allowable ice load will not be exceeded regardless of local ice thickness.

Vugraph 31

If a structure is designed based on limit force ice loads if has to be recognized that the initial momentum (or kinetic energy) of the ice feature has to be dissipated without generating higher loads than the "steady" limit force load. It is beyond the scope of this presentation to discuss this aspect of the problem in any detail, but previous work indicates that the various mechanisms shown in VG 31 can lead to dissipation of the initial momentum of a large ice feature.

Vugraph 32

In the case of an underwater berm, calculations show that a 10 x 10 km ice feature 50 m thick with an initial velocity of 0.5 m/sec can be brought to rest (Croasdale and Marcellus, 1981).

Vugraph 33

Another structural configuration which might be successful in resisting a thick ice feature is the sloping or conical structure. However, the advantage of the sloping structure diminishes as the ice thickness increases. Beyond a thickness of about 15 m it is not clear that the cone yields lower limit-stress loads than a vertical structure (especially if the global ice crushing pressure is 1.0 MPa or less). The pros and cons of sloping versus vertical structures for thick ice is an area for additional study and discussion.

CONCLUDING REMARKS

Vugraphs 34 and 35

In conclusion, the following points are summarized:

- Large-scale data obtained at real structures and Hans Island indicates lower global ice crushing pressures than predicted using indentation theory and small-scale ice strengths (e.g. 1.0 MPa effective global ice pressure versus say 5.0 MPa).
- A reasonably conservative value for pack ice driving forces over a 10 km width might be about 10^5 N/m (but higher over smaller widths).
- With an ice crushing strength of 1.0 MPa and with ice thicker than about 15-20 m, the advantage of a cone over a vertical structure may not exist (except perhaps in relation to structural vibrations induced by dynamic ice loads).
- On sandy soils, it appears that large production platforms could be designed for extreme ice features up to 40 m thick (if limit force ice loads can be shown to govern).
- When invoking limit force ice loads, the initial momentum of the ice feature has to be dissipated. (This could be done with an underwater berm.)
- More large-scale ice force measurements and their analysis (including pack ice forces) are required to refine the approaches and speculations discussed in this presentation.

ACKNOWLEDGMENTS

The author thanks Esso Resources Canada Limited for permission to make this presentation. The opinions expressed are those of the author and do not necessarily represent those of either Esso or its Affiliates.

REFERENCES

API Bulletin 2N 1981. API Planning, Designing and Construction of Fixed Offshore Structures in Ice Environment. API Dallas, Texas.

Cammaert, A.B. and T.T. Wong, 1983. Impact of Sea Ice on Offshore Gravity and Floating Platforms. 7th POAC, VTT, Helsinki.

Croasdale, K.R., 1980. Some Implications of Ice Ridges and Rubble Field on the Design of Arctic Offshore Structures. NRC Workshop on Sea Ice Ridging, Calgary, 1980. NRC Tech. Memo, 134, NRC, Ottawa.

Croasdale, K.R. and R.W. Marcellus, 1981. Ice Forces on Large Marine Structures. IAHR Ice Symposium. University of Laval, Quebec.

Croasdale, K.R., 1983. The Present State of Future Development of Arctic Offshore Structures. 7th POAC VTT, Helsinki.

Croasdale, K.R., 1985. Recent Developments in Ice Mechanics and Ice Loads. Behaviour of Offshore Structures, Elsevier Science Publishers, Amsterdam.

EIS, 1982. An Initial Probabilistic Assessment of Ice Loading on Beaufort Sea Structures. Prepared by CMEL for the Canadian Beaufort Sea EIS Partners, 1982.

Korzhavin, K.N., 1962. Action of Ice on Engineering Structures. CRREL Translation 260 (1971).

Sanderson, T.J.O., 1984. Theoretical and Measured Ice Forces on Wide Structures. IAHR Ice Symposium, Hansburg.

EXTREME ICE FEATURE - STRUCTURE INTERACTION

ISSUES OF INTEREST

- CAN STRUCTURES BE DESIGNED FOR THEM? (COVERED IN THIS TALK)
- SHOULD STRUCTURES BE DESIGNED FOR THEM? (NOT COVERED IN THIS TALK)

KRC/NOV 1986
VUGRAPH 1

OUTLINE OF TALK

- OVERVIEW OF LOGIC AND MECHANICS OF ICE STRUCTURE INTERACTION
- RELEVANCE OF CURRENT METHODS TO EXTREME ICE FEATURES
- SIGNIFICANCE OF FIELD MEASUREMENTS AND REAL WORLD EXPERIENCE
- SPECULATE ON TYPICAL EXTREME ICE FEATURE LOADS AND WHETHER WE CAN DESIGN FOR THEM (PERSONAL VIEW)

KRC/NOV 1986
VUGRAPH 2

DEFINITION OF EXTREME ICE FEATURE FOR THIS TALK

- GREATER THAN 15 - 20 M THICK
- TABULAR OR RIDGE-LIKE
- DISCRETE (I.E. LIMITED IN AREA AND WITHIN THINNER ICE)

KRC/NOV 1986
VUGRAPH 3

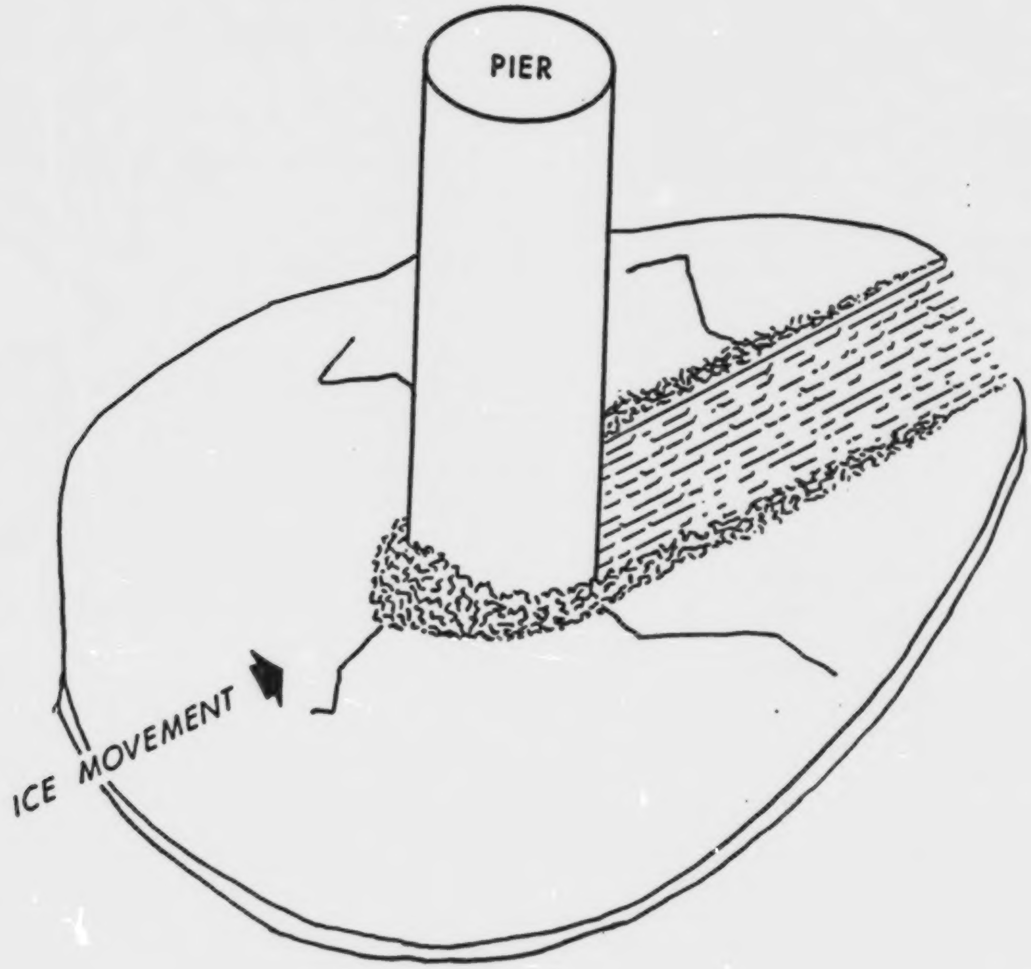
PIER
ICE MOVEMENT

ICE CRUSHING AROUND A PIER

VUGRAPH 4

ICE CRUSHING (INDENTATION)

- KORZHAVIN $p = Imk\sigma_c$

  $I = 1.0 \rightarrow 2.5$

  m = 0.9 FOR CIRCULAR PIERS

  K = CONTACT FACTOR (0.3-1.0)

  σ_c = UNIAXIAL COMPRESSIVE STRENGTH

- SIMPLE PLASTICITY (CROASDALE ET AL) $p = k\sigma_c(1+ 0.304 \frac{t}{b})$

  k = 1.0 FOR INITIAL BREAK OUT (OR MORE?)

  = 0.5 FOR CONTINUOUS CRUSHING

* PROBLEM IS DEFINING k AND σ_c (+ I)

KRC/NOV 1986
VUGRAPH 5

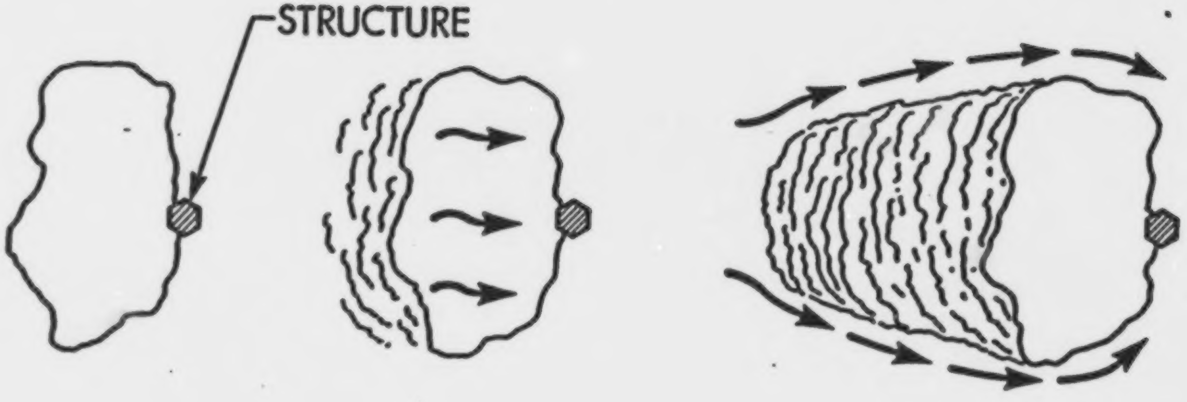

① INITIAL IMPACT BY LARGE ICE FEATURE (K.E. DISSIPATION)

② RIDGE BUILDING BEHIND ICE FEATURE (PLUS WIND DRAG)

③ PACK ICE DRAG ON STATIONARY RUBBLE

VUGRAPH 6

LIMIT STRESS

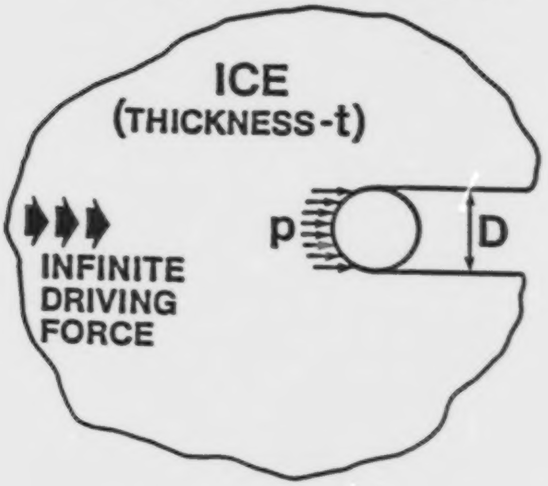
ICE
(THICKNESS-t)
INFINITE
DRIVING
FORCE
p
D

ICE LOAD = pDt

Limit-stress ice load governed by local ice failure

LIMIT MOMENTUM

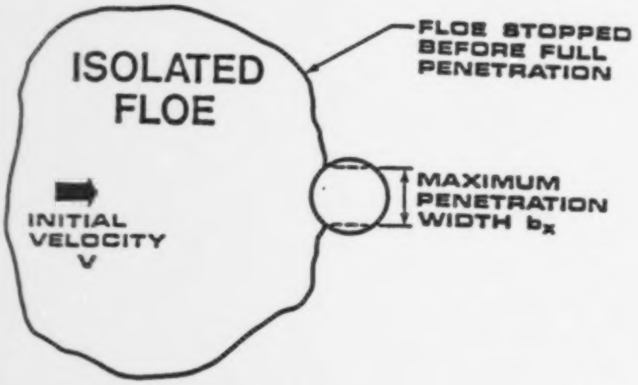
ISOLATED
FLOE
FLOE STOPPED BEFORE FULL PENETRATION
INITIAL
VELOCITY
V
MAXIMUM PENETRATION WIDTH b_x

Limit-momentum ice load governed by initial speed and mass of ice floe

LIMIT FORCE

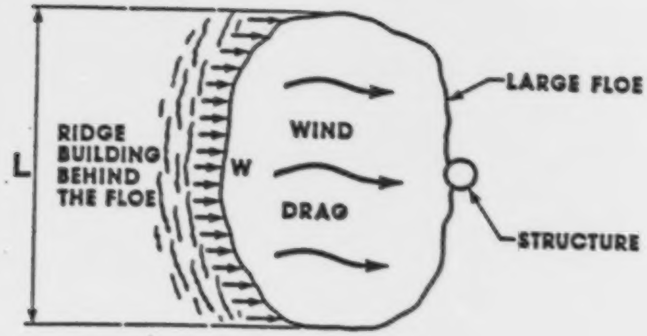
LARGE FLOE
RIDGE
BUILDING
BEHIND
THE FLOE
L
W
WIND
DRAG
STRUCTURE

Limit-force ice load governed by driving forces

LIMIT STRESS

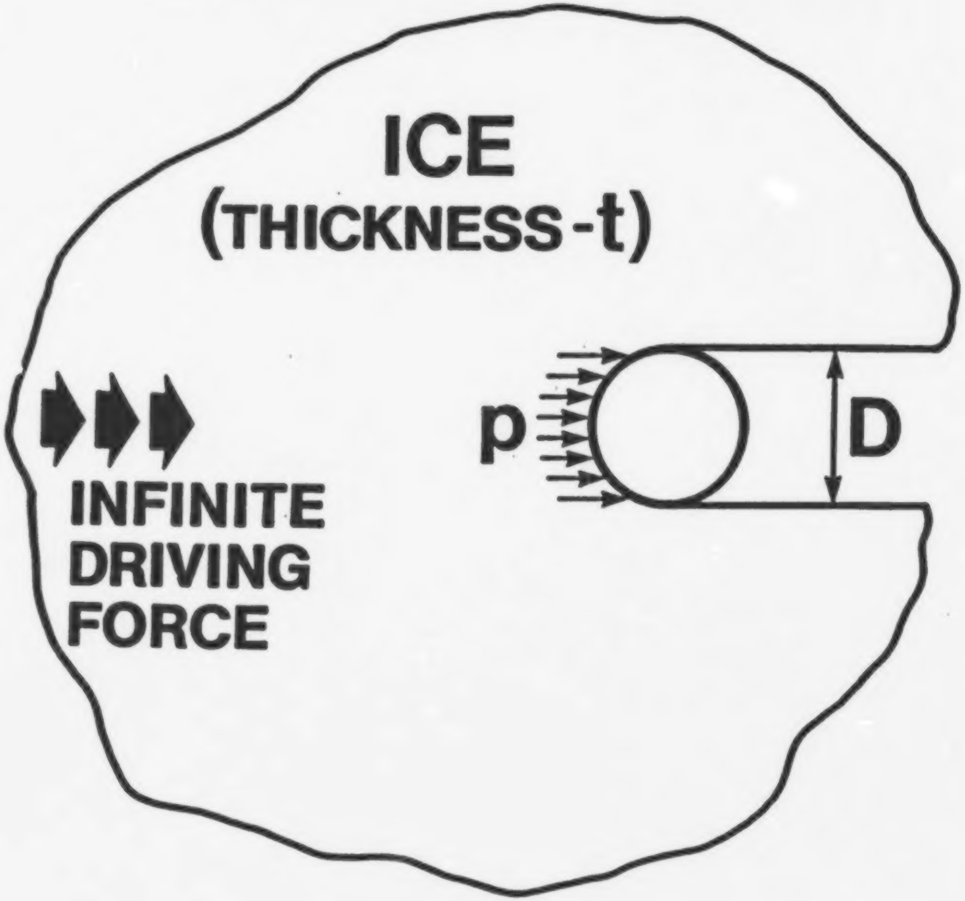
ICE
(THICKNESS-t)
INFINITE
DRIVING
FORCE
p
D

ICE LOAD = pDt

VUGRAPH 8

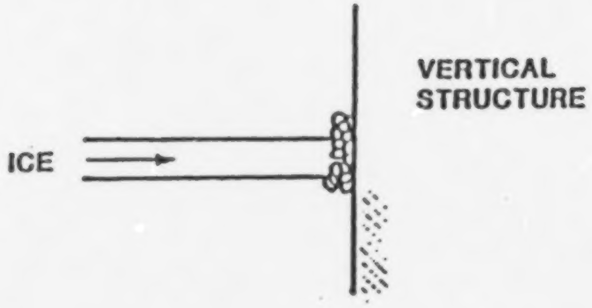
ICE
VERTICAL STRUCTURE

CRUSHING FAILURE

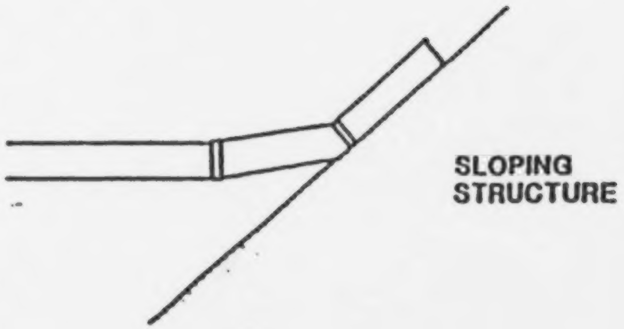
SLOPING STRUCTURE

BENDING FAILURE

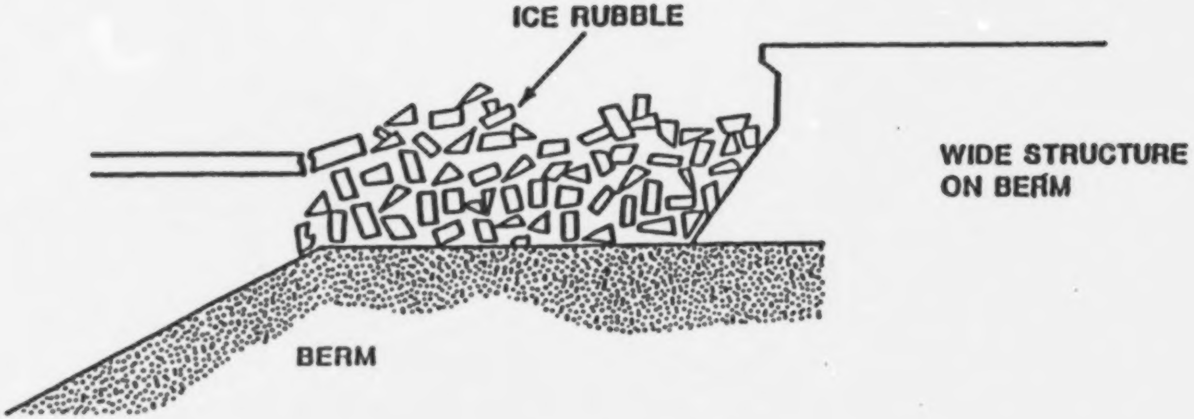
ICE RUBBLE
WIDE STRUCTURE ON BERM
BERM

RUBBLE BUILDING FAILURE

ICE FAILURE MODES

VUGRAPH 9

LIMIT MOMENTUM

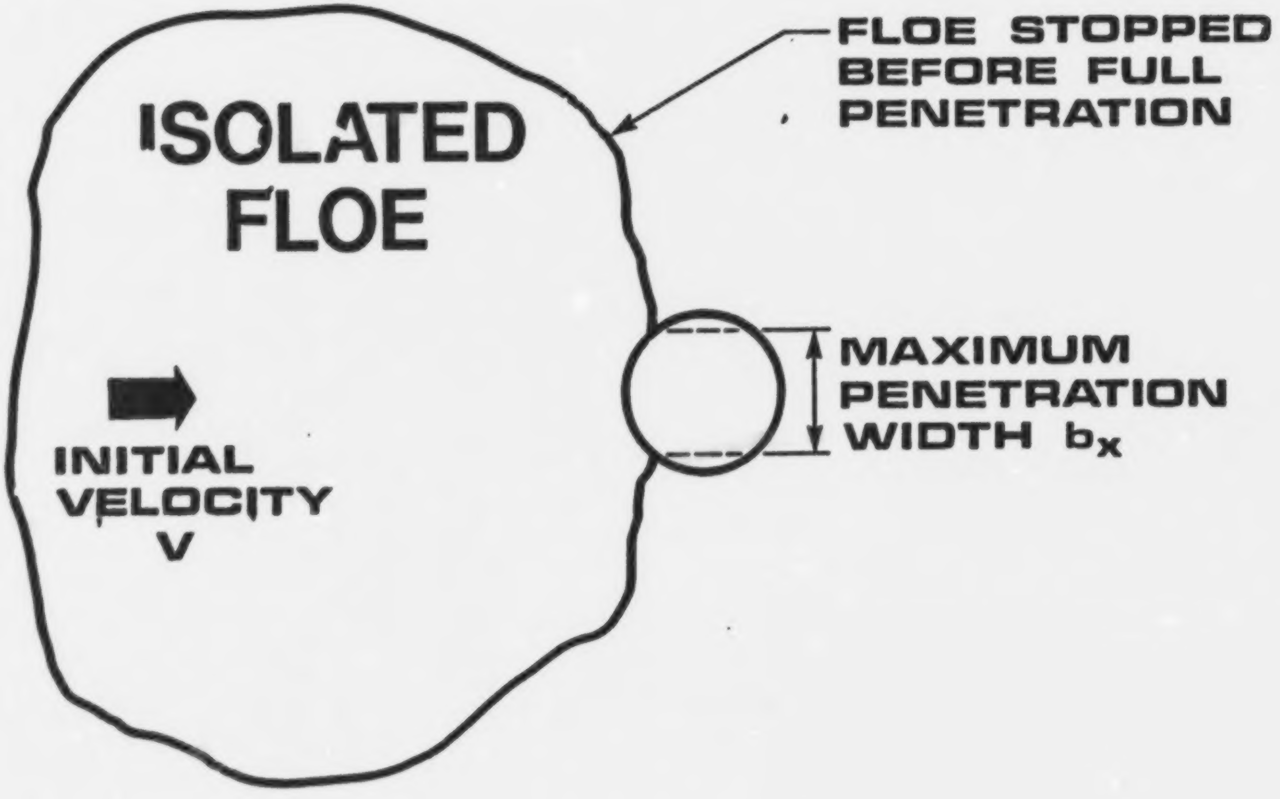
ISOLATED FLOE
INITIAL VELOCITY V
FLOE STOPPED BEFORE FULL PENETRATION
MAXIMUM PENETRATION WIDTH b_x

VUGRAPH 10

EQUATIONS FOR LIMIT MOMENTUM LOADS

ENERGY DISSIPATION

$$\underbrace{\int F\,dx}_{\text{WORK DONE BY ICE FORCE}} = \underbrace{1/2\ Mv^2}_{\text{INITIAL KINETIC ENERGY OF FLOE}} + \underbrace{\int P\,dx}_{\text{WORK DONE BY EXTERNAL FORCES (WIND AND CURRENT)}}$$

ICE FORCE

$$F = \underset{\text{EFFECTIVE ICE PRESSURE}}{p}\ \underset{\text{WIDTH AT PENETRATION x}}{b_x}\ \underset{\text{ICE THICKNESS}}{t}$$

VUGRAPH 11

LIMIT FORCE

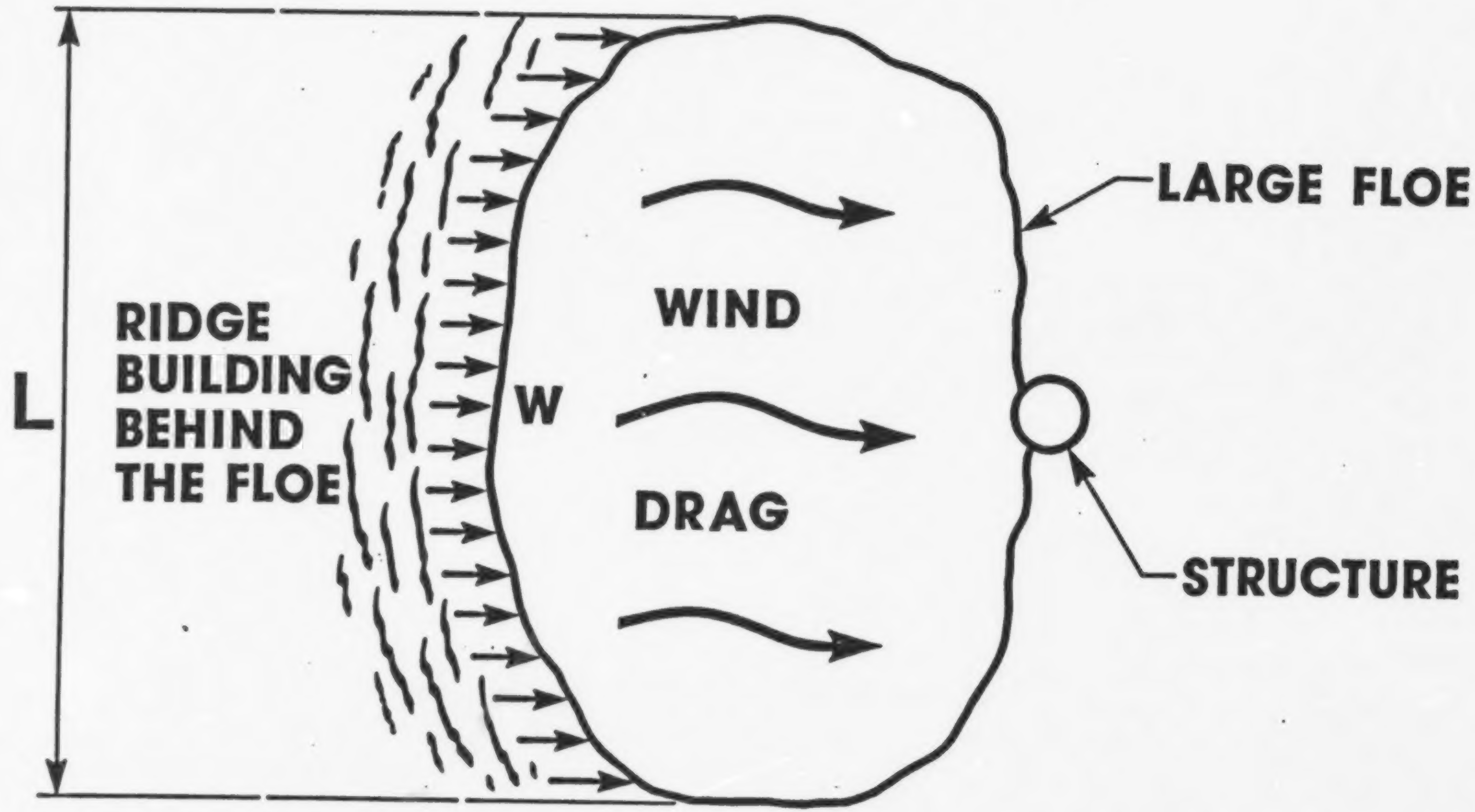
L
RIDGE
BUILDING
BEHIND
THE FLOE
W
WIND
DRAG
LARGE FLOE
STRUCTURE

VUGRAPH 12

LIMIT FORCE

ICE LOAD =

WIND DRAG + CURRENT DRAG + wL

VUGRAPH 13

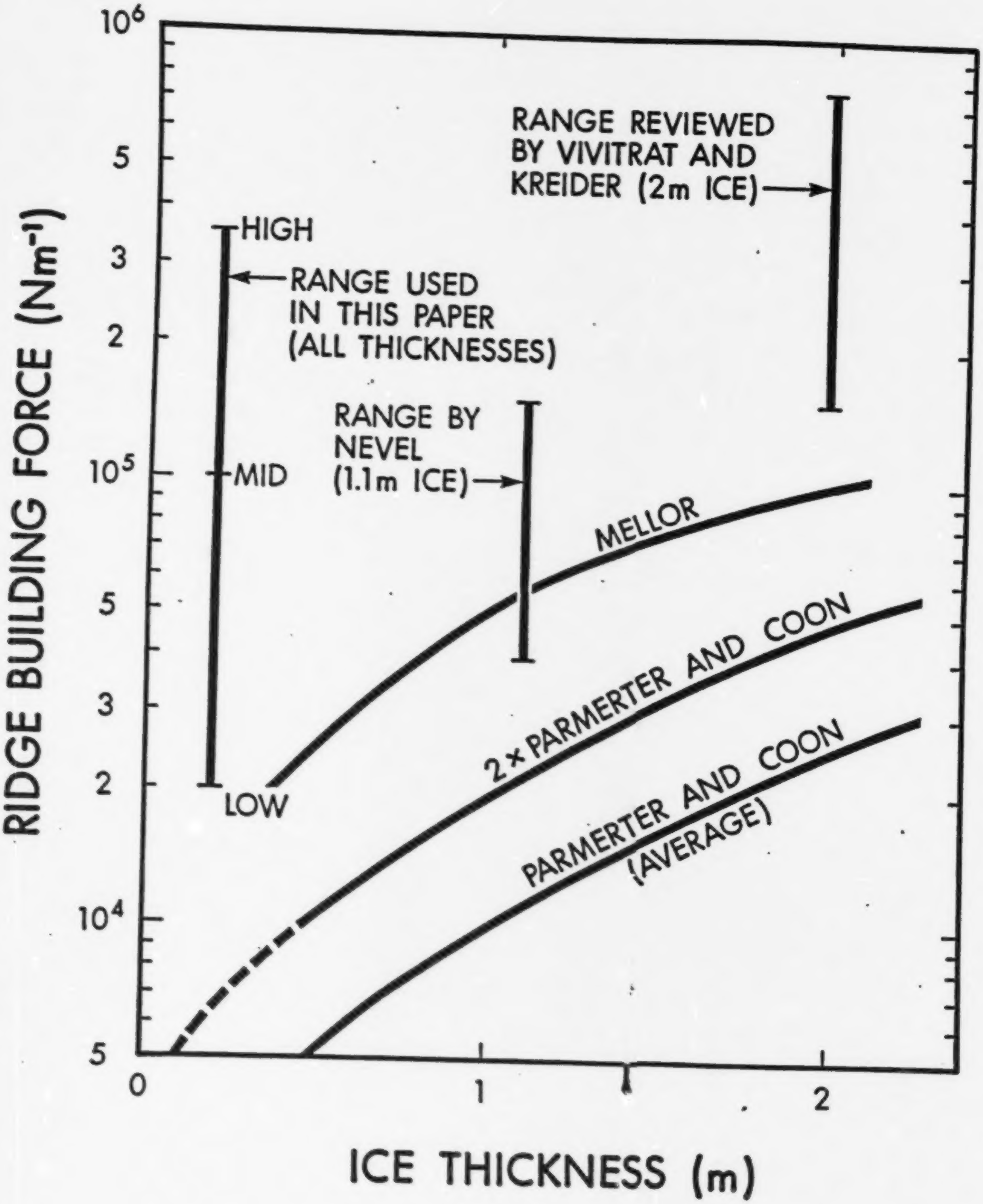

10^6
5
3
2
10^5
5
3
2
10^4
5
0
1
2
RIDGE BUILDING FORCE (Nm^-1)
ICE THICKNESS (m)
HIGH
MID
LOW
RANGE USED IN THIS PAPER (ALL THICKNESSES)
RANGE REVIEWED BY VIVITRAT AND KREIDER (2m ICE)
RANGE BY NEVEL (1.1m ICE)
MELLOR
2 × PARMERTER AND COON
PARMERTER AND COON (AVERAGE)

VUGRAPH 14

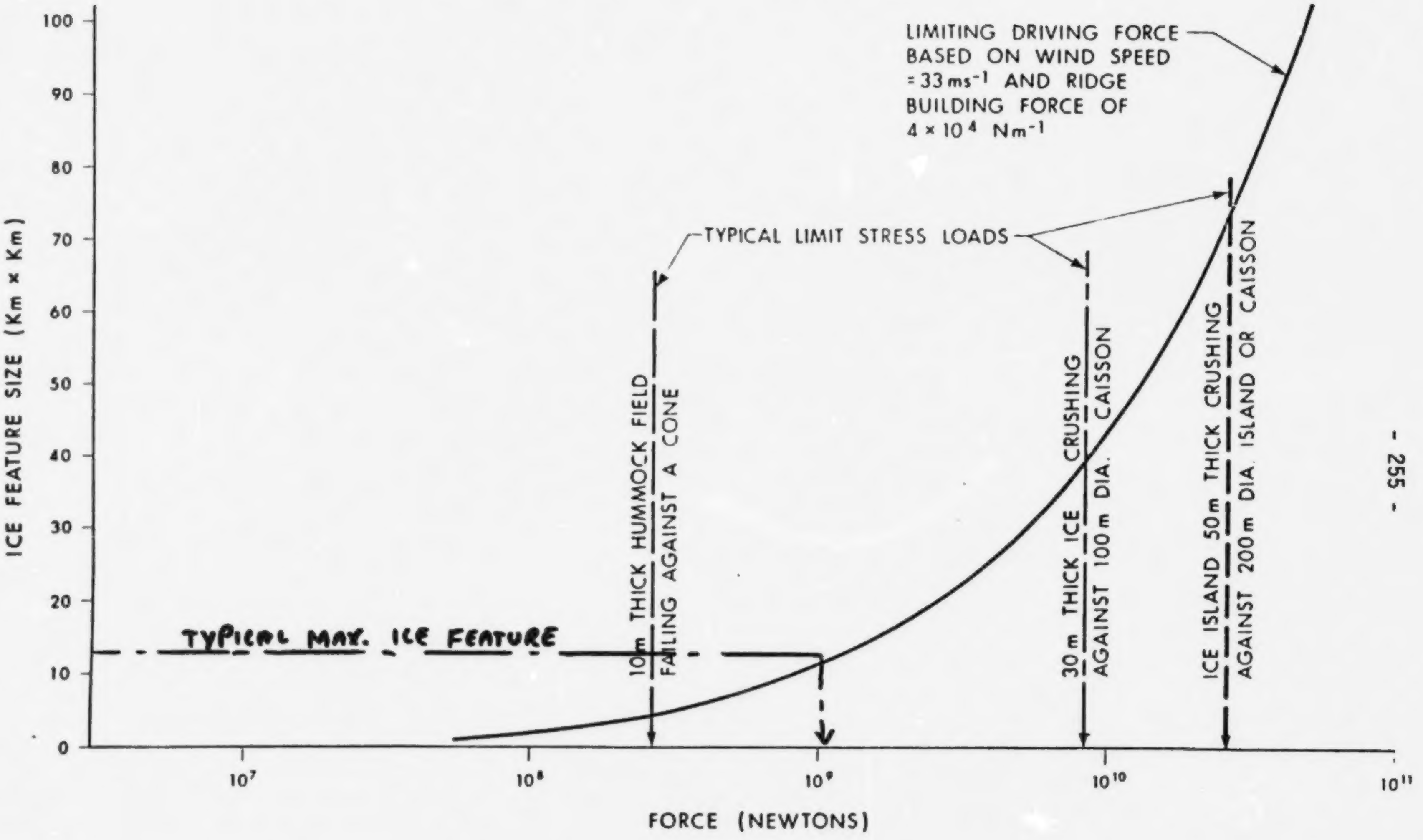

LIMITING FORCES

(AFTER INITIAL KINETIC ENERGY DISSIPATION)

VUGRAPH 15

(CROASDALE, 1980)

API 2N - CRUSHING

$$F = I\,K\,\sigma_c\,D\,t$$

σ_c — UNCONFINED CRUSHING STRENGTH

K — CONTACT FACTOR

I — INDENTATION FACTOR

KRC/NOV'86
VUGRAPH 16

ICE STRENGTH VS STRAIN RATE

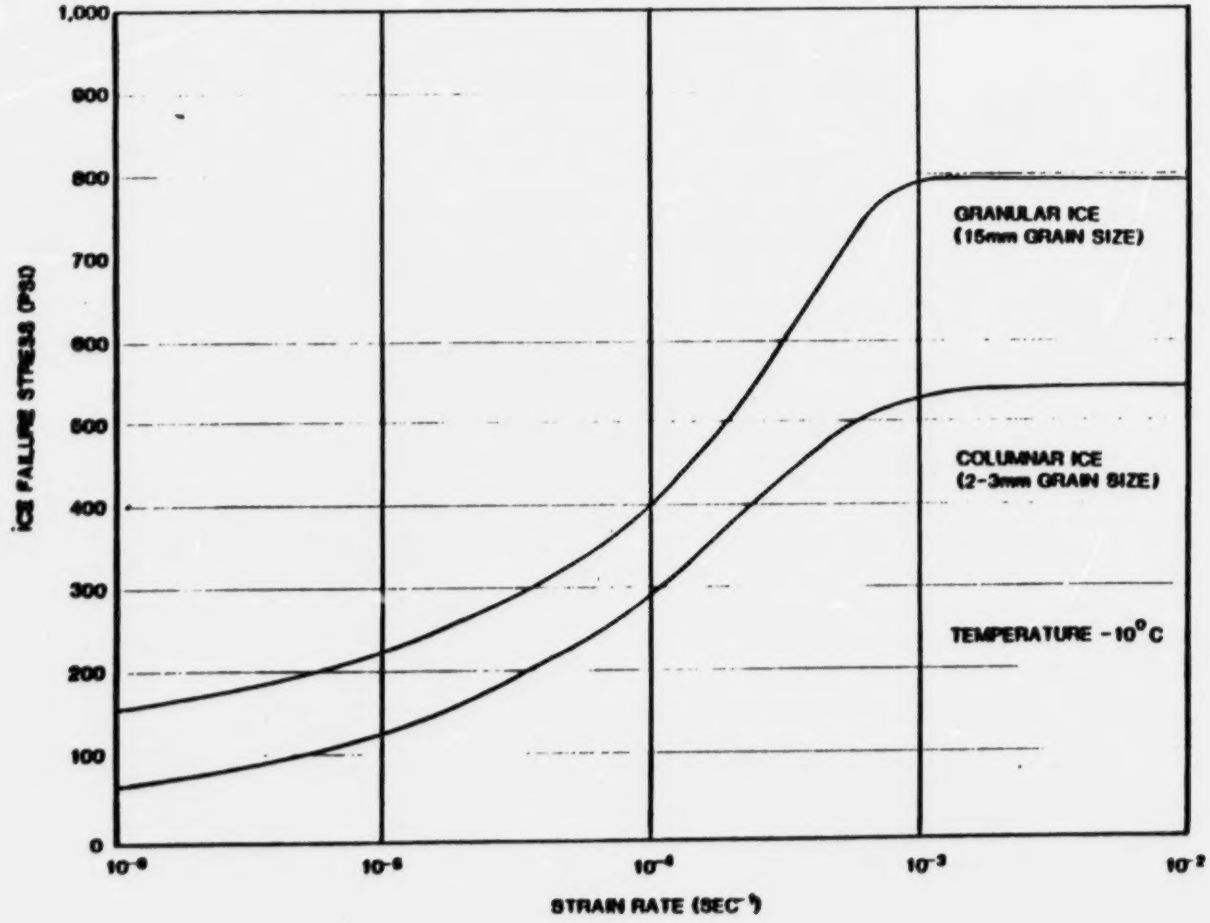

VUGRAPH 17

API 2N - ICE PRESSURES

A) COLUMNAR ICE; $-10°C$; $D/t \gg 10$; $\dot{\varepsilon} > 10^{-3}$
$I = 3.0$; $k = 0.6$; $\sigma_c = 550$ psi

EFFECTIVE ICE PRESSURE = 1200 PSI

B) GRANULAR ICE; AS ABOVE
$I = 1.2$; $\sigma_c = 800$ psi

EFFECTIVE ICE PRESSURE = 600 psi

KRC/NOV 1986
VUGRAPH 18

ICE LOAD BASED ON API 2N AND SMALL-SCALE ICE STRENGTHS

- 40 M THICK ICE
- GRANULAR ICE: FROM API - 2N
  p = 600 psi (4.0 MPa)
- STRUCTURE - 150 M DIA.

LOAD = 150 X 40 X 40 = 24,000 MN
OR 2,400,000 TONNES
OR 4,800,000 KIPS

(TYPICAL EXPLORATION CAISSON RESISTANCE = 100,000 TONNES)

KRC/NOV 1986
VUGRAPH 19

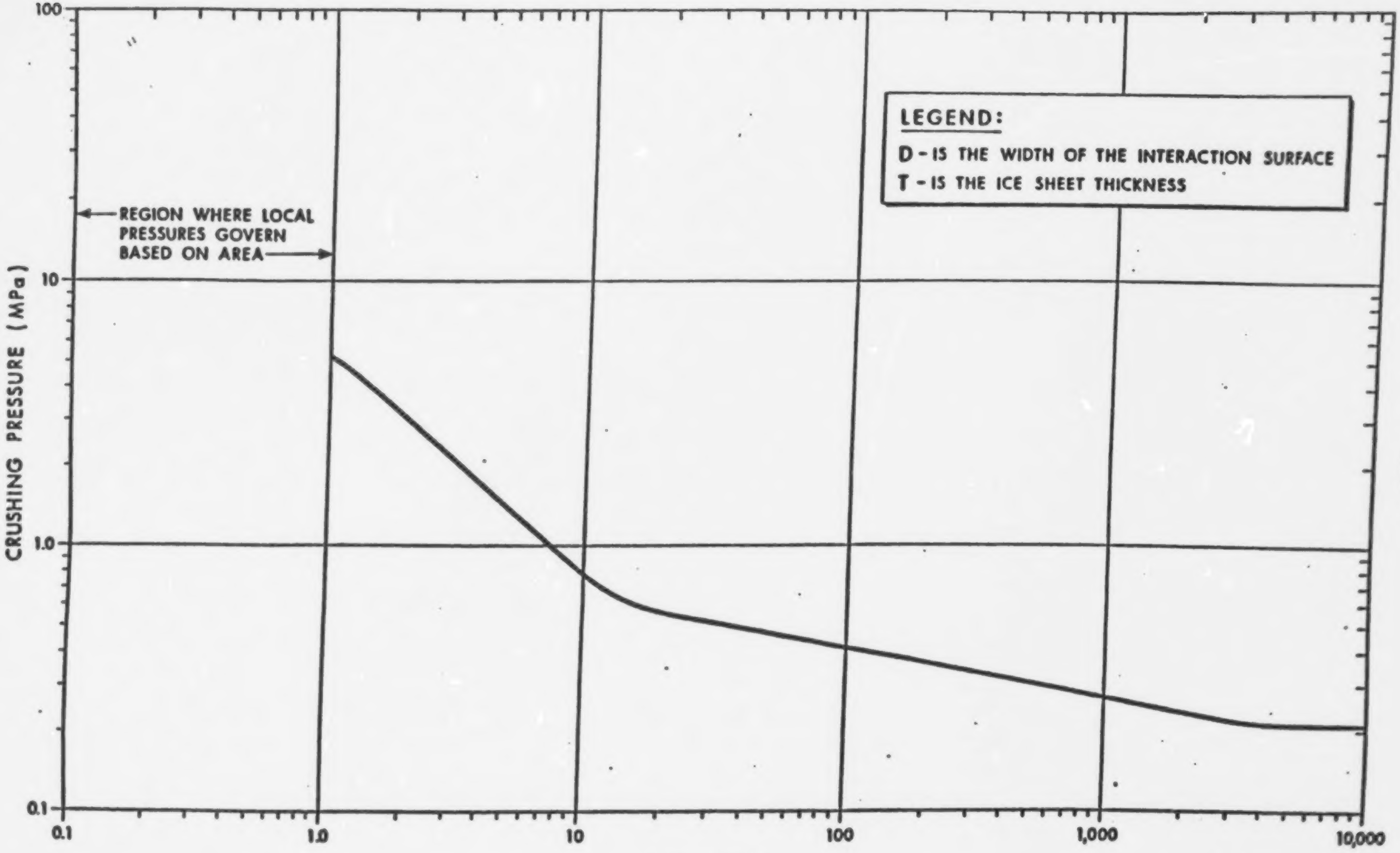

CRUSHING ICE PRESSURE VS. ASPECT RATIO (EIS)

VUGRAPH

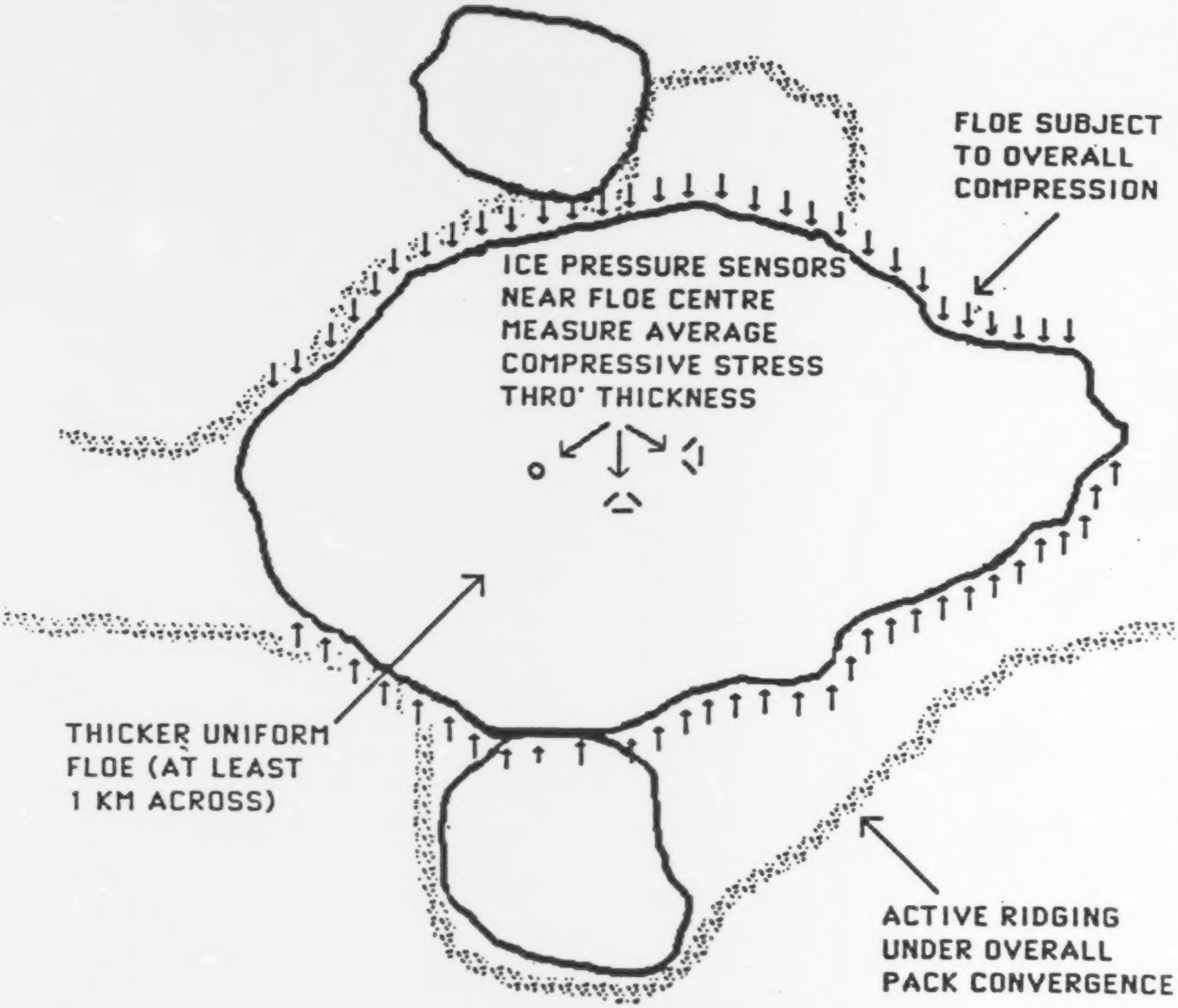
FLOE SUBJECT
TO OVERALL
COMPRESSION
ICE PRESSURE SENSORS
NEAR FLOE CENTRE
MEASURE AVERAGE
COMPRESSIVE STRESS
THRO' THICKNESS
THICKER UNIFORM
FLOE (AT LEAST
1 KM ACROSS)
ACTIVE RIDGING
UNDER OVERALL
PACK CONVERGENCE

OVERALLSCHEME
FOR MEASURING PACK-ICE FORCES

VUGRAPH 21

LOCATION OF STUDY

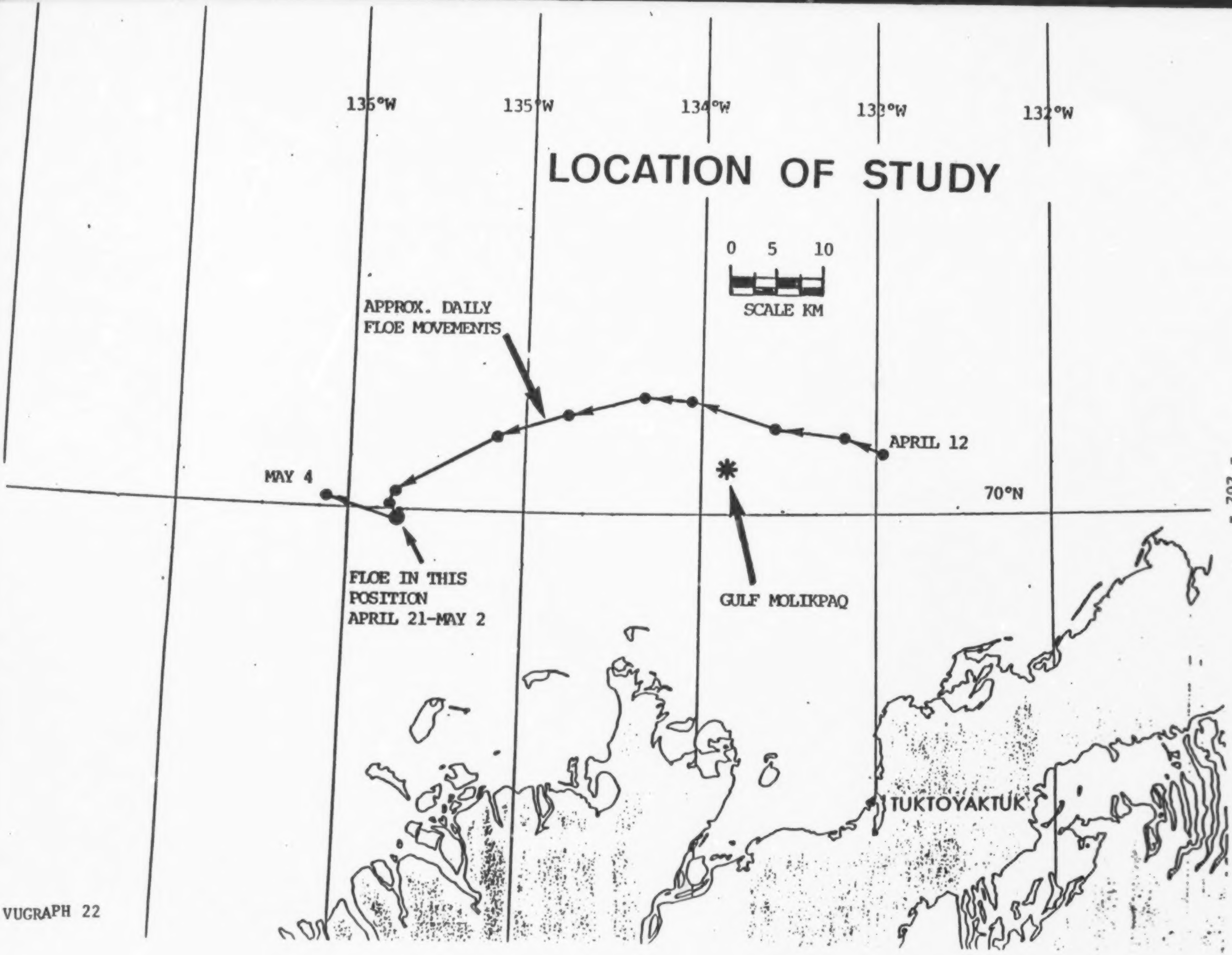
136°W
135°W
134°W
133°W
132°W
0 5 10
SCALE KM
APPROX. DAILY FLOE MOVEMENTS
APRIL 12
MAY 4
70°N
FLOE IN THIS POSITION APRIL 21–MAY 2
GULF MOLIKPAQ
TUKTOYAKTUK

VUGRAPH 22

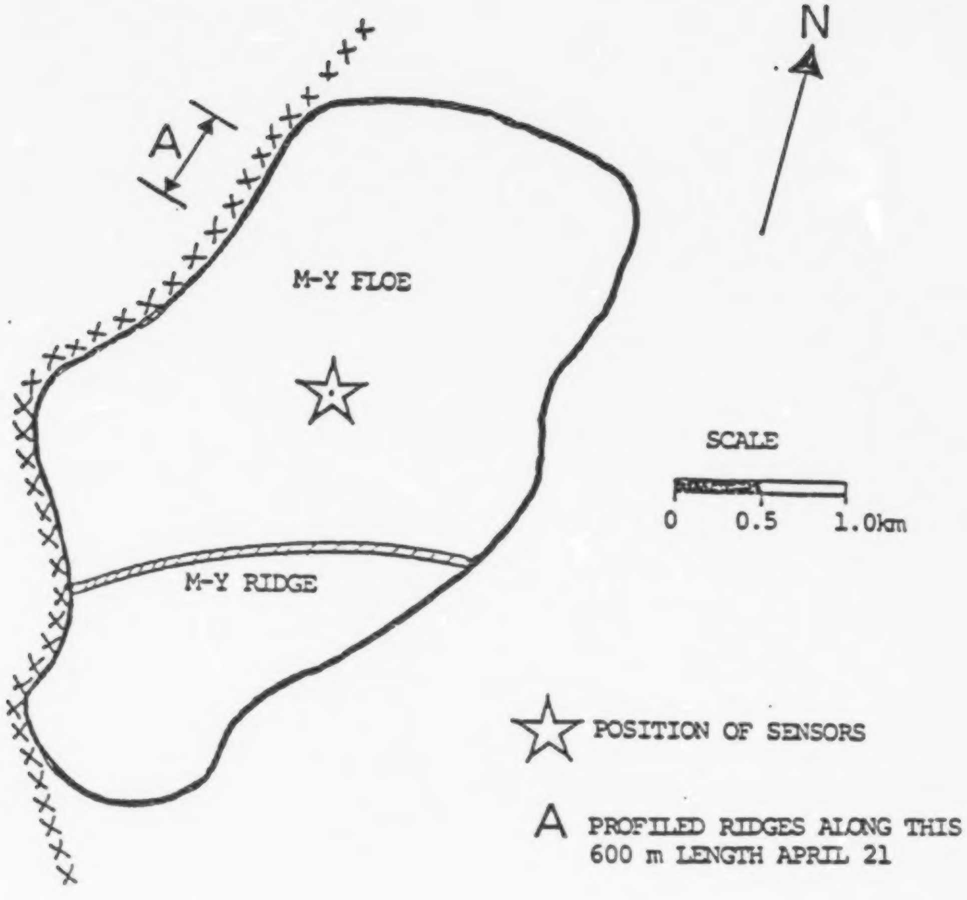
N
A
M-Y FLOE
SCALE
0
0.5
1.0km
M-Y RIDGE
POSITION OF SENSORS
A PROFILED RIDGES ALONG THIS 600 m LENGTH APRIL 21

RIDGING APRIL 21

VUGRAPH 23

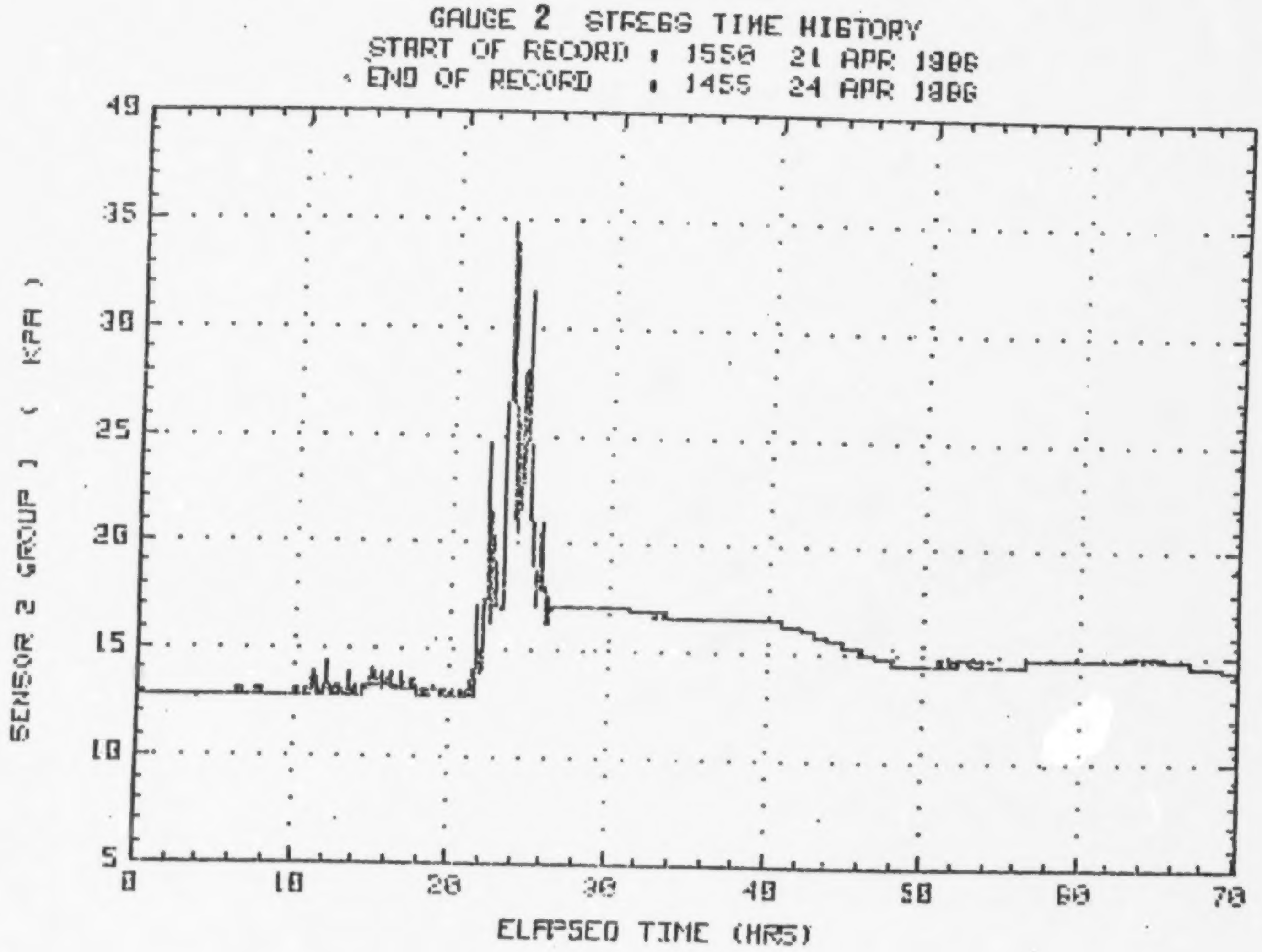

TYPICAL STRESS EVENT

VUGRAPH 24

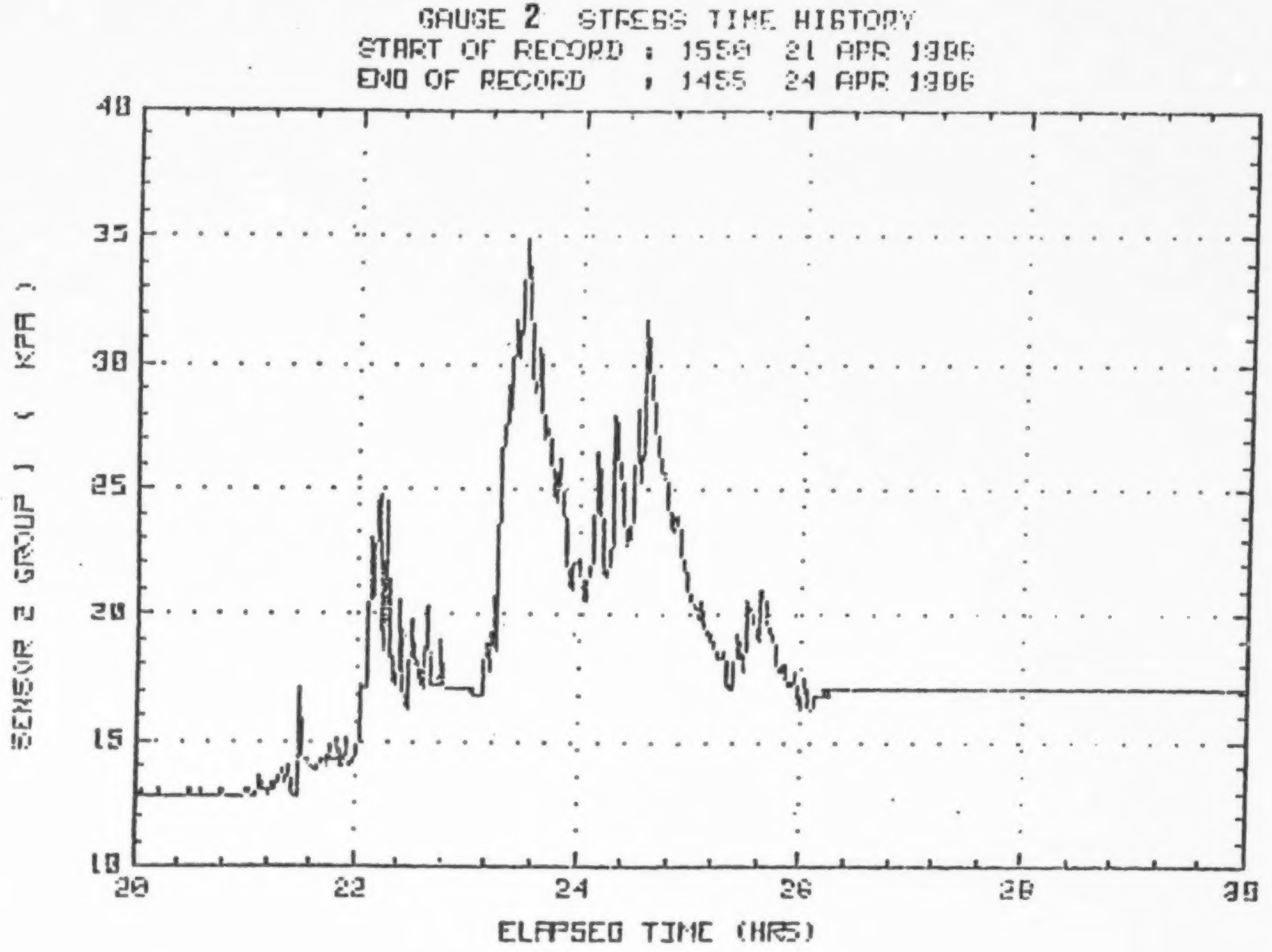

EXPANDED TIME SCALE

VUGRAPH 25

PACK ICE DRIVING FORCE EXPERIMENT (1986)
TENTATIVE RESULTS

- MAXIMUM STRESS EVENT DUE TO RIDGING AROUND FLOE $\simeq$ 25 kPa (4 psi)
- $w = \dfrac{\sigma}{t_{FLOE}}$
- FOR $t = 3$ m: $w = \dfrac{25 \times 10^3}{3} = 1.0 \times 10^4$ N/m
- ALLOW FACTOR OF 3 FOR ERRORS + UNCERTAINTIES GIVES 3×10^4 N/m FOR 5 km FLOE

KRC/NOV 1986
VUGRAPH 26

PACK ICE FORCES DEDUCED FROM MOLIKPAQ MEASUREMENTS

- QUOTED AS AT LEAST 500 kPa - 1500 kPa (OVER 1 KM ?) (FROZEN-IN ?)

- FOR 1.5 M 1st YEAR ICE
  w IS IN RANGE $7.5 \text{ X } 10^5$ N/m
  TO
  1.5×10^6 N/m

KRC/NOV 1986
VUGRAPH 27

SPECULATIVE PACK ICE FORCES AS FUNCTION OF FLOE WIDTH

WIDTH	W	MEASURED OR DEDUCED VALUES FOR W	STRUCTURE LOAD BASED ON W
km	N/m	N/m	TONNES-FORCE
1.0	10^6	$0.75-1.5X10^6$	100,000
5.0	$2 X 10^5$	$3 X 10^4$	100,000
10.0	10^5	?	100,000

KRC/NOV 1986
VUGRAPH 28

SPECULATIVE ICE LOADS DUE TO LARGE ICE FEATURES

- STRUCTURE DIA. = 15.0 m (VERTICAL SIDES)
- ICE CRUSHING PRESSURE = 1.0 MPa (140 psi)
- ICE FEATURE SIZE = 10 km
- DRIVING FORCE = 10^5 N/m

LOCAL ICE THICKNESS (m)	LIMIT-STRESS LOAD (TONNES)	LIMIT FORCE LOAD (TONNES)
10	150,000	100,000
20	300,000	100,000
40	600,000	100,000

KRC/NOV 1986
VUGRAPH 29

SLIDING RESISTANCE: OFFSHORE PRODUCTION PLATFORM - 40 m WATER

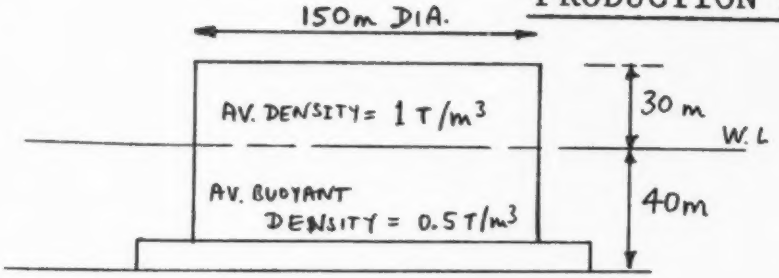
150m DIA.
AV. DENSITY = 1 T/m³
AV. BUOYANT DENSITY = 0.5 T/m³
30 m
W.L
40m

RESISTANCE = WEIGHT ON SEA FLOOR X TAN Ø

$$= \frac{\pi}{4} (150)^2 [\ (30x1) + (40 \times 0.5)]\ \tan 30^0$$

= 440,000 TONNES-FORCE

WITH F.O.S. = 2.0
ALLOWABLE ICE LOAD = 220,000 TONNES

KRC/NOV 1986
VUGRAPH 30

KINETIC ENERGY DISSIPATION

- VARIOUS LIKELY MECHANISMS

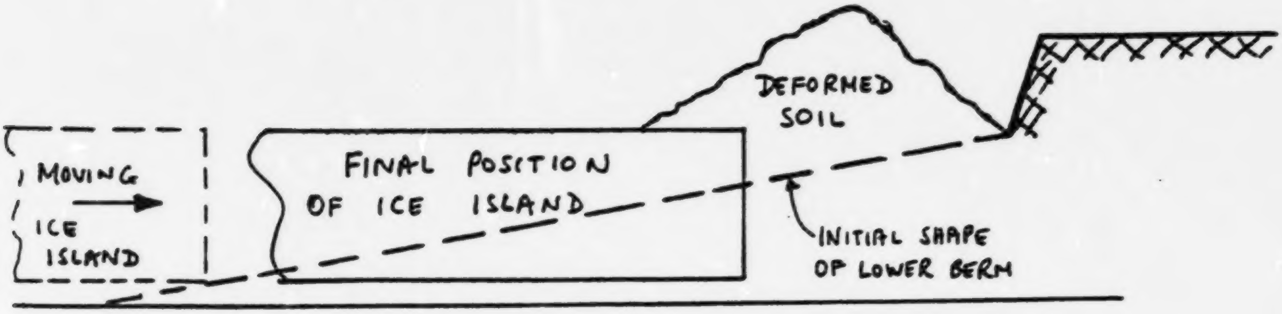
MOVING
ICE ISLAND
FINAL POSITION OF ICE ISLAND
DEFORMED SOIL
INITIAL SHAPE OF LOWER BERM

① - WORK DONE BY DEFORMATION AND LIFTING-UP OF SOIL IN LOWER BERM

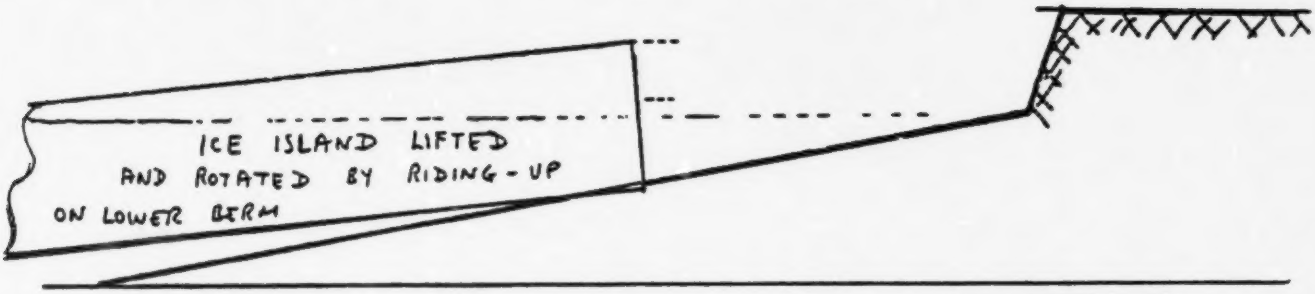
ICE ISLAND LIFTED AND ROTATED BY RIDING-UP ON LOWER BERM

② - WORK DONE IN LIFTING AND ROTATING ICE ISLAND

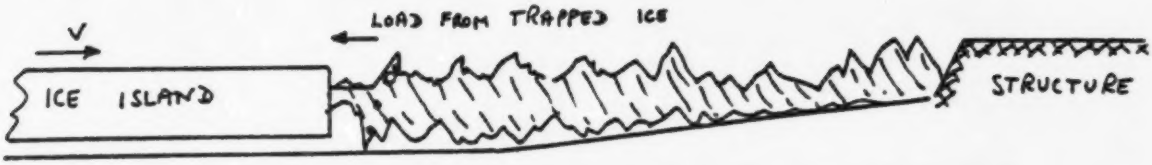
V
LOAD FROM TRAPPED ICE
ICE ISLAND
STRUCTURE

③ - WORK DONE BY TRAPPED ICE BETWEEN ICE ISLAND AND STRUCTURE (DEFORMATION + LIFTING)

VUGRAPH 31

KRc.

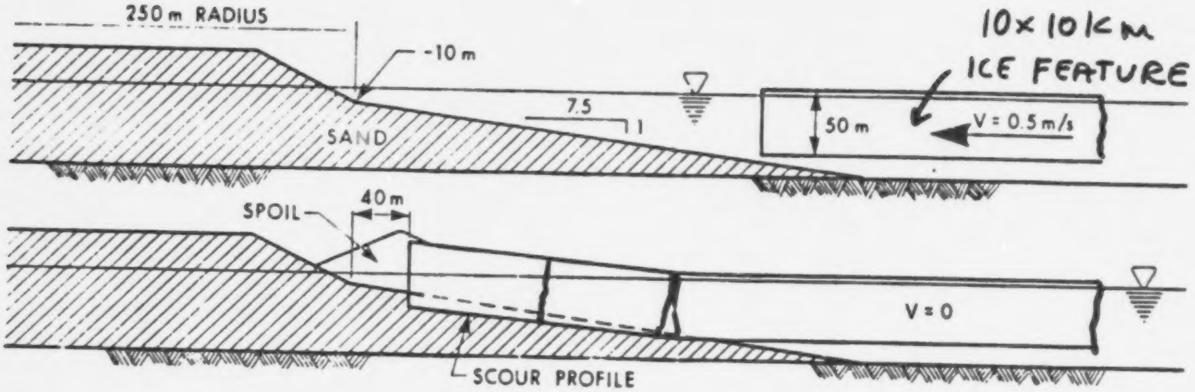
250 m RADIUS
-10 m
10× 10 km
ICE FEATURE
7.5
1
SAND
50 m
V = 0.5 m/s
SPOIL
40 m
V = 0
SCOUR PROFILE

ILLUSTRATION OF THE INTERACTION BETWEEN A 50 m THICK ICE FEATURE AND A BERMED ISLAND

TYPICAL 'ENERGY SINKS' (FROM THEORETICAL MODEL)

WORK BY SOIL FRONTAL FORCE – 53%
WORK BY SOIL BOTTOM FRICTION – 33%
POTENTIAL ENERGY GAIN OF ICE – 14%
100%

VUGRAPH 32

KRc.

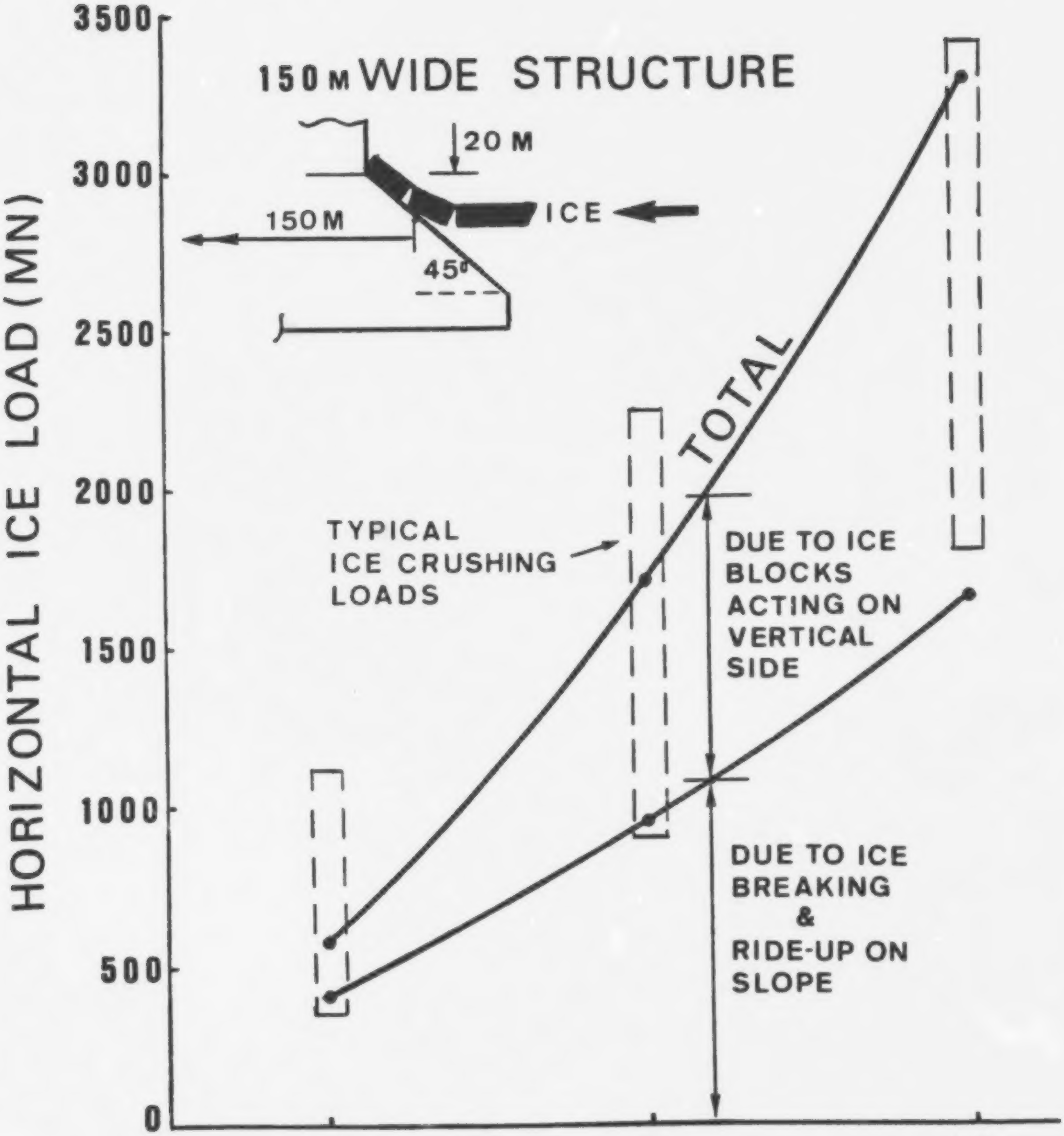
150 M WIDE STRUCTURE
20 M
150 M
ICE
45°
TOTAL
TYPICAL ICE CRUSHING LOADS
DUE TO ICE BLOCKS ACTING ON VERTICAL SIDE
DUE TO ICE BREAKING & RIDE-UP ON SLOPE
HORIZONTAL ICE LOAD (MN)
0
500
1000
1500
2000
2500
3000
3500
5
10
15
ICE THICKNESS (M)

VUGRAPH 33

1 OF 2

CONCLUDING REMARKS

- LARGE-SCALE DATA INDICATES LOWER LIMIT-STRESS LOADS THAN PREDICTED USING INDENTATION THEORY AND SMALL-SCALE STRENGTHS (E.G. 1.0 MPa EFFECTIVE GLOBAL ICE PRESSURE VS SAY 5.0 MPa)
- A REASONABLY CONSERVATIVE VALUE FOR PACK ICE DRIVING FORCES (E.G. RIDGING FORCES) OVER 10 km MIGHT BE 10^5 N/m (BUT HIGHER OVER SMALLER WIDTHS)
- AT 1.0 MPa ICE CRUSHING STRENGTH AND WITH ICE THICKER THAN ABOUT 15 - 20 m THE ADVANTAGE OF CONE OVER VERTICAL STRUCTURE MAY NOT EXIST (EXCEPT RE: DYNAMIC LOADS)

KRC/NOV 1986
VUGRAPH 34

2 OF 2

CONCLUDING REMARKS

- ON SANDY SOILS, LARGE PRODUCTION STRUCTURES CAN BE DESIGNED FOR EXTREME ICE FEATURES UP TO 40 m THICK (IF LIMIT FORCE LOADS CAN BE SHOWN TO GOVERN)

E.G. LIMIT STRESS LOAD = 600,000 TONNES
LIMIT FORCE LOAD = 100,000 TONNES
RESISTANCE = 440,000 TONNES

- WHEN INVOKING LIMIT FORCE LOAD, THE INITIAL MOMENTUM OF ICE FEATURE HAS TO BE DISSIPATED (UNDERWATER BERM MAY BE NEEDED)
- ALL THE ABOVE IS VERY SPECULATIVE (MORE LARGE-SCALE DATA NEEDED)

KRC/NOV 1986
VUGRAPH 35

NRC WORKSHOP ON EXTREME ICE FEATURES

Questions and Discussions Form

AUTHOR: K.R. Croasdale

PAPER: Extreme Ice Feature - Structure Interaction

DISCUSSION BY: B.D. Wright

DISCUSSION:

As always your presentation was excellent and outlined a number of very fundamental and important issues associated with extreme ice feature interactions and the associated "design loads". Although a slight digression, could you comment on the role of probabilistic ice loading models for the design criteria definition, particularly in relation to the rarity of extreme feature interactions?

AUTHOR'S REPLY:

There is no doubt in my mind that in considering the issue of loads on structures caused by extreme ice features one has to recognize the statistical and risk aspects of the problem. This, of course, has been done in the past, and several probabilistic ice load models and return-period based ice load criteria have been developed (including by yourself).

My talk has emphasized the deterministic aspects of the problem, and the likely forces associated with different interaction scenarios. This is useful in order to bracket the kinds of loads involved, but also to help identify the parameters which should be incorporated into a probabilistic model.

DISCUSSION BY: H.R. Kivisild

DISCUSSION:

Is it not true that even large (and thick) ice masses can be handled by sloping contact faces?

AUTHOR'S REPLY:

A large iceberg needs to be lifted by only about 1 m on a sloping face to absorb all its kinetic energy. So a sloping contact face is indeed an efficient means of absorbing energy during impact.

DISCUSSION BY: R. Gerard

DISCUSSION:

Why is it that the vast amount of experience with everyday bridge pier design codes and even load measurements continues to be ignored in the generation of design criteria for offshore structures?

AUTHOR'S REPLY:

As I mentioned in my talk, the starting point for engineers looking at ice loads on offshore structures was indeed bridge pier codes and experience. In fact, the API 2N formula for ice forces on a vertical structure is based on Korzhavin's equation. On the other hand, it was recognized that ice action on wide structures led to different kinds of ice failure processes than on a narrow bridge pier (e.g., non-simultaneous failures, ice rubble build-up, etc.). It was felt (and I think, quite rightly) that these different ice failure processes required new approaches, and that bridge pier codes were not appropriate.

Nevertheless, I am sure you are correct in suggesting that ongoing experience with bridges should not be ignored by offshore engineers; especially certain aspects of bridge pier loads such as dynamic response and local ice pressures.

ICE/STRUCTURE INTERACTION RESEARCH NEEDS

A Summary of Workshops Held in Calgary, 1986

by

Tom Zimmerman
Centre for Frontier Engineering Research

ABSTRACT

In May and June, 1986, a series of workshops dealing with ice/structure interaction was held in Calgary, Alberta. The workshops looked at the state-of-the-art of ice/structure interaction, identified gaps in the knowledge that currently exists in Canada and made recommendations regarding research needs. The invited participants included many experts in the field. The following seven areas were discussed:

1. Global and Local Ice Loads Including Dynamic Effects
2. Physical Modelling
3. Rubble Formation
4. Monitoring and Measuring Systems
5. Statistical and Probabilistic Aspects
6. Failure Criteria and Structural Response - Steel Structures
7. Failure Criteria and Structural Response - Concrete Structures

This paper summarizes the highlights from the workshop discussions and the recommendations regarding research needs.

INTRODUCTION

During the past twenty-five years, but especially during the last decade, significant research work has been completed which has focussed on the safe operation of ships and structures in the ice-infested waters of the Canadian offshore. Probably the most important thrust of this research, from the point of view of operational safety, has been directed at understanding the process involved when ice meets structure. The problem has specific parameters - in the arctic, the structures tend to be unique in form, in detail and in arrangement - the ice may exist in discrete features or in sheet form. On the east coast the structures tend to be more familiar in type - adaptations from the North Sea experience - but the ice component is even more challenging - the bergs ranging in size from those approaching the "maximum credible event" to smaller "bergy bits", driven at high speeds to impact on the structure.

Engineers have approached ice-structure interaction by separately examining existing information on the two components. Research on structures - steel, composite and concrete - has been in progress for decades, so that a reasonable understanding of the behaviour of the common elements has been achieved. Research on the mechanics of ice has been increasing in intensity as the importance of being able to operate in our cold environment strikes home. It is only, however, when engineers are faced with the problem of designing a specific structure to resist actual ice-forces over a significant life, that the weaknesses in our current state of knowledge are exposed.

Most of the research on structural components has used specimens that have proportions typical of structures designed for gentler climatic conditions - or even have their basis in building and bridge technology. When faced with ice features that exert loads thousands of times greater than those experienced on traditional structures, the designer is forced into arrangements that are massive by comparison; steel structures with thick plates, complex welds, and fatigue and impact susceptible details; and concrete structures with high strength concrete and congested reinforcing schemes.

Research on ice has been built on a base of small scale laboratory testing - typical of the materials and foundations technologies. The base, however, is inadequate to deal with an environment in which large scale effects dominate the behaviour - in which, for example, the ability to assess the load transfer through a matrix of jumbled ice rubble blocks is essential to the safety of a platform or vessel. While in the last ten years significant progress has been made in assessing these large scale effects, a unified approach which gives consistent results has not yet emerged.

During the months of May and June, this year, seven working sessions were convened, attended by experts in the various facets of ice-structure interaction. The groups were convened in an attempt to summarize the state-of-the-art of ice/structure interaction, to assess the accomplishments to date and to pinpoint the gaps that remain to be bridged.

Dr. Maurice J. Ruel, Director General, Environmental Protection, of the Canada Oil and Gas Lands Administration, addressed the Session on June 12. Dr. Ruel serves as Chairman of both the Panel on Energy Research and Development (PERD), and the Environmental Studies Revolving Funds.

Dr. Ruel outlined the considerable research effort, related to marine engineering for conventional energy systems, that is taking place within the overall framework of energy related research sponsored by the Government of Canada. In that context, workshop members were made aware of the longer term perspective of Government and of the primary objective of the research effort: "to ensure, through research and development, that there is sufficient technical knowledge for the federal government to discharge its policy, service, regulatory and jurisdictional responsibilities relating to the supply of crude oil, natural gas and electricity; and, to complement industry by providing technological support for maintaining near-term security in domestic oil and natural gas supply."

In terms of the ice/structure interaction problem, Dr. Ruel indicated that the more specific objectives are:

> "to develop and improve models, methods, and technologies required to define environmental design criteria;
>
> to improve techniques and technologies for offshore safety;
>
> and, to provide the necessary engineering and related research and development, for rigs and for systems on rigs to enable safe operations."

WORKSHOP FORMAT

The workshops were sponsored by Public Works Canada, and organized by the Centre for Frontier Engineering Research.

The steering committee, which set the scope of the workshops, consisted of:

Moe Cheung, of Public Works Canada, in Ottawa
Jack Clark, of C-CORE, in St. John's
Bob Frederking, of the National Research Council, in Ottawa
Brian Wright, of Gulf Canada Resources, Calgary
and Peter Adams, of the Centre for Frontier Engineering Research, in Edmonton

This steering committee set 3 objectives for the workshops:

Firstly, to assess the state-of-the-art of ice/structure interaction;

Secondly, to identify gaps in knowledge that currently exist in Canada;

and Finally, to make recommendations regarding research needs.

The committee also identified the seven general areas of interest that were considered during the workshops:

1. Global and Local Ice Loads, Including Dynamic Effects
2. Physical Modelling
3. Rubble Formation
4. Monitoring and Measuring Systems
5. Statistical and Probabilistic Aspects
6. Failure Criteria and Structural Response - Steel Structures
7. Failure Criteria and Structural Response - Concrete Structures

The seven sessions were conducted over a period of four days in May and June. Each session began with a keynote address by an invited speaker having an acknowledged degree of expertise in the area considered, and continued with a general discussion involving all participants.

The invited speakers: for Global and Local Ice Loads, was Norm Allyn of Swan Wooster Eng. Co., Vancouver; for Physical Modelling, Gary Timco, of the National Research Council's Hydraulics Lab in Ottawa; for Rubble Formation, Frank Bercha, of Frank Bercha & Associates, Calgary; for Monitoring and Measuring Systems, Dan Masterson, of Geotech, Calgary; for Statistical and Probabilistic Aspects, Ian Jordaan, formerly with DnV, now with Memorial University in St. John's; for Failure Criteria and Structural Response - Steel Structures, Laurie Kennedy, of the University of Alberta; and for Failure Criteria and Structural Response - Concrete Structures, Mike Collins, of the University of Toronto.

Proceedings of the workshops, containing the keynote addresses, along with summaries of the discussions and recommendations, are being distributed by COGLA. The comments contained in each keynote address are those of the author, and do not necessarily reflect the concensus of the workshop. However, in the discussion summaries and recommendations, every effort has been made to present the concensus of each working session.

RECOMMENDATIONS

I will now briefly discuss the recommendations of the workshops and describe the relative priorities among the seven topic areas, as seen by the workshop participants.

(See Appendix for detailed workshop recommendations.) In this way, I will attempt to establish an overall perspective for the research recommendations.

The consolidation of existing information and the acquisition of new information pertaining to global, semi-local and local ice loads was identified as the top priority for ice/structure research. The high cost of developing new information, particularly that resulting from large scale tests, is well recognized. Thus a balance is recommended between the re-examination of existing results and the selective pursuit of new testing programs. Of the areas considered, ice loading has the largest number of remaining unknowns and the potential for the greatest impact on the safety and economy of offshore development. Although a large volume of information has been developed, much of it is proprietary and has not been compared with other data sources or incorporated into the body of generally available information. Much of the existing information has been gathered to treat the effect of a single variable (such as strain rate, contact area, aspect ratio, etc.) while other variables which effect the data have been ignored. It is therefore difficult in many instances to directly compare data from different sources.

There have been significant developments, such as the establishment of the relationships between pressure and aspect ratio. Significant data gaps still exist, however, which force extrapolation of this and other concepts beyond the appropriate limits and thus detract from their use in detailed design.

Two major approaches are taken to the evaluation of ice loads: 1) the theoretical prediction of ice pressures from an ice mechanics approach, and 2) the direct measurement of ice pressures or loads. Both of these approaches deserve additional attention; the former to increase the understanding of failure processes and the latter for immediate use in design and for verification of various analytical models. The highest priority is assigned to the collection and consolidation of large scale field information concerning: the mechanical and physical properties of ice; qualitative information on failure modes for various ice-feature and ice-structure geometries; quantitative ice pressure data, for various ice-feature and ice-structure geometries; and static and dynamic response data for both ice and structures.

As the size of the general data base increases, more use will be made of probabilistic models to provide more consistent factors of safety for offshore structures. Further work, placing existing data into a probabilistic framework, will point to areas in which new information is required. It is important in this work, to maintain a close association between those collecting environmental data, those charged with inserting it in probabilistic models and those using the results in design.

There is a need to recognize that the ice loading data is required for the design of the structure and not only as a vehicle for the study of scientific concepts. Thus the design format must be considered in the initial stages of research plan formulation. Advice from the design community must be sought and agreement reached on which quantitities are essential to measure and how the recorded data should be categorized.

Another area of high priority is the study of rubble field morphology and the application of rubble fields to the protection of offshore structures. Rubble fields, whether naturally occurring or artificially generated, greatly influence the magnitude of the load that the ice feature transmits to a structure; grounded rubble fields having a beneficial effect by transferring the load directly to the foundation and non-grounded fields having the potential to actually increase the load on the structure. Rubble formation is recognized as a multi-modal process which results in a matrix of ice blocks; an assemblage having highly variable mechanical properties. Current thinking treats rubble piles as being composed of a Mohr-Coulomb material, but the full scale material properties are not well known. The potential impact of rubble fields on the safety and economics of offshore structures is of sufficient magnitude to warrant a major effort in this area.

The importance of increasing our understanding of how ice loads will impinge on offshore structures is reflected in the highest priority assigned to research dealing with ice loads. However, also recognized as a high priority item, with substantial impact on safety and economy, is the area of structural response. The current basis for formulating the response of steel, reinforced concrete and composite (steel/concrete) structures is largely based on research work and past experience with more traditional onshore structures, or offshore structures in milder climates. The design methods (often utilizing empirical equations) while proven suitable for these structures may not be appropriate for the more massive structures required in offshore, ice-infested areas.

For steel structures, the high research priorities involve the reassessment of the capacity of stiffened steel plates and the determination of the required material toughnesses and detail arrangements to prevent brittle fracture. The existing design rules based on the capacity of stiffened steel plates have their foundation in ship design (where relatively slender plates are used) and are overly conservative for the stockier elements used in offshore structures. This research alone has the potential of reducing the cost of a steel structure significantly.

The brittle fracture problem also has significant economic impact. Toughness requirements for the weld, heat affected zone and parent plate are hotly debated subjects. The new Canadian standard for offshore structures will likely include performance requirements, since agreement cannot be reached on specific toughness values. This approach may place Canadian steel producers at a significant disadvantage. To resolve this issue, research related to toughness requirements for welded details is recommended, along with a survey of the plate and weldment toughnesses of existing arctic structures and vessels.

Another area of concern for steel structures, is the development of serviceability guidelines related to local denting of the skin plate and the impact of local plate damage on the ability of the corresponding stiffening element to resist axial load.

The composite elements being considered for use in offshore structures (steel/concrete sandwich walls and concrete reinforced steel tubes) are considered to have significant potential, particularly because of their ability to distribute high local punching loads, and because of the great ductility they exhibit during failure. The use of structural elements which are relatively insensitive to the magnitude of local ice loads (for which the uncertainty is the greatest) will considerably improve both the safety and the economy of the structure.

For reinforced concrete structures, the research recommended involves the development of a rational approach for assessing the behaviour and strength of the massive, high strength, heavily reinforced elements required for offshore structures. The top priority in this regard should be given to the assessment of punching shear capacity. Current methods are based on the behaviour of bridge and building elements and are considered to be overly conservative, particularly for light weight and semi-light weight concrete. Again, guidelines dealing with serviceability concerns need to be developed.

A wide variety of monitoring and measuring systems are currently in use to measure ice actions and structural response. While it is generally felt that the rational use of existing measuring tools and methods can provide a reasonable degree of accuracy in predicting global ice loads on structures, there are a number of areas in this field in which significant developments can be made. At the top of this list is the development of improved approaches to the measurement of local and semi-local ice loads. Also of prime importance are improvements in measuring equipment and data processing techniques for dealing with the high frequency, dynamic response of the structure, the foundation, and the ice sheet.

Physical modelling in ice tanks is also thought to have the potential to provide information on the magnitude and distribution of local and semi-local ice loads. As current scale modelling technology does not allow this problem to be assessed, improvements in this regard seem warranted.

Emphasis should also be given to the collection of full scale field data with which models can be calibrated. In addition, improved modelling techniques should be developed to investigate dynamic, ice/soil/structure interaction problems.

In summary, the highest research priorities were identified as those dealing with the collection and consolidation of large scale field data dealing with: ice/structure static and dynamic response; and ice and rubble field properties and morphology. A high priority was also given to research dealing with structural response, i.e., the behaviour of the unique types of steel, concrete and composite structures used in the arctic and east coast offshore areas.

The seven areas considered during the workshops were selected as those having the greatest impact on the safe and economic development of offshore resources. Within the scope of the workshop series, research priorities have been identified, that when completed, will significantly enhance the ability of Canadian industry to provide safe, economical ice-resistant structures.

CLOSING COMMENTS

The structures now successfully operating in the Arctic are a tribute to the determination and dedication of all those involved. It is apparent, however, that for frontier development to proceed on an economical base, it is absolutely essential that each facility be designed to minimize costs. The research emphasis then, (a recurring theme within each of the expert groups gathered to focus on specific aspects of the problem) was CONSOLIDATE -

consolidate existing information - place that information in the design context - compare existing information from various sources - and finally ensure that the aggregated information is coincident with the experience gained from large scale field tests and from operations on existing structures.

The emphasis on large scale and operational experience carries with it two implications: first, it is essential that the framework for a particular project be established in consultation with the users of the research, so that the information will be developed in a form specifically suitable for design and construction.

Second, analytical or laboratory studies, performed in isolation from large scale field information, do not warrant a high priority. Such studies must be conceived as integral parts of a project that will be calibrated against the results of large scale field investigations or operational experience.

These two conditions dictate that more often a research project will involve a TEAM APPROACH, with an "owner" or "user" of the information, working together with design or construction specialists and linked to laboratory testing or research organizations. These linkages will, as a side effect, smooth the flow of information into the hands of the user and make it less likely that valuable research information will "sit on the shelf gathering dust".

As a final comment, it is timely to view the recommendations of this workshop series in the light of the significant effort by the Canadian Standards Association, supported by the Canadian Petroleum Association, and the

Canada Oil and Gas Lands Administration, which is focussed on the development of STANDARDS for fixed offshore structures. The standards development process entails a detailed, step-by-step, assessment of existing information within a framework of specific need. The effort thus identifies gaps in available information and focusses the research process. The Canadian climatic conditions, specifically ice and iceberg loadings, low temperatures, coupled with the unique structural arrangements developed to combat these conditions, have opened numerous opportunities to the Canadian research community. In working to close the gaps and produce standards for the design of safe and economical structures, technology will be developed that, as a by-product, will be saleable to the world. Thus the conclusions and recommendations of this workshop series are completely congruent with the needs of industry as specifically expressed during the process of standard development.

In summary, the Ice/Structure Interaction workshops served to identify the need to re-examine and CONSOLIDATE existing information - particularly that developed through large scale tests and operational experience - and to assess the information using a TEAM APPROACH, involving personnel with a knowledge of design and construction working in tandem with those expert in ice mechanics and structural response. The Canadian Standards Association activity related to the development of STANDARDS for offshore structures provides a convenient focus for this work and a practical display for Canadian expertise developed during the process.

APPENDIX

WORKSHOP RECOMMENDATIONS

GLOBAL AND LOCAL ICE LOADS INCLUDING DYNAMIC EFFECTS

RECOMMENDATIONS

1. An effort should be made to identify sources of existing ice pressure field data and where possible, collect and consolidate these data.

2. Encouragement should be given to operating companies to make selected tracts of proprietary field data available to the general scientific community where this can be achieved without compromising the competitive positions of the operators.

3. Attention should be given to the development of an approach to predicting ice loads which includes all factors currently recognized as affecting these predictions; strain rate, contact area, aspect ratio, geometry of structure, etc.

4. Emphasis should be given to the calibration of existing static and dynamic analytical models for large structures, rather than the development of more sophisticated models.

5. A high priority should be given to the collection of field data related to the static and dynamic response of ice, structure and foundation; the identification of mechanisms which force different modes of failure in the ice; and the determination of ridge building forces which limit the global load which can be transferred to a structure.

6. Consideration should be given to the establishment of standard measurement methods and quantities related to the collection of ice material properties in the field.

7. Attention should be given to determining the effect of high strain rates, large aspect ratios, large ice volumes, and large scale interaction mechanisms on ice forces.

8. Attention should be given to hydrodynamic and added mass problems associated with ice features.

PHYSICAL MODELLING

RECOMMENDATIONS

1. Continued support should be given to existing efforts in the area of model ice development and modelling techniques in general.

2. Emphasis should be given to the collection of full scale field data with which models can be calibrated.

3. Ice events should be modelled for which field data already exists and can be made available.

4. The feasibility of using physical models to determine semi-local ice load distributions should be investigated, and the required advances in modelling techniques determined.

5. Improved modelling techniques should be developed to investigate dynamic, ice/soil/structure interaction problems.

6. Increased emphasis should be placed on the integration and correlation of physical and numerical models.

RUBBLE FORMATION

RECOMMENDATIONS

1. Increased efforts should be made to identify individual modes of rubble generation and to determine what combinations of rubble generating processes are dominant.

2. Support should be given to field and laboratory work aimed at determining the properties of rubble piles, both naturally occuring and artificially produced.

3. A high priority should be given to the investigation of the use of rubble protected drilling systems.

4. Consideration should be given to the establishment of standard measurement methods and quantities related to the collection of rubble pile mechanical properties in the field.

5. Attention should be given to the area of rubble/soil/ structure interaction.

6. It is important to develop a better understanding of the mechanics of load transmission through broken ice sheets and rubble piles, and how load is transmitted to the structure and berm.

MONITORING AND MEASURING SYSTEMS

RECOMMENDATIONS

1. Emphasis should be given to the development of improved instrumentation arrangements for the evaluation of local and semi-local ice loads.

2. Encouragement should be given to the collection of visual data to help identify different failure modes and processes occuring during an ice event.

STATISTICAL AND PROBABILISTIC ASPECTS

RECOMMENDATIONS

1. An effort should be made to gain a consensus among those collecting environmental data, those conducting probabilistic analyses and those using the results in design, as to what specific ice parameters should receive the highest priority and in what format data should be taken to lend itself to probabilistic analyses.

2. Attention should be given to the identification of analysis techniques for reliably extrapolating limited data sets.

3. In order to add to the statistical data base, an effort should be made to identify sources of existing data and where possible to collect and consolidate this data.

4. More work is needed on probabilistic approaches to ice-mechanics. Techniques are required which will encompass the "weakest link" theories, including size effects and the effects of flaw size and distribution on the initiation of fracture in ice.

FAILURE CRITERIA AND STRUCTURAL RESPONSE
- STEEL STRUCTURES

RECOMMENDATIONS

1. A survey should be initiated to assess the materials, fabrication processes and subsequent performance of existing steel structures in the arctic, both on-shore and off-shore. Information to be gathered should include material specifications, actual material properties and repair and damage reports.

2. Attention should be given to the development of toughness requirements for welded joints. The relative severity of various configurations should be considered, as well as the properties of the weld, the HAZ and the parent plate. The effect of particular welding procedures should also be considered.

3. Consideration should be given to determining the effect on ultimate strength of local plastic deformations (denting) in the skin plate. The ability of a deformed plate and supporting stiffening element to carry axial loads should be determined.

4. Attention should be given to the revision of current stiffened plate design equations, as the current equations were developed for ship design and to a large extent are inappropriate for the less slender plates used in offshore structures.

5. Priority should be given to the development of analysis and design techniques for steel/concrete composite flat plate members subject to combined in-plane axial loads

and transverse punching loads. The ability of these members to resist impact loads and their performance from a brittle fracture point of view should be assessed.

6. Consideration should be given to the ability of composite and non-composite tubular members to resist ice impact loads. This information is crucial if jacket or semi-submersible structures are to be considered for use in ice environments.

FAILURE CRITERIA AND STRUCTURAL RESPONSE
- CONCRETE STRUCTURES

RECOMMENDATIONS

1. Attention should be given to a general reassessment of the empirical design equations used for reinforced concrete structures, to reflect member proportions, steel quantities, concrete strengths, and member configurations which are more appropriate for offshore structures.

2. In particular, a reassessment should be made of the strength reduction factors currently required for lightweight and semi-lightweight concrete for offshore structures, to take into account the items listed above.

3. Emphasis should be given to punching shear problems in the work recommended above. Consideration should be given to the beneficial effects of member edge restraint.

4. Attention should be given to the development of serviceability guidelines (limits on cracking) for reinforced concrete members for offshore structures.

5. Continued support should be given to basic research into the behaviour of reinforced concrete structural elements in those areas which have an impact on the design of offshore structures.

NRC WORKSHOP ON EXTREME ICE FEATURES

Questions and Discussions Form

AUTHOR: Tom Zimmerman

PAPER: Ice/structure Interaction Research Needs

DISCUSSION BY: R. Gerard

DISCUSSION:

This is more of a comment than a question. It seems to me that there is little feedback from designers to the general research population about what features are important to the design of various types of structures. Publication of bits and pieces of designs in conference proceedings that are not likely to be read by researchers in other but related fields does not really constitute effective feedback given the enormous amount of material that must be read these days. Rather there seems to be a need for some "synthesized" feedback. I believe workshops like you describe are a very worthwhile contribution along this line.

I would also like to take the opportunity to bemoan the marked lack of education in refereed engineering journals or papers that describe the design, and concerns in design, of the major structures.

METHODS OF RISK ANALYSIS

by F.G. Bercha**

The paper deals with application of risk analysis to extreme ice feature risk evaluation. The discussion is maintained on a relatively general plane, with simple illustrations from daily life as well as references to non-trivial risk analyses carried out in order to assess extreme ice feature risk. Following an introduction on the applications of risk analysis, techniques of risk analysis which can be used as a basis for the evaluation of ice risk are presented and described. A series of examples based on projects directed by the author covering extreme ice scour risk operations off the East Coast of Canada, and detailed risk and risk mitigation analyses of Arctic and East Coast ice and iceberg management programs are presented. Finally, the future of risk analysis is briefly discussed. It is concluded that risk analysis is a powerful tool for the evaluation of extreme ice feature risk.

---

* ©, 1986, F.G. Bercha and Associates (Alberta) Limited

**President, F.G. Bercha and Associates (Alberta) Limited, #301, 1220 Kensington Road N.W., Calgary, Alberta, Canada, T2N 3P5 (Telephone (403) 270-2221; Telex 03-827666); F.G. Bercha and Associates (Ontario) Limited, #450, 130 Slater Street, Ottawa, Ontario, Canada, K1P 6E2 (Telephone (613) 563-0555).

A. INTRODUCTION ON APPLICATIONS OF RISK ANALYSIS

What is risk? Generically, risk is defined as the chances of an undesired event; that is, risk is the probability of occurrence of an unwanted event. From a risk analytic point of view, this generic definition of risk is insufficient because it does not include some consideration of the magnitude or importance of the consequence. Accordingly, for the purposes of the present discussion, risk is defined as "a compound measure of the probability and magnitude of adverse effects" (Lowrance, 1976).

Obviously, risk analysis concerns itself with the quantification of risk and the generation of pertinent information on it. But where is risk analysis best applied and what sorts of events does it concern itself with? In a sense, we all use risk analysis everyday in arriving at decisions which involve the consideration of uncertain factors. We intuitively carry out a risk analysis when we select routes for driving to work, queues in which to line up at a bank teller or grocery check-out counter, a restaurant at which to have lunch, the task to begin from several tasks which have to be completed, and so on for many other elementary risk analytic scenarios. On a more complex plane, we carry out perhaps a relatively sophisticated risk analysis, when we choose rate and term of a mortgage, a new job, or a spouse. When we carry out the risk analyses for our decision in the above scenarios, we more or less intuitively identify the risks and manipulate the probabilities of causal factors in order to assess these risks. If we intuitively feel that the risk level is acceptable, we will proceed with the relevant alternative; if not, we may hesitate or choose an alternative with more acceptable risk levels.

In general, the more complex and undocumented the future scenario or phenomenon, the better the case there appears to be for carrying out formal risk analysis. In the case of extreme ice features, their very definition implies a paucity of data from which to make statistical predictions. Accordingly, extreme ice feature encounter risk may be considered a candidate for risk analysis as such ice features to a large degree constitute a phenomenon without history and are amenable to risk analysis through approaches involving the definition of causal factors for which we do have a physical and statistical understanding. For example, the occurrence of an extreme scour in the Beaufort Sea, as will be noted later, does not necessarily occur in accordance with the extrapolation of the data base for much smaller scours. Rather, one may have to approach the probabilistic prediction of scouring through a decomposition of the factors affecting the occurrence of extreme scours including presence of a sufficiently large ice keel, its strength, its inertia, and the co-presence of appropriate sloping penetrable sea bottom formations.

Now, to what extent should risk analyses be carried out; that is, are we interested only in the events initiating accidents, the chances of the accidents, or the ultimate consequences? In order to properly assess and understand risk, and to take advantage of all opportunities for risk mitigation, we need to carry out a complete risk analysis from initiating event to ultimate consequence.

Figure 1 illustrates the principal steps in the risk analysis process using the scenario of a MODU subjected to a hydrocarbon blowout. As may be seen, there are essentially two trains in the risk analysis process; that involving the initiating event risk analysis and that concerned with the consequence risk analysis. The illustration further subdivides each of these steps into substeps, and for each substep gives further elaboration for the physical example by briefly describing the analytic process through which one obtains a risk result, and the final quantity associated with that result. For the physical example noted, the following substeps constitute the risk analysis process:

(a) The definition of the MODU system, including the physical system and the operational scenarios associated with it.

(b) Evaluation of the initial risk probability and characteristics, in this case involving the probability of a blowout and its likely rate and duration of flow.

(c) Consequences on the system of various blowout severities. Such consequences include fire, explosion, structural damage, toxic gas.

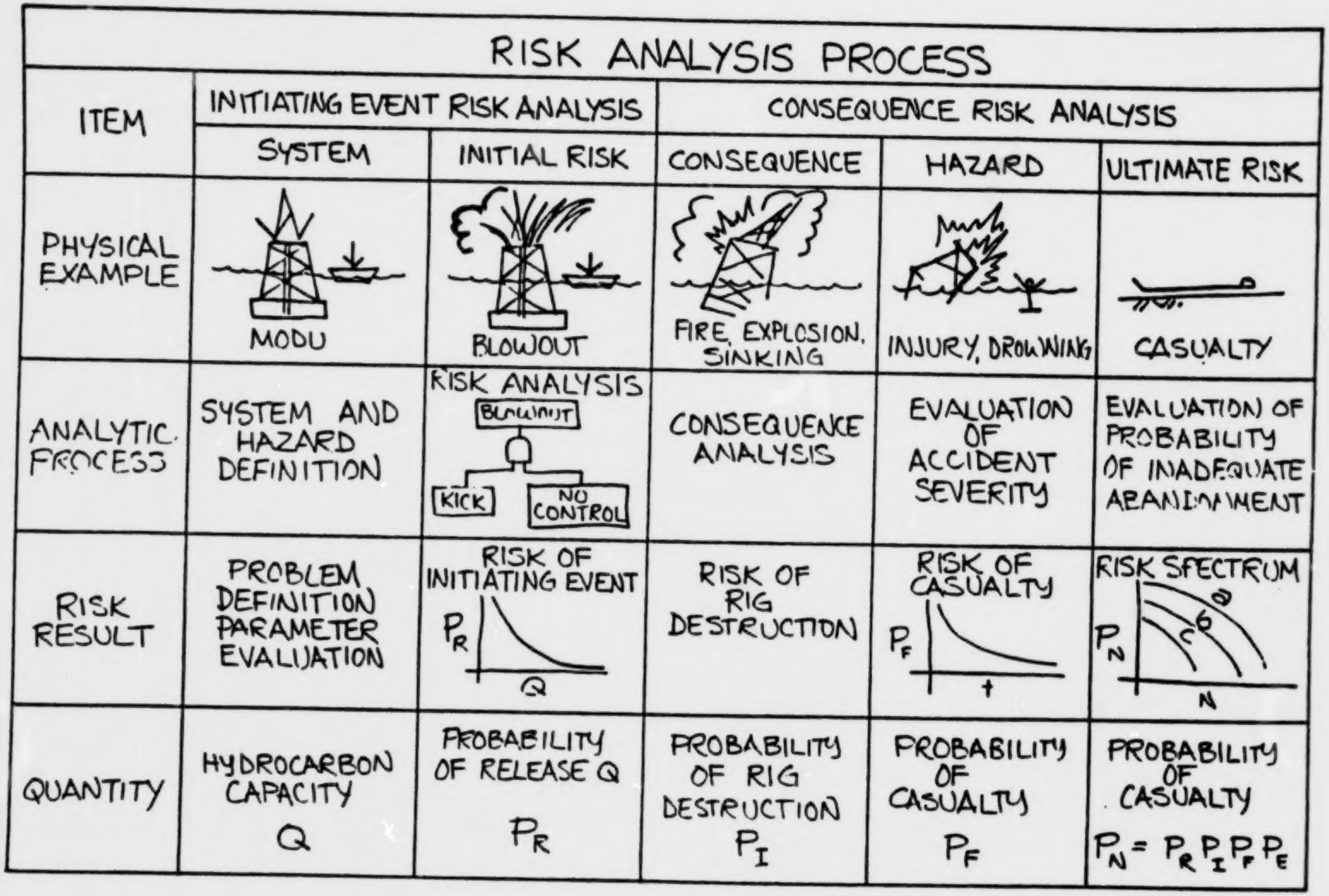

RISK ANALYSIS PROCESS

ITEM	INITIATING EVENT RISK ANALYSIS		CONSEQUENCE RISK ANALYSIS		
	SYSTEM	INITIAL RISK	CONSEQUENCE	HAZARD	ULTIMATE RISK
PHYSICAL EXAMPLE	MODU	BLOWOUT	FIRE, EXPLOSION, SINKING	INJURY, DROWNING	CASUALTY
ANALYTIC PROCESS	SYSTEM AND HAZARD DEFINITION	RISK ANALYSIS BLOWOUT KICK NO CONTROL	CONSEQUENCE ANALYSIS	EVALUATION OF ACCIDENT SEVERITY	EVALUATION OF PROBABILITY OF INADEQUATE ABANDONMENT
RISK RESULT	PROBLEM DEFINITION PARAMETER EVALUATION	RISK OF INITIATING EVENT P_R Q	RISK OF RIG DESTRUCTION	RISK OF CASUALTY P_F t	RISK SPECTRUM P_N a b c N
QUANTITY	HYDROCARBON CAPACITY Q	PROBABILITY OF RELEASE Q P_R	PROBABILITY OF RIG DESTRUCTION P_I	PROBABILITY OF CASUALTY P_F	PROBABILITY OF CASUALTY $P_N = P_R P_I P_F P_E$

FIGURE 1 THE RISK ANALYSIS PROCESS

(d) Hazard evaluation including consideration of the consequences of human exposure, probability of survival in the case of exposure, and probability of exposure until evacuation is accomplished, formulated as a probability of fatality as a function of time for various severity levels.

(e) Ultimate risk evaluation involves combining the probabilities of initial release, adverse effect on safety of rig, and human exposure to the hazard.

Thus, the process of risk analysis encompasses the entire set of scenarios from system definition to initiating event, to ultimate consequence. In the example given, human safety was considered the ultimate consequence. Other risk analysis objectives may involve the evaluation of economic loss, operational downtime, or environmental damage.

In the balance of this paper, details on methods of risk analysis applicable to extreme ice feature analysis will be presented, followed by references to several case studies carried out by the author.

B. METHODS OF RISK ANALYSIS

A large variety and range of risk analytic methodologies has been described in the literature. General descriptions of methodology are given by authors such a Fischoff et al. (1981), Schwing and Albera (1980); Slovak and Fischoff (1977). In the work of Burton et al. (1982), risk methodologies have been characterized as ranging from general qualitative evaluations to detailed simulation studies. Bercha et al. (1978a, 1979, 1980b, 1982a) also refers to several levels of risk analysis ranging from general evaluation through network analysis to discrete and continuous simulation methods. In accordance with the general description of methods of risk assessment provided by Bercha (1983), risk analysis methodologies are classified into the following three categories for the purposes of the present description:

(a) General risk evaluation mehtods.

(b) Network analysis methods.

(c) Monte Carlo methods.

This classification is advantageous not only because it represents an increasing level of input and output accuracy, modelling sophistication, methodology complexity, and information output detail, but also because it may be used as a good basis for the discussion of generation of input risk data and methods for evaluating risk mitigation measures. The general risk evaluation methods, which include statistical and probabilistic techniques as well as general empirical methods, are a good basis for the generation of inputs for the subsequent two techniques. These two techniques, the Network and Monte Carlo techniques, give a good deal of information regarding the causal structure of different risk scenarios, and accordingly are amenable to the analysis of risk mitigation methods. Because a relatively comprehensive discussion of these methods was given in the paper by Bercha (1983), only an outline with emphasis on those aspects most applicable to the present work shall be given herein.

1. General Risk Evaluation Methods

General risk evaluation methods are particularly useful for preliminary risk evaluation, and evaluation of input data for Network and Monte Carlo analysis. These general risk evaluation methods may be subdivided into Delphi methods (Salem and Soloman, 1980), bootstrapping methods (Fischoff et al., 1981), Bayesian methods (Burton, et al., 1982), general statistical methods (Bercha et al., 1983b), and general probabilistic methods (Rassmussen, 1981).

Delphi methods essentially consist of obtaining the opinions of many experts on the same subject. It has been found (Straugh, 1981) that the greater the number of experts interviewed, the better the accuracy of the opinion that is developed. These methods are useful in initial risk identification, particularly in areas where little history is available. Bootstrapping approaches are based on utilization of the level of risk that has been tolerated in the past as a basis for evaluating the acceptability of proposed risks. In essence, the techniques involve the utilization of comparative risk to define order of magnitude risk levels. Such techniques are particularly useful for evaluation of fault tree elements for which empirical data are not available although comparable situations have been documented.

Bayesian and general statistical methods involve analytical manipulation of empirical data to arrive at an evaluation of current risk. Bayesian techniques essentially consist of transformation of historical data for systems similar to the ones being evaluated through application of analytical and judgmental processes to transform that data. General probabilistic methods involve utilization of the principles of joint distribution analysis to evaluation of outcomes of simple combinations of events. For example, the Warner diagram illustrated in Figure 2 shows the probability of structural failure due to exceedance of certain probabilistic load levels.

As noted above, these techniques are particularly useful in the determination of input data for some of the more sophisticated risk modelling techniques described in the next two sections.

How valid is the input data? That clearly depends on the population of observations, the method of observation, and the way in which the data are used. If the statistical sample is valid, then its applicability in the analysis is to a large degree dependent on the similarity of the events of the data base to those described. When the conditions of the data base and the analysis are dissimilar, judicious use of Bayesian methods must be made. To a large degree, the end product of Bayesian transformation is an important function of the judgmental capabilities of the analyst. Very frequently, particularly in the case of unprecedented operations such as form the subject of the present discussions, although large statistically valid data samples are available for similar operations, the conditions associated with the similar operations are sufficiently dissimilar to those associated with the scenario being evaluated as to invalidate those data, at least for direct applicability. For instance, in the case of MODU accidents, a great deal of data are available for the Gulf of Mexico. Application of these data to operations off the East Coast must be done with a good deal of caution and judgment. Although the drilling operations as such are substantially the same, the environmental conditions affecting them are significantly different. Hurricanes are prevalent in the Gulf;

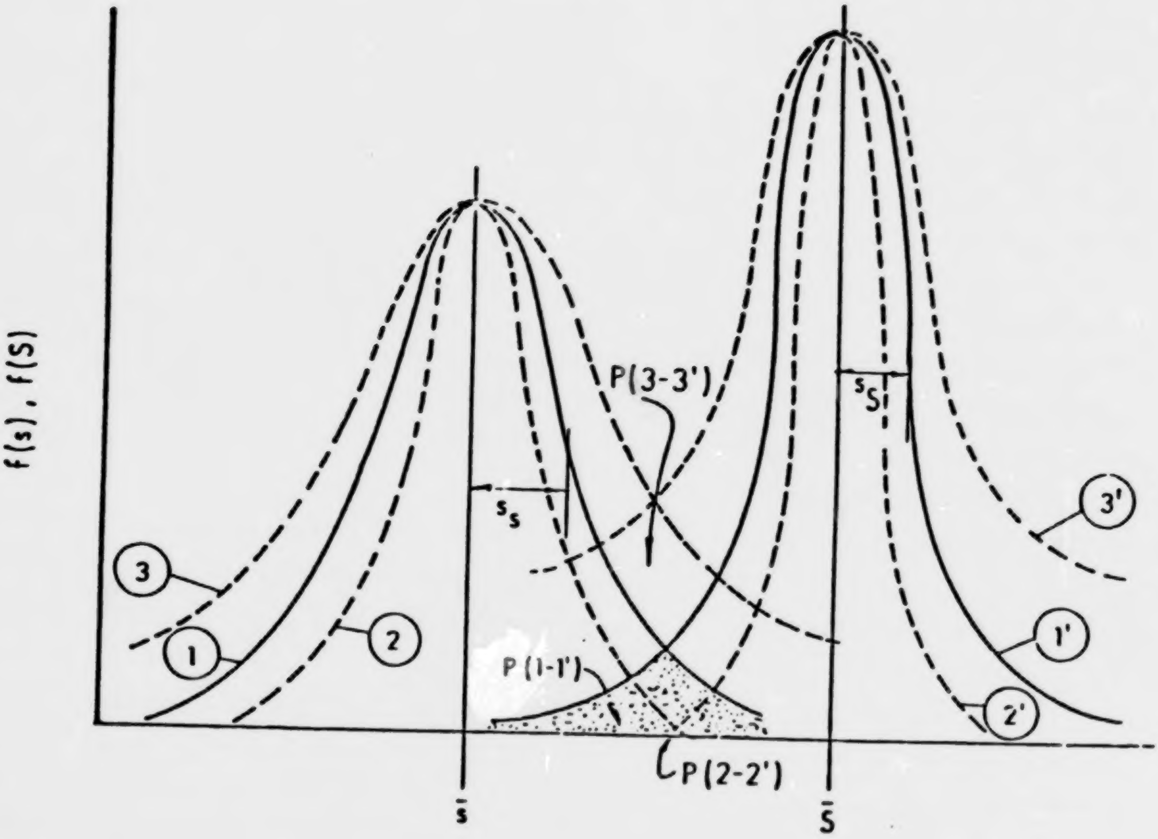

FIGURE 2 WARNER DIAGRAM (Bercha, 1977)

icebergs constitute the principal threat in the Hibernia area. One can actively manage icebergs but not hurricanes. The weather is predominantly cold in the northern area, while in the Gulf it is generally the opposite. Drilling is largely production oriented in the Gulf while it is principally exploratory in the Canadian waters. These differences in conditions and operations have to be taken into consideration when general statistical methods are utilized to generate data for input to the risk analysis.

2. Network Methodology

Network risk analysis methodologies include risk flow diagrams (Bercha, 1983), event trees (Denny et al., 1979), and fault trees (Chatterjee, 1974). All of these methodologies are essentially dependent on the concept of initial risk and consequence causal event interactions, which may best be illustrated by a description of fault tree methodologies.

Fault trees are graphic representations of event logic networks indicating the dependencies of events in causal chains. Figure 3 represents the principal structures of a fault tree. For event A to occur, either event B or C must occur. The gate connecting events B and C is called an OR gate since either of these would result in the occurrence of event A. However, events D and E, leading to the occurrence of event B, must both occur if event B is to take place; thus, they are connected through a structure called an AND gate. Further elaboration of the general applicability of fault tree techniques is presented in Bercha (1983).

Within the context of the analysis of risk mitigation measures, fault trees can be utilized either in a sensitivity analysis mode or in a direct analysis mode. In the sensitivity analysis mode, the effect of a subsidiary event probability variation on the resultant event probability is investigated through parametric manipulation of probabilities. For example, to define the sensitivity of event A to D in the sample fault tree, the probability expected for event D could be systematically multiplied by factors ranging from, say, one-tenth to 10, and the effect on A can be computed using the fault tree. If a

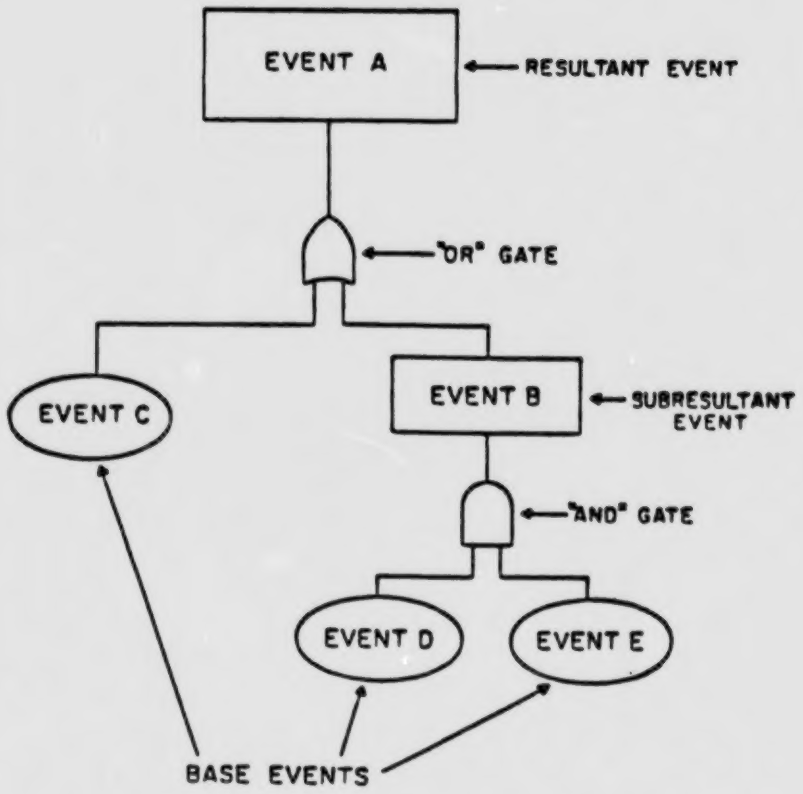
EVENT A
RESULTANT EVENT
"OR" GATE
EVENT C
EVENT B
SUBRESULTANT EVENT
"AND" GATE
EVENT D
EVENT E
BASE EVENTS

FIGURE 3 PRINCIPAL FAULT TREE STRUCTURES

small change in the probability of event D yields a significant change in event A, and if event D probability is susceptible to change, then measures which can be used to effect that change could be termed risk mitigation measures. The goodness of such measures from a practical point of view can be evaluated as a function of the ease with which these measures can be implemented, their costs, and their effectiveness. For example, if event A were a blowout, and event D were an operator error, and the application of additional training and onsite drills is likely to reduce the probability of operator error by, say, 50%, with the effect of reducing the probability blowouts by 25%, then the training and drills might be termed a feasible risk mitigation measure. Its precise feasibility would depend upon subsequent evaluation within the perspective of the total operation, cost, status quo of training, and so on. The best risk mitigation measures thus identified through fault trees might be subjected to a cost-benefit analysis as suggested in one of the examples in the next section.

In the direct analysis mode, rather than using fault trees in a sensitivity mode, all feasible risk mitigation measures identified may be evaluated through use of the fault tree.

3. Monte Carlo Methods

Monte Carlo or stochastic modelling is the systematic methodology for representing the outcome of a set of interactions involving a relatively intractably random character (Bercha, 1983); that is, the scenario is so complex and uncertain that one cannot intuitively idealize and understand it as a whole. This form of modelling is generally used as a method of simulation over a period of time; accordingly, simulation may progress as a series of constrained random draws spaced a time increment apart and progressing temporally. As an example, if the independent inputs to a fault tree diagram were all given as arbitrary probabilistic distributions, then the only way to truly evaluate the resultant event probability would be through a Monte Carlo simulation. In this case, a large number of sets of inputs would be drawn from the respective input distributions, resulting in a distribution of resultant event probabilities. In modelling an operation, on the basis of models of the unit processes, a set of outcomes of the operation can be modelled by a similar draw process.

The basic techniques of Monte Carlo modelling are again further discussed in Bercha (1983). Within the context of the present work, other than in evaluating fault trees, Monte Carlo methods may be utilized in the simulation of an operation, with the objective of evaluating operational risks including downtime, loss of production, or accidents. The results of such simulations will be further discussed within the context of risk mitigation in the next section.

C. EXAMPLES OF APPLICATION OF RISK ANALYSIS

The description of the examples given in this section emphasizes the use of risk analysis for evaluation of risk mitigation measures. The first two examples pertain to the initial risk of hydrocarbon drilling blowouts, with the first of them dealing generally with initial risk minimization and the second, more rigorously, with ways of evaluating cost-benefit of risk mitigation measures. The third and fourth examples deal with offshore drilling safety, and ways of mitigating safety risks. All examples are referenced to publicly available work for readers that are interested in further pursuing their development.

1. Offshore Blowout Risk Mitigation

In the work on probabilities of blowouts in the Beaufort Sea (Bercha, 1978) and Davis Strait (Bercha et al., 1978c), the principal objective of the work was to evaluate the likelihood of occurrence of blowouts and ways of reducing that likelihood. Specifically, in the Beaufort Sea study, a detailed fault tree analysis of blowout probabilities was carried out. At the time of the analysis, no drillship drilling history for that area was available. Through the analysis, it was found that the probability of blowouts, apart from depending strongly on the overpressure characteristics of the zones being drilled, was likely to be a very strong function of operator error. The sensitivity of the blowout probability to various factors was investigated through computerized fault trees to generate sensitivity graphs such as that shown in Figure 4. Here, it is profoundly evident that, apart from the environmental and geologic factors which are essentially immutable given that drilling will go on, the principal dependence of blowout risk appears to be to the human factors. Based on such analyses, recommendations were made pertaining to personnel training, conservative drilling policy, ice alert safety procedures, and other factors which could affect the operational response capability of the drilling system.

A similar evaluation carried out for drilling in the Davis Strait area revealed that blowout probabilities per se were likely to be significantly lower because of the considerably less hazardous geologic conditions in which drilling was likely to take place. Otherwise, causes of blowouts were found to be similarly dependent on human error with consequently similar risk mitigation recommendations.

2. Generalized Economic Evaluation Blowout Risk Mitigation Factors

Although the investigation described under this example (Bercha et al., 1983a) did not deal with offshore drilling, the methodology developed for it was sufficiently general and relatively novel enough to merit mention under the subject of the present paper. Specifically, it was desired to obtain some understanding of the relative feasibility of implementing different risk mitigation measures identified in an investigation of sour gas blowouts in Alberta. Table 1 summarizes the risk mitigation measures. These were identified, again, utilizing a fault tree sensitivity calculation approach. In order to appropriately evaluate the measures, it was necessary to estimate their effects on the probabilities of blowouts so that an evaluation of their cost expectation to reduce blowout costs might be obtained. Then, this cost reduction expectation was divided by the cost of implementing the appropriate measure in order to give a benefit-cost ratio.

Such an evaluation of cost expectation was carried out by combining all the cost expectations that could be evaluated for sour gas drilling blowouts utilizing a Monte Carlo procedure. From this cost spectrum or cost probability distribution, cost expectation reductions

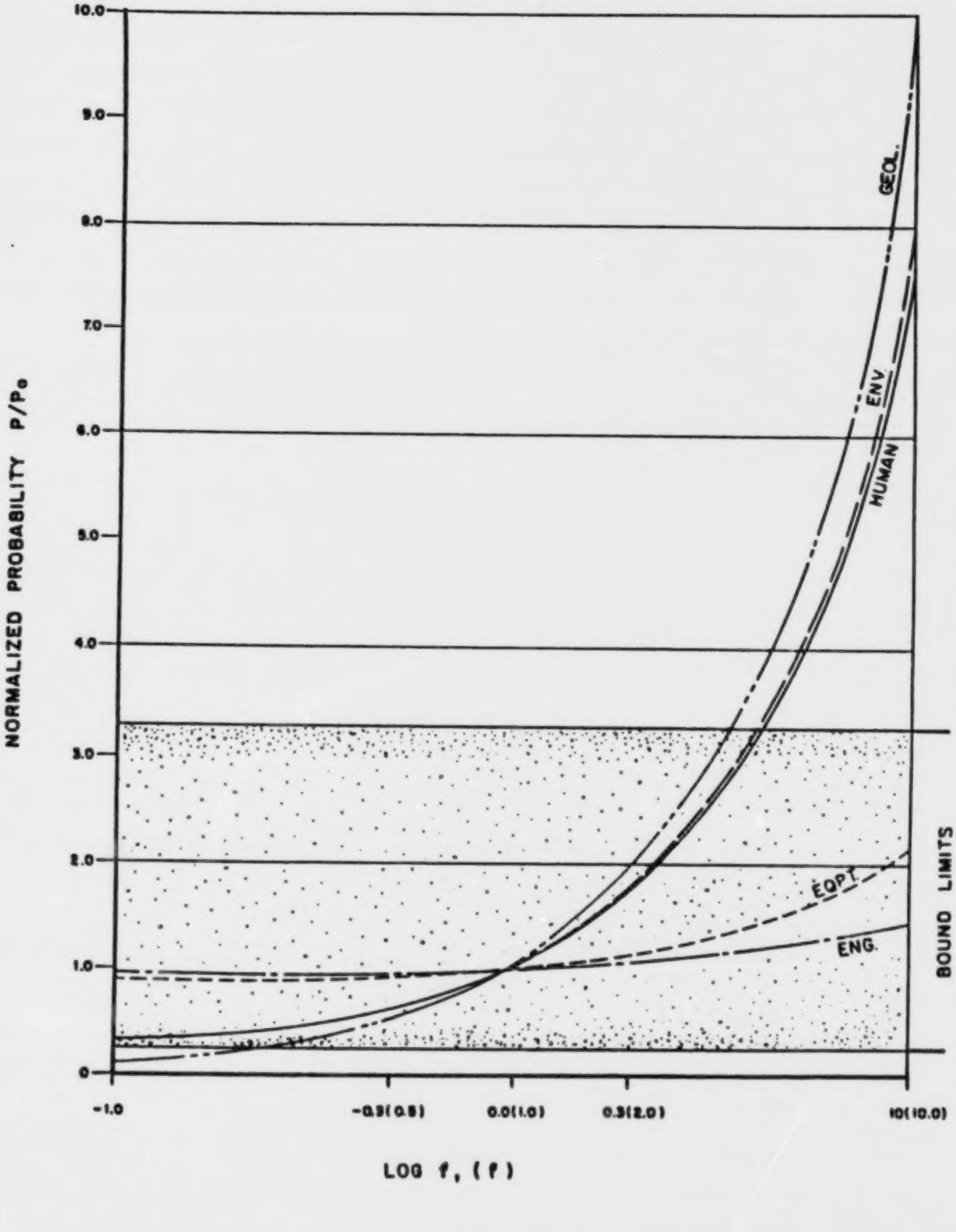

FIGURE 4 SENSITIVITY OF DRILLSHIP IN SUMMER TO FACTOR VARIATION

TABLE 1

BLOWOUT RISK MITIGATION MEASURES

(1) INCREASED ENFORCEMENT
(2) TRAINING
(3) SUMMER DRILLING
(4) CONSERVATIVE MUD PROGRAMS
(5) LIGHTING SOUR GAS BLOWOUTS
(6) CONTRACT RESPONSIBILITY
(7) EQUIPMENT INSPECTION
(8) SOUR GAS PERFORMANCE SPECS.

for blowouts of various severities were obtained in order to serve as a basis for the benefit-cost calculation. Results of this evaluation, for the risk mitigation factors mentioned in Table 1, were expressed in the form of benefit-cost ratios as shown in relative form in Figure 5. As previously suggested, the highest relative benefit-cost ratios were associated with those measures directed at reduction of human error.

Such analyses can be carried out for virtually any risk system, including the operation of MODU's off the East Coast. The results form a valuable guide for both regulatory and operational decision making regarding the thrust of risk mitigation procedures or regulations.

3. Beaufort Sea Safety Risk Mitigation

This study was directed at explicitly evaluating risk mitigation measures for increasing human safety of Beaufort Sea drillship drilling operations. Specifically, the risk of drowning or hypothermia as a result of immersion was addressed. Scenarios of a single man overboard from the drillship, a helicopter accident, and a drillship accident were considered. Various combinations of safety measures, as summarized in Table 2, were addressed for each of a series of scenarios. Clearly, all of these measures constitute risk mitigation measures as they are ways of improving the rescue or casualty reduction capability. The investigation was based on the utilization of modified fault tree techniques, in which varieties of seastate, accident scenarios, and safety measure combinations were investigated. Partial results in relation to risk mitigation were presented in graphical form such as that shown in Figure 6, in which the sensitivity of the probability of a fatality to the main system reliability is depicted.

4. MODU Safety Risk Mitigation

The authors recently carried out two studies of MODU casualty risks off the East Coast of Canada. Specifically, these included an investigation of semisubmersible drilling units operating on the Northeast Grand Banks (Bercha et al., 1982b) and an investigation of the risks associated with dynamically positioned drill units operating offshore Labrador (Bercha et al., 1983c). A wide variety of risk

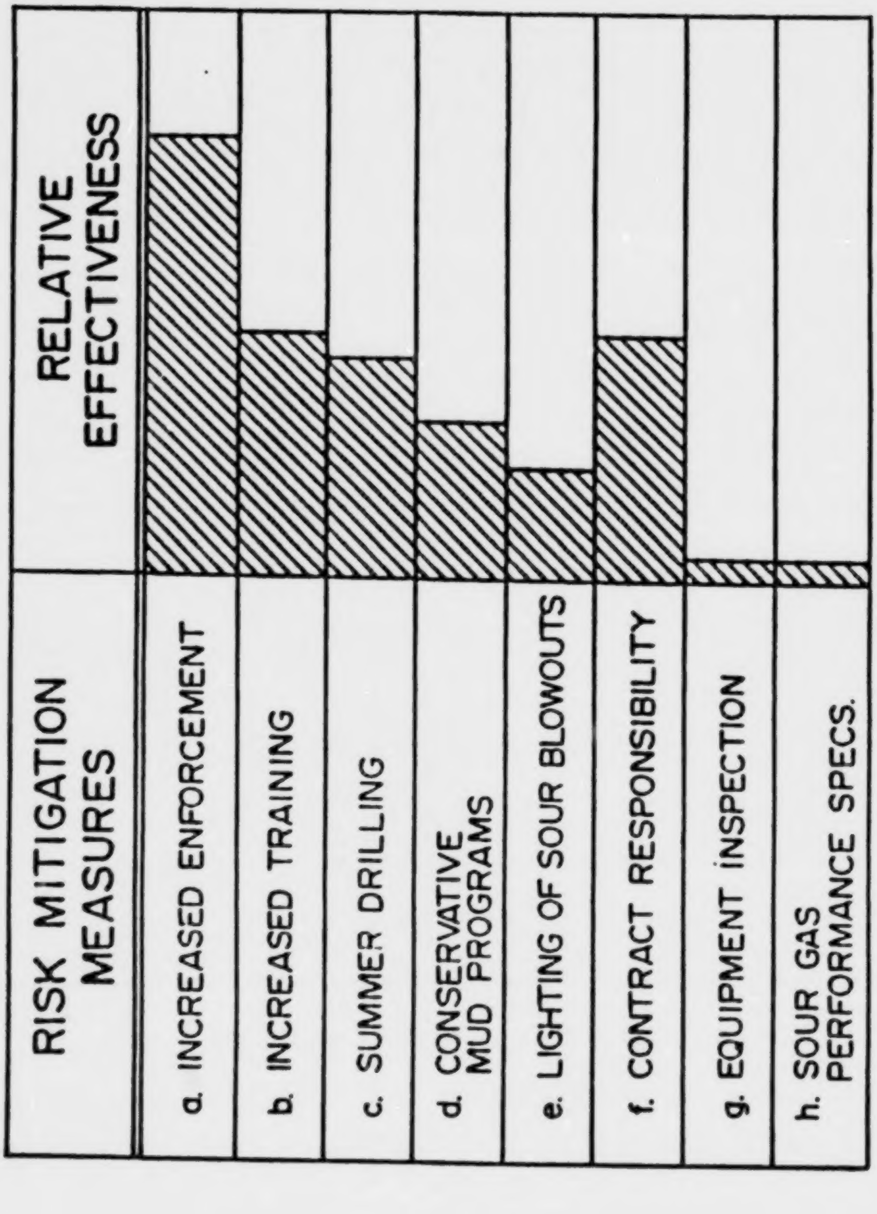

FIGURE 5 RELATIVE COST-BENEFIT OF RISK MITIGATION MEASURES

TABLE 2

TOTAL FATALITY EXPECTATIONS PER WELL

FOR SIGNIFICANT RESCUE MODES AND COMBINATIONS THEREOF

Scenario	Accident-Victim Density	Rescue Mode and Total Fatality Expectation										
		Standby	Zodiac	Lifeboat	Lifecraft	Helicopter	Rescue Swimmer	Standby + Zodiac	Standby + Lifeboat	Standby + Rescue Swimmer	Zodiac + Lifeboat	Zodiac + Helicopter
MOB	1.0	.41	.24	.30	.37	1.0	.46	.21	.23	.30	.20	.24
HDN	1.2	.81	.42	.51	1.08	.56	1.1	.37	.43	.94	.31	.42
HDD	1.2	.98	1.2	1.2	1.20	.60	1.2	1.07	1.06	.98	1.2	.60
DDS	.14	.03	.03	.03	.03	.04	.14	.02	.02	.03	.02	.02
DDC	.03	.03	.03	.03	.03	.03	.03	.02	.02	.03	.02	.02
TOTAL	--	2.26	1.92	2.07	2.71	2.23	2.93	1.69	1.76	2.28	1.75	1.30

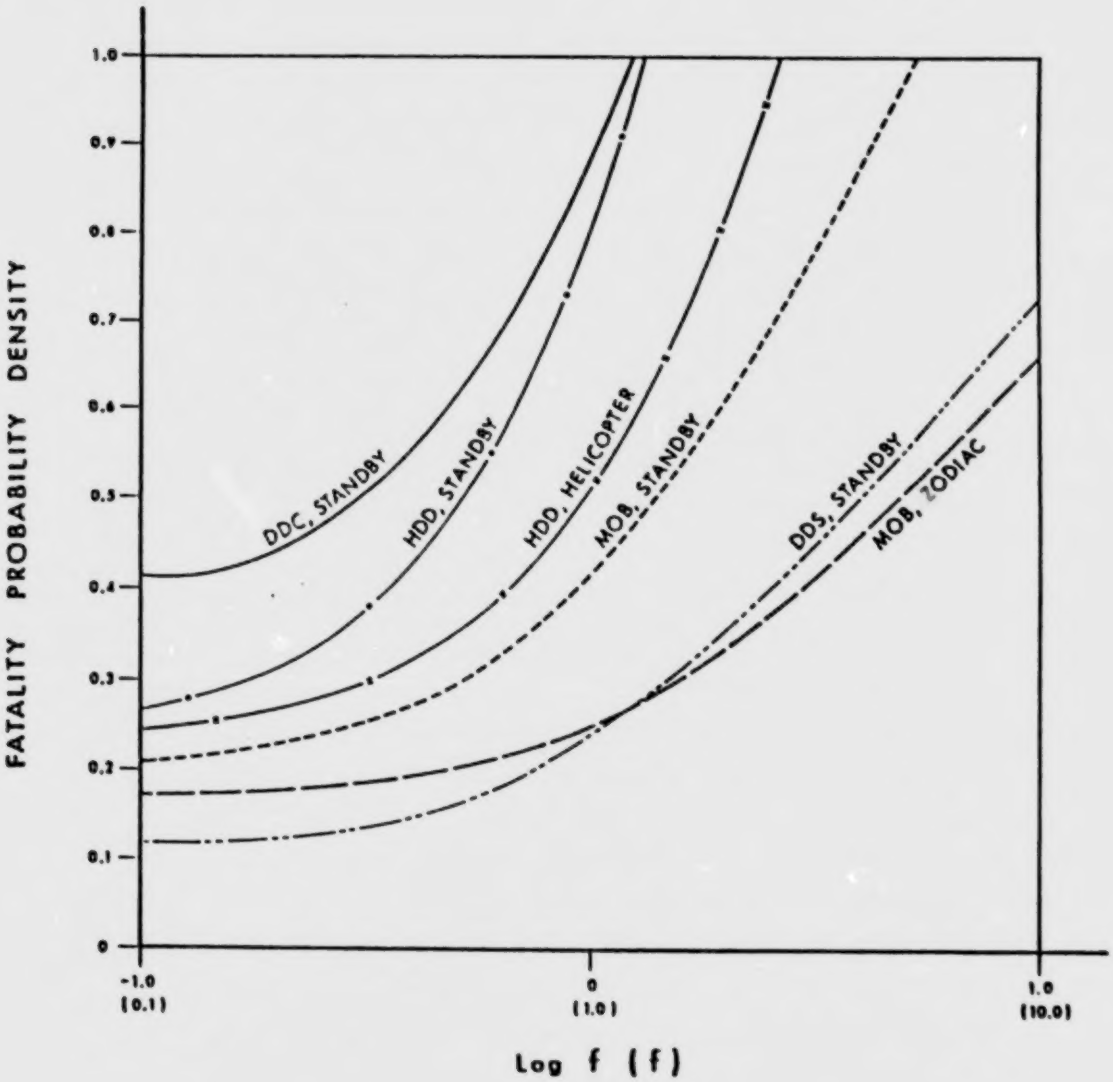

FIGURE 6 SENSITIVITY GRAPHS

mitigation measures, summarized in Table 3, was concluded to apply to both sets of operations. However, it was found that the risk of casualties was highly sensitive to the characteristics of the abandonment procedure. Fault trees depicting various abandonment scenarios were constructed as shown in Figures 7 and 8. Both abandonment casualties, as shown in Figure 7, and incomplete abandonment, as shown in Figure 8, were considered. It was found from the analysis that the following five types of measures are likely to have significant impacts on the risks of primary accidents associated with MODU's:

(a) Policies and procedures aimed at protecting equipment and personnel: The specification of operating limits, evacuation criteria, seasonal limits of operations, preventive maintenance and inspection.

(b) Measures aimed at improving personnel performance: Tranining, drills and exercises, safety management.

(c) Equipment, facilities, and support services: Evacuation systems, standby vessels, iceberg detection systems, and weather forecasting.

(d) Rig design: Stability and buoyancy specifications, both intact and damaged.

(e) Administration and enforcement of safety regulations: Jurisdictional issues, measures for encouraging compliance, accident reporting and analysis.

D. ROLE OF RISK ANALYSIS FOR EXTREME ICE FEATURES RISK EVALUATION

For the case of extreme ice features, the ice feature hazard event is regarded as an event without history thus, rather than attempt to fit distributions to a data base consistent with far lesser features than the extreme ice feature, the approach we take is a risk analytic one in which we decompose the extreme ice feature accident into its causal events.

Consider the case of ice island fragments in the Beaufort Sea. Clearly, here, a paucity of data exists and a frequency plot of data points may appear as Shown in Figure 9 - a somewhat perplexing data set to which to fit a distribution. Thus, we will then analyze the events

TABLE 3

RISK MITIGATION MEASURES

POLICIES AND PROCEDURES

- Operating Limits
- Operating Procedures
- Evacuation Criteria
- Emergency Equipment

PERSONNEL PERFORMANCE

- Safety Program, Commitment, Motivation
- Training
- Drills

EQUIPMENT AND SUPPORT SERVICES

- Evacuation System
- Iceberg Detection
- Environmental Forecasting
- Site Hazard Survey
- Drilling Instrumentation
- Handling Equipment

RIG DESIGN

- Environmental Conditions
- Rig Inspection/Review

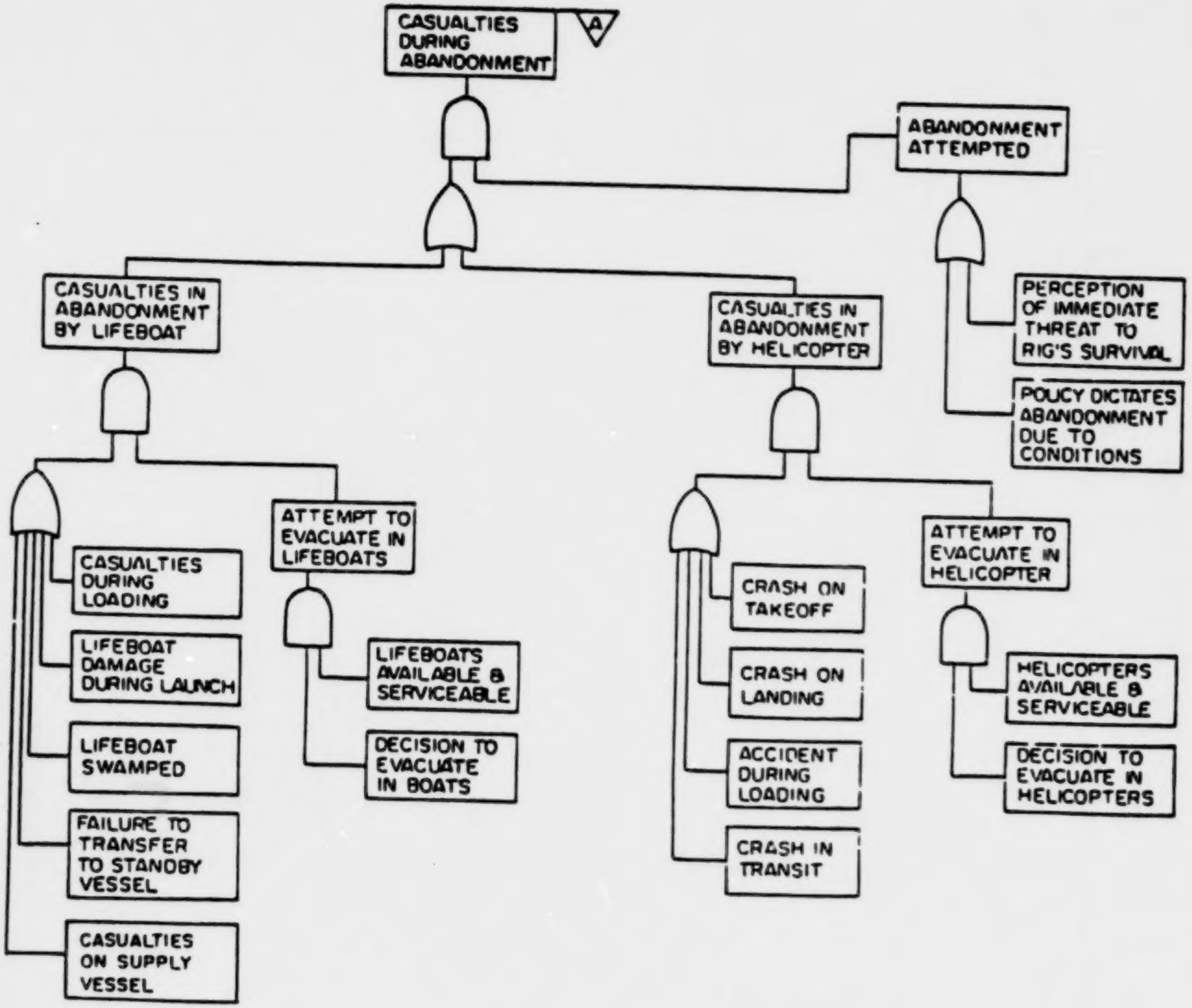
CASUALTIES DURING ABANDONMENT
A
ABANDONMENT ATTEMPTED
PERCEPTION OF IMMEDIATE THREAT TO RIG'S SURVIVAL
POLICY DICTATES ABANDONMENT DUE TO CONDITIONS
CASUALTIES IN ABANDONMENT BY LIFEBOAT
CASUALTIES IN ABANDONMENT BY HELICOPTER
CASUALTIES DURING LOADING
LIFEBOAT DAMAGE DURING LAUNCH
LIFEBOAT SWAMPED
FAILURE TO TRANSFER TO STANDBY VESSEL
CASUALTIES ON SUPPLY VESSEL
ATTEMPT TO EVACUATE IN LIFEBOATS
LIFEBOATS AVAILABLE & SERVICEABLE
DECISION TO EVACUATE IN BOATS
CRASH ON TAKEOFF
CRASH ON LANDING
ACCIDENT DURING LOADING
CRASH IN TRANSIT
ATTEMPT TO EVACUATE IN HELICOPTER
HELICOPTERS AVAILABLE & SERVICEABLE
DECISION TO EVACUATE IN HELICOPTERS

FIGURE 7 FAULT TREE FOR ABANDONMENT CASUALTIES

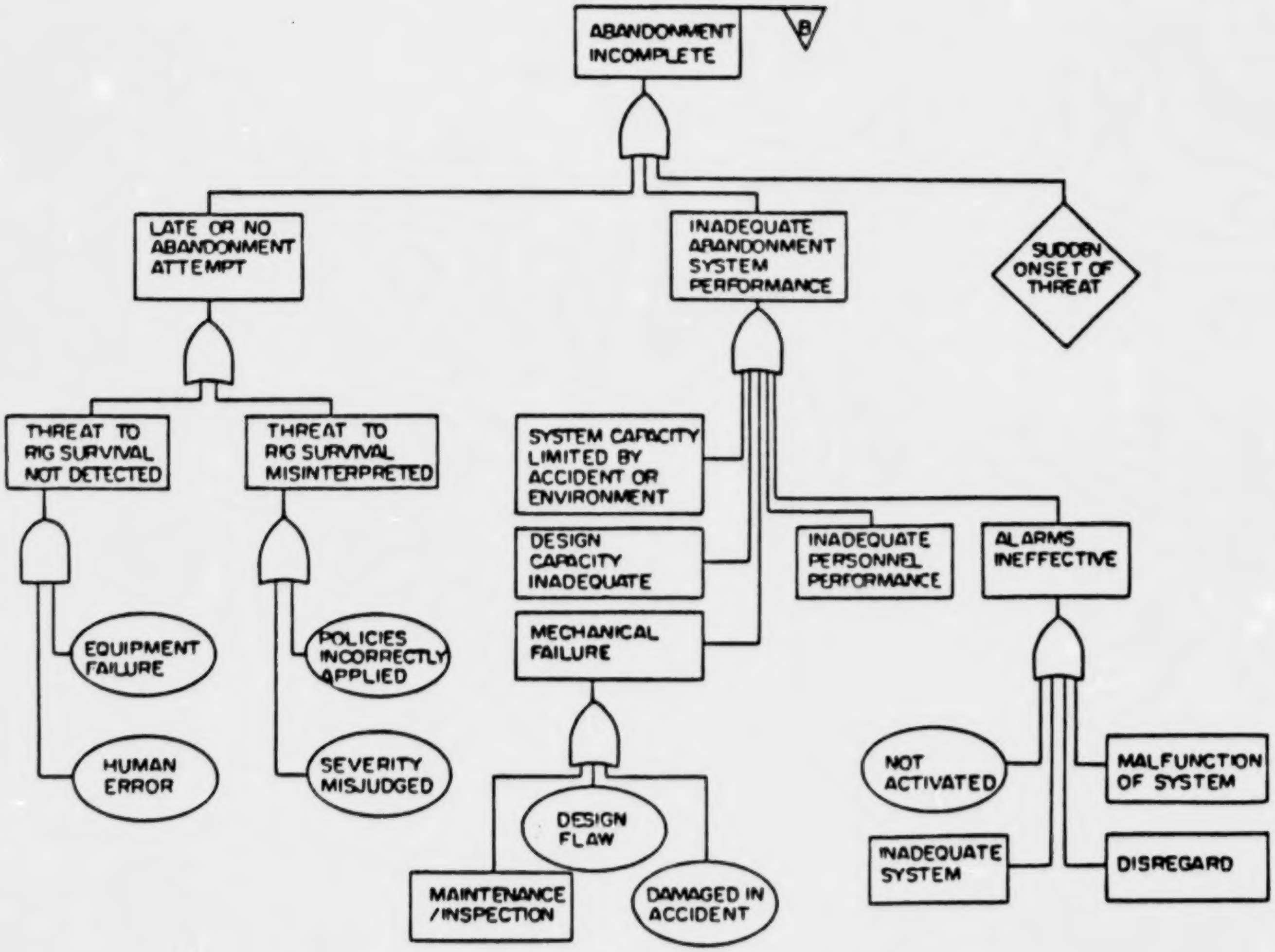
ABANDONMENT INCOMPLETE
B
LATE OR NO ABANDONMENT ATTEMPT
INADEQUATE ABANDONMENT SYSTEM PERFORMANCE
SUDDEN ONSET OF THREAT
THREAT TO RIG SURVIVAL NOT DETECTED
THREAT TO RIG SURVIVAL MISINTERPRETED
EQUIPMENT FAILURE
HUMAN ERROR
POLICIES INCORRECTLY APPLIED
SEVERITY MISJUDGED
SYSTEM CAPACITY LIMITED BY ACCIDENT OR ENVIRONMENT
DESIGN CAPACITY INADEQUATE
MECHANICAL FAILURE
INADEQUATE PERSONNEL PERFORMANCE
ALARMS INEFFECTIVE
DESIGN FLAW
MAINTENANCE /INSPECTION
DAMAGED IN ACCIDENT
NOT ACTIVATED
INADEQUATE SYSTEM
MALFUNCTION OF SYSTEM
DISREGARD

FIGURE 8 FAULT TREE FOR INCOMPLETE ABANDONMENT

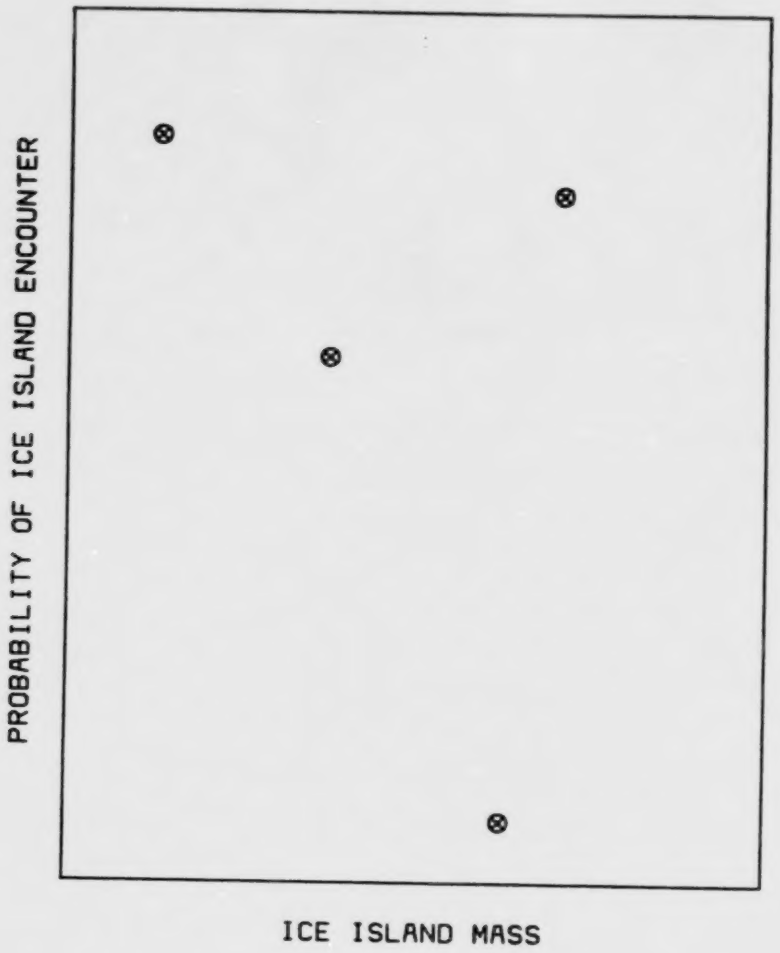

FIGURE 9 FREQUENCY PLOT OF ICE ISLAND DATA

leading to the presence of an ice island at a particular location. These events may include:

(a) calving of ice islands at arctic archipelago glaciers for West Greenland,

(b) flux entering archipelago,

(c) ways in which ice islands may find their way to the Beaufort Sea,

(d) flux entering the Beaufort Sea,

(e) distribution of ice island flux and mass distribution at given location,

(f) the necessary conditions including pack driving force, water depth, ice island draft, or encounter at a given location.

As illustration, the following description is based on a project recently carried out by the authors for Gulf Canada. In this case, the probability of extreme scour over a pipeline route had to be analyzed. The distribution approach was considered leading to a situation as depicted in Figure 10. Here, we see a very well behaved fit in the scour depth area up to roughly 3 meters. After that, however, any of the three distributions depicted will adequately fit the data but predict drastically different extreme scour results. Thus, a risk analytic approach was taken. Again, the occurrence of an extreme scour was analyzed within context of the causal events yielding a high-level fault tree as depicted in Figure 11. Now, utilizing existing data bases, it is possible to not only evaluate the probability of extreme scour occurrence, but also to understand the constituent events with the objective of mitigating associated risks.

In conclusion, it may be stated that a particularly viable approach for the analysis of extreme ice feature hazards is a risk analytic one. Utilizing Network methods of risk analysis, rather than attempting to fit distributions to a restricted data base, one reformulates the problem in terms of phenomena for which we do have probabilities and generates results with decreased bounds of uncertainty.

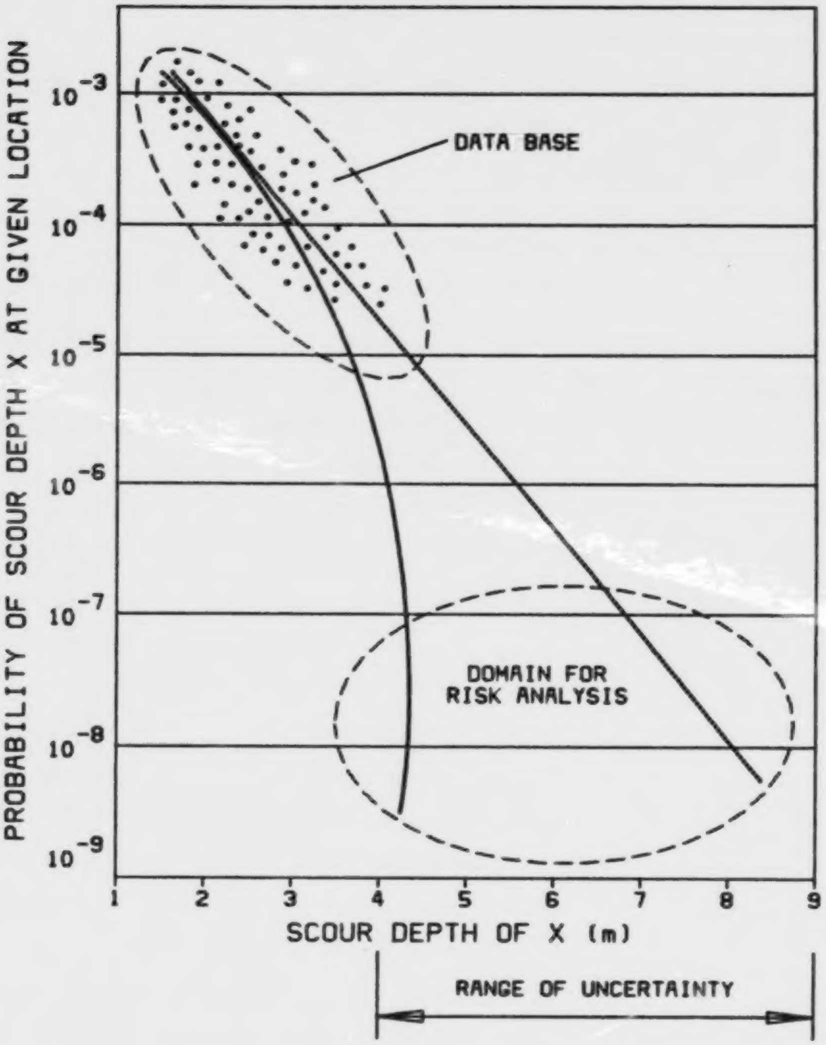

FIGURE 10 PROBLEM OF SCOUR DATA EXTRAPOLATION

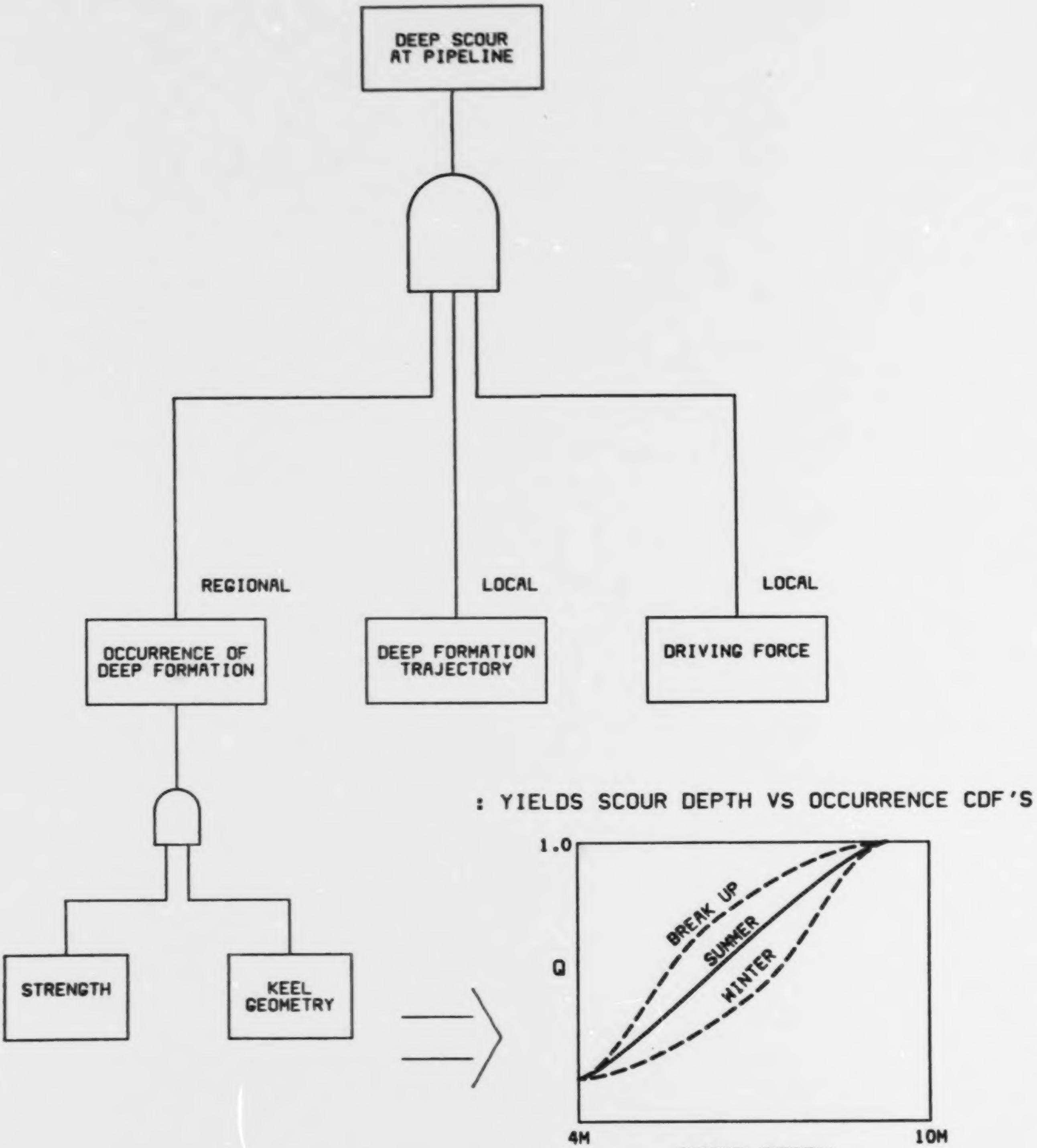
DEEP SCOUR AT PIPELINE
REGIONAL
LOCAL
LOCAL
OCCURRENCE OF DEEP FORMATION
DEEP FORMATION TRAJECTORY
DRIVING FORCE
STRENGTH
KEEL GEOMETRY
: YIELDS SCOUR DEPTH VS OCCURRENCE CDF'S
1.0
Q
BREAK UP
SUMMER
WINTER
4M
10M
SCOUR DEPTH

FIGURE 11 SCHEMATIC OF DEEP SCOUR ANALYSIS

REFERENCES CITED

Bercha, F.G. 1983. "Methods of Risk Assessment", International Workshop on Environmental Planning for Large-Scale Development Projects, Whistler, B.C.

Bercha, F.G. 1978. "Determination of Probabilities of Oil Blowouts in Canadian Arctic Waters", Offshore North Sea Technology Conference, Stavanger, Norway.

Bercha, F.G. and Associates Limited. 1983a. "Economic Risk from Sour Gas Well Drilling Blowouts in Alberta", Final Report, Energy Resources Conservation Board.

Bercha, F.G. and Associates Limited. 1983b. "Risk Analysis of Sour Gas Well Drilling Blowouts in Alberta", Final Report, Energy Resources Conservation Board.

Bercha, F.G. and Associates Limited. 1983c. "Risk Analysis of Drillship Units Operating Offshore Labrador", Final Report, Newfoundland Petroleum Directorate.

Bercha, F.G. and Associates Limited. 1982a. "Integrated Risk and Reliability Analysis - Extensions I and II, Arctic Pilot Project", Final Report, Petro-Canada.

Bercha, F.G. and Associates Limited. 1982b. "Risks Associated with Operations of Semisubmersibles off the Labrador Coast", Final Report, Newfoundland Petroleum Directorate.

Bercha, F.G. and Associates Limited. 1982c. "Monte Carlo Simulation of Downtime Risk Associated with Drilling Operations in Lancaster Sound and North Baffin Bay, Phase II", Final Report, Petro-Canada.

Bercha, F.G. and Associates Limited. 1981. "Integrated Risk and Reliability Analysis, Arctic Pilot Project", Final Report, Petro-Canada.

Bercha, F.G. and Associates Limited. 1980a. "Monte Carlo Simulation of Downtime Risk Associated with Drilling Operations in Lancaster Sound and North Baffin Bay, Phase I", Final Report, Petro-Canada.

Bercha, F.G. and Associates Limited. 1980b. "Determination of Probabilities of Oil Spills in Canadian Arctic Waters - Phase I", Final Report, Department of Fisheries and Environment.

Bercha, F.G. and Associates Limited. 1979. "Drillship Operation Simulation in Baffin Bay and Lancaster Sound", Final Report, Petro-Canada.

Bercha, F.G. and Associates Limited. 1978a. "Determination of Probabilities of Blowouts in Canadian Arctic Waters", Final Report, Department of Fisheries and Environment.

Bercha, F.G. and Associates Limited. 1978b. "Arctic Tanker Risk Analysis - Volumes I and II", Final Report, Canadian Marine Drilling Ltd.

Bercha, F.G. and Associates Limited. 1978c. "Davis Strait Exploratory Drilling Evaluation", Final Report, Department of Northern and Indian Affairs.

Bercha, F.G. and Associates Limited. 1977. "Analysis of Risk and Safety, Beaufort Sea Standby Vessels", Final Report, Department of Northern and Indian Affairs.

Burton, I. et al. (Ed.). 1982. "Living with Risk: Environmental Risk Management in Canada", Institute for Environmental Studies, University of Toronto.

Chatterjee, P. 1974. "Fault Tree Analysis; Reliability Theory and Systems Safety Analysis", Research Report ORC-74-34, Office of Naval Research.

Denny, V.E. et al. 1979. "Risk Assessment Methodologies: An Application to Underground Mine Systems". Risk Assessment and Perception.

Dixit, B. and Bercha, F.G. 1984. "CDU Ice Management Simulation", Verbal Presentation, Third International Offshore Mechanics and Arctic Engineering Symposium, New Orleans, Louisiana.

Fischoff, B. et al. 1981. Acceptable Risk, Cambridge University Press.

Hotzel, I.S. et al. 1984. "Simulated Oil Exploration Operations in Baffin Bay", Proceedings of the Third International Offshore Mechanics and Arctic Engineering Symposium, Vol. III, New Orleans, Louisiana.

Lowrance, W.W. 1976. Of Acceptable Risk, William Kaufman Inc.

Rasmussen, N.C. 1981. "The Application of Probabilistic Risk Assessment Techniques to Energy Technologies", Annual Review of Energy

Salem, S.L. and Solomon, K.A. 1980. Summary of Issues and Problems in Inferring a Level of Acceptable Risk, Santa Monica: Rand Collection, The Rand Corporation.

Schwing, R.C. and Albera, W.A., Jr. (Ed.). 1980. Societal Risk Assessment--How Safe is Safe Enough? New York: Plenum Press.

Slovik, P. and Fischoff, B. 1977. "On the Psychology of Experimental Surprises", Journal of Human Perception and Performance.

Straugh, R. 1981. Risk Assessment as a Subjective Process, Santa Monica: Rand Collection, The Rand Corporation.

REMOTE SENSING OF EXTREME ICE HAZARDS

AUTHORS

Eric Leavitt and Ray Lowry
INTERA Technologies Ltd.
Calgary, Alberta

ABSTRACT

The ability to operate safely in ice enfested areas has been enhanced by advances in the ability to monitor ice hazards using remote sensing methods. Sensors can be deployed on satellite, airborne or surface platform. Both visual or near infrared and microwave sensing have been applied to the ice monitoring problem. For real time operations the visual and near infrared systems available are limited by visiblity of the surface and the problem of getting the data to the customer reliably. Microwave sensors include both passive and active systems. The passive systems, mostly deployed on satellites so far have relatively low resolution for detection of most ice hazards. However the active systems, including Side Looking Airborne Radar, both real aperture and synthetic aperture, have been used successfully to monitor ice bergs, multiyear ice ,ice islands, etc. in real time operations. Lately, search radars have been used successfully to detect ice bergs of all sizes in variable sea states. Enhancements to surface marine radars are also improving their capabilities for use in hazard avoidance.

1. INTRODUCTION

The area of remote sensing of sea ice or other ice features is very broad. Thus, in order to provide some focus to this paper, we have concentrated on methods that are used for support of operations in ice. The capabilities and limitations of such systems are discussed in the following sections.

2. HAZARD DEFINITION

One of the first questions to be asked is, "What is an extreme ice hazard?" The answer to this question will depend on the capabilities and relative speed of the vessel in question and the location and time of year of the ice feature. It depends not only on the vessel's capabilities to withstand impacts or other encounters, but also on the systems available to detect and then avoid or otherwise manage the hazard. The avoidance or management of ice hazards is further discussed by R. Pilkington in "Options for Handling Hazardous Ice Features".

There are at least two facets to the remote sensing of ice features: (a) locating and tracking an ice feature using remote sensing techniques; and (b) presenting the information to the user in a timely manner and in such a way that he can interpret the data.

Hazard detection systems can have a tremendous effect on an operation's ability to function effectively in the ice, but only if these systems are used to their best advantage. The data must be reliably interpretable, and they must be available in a regular and timely fashion, as operators must be able to rely on them. Almost all operations will require more than one source of data; these multi-sensor and multi-temporal data must be integrated into coherent information for the use of the operators. An example is the use of a vessel's marine radar to track the ice motion relative to the vessel between daily overflights of airborne radars mapping large areas. By this means, the useful life of the airborne radar data is greatly extended.

2.1 Hazardous Ice Features

Icebergs

Icebergs floating in the open ocean are a very real and obvious hazard. They are generally classified by size as growlers (<100 m^2), bergy bits (100-300 m^2), small icebergs (300-2500 m^2) and medium and large icebergs. The larger icebergs are also classified by shape (for example, tabular, pinical, etc.). The degree of hazard presented by icebergs is fortunately proportional to their size, as is their ease of detection. However, for many vessels, an unexpected bergy bit encountered with a high differential velocity, caused either by a ship travelling at high speed or the bergy bit being driven by strong winds and waves, can cause substantial damage. Further, for radar, which is the prime sensor currently in use on most vessels, the difficulty of detection is directly related to sea state. In various radar trials which took place in project BERGSEARCH '84 (Rossiter et al., 1985), probability of detection for bergy bits was as low as 60% with waves of 2.9 m in height or less.

Ice islands are similar to icebergs in that they originate with ice formations on land. Although the formation mechanisms are different, and also less well known, as with icebergs they are essentially brine -free and very hard. Ice islands are rather rare but can be very large. For example, T3 was still some 22 km long when it was last seen in 1979-80.

Multi-year ice (or as it is now called, 'old ice') represents a hazard similar in some ways to icebergs. Because there is little brine to weaken the ice as compared to first- year sea ice, it is much harder than first- year ice and, when held in a matrix of first- year ice, represents a significant hazard.

Fortunately, ice which is salt- free tends to have a very different microwave signature than first- year ice, showing up much brighter, especially during the portion of the year when there is little melting. There is less surface reflection and absorption in salt- free ice; the radiation enters the ice and is scattered by a volume scattering mechanism. It is therefore a much brighter reflector.

Ice Islands

There are features within the ice pack, which can be described as ridges or hummock fields, that are sufficiently larger and stronger than the main pack, such that they constitute an extreme hazard. Features such as large shear ridges may build up over time until they are many times thicker than the surrounding ice and are very large in extent. Because they are composed of first- year ice, they can in fact be rather more difficult to detect using remote sensing technology.

For some applications, even first- year ice is a serious hazard. During the drilling of one well in the Gulf of Alaska, a semi-submersible rig was used which had no ice capability (Grittner et al., 1983). For various reasons, including insurance, it was necessary to ensure that sea ice came no closer to the rig than 75 miles. Remote sensing in this case was used to locate the leading edge of the ice.

Finally, we should remember that ice is not a constant medium. Particularly during the summer melt period, its properties for remote sensing vary, and this can have a dramatic effect on detection of hazardous ice features.

3. PLATFORMS AND SENSORS

The three sensor platforms are: satellite, airborne and ship or drilling. One can also think of ice hazard detection in terms of the following three scales:

1. Strategic
    - used for planning purposes, days to weeks in advance
    - low resolution in space and time may suffice
    - typically large area coverage
    - some delay in data reception can be tolerated

2. Tactical
    - planning a route or response, hours to one or two days in advance
    - kilometers to 10's of kilometers range
    - data required in near real time

3. Close range tactical scale
    - used to plan immediate course or avoid hazard
    - minutes to hours repeatability
    - several hundred meters to 10 -20 km range
    - need data in real time

Satellite systems can provide support for strategic and perhaps tactical requirements, airborne sensors can definitely provide support for both strategic and tactical requirements, and shipboard sensors can provide information for close range tactical requirements.

Details of various sensors are described in the following sections.

4. SATELLITE SENSORS

Satellite systems can be broadly grouped into those using visual or infrared wavelengths and those relying on passive or active microwave sensing.

Visual or near-infrared sensors include the high resolution sensors carried on the various Landsat satellites and now on the SPOT satellite. SPOT's high resolution (approx. 10 m) makes it useful for monitoring ice processes and icebergs. For example, SPOT is being used to monitor icebergs in the Antarctic. In general, the repeatability rate of these two satellite systems is too low to be of use in operational roles, as opposed to research or long -term monitoring roles. They also have difficulty in distinguishing multi-year ice from surrounding first- year ice.

The NOAA and Russian polar orbiting satellites have been used by operators. For example, the M.V. Arctic carries a Muirhead receiver and routinely receives the low resolution data product (4 km) from these satellites. The data are used to anticipate when the ice edge will be encountered and to plan airborne radar coverage. As described in Thompson (1986), the Swedish Meteorological and Hydrological Service has used the high resolution data available at Sondre Stromfjord, Greenland to provide course information to the Brostrom ore carrier, Thuleland. These systems are limited by cloud cover, resolution and data availability, but can provide a strategic overview and in some cases may provide sufficient tactical information to the user.

Microwave sensors offer the ability to sense the ice cover through overlying cloud cover and during the polar night. Table 1, from Thomas (1986), summarizes the satellite microwave sensors that are providing data over the polar regions. Frequencies lie in the range of 1-300 GHz (wavelengths from about 1 mm to 37 cm). Both active and passive systems can be utilized. One active system, SEASAT, which was an L-Band (1.275 GHz) Synthetic Aperture Radar System (SAR), was available briefly from July to October, 1978. New satellite SAR systems are being planned for deployment in the early 1990's.

Passive microwave sensors have been used to characterize the ice cover for more than a decade (Thomas, 1986). The maximum resolution of the sensors to date has been relatively low (approx. 30 km), but new systems are planned with higher resolution. Passive microwave sensors exploit the variable emissivities of different ice types to calculate the percentages of open water, first- year ice and multi-year ice. The usual approach is to use an equation that assumes that the observed emissivity is a summation of the emissivities of the various ice types for the given season and assumed snow cover. This is enhanced by simultaneously observing the ice at several frequencies and polarizations, as with the Scanning Multichannel Microwave Radiometer (SMMR) launched in 1978 aboard two NASA satellites, SEASAT and Nimbus 7. SMMR acquires data in both vertical and horizontal polarization at five frequencies: 6.6, 10.7, 18, 21 and 37 GHz.

As an example, Ph.D. Associates of Toronto has an algorithm that has been used to produce ice maps for the Atmospheric Environment Service (AES) Ice Centre.

TABLE 1. PAST, PRESENT AND PLANNED SPACECRAFT PROVIDING MICROWAVE DATA OVER POLAR ICE.

Spacecraft	Useful Lifetime	Sensors
Nimbus 5 (NASA)	1973-1976	Microwave Radiometer (ESMR)
SEASAT (NASA)	July - October 1978	SAR, SMMR, Radar Altimeter (ALT)
Nimbus 7 (NASA)	1978 to late 1980's	SMMR
Geosat (US Navy)	1985-1987	ALT
DMSP (US Air Force and Navy)	1986-mid 1990's	Microwave Radiometer (SMMI)
NROSS (US Navy/ NASA/NOAA)	1990-1993	ALT, SMMI
ERS 1 (Europe)	1990-1993	SAR, ALT
JERS 1 (JAPAN)	(1991-1993)	SAR
Radarsat (CANADA)	(1991-1996)	SAR, Radiometer

5. AIRBORNE SENSORS

The airborne sensors of most interest are Side Looking Airborne Radars (SLAR), either real aperture or synthetic aperture (SAR). There are other sensors that can be used, including passive microwave, laser, thermal infrared line scanner, etc. Before concentrating on SLAR or SAR capabilities, we should mention impulse radar and passive microwave systems.

Impulse radars take advantage of the fact that ice is relatively transparent to radar waves in the VHF band (e.g., 120 MHZ). The methodology is to transmit a short pulse from a transmitting antenna mounted on a helicopter or slow flying light aircraft at very low altitudes. Part of the pulse is reflected at the air-ice interface and the majority of the pulse is reflected at the ice-water interface. The systems do not work very well if there are large inhomogeneities in the ice cover, i.e., over an unconsolidated pressure ridge. Several systems have been developed and used successfully, e.g., Cambridge Consultants in cooperation with Exxon Production Research Co., EBA Engineering and Canpolar Consultants. Limitations include height of operation, ice thickness (either very thin or very thick (gt 10 m)), speed of data collection due to data rates and, as mentioned above, problems regarding ridges or unconsolidated ice due to too many reflecting corners. But these systems do have applications for obtaining ice thickness measurements at a much higher data rate than by using drilling.

Airborne passive microwave systems are similar to satellite systems. The ice cover is viewed in one or more frequencies (e.g., 37 GHz) and the emissivity is used to calculate the "temperature of the ice". One advantage of an airborne system relative to a satellite system is that the resolution is greater due to the lower altitude of operation. However, the resolutions of the systems are still too coarse to replace the use of SLAR or SAR.

5.1 Side Looking Airborne Radars (SLAR)

SAR and real aperture SLAR systems have been used operationally to monitor sea ice and icebergs since about 1980 in the Canadian and U.S. Arctic and east coast Canada (e.g., Shaw, 1986 and Leavitt et al., 1986).

A primary advantage of SLAR or SAR systems is that the return signal from multi-year ice, first- year ice, pressure ridges and glacier ice all have somewhat distinct signatures. These sensors are also, of course, independent of weather and ambient light conditions.

The ability to distinguish ice types at the frequencies typically used for SLAR or SAR is illustrated in Figures 1 and 2 for ice and icebergs respectively. A brief explanation is given below for each of the ice types.

1. First- Year Ice

Normally, a saline layer migrates into the snow cover and this layer acts as an efficient reflector. This causes the ice to appear relatively smooth to the radar, resulting in a rather low return (dark tones).

2. Older Ice

Older ice has gone through at least one melt season. It is less saline and the brine drainage has left behind small imperfections with only a small amount of salt. Any snow is relatively dry and fresh. The imperfections are of the scale of the radar wave (cms) and act as small isotropic radar scatterers. Isotropic scatters mean more energy is back- scattered, relative to smooth first- year ice, and older ice appears brighter.

3. Icebergs

Icebergs are an extreme case of fresh water ice. Bubbles or other air inclusions occupy up to 15% by volume. These inclusions also act as isotropic scatterers.

4. Ice Islands

Ice islands are similar to icebergs and can be similarily distinguished on SAR/SLAR imagery.

Some caveats about the use of SLAR systems include the following.
When first- year ice freezes at temperatures below -20 °C, salt is extruded from crystals and forms a saline layer on the surface. This combines with the "frost flowers" which form at these temperatures to make very efficient scattering centres, whose size is of the same order as the radar wavelength. These act as isotropic scatterers and the surface appears very bright. This ice is identified as first- year ice by comparison with previous imagery, by texture and by the shape of the features. It is normally possible to identify this as first- year by the fact that it occurs in leads or polynas.

During the early melt season, it is sometimes very difficult to distinguish between first- year ice and multi-year ice because once the snow on the surface is water saturated, the water dominates the backscattering process and the surface becomes very uniform in appearance.

The ability to distinguish between different ice types can be enhanced by the use of multiple frequencies or by considering the polarization of the return signal. However, such approaches raise the cost beyond that which is practical for operational, as opposed to research, programs. A more pragmatic and quite successful approach to this problem is to collect multi-temporal data and track the ice until the snow melt has progressed further to allow some distinctions to be made.

A special problem occurs with icebergs in open water where small bergs, bergy bits and growlers are not consistently detectable against a background of sea clutter. The BERGMAP 85' study (Rossiter et al.,1985), which compared several SLAR and SAR systems, found that 90 - 100% of small icebergs but only about 10-50% of growlers could be detected. Another problem is that it can be difficult to distinguish between icebergs and ships.

Shaw (1986) describes the use of the MARS SLAR to monitor icebergs on the Grand Banks. A partial solution to the detectability problem was to use 50 -100% overlap in area coverage to pick up bergs that might be missed on only one pass.

5.2 Search Radar

ESRF has also funded experimental use of a search radar to detect icebergs. Greg Warbansky of Husky-Bow Valley gave the following comments about this system to one of the authors (Leavitt) in a private conversation. The company used a Litton V3 Search Radar and Warbansky is currently writing up the results for publication. The V3 was a compromise and the more advanced V5 model has now been installed for further tests. The V3 has no pulse compression or scan- to- scan integration as does the V5. Husky-Bow Valley were able to detect bergs and bergy bits but had some trouble with growlers in high sea states.

The V3 performance overall was very encouraging; it was not noise- limited and Husky-Bow Valley were able to develop a good baseline data base. A big advantage for the search radar is that one sees ahead of the aircraft, which typically flies about 1500 ft above sea level. Thus, it is possible to vector the airplane to targets and determine visually whether they are bergs or ships. A given target is "seen" for 5 - 10 minutes, optimizing the ability to detect targets against a sea clutter background, as opposed to SAR or SLAR which only briefly views a given target. The radar can also be used to detect the ice edge but does not have sufficient resolution to be used within the ice pack itself. Because of the flight altitudes needed to maintain resolution, the aircraft range is also limited. However, it appears to be an effective method for surveying icebergs in an area like the Grand Banks.

6. MARINE RADAR

Research on the use of surface-based marine radar for imaging surface features has been carried out by the Communications Research Laboratory at McMaster University and by the Canadian Department of Fisheries and Oceans. A good review of this research is given in Haykin et al. (1985).

This work was conducted at the DFO's Borden Research Station on Baffin Island, Northwest Territories. Three separate field trips were undertaken during the spring in fast ice conditions, which made ground truthing easy. Recent work has focused on detecting icebergs in open water.

As discussed in Lewis and Currie (1984a and b), designing an ice imaging radar involves two elements: (a) specification of radar parameters for maximum effectiveness; and (b) specification of display techniques which maximize transfer of information to the operator.

Radar parameters which were varied in the studies referred to above include:

1. antenna beamwidth;
2. antenna height;
3. radar pulse length;
4. radar frequency; and
5. polarization.

Display techniques include:

1. edge detection and enhancement;
2. optimizing radar return dynamic range;
3. applying range normalization; and
4. exploiting color to increase the information content of the display.

Many of the radar parameters offer rather obvious improvements. For example, decreasing beamwidth or pulse length increases the resolution of the radar. Raising the height of the antenna offers a better grazing angle, etc.

Icebergs (and to a lesser extent multi-year ice) cause much greater depolarization in the scattered signal than does first- year ice. Figure 3 compares the like and cross polarized returns for a Ku band radar at Borden Island. The icebergs are more easily detected against a background of sea ice when the cross polarized signal is compared to the like polarized signal. It is apparently the air inclusions within the icebergs which lead to this effect. The average depolarization ratio for the icebergs studied was 11db (see Haykin et al., 1985).

Marine radar provides data continuously as a vessel proceeds through the ice or as the ice proceeds past a drill ship. Airborne imagery provides a once- or at most twice- daily snapshot of ice conditions. Normally, the ship or rig can be identified on the imagery at the time it is flown; however, as the ice and/or vessel moves, it can become difficult to keep track of one's position relative to the imagery. If the marine radar image can be matched to the airborne imagery (e.g., SAR), then it is possible to keep track of relative position and continue to use the SAR imagery for ice identification.

Canarctic Shipping and Transport Canada have been sponsoring research into integrated systems for several years (e.g., Canarctic Shipping Co., 1985). The combination of two sensors extends the usefulness of the imagery, making it more cost- effective. It also makes the marine radar a more effective tool for hazard avoidance since it becomes possible to indirectly identify ice types on the marine radar.

7. OTHER METHODS

There are, of course, other systems or techniques which could be or have been applied to the problem of detecting ice hazards. These include:

1. Coherent Radar

For example, the Swedish Defence Research Establishment has been working with Brostrom Shipping to apply coherent radar to the problem of detecting icebergs against sea clutter. As described in Larsson et al. (1986), the principle is that icebergs have a different doppler frequency spectra than sea clutter . They have collected data in an experimental mode which indicate that this is the case, and will be continuing research and development.

2. Phased Array Marine Radar (e.g., Haykin and Currie,1984)

This would provide improved resolution using an electronically steerable antenna array.

3. Ground Wave Effect Radar

This exploits the fact that HF waves tend to propagate along the air-ocean interface. NORTEC is working to develop a commercial system for deployment on the east coast of Canada. The potential exists for a range of about 300 -400 km.

4. Forward Looking Sonar

A hull monitored sonar can be used to detect iceberg keels, and both Canarctic and Brostrom have tested units. There are, however, propagation problems due to the varying depth of the ocean surface layer. The problem also exists of protecting the sensor from ice impacts. The data from such a sensor would have to be integrated with the marine radar display to fully identify targets.

9. ACKNOWLEDGEMENTS

We would like to acknowledge the people who contributed slides to our presentation, including Bob Gorman of Canarctic Shipping, Ed Lewis of DFO and Frank Bercha of Bercha and Assoc. We would like to thank Greg Warbansky of Husky-Bow Valley for permission to quote his remarks on the search radar. We would also like to thank the organizers of the conference for the opportunity to present these comments: Roger Pilkington and Ben Danielewicz.

10. REFERENCES

Canarctic Shipping Co. Ltd. 1985. Phase II Final Report, Shipboard Ice Navigation Support System.

Grittner, S.F., J.M. Karish and R.A. Stewart. 1983. Ice surveillance program to support the North Aleutian Shelf C.O.S.T. Well #1. Proc. POAC 83, Helsinki, Finland. Vol. 1. pp. 282-296.

Haykin, S. and B. Currie. 1984. A phased array radar for iceberg detection. CRL Report No. 121.

Haykin, S., B.W. Currie, E.O. Lewis and K.A. Nickerson. 1985. Proc. of the IEEE, Vol 73, No. 2, pp. 233-251.

Larsson, B., A. Nelander and G. Stenstrom. 1986. A high resolution pulse doppler radar for detection of small icebergs in Arctic sea routes. Proc. Polartech '86, Helsinki, Finland. Vol 1. pp. 358-363.

Leavitt, E., E. Krakowski and B. Mercer. 1986. An integrated ice monitoring system for Arctic offshore drilling. Proc. Polartech '86, Helsinki, Finland, Vol. 1. pp. 107-118.

Lewis, E.O. , B.W. Currie and S. Haybin. 1985. Effect of polarization on marine radar detection of icebergs. Proc. IEEE International Radar Conference. pp. 253-258.

Lewis, E.O. and B.W. Currie. 1984a. Effects of frequency and polarization on marine radar detection of ice targets in an ice cover. Proc. IAHR Ice Symposium 1984, Hamburg, Germany.

Lewis, E.O. and B.W. Currie. 1984b. Improved marine radar display for navigation in ice-covered waters. Proc. IAHR Ice Symposium 1984, Hamburg, Germany.

Rossiter J.R., L.D. Arsenault, E.V. Guy, D.J. Lapp, E. Wedler, B. Mercer, J. Dempsey and E. Mclaren. 1985. Bergsearch '84. Assessment of airborne imaging radars for the detection of icebergs. ESRF Report No. 016.

Shaw, V.L. 1986. Iceberg detection using SLAR. Proc. 10th Canadian Symposium of Remote Sensing, Edmonton, Alberta, Canada.

Thomas, R.H. 1986. Satellite remote sensing over ice. J. Geophys. Res. Vol. 91, no. C2, pp. 2493-2502.

Thompson, T. 1986. Sea ice surveillance by satellite. Proc. Polartech '86, Helsinki, Finland.

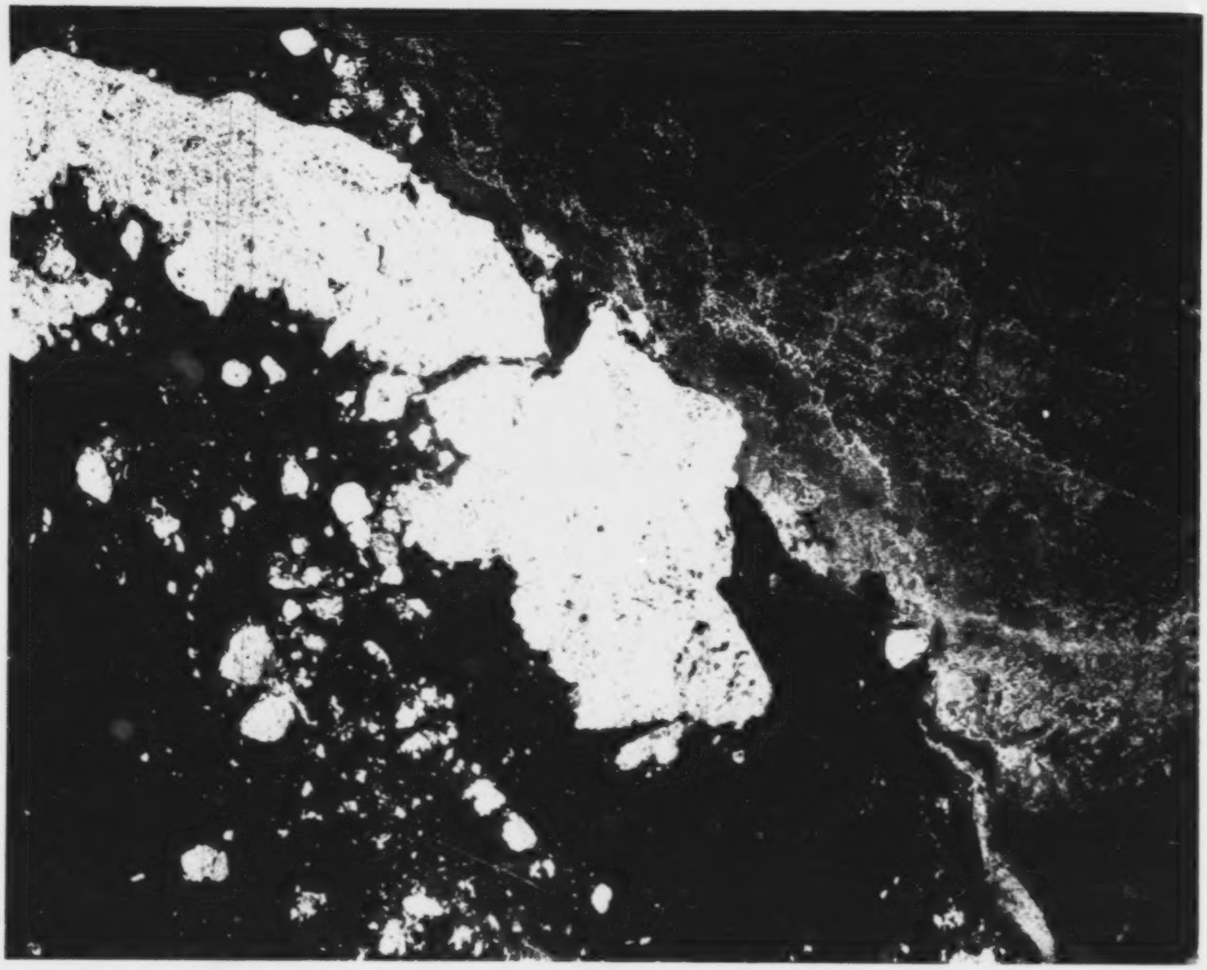

RADAR (SAR) IMAGE OF MACKENZIE BAY AREA, CANADIAN BEAUFORT SEA SHOWING FIRST-YEAR AND SECOND-YEAR ICE, SHEAR ZONE, DRILLING VESSELS AND ICEBREAKER TRACKS

Figure 1. A SAR image of old ice in first-year ice

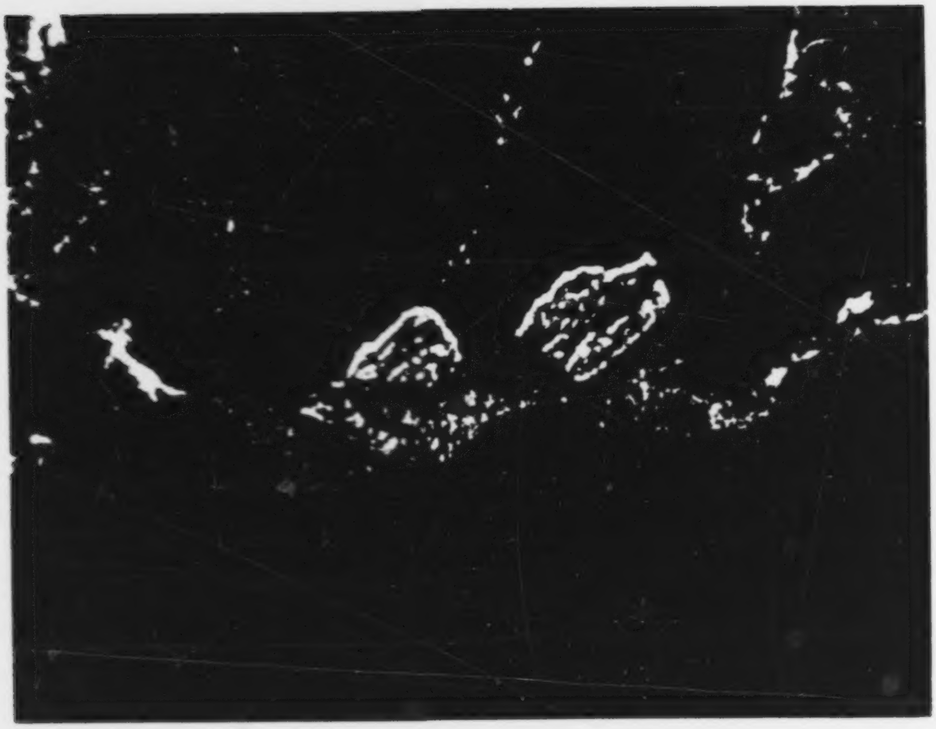

Figure 2. SAR image of two icebergs in first-year ice in Melville Bay, Greenland.

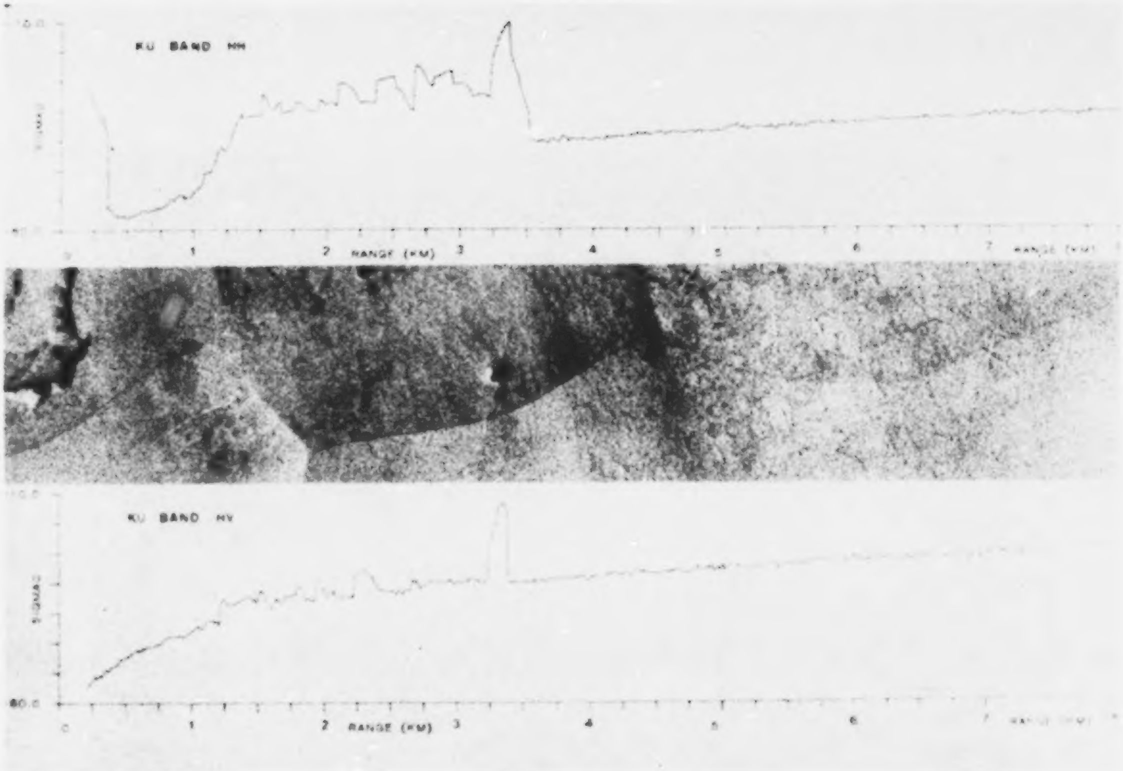

Figure 3. Plot of HH (top) and HV (bottom) for a Ku-band radar for two icebergs frozen in first-year ice (May 1983) from Lewis et al., 1985. A mosaic of the ice field is shown in the centre. Note that the iceberg at "A" is easily distinguishable in both returns. The iceberg at "B" is only distinguishable in the non-polarized (HV) return.

NRC WORKSHOP ON EXTREME ICE FEATURES

Questions and Discussions Form

AUTHOR: Eric Leavitt and Ray Lowry

PAPER: Remote Sensing of Extreme Ice Hazards

DISCUSSION BY: R. Pilkington

DISCUSSION:

How could one identify hummock fields in SAR/SLAR? How reliable is identification of ice shelves depending on location relative to aircraft flight path and orientation of surface waves?

AUTHOR'S REPLY:

Hummock fields are recognized on SAR imagery by their bright tone, very rough texture, and by their rather unusual shape. The tone and shape are easily recognized, even on the third and fourth generation photographic products often used in the Beaufort Sea. The texture can sometimes be lost in saturation on high contrast prints. By using a digital display, or by taking greater care in the production of hardcopy, this can be avoided. Digital displays are preferred, as they can display the full resolution, whereas hardcopy devices typically lose roughly half the resolution.

Because tone, texture and shape are all needed to accurately identify ice shelve fragments, it is necessary to have many pixels on a fragment. Given a 6 m pixel, this means fragments must be 'large' compared to 6 m for accurate identification. Few have been seen in open water, so the only useful data we have are from icebergs. Here the freeboard is the give-away as they tend to have very bright returns. How large a fragment must be to be 'iceberg-like' is unknown, but we suspect that the high return would show it to be an ice island fragment at a size smaller than that which the surface pattern could be resolved. Wave direction would not likely be a major factor.

OPERATIONAL RESPONSE TO HAZARDOUS ICE FEATURES

By G. R. Pilkington,
PILKINGTON and ASSOCIATES,
Box 23, Site 13, RR 4, Calgary,
Canada, T2M 4L4.

INTRODUCTION

Over the past two days we have heard about extreme ice features, their statistics, thickness, strength, etc and although the risk of one of these features ever hitting a structure is low, it is still a finite possibility. This paper reviews the operational reponses that would be carried out on an oil production structure in the Arctic if a hazardous ice feature should approach the structure.

The definition of an ice hazard depends on the particular structure. For example, to a semi submersible almost any ice is hazardous (Borthwick and Hadley, 1986). Gulf's conical drill rig, the Kulluk, can handle, with ice management, 10 / 10 thick first year ice in the early summer and several tenths of multi-year ice (Haverson and Pilkington, 1985), and Gulf's bottom founded Molikpaq structure can tolerate over 7 m of multi-year ice in winter (Wright et al, 1986). Floating vessels can tolerate relatively small hazards but they can react to the hazard by moving, whereas fixed structures cannot move and so have to be designed to withstand considerably larger hazards. Generally, in the case of a floating vessel, hazards are frequent (about once per year), but a fixed structure must be designed such that hazards are rare. Typically a bottom founded exploration structure (which is moved every year) would be designed for an environmental event that would cause significant damage every 20 years, whereas a production structure would be designed for an ice hazard with a significantly longer return period due to the duration of the production project and the higher economic and environmental risks.

ACCEPTABLE RISK

Defining an acceptable risk level for the design of a fixed offshore structure subjected to ice impact is difficult. It depends on the result of the damage:- does it involve human life or risk to the environment ?; what are the economic losses and is the owner of the structure willing to accept these losses (both structural damage and loss of production) ?; are the regulatory agencies willing to accept the risk levels ?

The proposed C. S. A. requirements for offshore structures (C.S.A. 1986) identifies two risk classes and a serviceability criterion;

Safety Class 1

Annual probability of failure 10^{-5}

In this case the failure of the structure would result in

a) Great risk to life,
b) High potential for environmental pollution,

Safety Class 2

Annual probability of failure 10^{-3}

In this case the failure of the structure would result in

a) Minimal risk to life,
b) Low potential for environmental pollution,

Serviceability

Annual probability of occurring 10^{-1}

This involves any event that only affects normal use and occupancy.

Safety Classes 1 and 2 represent the ultimate stress limit of the structure which would result in;

a) Loss of equilibrium of the structure,
b) Loss of bearing capacity of the structure,
c) Overturning instability,
d) Very large deformations.

"Serviceability" represents the limits which restrict normal use and occupancy, for example;

a) Deflection or rotation of members of structure,
b) Motions, such as vibrations,
c) Local damage,
d) Small displacements of structure.

The above risk levels can be quoted in terms of the life of the structure:

SAFETY	PROBABILITY PER YEAR for 1 year	PROBABILITY OF FAILURE OVER LIFE OF STRUCTURE (years)		
		10	25	40
CLASS 1	10^{-5}	.01%	.025%	.04%
CLASS 2	10^{-3}	1%	2.5%	4%
SERVICEABILITY	10^{-1}	66%	93%	98%

CALCULATION OF RISK

The probabilities quoted above incorporate both the probability of an environmental event occurring coupled with the probability that this event will cause a significant failure in the structure resulting in the indicated damage. An annual probability of 10^{-5} means that once in 10^5 years there is a "good"

(66 %) chance that the event will occur. Over this time the ice conditions will probably have changed significantly and the data used to predict the event will no longer be valid. However, it does indicate an event of very low probability.

The calculation of such loads is carried out by firstly considering the different interaction scenarios to determine those most likely to occur, then combining the different factors that affect the occurrence of the event using the Monte Carlo method or a product of probabilities (Bercha, this workshop). Combined in such calculations (Bercha and Griffin, 1985; Churcher et al, 1985; Dunwoody, 1983) are the probabilities of the extreme ice feature being in a particular location, and the distributions of the size, velocity, thickness, effective ice strength of the feature, plus wind and current strengths.

The probability of failure over the lifetime of the structure in the above table indicates that if there were 25 structures designed to these CSA standards, then it is expected that one would experience Class 2 damage every 40 years, whereas there is a very low probability that any one will experience Class 1 damage. Note that the normal damage risk levels for commercial buildings is about 1 % per year.

Such probability calculations are limited by lack of environmental information (see the summary of this workshop). For example there are only 2 years of data on hummock field distributions and sizes, and virtually no data on instantaneous drift speeds of large ice features (only 6 to 12 hour averages). Ice pressures are being measured on large structures (Wright et al, 1986), but there are no data on ice pressures for very thick ice features (i.e. 10 m and more), semi-global loads or ice bergs. Hence at present any production structure must be designed with a significant safety factor and during the first few years after a new structure is installed, the rig should be shut down whenever an ice feature approaches that is predicted to be capable of causing loads near the hazard design loads on the structure.

PASSIVE versus ACTIVE PROTECTION

Passive protection is built into the structure and includes such aspects as the weight, size, and resulting resistance of the structure; the shape of the walls-are they vertical and so cause crushing or sloping to initiate flexure which results in a lower effective ice failure pressure; and the presence of a berm which could either resist a thick ice floe directly or cause a rubble field to build up which would increase the resistance of the structure, dampen any dynamic loads and reduce local loads.

Based on this built-in passive protection, one calculates the maximum global loads the structure can tolerate. This paper discusses what one would do if an approaching ice hazard is estimated to exceed the capabilities of the passive resistance of a structure.

Because drilling and production operations take time to shut down, it is necessary to forecast the arrival of a hazardous ice feature and prepare accordingly- this is referred to as an "Alert Procedure ". Alert procedures are discussed for various structures by Wright and Weaver (1983), Dixit et al (1985), Churcher et al (1985), and Borthwick and Hadley (1986).

ALERT PROCEDURE

The alert procedure allows the operations staff to make a structure safe in the event of an impending hazard in a timely manner. Such procedures have been developed for all rigs used in the Arctic. Below is presented a general procedure similar to that used on the Kulluk and Molikpaq, but modified for use on a production structure.

The procedure is based on;

Hazard Time (HT) which is the time for the hazard to arrive at the rig,

Secure Time (ST) is the time to secure the well,

Evacuation Time (ET) is the time to evacuate the rig

In the case of a production structure, the time to remove all stored oil must be considered (if appropriate), ie.

Oil Removal Time (ORT)

If the hazard is approaching, then the time remaining before one of the above operations (ie. well securing, stored oil removal, or evacuation) must be initiated is given by

T = HT - (the larger of ST or ET or ORT)

and the operations conducted are dictated by whichever procedure results in the lowest value of T.

Typical times are:

ST is about 6 hours for one well and 3 hours for each subsequent well (Pidcock, 1987). Note that this is the same or less than required for an exploration well because of all the down hole valves and built-in safety systems.

ET is typically about 4 hours using a helicopter to evacuate 100 people, and considerably less if a nearby vessel can be used. However, it may take considerably longer if one has to rely on helicopters and the weather is bad. Normally if a hazard is approaching , non-essential people are evacuated early thereby reducing ET.

ORT may be anywhere from 0 hours if the structure has just been unloaded or if a pipeline is being used to about 3 days if ice conditions are such that a vessel can get to the structure easily. If ice conditions are such that the off loading vessel cannot get to the structure, ORT may by an entire winter. This indicates the need for an ice capable tanker to shuttle between the structure and oil storage in a nearby safe harbour.

A colour alert system is established depending on the value of T. For example,

T > 24 hours	GREEN	All Safe
24 > T > 12	BLUE	Early warning, increase monitoring
12 > T > 2	YELLOW	Warning. Keep constant watch of all alert times
T less than 2 hours	RED	Stop operating, secure wells, offload oil or start to evacuate rig.
HT less than ET	BLACK	Evacuate all personnel

This procedure -using time -is used in the Canadian Beaufort sea. On the East coast the alert procedure generally uses alert zones which are based on the maximum drift speed of the hazardous feature multiplied by alert times similar to those above (Borthwick and Hadley, 1986). The two systems are essentially the same, as HT above incorporates a reasonable forecasted ice drift rate which is continuously updated.

HAZARD TIME

The hazard time is not easy to determine. First one has to determine if a large feature is indeed a hazard to the structure and this depends on numerous factors.

Field decisions involve a review of SLAR or SAR imagery to identify any large, old ice features then a site investigation to study the feature more carefully. The site investigation involves determination of ice type, floe sizes, average thickness, edge and maximum thickness, pack ice thickness, is the feature frozen into the pack ice or are there cracks or leads around ?, ice thickness behind the ridges, etc. Once this has been done, it is then possible to determine if the feature is likely to be a hazard using a systematic calculation of limit stress and pack ice driving forces (Croasdale, this workshop), and the kinetic energy of the feature, as indicated below. The most important aspect of the ice feature is its thickness. This has generally been obtained in the past by visual inspection, drilling holes, surface profiles, and /or by side looking sonar systems lowered below the ice surface to profile ridge keels. A reliable, remote, fast, topside profiling system would greatly facilitate this operation. The three dimensional geometry of the ice feature is important in determining the load it might exert on a structure, and this, too, should be included in calculations of hazardous ice loads. If no site investigation can be made (due to weather or lack of availability of a helicopter), then the ice feature must be considered to be a hazard until an investigation can be made.

Here is provided a simple example of ice loading and hazard assessment for a production structure which is assumed to be octagonal in shape and approximately twice the size of Gulf Canada's Molikpaq (with four 120 m faces and 44m corners at 45 degrees).

A typical ultimate resistance of the assumed production structure would be about 200,000 tonnes, and the design hazard load (safety factor 1.5) would be 133,000 t. If the structure has vertical walls from the water line and to about 6m below, then thick ice will crush against the structure and the effective global ice failure pressure will be about 1 MPa for multi-year ice (Metge et al, 1981; Wright et al, 1986 and Sanderson, 1986). Thus loads of 200,000 and 133,000 tonnes (the ultimate and design hazard loads) result from impact from 10 m and 6.6 m thick, multi-year ice, respectively, assumming 100 % contact of the ice with the structure. Thus if the approaching ice feature contains significant areas of ice in excess of about 6.6 m thick, then it must be considered a potential hazard until more experience is gained.

Next it is necessary to determine if the pack-ice which drives the thick piece of ice is capable of generating these loads. This depends on the thickness of the pack ice, the size of the thick ice piece or floe, and the nature of the pack -ice/ thick ice bond (Croasdale, this workshop). If the bond between pack-ice and thick ice feature is well frozen then the failure pressure may be as high as 1.5 MPa, but if the bond is broken (i.e. cracks are evident in the pack ice surrounding the thick floe), then the maximum pack-ice pressure may be as low as 100 KPa (Wright et al, 1986). For pack-ice of 1 and 2 m thicknesses, the floe or thick ice feature must be at least 0.9 and 0.5 km wide for the frozen-in case and 13 and 6.5 km wide for the non-frozen case, respectively, for the pack ice to develop a driving force of 133,000 tonnes.

If the pack-ice is not able to generate the hazardous loads, the ice floe or thick ice feature may have enough kinetic energy by virtue of its mass and /or velocity to engulf the structure and develop the extreme loads. This depends on the shape of the structure and of the floe, and the thickness of the floe. Taking a worst case scenario of a floe engulfing the structure face on, if the floe is about 7 m thick, the floe must have at least 45

Giga Joules (GJ) of energy to develop 133,000 t. loads, which would require the floe to be about 40 km diameter for a drift velocity of 1 m/sec. If the ice is 10 m thick, the floe's energy must exceed 13 GJ, which requires a floe diameter of 30 km if the floe average thickness is 3m (again assuming a drift velocity of 1m /sec). If the ice thickness is 20 m, then loads approach 240,000 tonnes from the ice failing against the flat 120 m sides of the structure. In this case the floe needs to have just enough kinetic energy to allow the ice to develop complete contact with the side of the structure.

The above calculations would be conducted in the field to determine if a particular ice feature is a hazard, and if it is concluded to be a hazard then HT will be calculated and the appropriate Alert procedures will be followed.

LOCAL LOADS

In the case of local or semi-global loads (ie. loads over areas of 10 to 100 square meters) there is limited knowledge of the loads to use. The structure must be designed to reduce the effects of any local damage, for example, by segmenting ballast tanks.

It is difficulty to see how one could recognize a feature capable of causing "local" damage to a structure, and it is expected that one would ignore the problem until it happens then repair the damage as quickly as possible afterwards. Of course one must consider all the "local damage" scenarios and ensure that they will not lead to global failure of the structure (e.g by major losses of ballast or fill, which reduces the global resistance of the structure).

FORECASTING IMPACT

Once it has been determined that the ice feature is indeed a hazard to the structure, it is necessary to calculate HT, the time for the feature to reach the structure.

The forecast of the drift of a hazardous ice feature requires a forecast of winds and currents, and a calculation of the effects of these winds and currents, and of the Coriolis force on the feature. As indicated, reaction times of 5 days and more may be required for a production structure. Past experience indicates that winds forecast beyond about 24 hours are of little use for ice drift forecasting. Currents are generally not known at all and they are a major driving force for ice floes.

There are several models for forecasting ice drift in an open ocean that equate the wind, current, and Coriolis forces to the momentum of the ice floe or iceberg (Smith and Banke, 1983; Sodhi and El-Tahan, 1980; etc). For an ice covered ocean one has to include in-ice pressure. For this case models have been developed by Leavitt et al, 1981; Leavitt et al, 1983; Hibler, 1981 (this is a very large scale model); and I believe the

University of Washington has recently received a contract to continue this work. In some cases, these models can calculate the actual drift quite well when hindcasts are conducted with the actual measured winds, but on other occasions the hindcasts are not good. Thus at present, with the available wind forecasts and predictive models, ice floe predictions beyond a few hours are not too reliable and so are of limited use for tactical response. Models which use actual measured ice drift and wind data to obtain the important ice floe or iceberg parameters (e.g. drag coefficients, currents, added mass etc), and then use these parameters in subsequent predictions should provide better forecasts.

One tends to consider forecasting as being "right" or "wrong". If a floe was forecast to hit the structure and it didn't, then the forecast is "wrong"! In fact, forecasts should be considered as "probabilities".

For a period of up to 3 days, over which a reasonable wind forecast can be given, it is recommended that forecast error zones be developed based on actual, historic, ice drift trajectories. These error zones indicate for, say, 6, 12, 24 hours, and 2, and 3 days the size of the error that would be expected if one used a particular ice drift model. This provides the probability of an ice floe hitting the structure based on what it had done at that location in the past.

Beyond 3 days zones should be developed around the rig which use reasonable maximum ice drift velocities. For example, a 5 day maximum velocity of the ice might be 0.2 m/sec, giving a zone of 90 km diameter, and for 3 days the velocity might be 0.3 m /sec for a zone diameter of 72 km. Any hazardous ice feature entering these zones would initiate an alert, the features would be carefully tracked, and rig closure would commence as appropriate.

ACTIVE OPTIONS FOR HANDLING THE HAZARDS

If a hazardous ice feature (one capable of causing the design hazard loads on a structure) is identified updrift of the structure, what can be done to reduce the hazard once the hazardous feature has entered an alert zone ?

Explosives:

Considerable work has been done in this area which generally indicated that explosives would be ineffective in destroying icebergs as the ice is quite resilient to the blast despite its brittleness. A recent paper by Mellor (1983) reviews the methods of blasting ice and provides optimum charge quantities and locations which are verified in a paper by Fonstad et al(1982). The conclusions of the Mellor paper are that it is quite feasible to protect a structure against ice thrust, impact by sheet ice, multi-year ice ridges and small ice island fragments by means of explosives.

Ships:

It may be possible to break up hummock fields along their weak lines using ships, but it will not be possible to breakup ice islands or ice bergs. It would also be possible to break up the pack ice behind a large ice feature and so reduce the maximum pack ice pressure that drives the floe. However, this does not help if the ice feature has sufficient kinetic energy to generate the full limit stress loads as discussed above. Also, the floe may be so large that even the failing pack-ice pressure could cause problems.

Towing:

Ice bergs are frequently towed away from drill rigs on the east coast (Borthwick and Hadley, 1986) however, these are generally small bergs and it is unlikely that this method would be particularly effective against any berg or large ice feature that might be a threat to an offshore production structure at least with currently available vessels. In any event it would not be possible to tow a large ice feature in winter due to the surrounding ice pack.

REFERENCES

Bercha, F. G. and B. J. Griffin, Ice Risk to Offshore Production Operations, AOTC, 1985.

Borthwick, I.,and R. D. Hadley, Ice and Iceberg Contingency Planning and Management for Offshore Oil and Gas Operations, Polartech, 1986.

Churcher, A., D. Blanchet, B. Danielewicz, A. B. Dunwoody and A. Keinonen, Ice Loads on Bottom Founded MODU's for Operation in the Beaufort Sea, AOTC, Anchorage, 1985.

C. S. A. 1986, Proposed C. S. A. Recommendations for Offshore Arctic Structures.

Dunwoody, A. B., The Design Ice Island for Impact Against an Offshore Structure, Proceedings OTC, No 4550, Vol 2, pp 325-330, 1983.

Haverson, P. and G. R. Pilkington, Drilling in Ice from the Conical Drillship- Kulluk, AOTC, Anchorage, 1985.

Hibler, W. D., T. Udin and A. Ullerstig, Modelling Mesoscale Ice Dynamics using a Viscous Plastic Constitutive Law, POAC, 1981.

Leavitt, E., J. Sykes and T. T. Wong, A Sea Ice Model Developed for Use in a Real Time Forecasting System, POAC, 1981.

Leavitt, E., B. Mercer, and E. Krakowski, Real-Time Ice Forecasting in Support of Winter Drilling Operations in the Beaufort Sea, POAC, Helsinki, 1983.

Mellor, M., Protection of Offshore Arctic Structures by Explosives, POAC, 1983.

Metge, M., B. Danielewicz and R. Hoare, On Measuring Large Scale Ice Forces; Hans Island, POAC, Quebec City, 1981.

Pidcock, G. Private communication.

Smith, S. D., and E. G. Banke, The Influence of Winds, Currents and Towing Forces on the Drift of Icebergs, Cold Regions Science and Technology, No 6, pp 241-255, 1983.

Sodhi, D. S. and M. El-Tahan, Prediction of an Iceberg Trajectory during a Storm. Annals of Glaciology, 1: pp 77-82, 1980.

Wright, B., G. R. Pilkington, K. S. Woolner and W. H. Wright, Winter Ice Interactions with an Arctic Offshore Structure, IAHR, Iowa City, 1986.

Wright, B. and J. S. Weaver, Tarsuit Winter Alert Monitoring, OTC, paper 4518, pp 61 to 66, 1983.

ICE PRESSURES DURING THE IMPACT OF AN ICE MASS

by

H. R. Kivisild, D. Eng.
Lavalin Offshore Inc.

1. ABSTRACT

The collision of an ice feature with a structure creates variable contact pressures. The time average of these pressures is only a fraction of peaks and approaches unit energy to fail ice.

The unit energies can be applied to determine penetrations of structures and vessels into ice features. This defines contact areas and in its turn maximum contact forces.

2. Colliding extreme ice features cause critical loads

Critical forces are mostly from impacts. Static ice force is usually limited in open water. Static temperature load may be important in confined areas. Large continuous ice fields may exert dangerous forces but even these are more often than not amplified by dynamic action.

3. Static wind forces

As an example, wind blowing at 30 m/sec over rough ice is considered.

This wind will cause a shear of approximately

$$\tau = 2.2 \times 10^{-3} \times 1.4 \times 30^2 = 2.8 \text{ Pa}$$

If we consider action on a floe with a diameter of 3,000 m, the following static force is generated:

$$F_s = 7.07 \times 10^6 \times 2.8 = 19.8 \times 10^6 \text{ N} = 198 \text{ MN} = 20{,}000 \text{ ton}$$

This would cause the following load on a 100 m wide structure per lineal metre.

$$\frac{F_s}{B} = \frac{19.8}{100} = 0.2 \text{ MN/m}$$

These conditions generate a substantial force which still can be exceeded easily by dynamic action.

Thus, impact conditions must be investigated.

4. Dynamic effects

If the ice feature travels a short distance s from a stationary position until it reaches a structure, the following relationship may be written for the collision where the structure penetrates the ice floe by the distance Δ:

$$\int F_s \, ds = \int F_c \, d\Delta$$

For a short time period, the environmental drag F_s may be assumed to be constant. As an illustration, the contact load in collision is expressed by an average value. These substitutions give the following simple equation:

$$F_s \, s = F_{ca} \Delta$$

and the dynamic amplification is expressed by the ratio:

$$\frac{F_c}{F_s} = \frac{s}{\Delta}$$

The penetration of an ice feature needs typically to be in the order of a metre for severe load to be applied. This means that a load in the order of 10 m would suffice to amplify static loads by a factor of 10 in collision. Travel fetches of hundreds of metres give large amplifications.

5. Free moving ice features

The described effect has limitations from the braking effect of water resistance. It can be shown that the ratio of wind velocity to the speed of the mass stays below a limit, depending on the roughness of parameters, approximately

$$\frac{w}{v_\infty} = 40$$

and long travelling fetches would generate velocities which are expressed as follows:

$$\frac{v^2}{v_\infty} = 1 - \exp\left(-4.7 \times 10^3 \frac{s}{h}\right)$$

where:

s = travelling fetch
h = thickness of ice floe
v = collision speed of the ice feature
v_∞ = speed at infinite fetch

This expression may be written as follows:

$$\frac{v}{w} = \frac{1}{40}\left[1 - \exp\left(-4.7 \times 10^{-3}\,\frac{s}{h}\right)\right]^{\frac{1}{2}}$$

6. Intensity of the impact

The intensity of the impact is governed in certain occasions by momentum and in other conditions by the kinetic energy. Static conditions can be expressed by force.

The force relationship gives the following expression, valid for static conditions:

$$F_c = F_s$$

The momentum relationship gives the following expression, which is interesting for overturning and single load pulse effects.

$$\int F_c \, dt = mv$$

The energy relationship gives the following expression, which can be used to define penetrations:

$$\int F_c \, ds = \frac{1}{2} mv^2$$

The reaction of the ice mass will be discussed below

7. The collision process

There are two peaks which could be the critical parameters in the collision process.

There is a peak close to the initial contact. A strong impulse is given which changes the momentum of the ice feature and/or the momentum of the structure or the vessel in collision with ice.

A second peak can be equally important. Impulse and energy criteria determine how deep a structure or vessel will penetrate into the ice mass. The penetration often determines the largest load. This happens just as the ice mass is stopped. This peak exceeds the first peak by a wide margin when the ice load spreads as a structure or a vessel penetrates an ice mass.

8. The effects of ice properties

In addition to contact geometry, there are other factors in the relationship between pressures and dynamics, as shown below:

- ice properties depending on crystallography, salinity, temperature;
- size of loaded area and its position related to edge conditions;
- geometry of breaking including confinement and aspect ratio;
- impact velocity and its relationship to ice conditions;
- strain rate from impact speed and load area.

There are stochastic variables in the impact process such as ice properties.

Moreover, the process of breaking ice over a wide loaded area compared to the depth (or length) of loading, is itself a stochastic process. Spike load type failures create a stochastic process. Ductility and plastic flow reduce the importance of stochastic effects.

Simplified cases, such as instantaneous loads over a given area and pressures in a breaking sequence of infinite duration, lend themselves best to statistical analysis.

9. The long and short term effects of the ice load

Ice load is variable in time. The most rigorous way to consider this effect is by the use of an ice load algorithm which is used as a forcing function.

The duration of spikes in the breaking loads and their intervals are of the same order of magnitude as the free oscillation periods of various structural components. These facts indicate the application of ice force algorithms as forcing functions rather than the use of instantaneous loads as static loads.

Power spectra may be sufficient for many calculation.

Critical load times for structural elements are defined from general dynamics.

10. The determination of deepest penetration using the ice breaking energy concept.

Impulse and energy criteria yield maximum loads if the energy can be determined, which must be spent to achieve a given penetration into the ice mass. Penetration can give contact areas and thus forces.

The average energy of breaking ice per unit volume is expressed by the following equation:

$$\frac{E}{Q} = p_E \frac{\int F_b \; d\Delta}{\int A_b \; d\Delta}$$

Where F = force required to break ice,

A_b = ice area broken off,

Δ = penetration of indenter into ice,

p_E = energy per unit volume required to break ice,

E = work required to break off an ice volume V,

Q = volume of broken and removed ice.

The broken-off area may be assumed to be invariable during the short impact phase. In this case the quation can be written for unit energy as follows:

$$p_E = \frac{\int \frac{F_h}{A_b} \; d\Delta}{\int d\Delta} = \frac{\int p_b \; d\Delta}{\int d\Delta}$$

Certain modifications are required to use these equations with the impulse method. A time interval is introduced.

$$d\Delta = vdt$$

$$p_E = \frac{\int F_b \; vdt}{\int A_b \; vdt}$$

This equation can be simplified for short impulses where it may be assumed that:

$$v = \text{const}$$

that gives:

$$p_E = \frac{\int F_b \, dt}{\int A_b \, dt}$$

As above, the breaking area is constant in many applications.

$$A_b = \text{const}$$

and the equation becomes:

$$p_E = \frac{\int p_b \, dt}{t} = \frac{\int \frac{p_b}{v} \, d\Delta}{t}$$

or,

$$p_E t = \int \frac{p_b \, d\Delta}{v}$$

Where t = duration of the impulse.

Among other results, the last equation expresses the obvious fact that the impulse to create a flake is largest in the impact by a slowly moving floe. Also, obviously the ice floe has to be very large to possess sufficient momentum at a low speed.

11. Stochastic scale effects

In addition to size effects caused by different lengths of cracks under loads, here are numerous probabilistic theories indicating that a larger load area should have further reductions because of strength variations and crack distribution in the ice mass.

12. Stochastic time effects

As the impulse lengthens, so will an averaging process reduce average forces during one impulse to a figure which is approaching the pressure expressing energy to failure. This will happen in indefinitely long pulses during penetrations at a constant velocity.

$$p_e = \frac{\int_0^s p\,ds}{s} = \frac{\int_0^T pv\,dt}{\int_0^T v\,dt}$$

Where p_e = average channel pressure during the episode (pulse).

The other effect gives a high probability for pack loads in long penetrations. Also the probability of high loads increases for any impulse duration.

$$\max_{o<t<T_p} p_e = \max_{o<t<T_p} \frac{\int_0^{T_e} pv\,dt}{\int_0^{T_e} v\,dt}$$

Where T_e = duration of the episode (impulse),

T_p = duration of the collision,

v = impact velocity,

t = time variable,

p = contact pressure on the channel.

13. Database

As shown above, the parameters of the ice failing energy approach can be calculated from load histories of field and laboratory collision observations. We may mentioned Peyton 1968, Michel and Toussaint 1977, Kry 1978, 1980, 1987, Määttänen 1979, Blanchet & Michel 1981, Neill 1972, Bercha 1985 and Blenkarn 1970.

Excerpts from laboratory tests by Blanchet and Michel and from field measurements at Hondo Bridge in Alberta are attached as examples.

From these measurements it is obvious that unit energy required to fail ice is several times less than crushing strength. An average figure in the field is 1 MPa, but also 0.7 MPa can be associated with the highest peak loads.

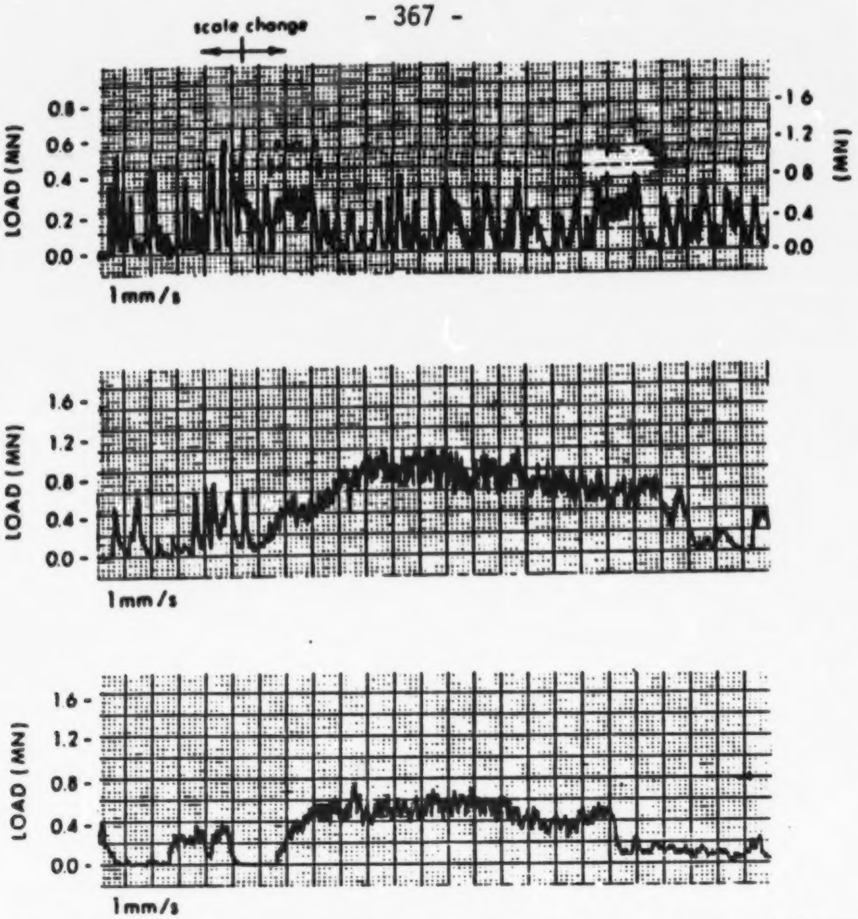

Examples of ice force histories for crushing failures at Hondo: (*a*) 12 April 1977, 03 h 47 min 16 s; (*b*) 26 April 1979, 16 h 49 min 29 s; (*c*) 26 April 1979, 16 h 51 min 40 s.

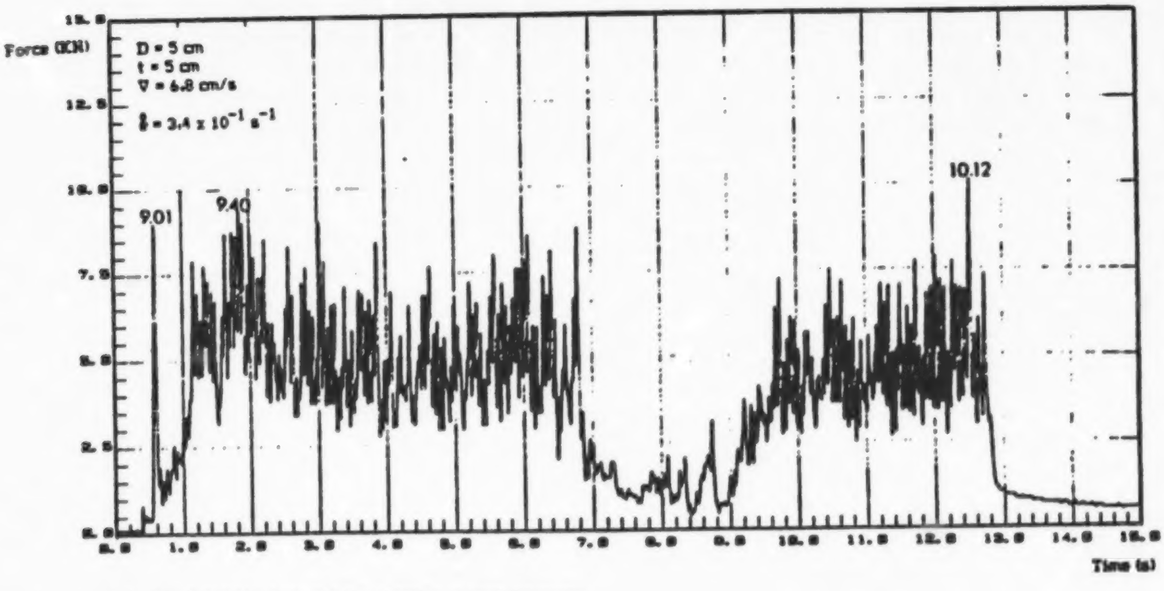

Laboratory indentation tests with flat indentors at Laval University
Test number 2 (Blanchet and Michel, 1981)

19. Application of results

A strong impulse at high pressures is applied at the initial contact. Depending on conditions, this can be the critical load. A slow impact gives the longest duration of critical pressures and thus the largest impulse. To deliver the required momentum, large ice features are required since the impact velocity is low.

A more usual maximum happens at maximum penetration of the ice feature by a structure or a vessel either by crushing or ride-up, or both.

To find that moment, unit energies in failing the ice mass should be used. These energies which are required to break and dislodge a unit of ice depend on the mode of failure, crushing or bending and other conditions as described anove. It was shown how equations can be written for the absorption of the kinetic energy of the ice feature. These energy equations define the maximum penetration and thereby the largest contact area.

Critical loads themselves are applied on the contact area at higher pressures than the failing energies. Compressive strengths, bearing capacities are reached. Spike pressures which are developed exceed unit failure energies several times.

In general, the application of formulae for ice breaking energy results in deeper penetrations by the colliding discrete mass than would be obtained if the penetration were estimated at ultimate failure stresses. Wedges and other mitigative steps need to be re-considered.

Dynamic analyses show that massive structures would respond to time average loads caused by light ice features (only a fraction of peaks). On the other hand, extreme ice features can cause sizeable impulses to be applied on large contact areas.

THE ULTIMATE EXTREME ICE FEATURE

ANTARCTIC ICEBERGS

(A summary of a paper present by R.B.Thomson)

The Antarctic is well-known for its enormous icebergs but little research has been done to enable an accurate assessment to be made of the total mass and number of icebergs produced each year.

The Antarctic icesheet of 25 million km^2, containing over 90% of the worlds ice and approximately 72% of its fresh water provides a vast reservoir for the production of icebergs. This is aided by around 2 million km^2 of iceshelves located around the coast of the Continent. These shelves, which are the source of around 70% of all Antarctic icebergs including the largest tabular bergs, are fed by huge glaciers, many moving several hundreds of kilometres down from the polar plateau. The June 1986 breakup of a large area of the Filchner Iceshelf is an excellent example of a major event for this produced three huge icebergs the largest measuring 284 by 86 km. Ice streams and outlet glaciers provide for the remaining 30% of Antarctic icebergs estimated to number around 100,000 produced annually. Of these only about 3% exceed 1km in greatest dimension.

Antarctic icebergs move around close to the Continent initially in the East Wind Drift and regional gyres before moving north into the Antarctic Circumpolar Current. There are a number of places around the Continent where winds and currents combine to turn icebergs north and these appear as great arcs of bergs stretching as far as the Antarctic convergence around latitude 52-54° S. Occasional sitings have been reported of icebergs in New Zealand waters (45°S) but few survive for long north of the Polar Front. The average lifetime of Antarctic icebergs is thought to be around six years. Measured average drifts vary from 4-13 km/day and the maximum recorded is 46 km/day.

Icebergs are only a minor hazard for Antarctic shipping. The greatest difficulty is that posed by the huge area (20 million km^2) of annual sea ice that surrounds Antarctica and which has trapped and destroyed many ships in the past. There being no offshore structures in the Antarctic any hazard by icebergs in this regard does not apply and this is probably one of the main reasons why an intensive study of icebergs has not yet been carried out in the Antarctic.

There has been a certain amount of speculation regarding icebergs as a potential source of fresh water which is an essential mineral in short supply in many parts of the world. Several studies undertaken in recent years have suggested that despite immense technical difficulties it appears to be feasible to select suitable icebergs and tow them to ports in those countries in the Southern Hemisphere where they would be available as fresh water at a fraction of the cost of alternative methods. The biggest technical problem appears to be that of how to harness the iceberg and accommodate its fresh water.

Current studies of icebergs in the Antarctic are limited to a few close studies of the calving mechanisms from glacier tongues and an internationally coordinated programme of reporting on all sightings. However, vast areas of the Antarctic are not seen from ships and aircraft and the possible use of satellites to provide a fuller coverage has yet to be fully studied. Indeed, research on Antarctic icebergs may not increase until such time as there is a practical requirement to do so, and probably that will not occur until significant resource related commercial activity is undertaken at sometime in the future.

NRC WORKSHOP ON EXTREME ICE FEATURES

Questions and Discussions Form

AUTHOR:	R. Thomson
PAPER:	The Ultimate Extreme Ice Feature - Antarctic Icebergs
DISCUSSION BY:	R. Pilkington

DISCUSSION:

You indicated that the freeboard of the Ross Ice wall is 80 m, suggesting a keel depth of 720 m. Do you see icebergs this deep?

You said you measured snow depths of 250 (?) ft. At what depth/pressure does snow change to ice?

AUTHOR'S REPLY:

The 800 km ice front of the Ross Ice Shelf varies from around 100 - 300 metres ASL rising rapidly towards the south to a maximum of about 1 km ASL. Where calvings of large icebergs have occurred the southern section of such a berg could therefore have a keel depth of 720 metres.

In drilling in east Antarctica we found a soft fern layer that increased in thickness from the coast to around 200 feet on the plateau. Very soft snow (dry drift) accumulates in the large troughs of the undulating surface to a depth of about 10-12 feet representing the annual accumulation. Below the fern layer our seismic shots indicated solid ice to a maximum of 15,800 feet in one location. It appears, therefore, that the transition from fern to ice occurs at about 200 feet inland where most accumulation is dry drift snow while near the coast where damp snow falls and accumulates, the change is as close as 10 feet. The change is within a few feet of the surface but in many places due to ablation by high winds the ice is almost continually exposed.

EXTREME ICE FEATURE MAPS OF THE ARCTIC OCEAN DERIVED FROM DATA RECORDED BY NUCLEAR SUBMARINES

Leonard A. LeSchack

Trident Arctic Exploration Ltd/LeSchack Associates, Ltd
3617, 608- 9th Street, S.W., Calgary, Alberta T2P 2B3

ABSTRACT

Under-ice profile data from Arctic Ocean cruises of USS SARGO (winter, 1960), USS SEADRAGON (summers of 1960 and 1962), and USS SKATE (summer of 1962), have been digitized and recorded on 9-track tape. Along with data recorded by HMS SOVEREIGN (spring, 1976), we have developed a total of 363 separate ice draft probability distributions (1-m depth intervals) covering the entire Arctic Ocean basin. Each draft distribution is derived from nominally 50-km lengths of contiguous profile data along each of the cruise tracks. These draft distributions also have been recorded on 9-track tape. Computations from these data are the basis for preparing contour maps of (a) mean ice depth, (b) standard deviation about the mean, (c) percent open water/thin ice, and (d) probability of encountering deep draft ice (>30 m). A Zycor, Inc. contour-tracing algorithm was used to map these four parameters on a North Pole-centered Transverse Mercator base. Geographical locations of extreme ice features are clearly depicted on these maps.

1. INTRODUCTION

For the past 15 years LeSchack Associates, Ltd. has been analyzing the under-ice profile data recorded by nuclear submarines cruising beneath the ice of the Arctic Ocean (LeSchack, 1983). These data provide the most reliable information to date on the temporal and geographical variations of sea ice depth, ice deformation, and distributions of thin ice and open water. Thus, these data are a good source of quantitative information for constructing and evaluating models of geographical distribution of ice draft probabilities, of surface heat transfer, and of sea ice dynamics in the Arctic Ocean. Several ice deformation parameters have been computed from all these data and maps of extreme ice features have been constructed. These maps should be of value to sea ice modellers, as well as for operational use.

Eighteen thousand kilometers of under ice profile data have been obtained from cruises of the USS SARGO, USS SEADRAGON, and USS SKATE (Figure 1), and in the East Greenland Sea from a cruise of HMS SOVEREIGN. The SARGO, SEADRAGON, and SKATE data, originally recorded on analog strip charts, were all digitized, and then recorded on magnetic tape cassettes in 1975 and 1976. Because few of the potential users of these data had cassette reading facilities, we transferred these data to standard 9-track magnetic tapes in 1985. The SOVEREIGN data, which are in a different format but also on 9-track tape, were provided by Scott Polar Research Institute. A general description of these data is given by Wadhams (1977).

2. DESCRIPTION OF THE SARGO, SEADRAGON AND SKATE DATA

The under-ice profile data were recorded with an upward-looking sonar as shown in Figure 2. They were recorded in analog form as shown in Figure 3.

Depth measurements were made directly from the analog charts with a line follower digitizer. The base from which all depth measurements were made is the water surface; this is determined by the characteristic reflection observed on the record when leads or polynyas are present (as small ones frequently are). The error in picking this water line may be as much as ± 1 m. The digitizer records X and Y data values along the profile by means of manually following the profile, from left to right, with an instrumented arm at the end of which is a pointer. The data points were digitized without sign starting from an origin positioned at the lefthand side of the record. The water line is at the top of the record. Only the first arrivals of recorded sound energy were digitized.

The digitizer recorded one two-digit depth value, Y, for every 0.01 inch of X-travel along the direction of the profile. Depth values were recorded in inches in increments of 0.1 inch on the record. This translates to a data point about every 2-6 m in the X-direction, depending on submarine speed, and depth increments of either 0.508 m, 0.975 m or 1.524 m in the Y-direction, depending on the original vertical scale of the analog record. As a result of the above, individual values of depth along deep keels are probably within ± 2 m and measurements along the profile are probably accurate to ± 10%, this error being largely a function of submarine speed variations. A typical original data cassette file is shown in Figure 4. These original files are now provided on 9-track tape.

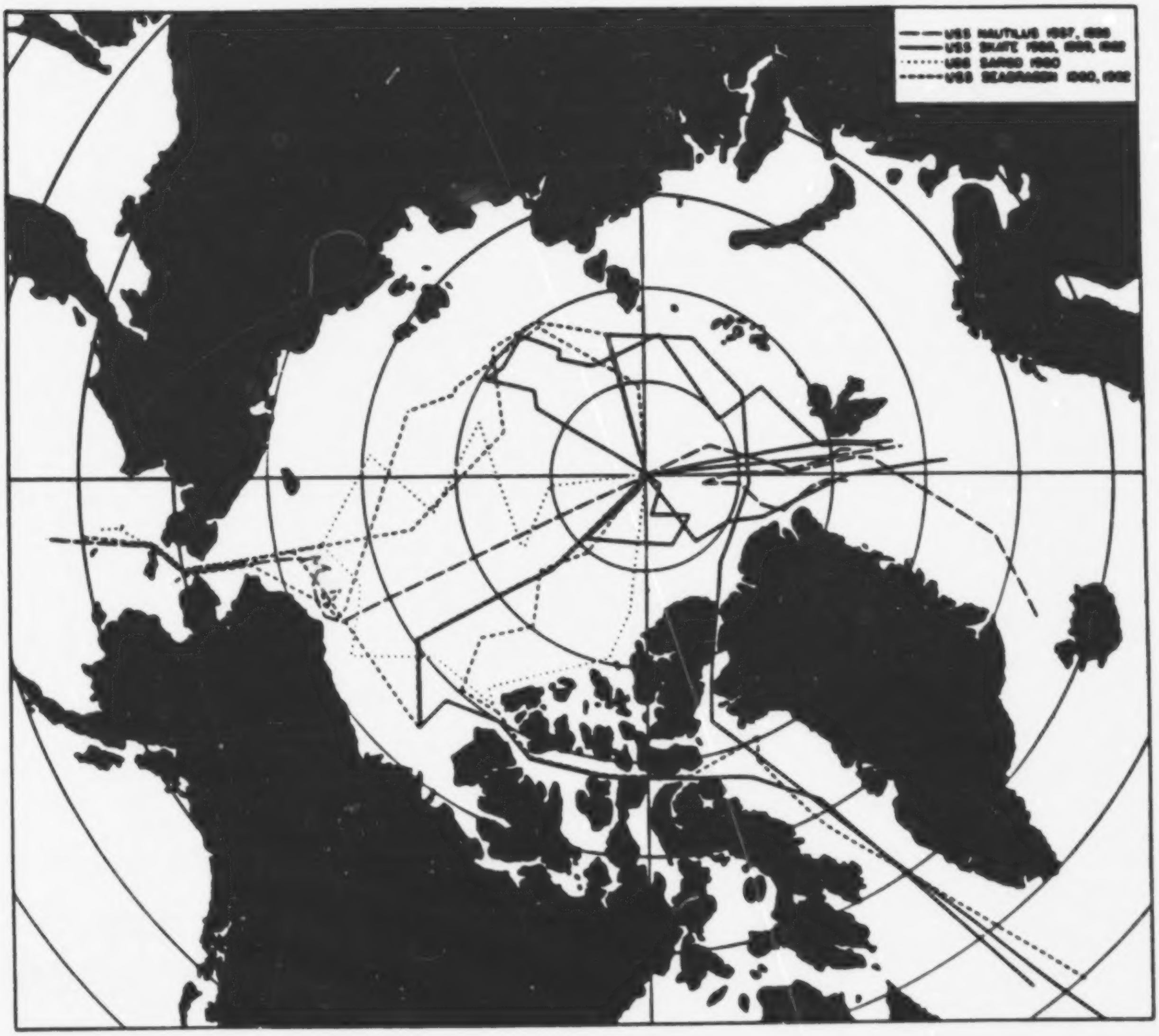
USS NAUTILUS 1957, 1958
USS SKATE 1958, 1959, 1962
USS SARGO 1960
USS SEADRAGON 1960, 1962

FIGURE 1: Cruise tracks of U. S. nuclear submarines in the Arctic Ocean (after Lyon, 1963).

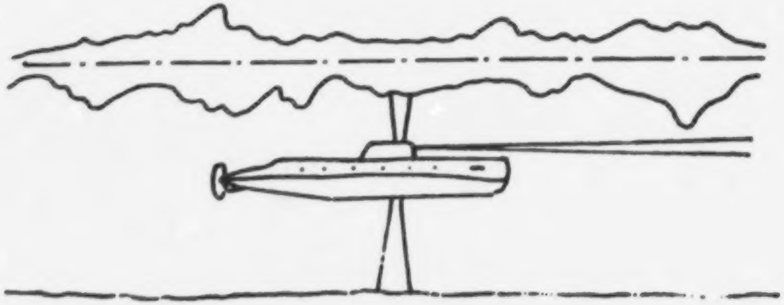

FIGURE 2: Sonar system for cruising under sea ice (after Lyon, 1963).

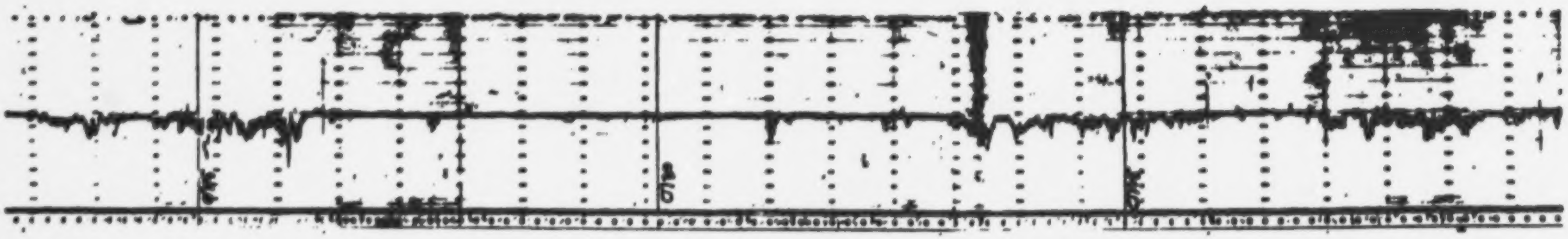

FIGURE 3: A 4-nautical mile submarine sonar under-ice segment recorded in the Chukchi Sea near Pt. Hope.

Header →

```
SRGOAI60 093245 14FEB.  /60, BC, 11/28/75          DX=04.99M POINTS = 1286
01 01 01 01 01 01 01 01 01 01 01 01 01 01 01 01 01 01 01 01 01 01 01 01 01
01 01 01 01 01 01 01 01 01 01 01 01 01 01 01 01 01 00 00 00 00 00 01 01 01
01 01 01 01 01 01 01 01 01 01 01 01 01 01 01 01 01 01 01 01 01 01 01 01 01
01 00 00 00 00 00 00 00 01 01 01 01 01 01 01 01 01 01 01 01 01 01 01 01 01
01 01 01 01 01 00 00 00 00 00 02 02 02 04 03 03 02 02 02 01 01 01 01 01 03
03 03 03 03 03 03 05 06 06 06 09 09 08 07 07 06 06 05 05 05 05 04 04 03 03
04 04 04 04 03 03 03 02 02 02 02 02 01 01 01 01 01 01 01 01 01 01 01 01 01
01 01 01 01 01 01 01 01 01 01 01 01 01 01 01 01 01 01 01 01 01 01 01 01 01
01 01 01 01 01 01 01 01 01 01 01 01 01 01 01 01 01 01 01 01 01 01 01 01 01
01 01 01 01 01 01 01 01 01 01 01 01 01 01 01 01 01 02 03 03 04 04 04 04 03
03 02 02 02 02 01 01 01 01 02 02 02 02 02 02 01 01 01 01 01 01 01 01 01 01
01 01 01 01 01 01 01 01 01 01 01 01 01 01 01 01 01 01 01 01 01 01 01 01 01
01 01 01 01 04 04 07 07 07 08 08 08 08 08 08 08 08 08 07 02 02 01 02 02 02
02 02 04 04 04 04 03 03 03 03 03 05 05 05 05 06 05 05 05 06 07 07 07 07 04
04 03 03 03 03 03 03 03 04 03 03 03 03 03 03 03 03 03 03 03 03 03 03 03 03
03 03 03 03 03 03 03 03 03 04 02 02 02 02 02 02 02 03 03 03 03 04 04 03 03
02 02 02 03 03 03 02 01 01 01 01 01 01 01 01 01 01 01 01 01 01 02 04 04 04
04 04 05 04 04 01 01 01 01 01 01 01 01 01 01 01 02 02 02 03 04 04 04 03 03
03 03 03 02 02 02 02 01 02 03 03 03 04 04 03 02 02 02 02 01 01 01 01 02 02
02 02 02 03 03 03 02 02 02 02 03 04 05 05 05 04 02 01 01 01 01 01 01 02 02
02 02 02 02 02 02 02 02 02 02 02 02 02 02 02 02 02 02 02 02 02 02 02 02 02
02 02 02 02 02 02 02 02 02 02 02 02 02 02 02 02 02 02 02 02 03 03 03 03 06
06 06 05 05 05 05 07 13 12 12 08 08 06 06 05 06 06 07 09 09 10 09 08 04 05
05 05 05 05 05 04 03 03 04 02 02 01 02 02 03 03 05 06 06 07 07 07 08 05 05
04 04 05 05 05 05 05 04 04 03 03 03 03 04 04 04 03 03 03 02 02 02 02 01 01
01 01 02 02 02 02 02 02 02 02 02 02 01 01 01 01 01 01 01 01 01 01 01 01 01
01 01 01 01 01 01 01 01 01 01 01 01 03 03 05 05 10 10 10 09 09 09 07 07 07
07 07 07 07 03 02 02 02 02 02 02 05 06 06 06 06 05 03 03 03 04 04 04 04 04
03 03 03 03 06 06 07 07 06 06 03 03 03 03 03 03 03 03 05 05 05 05 05 05 05
05 05 06 06 05 05 05 06 06 07 07 07 07 07 07 07 06 06 06 06 06 06 06 05 05
05 05 05 05 05 07 07 07 08 07 03 03 03 03 04 04 05 06 06 07 07 07 07 06 05
05 05 05 05 05 05 05 06 06 07 07 07 07 07 07 07 07 07 07 07 07 07 07 07 07
08 08 09 09 11 11 10 10 07 07 06 06 06 07 07 08 08 08 08 09 10 10 10 11 12
14 13 13 08 08 08 08 08 08 08 08 09 09 09 10 10 10 09 07 06 06 05 05 05 05
06 06 06 06 07 09 09 08 07 07 06 06 03 02 02 02 01 01 01 01 01 01 01 01 01
01 02 02 02 02 01 01 01 01 01 01 01 01 01 01 01 01 01 01 01 01 01 01 01 01
01 01 01 01 01 01 01 01 01 01 01 01 01 01 01 01 01 01 01 01 01 01 01 01 01
01 01 01 02 02 02 02 02 02 02 02 02 03 02 02 01 01 01 01 02 02 02 02 02 02
02 02 02 02 02 02 02 02 02 02 02 02 02 02 02 02 02 02 02 02 02 02 02 02 02
02 02 02 02 02 02 02 02 02 03 03 03 04 04 04 04 04 04 04 05 05 05 06 06 07
07 07 06 06 05 03 03 03 03 03 03 03 02 02 02 02 01 01 01 02 02 02 02 02 02
02 02 02 02 03 03 03 02 03 03 04 04 04 05 05 05 05 04 04 04 02 02 02 02 01
01 01 02 06 11 12 12 12 12 12 12 11 11 08 07 06 06 04 04 04 04 03 02 02 02
02 02 02 02 02 02 02 02 02 02 02 02 02 02 02 02 02 02 02 02 13 15 17 17 17
17 17 18 18 18 18 18 18 19 20 19 19 19 17 15 14 12 06 06 05 05 05 05 05 05
06 06 05 05 05 04 04 05 05 05 05 05 05 05 05 07 07 07 07 06 06 06 07 07 07
07 08 08 08 08 09 09 09 09 09 09 09 08 08 07 07 07 07 07 07 07 08 08 08 08
08 08 07 06 03 02 02 02 02 05 05 05 06 06 08 08 10 11 11 11 10 10 10 10 10
10 11 11 11 12 12 12 13 14 14 14 13 12 10 09 01 01 01 01 01 01 01 01 01 01
01 01 01 01 01 01 01 01 01 01 01 01 01 01 01 02 03 04 05 05 05 10 10 10 10
12 13 15 15 15 15 15 15 17 15 13 13 13 13 16 15 14 14 13 13 13 14 13 09 10
05 03 03 02 01 01 01 01 01 01 01
/*
```

End of file mark

FIGURE 4: A typical original data cassette file. There are generally between 12 and 25 of these original files included in a 9-track data file.

3. 50-KM SEGMENT ICE DRAFT DISTRIBUTION DATA

All the data described above have for convenience been grouped into contiguous 50-km (nominal length) segments, and draft distributions at 1-m depths have been computed. These distributions also have been recorded on 9-track tape. This tape contains 363 ice draft data files (in ASCII), each representing approximately 50 km of cruise track, along with "call up" lists of file names that permit accessing all data from a given cruise, all data with mean depths between 1 to 2 m, 2 to 3 m, ... up to 9 to 10 m, and all data on the tape. This tape can be used for creating the maps of extreme ice features to be discussed below. Table 1 shows a typical file of ice draft distribution as recorded on this tape.

4. MAPPING EXTREME ICE DEPTH PARAMETERS IN THE ARCTIC OCEAN

It can be seen from the foregoing that having 363 50-km ice draft data distributions similar to that shown in Table 1, maps of extreme ice depth parameters can be prepared for the Arctic Ocean. This has been done by computer using the Zycor Inc. contour tracing algorithm. The following maps have been prepared:

- mean under-ice draft; contour interval = 0.5 m
- standard deviation about the mean draft; contour interval = 0.5 m
- percent of ice surface thin enough for submarine surfacing (0 - 1 m deep); contour interval = 5%
- probability of finding deep draft ice (>30 m); plotted in terms of Log of probability, i.e., contours from -2.0 (1 chance in a 100) to -6.0 (1 chance in a 1,000,000), at intervals of -0.5

Each map is keyed to a North Pole-centered Transverse Mercator projection base. All maps are the same scale. The data used were a composite of all the data discussed above, plus data from the 1976 cruise of the USS GURNARD. The data for GURNARD were derived from Wadhams and Horne (1980). The justification for combining all the cruise data to make a composite of each parameter is that provided in LeSchack (1983). Although the simple statistical justification discussed therein can not be considered rigorous for the relatively small data sample used, experience so far has shown that as each new data set becomes available, its statistics compare favorably with those already developed for the same geographical area.

Mapping of the mean, standard deviation, and percent open water (or thin ice) were straight forward since individual values for each were already computed as shown in Table 1. For computing the probability of deep draft ice, rather than using the observed discrete probability values indicated by the actual draft frequencies, we chose to use the empirical negative exponential equation discussed by Brooks (1983) for

```
Cruise:                     SAR60
Date:                       13FE60
Identifier:                 061731-074500
Position:                   79.2N,110.5W
Mean (meters):              7.3
Standard Deviation:         4.3
PerCent Open Water:         3.18
Volume Page Number:         277-280
Segment Length (km.):       57.4
         Depth(m.)   No.of occurences
        Open Water          386
            0- 1            278
            1- 2            377
            2- 3            1255
            3- 4            1513
            4- 5            1130
            5- 6            1067
            6- 7            1056
            7- 8            841
            8- 9            845
            9-10            878
           10-11            651
           11-12            501
           12-13            424
           13-14            289
           14-15            227
           15-16            118
           16-17            93
           17-18            32
           18-19            29
           19-20            34
           20-21            40
           21-22            26
           22-23            16
           23-24            8
           24-25            13
           25-26            9
           26-27            4
           27-28            9
           28-29            -
           29-30            -
           30-31            -
           31-32            -
           32-33            -
           33-34            -
           34-35            -
           35-36            -
           36-37            -
           37-38            -
           38-39            -
           39-40            -
           40-41            -
           41-42            -
           42-43            -
           43-44            -
           44-45            -
           45-46            -
           46-47            -
           47-48            -
           48-49            -
           49-50            -
```

TABLE 1: A typical under-ice data record as recorded in our Universal Under-Ice Data Set. Given in the header is the submarine cruise, our identifier number, the approximate position of the midpoint of the segment, the weighted mean and standard deviation, the percent open water, the page numbers of where in LeSchack (1980a) these data can be found and the concatenated segment length.

computing deep draft probabilities. We did this because considerable scatter of the actual frequency values is noted at deep drafts when relatively small (i.e., 50 km) populations are used. On the other hand, the Brooks Equation appeared to universally fit all our data (some 18,000 km) very closely to depths of 30 m, and was thought to be a better predictor of deep drafts when small populations were used, than were the actual observed data frquencies. In using the Brooks Equation, all cumulative probabilities were normalized to unity at a depth of 3 m, the equilibrium thickness of ice (Maykut and Untersteiner, 1971).

We determined empirically, using the data set described above, for both physical and statistical reasons, that a 3-m depth value was also an appropriate constant to use as a "cutoff value" in evaluating the Brooks Equation. We chose 30 m arbitrarily as a depth for computing an extreme draft probability map, but obviously probability maps can be contoured for any chosen value. For ease in reading the deep draft probability map, the logarithm to the base 10 of the cumulative probability has been plotted.

5. WHAT THE MAPS SHOW

The maps show quantitatively, and in great detail, what in most cases has been generally known qualitatively: The Arctic winds and ocean currents cause compression of the ice against the Canadian Archipelago and the northern coasts of Greenland, and rarefaction in the northern reaches of the Beaufort, Chukchi, Laptev, Kara and Barents Seas. Not surprisingly, there is a similarity in contour patterns shown on the mean ice depth map with those shown on the standard deviation contour map; this relationship was suggested earlier by the correlations shown between these two parameters using GURNARD data, and presented in LeSchack (1980 b). The standard deviation map discussed here is far more detailed than the map presented in LeSchack (1983). The earlier map, although based on the same original data, lost much of the detail seen in the current map, owing to the need for broad areal averaging of these data to make a manageable task of the manual contouring process used to produce the 1983 map.

Intuitively, one would also expect similarity between the contour patterns of the probability map with those of the mean and standard deviation maps. This too is borne out from examination of these maps. Of particular interest is the close similarity between contour patterns of ice deformation for the Arctic Ocean theoretically derived by Hibler (1980) and those of deep draft probability developed from our empirical data.

The map of percentage of the ice surface that is either thin ice or open water exhibits somewhat different contour patterns from those of the other three maps. While increasing mean depth, standard deviation, and probability of encountering deep draft ice are all parameters generally associated with what Wadhams and Horne (1980) call "level" and "ridged" ice, the percentage of open water/thin ice is a map of what they call "thin ice", which comes from a different statistical population. This thin ice population is not necessarily caused by the compressive forces that create the increases in the values of the other three parameters.

The open water/thin ice map is expected to be of value to Arctic mariners as well as submariners. It is interesting to note, for example, that the successful voyage in 1977 of the Soviet nuclear icebreaker, "Arktika", to the North Pole was made almost entirely in, or close to, the clearly defined "channel" that comprises regions of sea ice that have greater than 5% thin ice or open water within them. Additionally, it should be noted that these regions containing 5% or more open water/thin ice comprise no more than half of the total region of permanent pack ice; the remaining half of the pack is presumably much less suitable for surface ship navigation of any sort, or for surfacing of submarines.

6. REFERENCES

Brooks, L. D., (1983), Statistical analyses of pressure ridge keel definitions and distributions, Proc. of 1983 Int'l Conf. on Port and Ocean Engineering Under Arctic Conditions (POAC-83), Helsinki, Finland, April 1983

Hibler, W. D. III, (1980), Modeling pressure ridge buildup on the geophysical scale, Proc. National Research Council Workshop on Sea Ice Ridging and Pileup, Calgary, October, 1980, NRC Tech. Mem. No. 134, pp 141-155

LeSchack, L. A., (1980 a), Arctic Ocean sea ice statistics derived from the upward-looking sonar data recorded during five nuclear submarine cruises, Tech. Rept. by LeSchack Associates, Ltd. under U.S. Offfice of Naval Research Contract # N00014-76-C-0757/NR 307-374, Sept. 1980, at U.S. Defense Documentation Center, Cameron Station, Alexandria, Virginia 22314

LeSchack, L. A., (1980 b), Correlation of under-ice roughness with satellite and airborne thermal infrared data, Tech. Rept. by LeSchack Associates, Ltd. under U.S. Ofice of Naval Research Contract # N00014-76-C-0757/NR 307-374, May 1980, at U.S. Defense Documentation Center, Cameron Station, Alexandria, Virginia 22314

LeSchack, L. A., (1983), Arctic Ocean ice deformation chart using sonar data recorded from nuclear submarines, Proc. of 1983 Int'l Conf. on Port and Ocean Engineering Under Arctic Conditions (POAC-83), Helsinki, Finland, April 1983

Lyon, W. K., (1963), The submarine and the Arctic Ocean, Polar Record, 11:75, pp 699-705

Maykut, G. A. and Untersteiner, N., (1971), Some results from a time-dependent thermodynamic model of sea ice, J. Geophys. Res., V 76, No. 6, pp 1440-1475

Wadhams, P., (1977), A comparison of sonar and laser profiles along corresponding tracks in the Arctic Ocean, AIDJEX/ICES Symp. on Sea Ice Processes and Models, Seattle, 6-9 Sept. 1977

Wadhams, P. and Horne, R. J., (1980), An analysis of ice profiles obtained from submarine sonar in the Beaufort Sea, J. Glaciology, V 25, No 93, pp 401-424

NRC WORKSHOP ON EXTREME ICE FEATURES

Questions and Discussions Form

AUTHOR: Len LeSchack

PAPER: Extreme Ice Feature Maps of the Arctic Ocean Derived from Data Recorded by Nuclear Submarines

DISCUSSION BY: Eric Leavitt

DISCUSSION:

Is there not a problem with stationarity in that the data reflect the particular time of the tracks and there is a limited number of tracks.

Ben made comment that they have found it necessary to separate data by time of year.

AUTHOR'S REPLY:

Yes, there is a problem because of the limited number of tracks. But they found generally good agreement where tracks have crossed. Also reasonable agreement with other indications, i.e., drift patterns, etc. Also agreement with classified data he has had access to.

Len commented on a problem of accepting data at face value. Just what surface is the sonar seeing? Also have problem with hyperbolic returns, i.e., multiple returns. Need to use care in pulling off depth values.

CHAIRMAN'S COMMENT:

The fact that the combination of data from a number of submarine tracks shown such distinct features would suggest to me that they are indeed genuine and probably even more localized than indicated, as averaging the data would tend to smear them out.

THE SURFACE WAVEFORMS ON THE ELLESMERE ISLAND ICE SHELVES AND ICE ISLANDS

G. Holdsworth
National Hydrology Research Institute, Saskatoon, Sask. S7N 3H5
and
Arctic Institute of North America, University of Calgary,
Calgary, Alberta, T2N 1N4

ABSTRACT

Surface waveforms are a dominant topographic feature of the ice shelves of northern Ellesmere Island and of the ice islands which are derived from them. Their exact mode of formation still remains unclear but it seems to involve a dynamic process associated with ice creep deformation during extreme events in the pack ice.

A systematic review of hypotheses advanced to explain the origin of the waves is presented. It is found that no new hypothesis seems to be necessary: only development of one particular theory combined with elements of another theory.

Justification for studying the origin and geometry of the surface waves is based on (1) satisfying safety requirements for aircraft operating on ice shelves and ice islands, and (2) obtaining the opportunity to study the fundamental dynamics of thin ice shelves and their interaction with the pack ice that is in intimate contact with them. The conclusions of this study have implications to the field of pack ice - structure interactions.

INTRODUCTION

The major ice shelves of the northern Ellesmere Island coastline and the ice islands that are derived from them are easily identified by the characteristic pattern of ridges and troughs in which bifurcations are common (e.g. Koenig et al, 1952). Wavelengths on the thickest shelf ice average about 235 m and amplitudes may reach 3.5 m (corresponding to ridge-trough differences or double amplitudes of 7 m). The origin of these waves has been discussed many times (Koenig et al, 1952; Hattersley-Smith, 1957; Crary, 1958, 1960; Lister, 1962; and Dorrer, 1971) but no general consensus seems to have been reached and no fully quantitative theories advanced. This paper is directed towards establishing a quantitative theory.

Because a characteristic wavelength: ice thickness ratio seems to exist and because of a ubiquitous bifurcation of ridges, this suggests that a dynamic process, involving ice deformation, may be the basic mechanism to be examined. This mechanism requires compression of the shelf perpendicular to the coastline. One obvious source for this compression is from the pack ice which is in intimate contact with the outer edge of all the ice shelves for most of the time. This mechanism has been suggested before but to my knowledge never fully investigated.

In order to test this theory initially, it is necessary to know the value of the flow stresses existing in the shelf and the level of extreme compressive stresses that may be transmitted from the pack ice into the shelf. Numerical simulations of ice shelf flow were carried out by MacAyeal and Holdsworth (1986) to determine the flow stresses existing in the Ward-Hunt Ice Shelf (WHIS) and the effect of a sea ice "back pressure" on the flow regime. Because of a current controversy surrounding the flow law for ice at low stresses, the emphasis of the above paper was redirected toward a study of the low stress rheology of shelf ice. However, some of the results of the numerical experiments involving sea ice "back pressure" applied to the WHIS model were presented in the above paper. These results showed that WHIS expansion due to creep could effectively be paralysed by applying a thrust along the outer edge of WHIS, of a magnitude compatible with our current knowledge of stress levels existing in a field of pack ice (Sanderson, 1984). Hibler (1984) has shown that the thickest pack ice and the highest stresses for the whole Arctic basin are concentrated along the northern coastlines of Ellesmere Island and Greenland.

In order to generate compressive strains within the shelf, it is evident that extreme pack ice thrusting must occur along the outer edge of the shelf. That these events may only occur over limited sections of the shelf edge and over limited periods of time, does not seem to present an insurmountable problem. Thus, as we shall see, the strain rate measurements that were carried out between 1964 and 1968 showing a net expansion over a small part of WHIS over those years in a direction perpendicular to the ridges (Dorrer, 1971) can be accommodated by the present theory.

Although ice island T-3 evidently did not originate from WHIS it is typical of the islands that are known to have calved from it. In April 1973, that segment of a former ice shelf was gripped in the pack ice, causing compressive strains to occur in the island, at the edge of which was a new pressure ridge. Rafting had caused a bending failure of the edge of the island. These latter features had formed prior to the strain measurements that were made on the central part of T-3 (Holdsworth and Traetteberg, 1973). It is not known whether the island had previously been under sufficient compression for a creep buckling instability to develop: the island still bore the imprint of a waveform assumed to have been inherited from the time when it was part of an ice shelf. This waveform was very subdued, evidently as a result of its rotational motion with respect to the variables that had shaped them: pack ice pressure, wind action, solar radiation and mass balance regimes. Nevertheless, for heavily laden aircraft landing on runways prepared on the surface of the ice islands, all traces of these waves must be removed. In April, 1973 a C-130 "Hercules" landed on a "bump", and by the time it had come to rest off the runway its main wing spar had snapped. The runway was oriented at a considerable angle to the axes of the remnant ridges, thus effectively lengthening the wavelength sensed by the aircraft. Resonance of the air-frame could have been set up as the aircraft travelled over these ridges. Attention to this problem is being addressed on "Hobson's" ice island that calved from WHIS in 1983 (Jeffries and Serson, 1983).

REVIEW OF HYPOTHESES ADVANCED TO EXPLAIN THE ORIGIN OF THE SURFACE WAVES

The following list of hypotheses were classified by Lister (1962) into two classes: generic and superimposed. In the former case the waves would form during the formation of the shelf. Thus, the first five wave mechanisms could be broadly considered "generic", although Lister did not include this many in his discussion of the subject. The list of hypotheses are as follows:

(1) The thermal stress hypothesis, in which temperature changes (in this case rapid temperature increases) cause compressive strains which lead to buckling (Wright and Preistley, 1922; Zubov, 1955).

(2) The pressure hypothesis, in which pressure form the pack ice compresses the shelf roughly at right angles to the coastline (Debenham, 1954; Zubov, 1955). Although not stated, this implies that a creep buckling instability develops in the shelf.

(3) The pressure ridge stacking hypothesis in which "hedges" of stacked ice alternate with sections of undeformed ice. A smoother "waveform" would subsequently evolve by drifting of snow (Hattersley-Smith, 1957; Lister, 1962).

(4) The glacier compression hypothesis, where flow of glaciers into the shelf causes folding of ice (Marshall, 1960).

(5) The tidal action hypothesis, in which the ice is deformed as the tide progresses into the coast. The shelf is assumed to be floating everywhere except where it is gripped to the coast (Debenham, 1954).

(6) The sief-type snow dune hypothesis, where linear dunes form parallel to the coastline which was taken to be the direction of the prevailing winds. The ridge and trough structure was preserved during a surface ablation phase, such as exists at

present. Thus, these are paleo-features, since sief dunes are not now seen to form. This theory is attributed to Hattersley-Smith, (1957).

(7) The meltwater lake alignment hypothesis, in which prevailing winds blowing parallel to the coastline over a randomly distributed array of meltwater lakes cause them to become elongated. These "ribbon" lakes grow by wave action on the down wind end, the rate increasing as the fetch increases (Crary, 1958).

These hypotheses will now be discussed in order.

(1) The thermal hypothesis appears weak, as there will be periods of rapid temperature decrease, with associated tensile stresses, which would either just counteract any tendency towards buckling or lead to cracking. Thermal stresses can be significant (Sanderson, 1978) but they would only affect the upper 15 m of the shelf.

(2) The pressure hypothesis is the one developed in this paper and combined with (7).

(3) This hypothesis requires an extraordinary uniform stacking sequence, and then relies on another (aeolian) mechanism to finish the process off. It is thus a hybrid mechanism, and as Lister states, the smoothing process by drift might just tend to fill in the troughs. However, this is not the issue, but rather the first (dynamic) part of the process.

(4) The glacier compression hypothesis is tenable where glaciers flow into ice shelves. Whereas this hypothesis can hardly be invoked for the WHIS it can evidently be applied elsewhere (e.g. Milne Ice Shelf). Because we are seeking a general mechanism that applies to all shelf ice, this mechanism will not be considered further.

(5) The tidal action hypothesis is obscure. A damped waveform does occur near the "hinge zone" of tide-water glaciers, but the extent of this effect is insignificant in the present case (Holdsworth, 1971).

(6) The sief dune hypothesis rests on the belief that the ridges formed during an earlier cold phase (e.g. the Little Ice Age) when there was also a positive surface net mass balance. Furthermore, the East-West winds would have to have been much stronger than today, since sief-type snow dunes are not observed today, whereas barchan dunes are (B.T. Prager, personal communication). Sief-type snow dunes do not seem to have been reported in the literature. If, however, the ridges are allowed to form in this way, then they could be perpetuated by the presence of meltwater lakes which form in the troughs as they do today. No explanation is offered, either in this hypothesis or or the hypothesis (7) of Crary, as to why the wavelength is so uniform and why it is that particular value. Hypothesis (2) will now be developed and discussed.

PACK ICE PRESSURE HYPOTHESIS

Ice shelves have an inherent tendency to expand under gravity induced stresses (Weertman, 1957) unless they are constrained in some way. The stresses associated with this creep are very low for a shelf only about 47 m thick (of order 0.02 MPa). It has been shown by numerical modelling that WHIS possesses a flow divide (MacAyeal and Holdsworth, 1986) and that by cumulative creep away from this divide, a measureable flow rate is attained at the outer edge. This is of order 1 m yr^{-1}. The model results were compared with the only measurements of flow rate and strain rate made on the shelf (Dorrer, 1971). These data were obtained over a 4-year period and showed that the shelf was expanding in the direction of flow over that particular time interval. This was a net result and does not preclude a period or periods of contraction. Further, there was also a significant shear strain component, indicating that marginal drag effects are important at that site.

Using published values of the flow law parameters and taking account of the brine content in the shelf, and its effects on the flow law, as well as including a back pressure term, it was possible to match the field data in some of the model runs. By increasing the back pressure, the shelf motion can effectively be paralysed and even reversed. The stress level in the pack ice at this stage is in excess of 0.1 MPa as was evidently the case for pack ice surrounding ice island T-3 in April, 1973.

The next step is to consider models that would lead to a prediction of the edge thrust that would be required to cause a creep buckling instability. Then it would be necessary to determine if the corresponding stress levels that this would imply for the pack ice are realistic or not. Also, from such instability modelling, it should be possible to obtain an estimate of the wavelength/thickness ratio.

BUCKLING MODELS

Using an energy balance model and an equation derived for a linear elastic material recast into a form describing a linear viscous material, Hochstein (1967) presented an inequality that related the axial thrust supplied, to the wave number of the folds and to the density of sea water. Although that situation is not identical to the present one, in principle, the same type of stability criterion could be applied. However, the derivation of the equations (attributed to Jeffries, 1959) seems to imply an inconsistency and, therefore, the result cannot be assumed to be quantitatively reliable. Furthermore, viscous theory is substituted for elastic theory in a rather ad hoc way. However, the results, surprisingly, are of the right order of magnitude.

The buckling criterion established was

$$P_s > \rho_w \, g/K^2$$

where P_s is the thrust, where ρ_w is the density of sea water and $K = 2\pi/L$ is the wave number ($L = 230$m). The axial stress in the Ward-Hunt Ice Self (thickness $H = 47.5$ m) is $P_s/H = 0.3$ MPa. For multi-year sea ice ($H = 12$ m: $L = 60$ m) the corresponding stress P_s/H would have to exceed a value of about 0.08 MPa.

These stress levels in the shelf and in the multi-year sea ice would imply the existence of stresses in the pack ice between about 0.8 MPa and 3 MPa. However, since the applied thrust is not purely axial but eccentric, then the tendency towards buckling should occur at sea ice stress states much lower than these. Furthermore, there is no time factor integrated into this model.

A more complete theoretical analysis of the plastic creep buckling of floating shelf ice was made by Collins and McCrae (1985). They found an instability criterion expressed by:

$$P_c > 0.3\ \rho_i\ g\ H$$

where P_c is the vertically averaged axial stress in the shelf, ρ_i is the density of the shelf and H is the total thickness. Using the appropriate values in this expression, it is found that for WHIS

$$P_c > 0.13\ \text{MPa}$$

Depending on the thickness of the sea ice, the stress in the pack ice might exceed this value by up to a factor of 10.

The above analysis is based on a parallel fold-like instability and it predicts a dominant wavelength corresponding to the critical stress, P_c. The dimensionless wavelength at the critical stress is given as:

$$\lambda_c = 2\pi/KH = L/H$$

According to the theory, $\lambda_c = 2.5$ to 3 corresponding to a value of $n = 3$ in the power flow law. Since this obviously does not agree with observations ($L/H = 5$) an argument was developed to raise λ_c to 4.2.

The theory developed by Smith (1979) shows that for a layer of highly non-linear material undergoing parallel folding:

$$4 < \lambda_c < 6 \text{ , quite generally.}$$

DISCUSSION OF THEORY VERSUS OBSERVATION

For the Ward-Hunt Ice Shelf, the dimensionless wavelength for the thickest ice at present is 230/47.5 = 4.8 and for the re-entrant ice it is 60/12 = 5, which is in good agreement with the last two theoretical model results. When we examine the critical stress needed to cause an instability, there is much more uncertainty. The reasons for this may be that the theory is imperfect (no account has been taken of the time scales involved) and definitely that we have not taken into account the fact that the thrust is eccentrically applied, and thus the thrust, and hence the depth-averaged stress in the pack ice needed to initiate buckling in the shelf or the re-entrant ice will be less than the values given above.

Returning to the data of Dorrer (1971), it was noted by that author that his results seemed to support the hypothesis of Hattersley-Smith (1957). The modelling of the creep of WHIS and the scenario for the development of creep buckling in WHIS developed below, show that this conclusion was not justified.

CREEP BUCKLING INSTABILITY IN THE WARD-HUNT ICE SHELF

As we have seen, ice of different thickness associated with WHIS possesses surface undulations but the dimensionless wavelength remains about the same ($\lambda_c = 5$). This data pertains only to young shelf ice or potential shelf ice and very old shelf ice.

So far, there have not been any direct measurements made at the base of the WHIS. The basal geometry in particular is of great interest, since it has a direct bearing on such processes as deformation mode, basal boundary thermodynamics and mass balance.

There are strong indications that basal geometry of WHIS is only slightly undulating or very nearly flat. For perfect small-scale isostatic equilibrium, large basal bulges would have to be present to compensate the surface ridges. Since many of the trough lakes are very nearly at sea level, this would imply a fractionally thin shelf at that point. There is no evidence for this being the case. On the other hand, if a buckling mode of deformation is accepted, then how is a parallel folding geometry compatible with what we think the present geometry is?

Evidence for an essentially flat or only slightly undulating bottom comes from several sources:

(1) Impulse radar measurements by Prager (1983) for eastern WHIS have been corrected according to the known geometry of the surface and the result is that the basal geometry is nearly flat (B.B. Narod, personal communication 1986).

(2) Impulse radar measurements made above ice island T-3 show a similar result (J. Rossiter and E. Leavitt, personal communication).

(3) Submarine sonar records from a traverse under T-3 showed the bottom of the ice island to be essentially flat (L. Leschack, personal communication).

The following scenario is designed to take account of theory and observation as far as the Ward-Hunt Ice Shelf waveforms are concerned.

(a) Because logs have been found in Disraeli Fiord this indicates that thick shelf ice was not in existence at some former time. Furthermore, currents were such as to drive logs into the fiord. As growth of the proto-ice shelf took place, both areally, away from the coast and vertically, the outer edge was periodically subjected to extreme thrust events from the pack ice. These events may have return times of years or even decades, and as the ice shelf thickened, which the ice core evidence shows, the thrust required to cause compressive creep would also increase in proportion. Thus, the return times of the "critical" thrusts in the pack ice would also be expected to increase. Note that in the previous application of instability theory, no mention was made of time scales. This may be an important factor in setting the level of the critical stress and it is, of course, very important in the subsequent creep process.

If an instability has occurred and parallel folding takes place, then we expect a characteristic wavelength to be set up according to the thickness. Thrusts may be very localized during one particular event but may occur at any point along the ice shelf edge. Judging by the geometry of the folds in multi-year sea ice (e.g. see Hattersley-Smith, 1963), the length scale of the extreme thrust front may be less than 1 km. This is the interpretation of the peculiar ridge geometry: terminating and bifurcating ridges, which indicate non-homogeneous strain. As the shelf ice thickens, however, the eccentricity of the edge thrust increases, thus in principle making it easier for an instability to get started.

(b) After the release of the critical compressive stress, and assuming that a waveform was locked in, the shelf would resume its outward expansion, due to gravity driven tensile stresses and the waveform begins to be subdued. Wave crests tend to subside and wave troughs to rise due to buoyancy forces.

The assumption is now made that the creep (recovery) strains and hence displacements are smaller than geometry changes caused by hydro-thermo-dynamic processes acting at both boundaries, for the upper surface in summer and for the lower surface all year. The important processes are surface lake hydrology and basal freezing, or melting.

(c) If the surface waveform survives into the summer, then meltwater lakes collect in the troughs, which because of their higher albedo preferentially overdeepen. These lakes will tend to migrate or elongate due to wave action which increases as the fetch increases. It has been found that the prevailing winds (but not the strongest winds) are east-west, or nearly parallel to the axis of the troughs (Crary, 1960).

(d) As the shelf thickens, either by superimposed ice accumulation at the surface or by basal ice accumulation by freezing of fresh or salt water, the geometry is modified. The summer season processes are essential to preserving the surface waveform. At the base, preferential ice accretion in the hollows and preferential ablation of the basal bumps by water currents would seem to be capable of smoothing out the bottom geometry.

(e) Given this new geometry, another extreme event may now be superimposed on the shelf, which, if it is thicker than before, buckles with a longer wavelength. The processes described in (c) and (d) acting faster than subsequent creep recovery processes then modify the shelf into a new form. The shift from a lower characteristic wavelength to a higher one would be very gradual and indeed even some earlier wavelengths may become "trapped". If one wanted to trace the geometry changes as the shelf thinned then similar arguments could be applied. If a limiting or "steady state" thickness was attained then any future compression events would only tend to reinforce the existing waveform.

(f) If some areas of the shelf have not been subjected to a "critical" thrust, then bridging between deformed areas might be brought about by east-west migration of trough lakes, as given in hypothesis(7).

The western sector of WHIS contains considerable brine, particularly below a depth of abut 25 m, whereas the eastern sector does not contain significant brine. This is evident from ice core work and particularly from airborne radar depth sounding.

Brine in the lower half of the shelf, where temperatures are warmer than above will increase the tendency for lowering the "effective" viscosity of the ice. This assymetry of ice properties increases the tendency for an instability to develop (Biot, 1965). These observations would suggest that the western part of the shelf would be more easily deformable than the eastern part (see MacAyeal and Holdsworth, 1986).

On this model then, the shelf, in attempting to build up and spread by slow creep, is temporarily compressed. Once a waveform is "locked in" on the surface, long-term creep will, in principle, stretch the wavelengths. Thus, strictly, any statistical treatment or study of observed wavelengths at any particular time, with respect to theoretical treatments of buckling processes, should take into account any changes in wavelengths since formation. This has not been done here. The corrections are thought to be small, but should be investigated.

SUMMARY AND CONCLUSIONS

It has been argued that a possible explanation for the existence of a characteristic waveform on Ellesmere Island ice shelves and in particular on the Ward-Hunt Ice Shelf, is by compression from the pack ice. Surface lake hydrology subsequently plays a significant part in perpetuating the waves. The peculiar but common feature of bifurcating ridges is explained by nonhomogeneous strain which is caused by piecemeal compression of only restricted sections of the shelf at any one time. The processes involved in the evolution of the waves are summarized in Figure 1.

Forces required to be transmitted through the pack ice into the shelf are evidently significantly higher than most forces estimated or meaured in situations where less thick ice interacts with fixed offshore structures. However, this issue should not be allowed to detract from the present hypothesis. Firstly, the pack ice here is the thickest for the whole Arctic basin, ridging can be extremely intense and currents and winds can conspire to exert long-term compression on the shelf ice. Secondly, it is the extreme event which is expected to initiate buckling; lower but longer term compression may still be capable of causing compressive creep with amplification of the initial waveform. In the much longer term, net expansive creep of the shelf will dominate, so that data such as Dorrer's (1971) may still be compatible with this hypothesis. Waveforms that "invade" undeformed areas of the shelf, by the process of lake migration are superimposed forms. The structural waves evidently change wavelength as thickness changes occur but stabilize when the shelf reaches "steady state".

A conclusion of this study and of the literature review on which it is based, is that, most likely, the Ward-Hunt Ice Shelf owes some of its long-term existence to the confinement provided by the pack ice field along its periphery. The hypothesis presented here should be applicable to the other ice shelves on Ellesmere Island, except where it can be shown that other processes capable of compressing and buckling floating ice are acting. This would include instances where land glaciers flow into floating ice masses (Jeffries 1986b).

ACKNOWLEDGEMENTS

Observations made on the Ward-Hunt Ice Shelf in April and May 1983 contributed to some of the ideas expressed in this paper. The extensive literature (not all cited) on the Ward-Hunt Ice Shelf proved quite invaluable in making this study. The coordinator and staff of the Polar Continental Shelf Project, Ottawa, are kindly thanked for their logistic support. I also thank those who provided constructive criticism of the first draft of this paper presented at the Workshop.

This paper is published with the approval of the Director, National Hydrology Research Institute. A more detailed version is in preparation.

REFERENCES

Biot, M.A. 1965. Mechanics of incremental deformations, New York, J. Wiley.

Collins, I.F. and I.R. McCrae 1985. Creep buckling of ice shelves and the formation of pressure rollers, Journal of Glaciology 31 (109): 242-252.

Crary, A.P. 1960. Arctic ice island and ice shelf studies, part II, Arctic 13 (1):32-50.

----------- 1958. Arctic ice island and ice shelf studies, part I, Arctic 11 (1): 3-42.

Debenham, F. 1954. The ice island of the arctic: an hypothesis, Geographical review 44: 495-507.

Dorrer, E. 1971. Movement of the Ward-Hunt Ice Shelf, Ellesmere Island, N.W.T., Canada, Jornal of Glaciology 10 (59): 211-225.

Hattersley-Smith, G. 1957. The rolls on the Elesmere Ice Shelf, Arctic 10 (1): 32-44.

--------------------- 1963. The Ward-Hunt Ice Shelf recent changes in the ice front, Journal of Glaciology 4 (34): 415-24.

Hibler, W.D. III 1984. Ice dynamics US Army CRREL Monograph 84-3.

Hochstein, M.P. 1967. Pressure ridges of the McMurdo Ice Shelf near Scott Base, Antarctica, New Zealand Jounal of Geology and Geophysics 10 (4): 1165-68.

Holdsworth, G. 1971. Calving from Ward-Hunt Ice Shelf 1961-62, Canadian Journal of Earth Sciences 8(2): 299-305.

Holdsworth, G. and Traetteberg, A. 1973. The deformation of an arctic ice island, Proc. Second Intern Conf on Portland Ocean Engineering under Arctic Conditions, University of Iceland Reykjavik.

Jeffreys, H. 1959. The Earth, Cambridge University Press.

Jeffries, M.O. 1986. Ice island calvings and ice shelf changes, Milne Ice Shelf and Ayles ice Shelf, Ellesmere Island, N.W.T, Arctic 39 (1): 15-19.

--------------- 1986b. Glaciers and the morphology and structure of Milne Ice Shelf, Ellesmere Island, N.W.T. Canada, Arctic and Alpine Research 18 (4): 397-405.

Jeffries, M.O. and Serson, H. 1983. Recent changes at the front of Ward-Hunt Ice Shelf, Ellesmere Island, N.W.T., Arctic 36 (3): 289-290.

Koenig, L.S.; Greenaway, K.R.; Dunbar, M.; Hattersley-Smith, G.F. 1952. Arctic Ice Islands, Arctic 5 (1) 67-103.

Lister, H. 1962. Heat and mass balance at the surface of the Ward-Hunt Ice Shelf 1960, AINA Research Paper No. 19.

Lyons, J.B. and Ragle, R.H. 1962. Thermal history and growth of the Ward-Hunt Ice Shelf, IASH Publication No 58: 88-97.

MacAyeal, D. and Holdsworth, G. 1986. An investigation of low stress ice rheology on the Ward-Hunt Ice Shelf, Journal of Geophysical Research 91 (B6): 6347-58.

Marshallm, E.W. 1960. Structure and stratigraphy of T-3 and Ellesmere Ice Shelf Scientific Studies at Fletcher's Ice Island T-3, Geophysics Research Paper No 63, Air Force Cambridge Research Center: 45-57.

Prager, B.T. 1983. Digital signal processing of UHF radio echo sounding data from northern Ellesmere Island, M.Sc. Thesis, University of British Columbia Canada.

Sanderson. T.J.O. 1978. Thermal stresses near the surface of a glacier Journal of Glaciology 20 (83): 257-283.

----------------- 1984. Theoretical and measured ice forces on wide structures, Proc. 7th Intern. Symp. on Ice, (Hamburg) 4: 151-207.

Smith, R.B. 1979. The folding of a strongly non-Newtonian layer, American Journal of Science-279: 272-287.

Weertman, J. 1957. Deformation of floating ice shelves, Journal of Glaciology 3 (21): 38-42.

Wright, C.S. and Preistley, R.E. 1922. Glaciology Harrison (London).

Zubov, N.N. 1955. Arctic Ice, Moscow (Translation).

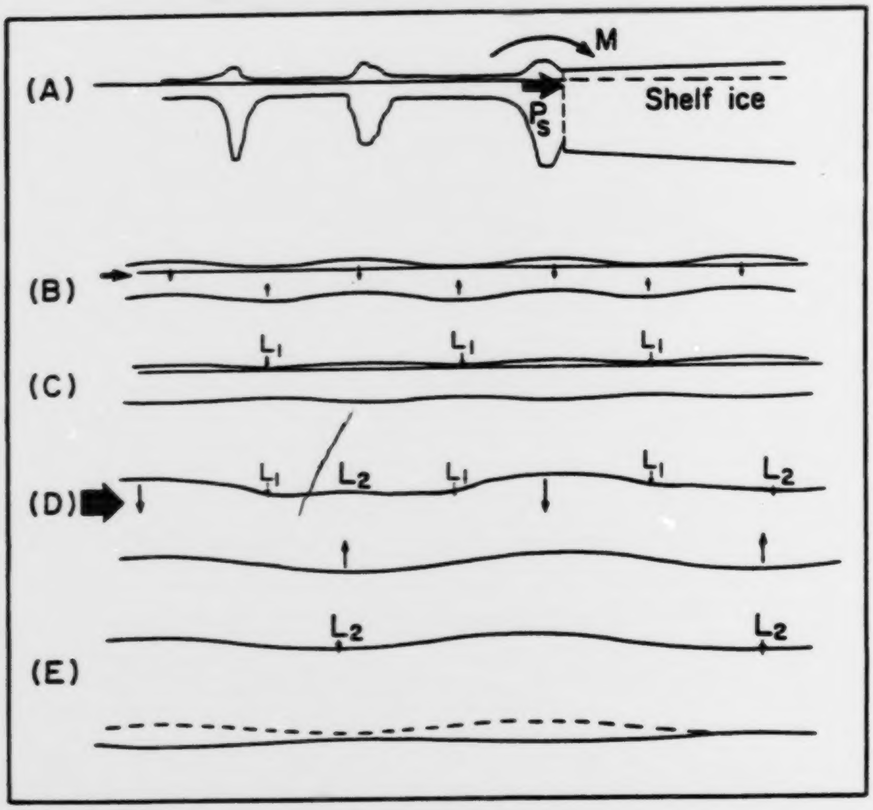

Figure 1. (A) Concept for transmitting axial thrust (P_s) and bending moment (M) from the pack into the edge of the shelf ice. (B) Buckling of a thin proto-ice shelf. Vertical arrows indicate creep directions of troughs and crests, after removal of the horizontal thrust. (C) Hypothetical shelf geometry developed without further buckling. Meltwater lakes (L_1) have formed and are "locked in". (D) After thickening of the shelf from stage (C), a new critical thrust, causes buckling with a new wavelength ($\lambda_c \approx 5$). Sites marked L_2 are where new lakes will tend to form. (E) Hypothetical shelf geometry at "final" steady state thickness. Old lakes (L_1) have been erased and new lakes (L_2) dominate. Basal freezing and subsidence of original hollows (under anticlines) have caused smoothing of the base. Note that this is a highly simplified sequence and many intermediate steps are envisaged.

NRC WORKSHOP ON EXTREME ICE FEATURES

Questions and Discussions Form

AUTHOR: G. Holdsworth

PAPER: The Surface Waves Forms on the Ellesmere Island Ice Shelves and Ice Islands

DISCUSSION BY: G.R. Pilkington

DISCUSSION:

1. As the ice shelf thickens, the buckling phenomenon must be more dominant than the along-shore wind-menting effects. Would you expect this to be the case?

2. You suggested that once the melting effect starts it propagates. Would you not expect to find long wavelength undulations that have propagated into areas of thinner ice?

AUTHOR'S REPLY:

1. As the ice shelf thickens the "old" wavelengths (λ_1) remain locked in (but can propagate parallel to ridge lines) until another "extreme" thrusting event occurs. Then a new wavelength appears (λ_2). Superimposed on this waveform will be the old (shorter) wavelengths (λ_1's) which will slowly be erased:

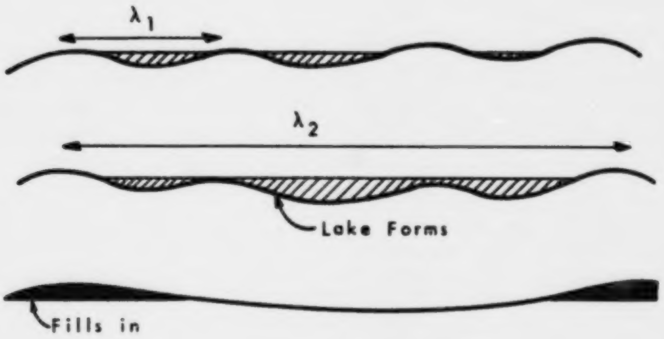

2. Once the meltwater lake-wind propagation mechanism is underway there is no reason for it not to invade a thinner section of shelf if this exists. If waves (of shorter wavelength λ) already exist there, then the result will be a bimodal distribution (if it could be distinquished). Certainly there is a significant variance in λ's measured in some sections of the shelf.

DISCUSSED BY: G.R. Pilkington

DISCUSSION:

Martin Jeffries showed results that indicate that the high spots on the top of the ice shelf correspond to low spots on the bottom which is just the opposite to what you postulated. Any comments?

AUTHOR'S REPLY:

The current "belief" is that the bottom surface "reflects" the top surface geometry but with some scale factor applied. It seems as if this factor is 1. Initially, I consider the shelf to buckle, i.e., parallel folding occurs, but then after the compressive stress is released, anticlines tend to subside and synclines tend to rebound upwards; at the same time the arched sections of the lower surface may become filled in with frozen fresh- or salt-water depending on where the boundary between these two water boundaries is. The "final" result is that the base passes through a flat stage and then becomes slightly bummocked (lower surface ridges). Submarine sonar data seem to support this picture at least for Ice Island T-3 (L. LeSchack private communication). Therefore, M. Jeffries' conceptual drawing and my model are not at variance. I present the stages of my model in a 3 part figure below:

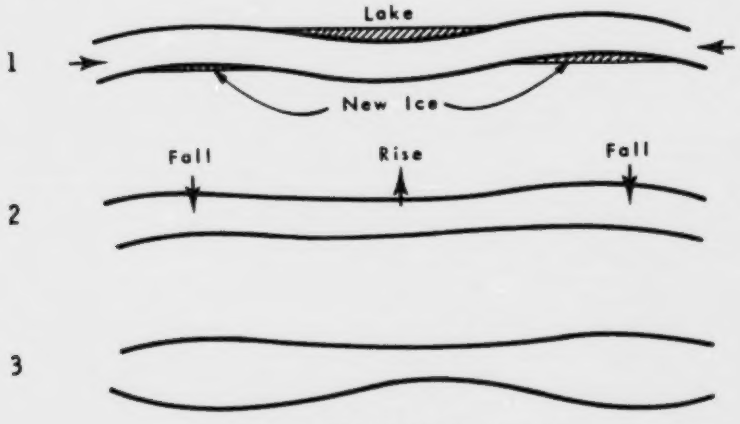

"PSEUDO" Stationary

OXYGEN ISOTOPE EVIDENCE OF FRESHWATER POOLS AND ICE ACCRETION BELOW MULTIYEAR LANDFAST SEA ICE, NORTHERN ELLESMERE ISLAND.

Martin O. Jeffries
Geophysical Institute
University of Alaska
Fairbanks
Alaska 99775-0800

ABSTRACT Salinity and oxygen isotope measurements from thick sea ice cores off the north coast of Ellesmere Island are briefly examined. Data from undeformed MLSI show evidence of pronounced annual layers that arise from ice growth associated with freshwater-seawater stratification below the ice. Furthermore, a large part of the "sea ice" is composed of freshwater. Annual layers are not evident in a core from deformed MLSI which has salinities of as much as 12.1 o/oo. Oxygen isotope values at the bottom of the core indicate that freshwater-seawater stratification occurred only after deformation.

INTRODUCTION

The most striking ice features off the north coast of Ellesmere Island are the ice shelves from which ice islands calve periodically (see Jeffries, this volume). However, in addition to the ice shelves there are large areas of thick, multiyear landfast sea ice (MLSI)(Jeffries and Serson 1986). MLSI has existed for many years at numerous locations, having grown since ice island calvings. With the exception of a study of the ice plug in Nansen Sound (Serson 1972), there have been no investigations of MLSI. Each spring since 1982, I have worked in this region and taken the opportunity to drill some ice cores in the MLSI. In this paper I present some results of salinity and stable oxygen isotope analysis of ice cores.

OXYGEN ISOTOPES

Sea ice growth involves the rejection of brine from the ice to the water. Further brine loss occurs as the ice ages. Compared to the loss of brine during ice growth and aging, only a negligible isotopic fractionation occurs between the light (^{16}O) and heavy (^{18}O) oxygen isotopes. Therefore, the isotopes are conservative tracers and potentially a valuable additional tool for sea ice core interpretation.

Oxygen isotope abundances are commonly expressd on a δ ("del") scale as follows,

$$\delta^{18}O\ (o/oo) = \left\{ \frac{(^{18}O/^{16}O)_s}{(^{18}O/^{16}O)_{SMOW}} - 1 \right\} \times 10^3$$

where o/oo is parts per thousand or per mille, $^{18}O/^{16}O$ is the ratio of the number of ^{18}O and ^{16}O atoms in s, the unknown sample and in a standard, SMOW (Standard Mean Ocean Water; Craig 1961).

SMOW has a constant value, close to zero parts per thousand, in all the deep ocean waters of the world. On the other hand, the worldwide isotopic composition of precipitation varies considerably, with the greatest deviations from zero occurring in the polar regions. Along the north coast of Ellesmere Island, snow has a mean δ value of -31.0 o/oo (Jeffries 1985) and snow meltwater has a similar value. Therefore, a considerable difference exists between the isotopic compositions of seawater and freshwater in this region. This should be evident in MLSI ice cores as a record of ice growth associated with the changing water structure below the ice.

RESULTS

Figure 1 illustrates the salinity and $\delta^{18}O$ profiles in 3.8m thick sea ice a short distance east of Markham Ice Shelf. Both the profiles show regular variations that have a cycle of 0.5m. Salinity and oxygen-18 are linearly related with a correlation coefficient of 0.85. Likewise, the salinity profile of a core (Fig. 2) from Milne Re-entrant at the front of Milne Ice Shelf also has a 0.5m cycle. This core is from ice almost 10m thick and the salinity and $\delta^{18}O$ profiles both show the same pattern of variation; low salinity/ low $\delta^{18}O$ layers near the surface and around 4m depth while contrasting high salinity/high $\delta^{18}O$ layers occur around 2m and 7m. Salinity and $\delta^{18}O$ are linearly related with a correlation coefficient of 0.78. Below 7m depth it is noted that δ values are quite homogeneous with a mean value of -3.9 o/oo (Fig. 2).

Ice core 85-4 was drilled in a 10m thick hummock at the front of west Ward Hunt Ice Shelf. The salinity and oxygen-18 profiles are shown in Fig.3. The ice has a mean salinity of 2.92 o/oo with a distinctive broad salinity peak and salinity maximum of 12.1 o/oo in the region of 5m depth. From the surface to almost 8m there is little ^{18}O variation about the mean δ value of -3.6 o/oo. Below 8m the δ values become much more negative with a minimum of -20.7 o/oo.

DISCUSSION

Since the massive calving that occurred in 1961-62 (Hattersley-Smith 1963), multiyear ice has become established at the front of west Ward Hunt Ice Shelf. The rough, hummocky surface of old, weathered pressure ridges indicates that the ice was deformed at some time in the past. However, other large areas of MLSI in this region (represented by ice cores 84-1 and 85-8) show few surface signs of past deformation. Salinity and $\delta^{18}O$ profiles in undeformed ice contrast with those in the deformed ice.

Friedman et al. (1961) presented evidence of stable isotope variations associated with annual salinity layers in pack ice. Weeks and Ackley (1982) discuss annual layers in detail. In this study, the salinity and $\delta^{18}O$ variations in undeformed ice are attributed to water stratification below the ice and annual variations in the salinity and ^{18}O content of the water from which the ice grows. In summer, fresh meltwater from the surface of the ice forms pools beneath the ice. When this water freezes the ice is of lower salinity and has lower (more negative) $\delta^{18}O$ values than ice that subsequently forms in the winter from more saline water with more positive δ values. The annual layers suggest that the ice in ice cores 84-1 and 85-8 is approximately 8 and 20 years old respectively.

It is noted that the total range of δ values is greater than the range of individual annual fluctuations. This can be attributed to variations in the amount of freshwater that pools beneath the ice and the degree to which it mixes with seawater, in a given year. In the case of the low salinity layer at 4m in core 85-8 (Fig.3), this must be due to a pronounced water stratification and year-round persistence of a layer of water with negligible salinity and negative δ values that undergoes only a small seasonal change of composition. Conversely, the high salinity layers at 2m and 7m are evidence of year-round persistence of a layer of high salinity water with δ values much closer to SMOW. The isotopically homogeneous layer below 7m can be accounted for by an absence of water stratification when the ice was underlain year-round by seawater.

In core 85-4, the upper 8m of isotopically homogeneous ice represents deformed ice that contains pockets of trapped brine. Freshwater, with more negative δ values, was pooled and mixed with seawater below the ice only after ice deformation and the establishment of more stable ice conditions. Ice freezing from this water would, therefore, also have more negative δ values. As noted in the previous section, the mean annual accretion rate is about 0.5m. Therefore, the lowermost 2m of ice perhaps represents 4 years of growth since 1981, the core having been drilled in spring 1985. Deformation of the ice probably occurred in 1980-81. This agrees with the known accretion history of sea ice at the front of Ward Hunt Ice Shelf (H. Serson personal communication).

CONCLUSION

Deformed and undeformed multiyear landfast sea ice as much as 10m thick has been found off the north coast of Ellesmere Island. The $\delta^{18}O$ variations in the MLSI are evidence of a considerable input of freshwater to the system. Indeed, some of the "sea ice" is composed largely of freshwater. This is particularly true of the undeformed ice where annual salinity and $\delta^{18}O$ layers can be attributed to water stratification below the ice. The preservation of the annual layers is evidence of long-term congelation ice growth and the absence of deformation. Annual layers are not evident in the deformed ice and negative δ values associated with some measure of recent freshwater-seawater stratification are found only in ice near the bottom.

ACKNOWLEDGEMENTS

This work was made possible through the support of the Polar Continental Shelf Project, Defence Research Establishment Pacific, Arctic Institute of North America, Gulf Canada, Dome Petroleum and Petro-Canada when I was a graduate student at the University of Calgary, Dept. of Geography. Dr. H.R. Krouse of the University of Calgary, Dept. of Physics kindly undertook the stable isotope analysis. Work at the Geophysical Institute, University of Alaska is supported by the U.S. Dept. of Energy (Morgantown Energy Technology Centre, W. Virginia).

REFERENCES

Craig, H. 1961. Science 133 : 1833-1834.
Friedman, I., Schoen, B. and Harris, J. 1961. Journal of Geophysical Research 66 : 1861-1864.
Hattersley-Smith, G. 1963. Journal of Glaciology 4 : 415-424.
Jeffries, M.O. 1985. PhD Thesis, University of Calgary.
Jeffries, M.O. and Serson, H.V. 1986. Annals of Glaciology 8 : 96-99.
Serson, H.V. 1972. Defence Research Establishment Ottawa. Technical Note 72-6
Weeks, W.F. and Ackley, S. 1982. CRREL Monograph 82-1.

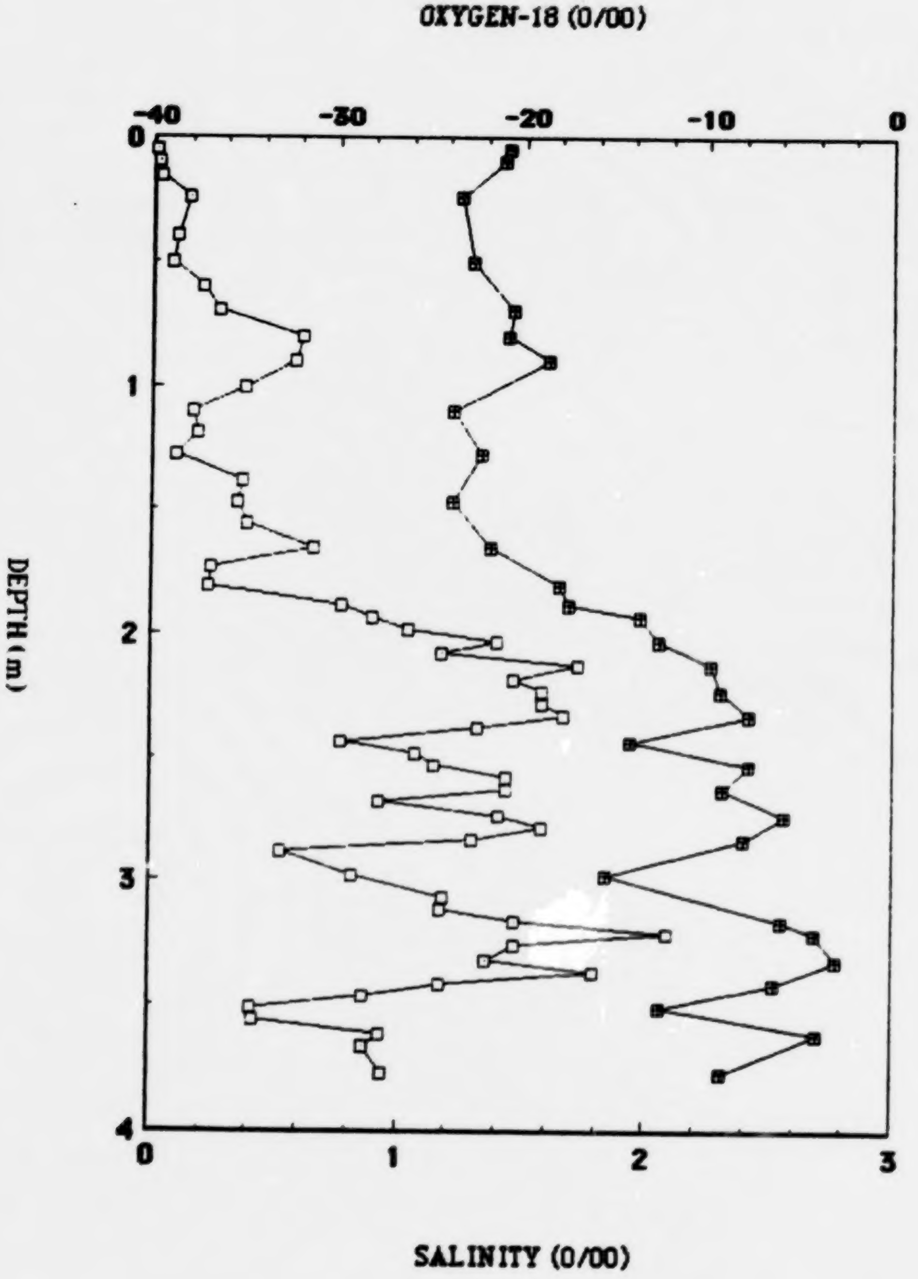

Fig. 1: Salinity (left) and O-18 (right) profiles, ice core 84-1.

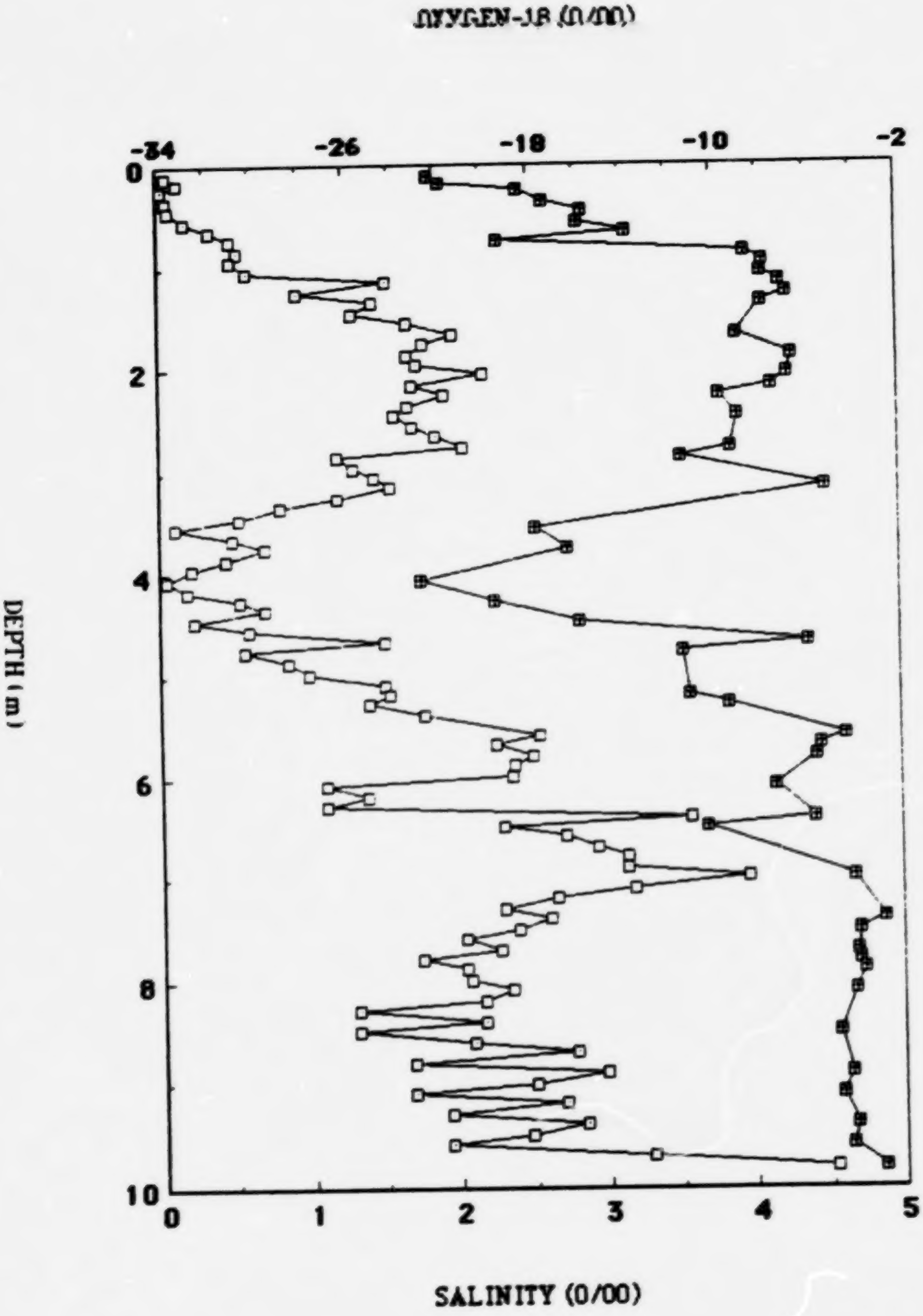

Fig. 2: Salinity (left) and O-18 (right) profiles, ice core 85-8

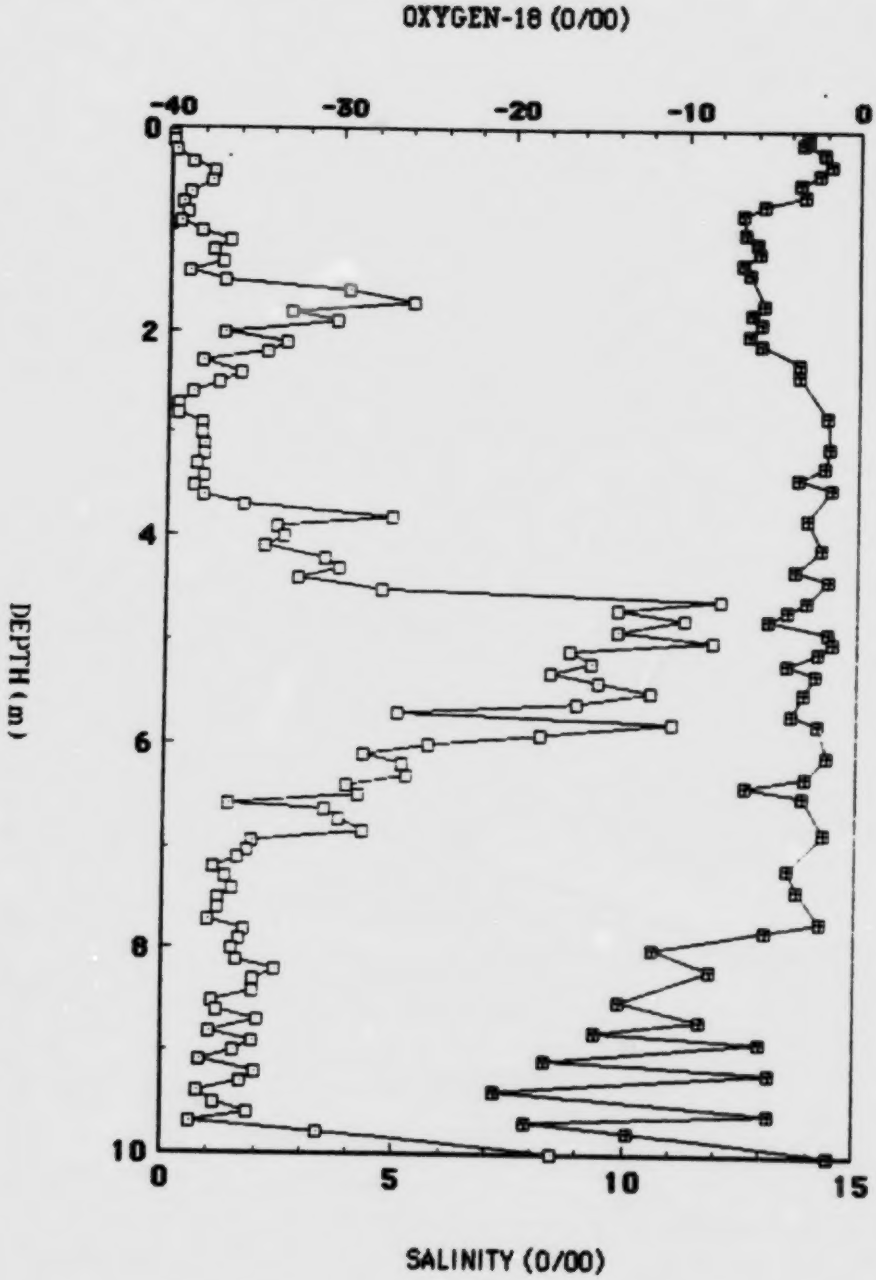

Fig. 3: Salinity (left) and O-18 (right) profiles, ice core 85-4.

PRELIMINARY OBSERVATIONS ON COMPRESSIVE STRENGTH, DEFORMATION AND POISSON'S RATIO OF ICEBERG ICE

by

Nirmal K. Sinha and R. Frederking

INTRODUCTION

Icebergs represent a hazard, both to navigation and to offshore structures on the East Coast of Canada. Little information, however, is available on the strength and deformation of ice taken from an iceberg. To the authors' knowledge the only data available in the open literature are those of Gammon et al (1983) and El-Tahan et al (1984), who performed uniaxial compressive strength tests under constant displacement rates or nominal constant strain rates. Gammon et al (1983) carried out a number of tests on cylindrical specimens under constant strain rate control. The rate for all tests was fixed at 1×10^{-3} s^{-1} and test temperature ranged from -3.5°C to -6°C. Failure was premature and at stresses ranging from 4.75 MPa to 6.72 MPa. El-Tahan et al (1984) measured specimen strains during their tests but no data were provided on how the strain rates varied during the tests. They performed their tests at relatively high rates with mean strain rates in the range 8.2×10^{-4} s^{-1} to 5.8×10^{-2} s^{-1} and reported that the failures were all brittle-type fractures.

The present study was carried out at relatively low strain rates primarily to understand the upper yield type of response which is more amenable to simple analysis. This study has been carried out with closed-loop controlled constant specimen strain rates (strain measured on the specimen) and lateral strains were measured.

ICE CHARACTERISTICS

Tests were carried out on ice obtained from a large block, approximately 10 m^3 in volume, which had fallen from an iceberg. The sail height of the iceberg was 15 m, and it was immobilized in the land-fast sea ice in Lancaster Sound near Adams Island (73°45'N, 81°30'W) at the mouth of Navy Board Inlet. Ice was sampled in early March 1983 in the form of 350 mm cubes and stored in heavy duty cardboard boxes kept outside at air temperatures in the range of about -35°C. Within two days after sampling, these boxes were transported south in unheated compartments of aircraft. The first leg of the journey took the boxes from the field station in Borden

Peninsula to Nanisivik in northern Baffin Island. They were then flown to Montreal in a connecting flight. Immediately after arrival in Montreal, they were transported in an unheated van to Ottawa. The air temperature was about -5°C during the last leg of the journey. Total time in transit was 15 hr. The temperature of the ice blocks were measured after arrival in Ottawa and found to be in the range of -10°C to -15°C. The blocks were then stored in a cold room at -10°C, the same temperature at which the mechanical tests reported here were carried out in November-December, 1983.

Although the blocks were apparently solid, cracks or crack like features were visible in all of them. Moreover the ice was bubbly and elongated bubbles were oriented in a preferred direction. Some of the blocks fell apart into pieces when attempts were made to cut them into smaller units. One of the blocks was structurally solid enough to be subsectioned. Six specimens with finished dimensions of 100 mm × 100 mm × 250 mm were made from this block using a band saw, a milling machine and a lathe kept inside a cold room at -10°C.

All specimens were made with their long directions parallel to the long axis of the bubbles in order to avoid or minimize the effect of the anisotropy associated with the bubbles. Thin sections corresponding to the specimen tested at a strain rate of $1 \times 10^{-7}\ s^{-1}$ are shown in Figure 1. Thin sections were made parallel to the top, front and right faces of the test specimen. It can be seen in the front thin section that a significant number of the grains are elongated with their longer dimensions parallel to the length of the specimen and hence the elongation of the bubbles. This is more evident in Figure 2 which shows traces of the grains in a thin section and the corresponding fabric diagram. There are indications that the elongation of the grains and the bubbles tends to be parallel to the basal plane of many of the grains. Nakawo and Wakahama (1981) noted that bubbles in glaciers are elongated normal to the flow direction. Thus the chosen long axis of the specimens, hence the axis of compression applied during the present tests, could be normal to the flow of the glacier from which the present iceberg calved.

The average cross sectional area of the grains in this ice was 56.8 mm^2, giving an equivalent grain diameter of 8.5 mm if all grains are assumed to be circular in cross section. This assumption gives only about 12 grains across the specimen width. According to Jones and Chew (1981), the specimen should be at least 12 times the grain diameter so that the maximum yield stress may be independent of the ratio between specimen size and grain size. Thus, in spite of choosing an apparently large specimen size, only the minimum requirement for avoiding the geometric effect was met.

Ice density for each specimen was determined, prior to the test, from the mass and the dimensions. The average density for the six specimens were found to be 892 ± 4 kg m^{-3}, which gives an average porosity of 2.8%.

TEST PROCEDURES

Uniaxial closed loop controlled constant strain rate tests were performed using a 1 MN capacity servo-hydraulic test system with the controlling, 200 mm long, displacement gauge mounted directly on the samples. Axial load was applied across the 100 × 100 mm faces. Details of the test techniques used here, particularly the method used for mounting the controlling gauge, can be found in Sinha (1986). Two displacement gauges were also mounted in the central area of the specimens to measure lateral deformations in two mutually orthogonal planes perpendicular to the loading direction. It can be seen in Figure 3 that the controlling gauge monitors and controls the average axial deformation of 40% of the specimen volume, i.e., the area of 50 mm wide and 200 mm long covered by this gauge. In comparison, the lateral gauges averaged the transverse strains in the central 50 mm long section or about 20% of the total specimen volume. Since the strain levels involved were very small (less than 0.3%) and since the specimens deformed with no detectable bulging or shape change, it may be assumed that the deformation was homogeneous during the test and thus well represented by the measurements.

RESULTS AND ANALYSIS

Tests were carried out at strain rates of 1×10^{-7} s^{-1}, 1×10^{-6} s^{-1}, 1×10^{-5} s^{-1}, 3×10^{-5} s^{-1}, 1×10^{-4} s^{-1} and 3×10^{-4} s^{-1}. An upper yield type failure was noticed in all the tests in the strain rate range of 1×10^{-7} s^{-1} to 1×10^{-4} s^{-1} (Figure 4). The test at 1×10^{-5} s^{-1} was less than ideal; the specimen cracked during the early period but did not shatter. Premature splitting type of failure with subsequent shattering occurred, however, at a strain rate of 3×10^{-4} s^{-1}.

Detailed histories for the tests carried out at strain rates of 1×10^{-7} s^{-1} and 1×10^{-4} s^{-1} are shown in Figures 5 and 6 respectively. The slower test covers a test time of about 5.5 hours whereas the faster test was over in about half a minute. These figures show clearly the effect of stress or strain level and the loading history on the effective (secant) modulus, $E_e = \sigma_1 / \varepsilon_1$ and the strain ratios, $\mu_{21} = \varepsilon_2 / \varepsilon_1$ and $\mu_{31} = \varepsilon_3 / \varepsilon_1$ (σ_1 and ε_1 are the axial stress and strain respectively and ε_2 and ε_3 are the transverse strains). The monotonically increasing transverse strain rates at 1×10^{-4} s^{-1} is indicative of increasing cracking activities and the corresponding dilatation effect (strain ratio greater than 0.5). In comparison, the transverse strain rates at 1×10^{-7} s^{-1} show a gradual approach to a quasi equilibrium value amenable to primarily visco-elastic flow with little cracking activity (Sinha, 1982).

The dependence of the maximum stress, σ_{1f} on strain rate is shown in Figure 7 which also shows the strains and strain ratios at failure. It can be seen that the strength at 1×10^{-5} s^{-1} could have reached a higher value if the specimen had not cracked prematurely. On the whole, the rate effect on strength is clearly visible. No rate effects, however, are noticeable in the case of failure strain or in the corresponding strain ratios. Moreover, no apparent anisotropy in the transverse strain is noticeable.

The dependence of failure modulus, $E_f = \sigma_{1f} / \varepsilon_{1f}$ on strain rate and the rate sensitivity of E_f is shown in Figure 8. This illustration also shows the dependence of average strain ratio, $(\mu_{21}^f + \mu_{31}^f) / 2$, at failure on strain rate.

DISCUSSION

So far, no data are available in the open literature on the dependence of strength of iceberg ice on strain rate for conditions where the specimen deformations were monitored and controlled by a closed loop system. In fact, this type of data are not even available for freshwater isotropic ice. However, such data are available for laboratory grown freshwater transversely isotropic columnar-grained S-2 ice at -10°C with load applied in the plane of isotropy (Sinha, 1982) (the dotted line in Figure 7). The two sets of results seem to agree well at strain rates of about 1×10^{-6} s^{-1} or below, the same range in which little cracking activity was reported for the S-2 ice. The failure strains for the S-2 ice increased from 4×10^{-4} at 5×10^{-7} s^{-1} to about 1.4×10^{-3} at 1×10^{-4} s^{-1}. These strains are comparable and, in fact at the higher strain rates, are almost identical for the two types of ice.

CONCLUSION

Iceberg ice exhibiting elongated grains and bubbles with an oriented fabric, was tested uniaxially at -10°C under closed-loop controlled constant specimen strain rates with load applied parallel to the long axis of the grains and hence the bubbles. The average grain size was 8.5 mm and the porosity was 2.8%. An upper yield type of failure occurred in the strain rate range of 1×10^{-7} s^{-1} to 1×10^{-4}. The strength increased from 1.1 MPa to 4.9 MPa in this range. Premature fracture occurred at a stress level of 5.5 MPa for a strain rate of 3×10^{-4} s^{-1}. Axial failure strains were less than 0.2%. Deformation modulus at peak stress increased from 0.6 GPa to 6.0 GPa. With deformation the transverse strain rate asymptotically approached a constant value at 1×10^{-7} s^{-1} but the transverse strain rate monotonically increased at 1×10^{-4} s^{-1}. Strain ratio at failure increased from 0.32 at 1×10^{-6} s^{-1} to 0.64 at 3×10^{-4} s^{-1}. This increase is associated with the increase in cracking activity.

ACKNOWLEDGEMENT

This research was partially funded by Task 6: Conventional Energy Sources of the Canadian Government's Energy R&D Program as part of a project being carried out for Transport Canada. The authors are grateful for technical assistance to C.A. Bjerkelund, R. Jerome and J. Neil.

REFERENCES

El-Tahan, H., Swamidas, A.S.J., Arokiasamy, M. and Reddy, D.V. (1984). Strength of iceberg and artificial snow ice under high strain rates and impact loads. Proc. 3rd Offshore Mechanics and Arctic Eng. (OMAE) Symp., pp. 158-165.

Gammon, P.H., Gagnon, R.E., Bobby, W. and Russell, W.E. (1983). Physical and mechanical properties of icebergs. Proc. 15th Annual Offshore Technology Conf., May 2-5, Paper No. OTC 4459, Vol. 1, pp. 143-150.

Jones, S.J. and Chew, H.A.M. (1981). On the grain-size dependence of secondary creep. J. Glaciology, Vol. 27, No. 97, pp. 517-518.

Nakawo, M. and Wakahama, G. (1981). Preliminary experiments on the formation of elongated air bubbles in glacier ice by stress. J. Glaciology, Vol. 27, No. 95, pp. 141-146.

Sinha, N.K. (1982). Constant strain- and stress-rate compressive strength of columnar-grained ice. J. Materials Science, Vol. 17, No. 3, pp. 785-802.

Sinha, N.K. (1986). Young Arctic frazil sea ice: field and laboratory strength tests. J. Materials Science, Vol. 21, No. 5, pp. 1533-1546.

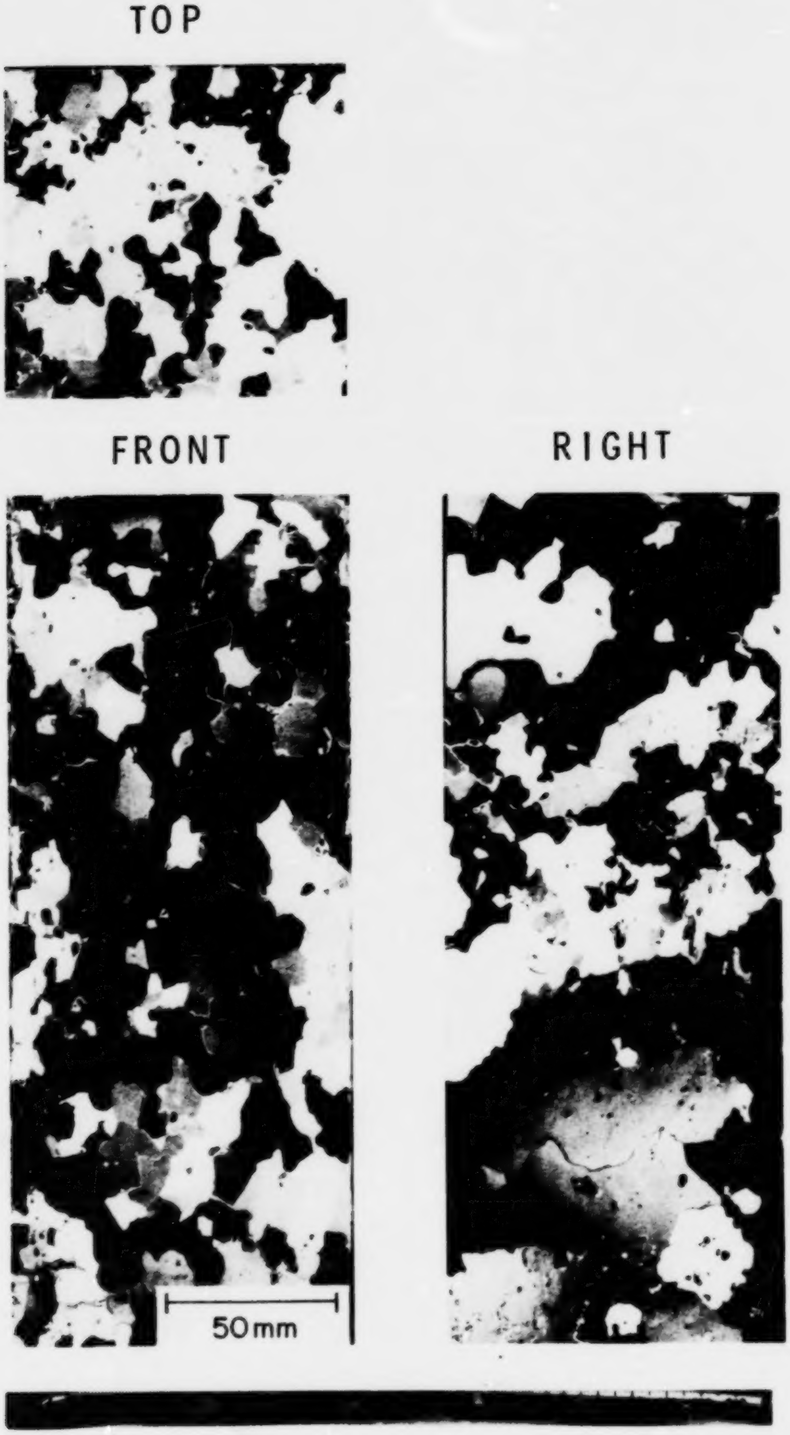
TOP
FRONT
RIGHT
50mm

FIGURE I THIN SECTIONS OF ICEBERG ICE SEEN THROUGH CROSSED POLAROIDS

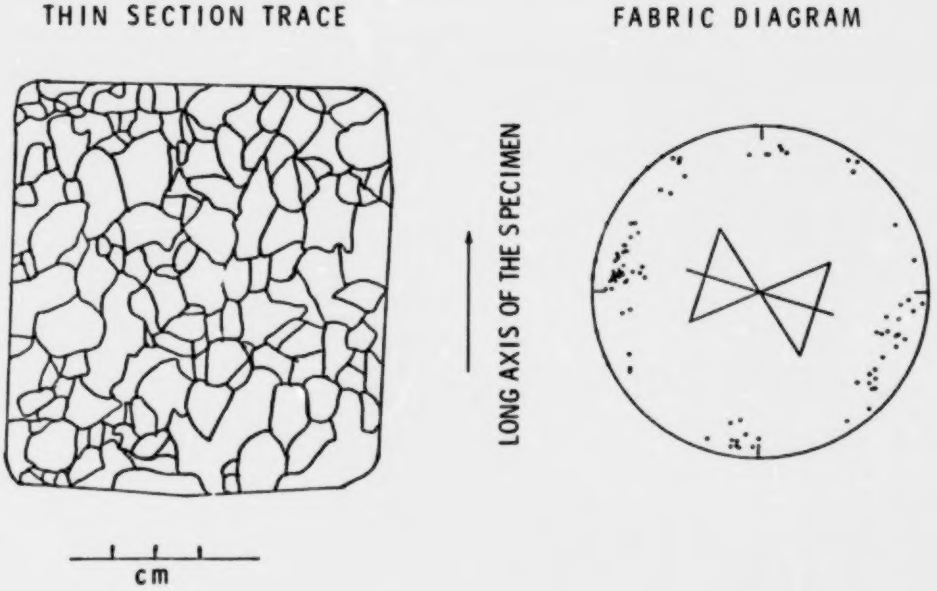
THIN SECTION TRACE
FABRIC DIAGRAM
LONG AXIS OF THE SPECIMEN
cm

FIGURE 2 TRACE OF A THIN SECTION AND THE CORRESPONDING FABRIC DIAGRAM FOR ICE SPECIMEN TESTED AT A STRAIN RATE OF $1 \times 10^{-7}\ s^{-1}$

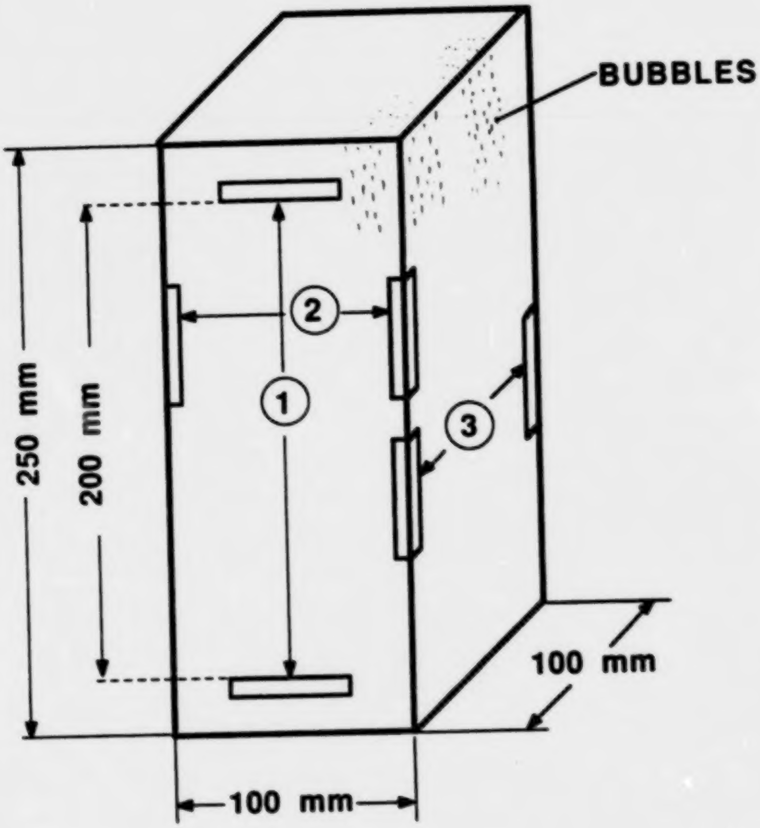
BUBBLES
250 mm
200 mm
100 mm
100 mm
①
②
③

FIGURE 3 LOCATION OF THE DISPLACEMENT GAUGES. OUTPUT OF GAUGE I WAS USED TO CONTROL THE STRAIN RATE IN THE CLOSED-LOOP SYSTEM.

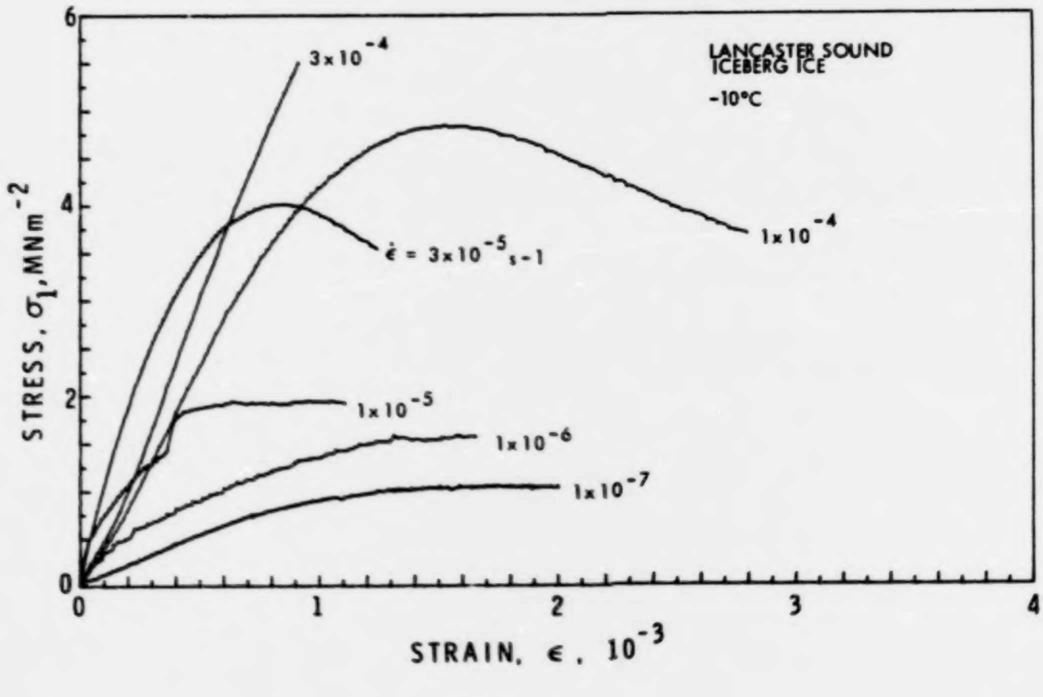

FIGURE 4 STRESS-STRAIN DIAGRAMS FOR ICEBERG ICE SUBJECTED TO TRULY CONSTANT STRAIN RATE

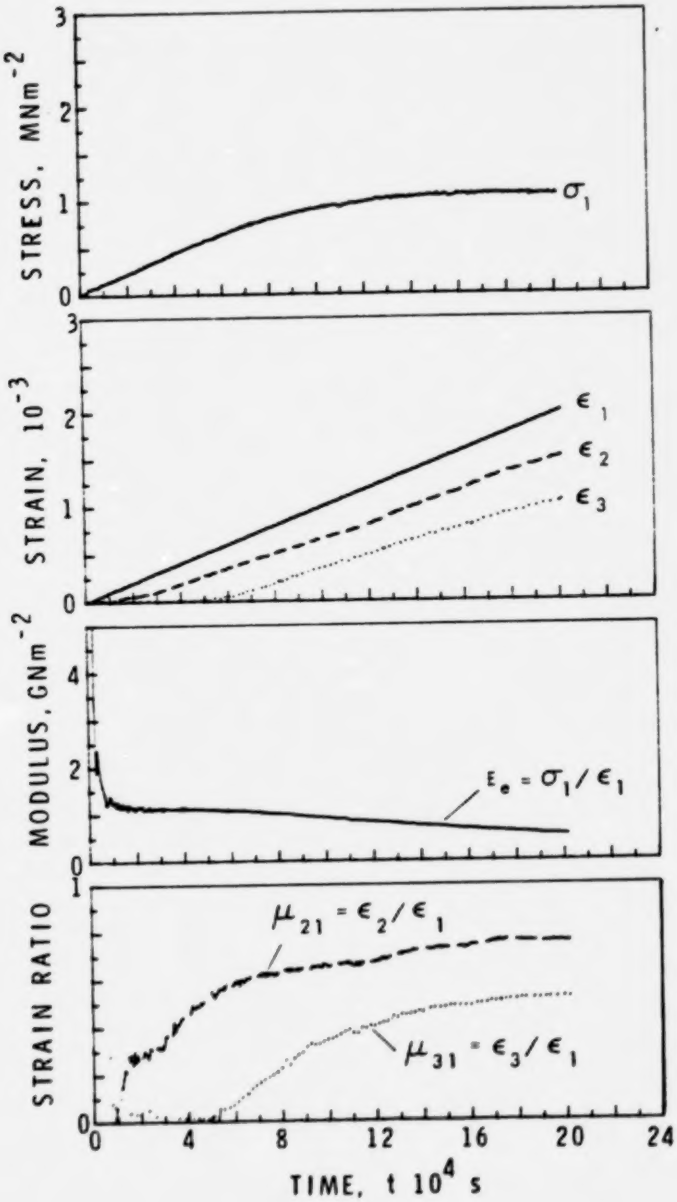

FIGURE 5 STRESS, STRAIN, EFFECTIVE MODULUS AND STRAIN RATIO HISTORIES AT STRAIN RATE OF $1 \times 10^{-7}\ s^{-1}$

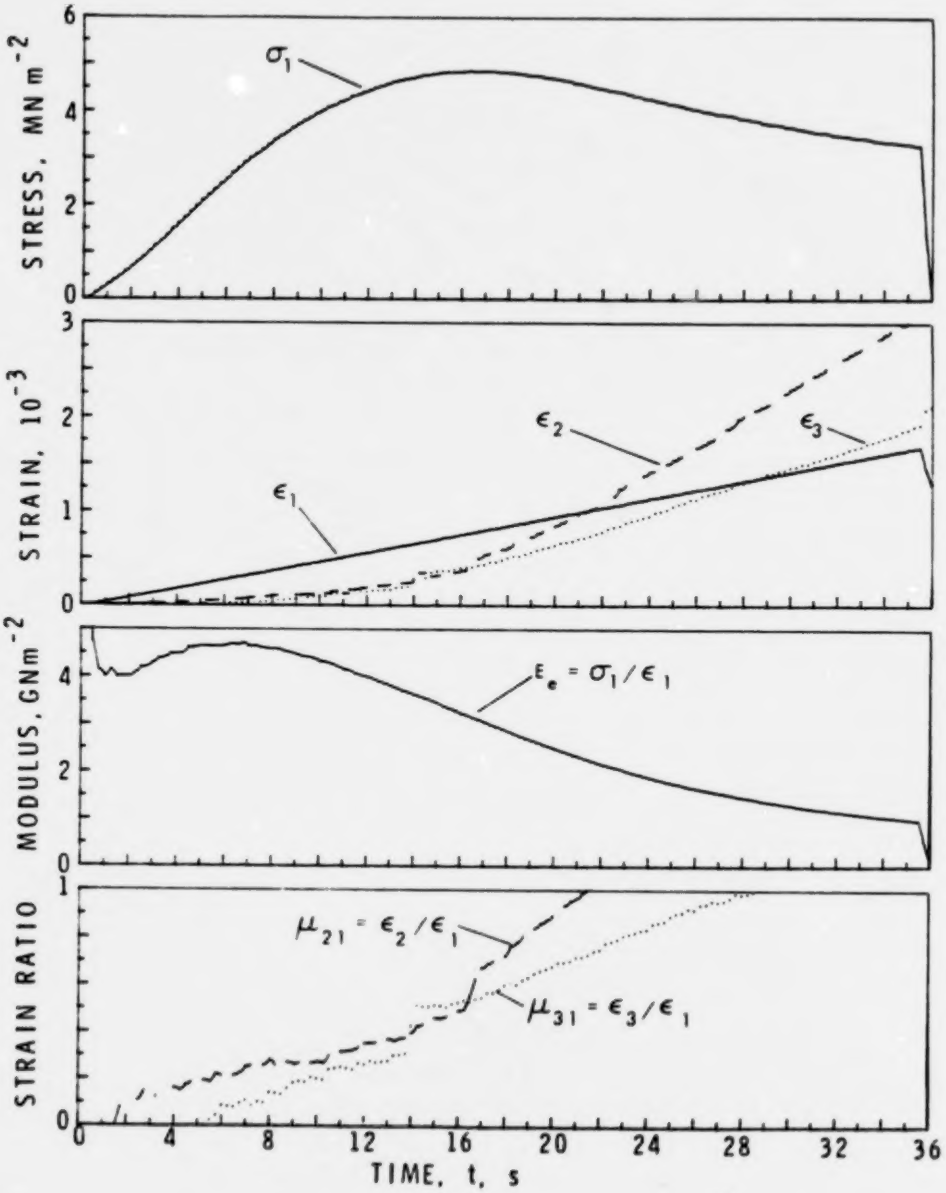

FIGURE 6 STRESS, STRAIN, EFFECTIVE MODULUS AND STRAIN RATIO HISTORIES AT STRAIN RATE OF 1×10^{-4} s^{-1}

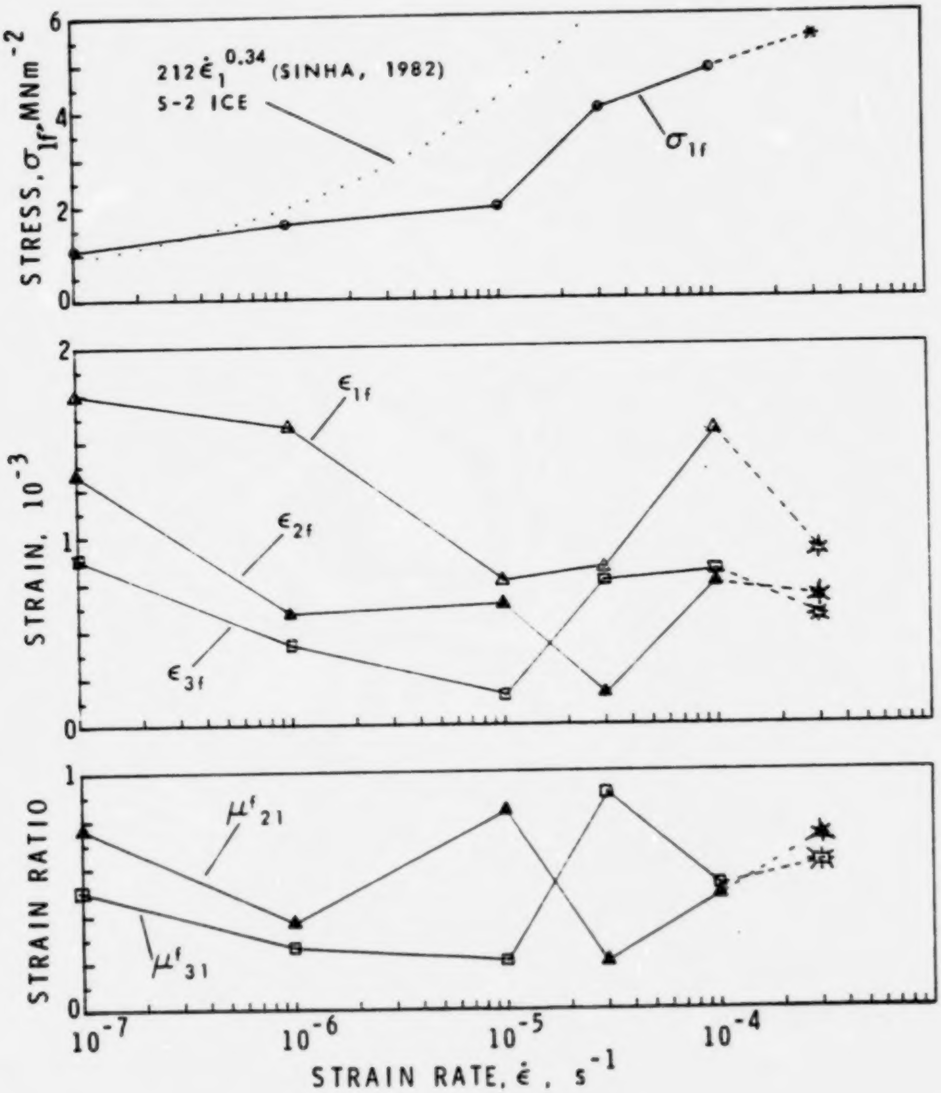

FIGURE 7 STRAIN RATE DEPENDENCE OF FAILURE STRESS, STRAIN AND STRAIN RATIO AT -10°C

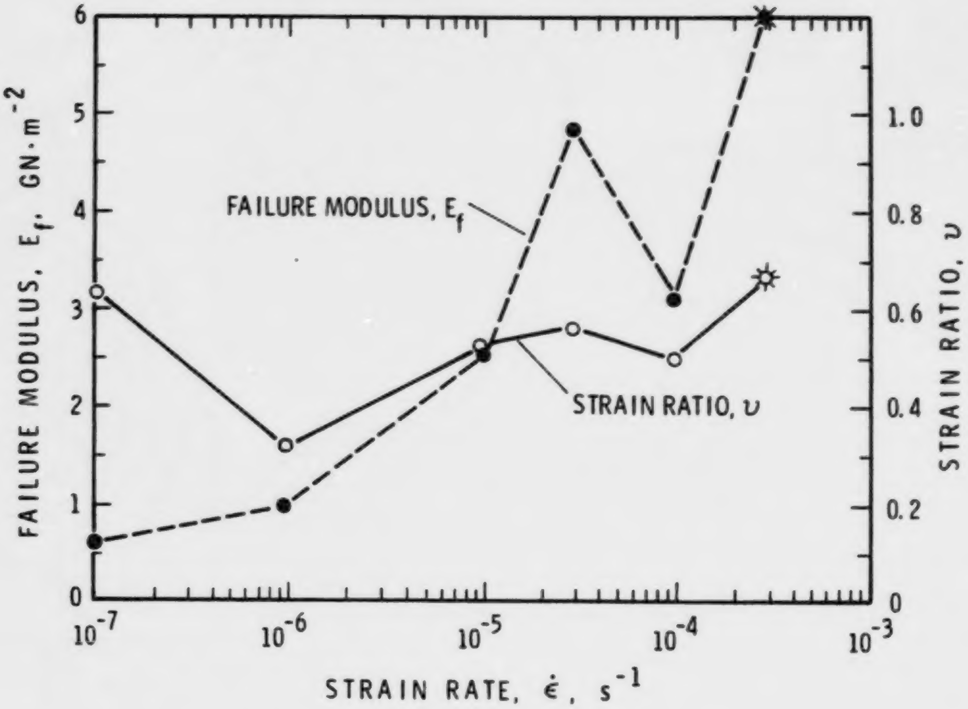

FIGURE 8 FAILURE MODULUS AND RATIO OF LATERAL TO AXIAL STRAIN AT FAILURE FOR ICEBERG ICE AT -10°C

NRC WORKSHOP ON EXTREME ICE FEATURES

Questions and Discussions Form

AUTHOR:	Nirmal K. Sinha and R. Frederking
PAPER:	Preliminary Observations on Compressive Strength, Deformation and Poisson's Ratio of Iceberg Ice
DISCUSSION BY:	R. Gerard

DISCUSSION:

A tremendous amount of effort has gone into defining the strength of small samples in carefully controlled experiments. Presumably though, the in-field strength is a function of large imperfections in the ice; large cracks, etc. Is there not as much need, for design rather than contributions to material science, to document these features, how to characterize them and to determine their influence and strength as there is to refine more and more the small sample strength? There seem to be a large imbalance in the effort on the two subjects.

AUTHOR'S REPLY:

Carefully controlled experiments are required to understand the rheological and hence mechanical properties of a material including ice. This knowledge helps us to understand the large-scale behaviour. In fact, the 'imbalance' mentioned above is decreasing every day and we are getting more and more a balanced picture.

DISCUSSION BY: G. Holdsworth

DISCUSSION:

Is it possible that the fine bubble trajectories that are shown so well in your slides are a feature related to the removal of the cores or samples? Alternatively, could surface exposure of the ice to "weathering" be a factor? Do you find these features at greater depths? How do you believe they affect the mechanical properties of the ice.

AUTHOR'S REPLY:

We sampled ice in the form of blocks, not cores. It is certain that these features are inherent characteristics of iceberg ice and most probably they correspond to thermally induced cracks. They could also represent air bubble layers developed due to the consolidation or compaction of snow layers on the glacier bed. It is difficult to say anything certain on the origin of these features. I do not know whether they are present at greater depths. If they are due to thermal cracks - then probably they are not present at greater depths where temperature does not change as quickly as it could near surface zones.

They certainly play a role in the deformation and fracture of ice, and the interpretation of mechanical test data must take into consideration the texture of the ice along with the structure and the fabric. In fact, we are already in a position to take into account the effect of bubbles and microcracks in our rheological model and thereby predict, more precisely than before, strength and deformation properties.

DISCUSSION BY: Martin Jefferies

DISCUSSION:

In the ice that accumulates at the surface of the ice shelves we find many examples of the "milky way" bubble features that you mentioned. When we drill ice cores in this ice which is freshwater ice and cold (-25°C to -15°C) the cores often shatter in smaller pieces. Do you think the "milky way" features are structural weaknesses that not only contribute to the break-up of ice cores, but also cause large scale weaknesses?

AUTHOR'S REPLY:

Yes, the "milky way" bubble features are probably structural weaknesses in the ice, brought about by mechanical and thermal stresses. On occasion I have taken pieces of shattered ice and fitted them back together; the breaks often occurred along the "milky way" weaknesses.

DISCUSSION BY: Rick Weiss

DISCUSSION:

(1) Measurements of transverse strain are not averaged over a length of specimen as is the normal strain.

(2) Measurements of transverse strain can be significantly affected by size and orientation of individual anisotropic grains when there are only a few grains across the width of the specimen.

AUTHOR'S REPLY:

(1) Measured transverse strain represent the central area of the specimen as can be seen in Figure 3.

(2) As can be seen in the text, the number of grains across the width of the specimen was not large but perhaps sufficient.

ICE INTERACTIONS WITH THE MOLIKPAQ

by

B. Wright and G.R. Pilkington
Gulf Canada corporation
Calgary, Canada

The reader is referred to the paper "WINTER ICE INTERATIONS WITH AN ARCTIC OFFSHORE STRUCTURE" by Wright B., G.R. Pilkington, K.S. Woolner and W.H. Wright, in IAHR Proceedings, Iowa City, 1986.

SUMMARY

OF A PRESENTATION GIVEN BY

VEGAR STEIRO AND STEIN STORLI

OF THE

NORWEGIAN PETROLEUM DIRECTORATE

The first production licenses on the Norwegian Continental Shelf were granted in 1965, and the first well was drilled the following year.

14 July 1972, a unanimous Storting approved establishment of the Norwegian Petroleum Directorate (NPD). At the same time, the Ministry of Industry was strengthened by the establishment of a separate Division for Petroleum and Mining. It was decided that NPD should be located in Stavanger, where the activities started April 1973. In 1978, matters concerning petroleum and energy were removed from the Ministry of Industry upon the establishment of the Ministry of Petroleum and Energy, and in 1979 the constitutional responsibility for matters concerning working environment, safety and emergency preparedness on the Continental shelf were transferred from the Ministry of Petroleum and Energy to the Ministry of Local Government and Labour. This had the effect of making the NPD responsible to two ministries. NPD works as technical advisor to these ministries.

In connection with the start of exploratory drilling off the coast of North Norway in 1980, the directorate set up its own regional office in Harstad.

FUNCTIONS

The NPD executes regulatory control of the petroleum activities on the Norwegian Continental Shelf and Svalbard.

The main functions of the Directorate are:

- to verify that petroleum activities are carried out in accordance with the current petroleum laws
- to ensure that petroleum activities do not prevent other activities from being carried out
- to map petroleum resources
- to undertake geophysical and geological exploration for the authorities
- to collect and interpret geological, geophysical and other technical data
- to ensure that the petroleum resources are exploited properly
- to maintain contact with scientific and educational institutions and to make available to them data that are no longer confidential
- to undertake petroleum economic planning and control of

all phases of petroleum activity and to administrate royalty and area fees

- to award scientific and commercial reconnaissance licenses.

From 1966 to the present the total drilling activity has been:

532 exploration wells offshore
370 development wells offshore
12 exploration wells onshore (Svalbard)

The shelf south of the 62nd parallel represents only 15 per cent (144 000 km) of the total Norwegian Shelf (1 mill. km). The NPD has estimated the total probable recoverable reserves on the Norwegian Shelf to be close to 5 000 million ton oil equivalent.

After further drilling in the Norwegian part of the North Sea, and only a handful of wells on the remaining 85 per cent of the Shelf, the reserve estimates were increased to about 6 000 million tons.

North of the 62nd parallel there has been only exploration drilling:

37 wells on Haltenbanken
6 wells on Trænabanken
4 wells on Nordland II
31 wells on Troms I

When discussing the development of the Norwegian Barents Sea, the onshore Spitsbergen area is an integrated part. A total of 12 wells have been drilled on Spitsbergen as shown in Figure 3.

Onshore development

The onshore areas of the Norwegian Arctic are limited to the Svalbard islands. Extensive geologic mapping has been performed for many decades.

The first commercial exploration well aimed at oil or gas prospects was spudded in 1963 by Norsk Polarnavigasjon.

No commercial discoveries have been made on Svalbard so far, although numerous shows have been encountered. Thick sediments with rich source rocks, reservoir rocks, cap rocks and significant structures have been proved. A general trend of the reservoirs is the low porosity. The low porosity causes high rock velocities which have been reported from several seismic investigations on the Spitsbergen islands. The exception is the Kong Carls Island in the eastern part of the archipelago where highly porous reservoir rocks have been found. Kong Carls island is, however, included among the areas with a national park status implying no commercial activities.

The maturity of the source rocks shows variations and may also represent a problem in some areas.

One well is presently being drilled. The operator is the Soviet company Arktikugol. The well their second petroleum exploration well in Vassdalen, close to the Van Mijenfjord. It was spudded in January 1985 and was planned to be finished late summer of 1986. According to NPD's knowledge, 1987 is a more probable time of finishing. The well is part of the work obligation necessary to keep a number of licenses.

There has been seen an increased interest in exploration on the Spitsbergen islands the last years. BP acquired seismic profiles on a glacier SE of the Svea mine in 1985 and they carried out a more extensive survey in 1986. Further, Norsk Hydro has made an agreement with Store Norske Spitsbergen to jointly do petroleum exploration on the licenses of Store Norske south of Longyearbyen. Statoil continues to have an active interest in the area, and they carried out seismic on glaciers this year. Norsk Polarnavigasjon is also planning further drilling on their licenses. In addition, several groups of varying degrees of seriousness have asked for and managed to raise money for petroleum exploration on Spitsbergen. Additional wells are accordingly expected in the coming years.

Three main reasons appear to be the driving mechanism for the increased interest in the area:

1. "New" geological model
   Although high risk due to the high velocities linked to the tight rocks in general, part of the deposits might have been sheltered from the hydrothermal activity, which presumably filled the previously porous rocks. Even if such beds of present optimal position are not expected to have widespread regional appearance, they could be important locally.

2. Research aspect
   Surveys like the one of BP have important scientific elements. Seismic profiles on glaciers have never been acquired before for commercial use. Mastering such technology is important and applicable several other places in the Arctic - and the Antarctic. The work is pioneering in the sense that exploration for hydrocarbons is in ice covered areas.

3. Most of the stratigraphic horizons to be found offshore are exposed onshore the Svalbard islands.
   Knowledge of the geology of the islands is accordingly very important for the understanding of the geology of the Barents Sea.

Since the areas opened for petroleum activities have been expanded significantly towards the north during the last years (see Figures 1 and 4), the third item might be the most important argument for the oil companies to work on Svalbard.

Offshore development

Barents Sea

Offshore exploration drilling commenced in June 1980. 31 wells had been completed by the end of 1986. All wells have been drilled in the Troms I area, shown in Figures 5 and 7. The number of wells drilled annually is shown in Figure 6.

The Troms I area is the only part of the offshore Norwegian Arctic where commercial exploration drilling has occured.

The drilling results are considered very encouraging. The wells have demonstrated good potential reservoir rocks and rich source rocks in several horizons.

Several gas discoveries have been made. Proven recoverable resources total around 210 x $10^9 m^3$ (9 TCF). Table 1 shows the resource estimates published NPD.

Proven resources on Troms I.

Albatross	34,3
Askeladd	52,0
Snøhvit	74,4
Snøhvit Nord	3,3
7119/12 (1)	3,6
7120/07	24,3
7120/12	14,8
SUM	206,7

The lack of infra-structure, long distance to a possible market and the water depth of the area makes it necessary to find more gas and oil before commercial development on a large scale can take place. Good oil shows have also been encountered, but limited reservoirs are established. The most significant is an extensive 15 m thick zone in the Snøhvit structure.

The most interesting indications of oil might be those of the first well drilled in the Loppa Ridge. It encountered several hundred meters of oil shows in carbonate and clastic rocks of Permian and Carboniferous. All the previously discovered resources mentioned above are from Jurassic or Triassic sandstones. Subsequent testing revealed that the majority of the oil is residual and only minor amounts were produced. The amount of water, however, showed that the production capasity of the rocks is good.

Further studies to find the relation between the oil shows and its source are very important, i.e. to find out if we have a different and perhaps older source rock than that of the oil in Snøhvit. So far, the studies indicate a different source for the oil in the carbonates than found in the Troms I area.

Several analyses of organically rich shales from different stratigraphic horizons encountered in a number of wells in the Troms area have shown that they are potential source rocks for both oil and gas. It is therefore reasonable to assume that significant amounts of oil as well as gas must have been generated in the general area.

As shown in Figure 4, the areas which are going to be opened for future exploration for oil and gas are mainly in the north. The ice conditions are shown in Figure 7 and Figure 8. The exploration activity will in a few years time be within areas where there is drifting pack ice in the winter. This will require techology which has been tested and proven in other areas of the world.

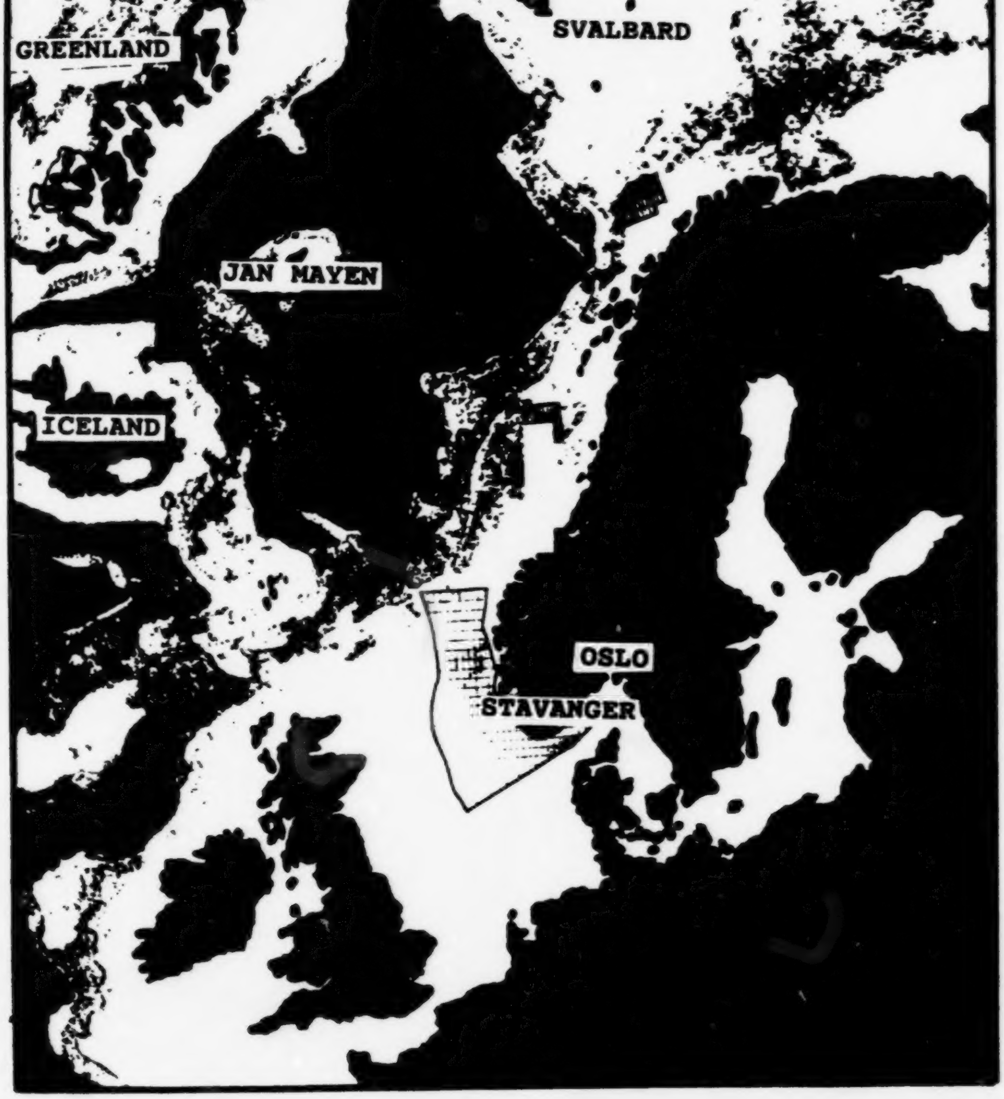
GREENLAND
SVALBARD
JAN MAYEN
ICELAND
OSLO
STAVANGER

Fig. 1

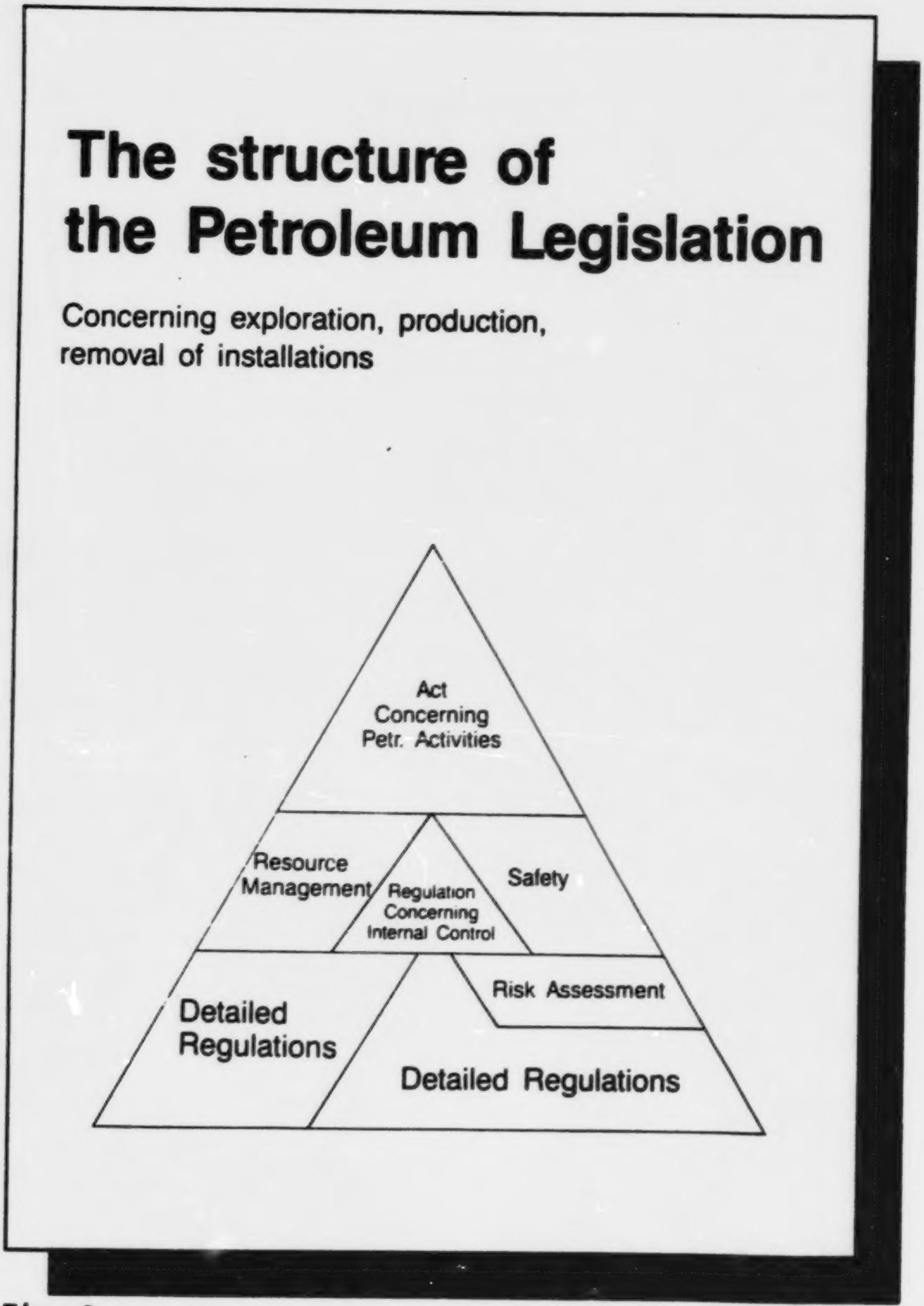

The structure of the Petroleum Legislation

Concerning exploration, production,
removal of installations

Act
Concerning
Petr. Activities
Resource
Management
Regulation
Concerning
Internal Control
Safety
Risk Assessment
Detailed
Regulations
Detailed Regulations

Fig. 2

S -

Well locations on Svalbard

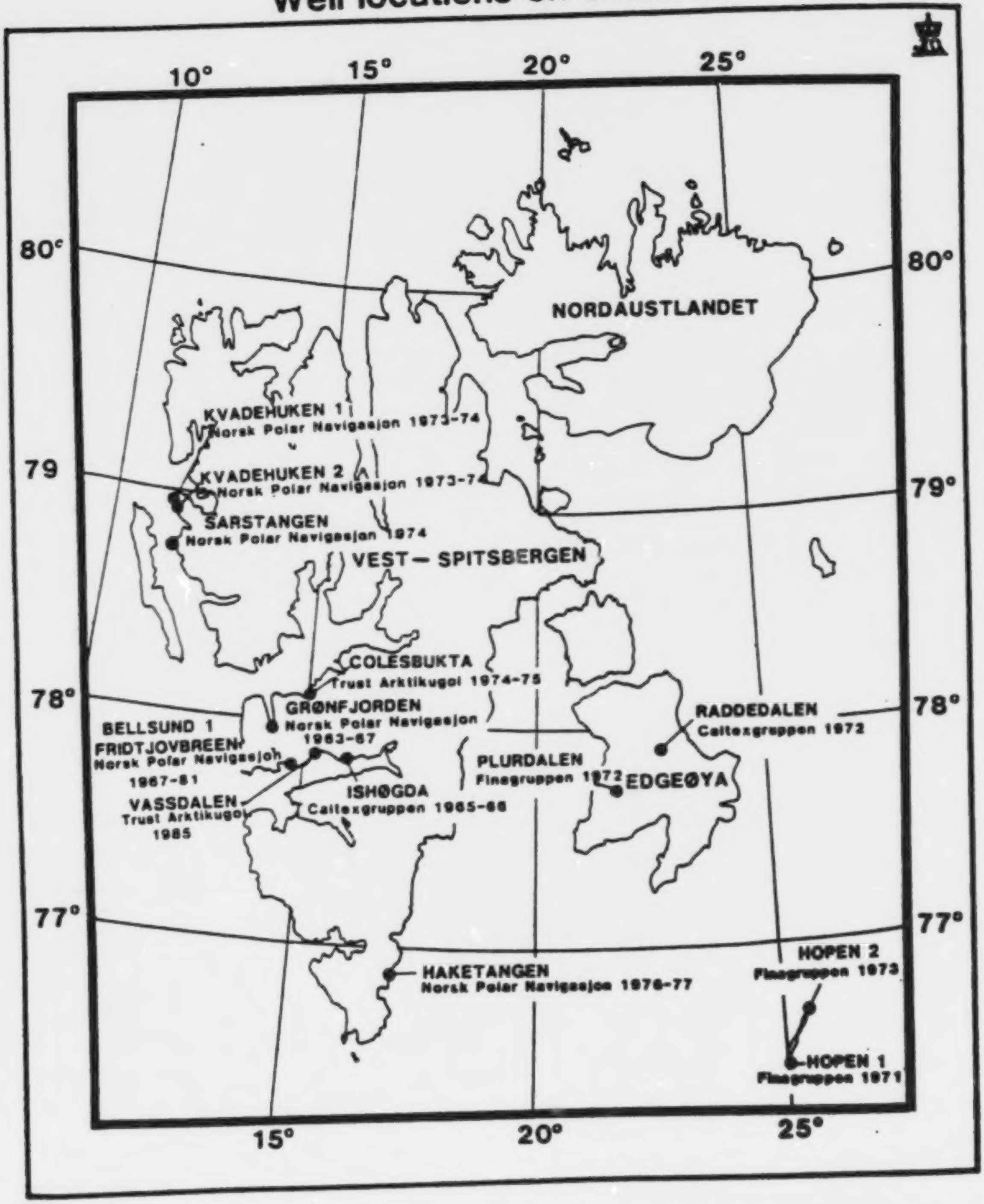
10°
15°
20°
25°
80°
80°
79
79°
78°
78°
77°
77°
15°
20°
25°
NORDAUSTLANDET
KVADEHUKEN 1
Norsk Polar Navigasjon 1973-74
KVADEHUKEN 2
Norsk Polar Navigasjon 1973-74
SARSTANGEN
Norsk Polar Navigasjon 1974
VEST — SPITSBERGEN
COLESBUKTA
Trust Arktikugol 1974-75
GRØNFJORDEN
Norsk Polar Navigasjon
1963-67
BELLSUND 1
FRIDTJOVBREEN
Norsk Polar Navigasjon
1967-81
VASSDALEN
Trust Arktikugol
1985
ISHØGDA
Caltexgruppen 1965-66
PLURDALEN
Finagruppen 1972
EDGEØYA
RADDEDALEN
Caltexgruppen 1972
HAKETANGEN
Norsk Polar Navigasjon 1976-77
HOPEN 2
Finagruppen 1973
HOPEN 1
Finagruppen 1971

Fig. 3

FUTURE EXPLORATION AREAS NORTH OF STAD

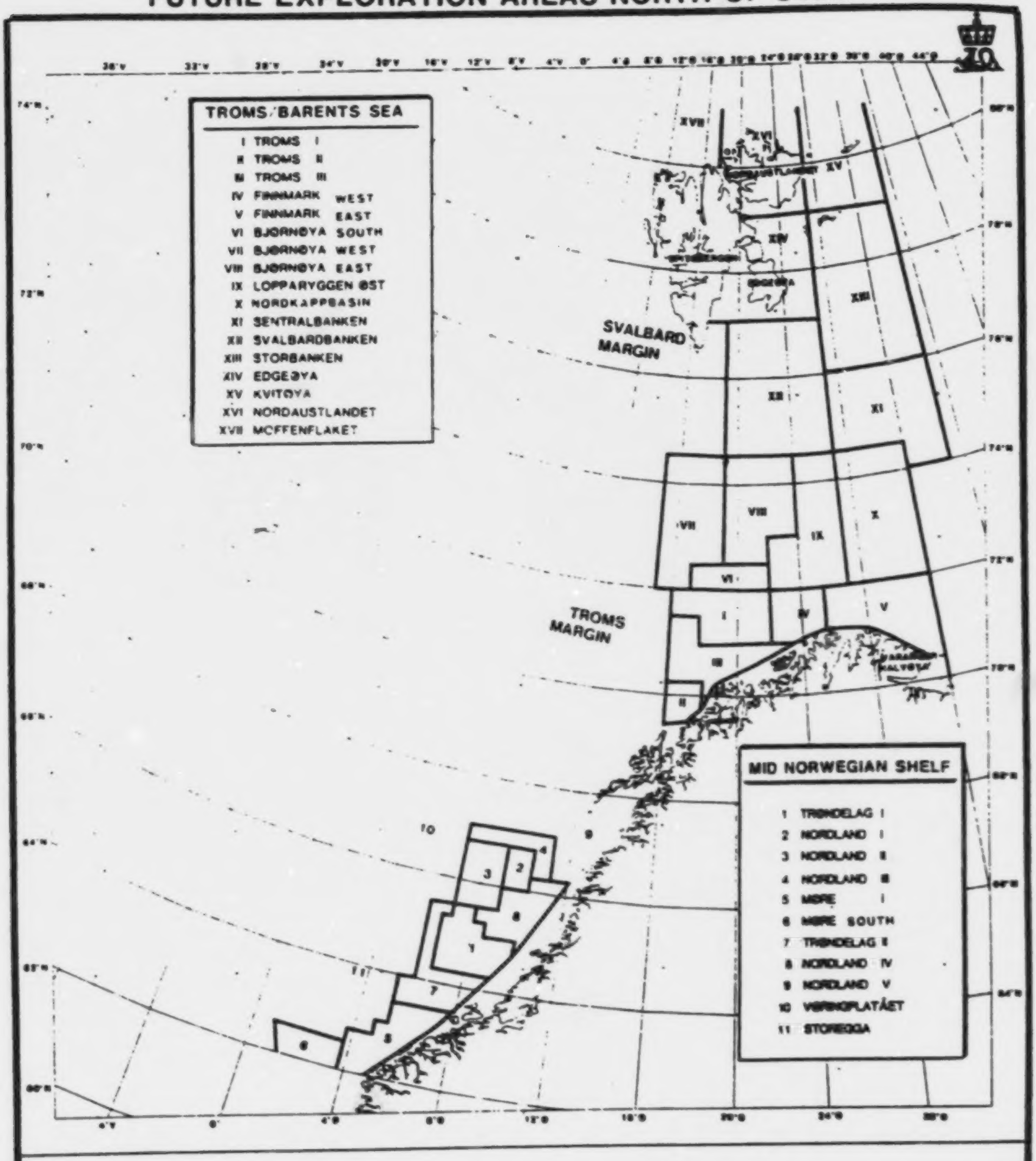
TROMS/BARENTS SEA
I TROMS I
II TROMS II
III TROMS III
IV FINNMARK WEST
V FINNMARK EAST
VI BJØRNØYA SOUTH
VII BJØRNØYA WEST
VIII BJØRNØYA EAST
IX LOPPARYGGEN ØST
X NORDKAPPBASIN
XI SENTRALBANKEN
XII SVALBARDBANKEN
XIII STORBANKEN
XIV EDGEØYA
XV KVITØYA
XVI NORDAUSTLANDET
XVII MOFFENFLAKET
MID NORWEGIAN SHELF
1 TRØNDELAG I
2 NORDLAND I
3 NORDLAND II
4 NORDLAND III
5 MØRE I
6 MØRE SOUTH
7 TRØNDELAG II
8 NORDLAND IV
9 NORDLAND V
10 VØRINGPLATÅET
11 STOREGGA
SVALBARD MARGIN
TROMS MARGIN
XVII
XVI
XV
XIV
XIII
XII
XI
X
IX
VIII
VII
VI
V
IV
III
II
I
1
2
3
4
5
6
7
8
9
10
11

REGIONAL SEISMIC SURVEYS IN NORWEGIAN SEA AND BARENTS SEA

Fig. 4

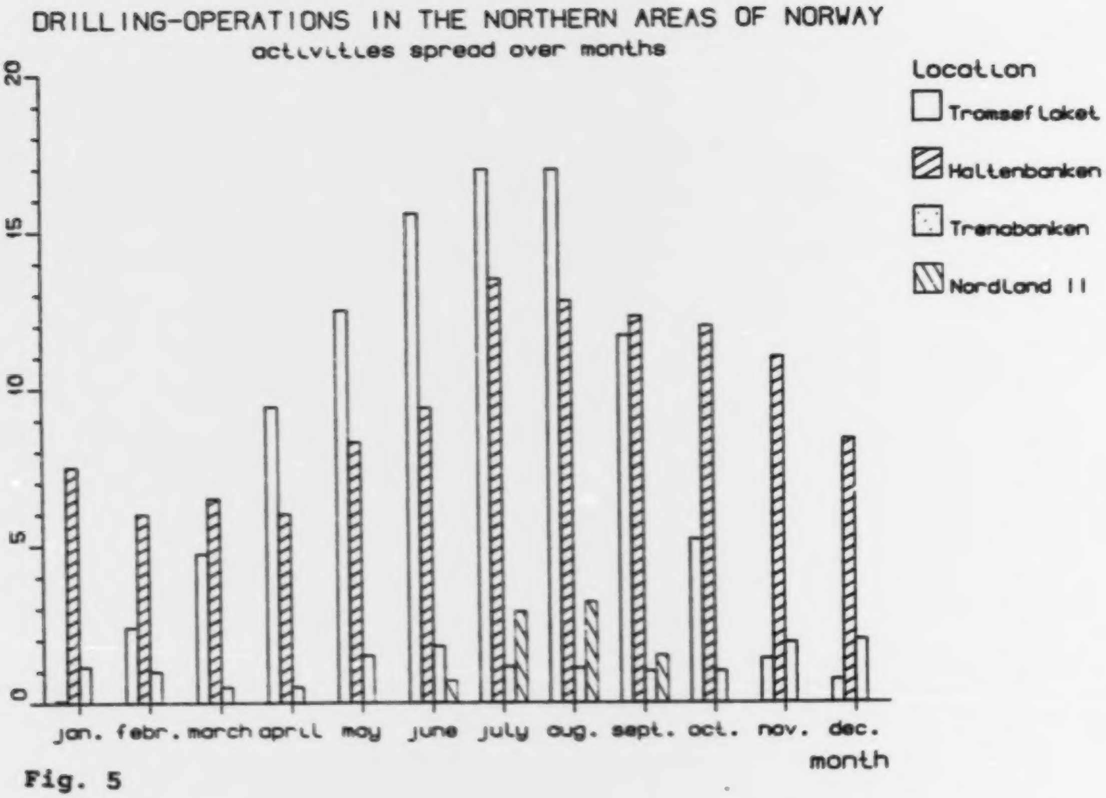
DRILLING-OPERATIONS IN THE NORTHERN AREAS OF NORWAY
activities spread over months
0
5
10
15
20
jan.
febr.
march
april
may
june
july
aug.
sept.
oct.
nov.
dec.
month
Location
Tromsøflaket
Haltenbanken
Trænabanken
Nordland II

Fig. 5

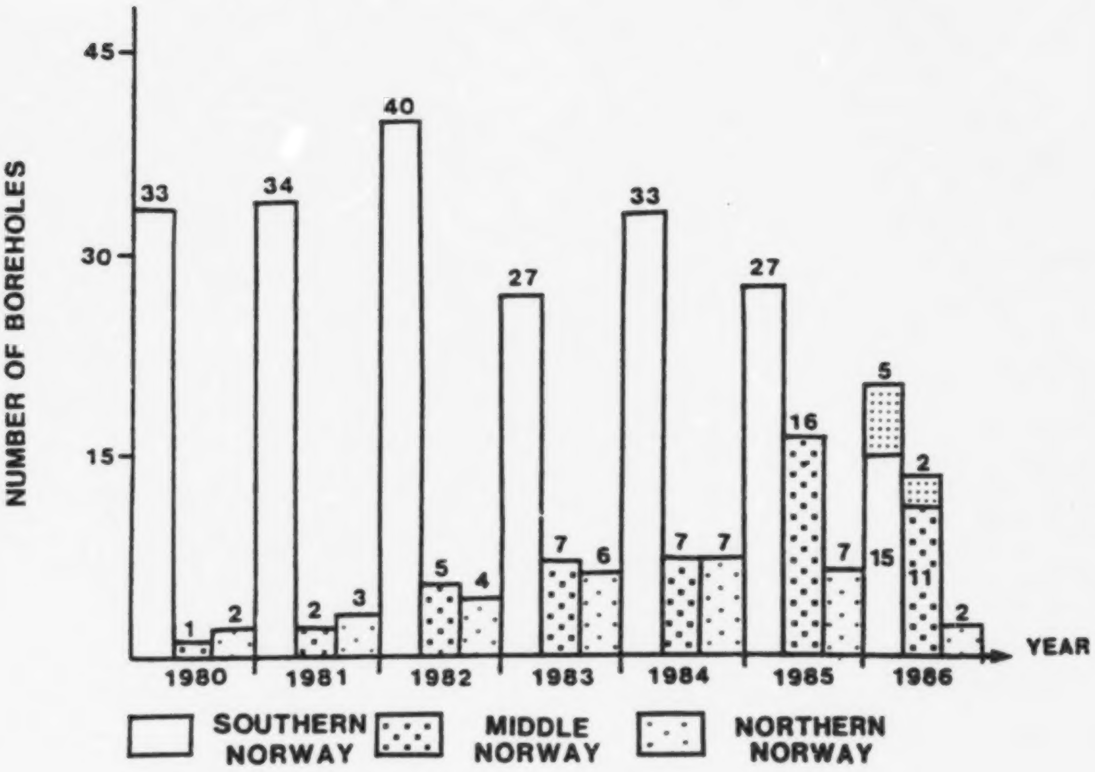

EXPLORATION DRILLING

EXPLORATION WELLS SPUDDED PR. YEAR

Fig. 6

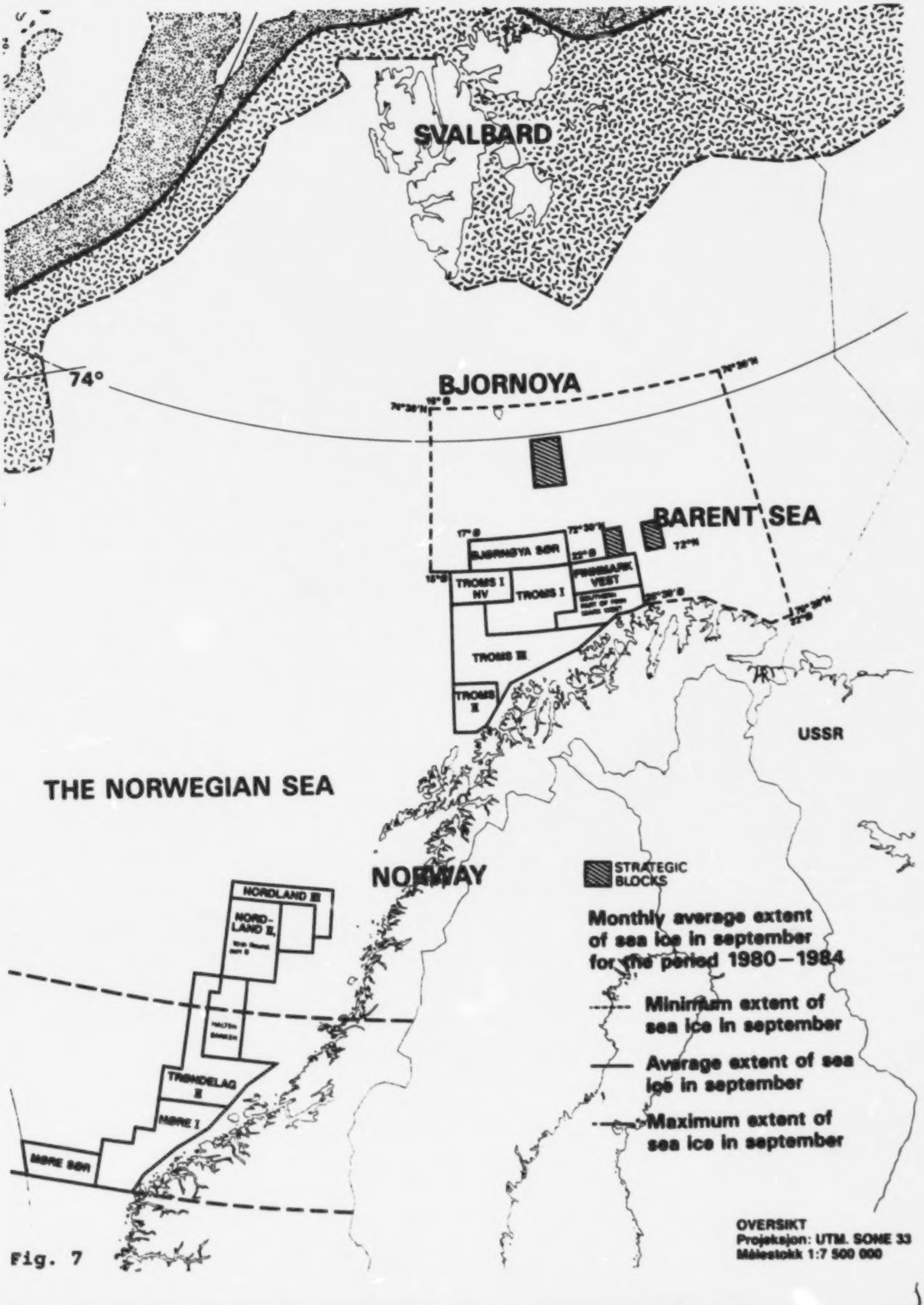
SVALBARD
74°
BJORNOYA
74°30'N
15° E
74°30'N
BARENT SEA
17° E
72°30'N
22° E
72°N
BJORNOYA SØR
15° E
TROMS I NV
TROMS I
FINNMARK VEST
22°30' E
70°30'N
32° E
TROMS III
TROMS II
USSR
THE NORWEGIAN SEA
NORWAY
NORDLAND III
NORD-LAND II
HALTEN-BANKEN
TRØNDELAG II
MØRE I
MØRE SØR
▨ STRATEGIC BLOCKS
Monthly average extent of sea ice in september for the period 1980—1984
Minimum extent of sea ice in september
Average extent of sea ice in september
Maximum extent of sea ice in september
OVERSIKT
Projeksjon: UTM. SONE 33
Målestokk 1:7 500 000

Fig. 7

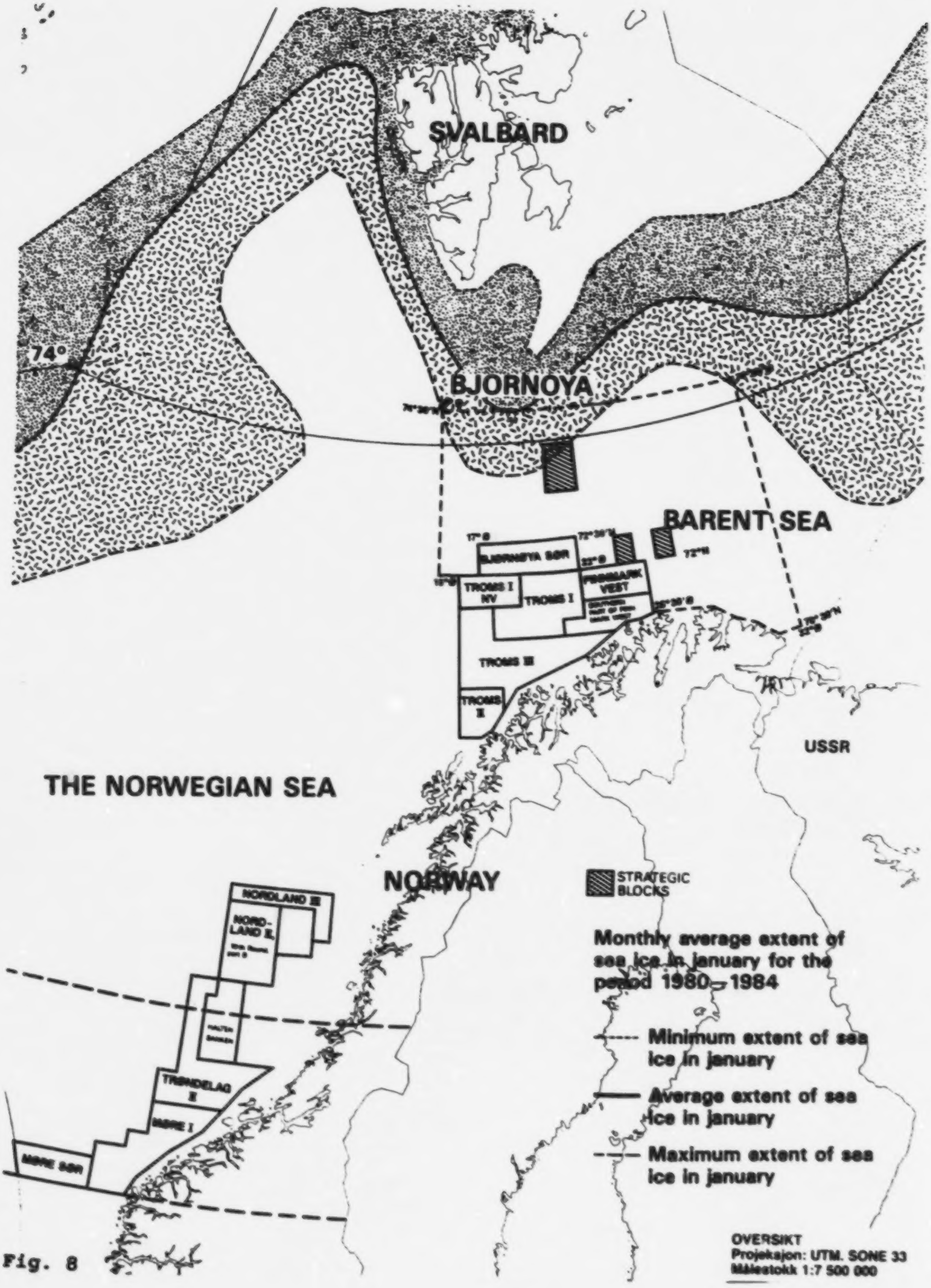
SVALBARD
74°
BJORNOYA
BARENT SEA
17° Ø
BJØRNØYA SØR
72°30'N
22° Ø
72°N
TROMS I NV
TROMS I
FINNMARK VEST
22°30'Ø
TROMS III
TROMS II
USSR
THE NORWEGIAN SEA
NORWAY
NORDLAND III
NORD-LAND II
HALTEN BANKEN
TRØNDELAG II
MØRE I
MØRE SØR
STRATEGIC BLOCKS
Monthly average extent of sea ice in january for the period 1980 – 1984
Minimum extent of sea ice in january
Average extent of sea ice in january
Maximum extent of sea ice in january
OVERSIKT
Projeksjon: UTM. SONE 33
Målestokk 1:7 500 000

Fig. 8

CURRENT RELEVANT RESEARCH ACTIVITIES OF THE ATTENDEES AT THE WORKSHOP

Attendees at the workshop were requested to identify their current areas of research, relevant to the workshop topic of extreme ice features.

Jackie Richter-Menge: CRREL

- Failure mechanisms of first year ice,
- Tensile tests starting in the new year,
- Studies in fracture mechanics,
- Development of an ROV to probe and map the bottom of the ice,
- Thermal drill to drill large holes in the ice, for determining the thickness of floes and installing ice stress sensors.

Vegard Storeli: Norwegian Petroleum Directorate

- Continuing to collect environmental data on the conditions around Svalbard in support of drilling in this area (drilling is presently being conducted in this area in the summer),

Jean-Paul Nadreau: C-CORE

- Requesting funds from NSERC to conduct a dynamic analysis of Gulf's Molikpaq structure, both physically and mathematically.
- Triaxial testing of ice; tensile tests in a multiaxial stress state,
- Indentation tests with large indentors.

NIRMAL SINHA: NRC

- Improving the borehole jack as an in situ method of testing ice.

Hans Kivisild: Lavalin

- Studying ice forces caused by fragmented river ice.

Tom Zimmerman: C-FER

- Studying the structural response of a composite wall.

Maher Nessim: DNV

- Studying the extreme loading of a structure in ice (13 companies),
- Scour optimization model.

Ken Wickwire: Nortek

- Working on a ground radar system capable of tracking ships and icebergs out to 300 km from shore. Three to seven stations should be enough to map the entire coast of Labrador.

John Sykes: U. of Waterloo

- Image analysis of SAR, SLAR and marine radar.

Ben Danielewicz: Canmar

- Thick multi-year ice statistics in support of operations.

John Sun: Unical

- His company is involved in the ice-structure model being developed by DNV (Maher Nessim).

Rick Weiss: Exxon

- Developing model to predict ice island impact,
- Ice island-structure interaction model,
- Methods of mitigating risk of ice island interactions using protective berms, and means of destroying features using, for example, coal dust,
- Statistics of ridges using an impulse radar which is good to 10 m (CCL's),
- Developing a rapid hole drilling system using hot water,

- Studying the gross properties of ice islands and hummock fields,
- Studying the 3 D shape of ridges using a sonar system,
- He indicated that he needed a device to drill large diameter holes in ice.

Eric Leavitt: Intera

- Studying the remote sensing of ice features,
- Working with Canarctic on their mission with MV Arctic into the high Arctic. Project should get about 100,000 to 200,000 km of good ice information,
- Intera will have a second SAR in 4 weeks time,
- New radar will be used on MIZEX project this spring, and will be used to image the East Greenland Sea and downlink the information to a ship,
- CCL have an ice thickness radar on a project in the Barents Sea, Intera is hoping to conduct simultaneous SAR if project goes ahead,
- There will be a submarine transect under the Greenland Sea for which the route will be published; Intera will fly their SAR along submarine route.

Bill Sackinger: Geophys. Inst., Fairbanks, Alaska

- Studying natural sea spray icing,
- Ice islands; calving, trajectories, probability of encounter, ice strength, etc.,
- Thickening an area of ice in the Gulf of Bothnia which will be pulled against a lighthouse to measure loads.

Martin Jeffries: Geophys. Inst., Fairbanks, Alaska

- Same as Bill above,
- He has a lot of ice cores from Hobson's ice island on which to do isotope studies,
- Will be monitoring the ice shelves for losses and regrowth,
- Interested in the thick multi-year landfast ice.

Len LeSchack: Trident Arctic Ltd. Canada

- Data presented in workshop,
- Just finished a study involving a submarine pass with laser overflight and the relationship between ridge keels and sails.

Paul Spencer: Geotech.

- Developing stress sensors,
- Constructing large ice structures by spraying.

Gerry Holdsworth: AES

- Continuing studies of Ward Hunt ice shelf,
- Applied calving model to Ward Hunt,
- Studying back pressure effect from pack ice,
- Calving model is not sophisticated but giving right shape,
- Conducting experiment in 1988 with Nirmal on low stress/low strain (.01 MPa).

Bob Thompson: Antarctic Inst., New Zealand

- Providing support role for airstrips, etc. at McMurdo,
- Put strain gauge on Erebus glacier hoping it calves,
- Collecting iceberg sightings,
- Studying icebergs in Ross Sea with satellites (size, shape and drift).

Brian Wright: Gulf Oil

- Curtailing Beaufort sea operations,
- Kulluk, Molikpaq and icebreakers in a safe winter harbour,
- Last summer loaded tanker with 300 000 bbls of oil from Amauligak,
- Conducting dynamic analysis of the Molikpaq.

NRC EXTREME ICE FEATURES WORKSHOP ATTENDEES

Dr. Frank Bercha
F.G. Bercha (Alberta) and
Associates Ltd.
301, 1220 Kensington Rd., N.W.
Calgary, Alberta

Tel. No.: (403) 270-2221

Mr. Dave L. Chiang
Science Application International
Corporation
1710 Goodridge Drive
McLean, Virginia 22102
U.S.A.

Ms. Shawn Cornett
Dome Petroleum
Box 200
Calgary, Alberta

Mr. K. Croasdale
Esso Resources Ltd.
339 - 50 Ave. S.E.
Calgary, Alberta
T2G 2B3

Tel. No.: (403) 259-0386

Mr. Ben Danielewicz
Dome Petroleum
Box 200
Calgary, Alberta

Tel. No.: (403) 231-1957

Robert Gerard
University of Alberta
Edmonton, Alta.
T6G 2G7

Tel. No.: (403) 432-2066

Eugene V. Guy
Memorial University of
Newfoundland
St. John's, Newfoundland
A1B 3X5

Tel. No.: (709) 737-8354

Mr. Chris Hill
#201, 727 - 3 Ave. N.W.
Calgary, Alberta
T2N 0J3

Tel. No.: (403) 283-8712

Dr. G. Holdsworth
National Hydrology Research
Institute
Environment Canada
# 11 Innovation Blvd.
Saskatoon, Saskatchewan

Tel. No.: (306) 975-5785

S. Hotzel
28 Hawkhill Way N.W.
Calgary, Alberta
T3G 2L1

Tel. No.: (403) 239-5609

Dr. Martin Jeffries
The Geophysical Institute
University of Alaska
Fairbanks, Alaska
U.S.A.

Tel. No.: (907) 474-5257

Dr. I. Jordaan
Memorial University of
Newfoundland
St. John's, Newfoundland
A1B 3X5

Dr. Hans R. Kivisild
Lavaline Offshore Inc.
909 - 5th Ave. S.W.
Calgary, Alberta
T2P 3G5

Tel. No.: (403) 294-2538

Vlodek Laskow
Arctic Research and Development Ltd.
P.O. Box 85
Bragg Creek, Alberta
TOL OKO

Tel. No.: (403) 949-2134

L. LeSchack
Trident Arctic Exploration Ltd.
3617, 608 - 9th St. S.W.
Calgary, Alberta
T2P 2B3

Dr. Jim Lever
C-CORE
Memorial University of Newfoundland
St. John's, Newfoundland
A1B 3X5

Mr. Ray Lowry/Eric Leavitt
Intera Technologies Ltd.
12 flr., 519 - 5 Street S.W.
Calgary, Alberta
T2P 3S2

Tel. No.: (403) 266-0900

Dr. Jean-Paul Nadreau
C-CORE
Memorial University of Newfoundland
St. John's, Newfoundland
A1B 3X5

Maher Nessim
Det Norske Veritas Canada Ltd.
1110, 10201 Southport Rd. S.W.
Calgary, Alta.
T2W 4X9

Tel. No.: (403) 253-3422

G.R. Pilkington
G.R. Pilkington and Associates
Box 23, Site 13, R.R. 4
Calgary, Alberta
T2M 4L4

Tel. No.: (403) 239-0370

Ms. J. Richter-Menge
Cold Regions Research and
Engineering Laboratory
Hanover, New Hampshire 03755
U.S.A.

Tel. No.: (603) 646-4100

Professor Bill Sackinger
The Geophysical Institute
University of Alaska
Fairbanks, Alaska
U.S.A.

Tel. No.: (907) 474-7865

Dr. N.K. Sinha
Institute for Research in
Construction
National Research Council of
Canada
Ottawa, Ontario
K1A 0R6

Tel. No.: (613) 993-3802

Dr. Harold Shoemaker
U.S. Dept. of Energy
P.O. Box 880
Morgantown, West Virginia 26507
U.S.A.

Dr. Paul Spencer
Geotech Engineering
4500 - 5 St. N.E.
Calgary, Alberta

Tel. No.: (403) 230-4128

Mr. G. Spedding
Esso Resources Ltd.
339 - 50 Ave. S.E.
Calgary, Alberta
T2G 2B3

Tel. No.: (403) 259-0335

John Sun
Unocal
376 South Valencia Ave.
Brea, CA 92621
U.S.A.

Tel. No.: (714) 528-7201

Mr. Vegar Steiro
P.O. Box 787
9401 Harstad
Norway

Mr. Stein Storeil
Norwegian Petroleum Directorate
P.O. Box 600
4001 Stavenger
Norway

Professor J. Sykes
Department of Civil Engineering
University of Waterloo
Waterloo, Ontario
N2L 3G1

Mr. M.D. Thomas
COGLA
Box 1500
Yellowknife, N.W.T.
X1A 2R3

Tel. No.: (403) 920-8178

R.B. Thomson
New Zealand Department of Scientific
and Industrial Research
Antarctic Division
P.O. Box 13247
214A Oxford Terrace
Christchurch, N.Z.

Dr. Ronald I. Verrall
Defence Research Establishment
Pacific
DREP
FMO
Esquimalt, B.C.
VOS 1BO

Tel. No.: (604) 380-2912

Dr. R.T. Weiss
Exxon Production Research Co.
P.O. Box 2189
Houston, Texas 77252-2189
U.S.A

Tel. No.: (713) 965-4763

Kenneth Wickwire
NorTek Engineering Inc.
#501, 220 LeMarchant Road
St. John's, Newfoundland
A1C 2H8

Tel. No.: (709) 739-6749

W. Wright
Gulf Canada Corp. Ltd.
401 - 9th Ave. S.W.
Calgary, Alberta
T2P 2H7

Tel. No.: (403) 233-3896

Mr. Tom Zimmerman
C-FER
Building 7-A
University of Edmonton Campus
Edmonton, Alta.
T2G 2E2

Tel. No.: (403) 432-5108

NATIONAL RESEARCH COUNCIL OF CANADA

ASSOCIATE COMMITTEE ON GEOTECHNICAL RESEARCH

LIST OF TECHNICAL MEMORANDA

NOTE: Copies of out-of-print Technical Memoranda can be duplicated at $0.34 per page, $3.40 minimum, in Canada, and obtained by directing a request to the Canada Institute for Scientific and Technical Information, National Research Council, Canada, Building M-55, Ottawa, Ontario, K1A 0R6.

NOTE: All orders for publications must be prepaid and should be addressed to the Publications Section, National Research Council, Canada, Building R-88, Ottawa, Ontario, K1A 0R6.

Nos. 1-8 - Previously Classified - now out-of-print.

* 9 Proceedings of the 1947 Civilian Soil Mechanics Conference. August 1947.

* 10 Proceedings of the Conference on Snow and Ice, 1947. October 1947.

* 11 Proceedings of the 1948 Civilian Soil Mechanics Conference. October 1949.

* 12 Index to Proceedings of Rotterdam Soil Mechanics Conference, Soil Mechanics Bulletin No. 1. May 1949.

* 13 Canadian Papers: Rotterdam Soil Mechanics Conference. June 1949.

* 14 Canadian Papers presented at the Oslo Meetings of the International Union of Geodesy and Geophysics. December 1949.

15 Canadian Survey of Physical Characteristics of Snow-Covers, G.J. Klein. April 1950.

* 16 Progress Report on Organic Terrain Studies, N.W. Radforth. April 1950.

* 17 Proceedings of the 1949 Civilian Soil Mechanics Conference. April 1950.

* 18 Method of Measuring the Significant Characteristics of the Snow-Cover, G.J. Klein, D.C. Pearce, L.W. Gold. November 1950.

* 19 Proceedings of the 1950 Soil Mechanics Conference. April 1951.

* 20 Snow Studies in Germany, Major M.G. Bekker, Directorate of Vehicle Development, Department of National Defence. May 1951.

* 21 The Canadian Snow Survey, 1947-1950, D.C. Pearce, L.W. Gold. August 1951.

* 22 Annual Report of the Canadian Section of the International Society of Soil Mechanics and Foundation Engineering (June 1950 - June 1951), Soil Mechanics Bulletin No. 2.

* 23 Proceedings of the Fifth Canadian Soil Mechanics Conference, January 10-11, 1952. May 1952.

* 24 A Suggested Classification of Muskeg for the Engineer, N.W. Radforth. May 1952.

* 25 Soil Mechanics Papers Presented at the Building Research Congress 1951. November 1952.

26 Annual Report of the Canadian Section of the International Society of Soil Mechanics and Foundation Engineering (June 1951 to June 1952). Soil Mechanics Bulletin No. 4. December 1952.

* 27 Proceedings of the Sixth Canadian Soil Mechanics Conference, Winnipeg, December 15-16, 1952. May 1953.

* 28 The Use of Plant Material in the Recognition of Northern Organic Terrain Characteristics, N.W. Radforth. March 1954.

* 29 Construction and Maintenance of Roads over Peat, F.E. Dryburgh and E.R. McKillop (Reprinted with Permission of D.S.I.R., Great Britain). July 1964.

30 Canadian Papers Presented at the Third International Conference on Soil Mechanics and Foundation Engineering. July 1954.

31 The International Classification for Snow. (Issued by the Commission on Snow and Ice of the International Association of Hydrology.) August 1954.

32 Annual Report of the Canadian Selection of the International Society of Soil Mechanics and Foundation Engineering. June 1953 to June 1954. Soil Mechanics Bulletin No. 5. July 1954.

* 33 Proceedings of the Seventh Canadian Soil Mechanics Conference, Ottawa. December 10-11, 1953. September 1954.

* 34 Palaeobotanical Method in the Prediction of Sub-surface Summer Ice Conditions in Northern Organic Terrain, N.W. Radforth. March 1955.

* 35 Proceedings of the First Regional Soil Mechanics Conference, Fredericton, April 23-24, 1954.

* 36 Proceedings of the Eighth Canadian Soil Mechanics Conference, Ottawa, December 16-17, 1954. April 1955.

37 Guide to the Field Description of Soils for Engineering Purposes. December 1955. Price $0.60

37F Guide d'Identification sur Place des Sols. NRC 3813F. March 1958, Price $0.30.

* 38 Proceedings of the Western Muskeg Research Meeting. 2 March 1955. September 1955.

* 39 Range of Structural Variation in Organic Terrain by Dr. N.W. Radforth. March 1956.

40 Annual Report of the Canadian Section of the International Society of Soil Mechanics and Foundation Engineering (June 1954 - December 1955). Soil Mechanics Bulletin No. 6. May 1956.

* 41 Proceedings of the Ninth Canadian Soil Mechanics Conference, Vancouver. December 15-16, 1955. October 1956.

* 42 Proceedings of the Eastern Muskeg Research Meeting, February 22, 1956. October 1956.

43 Muskeg Access with Special Reference to Problems of the Petroleum Industry by Dr. N.W. Radforth. November 1956.

44 Guide to a Field Description of Muskeg. Prepared by I.C. McFarlane. January 1957. Price $0.10.

* 45 Peat in Canada and Britain, Economic Implications. N.W. Radforth. (Reprinted from Journal of the Royal Society of Arts, Vol. CIV.) November 9, 1956.

* 46 Proceedings of the Tenth Canadian Soil Mechanics Conference, Ottawa. December 16 and 17, 1956.

* 47 Proceedings of the Third Muskeg Research Conference, February 20-21, 1957. July 1957.

48 The Nicolet Slide, J.E. Hurtubise and P.A. Rochette. May 1957.

49 Permafrost - A Digest of Current Information. August 1957.

50 The Mechanism of Flow Slides in Cohesive Soils, G.G. Meyerhof. September 1957.

* 51 Engineering Problems Involving Pre-Consolidated Clay Shales by R.M. Hardy.

52 Canadian Papers Presented at the Fourth International Conference on Soil Mechanics and Foundation Engineering, London. August 1957.

* 53 Proceedings of the Eleventh Canadian Soil Mechanics Conference, Ottawa. December 9-10, 1957.

* 54 Proceedings of the Fourth Muskeg Research Conference, March 11, 1958. August 1958.

55 Annual Report of the Canadian Section of the International Society of Soil Mechanics and Foundation Engineering for Year Ending June 1958, including Membership List of the Canadian Section. Prepared by C.B. Crawford. September 1958.

* 56 The Bearing Strength of Ice. A Symposium sponsored by the Associate Committee on Soil and Snow Mechanics, held at the Building Research Centre, National Research Council, Canada, Ottawa, April 16-17, 1958. Price $0.50.

* 57 Muskeg Impedence Factors Controlling Mobility, N.W. Radforth and J. Evel.

58 Muskeg Access: The Slipe-Haul Method. James Cuthbertson and N.W. Radforth. April 1959.

59 Proceedings of the Twelfth Canadian Soil Mechanics Conference. December 8-9, 1958. April 1959.

* 60 Proceedings of the Permafrost Research Conference at the Building Research Centre, Ottawa, March 27, 1958.

61 Proceedings of the Fifth Muskeg Research Conference, March 4, 1959. May 1959.

62 Annual Report of the Canadian Section of the International Society of Soil Mechanics and Foundation Engineering for Year Ending June 1959, including Membership List of the Canadian Section. Prepared by C.B. Crawford. August 1959.

63 Proceedings of the Thirteenth Canadian Soil Mechanics Conference, 10-11 September 1959. June 1960.

64 Snow Road Preparation in Scandinavia. March 1960.

* 65 Annual Report of the Canadian Section of the International Society of Soil Mechanics and Foundation Engineering for Year Ending June 1960, including Membership List of the Canadian Section. Prepared by C.B. Crawford. August 1960.

66 Snow Depth and Snow Density at Resolute, Northwest Territories by R.W. Longley, University of Alberta. Reprinted from Journal of Glaciology, Vol. 3, No. 28, Oct. 1960, pp. 733-738.

* 67 Proceedings of the Sixth Muskeg Research Conference, 20-21 April 1960. February 1961.

* 68 Annual Report of the Canadian Section of the International Society of Soil Mechanics and Foundation Engineering for Year Ending May 1961,

including Membership List of the Canadian Section. Prepared by C.B. Crawford. June 1961.

* 69 Proceedings of the Fourteenth Canadian Soil Mechanics Conference, 13-14 October 1960. June 1961.
2-4 February 1972. NRCC 12498. Price $5.00

70 Proceedings of the Symposium on Air Bubbling, Ottawa, 11 May 1961. December 1961.

* 71 Proceedings of the Seventh Muskeg Research Conference, December 1961.

72 Canadian Papers Presented at the Fifth International Conference on Soil Mechanics and Foundation Engineering, Paris. July 1961.

* 73 Proceedings of the Fifteenth Canadian Soil Mechanics Conference, 8-9 November 1961. June 1962.

74 Proceedings of the Eighth Muskeg Research Conference, 17-18 May 1962. October 1962.

* 75 Annual Report of the Canadian Section of the International Society of Soil Mechanics and Foundation Engineering for Year Ending June 1962, including Membership List of the Canadian Section. June 1962.

76 Proceedings of the First Canadian Conference on Permafrost, 17-18 April 1962. January 1963.

77 Proceedings of the Atlantic Provinces Regional Seminars on Muskeg, 15, 17 and 19 October 1962. December 1963.

78 Symposium on the Heat Exchange at Snow and Ice Surfaces, 26 October 1962. October 1963.

79 Guide to a Field Description of Permafrost for Engineering Purposes. Prepared by J.A. Pihlainen and G.H. Johnston, October 1963. Price $0.10.

80 Annual Report of the Canadian Section of the International Society of Soil Mechanics and Foundation Engineering for Year Ending June 1963, including Membership List of the Canadian Section. October 1963.

81 Proceedings of the Ninth Muskeg Research Conference, 21-22 May 1963. April 1964.

82 Proceedings of the Sixteenth Canadian Soil Mechanics Conference, 12 and 14 September 1962. January 1964.

83 Proceedings of a Conference on Snow Removal and Ice Control, 17-18 February 1964. October 1964. Price $1.50

84 Annual Report of the Canadian Section of the International Society of Soil Mechanics and Foundation Engineering for Year Ending June 1964, including Membership List of the Canadian Section. October 1964.

85 Proceedings of the Tenth Muskeg Research Conference, 21-22 May 1964. May 1965.

86 Proceedings of the Canadian Regional Permafrost Conference, 1-2 December 1964. September 1965.

87 Proceedings of the Eleventh Muskeg Research Conference, 6-7, May 1965. May 1966.

88 Canadian Papers Presented at the Sixth International Conference on Soil Mechanics and Foundation Engineering, Montreal, September 1965. December 1965.

89 Annual Report of the Canadian Section of the International Society for Soil Mechanics and Foundation Engineering for Year Ending June 1966, including Membership List of the Canadian Section. September 1966.

90 Proceedings of the Twelfth Muskeg Research Conference, 19-20 May 1966. March 1967.

91 Annual Report of the Canadian Section of the International Society for Soil Mechanics and Foundation Engineering for Year Ending June 1967, including Membership List of the Canadian Section. November 1967.

92 Proceedings of a Conference on Ice Pressures Against Structures, March 1968. Price $3.50.

93 Manual on Snow Removal and Ice Control in Urban Areas. November 1967. Price $1.50.

93F Manuel de Dēneigement et de la Lutte Contre le Verglas dans les Rēgions Urbaines. March 1969. Price $1.50.

94 Annual Report of the Canadian Section of the International Society for Soil Mechanics and Foundation Engineering for Year Ending June 1968, including Membership List of the Canada Section. November 1968.

95 Report of the Geotechnical Sciences to the Solid-Earth Science Study Group of the Science Council of Canada. April 1969.

96 Proceedings of the Third Canadian Conference on Permafrost, 14-15 January 1969.

97 Annual Report of the Canadian Section of the International Society for Soil Mechanics and Foundation Engineering for Year Ending December 1969, including Membership List of the Canadian Section. February 1970.

* 98 Proceedings of a Conference on Ice Engineering and Avalanche Forecasting and Control. (Sixth Snow and Ice Conference, Calgary, 23-24 October 1969.) November 1970. Price $1.00

99 Proceedings of the Thirteenth Muskeg Research Conference, 7-8 May 1970. November 1970. Price $1.00.

100 Annual Report of the Canadian Section of the International Society for Soil Mechanics and Foundation Engineering for Year Ending December 1970, including Membership List of the Canadian Section. March 1971. Price $1.00.

101 Workshop on the Action of Ice on Structures, 12-13 November 1970. April 1971. Price $1.00.

102 Proceedings of the Fourteenth Muskeg Research Conference, 10-11 May 1971. January 1972. Price $1.00.

103 Proceedings of a Seminar on the Permafrost Active Layer, 4-5 May 1971. December 1971. Price $1.00.

104 Proceedings of Canadian Northern Pipeline Research Conference, 2-4 February 1972. (NRCC 12498) Price $5.00.

105 Annual Report of the Canadian Section of the International Society for Soil Mechanics and Foundation Engineering for Year Ending December 1971, including Membership List of the Canadian Section. June 1972. Price $1.00

106 Summary of Current Research on Snow and Ice in Canada. June 1972. Price $1.00.

107 Seminar on Ice Jams in Canada, 7 May 1973. July 1973. Price $1.00.

108 Proceedings of a Seminar on the Thermal Regime and Measurements in Permafrost, 2-3 May 1972. October 1973. Price $1.00.

109 Proceedings of National Conference on Urban Engineering Terrain Problems, 7-8 May 1973. (NRCC 13808) Price $5.00.

110 Proceedings of the Fifteenth Muskeg Research Conference, 14-15 May 1973. March 1974. Price $1.00.

111 Permafrost Terminology. NRCC 14274. Price $3.00.

111F Terminologie du Pergélisol. NRCC 14274F. Price $3.00.

112 Annual Report of Canadian Section ISSMFE including Membership List of Canadian Geotechnical Society. September 1974. Price $1.00.

113 Proceedings of a Symposium on Permafrost Geophysics, 27-28 February 1974. November 1975. Price $1.00.

114 Proceedings of a Research Seminar on Thermal Regime of River Ice, 24-25 October 1974. Price $1.00.

115 A Survey of Snow Engineering Research Needs in Canada, March 1975. Price $1.00.

116 Proceedings of the Sixteenth Muskeg Research Conference, 7 October 1975. March 1976. Price $1.00.

*117 Russian-English Glossary of Permafrost Terms - Poppe & Brown. May 1976. Price $1.00

118 Summary of Current Research on Snow and Ice in Canada 1975-76. March 1976. Price $1.00.

119 Proceedings of a Symposium on Permafrost Geophysics, 12 October 1976. Price $1.00.

120 Proceedings of a Workshop on Avalanche Control, Forecasting & Safety, 1-4 November 1976. February 1978. Price $1.00.

121 Workshop on the Mechanical Properties of Ice, 24-25 January 1977. October 1977. Price $1.00.

122 Proceedings of Seventeenth Muskeg Research Conference, 4 October 1977. June 1978. Price $1.00.

123 Proceedings of Workshop on Bearing Capacity of Ice Covers, 16-17 October 1978. May 1979. Price $3.50.

124 Proceedings of a Symposium on Permafrost Field Methods and Permafrost Geophysics, 3-4 October 1977. April 1979. Price $3.50.

125 Peat Testing Manual. May 1979. Price $3.00.

126 Results of a Survey of Research in Geotechnics at Canadian Universities. November 1979. Price $5.00.

127 Proceedings of the Eighteenth Muskeg Research Conference, 15 August 1979. June 1980. Price $7.50.

128 Proceedings of Symposium on Permafrost Geophysics (No. 5), 13-14 November 1978. Price $8.50.

129 Workshop on Winter Roads, 18-19 October 1979. Price $5.00.

130 Proceedings of Workshop on Permafrost Engineering, 27-28 September 1979. Price $7.00.

131 Mineral Terrain Terminology. NRCC 20010. Price $5.00.

132 Guidelines for Weather, Snowpack and Avalanche Observations. Revised Edition 1986. Price $5.00

133 Proceedings of Avalanche Workshop, 3-5 November 1980. Price $10.00.

134 Proceedings of Workshop on Sea Ice Ridging and Pile-up. January 1982. Price $10.00.

135 Geotechnical Aspects of Waste Disposal. July 1983. Price $5.50.

135F Aspects Géotechniques de l'Elimination des Déchets. Prix $5.50.

136 Workshop on Ice Scouring, 15-19 February 1982. Price $14.00 (NRCC 24708).

137 Proceedings Fourth Canadian Permafrost Conference, The Roger J.E. Brown Memorial Volume. March 1981. (NRCC 20124) Price $50.00 Book Rate, $53.00 First Class Canada, $56.00 First Class U.S.A.

138 Proceedings - Advances in Peatland Engineering, 25-26 August 1986. (NRCC 26012) Price $25.00. (Copies available through the Conference Services, NRCC. and BiTech Publishers Ltd., 902 - 1030 W. Georgia Street, Vancouver, B.C., V6E 2Y3.

139 Proceedings of the Workshop on Subsea Permafrost, November 18, 1985, and Pipelines in Permafrost November 19, 1985. November 1986. (NRCC 26706) Price $10.00.

140 Proceedings of Workshop on Snow Property Measurements, 1-3 April, 1985. Compiled by R. Kry. (NRCC 27594) Price $25.00

141 Proceedings of Workshop on Extreme Ice Features, 3-5 November, 1986. Compiled by G.R. Pilkington. (NRCC 28003) Price $ 20.00